Technical Discussions of
Offsite Safety Programs For
Underground Nuclear Detonations

DISTRIBUTION STATEMENT A
Approved for Public Release
Distribution Unlimited

United States Atomic Energy Commission
Nevada Operations Office

MAY 1969

20000920 209

LEGAL NOTICE
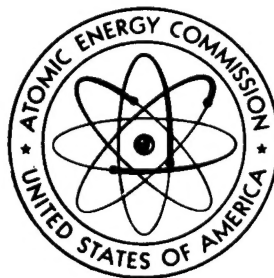
Technical Discussions of Offsite Safety Programs For Underground Nuclear Detonations

United States Atomic Energy Commission

Nevada Operations Office

MAY 1969

CONTENTS

CHAPTER 12

CHAPTER 13

CHAPTER 14

CHAPTER 15

Chapter 1

SAFETY RESPONSIBILITIES OF NEVADA OPERATIONS OFFICE

Robert E. Miller, *Manager*
U.S. Atomic Energy Commission, Nevada Operations Office, Las Vegas, Nevada

The Nevada Operations Office of the Atomic Energy Commission has at present a prime responsibility for the execution and safety of all underground nuclear detonations carried out by the United States Government. This is a responsibility that has not been taken lightly in the past and continues to occupy a cardinal position in all NVOO test activity; specifically, at the Nevada Test Site, central Nevada test area, and at the Aleutian Island of Amchitka.

The process of detonating a nuclear device never can be assumed to be free from danger or risk. Based on our experience with more than 465 announced nuclear detonations including some 270 underground explosions at the Nevada Test Site, the status of our safety knowledge and damage prevention capability indicates that these experiments can be conducted safely. A definition of safety which reflects the philosophy of the NVOO is:

> "A nuclear device can be detonated safely when it is ascertained that the detonation can be accomplished without injury to people, either directly or indirectly, and without unacceptable damage to the ecological system and natural and man-made structures."

Through the investigations and procedures which are discussed in detail in the papers which follow, I am confident that the reader will obtain an even greater appreciation of the scope of the NVOO safety effort.

I would like to summarize briefly the actions and procedures taken for a nuclear test. Potential hazards are investigated and plans and safety procedures are placed in effect well before and continued after the detonation of a nuclear device to assure the safety of all personnel and property both on and offsite. To insure that all detonations are conducted in accord with this concept of public safety, two concurrent programs have been established by NVOO.

The first program is associated with safety measures taken at the time of a test such as evaluating the hazards that might be associated with the underground nuclear detonation; preparing of safety plans; and documenting and evaluating the postshot effects.

The second program involves long-range studies and is a continuous effort to expand our understanding of event-related phenomena. The long-range program objectives are: to improve prediction capabilities, to develop improved safety precautions at less cost for future projects, and to develop capabilities for both new programs and those which are still in the theoretical stage.

The two safety programs are closely interrelated and provide a sound and meaningful foundation for safety appraisals by NVOO. The long-range program relies on data and analysis of the project-associated program, which in turn benefits from the improved prediction capability that results from the long-range studies.

The subject matter presented in this volume covers many disciplines, in varying degrees of complexity. It represents most of the effort being expended in the Safety Program by the AEC/NVOO with the exception of certain specialized studies for Plowshare. The abundance of available material pertaining to these subjects obviously precludes a totally comprehensive treatment. It is instead, the intention of the authors to offer the reader when applicable, a broad technical discussion of their specialties, utilizing all appropriate mathematical and theoretical considerations. The programs, methods and interpretation of data described in the following chapters are subject to change from time to time due to the acquisition of additional data, improved methods of analysis, improved understanding of the physics involved, and program reevaluation. However, this format emphasizes the theoretical and to a lesser extent, the practical aspects of current safety methods based on our present programs.

Chapter 2

HISTORY OF U.S. NUCLEAR TEST PUBLIC SAFETY PROGRAMS

Henry G. Vermillion, *Director, Office of Public Affairs*
U.S. Atomic Energy Commission, Nevada Operations Office, Las Vegas, Nevada

In the history of United States nuclear testing the record of public safety has been exceptionally good. Two minor and incidental injuries to persons away from official test sites have been verified, and for these the Atomic Energy Commission paid medical bills. There is some concern among the scientific community about the long-range effects of minute additional amounts of radioactivity on the human race. This concern is not limited to nuclear weapons, and it will not be taken up at this time.

As is the case in most progressing programs, the Safety Program associated with nuclear testing has been progressively improved through new technology and more and more sophistication. As a consequence, public safety has been greatly enhanced. It must be added that increased funding necessary for the Safety Program has paralleled that for the testing program because of similar changes in complexity and sophistication. However, it also has stemmed from the need to evaluate new testing methods, to make sure that they do not endanger the safety of offsite populations.

To explain the point, in the years during which U.S. nuclear explosions were all in the atmosphere except for a few in the ground not far under the surface, the public safety concerns were for airborne radioactivity, air blast, and the brilliant flash of light which could cause eye injury.

Now the concern about air blast has all but vanished in our typical deep underground tests, the flash has completely disappeared, and the concern about radioactivity continues but on a changed basis. New concerns involve possible effects of underground tests on ground water, in perhaps contaminating it or changing its availability, and the possible effects of earth motion on natural or man-made structures.

This account covers the period from Trinity, the first test in New Mexico in 1945, to the present, although some of the statistics may not come quite up to today. It covers all continental United States nuclear explosive tests and one which was conducted by the Department of Defense

below the surface of Amchitka Island in the Aleutian Chain of Alaska.

When testing began at the Nevada Test Site in 1951, public health and safety protection was organized on a basis adequate for the conditions and time. Offsite radiation was monitored, and road blocks were set up to prevent motorists from entering areas where the fireball could be seen directly. After a few years, the U.S. Public Health Service was brought into the test organization, and soon afterward provided all of the skilled offsite radiation monitors who also provided two-way communications links with nearby offsite residents.

It may be of interest to note that when controversy over the effects of fallout emerged strongly during the early 1950's, the hazards of principal concern were the possible somatic effects of strontium-90 uptake by humans and its possible long-term effects when assimilated into the skeletal structure, and the possible long-term genetic effects of low-level radiation doses to the population.

In those years, the gamma spectrometer, which now is so widely used, was in early development, and the capability for differential analysis of a spectrum of isotopes existed principally in chemistry laboratories where processes were long, tedious, and difficult. With the development of improved instrumentation providing rapid determination of concentrations of short-lived fission products, there developed a new concern for the radioactive iodine isotopes — principally iodine-131.

When the gamma spectrometer came into fairly widespread use in the late 1950's and early 1960's, what had been difficult became relatively easy, and capabilities that had been concentrated in a few locations became scattered widely across the nation. Simple identification of the various radioactive isotopes of iodine in the atmosphere, on vegetation and in milk did not increase the hazard, but it did increase the awareness of many scientists of the possibility of hazard. Thus it was that concern over the iodine isotopes — principally iodine-131 — came to the forefront as compared with the older concern over strontium-90.

The finding of radioiodine at unexpectedly high levels in milk in the Salt Lake City area in mid-1962, following a period of atmospheric testing, led to a reassessment by numbers of theorists of what might have been the doses to thyroids of persons, particularly babies and small children, living in areas of Utah and Nevada when the most fallout occurred there from atmospheric tests. The theorists reviewed data on external gamma levels or levels of gross beta activity in air, for various offsite locations, which had been compiled from AEC reports and attempted to translate these data into concentrations of radioactivity in milk. From these predictions, efforts were made to estimate thyroid exposures to a hypothetical individual. These studies indicated that the higher thyroid exposures might have occurred in the vicinity of St. George, Utah.

The U.S. Public Health Service conducted a study in 1965-66 of all school children of the appropriate age group in Washington County, Utah, the County in which St. George is located. A control group of similarly aged school children was chosen for study in Graham County, Arizona, where there had been no thyroid exposures resulting from nuclear testing.

The method doctors used to identify thyroid abnormalities was to palpate or feel the thyroid glands of each child. Children who seemed to have an abnormality were noted, and this group then was examined by nationally recognized thyroid experts. In Utah, children who seemed to have gross abnormalities then were taken to a Salt Lake City medical center for intensive examination.

The results of the thyroid study were examined during a special study on Pathological Effects of Thyroid Irradiation by the National Academy of Sciences (NAS), and reported by the NAS December 1966. The report stated: "Examination conducted in 1965 of school children in Washington County, Utah, revealed several thyroid abnormalities, but nothing which can be specifically ascribed to radiation as an etiological agent. Because of the fact that Washington County residents seem, historically, to have had a relatively high prevalence of thyroid disease and because children in Utah outside Washington County and in Northern Arizona at the time of fallout showed the same frequency of the more severe thyroid abnormalities as did the children who were in residence within the County, it is not possible, from this particular study, to ascribe any degree of significance to radiation exposure."

The test organization in its underground test work maintains close surveillance over any release of radioactivity whether from a Plowshare cratering experiment where some release is anticipated, or from a contained test where the release is accidental. In either case, most of the fission products are trapped underground. Of these, the radioiodines are believed to be of the most concern.

When the first full-scale contained underground test, Rainier, was conducted in September, 1957, little was known of the effects of deeply buried high-yield underground explosions, nuclear or otherwise. Rainier had a yield of about 1,700 tons of TNT equivalent. All radioactivity was contained underground, and a new means for lessening fallout had been found. The method was devised by the University of California Radiation Laboratory, now known as the E. O. Lawrence Radiation Laboratory, at Livermore. Rainier was fired in a chamber at the end of a hooked curve in a mined tunnel. Later, the Los Alamos Scientific Laboratory designed a drilled vertical shaft system of placement for experiments to determine the nuclear safety in handling or storage of weapons. Most U. S. underground tests now are conducted at the bottom of straight drilled vertical shafts, although tunnels still are used on occasion when special instrumentation is required.

From the end of July, 1962, all U.S. nuclear testing in the United States proper — exclusive of Pacific islands and waters — has been underground, with all tests designed for complete containment except for several Plowshare earth moving experiments in which some release of radioactivity was anticipated. Signing of the Limited Test Ban Treaty in 1963 made it mandatory that all nuclear tests be conducted underground.

It may be of some interest to look at the record of performance in atmospheric test days.

The highest radiation exposure believed received by any individual beyond the boundaries of the Nevada Test Site during 84 atmospheric detonations between January 1951 and July 1962 was 13.5 roentgens, and the next highest was 10.5 roentgens. The highest estimated exposure to any community was about 6 roentgens. At most inhabited places within 200 miles of the test site, radiation doses were far less than a roentgen. Onsite, one employee accidentally received a dosage of 39 roentgens.

It may be noted in contrast that, in release of radioactivity from a Plowshare earthmoving experiment, or accidental release from a test designed for containment, offsite measurements are almost always very low, that is, in thousandths of a roentgen (milliroentgen) and usually a very few thousandths — sometimes in fractions of a thousandth of a roentgen.

During atmospheric test years, particularly the first few, the AEC paid approximately $50,000 for air blast dam-

4

age, principally for windows in Las Vegas. During later years air blast predictive capability was increased, and blast damage was almost eliminated. The brilliant flashes of light during atmospheric tests caused some temporary impairment of vision for a few persons offsite, and some eye damage to military personnel participating in onsite exercises. Only one military man, who sneaked a look at the fireball over his shoulder, is known to have suffered permanent eye damage to one eye in which vision was reduced from 20/20 to 20/100. His other eye was shielded by his nose and was not damaged.

In early 1962 the AEC established the Nevada Operations Office to administer its nuclear weapons and Plowshare explosive test programs. About that time, the relatively new problems of how to understand, control, or minimize possible effects of large underground nuclear detonations began to command an increasing share of the attention of the test organization.

It should be explained that the Nevada Operations Office of the AEC administers any nuclear explosive test site under AEC authority, and provides a Test Manager who has immediate authority to control onsite and offsite safety conditions of any test, such as whether to fire on schedule or postpone. However, the total test operation is performed by a test organization composed of all elements including scientific, technical, construction, logistics, and so on, including a strong public safety element. The design of each test is the responsibility of a sponsoring scientific organization such as an AEC scientific laboratory or the Defense Atomic Support Agency of the Department of Defense. Various scientific-technical contractors to the Nevada Operations Office, plus elements of other Government agencies, measure effects of nuclear explosions, perform studies and with their own data or that of others provide to the operating organization the ability to predict the effects of an underground test, and the downwind intensities of a planned or accidental release of radioactivity.

In the field of meteorological recording, research and prediction the work is done by the Air Resources Laboratory, Las Vegas, of the Environmental Science Services Administration of the U.S. Department of Commerce — formerly known as the U.S. Weather Bureau's special unit in Las Vegas. The Laboratory provides not only predictions of wind speeds and directions, but also of possible downwind radiation intensities should radioactivity be released either from an earthmoving test or accidentally. During the unit's 12 years in Las Vegas its personnel have gained an extremely sophisticated knowledge of weather patterns in and around the Nevada Test Site.

The U.S. Public Health Service unit in Las Vegas, during its 14 years of providing offsite radiation monitoring and surveillance for the AEC, has helped establish and maintain good relations with persons living around nuclear detonation sites. Its personnel have become immensely more sophisticated in skills, techniques and abilities. The number of its personnel also has increased greatly to meet the new challenges. Oliver A. Placak, now retired, was the first Officer in Charge of the Public Health Service unit supporting the test organization in Las Vegas, and later was Director of the Southwestern Radiological Health Laboratory (SWRHL) of the PHS which was established in Las Vegas. The SWRHL now occupies four handsome buildings on the campus of the University of Nevada, Las Vegas. Dr. Melvin W. Carter is its present Director.

It may be of interest that a beef herd was established on the Nevada Test Site in 1957 and was later turned over to the Public Health Service to administer. The principal purpose of establishing the herd was to learn whether grazing on desert browse in the immediate vicinity of nuclear tests would have any adverse effects on the animals. Autopsies have been performed on animals from four generations. All of the tissues examined appeared normal and healthy. The PHS also operates a dairy cattle herd at the test site, principally for performing experiments on the passage of artificially fed radioiodine from the food chain, through the animal and into milk.

In 1957, a Panel of Safety Consultants was appointed to advise the Manager, NVOO, on certain public safety matters related to the effects of underground tests. Most of the original appointees were recommended by the National Academy of Sciences as experts in their fields of geophysics, hydrology, geology and so on. Although there have been changes in membership, the Panel still carries on its original function.

As a result of underground nuclear testing experience, geophysicists were delighted to learn that earth shock signals of a known character and strength could be utilized for their measurements of the makeup of the earth. Though not by design, seismic profiling studies benefited greatly from the underground explosion data.

When test explosions began to be larger, however, regional offsite effects of ground motion became an obvious potential problem. Secretary of Defense McNamara, in testimony to Congress in 1963 on the Limited Test Ban Treaty, said that it appeared likely that underground tests of up to one megaton could be conducted safely at the Nevada Test Site.

By that time the AEC test organization's prediction capability had been enhanced in two ways. An expanded network of local and regional seismic recording stations had been started through the personnel and facilities of the U. S. Coast & Geodetic Survey. The firm of Roland F. Beers, Inc., of Alexandria, Virginia (now Environmental Research Corporation), had been put under contract to interpret the seismic recordings provided by the USC&GS, and to provide a predictive capability for ground motions from future tests at various distances.

Ground motion from an underground test was first felt in Las Vegas in September 1963, seconds after the Bilby event of about 200 kilotons. Although relatively few persons felt the motion, and a large gap exists between motion that can be felt and that which can damage buildings, the question of how to translate the ground motion prediction into possible effects on buildings was still unresolved.

The AEC, to obtain better information, then employed John A. Blume and Associates of San Francisco, a firm long familiar with earthquake effects on structures, and experienced in engineering structures designed so as to minimize earthquake damage, as the final link in the chain of cause, measurement, effect, and predictive capability. Blume was retained to interrelate Beers' earth motion predictions and their probable effects on man-made structures. The capabilities of each member of this three-way team, and the linking of their efforts, have been sharply upgraded over the past several years.

From the beginning of underground testing, questions have been asked by the public about a possible relationship between underground nuclear explosions and earthquakes, particularly whether the explosions could cause or trigger earthquakes along known major geologic faults such as the San Andreas Fault in California.

Obviously, any answer has to be based on inferences and theory. Studies have shown no basis for believing that underground nuclear explosions induce activity along distant fault lines. There is recent evidence that higher yield explosions may cause movement along nearby fault lines — within a few miles — and that they may result in aftershocks in the near vicinity, as many earthquakes do. In such cases, some of the aftershocks may result primarily from settling of the rock broken by the explosion. To date, all observed shocks after events have resulted in considerably less energy release than that of the original explosion, and have been quite close to the ground zero area. Seismic experts associated with the test program are watching the phenomenon closely.

From the earliest days of contained underground testing, the possible effects of nuclear explosions on ground water have been a source of concern to the test organization and to the public. The AEC long ago began drawing on the expertise of the U. S. Geological Survey, which established a permanent unit at the Nevada Test Site and provided backup from its offices in Denver.

Some years back the Nevada Operations Office sought a contractor to assess possible transport of radionuclides in ground water, and obtained the services of Hazleton-Nuclear Science Corporation, now a part of Isotopes, Inc.

The USGS has drilled numbers of hydrological test holes close in to and farther away from underground nuclear test sites, but to date no radionuclides have appeared in underground water in any of the holes. As a result, the Isotopes, Inc., work has been largely theoretical in nature, confined to the laboratory, the computer, and the drawing board, and is based on water travel speeds and paths obtained from the USGS studies.

The University of Nevada's Desert Research Institute provides a consulting service on underground water. Dr. George B. Maxey, a member of the Institute staff and a hydrologist long familiar with Nevada Test Site geology and hydrology, is a member of the team dealing with underground water studies, assessments, and predictions at the test site.

The greater sophistication in approach to all phases of test safety as the years have progressed also has led to a greater diversity of review boards, committees, panels, subcommittees, and individuals who are concerned with specific facets of public safety. As an example, there is a Nevada Test Site Planning Board which has subcommittees on ground shock and on radioactive effluent release — the planned or accidental escape of radioactivity to the atmosphere. The NTS Planning Board, made up of senior representatives of all organizations with substantial interests in the use of the Nevada Test Site (and through logical extension all nuclear explosive sites) hears reports made by its subcommittees and makes recommendations to the Manager of the Nevada Operations Office on public safety matters as well as on budgeting, scheduling, and many other matters.

The Test Evaluation Panel established about five years ago considers in minute detail all aspects of containment of underground tests. This Panel is chaired by the Nevada Operations Test Manager with representatives from the AEC scientific laboratories and the Department of Defense. The principal purpose of the extremely close examination given to containment of radioactivity relates

6

to conducting the test within the constraints of the Limited Test Ban Treaty, but this action inherently takes the interests of public safety into full account.

In fact, through the years of underground testing, the test organization's philosophy has been that every reasonable effort must be made to make sure that no release of radioactivity occurs from a test designed to contain its radioactivity underground. All safety measures are taken under the assumption that the most radioactivity that possibly can escape, will escape. The concern at the highest administrative levels of the Atomic Energy Commission is evidenced by a written constraint from the General Manager to those managing nuclear test operations which instructs them to: "Take every precaution necessary including the delay or postponement of any shots, to reduce to a minimum the hazards, both to the public and to onsite personnel, from any nuclear detonation."

This historical account could conclude with the findings to date from some of the evolving programs described, but others in the presentations have detailed knowledge of results. However, it may be fair to sum up by saying:

1. The test organization has steadily improved its capability for designing and constructing underground test facilities so they will not leak radioactivity to the atmosphere, or that any escape will be small if it occurs in spite of all precautions. It may be of interest that of the tests that have resulted in accidental escapes since the Limited Test Ban Treaty has been in effect, all have been of low yield (zero to 20 kilotons) except one that was in the low-intermediate range of 20 to 200 kilotons.

2. There is no indication that underground test explosions have any effect on the quantity of water available in springs or wells except perhaps very close to the shot point during the passage of the pressure surge. There is no evidence that radioactivity in ground water as a result of underground tests will offer any public health hazard.

3. A positive program exists for predicting with good accuracy ground motions that will result from future tests, and for predicting any potential damage to structures. Past detonations have not resulted in damage beyond a few miles from the shot point. Any future increases in yield will be in careful steps upward so the effects of past explosions can be evaluated fully, and reasonable effects extrapolations made.

Chapter 3

REVIEWS TO INSURE SAFETY OF NUCLEAR OPERATIONS

Robert H. Thalgott, *Test Manager*
U.S. Atomic Energy Commission, Nevada Operations Office, Las Vegas, Nevada

The Atomic Energy Commission is responsible for public safety for all U.S. nuclear detonations. Within the continental United States, the Commission implements this responsibility through its Nevada Operations Office.

The Nevada Operations Office conducts those studies and reviews which are necessary to predict reliably the effects of nuclear detonations which may affect the safety of people and property. We do not consider ourselves infallible in defining safety problems or arriving at credible and practical solutions to these problems. For this reason recognized experts in the pertinent scientific disciplines are consulted. These disciplines include but are not limited to: health physics, radiobiology, seismology, hydrology, geology, structural effect from ground motion, and rock mechanics.

This continuing effort on the part of NVOO, its contractors, and consultants, has permitted the nuclear weapons testing program to go forward essentially without injury to the public or damage to property.

Preparation for the safe conduct of an event is based upon prediction of the effects of the maximum credible accident which could befall that event. Necessary steps are taken as indicated by the predictions to ensure that *NO* limits or guides are exceeded. Precautionary measures are taken to ensure that public safety will be protected, should an accident materialize. NVOO measures and documents the actual effects in order to take emergency action to protect life and property, if necessary, and to accurately identify the effects to improve the accuracy of the predictive effort for future tests.

There are two very important aspects to the predictive and measurement efforts. First, in order to successfully carry on tests, the neighboring population outside the Test Site must be protected from injury. The people must also be adequately informed. Only by dependable predictions can this be done satisfactorily. Good public relations with these people means informing them of the possible effects of the event prior to its execution and having that information as accurate as possible.

The second very important function of the measurement effort is to be able to form a firm basis for settlement of valid damage claims and to protect the Government against invalid claims. We must ensure that every effort is made to obtain correct measurements and that these measurements are properly interpreted and made accessible to the public and interested organizations. It is important that the people and interested organizations not only be assured that all steps are taken for protecting the public, but also that they be made aware of the extent and nature of this effort.

Prior to any nuclear detonation there are a series of reviews to ensure that the detonations are conducted safely and within the constraints of the Limited Test Ban Treaty. To achieve the safety in nuclear testing that we desire, a system for review and approval was developed. Figure 3.1 illustrates this system. All nuclear tests do not necessarily involve all of the individual steps depicted; however, unusual tests do receive reviews from the entire system. Table I shows a listing of various safety review organizations.

The sponsoring laboratory performs safety evaluations related to nuclear systems safety, that is, procedures associated with assembly of the device, transportation, and emplacement as well as the detonation system. These nuclear safety procedures are later independently reviewed by a group of knowledgeable persons (nuclear safety survey group or nuclear safety study group) and when appropriate, recommendations are made to improve or assure safe assembly, transportation, etc.

The laboratory independently evaluates and assesses those man-made and natural mechanisms which influence containment of the explosion. Each event is then reviewed several times by a Test Evaluation Panel composed of individuals with considerable experience in nuclear testing. The organizations furnishing such individuals are the Los Alamos Scientific Laboratory, Lawrence Radiation Laboratory, Sandia Laboratory, Department of Defense, Air Resources Laboratory — Las Vegas, U.S. Public Health Service, AEC, and independent consultants. Every aspect of the event which

9
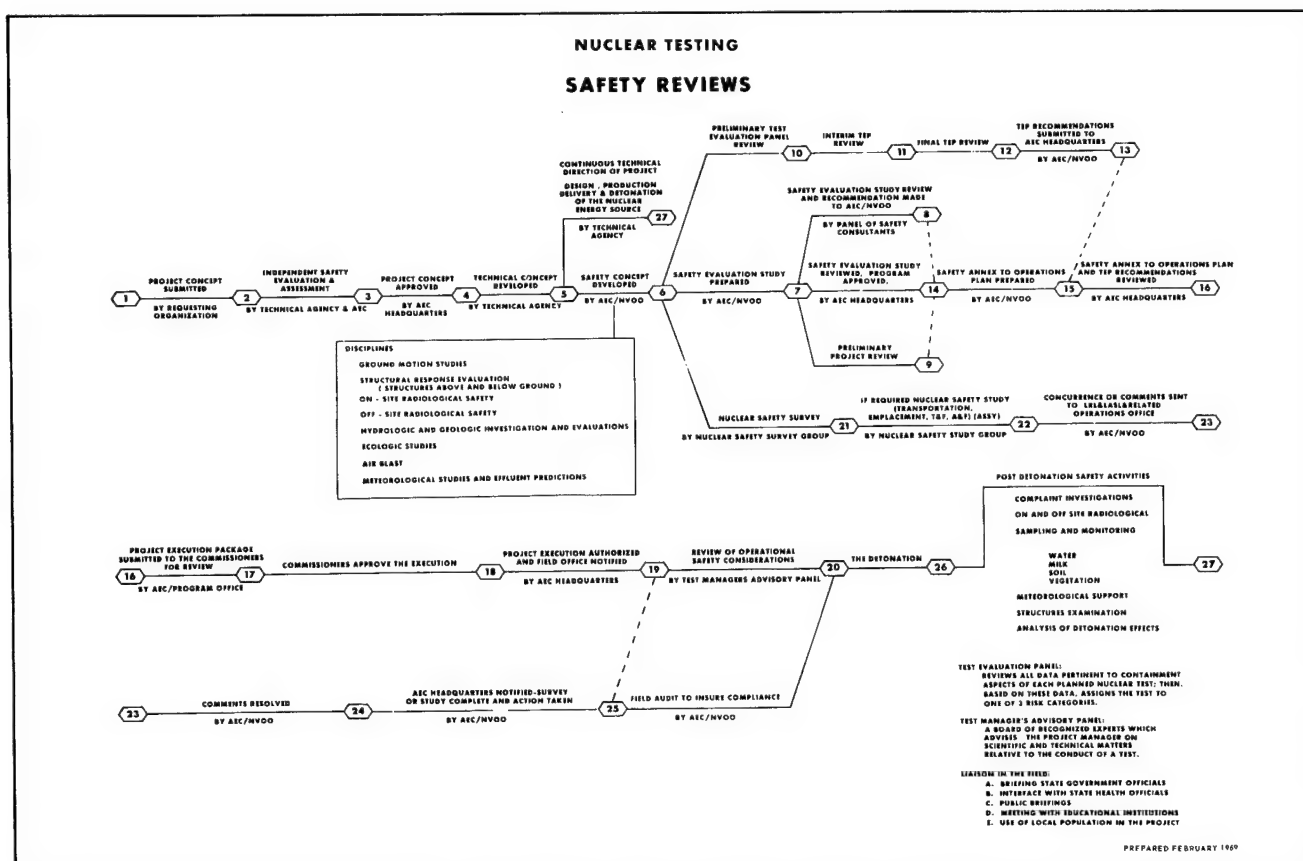
Figure 3.1. Safety Reviews in Nuclear Testing.

might affect containment is reviewed by this Panel several times as preparations for the event are made. A detailed study of the geological features around the shot point is made by the U.S. Geological Survey and presented to the Panel. If there are indications of possible faults or other geologic anomalies which may affect containment, new shot points are recommended by the U.S. Geological Survey. Additional geological information is also obtained by the U.S. Geological Survey from satellite holes drilled to accommodate instrumentation around the emplacement hole. A careful study is made of the drilling, casing, and grouting history of each of the emplacement and satellite holes to ensure that there will be no man-made path to the surface. If there are indications that grouting and casing have left voids, corrective measures are taken or the hole is abandoned.

The proposed stemming plan (that is, the method to be used for filling the emplacement and instrument holes) is reviewed by the Test Evaluation Panel. If there are doubts as to the capability of the stemming material to contain radioactivity, then appropriate changes are made in the stemming plan. The stemming may range from alternate layers of pea gravel and fine sand to complete cementing of the entire length of the hole, depending upon the shot, media, and the location. The same type of review is made to assure containment of a test to be made in a tunnel instead of a drilled hole.

AEC Headquarters staff, and finally the Commission, reviews the safety of each event, and if they are satisfied, grant authority for its execution.

Even though these reviews are made and every possible precaution has been taken to ensure that no radioactivity will reach the surface, preparations for detonation of the device assume that the maximum credible release of radioactivity will occur. Plans are made for the prompt evacuation of populated areas on or off the Nevada Test Site should a release of radioactivity occur with unacceptable levels of radiation predicted.

The U.S. Public Health Service places offsite radiation monitors in the downwind direction in order that we may get full documentation and take corrective action if there is an accidental release.

The Test Manager has established an Advisory Panel made up of specialists in meteorology, radiation, and medicine to advise him as to the hazards to be expected from each event. Other disciplines are added to the Panel

TABLE I. SAFETY ORGANIZATIONS FOR NUCLEAR DETONATIONS

ORGANIZATION	ORGANIZATION CHARTER	MEMBERSHIP	REVIEWS ARE PERFORMED	
			No. of Times	During Phase
I. FIELD ORGANIZATIONS **A. Sponsoring Laboratory**	Review to determine feasibility of fielding experiment.	Appropriate laboratory personnel (LASL, LRL, DASA, Sandia Corp.)	Continuing	I, II, III
B. Ground Shock Subcommittee	Advise the Manager, NVOO, through the NTS Planning Board on seismic problems which may affect the NTS or STS facilities and programs.	Sandia Corp., NVOO, LASL, LRL, TC/DASA	Continuing	II
C. Radioactive Effluent Subcommittee	Advise the Manager, NVOO, through the NTS Planning Board of the adequacy of NTS radiation measurement systems. Evaluates radiation effluent data from nuclear tests and reports their findings through the NTS Planning Board.	LASL, NVOO, Sandia Corp., AFSWC, LRL, AFTAC, TC/DASA	Continuing	II
D. NVOO Panel of Safety Consultants	Composed of some of the most eminent people in the fields of geology, hydrology, rock mechanics, soil mechanics, earthquake seismology, etc., to evaluate programs conducted under the long-range study program and prepare safety evaluations for specific events and series of events.	G. B. Maxey, University of Nevada L. S. Jacobsen, Calif. Inst./Tech. N. M. Newmark, Univ. of Ill. D. U. Deere, Univ. of Ill. T. F. Thompson, Geol. Engrg. L. G. von Lossberg, Sheppard T. Powell & Assoc. S. D. Wilson, Shannon & Wilson, Inc.	As requested by Manager, NVOO	II
E. Test Evaluation Panel	Advises the Manager, NVOO, on the containment aspects of proposed nuclear explosive tests. Performs periodic reviews of technical data and containment plans to determine their adequacy in assuring compliance with the Limited Test Ban Treaty.	NVOO, LASL, LRL, Sandia Corp., USPHS, ESSA/ARL, DASA	Bimonthly	II
F. Test Manager's Advisory Panel	A panel composed of experienced advisers who are recognized experts on radiation, weather, fallout, and other subjects. The Panel examines predictions of the effects of each event and evaluates field preparations designed to minimize predicted hazards.	NVOO, LASL, LRL, Sandia Corp., USPHS, ESSA/ARL, Medical Consultants	D-1 Days and D-Days for each event	III
G. Nuclear Weapons Safety Program Survey/Study Groups	Nuclear Safety Survey and Study Groups are convened to assure that prior to beginning any operation involving atomic weapons, positive measures are provided to prevent an accidental or unauthorized nuclear detonation.	NVOO, SAN, ALOO, Sandia Corp., LRL, LASL	Continuing	II
II. AEC HEADQUARTERS ORGANIZATION **A. Divisions of Military Application and/or Peaceful Nuclear Explosives**	Compiles, reviews, and submits pertinent event related documents to AEC Commissioners.	DMA and/or DPNE Staff	Continuing	II
B. Division of Operational Safety	Reviews safety plans on special events.	DOS Staff	As required	II
C. AEC Commissioners	Review events and grant execution authority.	Commissioners	Continuing	II

February 1969

Phase I - Conceptual
Phase II - Planning
Phase III - Field Execution

as conditions warrant. The Panel is chaired by a scientific advisor who is familiar with the nuclear device, timing and firing systems, and program objective.

Although the Test Manager's Advisory Panel may meet several times, months in advance, to discuss specific problems on difficult or unusual shots, the Panel always meets the day before the detonation to hold a readiness briefing in which the control plans are reviewed. A complete weather picture with predictions for shot time meteorological conditions is given and review made of the preparation for onsite and offsite population control. The Advisory Panel meets continuously in the period immediately prior to firing to insure that the predicted conditions have indeed come to pass and that the meteorological conditions are acceptable at the time of firing. If it is determined that, with the maximum credible accident, the test can be safely carried out, recommendation is made to the Test Manager to proceed with the detonation. The Test Manager's Advisory Panel also reviews the last-minute preparation to ensure that all of the recommendations of the Test Evaluation Panel regarding containment have been, in fact, carried out in the field.

Complete field preparations are made to document even the smallest release of radioactivity. A system of remote reading monitoring instruments is installed around ground zero and in most cases a remote reading instrument is in the emplacement hole; there is also a ring of air samplers around the ground zero site. We have in the air at shot time at least two airplanes — one equipped with monitoring instruments, the other with sampling equipment. Should there be a release of radioactivity, the monitoring plane makes passes over ground zero and through the radioactive cloud and then keeps track of the leading edge of the cloud. The sampling plane comes in through the cloud and takes samples. These samples are immediately brought back to the Southwestern Radiological Health Laboratory for analysis so that we know exactly what radionuclides are present.

Two additional monitoring planes are also utilized as necessary. These planes are equipped with extremely sensitive detection instruments and with proper equipment aboard to analyze constantly the radioactivity picked up by the detectors. This then provides us with immediate and continuing knowledge of the cloud's contents. The sensitivity of these instruments is such that they can detect changes from natural radon concentrations and are able to discriminate between the debris in the cloud and the natural radioactivity which is always around us. The tracking effort of these planes is used to position ground monitors in areas which may have been or will be affected. These ground monitors then go through the sampling procedures as described in Chapter 14 by the U.S. Public Health Service.

As you perhaps know, testing has been carried out at the Nevada Test Site for 17 years — underground detonations for about 11 years. We maintain three or more camp sites constantly. The largest of these is Mercury. There are also camps in the forward area, one near the CP, and one at Area 12. The population at these camps may vary from 500 to 2,500 people. Although this relatively large number of people live and work within a few miles of the ground zero of even the largest yield tests, there has never been an injury among them as a direct result of a detonation.

We are constantly striving to improve the accuracy of our prediction capabilities in all areas, and have made much progress. We also have come a long way in devising techniques to assure the containment of radioactivity during shot and postshot related activities. This progress in prediction capability and containment techniques was necessitated by the increased complexity of experiments. In the last analysis all those involved in the test program recognize the potential hazards involved. Therefore, we rely on a proven system based upon taking those actions necessary to protect against the effects of the maximum credible accident.

Chapter 4

PHENOMENOLOGY AND CONTAINMENT OF UNDERGROUND NUCLEAR EXPLOSIONS

Lawrence S. Germain; *Associate Division Leader, L Division,* and J. S. Kahn; *Group Leader, Geosciences Group*
Lawrence Radiation Laboratory, University of California, Livermore, California

INTRODUCTION

This chapter will deal with some aspects of the phenomenology of underground nuclear explosions. It is divided into four general sections.

First, we shall examine the rather extensive history of routine underground explosions and note that, from a pragmatic point of view, a nuclear explosion can be contained by putting it underground. Those few cases where some radioactivity was released will be examined to see if they can be categorized or if there were extenuating circumstances.

Second, we shall describe the calculation of early-time phenomenology—the interactions between a nuclear explosion and the media surrounding it during the first few tenths of a second after the explosion. We shall attempt to substantiate these calculations by showing how well they agree with actual measurements.

Third, we will present a parallel discussion of the calculation of late-time phenomenology and the verification of these calculations by field observations.

Fourth, we shall address the question of how containment is affected by geological features such as faults and joints.

Before going into our detailed discussion, let us describe in general the phenomena involved in an underground nuclear explosion. Picture a 10-kiloton (kt) source buried 750 ft below the desert surface in Yucca Flat. When the nuclear detonation occurs, this large amount of energy is produced in a very short time, perhaps about 10 sec. The material in the nuclear device is not only instantly vaporized but also raised to a temperature of several million degrees Kelvin. A strong shock moves from this hot, high-pressure region, vaporizing some of the surrounding earth. At this point, a cavity has been formed, having a radius of about 15 ft and containing rock vapor at a pressure of about 1 megabar (Mbar: one-million atmospheres). The cavity continues to expand for about 100 milliseconds (msec),

until its pressure drops to a value about equal to the ambient hydrostatic overpressure (ρgh). For 750 ft of alluvium this would be about 50 bars. The cavity now has a radius of about 100 ft.

While the cavity is growing, the main shock from the explosion is moving towards the ground surface. It arrives there about 100 msec after the explosion and causes the surface to rise momentarily by about a foot; then the shock is reflected back as a rarefaction. The passage of the main shock causes failure in much of the material between the shot point and ground surface. The failure may be either brittle or plastic, depending on the stress conditions and the properties of the material.

The foregoing describes what we shall term early-time phenomenology; late-time phenomenology commences after the cavity has been stabilized and shocks and elastic waves have been dissipated. At about this time the rock gases condense, leaving water vapor as the most important component of the cavity gases. The cavity gases cool by simple Newtonian heat transfer to the cavity wall, and consequently the cavity pressure drops. Continued cooling leads to condensation of some of the more condensable cavity gases (such as water). The transfer of heat from the gases to the surrounding rock establishes a high thermal gradient in the cavity wall, resulting in cracking and flaking of the cavity surface. This in turn enhances the cooling rate by mixing earth into the cavity gases.

Ultimately, after a period which may be minutes or may be hours, as a result of both decrease of cavity pressure and cracking in the cavity wall, the cavity can no longer support itself and collapses. The collapse propagates upward in a few seconds through the material which has been cracked by the explosion and forms a chimney of rubble. The rubble quenches the remaining condensable gases in the cavity. Figure 4.1 is a photograph of a cavity that did not completely collapse. It shows how a typical cavity would look as collapse begins, after some rubble has fallen from the
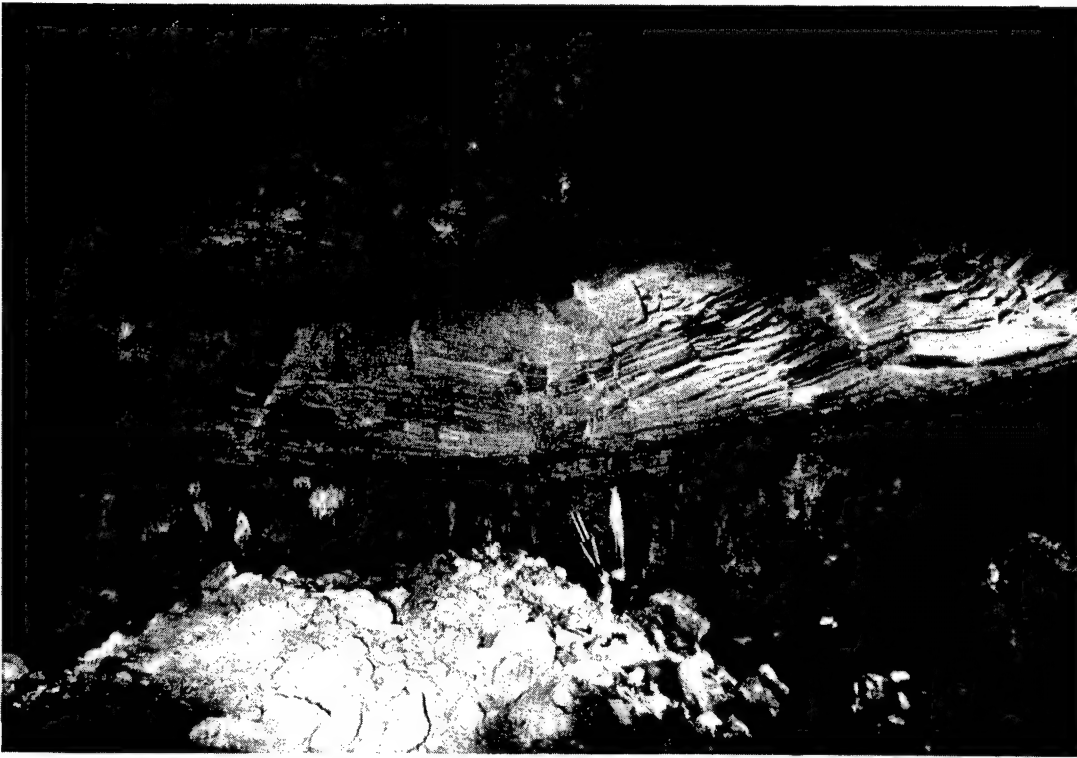
13

Figure 4.1. Cavity Formed by an Underground Nuclear Explosion. The Man Standing on the Rubble Pile (Arrow) Indicates the Scale.

Figure 4.2. Formation of a Subsidence Crater.

14

roof to the floor. If the chimney does not encounter rock which is strong enough to support a roof span of about one cavity diameter, as is frequently the case when alluvium is the emplacement material, collapse will continue to propagate upward and will reach the surface and form a crater. A typical subsidence crater, at the moment of formation, is shown in Figure 4.2. For our sample shot we would expect a crater about 200 ft in radius and perhaps 50 ft deep.

The remaining noncondensable cavity gases, now at a pressure of only a few pounds per square inch (psi), are trapped in the rubble and can now reach the surface only by a long and tortuous path.

PAST EXPERIENCE

We have chosen to examine the population of nuclear-test shots having these two properties in common:

1. They were all fired in vertical holes without line-of-sight pipes or other direct communication with the surface.

2. They were all fired after the resumption of nuclear testing in 1961.

Table I summarizes this population by dividing it into intervals of yield and intervals of scaled depth of burial. Within each category, the total number of events in which there was significant leakage are indicated. "Significant leakage" is defined as a total release of radioactivity of more than 100 curies (Ci).

Scaled depth of burial is the actual depth divided by the cube root of the yield; it is a convenient number of use because, assuming that the energy from a shot is dissipated uniformly in the volume around the shot point (hence the cube-root factor), the pressure arriving at the surface will be the same for all shots having the same scaled depth of burial in the same material.

Consequently, most rules of thumb concerning successful containment are expressed in terms of scaled depth of burial.

As stated above, we set the dividing line between successful containment and significant leakage, in terms of total release, at 100 Ci. Expressing total release in curies (1 Ci = 3.7×10^{10} disintegrations per second) is not completely unambiguous, since the release of a given number of atoms of a given species will produce different numbers of disintegrations per second, depending on the time of detection. We have therefore adopted the practice of converting all measurements to the number of disintegrations which would be given at 12 hr after release time (R). In essence, our quoted total release is that activity which would be given if one could capture all of the released material in one place at R + 12 hr. The seemingly arbitrary limit of 100 Ci was chosen because, in general, the release must go well above 100 Ci before one has to worry about offsite detection of the activity.

Table I indicates that there was significant leakage in 10 events. The amount of radioactivity that was leaked in these events varied from 200 Ci up to 10^5 or 10^6 Ci. Three events vented through ground fissures within the first minute after shot time. Of these three, only one had a scaled depth of burial greater than 350 ft/kt$^{1/3}$. In general, the others did not leak radioactivity until after collapse. A detailed examination of the 10 events that leaked reveals that five of them were atypical in that they were fired in dolomite (a carbonate rock), were located very close to a fault, or involved unusual downhole geometries. The other five were all in the low or low-intermediate yield range.

The one event of low-intermediate yield that showed some leakage was fired in water-saturated dolomite. In such a medium, one would expect that the shot would

TABLE I. TOTAL POPULATION OF EVENTS, CATEGORIZED BY YIELD (W) AND SCALED DEPTH OF BURIAL (SDOB)

(ft/kt$^{1/3}$)	Low yield W ≤ 5 kt Events	Leakage	5 < W ≤ 20 kt Events	Leakage	Low-intermediate yield 20 < W ≤ 200 kt Events	Leakage	Intermediate yield 200 < W ≤ 1000 kt Events	Leakage	High yield W > 1000 kt Events	Leakage	Totals Events	Leakage
≤ 350	3	1	8	1	3	0	0	—	0	—	14	2
> 350 ≤ 400	2	1	16	1	11	1	4	0	1	0	34	3
> 400 ≤ 450	14	1	16	0	12	0	1	0	0	—	43	1
> 450 ≤ 500	20	2	9	0	9	0	0	—	0	—	38	2
> 500 ≤ 600	28	2	4	0	5	0	0	—	0	—	37	2
> 600 ≤ 800	15	0	8	0	1	0	0	—	0	—	24	0
Totals	82	7	61	2	41	1	5	0	1	0	190	10

15

produce a large quantity of noncondensable CO_2 gas, which would not be present in any shot of the same yield in tuff or alluvium. It is reasonable to assume that the noncondensable CO_2 eventually diffused to the surface, bringing with it noncondensable fission products. Our experience with detonations in carbonate rock is limited, but it suggests that radioactivity is more likely to be released from a detonation in carbonate rock than from detonations in other formations.

The picture that emerges from these observations is one of some concern for seepage of radioactive gases from low-yield shots but remarkable success with containment in the higher-yield shots. The seepage from low-yield shots has seldom posed a serious problem and indeed has seldom been detectable offsite. Our success in containing high-yield events is encouraging.

EARLY-TIME PHENOMENOLOGY

Calculational Methods

In any underground nuclear explosion, the shock front that propagates from the shot point carries with it energy from the explosion, and it distributes this energy by doing work on the surrounding material. In the process, the material undergoes changes in both its physical and mechanical states. If enough energy is deposited in the material, the material will vaporize or melt, changing its physical state, or it may crush or crack.

Special computer codes have recently been developed for predicting the close-in phenomena of underground nuclear explosions; they are based on the laws of physics and the knowledge of the properties of the materials in which the detonations occur. As a consequence, a better understanding of experimental observations and measurements has evolved.

A spherically symmetric, Lagrangian, hydrodynamic-elastic-plastic code called SOC is now being used in making these calculations.[1] A similar code in two dimensions, TENSOR, is also available.[2] The general calculational procedure in these codes is described below.

Procedure[3]

Clearly, the rock vapor causes stresses in the surrounding medium. The equation of motion provides a functional relationship between the applied stress field and the resulting acceleration of each point in the medium. Accelerations, when allowed to act over a small time increment, Δt, produce new velocities; velocities produce displacements, displacements produce strains, and strains produce a new stress field. Time is advanced by Δt, and the cycle is repeated. The time increment is determined by an independent stability condition which requires the increment to be smaller than the time necessary for a compressional wave to travel across the smallest zone.

Two areas in the above loop need further discussion: (1) the manner in which the stress field produces accelerations, and (2) the manner in which the strain field is coupled to the stress field through the equation of state of the medium. We limit the discussion here to spherical symmetry, and we attempt to interpret the equation of motion and medium behavior in a general way.

The fundamental equations of continuum mechanics (conservation of mass, linear momentum, and angular momentum) combine to produce the Eulerian equation of motion:

$$\rho u_R = -\left(\frac{\partial P}{\partial R} + \frac{4}{3}\frac{\partial K_s}{\partial R} + 4\frac{K_s}{R}\right) \quad (1)$$

and the stress tensor in the spherically symmetric coordinate system is written as the sum of an isotropic tensor and a deviatoric tensor:

$$\begin{bmatrix} T_{RR} & 0 & 0 \\ 0 & T_{\theta\theta} & 0 \\ 0 & 0 & T_{\phi\phi} \end{bmatrix} \quad (T_{\theta\theta} = T_{\phi\phi})$$

$$= \begin{bmatrix} -P & 0 & 0 \\ 0 & -P & 0 \\ 0 & 0 & -P \end{bmatrix} \quad (2)$$

$$+ \begin{bmatrix} \frac{4}{3}K_s & 0 & 0 \\ 0 & \frac{2}{3}K_s & 0 \\ 0 & 0 & \frac{2}{3}K_s \end{bmatrix}$$

where

ρ = density,

$\dot{u}_R$ = particle acceleration,

R = space variable (radius),

P = mean stress,

$T_{RR}, T_{\theta\theta}, T_{\phi\phi}$ = radial and tangential stresses, and

K_s = stress deviator.

We see from equation (2) that

$$P = -\frac{1}{3}(T_{RR} + T_{\theta\theta} + T_{\phi\phi})$$

16

and

$$K_s = \frac{T_{\theta\theta} - T_{RR}}{2}. \tag{3}$$

Equation (1) shows that the two stresses causing the acceleration are P and K_s. When this equation is differenced we obtain a functional relation between stress gradients and the acceleration of a point in the medium. The forces that are driving the stress wave, P and K_s, are invariant tensor quantities in the one-dimensional formulation.

The first invariant of the stress tensor, I_1, is given by

$$I_1 = T_{11} + T_{22} + T_{33}.$$

Thus

$$P = -\tfrac{1}{3}I_1 \text{ and}$$

$$K_s = \tfrac{1}{2}\sqrt{3I_{2D}},$$

where I_{2D} is the second invariant of the deviatoric stress tensor.

Initial conditions for such a problem involve specifying the properties of the vaporized rock. Equilibrium equations of state have been developed for various natural materials in which underground nuclear and high-explosive detonations have occurred. A set of assumptions was made to obtain the gas equation of state.[4] One of these was that the materials behave like a perfect gas of molecules and ions below about 3 electron volts (eV) and like a perfect gas of atoms, electrons, and nuclei above 3 eV. At liquid and solid densities, the experimentally determined Hugoniot equation of state was used, and the state points were obtained from interpolation between the Hugoniot measurements and points at about 50 eV.

The adiabatic expansion of a gas is calculated using another set of assumptions, namely, that the required increase in enthalpy to cause vaporization — 2800 calories per gram (cal/g) for a silicate rock — is equal to the "waste heat" when the Hugoniot is assumed to be the unloading curve. (See Figure 4.3.) The initial pressure of the gas vapor is equal to the pressure of vaporization, and its initial density is equal to the bulk density of the material.

A series of calculations[4] has shown that the radius of vaporization, R_V, depends on the yield, W, and the energy of vaporization, E_V:

$$R_V = 1.524 \, W^{1/3} \, E_V^{-0.256},$$

where R_V is in meters, W is in kt, and E_V is in 10^{12} ergs per cubic centimeter (cc).

E_V is related to the pressure of vaporization and specific volume by:

$$E_V = \frac{1}{2}\frac{P_V \Delta V}{V_0},$$

where

P_V = pressure of vaporization,

ΔV = specific volume change, and

V_0 = initial specific volume.

The energy density in the gas is independent of the yield, since R_V^3 is proportional to W. The internal energy of this gas in cal/g is given by

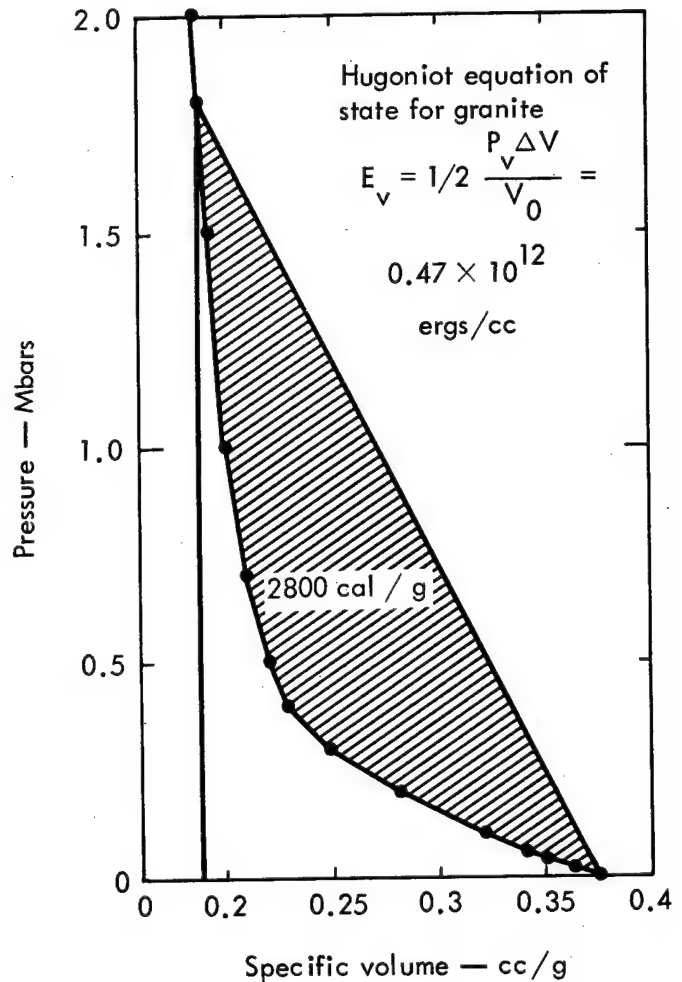$$E_0 = \frac{10^{12}}{\tfrac{4}{3}\pi \rho_0 (R_V^{1 \text{ kt}})},$$

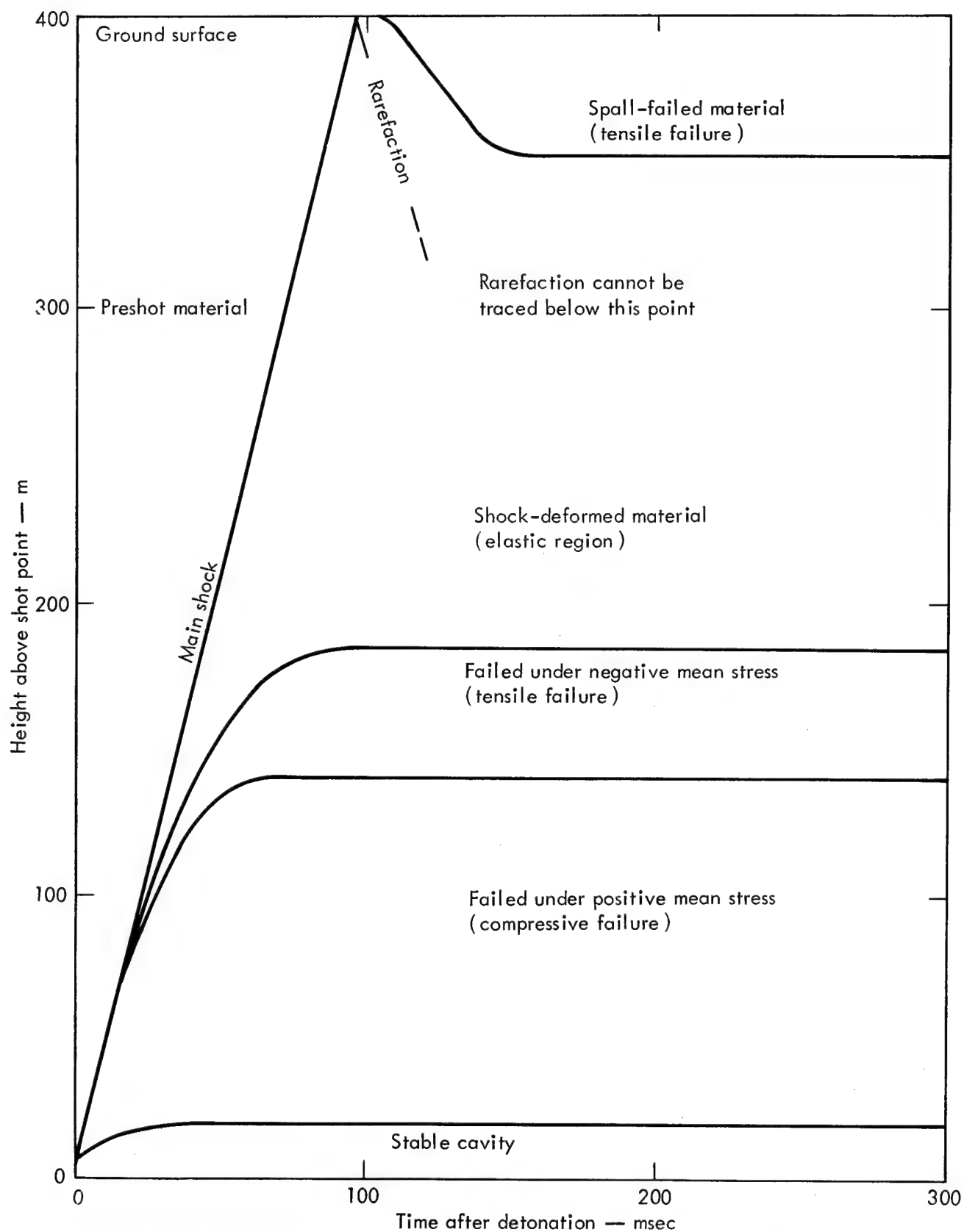Figure 4.3. Shock Hugoniot for Granite (Shaded Area Represents "Waste Heat").

17

Figure 4.4. Calculated Effects of a Deeply Buried 10-kt Nuclear Explosion on the Surrounding Medium. Depth: 400 m; Medium: Lewis Shale[5].

where

$$R_V^{1 \ kt} = 1.524 \ E_V^{-0.256}, \text{ and}$$

$\rho_0 = $ bulk density of the material.

The rock gas is then allowed to expand adiabatically from the point defined by ρ_0, E_0, and P_V according to the equilibrium equation of state derived as described above.

Results

Histories of the effects of 10-kt underground nuclear explosions on the surrounding media, as calculated by the SOC code, are shown in Figures 4.4 and 4.5. In Figure 4.4 the explosion is at a depth of 400 m, while in Figure 4.5 it is at a depth of only 150 m. The two histories are significantly different. At a depth of burial of 400 m, the cavity growth is unaffected by the rarefaction from the surface, since it is so weak as to be imperceptible by the time it has reached the cavity. However, at a depth of burial of 150 m, the returning rarefaction allows renewed growth of the cavity by reducing the ambient pressure below that of the cavity.

The ability of the rarefaction from the surface to affect the cavity has been called the "gas-acceleration" phase of cavity growth. This gas-acceleration phase occurs if the surface is close enough to the explosion

point to affect cavity growth. The expanding cavity can, in effect, sense the direction of the free surface and expand preferentially in that direction. When this occurs, one might have serious questions about the adequacy of containment. If, however, the gas-acceleration phase does not occur, the explosion is essentially in an infinite medium and is unaffected by the free surface. For these reasons we feel that the absence of the gas acceleration phase in the result of a calculation is a good physical criterion for the preclusion of dynamic venting.

A second difference between Figures 4.4 and 4.5 is the absence of the elastic region at the 150-m depth of burial. In essence, at this depth one could expect the rock to fail by some mechanism at all points between the shot point and the surface.

Rock in this region can fail in a number of ways. There is a region immediately outside the cavity in which the temperature exceeds the melting point but not the vaporization point of the rock. Thus a relatively thin region of melt is produced. (This region is too thin to be conveniently shown in the figures.) Outside the melt zone there is a region where the material fails under compressive load with the passage of the shock. This is the region labeled "compressive failure" in the figures. However, the failure mechanism may be either plastic flow (ductile failure) or fracture (brittle fail-
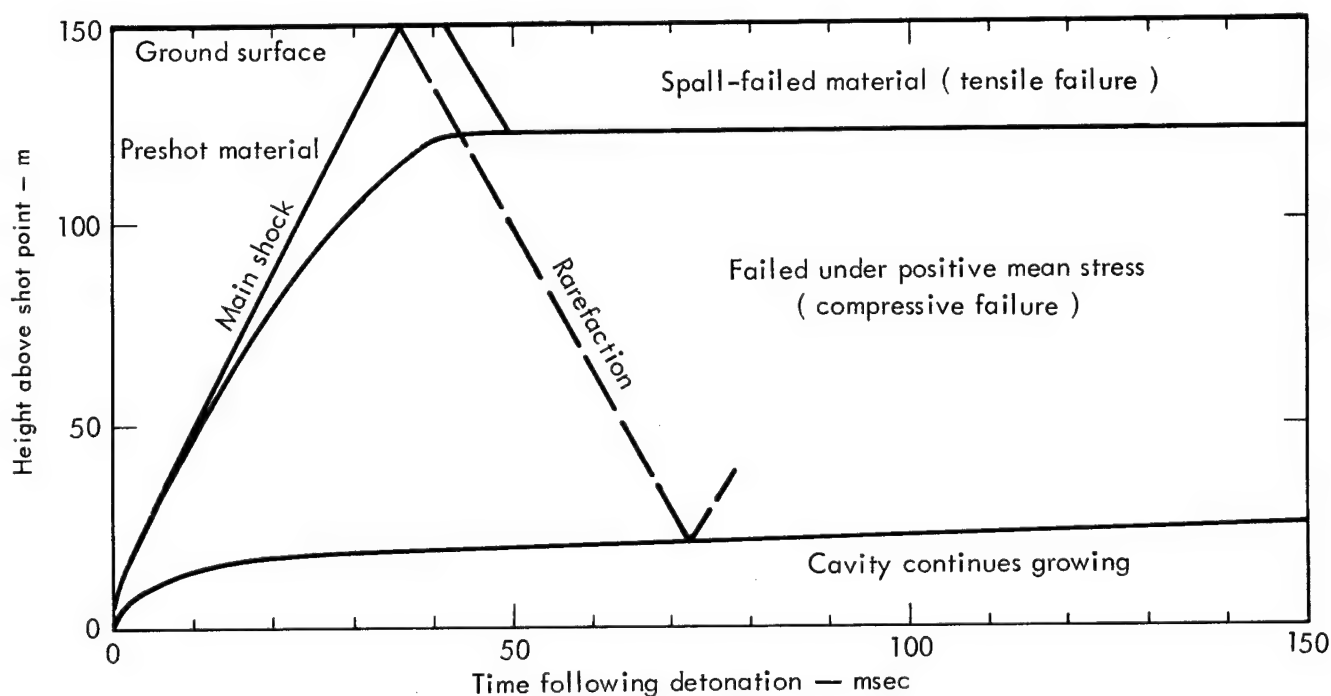

Figure 4.5. Calculated Effects of a Near-Surface 10-kt Nuclear Explosion on the Surrounding Medium. Depth: 150m; Medium: Lewis Shale[5].
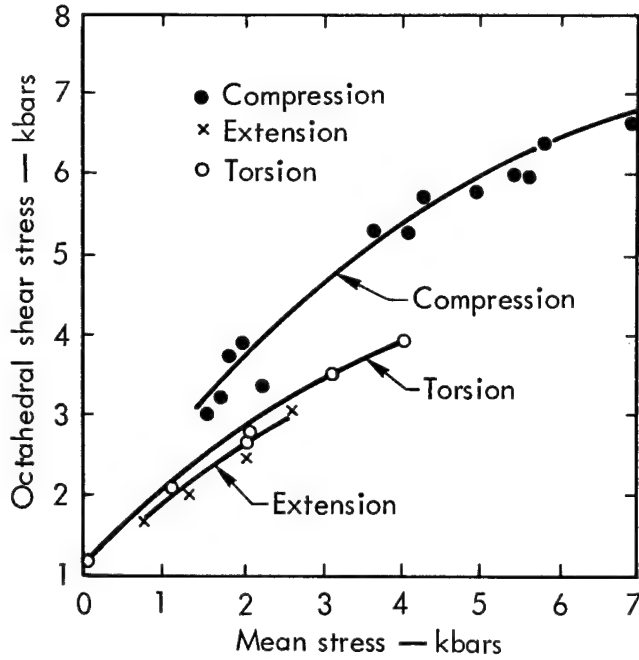
19

Figure 4.6. Octahedral Shear Stress Versus Mean Stress
for Dolomite.

Figure 4.7. Y Versus Mean Stress for Dolomite.

ure). In the region labeled "compressive failure," if brittle failure occurs the cracks will be in the direction of greatest compressive stress, i.e., radial, or at some shear angle to the radius. Upon unloading by the following rarefaction, annular cracks will also be produced. Beyond the zone of compressive cracking is a region where a shock stress is not large enough to cause compressive failure, but tensile cracking is produced in the unloading phase. Again, these cracks are annular. This region is labeled in Figure 4.4 as "Failed under negative mean stress (tensile failure)." A slightly different form of tensile cracking is produced near the surface, where the rarefaction reflected from the surface will produce a tension. The resulting tensile failure is called spall and is so labeled in the figures.

To calculate the extent of fracturing produced by the source, one must know the "strength" of the medium as a function of the state of stress. A direct approach is to plot the octahedral shear stress, which is equal to $(2I_{2D}/3)^{1/2}$, versus the mean stress, P_m, which is equal to $-I_1/3$. The results of various destructive tests (compression, extension, and hollow torsion) are shown for dolomite in Figure 4.6. The plot clearly does not give a consistent failure surface when the test type is changed.

However, it has been found (Figure 4.7) that a consistent failure surface results if we define "strength" as a function, Y, as follows:[6]

$$Y = \frac{3}{4}\left[(3I_{2D})^{1/2} + \frac{I_3}{|I_3|}\left(\frac{|I_{3D}|}{2}\right)^{1/3} \right]$$

To review the various stress invariants let us write a general stress tensor:[7]

$$\begin{bmatrix} T_{11} & T_{12} & T_{13} \\ T_{21} & T_{22} & T_{23} \\ T_{31} & T_{32} & T_{33} \end{bmatrix} \qquad (T_{ij} = T_{ji}),$$

and write the stress deviators

$$T_1 = P_m + T_{11},$$

$$T_2 = P_m + T_{22},$$

$$T_3 = P_m + T_{33}.$$

then

$$I_3 = T_{11}\, T_{22}\, T_{33} \cdot 2T_{12}\, T_{33}\, T_{31}$$
$$- T_{11}\, T_{23}^2 - T_{22}\, T_{31}^2 - T_{33}\, T_{12}^2,$$
$$I_{2D} = T_1\, T_2 + T_2\, T_3 + T_3\, T_1 - T_{12}^2 - T_{31}^2,$$
$$I_{3D} = T_1\, T_2\, T_3 + 2T_{11}\, T_{23}\, T_{31} - T_1\, T_{23}^2$$
$$- T_2\, T_{31}^2 - T_3\, T_{12}^2.$$

20
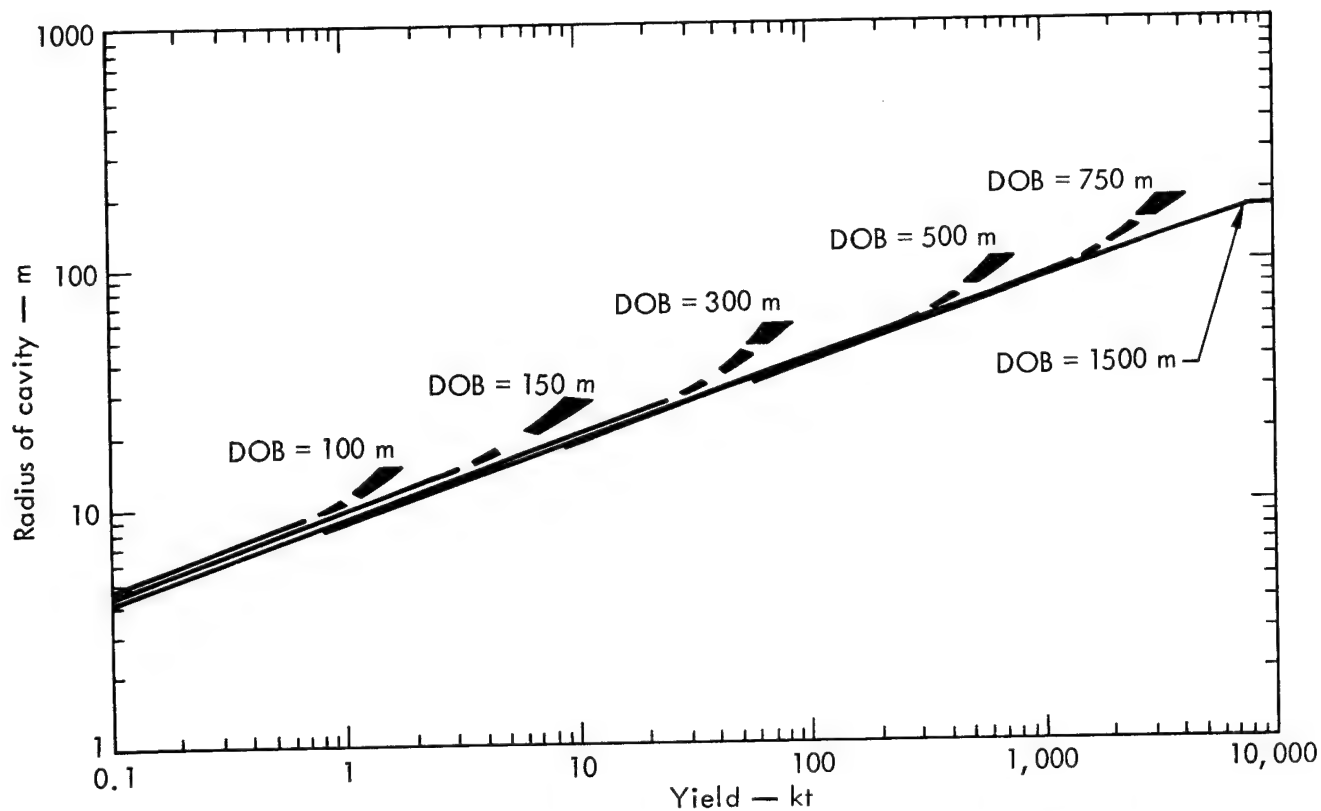
Figure 4.8. Radius of Cavity Versus Yield at Various Depths of Burial (DOB); SOC Model Study in Lewis Shale[5].
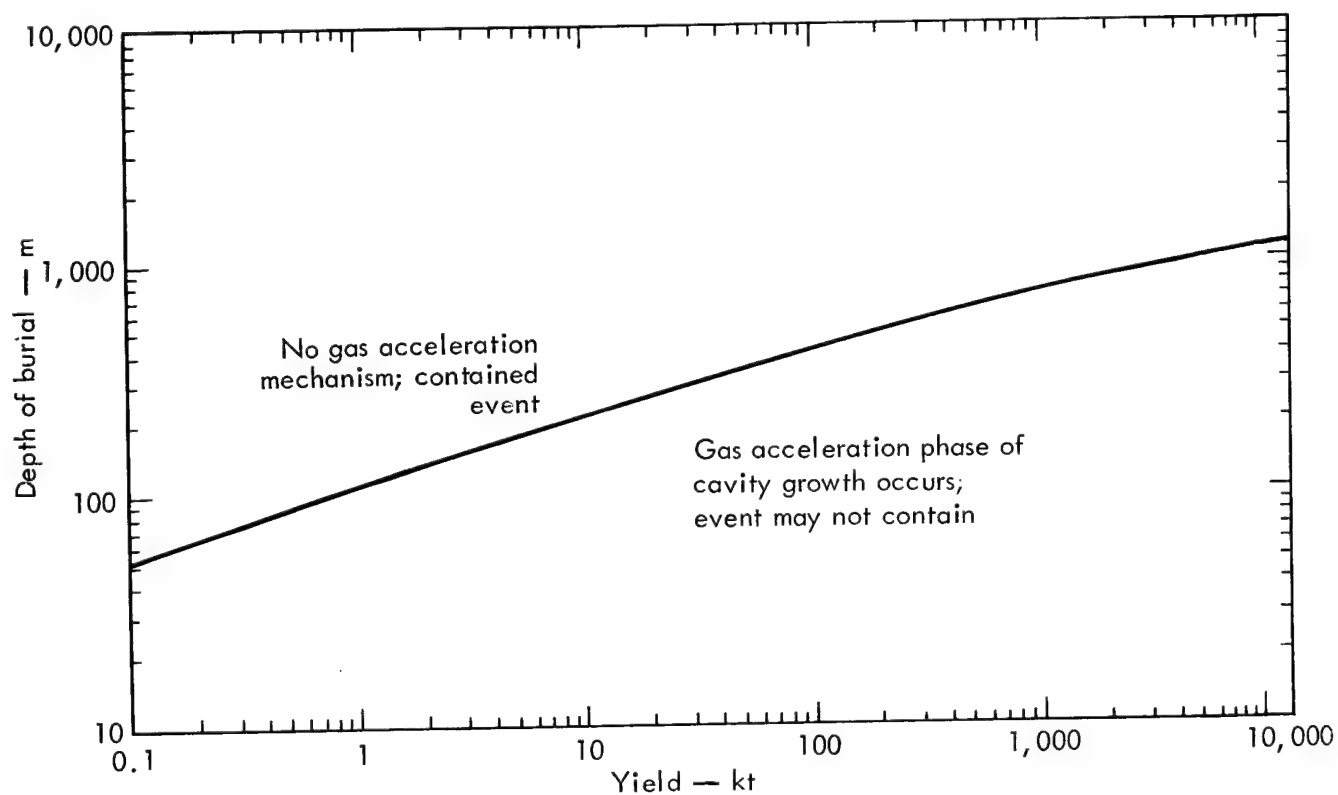
Figure 4.9. Burial Criteria (Gas Acceleration in Lewis Shale).

Radius of cracking

Lewis shale: 200 m

Pictured Cliffs sandstone: 176 m

Hardhat granite: 170 m

Handcar dolomite: 115 m

Radius of cavity

Hardhat granite: 33 m

Lewis shale: 30 m

Pictured Cliffs sandstone: 27.5 m

Handcar dolomite: 24 m

Scale 1 in. = 40 m

Yield: 30 kt
Depth of burial: 300 m

Figure 4.10. Radius of Compressive Cracking and Cavity as a Function of Medium: Calculation Model Study.

One should by no means assume that rock failure at all levels between the shot point and the surface implies the presence of an easy path by which radioactivity can reach the surface, thus causing delayed seepage. On the contrary, both field experience and calculations tell us that the time required for gas to diffuse through these cracks under the driving force of cavity pressure is long compared to the time it takes for cavity pressure to decay. This will be discussed in more detail later. (See Seepage of Radioactivity.)

The onset of the gas-acceleration phase of cavity growth can be determined by inspecting the value of the cavity radius as a function of yield (Figure 4.8). At depths where there is no gas-acceleration phase, the cavity radius increases as $W^{1/3}$. There comes a point, however, where cavity radius begins to increase rapidly with further increase of yield; this rapid increase indicates the onset of gas acceleration. An estimate of the point at which each curve in Figure 4.8 deviates from linear when plotted against yield gives a criterion for depth of burial by the gas-acceleration model in Lewis shale (Figure 4.9). When compared with current practice the criterion is seen to be consistent in the yield region where most of our experience lies (1 to 50 kt), and the comparison indicates

that our current practice is quite conservative in the higher yield range.

Using a criterion like gas acceleration instead of a rule of thumb places the subject of containment on a firmer technical footing, but it also introduces complications. The gas-acceleration crit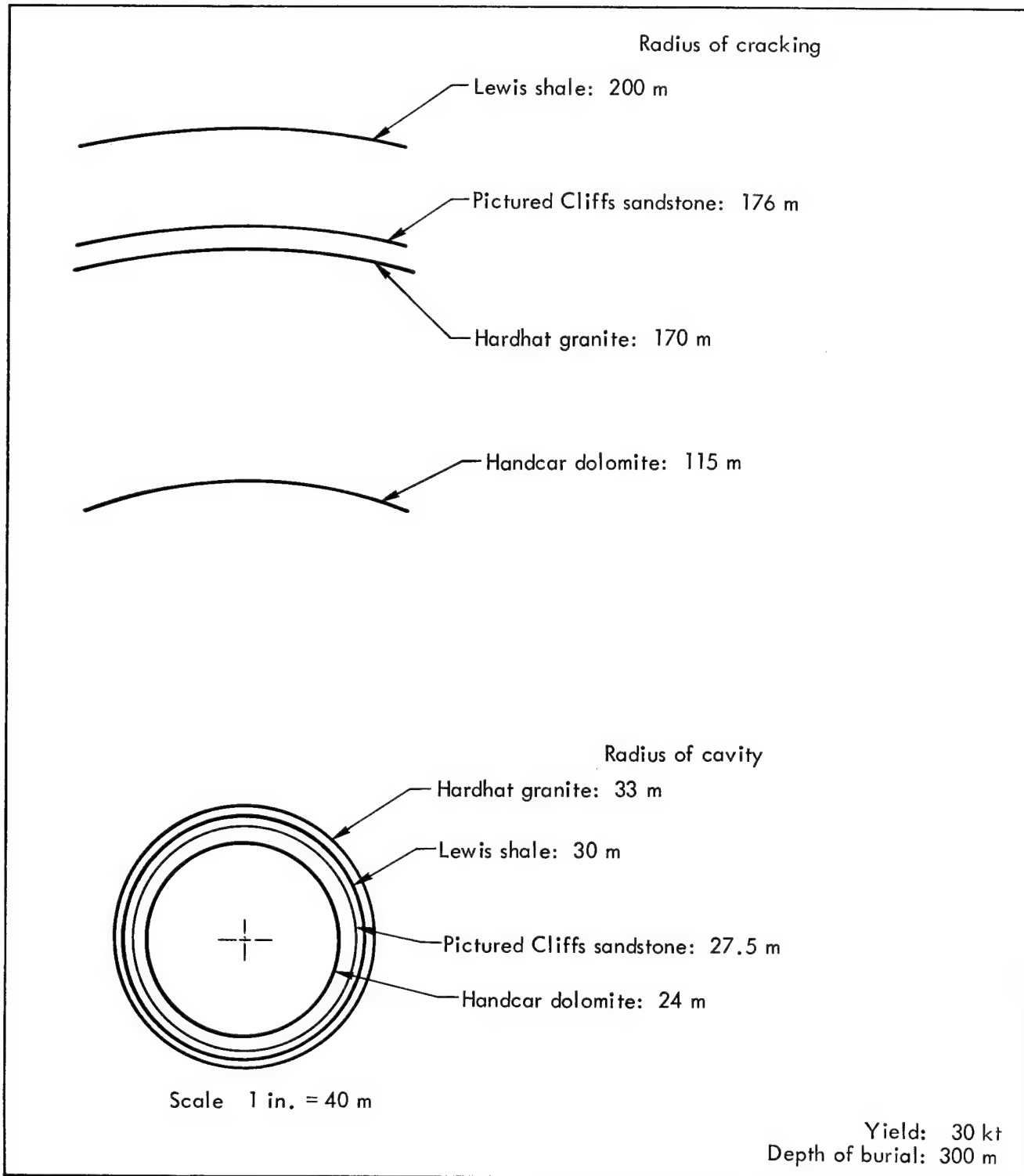erion is, like containment itself, clearly dependent on material properties, since it arose from a calculation which involved material properties. The extent of this material dependence is suggested in Figures 4.10 and 4.11. Figure 4.10 shows cavity radii and failure radii for the same yield and depth of burial in several different media. Figure 4.11 shows the depth-of-burial criterion derived from gas acceleration for several different media.

The rock property which probably has the greatest effect on the presence or absence of the gas-acceleration phase is compactability, the nonreversible compression caused by elimination of void spaces. Since this compression is done under considerable shock pressure, much energy in the form of $P\Delta V$ work is locally deposited as internal energy and thus removed from the energy available to the hydrodynamic shock. Removal of energy from the shock will in turn remove energy from the returning rarefaction and thus inhibit the gas-acceleration phase. Compactability is strongly
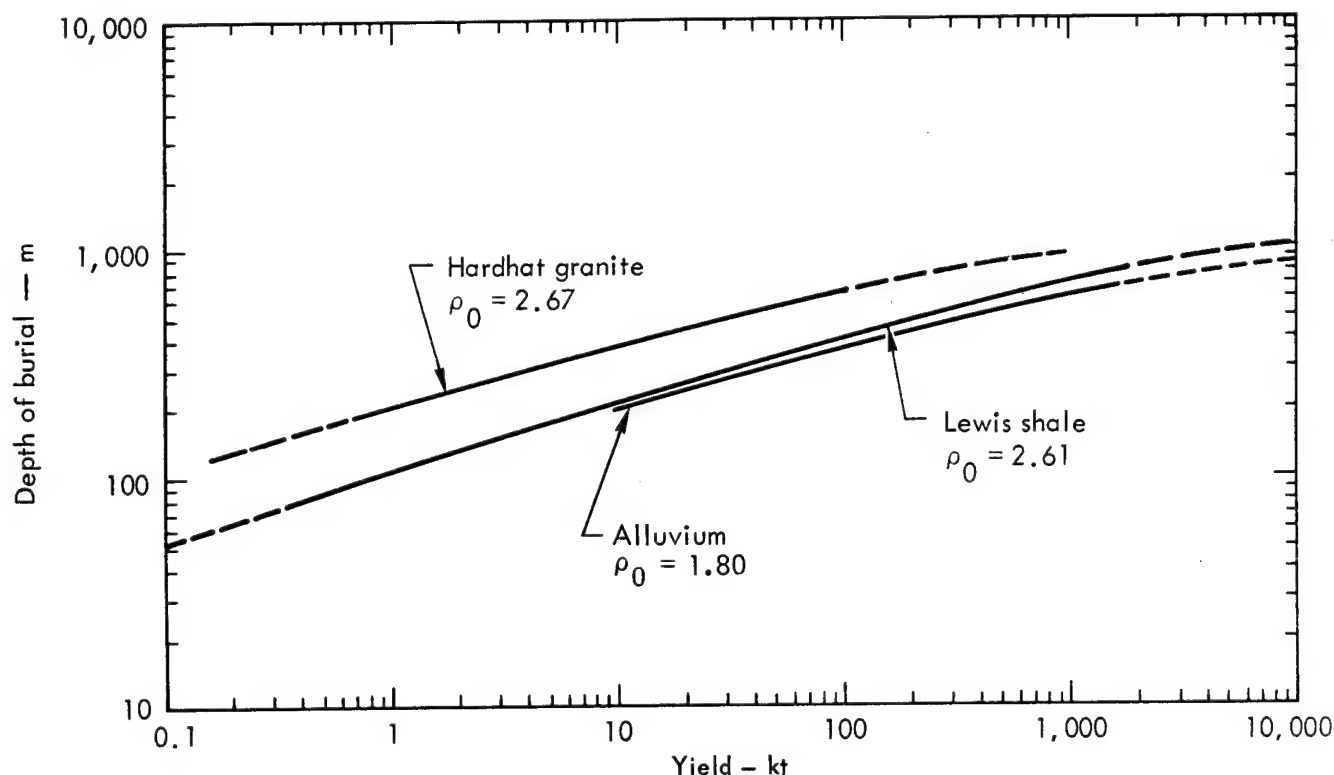

Figure 4.11. Depth-Verus-Yield Criterion for Gas Acceleration as a Function of Medium.

23

related to the porosity, ratio of void volume to total volume, and degree of saturation (how much of the void volume is full of water) of the medium. At present these quantities are difficult to determine unless one obtains samples of the media in the neighborhood of the explosion. However, one can get some help in evaluating compactability from more easily measured properties, such as density and sonic velocity.

Shock velocity within the medium is clearly important since it determines the interval between the explosion and the arrival back at the cavity of a signal reflected from the surface. The shorter this interval the more probable is a gas-acceleration phase, because one has caught the cavity in an earlier stage of its growth.

The exact shape of the PV curve of the material is also important. If the PV curve shows considerable curvature (refer to Figure 4.3), the velocity of the rarefaction following the shock (given by the local slope at the appropriate value of P) will be higher than that of the shock itself (given by the average slope from $P = 0$ up to P). Thus the following rarefaction will catch up to the shock and weaken it. Again, any weakening of the shock will weaken the gas-acceleration phase of cavity growth.

Comparison of Calculations and Experiments

There have been many experiments in which nuclear phenomenological effects have been both predicted and measured. Typical examples in different rock materials are the Piledriver, Salmon, Gasbuggy, and Cabriolet Events. Cabriolet was a cratering experiment, and the other three were contained underground events.

Piledriver Event

Piledriver was an approximately 60-kt explosion in granite at the Nevada Test Site (NTS). The mechanical properties of this granite had been previously determined for the Hardhat experiment, and those equation-of-state (EOS) data served as the EOS data for the analysis of Piledriver.

Calculations [8]

Two SOC code runs were made, one vertically with the free surface 463 m above the device, the other horizontally with a constant overburden of 463 m and no free surface. These calculations are summarized in Figure 4.12. Here a plot of cavity radius as a function of time demonstrates the role that the free surface plays in the physics of cavity formation. The two SOC runs are identical until the rarefaction arrives back from the free surface to the growing cavity. This wave is large enough to cause significant changes in cavity growth rate, as evidenced by the slope change for the vertical SOC run at about 2×10^2 msec. This phenomenon is recognized as the gas-acceleration phase of
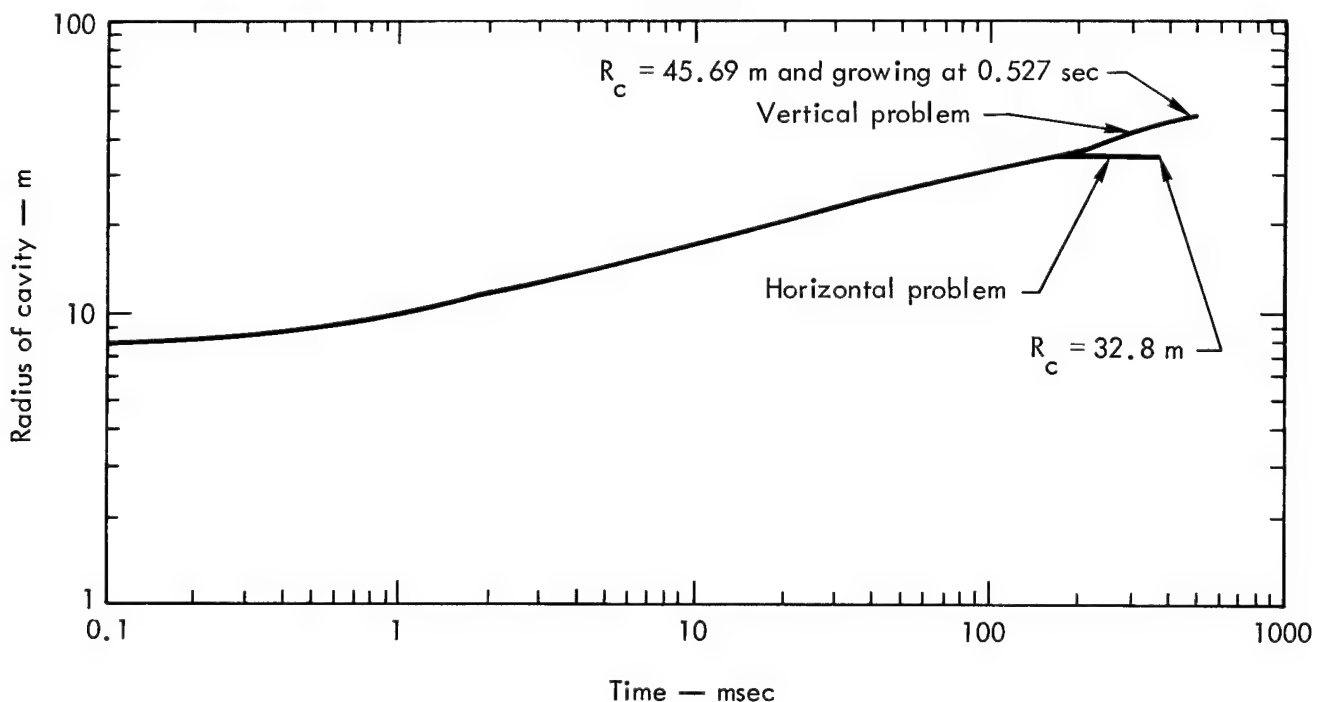

Figure 4.12. Calculated Growth History of the Piledriver Cavity.

cavity growth, which has been previously described. In spite of the fact that the vertical calculations indicated gas acceleration, the explosion contained.

The calculated cavity radius was approximately 46 m and still growing at 0.527 sec. Shock-induced cracking was predicted to extend at least 237 m above the shot point. It was further pointed out that if the tensile strength of the rock materials would not permit a roof span of one cavity diameter to be stable, then the roof would collapse beyond the induced cracking zone or until the bulked rock filled the void to a point of equilibrium.

Measurements [9]

Chimney height was placed at 277 m above the shot point, and the cavity radius at 44.5 m. Calculated and measured peak pressure and peak particle velocity are compared in Figure 4.13. The observed measurements are consistent with the vertical calculations, indicating that the gas-acceleration role as currently simulated has converged or is converging on reality.
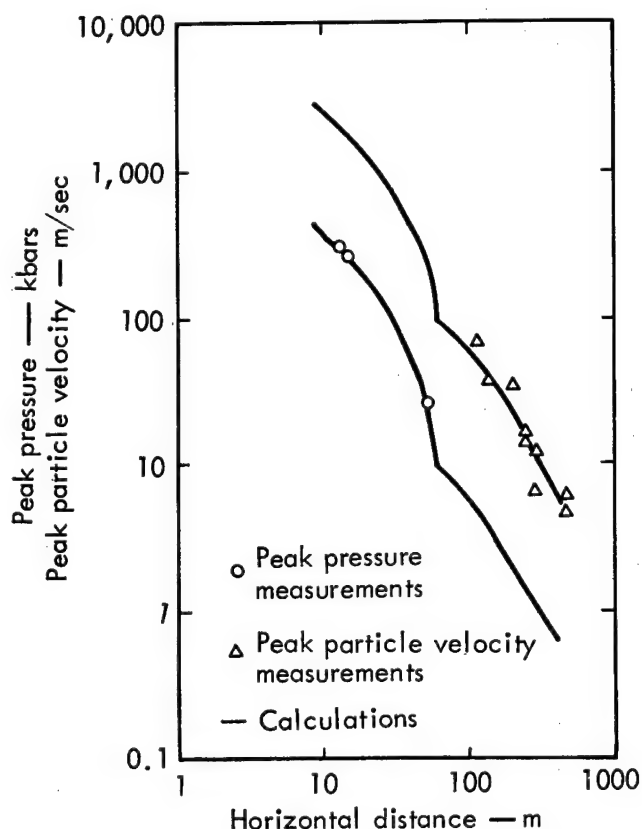

Figure 4.13. Peak Pressure and Peak Particle Velocity Versus Distance: Piledriver Event.

Salmon Event

Salmon was an approximately 5-kt nuclear explosion buried at 827.8 m in the Tatum Salt Dome near Hattiesburg, Mississippi. It was detonated in October 1964. The salt dome consists of nearly vertical beds of NaCl and $CaSO_4$ with a composition of 90 percent NaCl, 10 percent $CaSO_4$. The top of the dome is flat, about 375 m below sea level and about 1600 m wide. It is capped by approximately 140 m of anhydrite (nearly pure $CaSO_4$), above which is a few meters of gypsum, which in turn is overlain by about 38 m of limestone. Above these sediments is about 275 m of sand and clay [10].

Calculations

One-dimensional SOC calculations were run vertically above the working point. The material parameters used in the calculations are summarized in Table II. These first series of calculations (preshot) were performed by Rogers; [11'] the following description is taken freely from his work.

Bulk and shear moduli were used which agreed with the experimental seismic compressional and shear wave velocities. The p-μ* data were based on static and dynamic compressibility data for salt. The density used, 2.2 g/cm^3, was in agreement with laboratory analysis. A tensile strength of 10 bars was arbitrarily selected to indicate that the salt has some coherence on a large scale. The overburden of 181 bars at shot depth was added to this for determining the stress limit above which cracking occurs, so any reasonable value for the tensile strength has only a small effect on the calculated radius of cracking. The Tatum salt is impure, which implies a low bulk tensile strength. Anhydrite exhibits a sluggish phase transition in the pressure range of about 20 to 30 kilobars (kbars), and the effect of this on the 9 percent impurity in the salt was included in the code by setting the bulk compressive strength (Y_0) of the salt at 25 kbars. The input parameters for the overlying layers of anhydrite, limestone, and sediments were selected on the basis of data available at the time. No extensive p-μ curves were necessary for rock other than salt, since the pressure outside the salt dome was low enough to be described by the elastic constants and one point on the p-μ curve set to agree with the bulk modulus.

---

*Tables in which pressure is tabulated as a function of shock compression ($\mu = \rho/\rho_0 - 1$) for a material in its initial state and in its crushed state.

TABLE II. INPUT DATA FOR SALMON PRESHOT CALCULATIONS (VERTICAL COMPONENT)

Parameter[a]	Salt	Anhydrite	Limestone	Sediments	
Overburden pressure at shot depth, kbar	0.181				
K, kbars	245	555	468	108	182
G, kbars	122	308	324	12.8	68
ρ_0, g/cc	2.2	2.92	2.5	2.0	1.9
T_0, kbar	0.01	0.01	0.01	0	0
K_0, kbar	0.600	0.20	0.1	0	0
K_1, kbar	0.100	0.10	0.1	0	0
K_2, kbar	0.050	0.05	0.05	0	0
Y_0, kbars	25	100	100	10	0
Y_1, kbar	0.500	0.1	0.1	0.005	0
Γ	1.5	2	2	2	2
Yield, kt	5.0				

		Salt Hugoniot			
p	μ	p	μ	p	μ
0	0.0	25	0.0828	300	0.53
1	0.00447	40	0.123	400	0.63
2	0.0085	60	0.173	600	0.795
5	0.02027	80	0.219	900	0.98
8	0.0318	100	0.255	1200	1.13
11	0.0426	150	0.34	2000	1.35
15	0.0554	200	0.41		

[a] K = bulk modulus; G = shear modulus; ρ_0 = initial density; T_0 = initial tensile strength; K_0 = dynamic elastic limit; K_1 = low-strain-rate elastic limit; K_2 = static elastic limit; Y_0 = confined crushing strength; Y_1 = compressive strength of cracked material; Γ = Grüneisen parameter.

A postshot calculation was also made, with a new set of gas tables, to describe the central cavity pressure and with new experimentally determined compression data for the Tatum salt in the low-pressure range (40 kbars).

The value of the total internal energy in the material that will cause vaporization, E_V, used to determine the amount of salt vaporized is based on the waste heat concept, with the Hugoniot as the release adiabat and the heat of vaporization being about 1 kcal/g. For the 5 kt of energy dumped into a central sphere of iron gas of density 2.58 g/cc and 25-cm radius, the surrounding salt was vaporized to a radius of 3.7 m.

Subsequent calculations were started with the 5 kt of energy dumped into a central region of salt gas having a density of 2.0 g/cc and a radius of 2 or 3 m. With these inputs in the vertical calculations, the cavity growth stops at a radius of about 24 m in about 100 msec (Figure 4.14). In the horizontal calculations, the cavity radius also goes to about 24 m in 100 msec, but then shrinks back to about 22 m at later time (250 msec). The pressure inside the complete cavity obtained from the pre-shot calculation was about 100 bars and less than the 181-bar overburden. The postshot calculation with the more accurate gas tables gave a value slightly higher than the preshot calculation, but

the difference was not significant. Since the code does not include condensation or heat transfer, the real conditions at late time after the shot have not been completely treated.

As shown in Figure 4.14, the salt was predicted to fail with the shock front up to about 25 m radius. The salt originally at 25 m is displaced to 35 m as the cavity expands. The failure associated with the shock front is directly related to the 25-kbar value used for the confined crushing strength (Y_0). A calculation was made with the value of Y_0 set high so that no failure could occur with the shock front. This calculation showed the material to exceed its tensile strength to about 33 m radius before any effects of reflected waves from overlying layers occurred. Whether the material fails by crushing or cracking depends on the interaction of crushing strength and tensile strength, and in either case the material exhibits considerable plastic flow [12]. Cracks do not stay open very long, and in the real world (distinguished from the

computer mathematics) any cracks found will close again by flow of the salt under overburden pressures. After the dynamic aspects of the explosion, the cavity will settle into static equilibrium, with the radial stress on the cavity wall dropping essentially to zero and tangential stress going into compression to sustain the overburden. If this tangential compressive stress is less than the strength of the material at the cavity wall, the cavity will remain open.

The plastic flow region (without actually cracking open) is controlled in the code primarily by the value of the low-strain-rate elastic limit (K_1), i.e., the maximum stress difference allowed for a material between principal directions for the cracked state of the material. The value of 100 bars was selected on the basis that the experimental tensile breaking strengths, where plastic flow would presumably start, were above this value. This stress limit is used on the rising part of the front when the code says it is no longer a
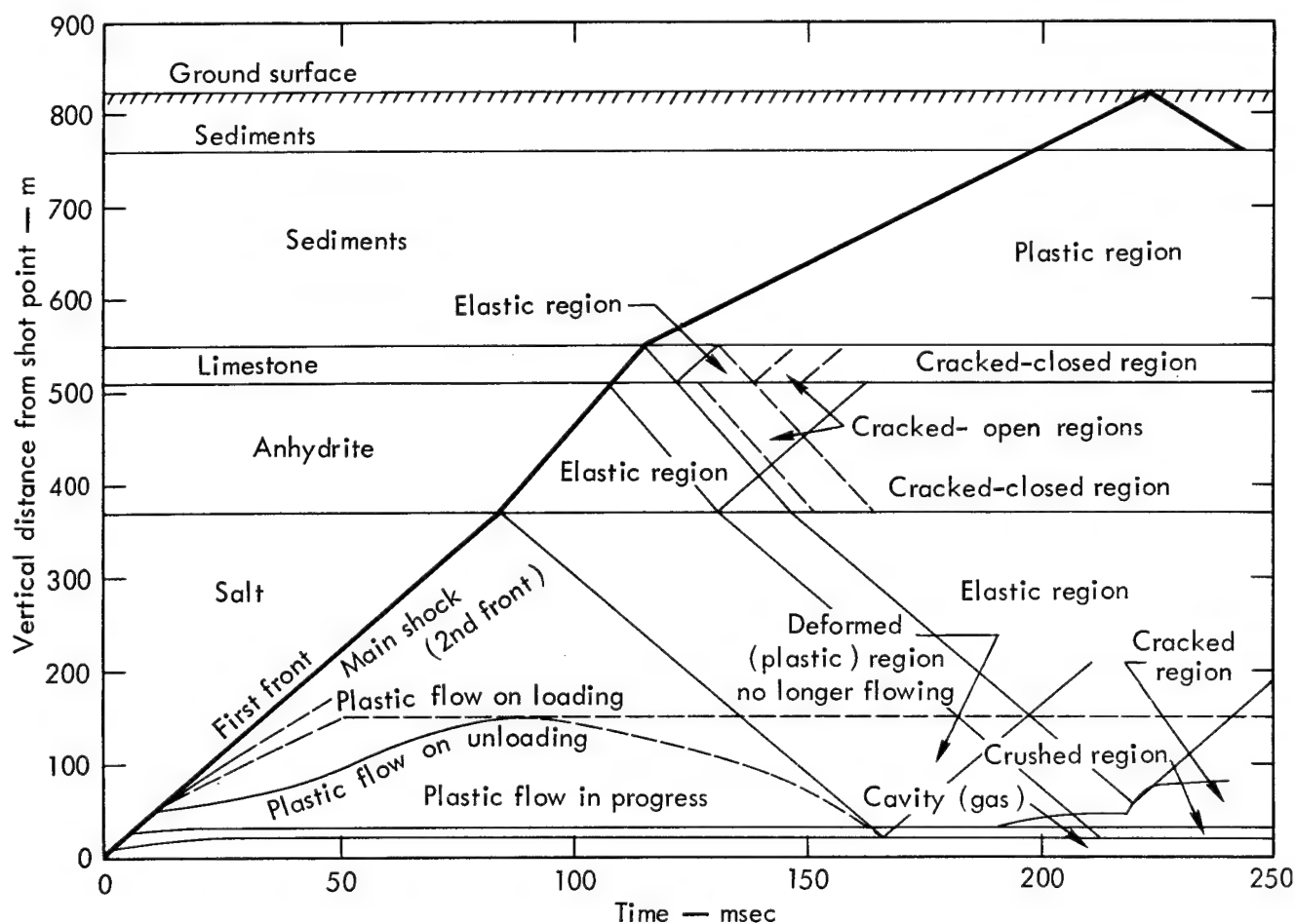

Figure 4.14. Preshot Calculations of Shock-Wave Arrival Times and Rock Alterations for the Salmon Event.

27

sharply rising front and on the unloading region behind the shock front. The calculated time-distance history of when the flow is occurring is also shown in Figure 4.14. On the basis of the 100-bar value for K_1, flow occurs out to about 150 m. The value of K_1 that best represents the Tatum salt is not known, however, and this value of 150 m might be on either side of the true value.

Calculated wave shapes for the intermediate range from the horizontal calculation are given in Figure 4.15. Plots for a vertical calculation are similar, except that overburden is different for each radius, and waves reflected from the various boundaries complicate the late-time shape of the wave. The effect of the stress deviator K_s (the maximum stress difference allowed between principal directions for dynamic conditions) in determining the magnitude of the precursor is seen in the "knees" in the plots.

The ground-surface vertical-motion calculations for a point directly over the shot point are shown in Figure 4.16. These calculations involve the

properties of all the material overlying the shot point, and agreement was fair only when more refined input data — "postshot" — were used.

Measurements

Calculations and experimental data for the arrival time of the shock front, or first disturbance, are compared in Figure 4.17. The preshot and postshot calculations agree with experimental data, since all points fall on the same curve.

Figure 4.16. Calculated and Measured Vertical Motion of the Ground Surface Directly Over the Salmon Shot Point.
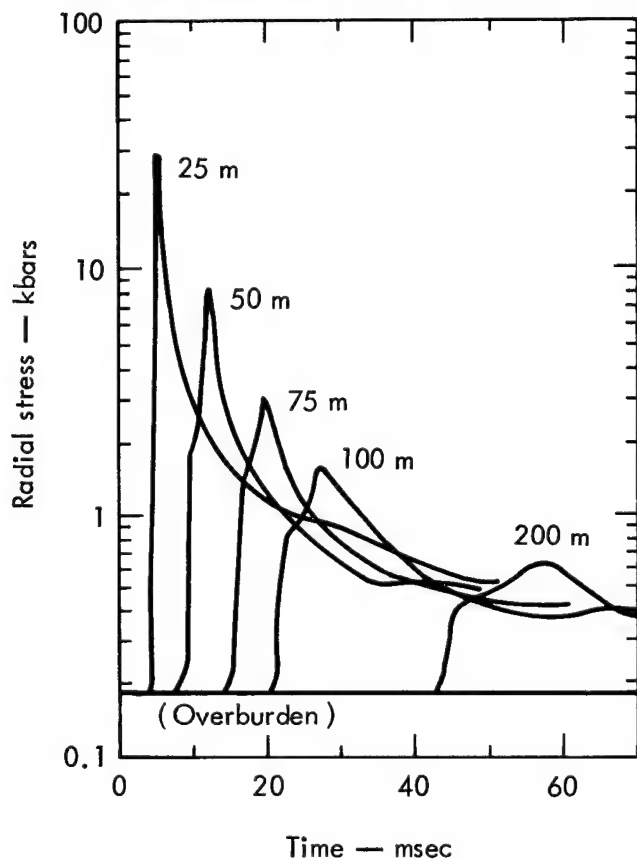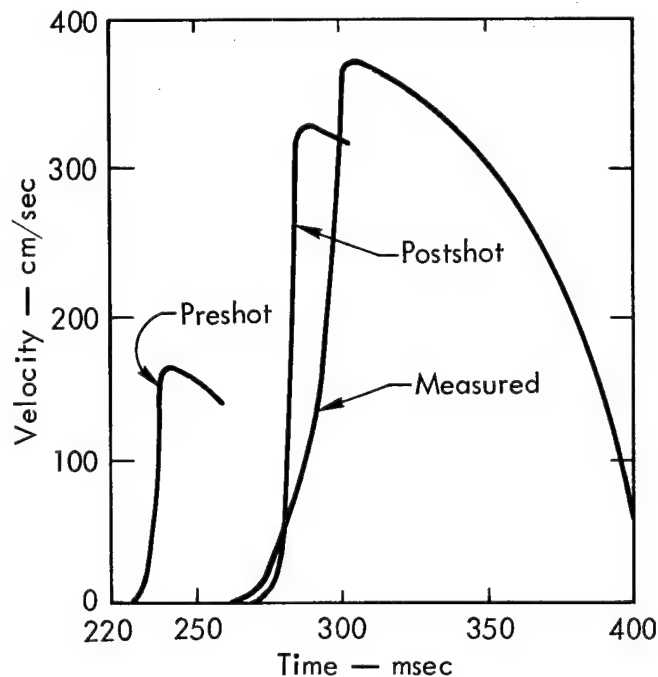

Figure 4.15. Calculated Radial-Stress-Wave Profiles at Several Locations in the Horizontal Direction From the Salmon Shot Point.
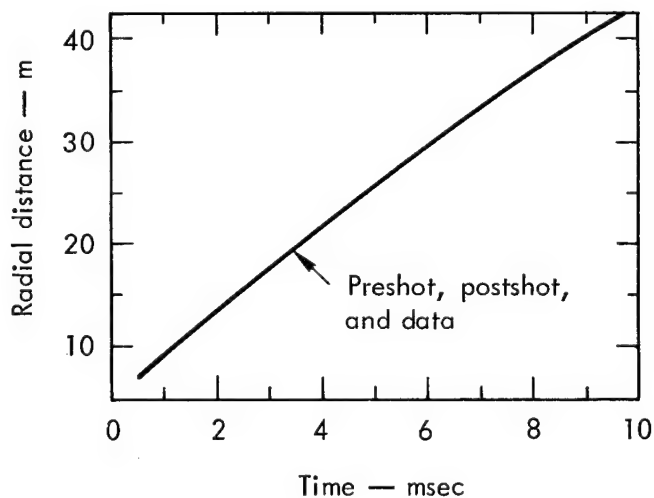

Figure 4.17. Calculated and Measured Shock-Wave Arrival Times Near the Salmon Shot Point.
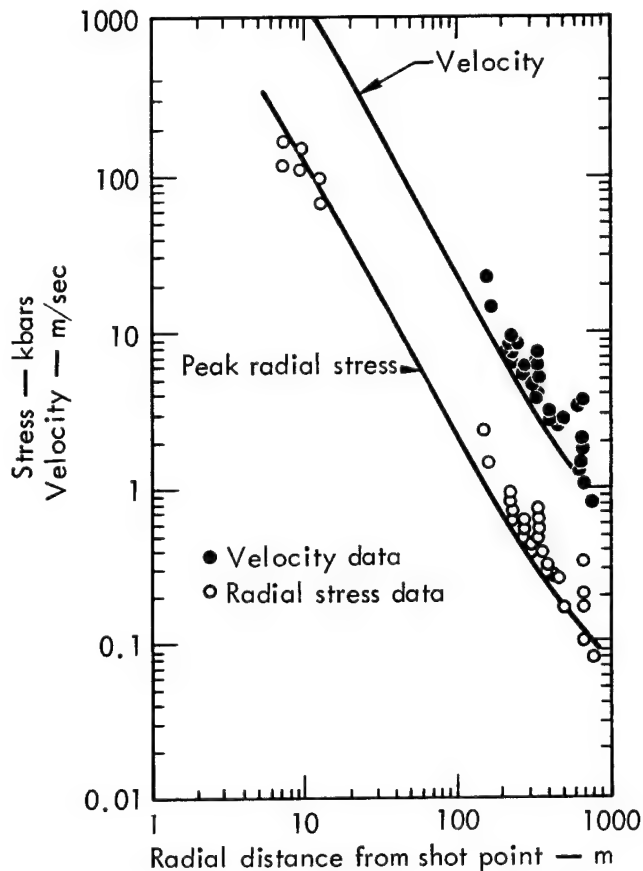
Figure 4.18. Calculated Peak Radial Stress and Peak Material Velocity Compared With Field Data From the Salmon Event.

Calculated peak velocity and peak radial stress are compared with the field data in Figure 4.18. The experimental data do not measure radial stress directly, but it can be approximated from the velocity data and the assumption that the wave is elastic with the stress given by

$$\sigma_r = \rho_0 \, C_0 \, U_p,$$

where

σ_r = radial stress,
ρ_0 = density,
C_0 = sound speed, and
U_p = particle velocity.

The calculations of peak velocity and peak radial stress are generally about 50 percent lower than the experimental data. The experimental ground-free-surface vertical motion shown in Figure 4.16 is nearly matched by postshot calculations.

The cavity radius determined by pumping the cavity full of air was measured to be about 17 m. Measurements of the increase in pressure as a function of time and rate of air injection show that there is some additional volume, presumably in cracks or fissures connected to the cavity. The total volume of the fissures connected to the cavity is small compared to the main cavity volume (10 to 25 percent), and when this volume is added to the spherized cavity the radius is increased a few meters. The difference between 17 m and 24 m predicted by Rogers is not small. This anomaly was not resolved until refinements were recently made in the SOC input[6].

The static elastic limit assumed by Rogers was 50 kbars. The failure model developed by Cherry and others,[6] using EOS of Tatum salt material, allowed for a brittle-ductile transition at 68 bars mean pressure. This implies a stronger salt and predicts a cavity radius of approximately 16 m, which agrees closely with the measured radius.

It is instructive to note that with a more accurate EOS and more sophisticated modeling, such as the

Figure 4.19. Hugoniot Data for Lewis Shale and Pictured Cliffs Sandstone.

Figure 4.20. Hydrostatic Compressibility of Dolomite, Granite, Sandstone, Shale, and Coal.

Figure 4.21. Material Failure Criteria for Sandstone, Shale, and Coal.

30

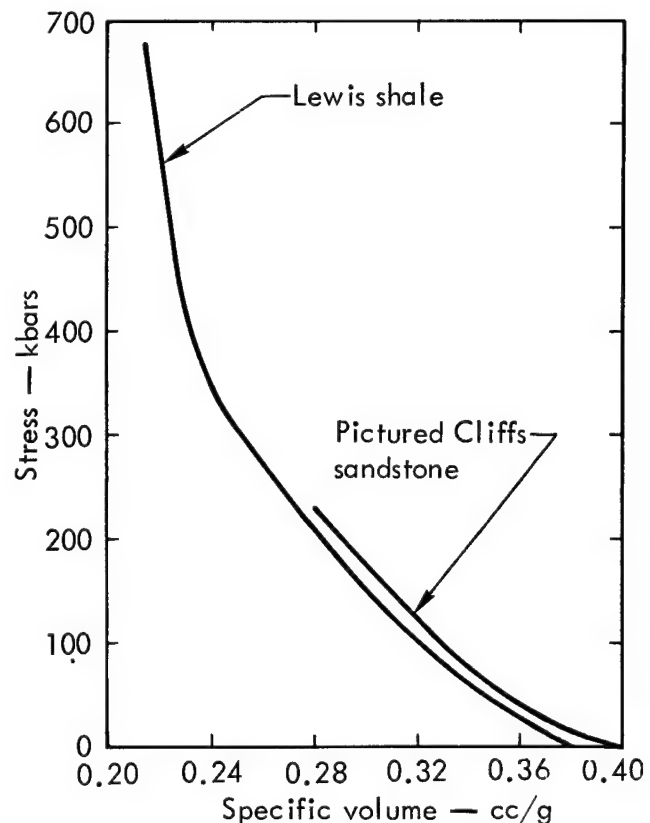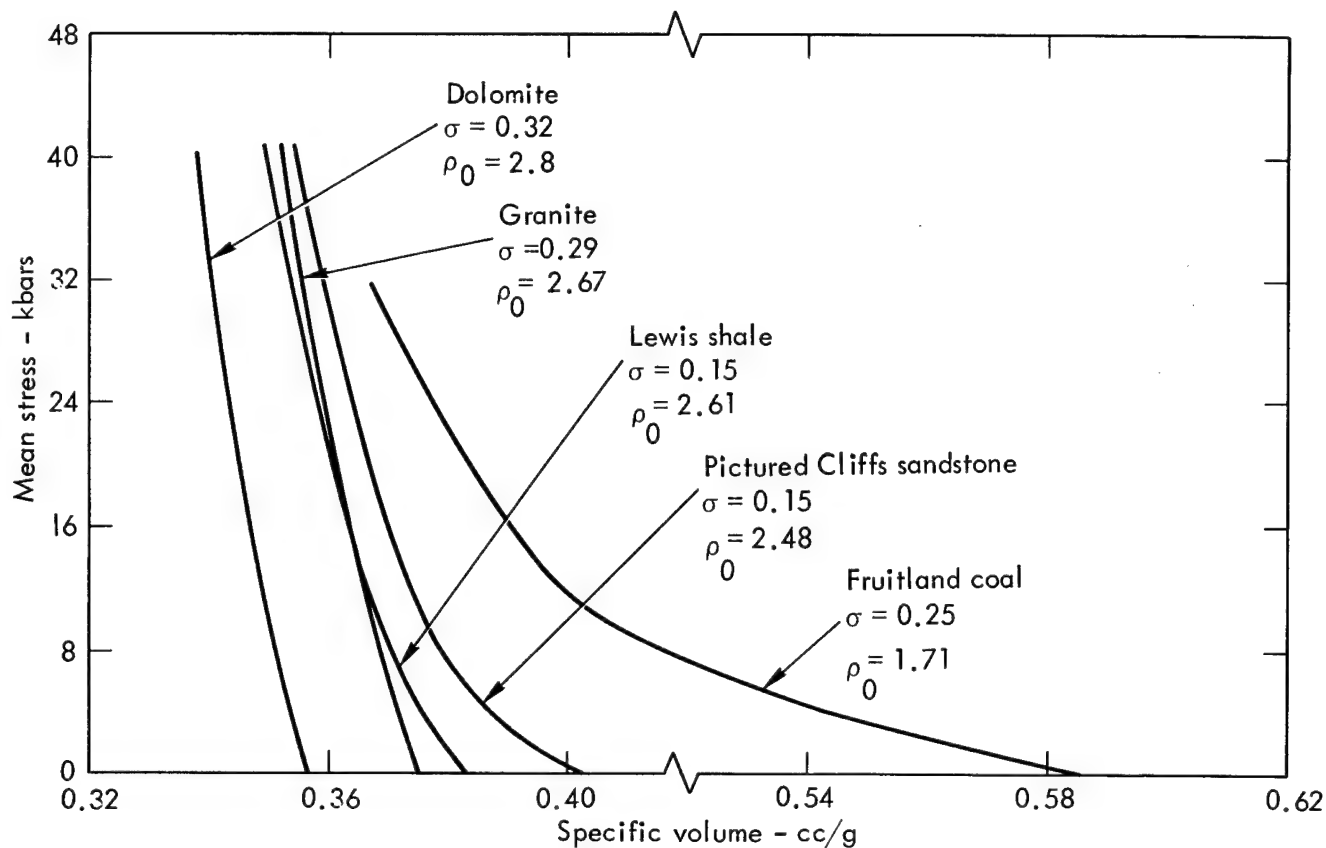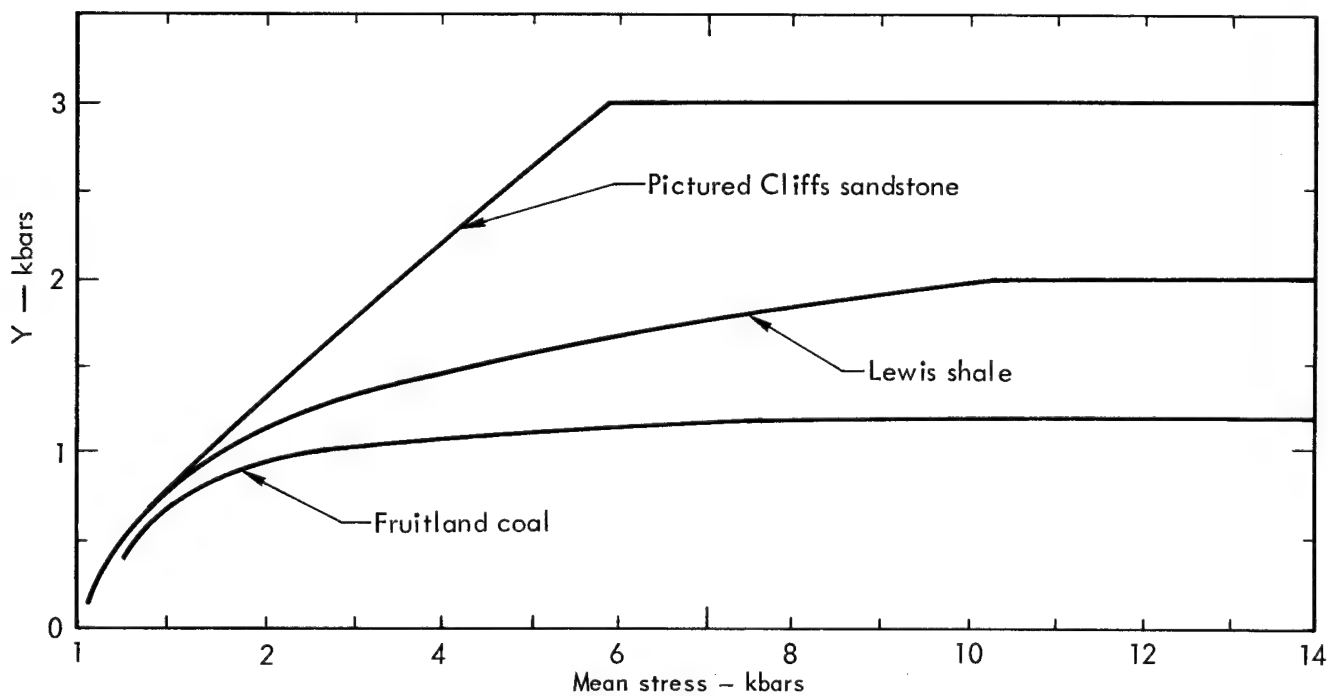failure models recently developed, the simulated phenomenology converges on the real world. This point was also confirmed when Cherry computed peak velocity and peak radial stress with the more accurate EOS of salt. Here there was better agreement with the measured data in Figure 4.16.

Gasbuggy Event

The Gasbuggy experiment was conducted within a sequence of horizontal sediments at a depth of 4240 ft. The energy source was a 26-kt nuclear device. A generalized stratigraphy from the shot point to 3300 ft is:

DEPTH (ft)	FORMATION
3300 to 3650	Sandstone (Ojo Alamo)
3650 to 3800	Shale (Kirtland)
3800 to 3882	Shale-coal (Fruitland)
3915 to 4202	Sandstone (Pictured Cliffs)
4202 to shot point	Shale (Lewis)

This layered geometry dictated a need for careful equation-of-state descriptions of the Lewis shale and the Pictured Cliffs sandstone [13]. The shock Hugoniot data to approximately 680 kbars for Lewis shale and approximately 200 kbars for the Pictured Cliffs sandstone are illustrated in Figure 4.19. The sediments above the Pictured Cliffs were tested to less than a few kilobars, since higher pressures were not expected at these levels. A description of the hydrostatic compressibility of the Lewis shale, Pictured Cliffs sandstone, and Fruitland coal in comparison with granite (Piledriver, Hardhat) and dolomite (Handcar) may be seen in Figure 4.20. The criteria for material failure are derived and defined by Cherry and others,[6] and are illustrated in Figure 4.21. For a given material and a given mean stress, failure is defined when Y, a function of the material stress invariants, equals or exceeds the upper value of the material failure curve illustrated in Figure 4.21. For example, failure will occur at a mean stress of 8 kbars in Lewis shale when $Y \geq 1.7$ kbars, and in the Pictured Cliffs sandstone when $Y \geq 3$ kbars. These data, along with the data in Table III, are the estimates of the parameters used to generate the equations of state necessary for the Gasbuggy calculations.

Calculations

Two one-dimensional calculations using the SOC code were run [3]. The first treated all material above 3195 ft as Pictured Cliffs sandstone. This calculation predicted failure, i.e., cracking, out to approximately 390 ft, and a cavity radius of 78 ft.

The second run included the different layers above the Pictured Cliffs formation. Here material property differences, specifically those of the Fruitland coal, play a major role in determining the interaction of materials and source. Note the differences in density, compressional velocity, compressibility, and Poisson's ratio indicated in Table III. With these parameters now in the code, it was predicted that the highly compressible coal would act as an energy sink and in this way significantly lower the failure criteria below the values determined in the first calculations, at distances somewhere above the base of the coal. Based on these new input parameters, the chimney was predicted to extend only 334 ft vertically, stopped by the coal bed, but fractures could ex-

TABLE III. PARAMETERS USED IN GENERATING EQUATIONS OF STATE FOR THE GASBUGGY CALCULATIONS

Material	Region thickness (ft)	Density (g/cc)	Compressional velocity log (ft/sec)	Total water content (wt %)	Compressibility (Mbar)	Poisson's ratio	Heat of vaporization[a] (ergs/cc × 10^12)	Heat of fusion[a] (ergs/cc × 10^12)
Lewis shale	Shot point to 4202	2.61	13,700	3.5	0.191	0.15	0.4759	0.1259
Pictured Cliffs sandstone	4202 to 3915	2.48	13,520	4.5	0.134	0.15		
Fruitland coal	3915 to 3882	1.71	8,850		0.0602	0.25		
Fruitland shale	3882 to 3800	2.49	11,700		0.132	0.15		
Kirtland shale	3800 to 3650	2.58	14,070		0.240	0.15		

[a]Heats of vaporization and fusion for SiO_2.

tend around the device up to 425 ft. Preliminary time-of-arrival data are compared with calculated data in Figure 4.22.

Measurements

Postshot investigations by Korver and Rawson [14] indicate that the cavity top is probably at approximately 3850 ft, or 325 ft above the working point, indicating a significant role played by the compressible coal in halting the chimney growth. The radius of fractures is estimated at 480 ft.

In general, there is very good agreement between measurements and those calculations which include the different rock materials above the shot point.

Cabriolet Event

The Cabriolet Event was a 2.5-kt Plowshare nuclear cratering experiment in volcanic trachyte at NTS. It was detonated in January 1968.

Calculations

The basis for the Cabriolet calculations had already been established [3]. Figures 4.23 through 4.25 summarize the *in situ* hydrostatic compressibility, seismic velocity measurements, and density measurements for the rocks at the Cabriolet site. The break in the velocity curves at 28 to 35 m from the surface was the criterion for selection of the density inputs indicated on Figure 4.25.

Figure 4.26 is the predicted peak radial stress as a function of distance about the shot point. The particle velocity versus distance at 135 msec is illustrated in Figure 4.27

Figure 4.28 represents the throwout calculation at 135 msec. All zones whose velocities were great enough to pass the free surface were removed from the grid.

Cabriolet Code Verifications

Data collected on the Cabriolet experiment are still being reduced. The apparent radius was 178 ft, compared with a predicted 170 ± 40 ft. Preliminary data from a slifer positioned 25 ft from the emplacement hole indicate good agreement between calculated shock position and actual shock position as a function of distance and time.

LATE-TIME PHENOMENOLOGY

Cavity Cooling

Calculations

The cooling of cavities produced by nuclear explosions is being investigated by Chapin [15] with two calculational models. The first model simulates the thermodynamics of the cavity from the time at which hydrodynamic expansion ceases (on the order of tenths of a second) until cracked material over the cavity drops into the cavity and collapse starts. The second model numerically describes the cooling of the cavity gas during collapse when relatively cool wall material is falling through the cavity.

Results of a SOC or TENSOR calculation are used to obtain the size and shape of the cavity and the energy and density of the cavity gas, which are initial conditions for Chapin's first cooling model. In this model, the following assumptions are made:

1. Gas properties are constant throughout the cavity, since rapid mixing is taking place.
2. The effect of natural convection in the cavity, which might induce thermal gradients in the gas, is small and can be ignored.
3. The material in the cavity is a binary mixture of SiO_2 and H_2O.
4. The cavity gas is optically thick and emits blackbody radiation to the wall.
5. The wall is a perfect absorber. (Scattering properties of the gas and reflecting properties of the wall surface are not known.)
6. Convective and radiative heat transfer are independent.
7. The wall conditions are uniform.
8. Melted wall material is instantly removed from the walls, and all of the water contained in the melt is added to the cavity gas.
9. The cavity volume is constant.
10. All of the heat released from the cavity during condensation of the rock gas is due to the condensation process.

Starting with the initial conditions in the cavity as it is a few tenths of a second after the explosion (a pressure near overburden and a temperature of a few thousand degrees Kelvin), Chapin uses equations of state for SiO_2 and H_2O to determine the thermodynamic properties of the cavity gas. By calculating a heat trans-
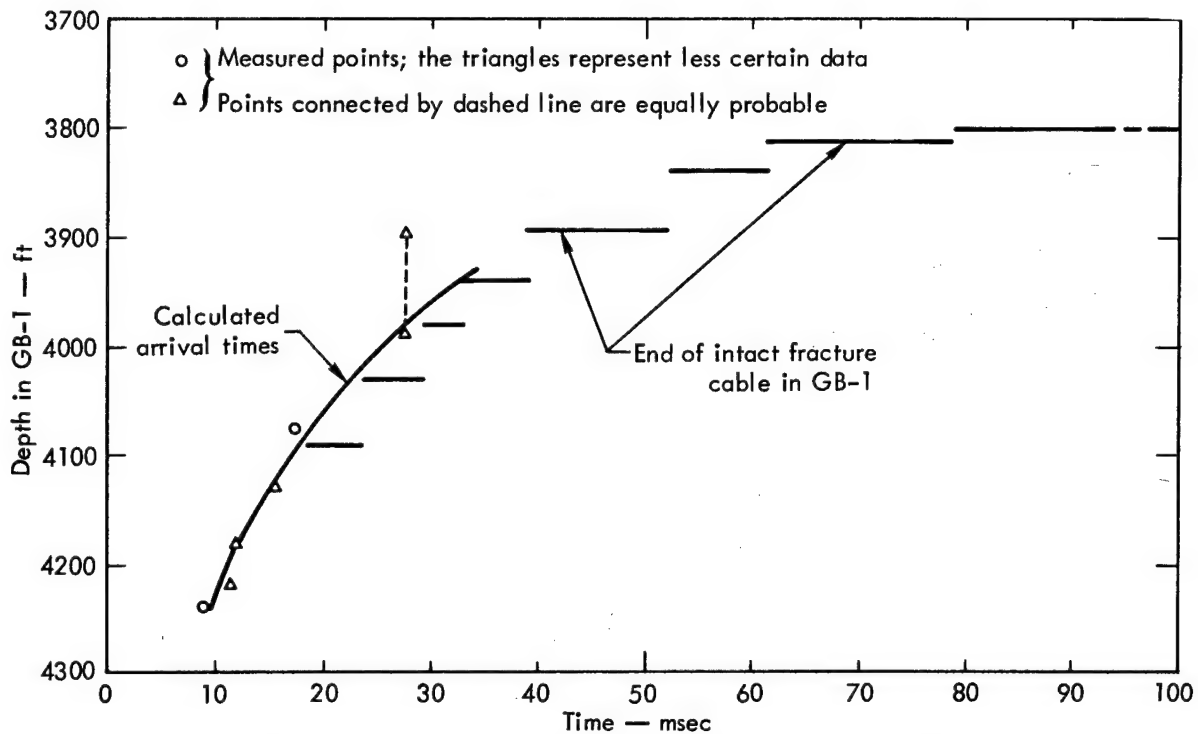
Figure 4.22.   Time of Arrival of First Motion at Various Radial Distances.
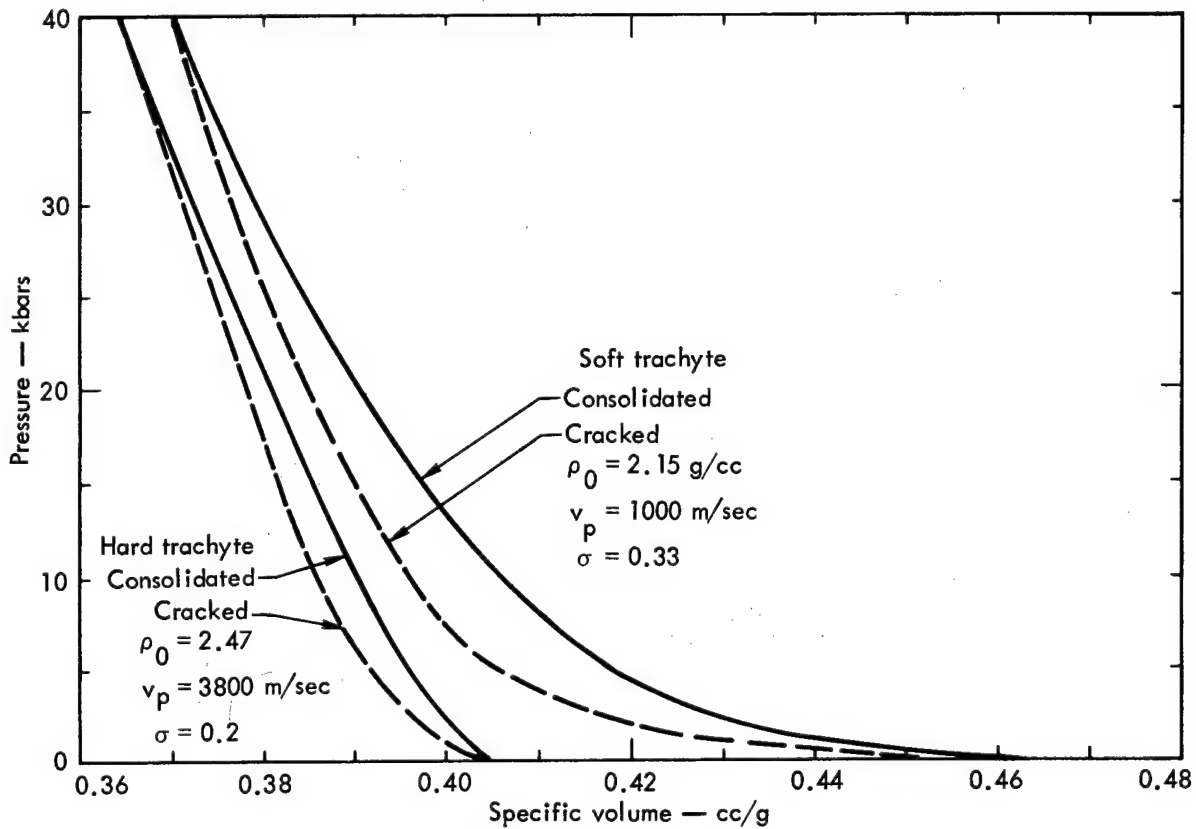
Figure 4.23.   Hydrostatic Compressibility of Consolidated and Cracked Soft Trachyte.

33
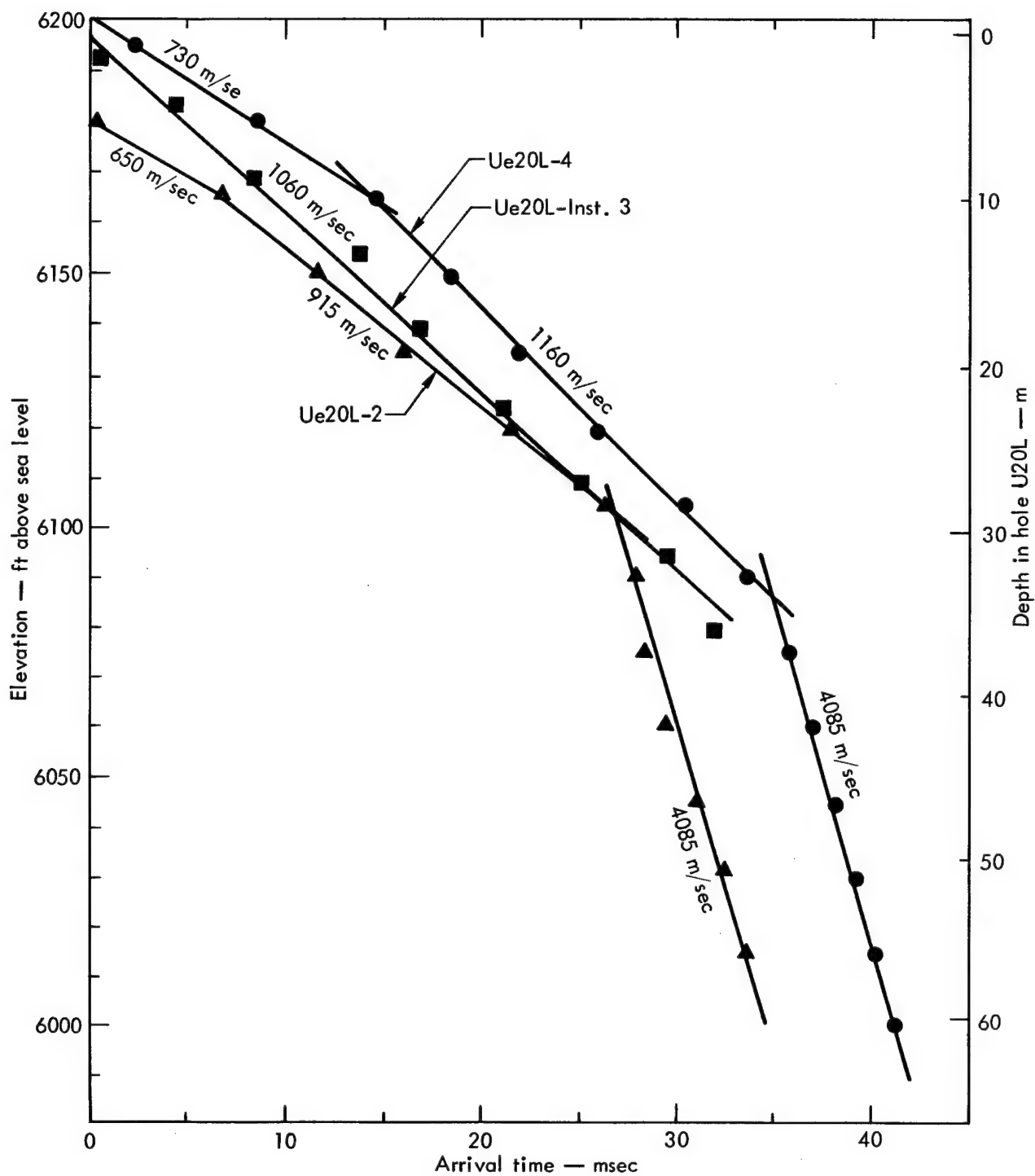
Figure 4.24. Seismic Velocity Data from Cabriolet Site.

34
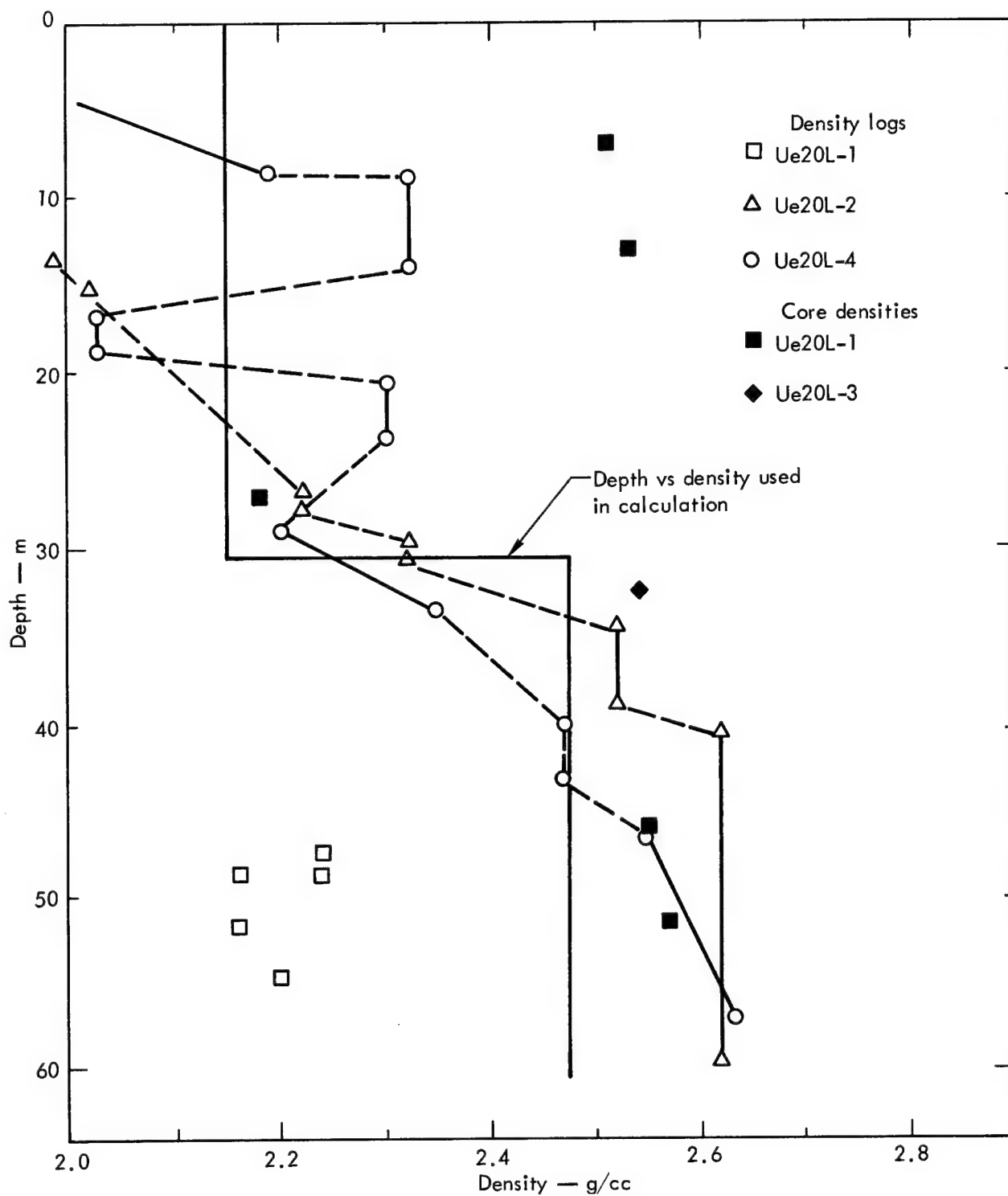
Figure 4.25. Density Measurements in the Vicinity of the Cabriolet Emplacement Hole.
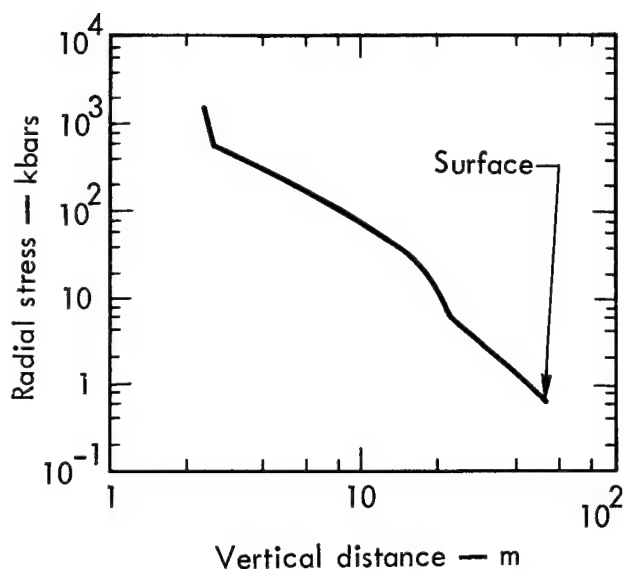
Figure 4.26. Predicted Peak Radial Stress as a Function of Distance About the Cabriolet Shot Point.

fer rate which includes radiation and convection, one determines the energy transferred to the cavity walls during a time interval Δt. The energy transferred to the walls is allowed to melt rock and vaporize water in the rock. The vaporized water is added to the cavity gas over the time Δt, and the increase of water density in the cavity is calculated. The increased density and decreased energy in the cavity at the time $t_0 + \Delta t$ result in a lowered temperature and pressure. This process is repeated by finite differences to obtain the time-history of the cavity.

A point will be reached where the gaseous rock can condense. While the gas is condensing the heat-transfer rate is held constant at its value just before condensation. All of the energy released by the cavity during rock condensation is assumed to be due to the condensation process, and the temperature of the cavity gas remains constant.

After the rock has condensed, the cavity is all steam; thus only the equation of state for water is needed. When the cavity temperature drops below the vaporization temperature of rock, heat transfer may be approximated by conduction into the walls. At this point, the
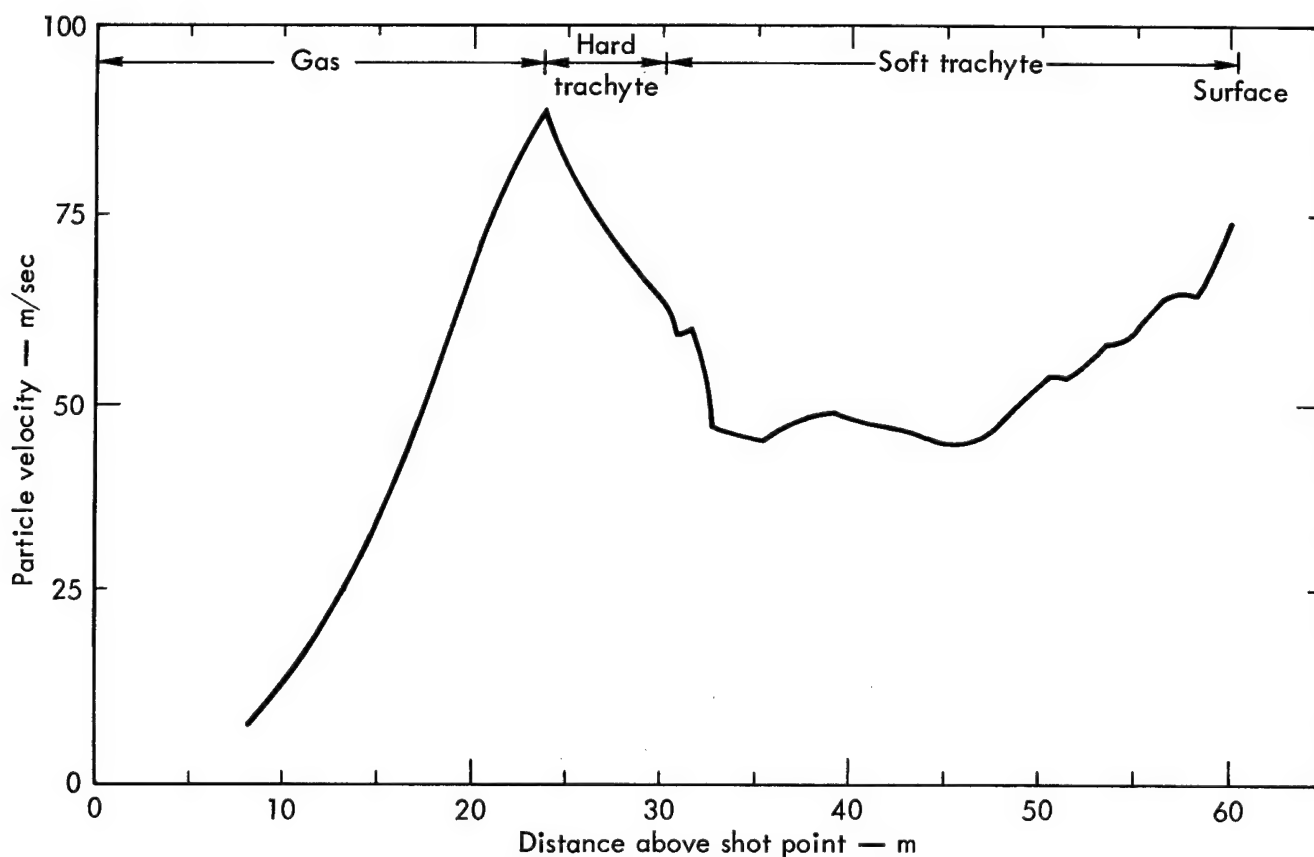
Figure 4.27. Calculated Particle Velocity Versus Distance Above Cabriolet Shot Point at 135 msec.

36
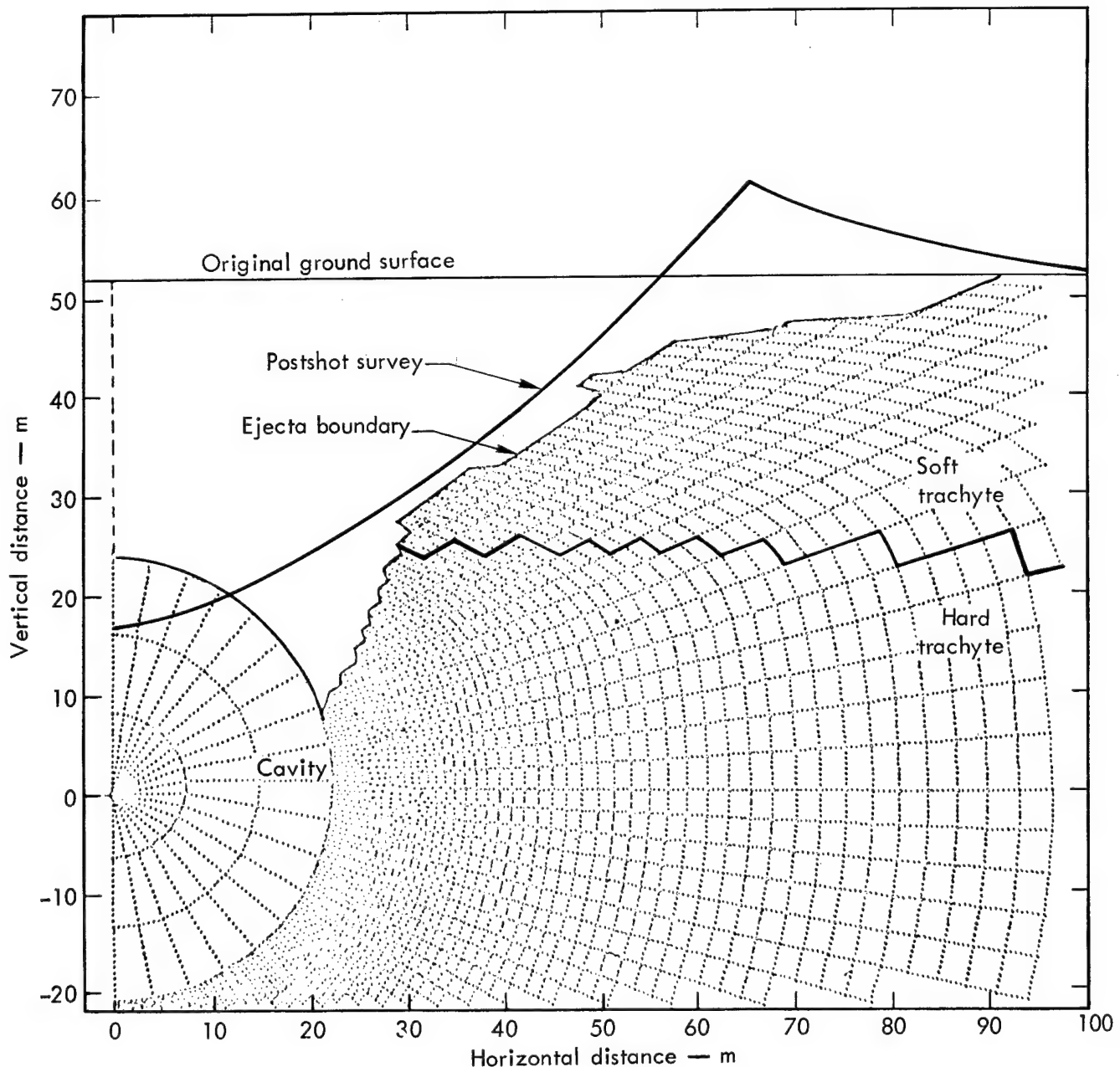
Figure 4.28. Throwout Calculation at 135 msec for a 2.5-kt Nuclear Explosion in Layered Trachyte (Cavity Pressure = 48 bars).

TRUMP code,[16] which solves the heat-conduction equation with thermal-conductivity variables in space and time, can be used to calculate the heat-transfer rate. However, if a constant value for the thermal conductivity can be chosen, the heat-transfer equation and its boundary conditions in spherical coordinates can be simplified, and the heat-transfer rate can be calculated without TRUMP.

By using the heat-transfer rate due to conduction (from TRUMP or the analytical solution), Chapin's finite difference model can be continued to calculate the

decrease in cavity pressure and temperature during the conduction phase.

Chapin's cavity-collapse model starts at a time when the cavity pressure is less than overburden. Collapse is visualized as a shower of debris into the cavity from the cracked material over the cavity. The model considers particles as they fall from the cavity roof. Each particle is allowed to trap some of the cavity gas in the bottom of the cavity, and the remaining gas in the cavity rises to replace the particle. The particles fall by gravity, hence they remain in the cavity

for a certain time. The particles are assumed to be spheres initially at a temperature T_0, and a rate for convective heat transfer to the particles from the cavity gas is calculated. This energy is then removed from the cavity gas. A rate and an average size at which particles enter the cavity are estimated. The rate of removal of mass and energy from the cavity gas can then be calculated. Using a water equation of state for the cavity gas, the pressure and temperature of the remaining cavity gas can be found. By advancing the equations with respect to time, the time-history of the cavity gas as it rises to replace wall particles can be calculated. Comparisons between Chapin's model and experimental results are incomplete. Preliminary analyses indicate that good agreement can be achieved between the model and the observations discussed below. (See Figure 4.29.)

Measurements

In one case where good cavity-pressure measurements were obtained from 45 sec postshot until collapse, simple Newtonian cooling of a steam-filled cavity was

adequate to match the experimental data:[17]

$$(T - T_\infty)/(T_0 - T_\infty) = e^{-(hA/C_v n)t},$$

where:

t = time,
T = temperature at time t,
T_0 = T at $t = 0$,
T_∞ = T at $t = \infty$ (ambient temperature),
h = surface heat transfer coefficient,
A = surface area,
C_v = molar heat capacity at constant volume, and
n = total moles of material in cavity.

The Newtonian cooling calculation and the experimental values are compared in Figure 4.29. Best agreement was obtained by assuming a heat-transfer coefficient of about 0.01 cal/cm^2-sec-°K. Note that at about 7 min after the shot, the measured pressure begins to deviate significantly from the best-fit curve. The deviation is probably the result of condensation of water vapor.
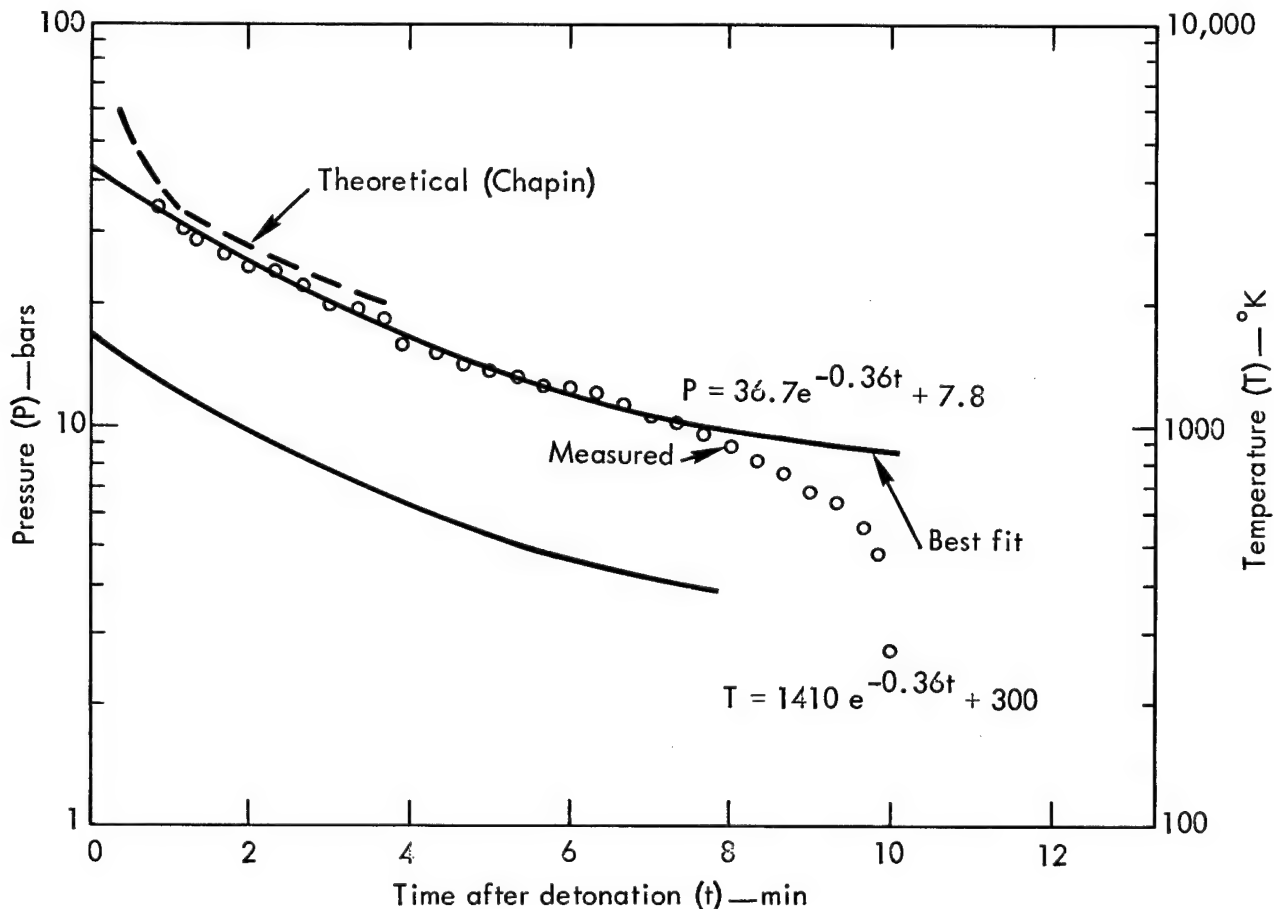

Figure 4.29. Comparison of Measured Pressure, Theoretical Pressure, and Best-Fit Pressure and Temperature Curves.

Seepage of Radioactivity

Calculations

The POROS code has been developed and successfully used by Rodean to simulate gas flow through porous materials[18]. POROS is one-dimensional with options for planar, cylindrical, or spherical coordinates; any set of units may be used. A number of boundary conditions may be applied to either the Darcy or the non-Darcy (laminar or turbulent) flow it calculates. The thermodynamic process may be adiabatic or isothermal throughout the system, or it may involve local temperature equilibrium between the gas and porous material. A POROS calculation could start at about the end of Chapin's cavity-collapse model, when heat transfer between the cavity gas and the rock particles is no longer significant.

Darcy flow assumes that inertial forces are negligible. The Darcy equation is a reduced Navier-Stokes equation which equates the pressure gradient with viscous forces and potential body forces. In POROS, the body forces on the gas or fluid are also neglected, and only the viscous forces resist the gas motion. Darcy flow can be used for flows down to a Reynolds number of about 1, where the diameter of a grain size is used for the length parameter. The non-Darcy "turbulent" flow considered by POROS reduces to the Darcy equation by the use of another constant that effectively multiplies the permeability constant. POROS treats the viscosity of the gas, the Reynolds number, and the porosity and permeability of the sand as constants; however, it would require only a minor change to treat them as functions of thermodynamic variables or position.

POROS was used to simulate some laboratory tests of a high-pressure (250 psi) gas through 20 ft of typical sands used for stemming at NTS. Pressure versus time-histories were both measured and calculated at stations located 5, 10, 15, and 20 ft from the initial gas/sand interface. Results compare very well for the 5- and 10-ft stations, but differ slightly at the 15-ft station and more at the 20-ft station. Generally, the "turbulent" non-Darcy calculations give better agreement with the data.

Measurements

Although the agreement between calculations and the laboratory experiments cited above is promising, there have been no meaningful comparisons between POROS calculations and data from nuclear shots. While we expect this calculational tool to be of increasing use in the future, at present one must seek an understanding of seepage of radioactivity by examining our field experience.

Delayed seepage of radioactivity may occur in an otherwise contained underground nuclear shot as a result of the upward travel of radioactive gases in the chimney which forms by progressive collapse of the material overlying the initially produced cavity. Aron[19] has reviewed data from 28 underground nuclear shots of yields ranging from a fraction of a kiloton to approximately 1000 kt, to examine the relationship between nuclear explosive yield and the height to which radioactive gases rise in the chimney. The following is taken freely from Aron's work.

The 28 events were chosen according to the following criteria:

1. The postshot hole drilled to determine the height of radiation in the chimney must have been drilled vertically down into the chimney within one cavity radius of a vertical line through the working point (most postshot holes prior to mid-1964 met this requirement), or, if the postshot hole was drilled at a slant from the outside the chimney, the bit must have entered the chimney at a height above that at which radiation was detected.

2. A record must have been available of the depth of the bit at the time radiation was detected.

Relationship Between Yield and Rubble Volume

The radioactive gas propagates up to the chimney toward the surface by displacing the collapsing chimney rubble and by diffusion. As a result of heat transfer between the hot gas and cold rubble, the gas is cooled and finally condenses. Therefore, the larger the yield, the greater the amount of gas and the more rubble necessary to condense the gas.

It was assumed for the purpose of this study that the cavities were spherical, that the chimneys were right circular cylinders with the same radius as the cavity, and that the gradation of the chimney rubble was the same for all events. Thus, the chimney volume, V, up to a height, h, above the working point can be computed as:

$$V = \frac{2}{3} \pi R_c^3 + \pi R_c^2 h,$$

where

R_c = the cavity radius.

There is usually a considerable uncertainty in the cavity radius. It is clear from the above formula that large uncertainties in radii will produce large uncertainties in chimney volumes, In addition, cavities are not always spherical.

The data give one of two possible values of h: (1) the location of the bit when radioactivity is first detected at the surface; or (2) the location of the bit when loss of circulation of drilling fluid (LOC) occurs. LOC always occurs either at the same level or higher than the location of the bit when radioactivity is first detected at the surface. Since we wish to arrive at a conservative relationship between yield and the volume of rubble necessary to quench the contaminated gas and stop movement of noncondensable gases to the surface, we shall assume that a column of rubble at least up to the LOC point is required. An envelope can then be derived, such that it gives a volume greater than that of the rubble column up to LOC for all these 28 cases. This envelope can be expressed as

$$V = 4.67 \times 10^6 \, W^{0.754}, \quad (4)$$

where

V = volume in ft^3, and
W = yield in kt.

For events with yields less than 10 kt, the volume-yield line approximates the surface of the earth. However, for higher yields, the line is generally below the surface. This means that by using the present depth criteria, radiation will not rise as close to the surface for higher yields as for lower yields. If data with less uncertainty were available for the depth where radiation was encountered, this conservative line could be moved downward and thus be even more meaningful.

Maximum Depth of Burial at which Radiation will Rise up the Chimney to the Surface

Another way to examine the volume of chimney rubble is to plot, for various yields, the maximum depth of burial at which radiation will propagate up the chimney to the surface. This depth is computed as follows: The volume, V, of rubble in the chimney up to the height, h, to which radiation rises is

$$V = \frac{2}{3}\,\pi R_c^{\,3} + \pi R_c^{\,2}\, h = \pi R_c^{\,2}\!\left(\frac{2}{3} R_c + h\right). \quad (5)$$

Using the predicted cavity radius for tuff, R_{cp},

$$R_{cp} \approx 312 \, \frac{W^{1/3}}{(\rho d)^{1/4}} \quad (6)$$

where

W = yield in kt,
ρ = density in g/cc, and
d = depth of burial in feet.

We substitute in equation (5) to get

$$V = \pi (312)^2 \, \frac{W^{2/3}}{(\rho d)^{1/2}} \left[\frac{2}{3}\left(312 \, \frac{W^{1/3}}{(\rho d)^{1/4}} + h\right)\right]. \quad (7)$$

Now if we let d equal h and assume that $\rho = 2.1$ g/cc, we get, after some algebraic manipulation,

$$V = 2.13 \times 10^5 \left(\frac{168\,W}{h^{3/4}} + W^{2/3} h^{1/2}\right). \quad (8)$$

By using equation (4), the curve for tuff in Figure 4.30 can be drawn. The alluvium curve in Figure 4.30 was drawn in similar manner, except that the predicted cavity radius and density were:

$$R_{cp} = 296 \, \frac{W^{1/3}}{(\rho h)^{1/4}},$$

$$\rho = 1.9 \text{ g/cc}.$$

The dashed parts of the curves represent extrapolation, since there is little or no experience with those yields in that soil material. These two curves represent the minimum depth of burial necessary to create sufficient chimney rubble to quench and to stop the displacement and diffusion of the contaminated gas up the chimney.

Although it would appear that the curves derived in Figure 4.30 are very conservative as a result of using equation (4), a few words of caution are in order. Cavity radius for individual events cannot be predicted very accurately. Also, there will be errors in estimating average overburden pressure because of lack of detailed knowledge of density. The distance from the working point to the postshot surface is not the depth of burial, d, as assumed in equation (4), but rather d less the depth of the crater formed. When Figure 4.30 is compared with current practice, we can conclude that current practice is conservative below 1 kt and above 10 kt, and realistic in the region between 1 and 10 kt. However, this is exactly the region where most of our experience lies, and only a few events in this region have seeped a significant amount of radioactivity. (See PAST EXPERIENCE.)
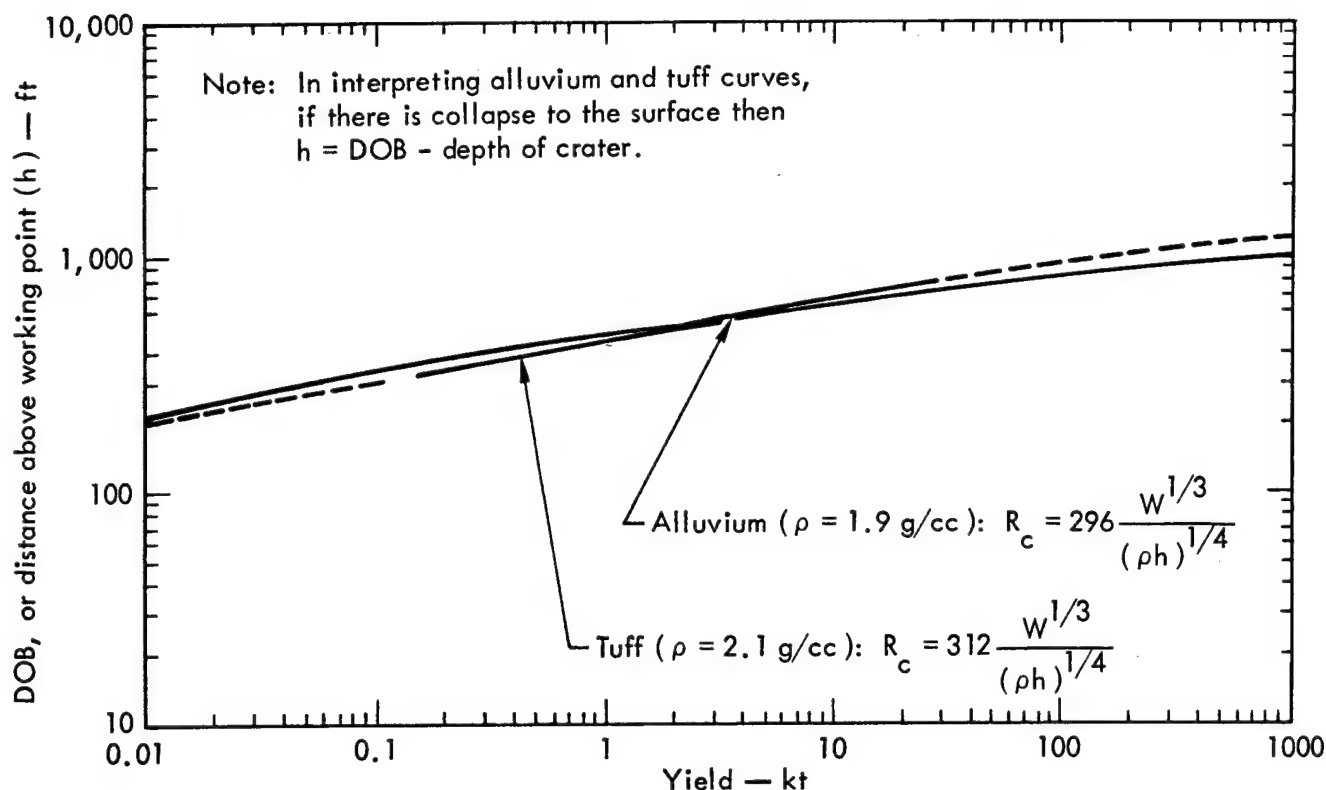
40

Figure 4.30. Calculated Maximum Depth of Burial (DOB) at Which Radiation Will Rise up the Chimney to the Surface in Alluvium and Tuff.

Distance from Surface to Top of Radioactivity in Chimney

Figure 4.31 illustrates another method of demonstrating with the available data that venting by the propagation of gas up the chimney is less probable at high yields. This figure is a plot of distance from the surface to where radiation was first encountered as a function of yield. Since there is considerable uncertainty in the radiation location, the curve is drawn to be conservative.

The information in this figure is independent of cavity radius; therefore, the uncertainty in cavity radius does not hinder its interpretation. This figure shows again that for yields above 10 kt the distance between the surface and detectable radiation increases with yield.

Conclusions

There appears to be a relationship between yield and volume of rubble necessary to quench the condensable contaminated gases rising up the chimney to contain the noncondensable contaminated gases.

At yields greater than 10 kt, the distance between the surface and the highest point to which radiation rises up the chimney becomes greater as the yield increases.

Seepage due to radiation propagating up the chimney during collapse is less probable for yields greater than 10 kt, and the probability decreases as the yield increases.

CONTAINMENT AND GEOLOGICAL STRUCTURES

Structures which may be potential vent paths are the man-made discontinuities formed by the drilling of emplacement or instrument holes, or the geological discontinuities of faults or joints. The man-made discontinuity is resolved by carefully stemming the holes with sand and gravel, grout, or combinations of these. The properties of the stemming materials are matched as nearly as necessary to the properties of the surrounding rock. There have been few problems in this specific engineering area. Emplacement holes are successfully stemmed, and with few exceptions they have not acted as vent paths.

Whereas the positions of drilled holes are known within inches, the positions of faults are much less precisely known. Fault motion cannot be predicted with confidence. Our operational procedure has been to avoid emplacing explosives on or immediately adjacent to known major or sensitive faults. We follow this policy not because we can predict with certainty that these sites would generate vent paths, but simply because it eliminates any possibility that they might.

41
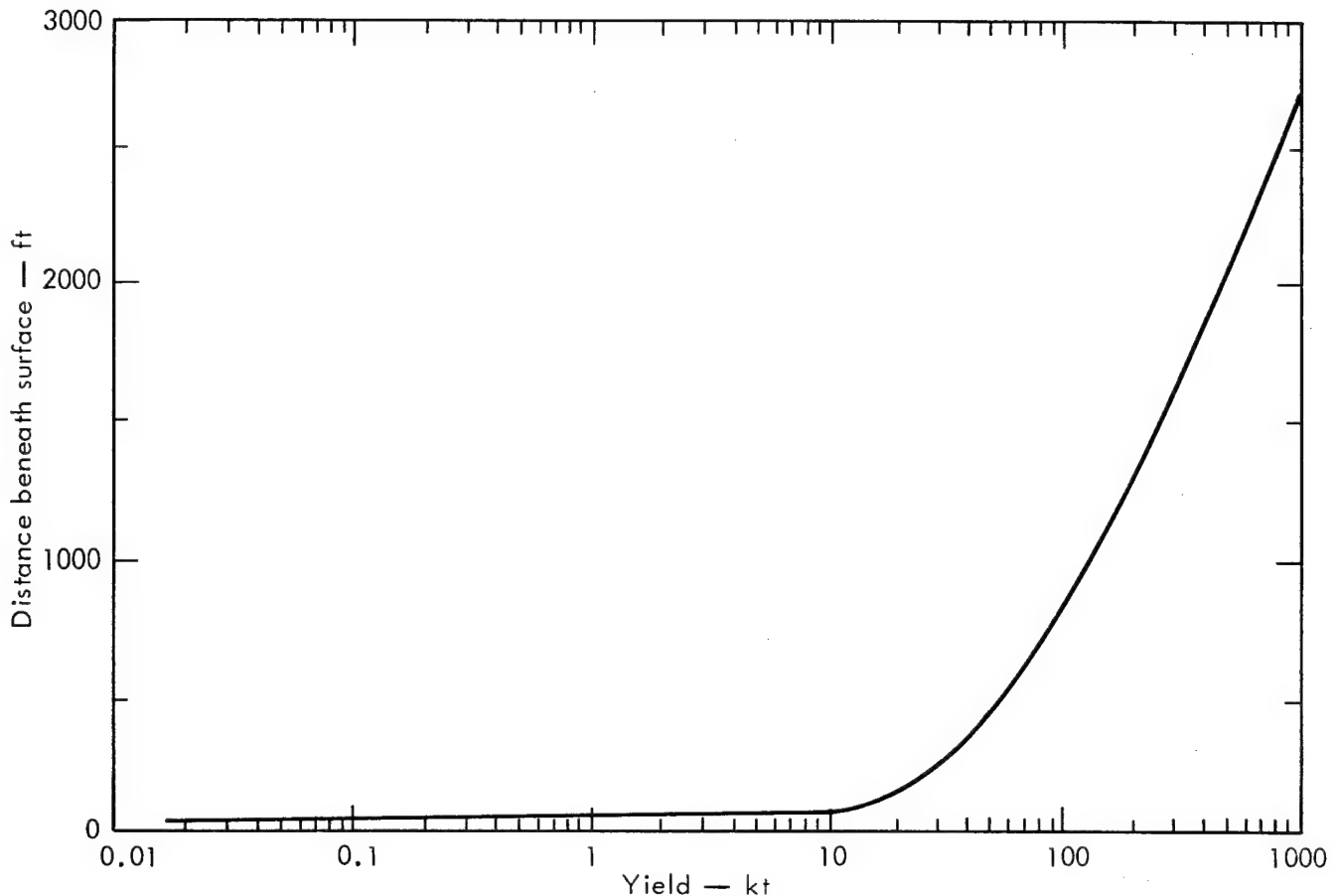
Figure 4.31.   Distance From Surface to Top of Radioactivity in Chimney.

Surface Fracture Patterns and Their Origins

Geologic fracture patterns associated with underground nuclear explosions fall into three general types:

- Radiosymmetric Fracture Patterns

  This group includes both radial and concentric fractures that combine to form a pattern whose center of symmetry is ground zero. Individual fractures may be as long as a few tens of feet, and the whole pattern usually extends up to 500 $W^{1/3}$ ft. The fractures are caused by doming, spalling, and collapse.

- Bisymmetric Fracture Patterns

  These are fractures with a strong preferred orientation, more or less bilaterally symmetrical with respect to a surface line through ground zero. They are usually tens of feet long but may be several hundred feet long; the pattern may extend up to 1000 $W^{1/3}$ ft. These fractures are thought to be controlled by joints.

- Linear Fracture Patterns [20]

  Linear-fracture zones may range from a few feet to several hundred feet wide and from a few feet to thousands of feet long. These fractures are thought to be most likely associated with faults and therefore extend to depths of hundreds to perhaps thousands of feet.

The above generalized descriptions of fault or fracture patterns are of little help in predicting containment or dynamic venting. For the purposes of containment, it has been suggested that the terms "sensitive" and "insensitive" be applied to faults as a guideline for their motion potential. "Sensitive" is understood to apply to those faults along which an explosion causes or triggers some displacement for thousands of feet. "Insensitive" applies to all other faults.

Sensitive faults cannot be positively identified without a large nearby explosion, nor can the mechanisms of motion be expressed rigorously. Hence, it is impossible to predict fault motion. There is considerable correlation between sensitive faults as defined above and those that have experienced motion in recent geological time — i.e., the past million years.

42

Figure 4.32. Typical Cross Section Through Yucca Flat (U. S. Geological Survey).

43

Figure 4.33. Yucca Fault and Area 3 Fault and Locations of Events That Caused Known
Movement Along Them.

44

Yucca Flat Faults

Yucca Flat is a 10- by 20-mile area covered with alluvium. Tertiary tuff underlies the alluvium, and the tuff is underlain by carbonates. The valley is surrounded by hills of tuff which are underlain by pre-Tertiary sediments and intrusives.
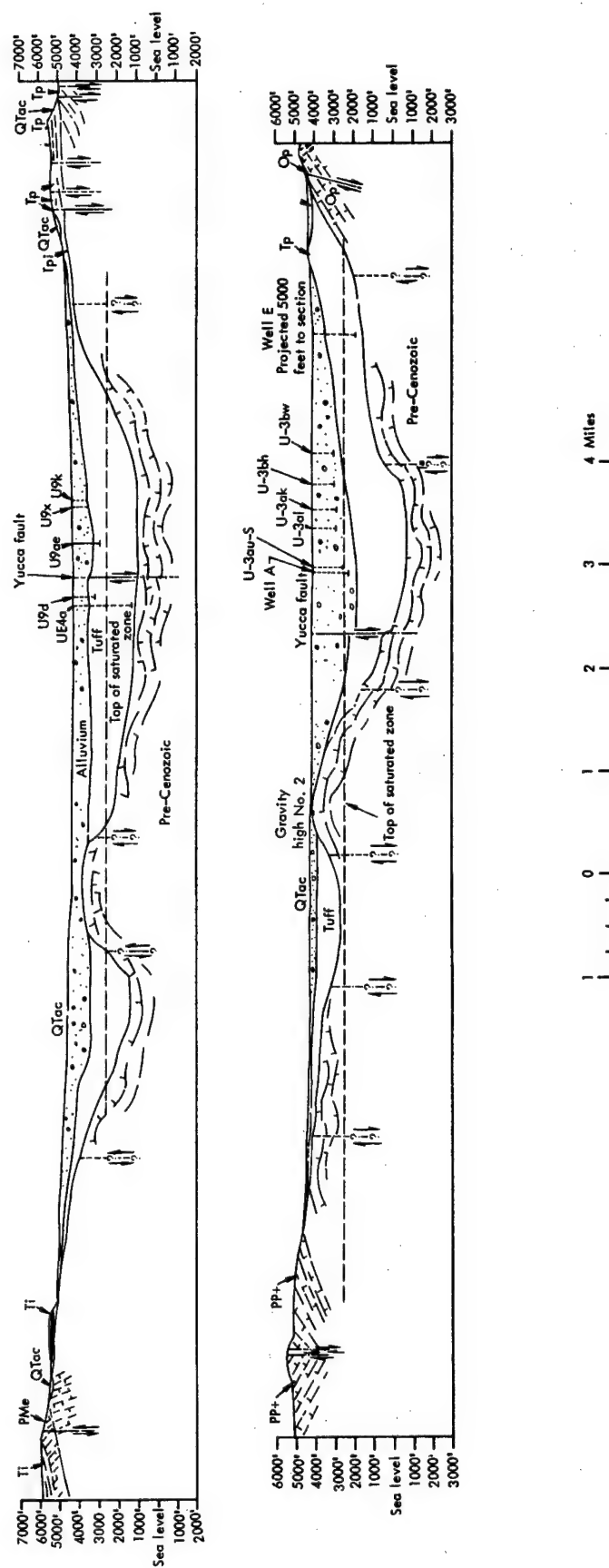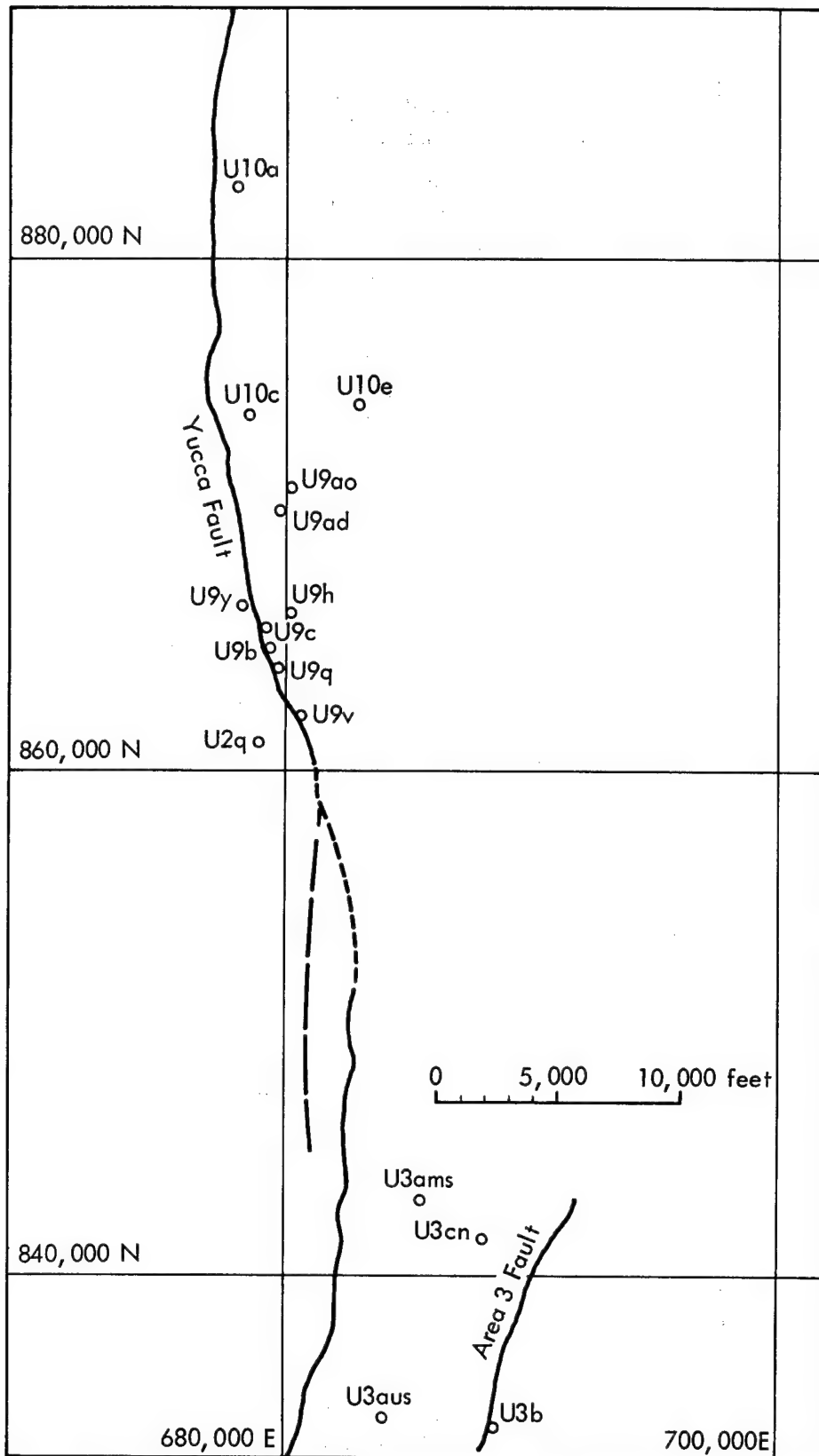
Two typical cross sections through the valley are shown in Figure 4.32. The unconformable relation of the alluvium resting on the tuff, which in turn rests on the pre-Tertiary rocks, is clearly seen.

Motion Studies

1962 to 1968

During the period of 1962 to 1968, the U. S. Geological Survey studied the motion of faults in Yucca Flat as a result of nuclear tests by examining surface areas adjacent to ground zero before and after the tests. The two predominant sensitive faults in Yucca Flat are the Yucca Fault and the Area 3 Fault (Figure 4.33). The Yucca Fault extends north and south probably the whole length of the valley. In its northern extension, the surface expression is a 20-ft escarpment in alluvium.

The vertical displacement on the east is 100 ft in tuff. The downthrown side in both instances is on the east. The Area 3 Fault trends approximately 10° east and is about 2 miles east of the Yucca Fault in the middle of the valley. There is little surface expression of this fault.

Dickey[21] reports that faulting on the Yucca Fault and Area 3 Fault due to nuclear explosions is expressed as small vertical displacements, perhaps several inches, or as cracking extending for thousands of feet, with no vertical displacement.

Table IV summarizes significant data on the effects of 16 shots fired in the vicinity of these faults. Among the 16 events instrumented, fault motion was observed in 11; of these 11, one vented. Visible ground heaving was observed on two events, Sacramento and Bilby. While only one of the 11 events showing fault motion vented, there were two out of the total of 16 events that showed dynamic venting associated with ground fissures which apparently intersected surface ground zero, the emplacement hole, or the working point. In addition, one event showed late-time seepage.

TABLE IV. CHARACTERISTICS OF 16 EVENTS IN THE VICINITY OF YUCCA FAULT AND AREA 3 FAULT

Event	Site	Yield (kt)	Contact[a] depth (ft)	Depth (ft)	Radius (ft)	Volume (10^3 cu. yards)	Collapse time (min)	Remarks
1. Yucca Fault								
Stillwater	U9c	2.8 ± 0.3	1250 A-T	40.0	206	53.4	9.0	No vent; fault motion
Cimarron	U9h	11.9 ± 0.2	1210 A-T	36.0	259	67.5	44.0	No vent; no fault motion
Aardvark	U3ams	38 ± 0.6	>900 A-T 3000 T-P	73.5	479	641.0	105.2	No vent; 18,000 ft of fracturing along fault, 5 in. vertical displacement
White	U9b	Low	1100 A-T	51.0	243	112.9	12.0	No vent; fault motion
Haymaker	U3aus	45.5 ± 1.5	>1520 A-T	108.9	461	914.6	24.88	No vent; fault motion
Sacramento	U9v	Low	>1000 A-T	70.0	225	87.0	6.0	Visible ground heaving
Wichita	U9y	Low	1500 A-T	58.0	222	61.5	5.35	Vented through fissure 50 ft from GZ; no fault motion
Mississippi	U9ad	Low-intermediate	1435 A-T 3250 T-P	125.0	444	815.7	67.5	Probable fault motion
Bilby	U3cn	~200	850 A-T 2700 T-P	85.6	728	2061	31.0	No vent; 15,000 ft of fracturing along fault; 4 in. vertical displacement; surface heaved ~150 in.
Roanoke	U9q	Low	>1000 A-T	5.0	47.9	0.68	15.0	Seepage around cables; no fault motion
Fore	U9ao	Low-intermediate	1380 A-T 3050 T-P	125.0	463	1451	128.0	No vent; fault motion 3 in. vertical
Klickitat	U10e	Low-intermediate	555 A-T 1950 T-P	122.8	467.5	11.51	78.2	No vent; fault motion
Dub	U10a	Low	1130 A-T	97.0	87.4	83.3	51.0	Fault motion; vertical walls in crater
Turf	U10c	Low-intermediate	1710 A-T	93.0	560	1180	680.0	No vent; fault motion 12 in. vertical
Crepe	U2q	Low-intermediate	1100 A-T 3300 T-P	64.6	350	304	125.0	2 in. vertical motion
2. Area 3 Fault								
Bandicoot	U3bj	Low	1500 A-T	124.5	301	374	5.17	Vented through fissure; small vertical motion
Bilby	U3cn	~200	850 A-T 2700 T-P	85.6	728	2061	31.0	Surface heaved ~150 in.; vertical displacement ~6 in.; 9,000 ft of fracturing along fault

[a] A-T indicates the contact between alluvium and tuff. T-P indicates the contact between tuff and paleozoic rock.

In order to determine the time sequence of motion of the Yucca Fault relative to the detonation of a nuclear explosive, a photographic study of fracturing was conducted as part of the Commodore Event. The significant results of this study are summarized below:

1. Yucca Fault ruptured at about the time of arrival of the first seismic wave, 0.564 sec after detonation. Fault motion lasted for 0.056 sec.

2. Ground motion caused by the seismic wave lasted for about 3 sec. Two distinct phases were associated with this motion. The first, lasting 0.5 sec, had a relative amplitude of 2 in. The second, lasting for approximately 2.35 sec, had a relative amplitude of 11 in.

3. Fracturing around ground zero was strongly oriented to the northeast and originated about 800 ft southeast of ground zero.

4. Radial and concentric fractures were not evident before the collapse over the explosion point.

Agile Event

As of May 27, 1967, the only documented motion on the Yucca Fault occurred in the Agile Event. Here the explosion caused motion on the Yucca Fault as far as 5000 ft northeast and 6000 ft southeast of the site (U2v). The maximum vertical displacement was 0.3 ft.

East Branch of Area 3 Fault and Area 7 Fault

Other sensitive faults in Yucca Flat are the east branch of Area 3 Fault and the Area 7 Fault. The latter, and the two fracture zones west of site U4c,* may be classified as sensitive only on the basis of motion caused by explosions. Evidence for movement in recent geologic history is lacking.

---

*The Zaza Event in site U4c generated two linear-fracture zones 2000 and 2800 ft west of ground zero in addition to the normal fractures expected around ground zero. The significance of these two sets of fractures is that they continue for thousands of feet, far beyond what is normally expected in Yucca Flat. Thus it has been inferred that they represent hidden faults.

Pahute Mesa Faults

The Pahute Mesa area has a thick cover of relatively flat-lying Tertiary volcanic rocks which are locally disturbed by small rhyolite intrusives and cut by numerous northward-trending high-angle faults[22]. The cross section in Figure 4.34 is a few miles north and northeast of the Timber Mountain caldera, and the west end of the cross section extends into the Silent Canyon caldera, where the volcanic sequence is much thicker than to the east.

The Tertiary rocks are assumed to overlie a series of thrust plates composed of uppermost pre-Cambrian to middle Paleozoic sediments which, in turn, unconformably overlie the pre-Cambrian basement complex. The thrust sequence, for the most part, has been projected northwestward from the Yucca Flat area. The Paleozoic rocks are folded where they are exposed at the south end of the Belted Range, and the rock comprising the thrust plates at depth are presumed to be moderately to strongly folded. A general west dip is projected for the thrust plates and assumed for the top of the pre-Cambrian complex. By analogy with other caldera, the Silent Canyon caldera may be underlain by a granite intrusion of similar age.

The fractures resulting from nuclear explosions in Pahute Mesa have been recently reviewed[20]. Most of the fractures opened by the explosives are on or near previously mapped faults. In most instances, the displacements along the explosion-produced fractures are in the same direction as those in the original structures. In some instances, explosion-produced fractures were opened by subsequent explosions. Lateral movement on some of the fractures indicates that a horizontal component of stress is present in the mesa.

The following description is an example of a typical interaction between a nuclear explosion and the Pahute Mesa stratigraphy.

"An intermediate yield explosion at the U19as site... formed numerous small fractures along the cableway, roads, and other ground compacted by man. Fluffed ground and overturned stones were seen as far as 2000 feet from GZ. Thirteen hundred feet northwest of ground zero is a fracture about 1,500 feet long which was opened by the U20g explosion and reopened by the U19as explosion. Maximum displacement was 2 inches down on the northwest. Twenty-five hundred feet farther northwest are three other fractures opened by the U20g event and reopened by the U19as explosion. The only other significant fractures caused by the U19as explosion developed in a northeast-trending zone about 5,000 feet long that passes just east of ground zero."[20]

Figure 4.34. Geological Section from Pahute Mesa East.

Conclusions

From these observations and other studies, we draw the following conclusions:

1. Yucca Fault is more sensitive than the Area 3 Fault, and movement along these faults is not systematic.

2. Yucca Fault motion has occurred most often at scaled distances up to 1000 $W^{1/3}$ ft, Area 3 Fault at distances of up to 500 $W^{1/3}$ ft.

3. Pahute Mesa motion is associated with pre-existing structural discontinuities. The general linear alignment of the extensively long cracks indicates motion on faults which may extend to considerable depths. The likelihood of venting on Pahute Mesa faults is probably of the same order of magnitude as venting on the faults in in Yucca Flat, with which LRL and LASL have had their most extensive experience.

Our current thinking is that faults intersected by expanding cavities are not significant vent paths by the nature of the phenomenology of cavity growth. As soon as the shock vaporizes and melts the rock surrounding the explosive, a liquid seal under megabar pressures closes off the rock from the expanding cavity. Faults of joints which may have extended into the cavity, or lie adjacent to or a short distance from the explosion, are closed as the shock wave moves through the rock and remain closed as the cavity begins to expand into the rock. The "crack" that was part of the fault or joint no longer exists as a crack but rather as a tightly sealed fracture indistinguishable from the rock surrounding it. In some instances, as the rock outside of the cavity begins to unload, pre-existing cracks will begin to open. These cracks will progress back toward the cavity wall, which is now covered with a film of liquid. They may indeed progress through the elastic

Figure 4.35.   Wall of a Tunnel Dug Into the Vicinity of the Cavity of an Underground Nuclear Explosion. The Dark Areas (Arrows) Are Injected Melt That Has Been Quenched in Cracks Within Cold Country Rock.

48

region, through the plastically deformed region, and into the recrystallized zone, and then open into the liquid-melt coating on the cavity wall. Under these circumstances, with the pressure in the cavity greater than the pressure in the crack, melt will be injected into pre-existing cracks or into some randomly generated crack.

It is conceded, therefore, that under certain geologic geometries pre-existing cracks may act as potential sites for deposition of liquid melt. This phenomenon occurs near or at the end of cavity growth, and the crack paths act as surfaces upon which to quench the melt, condense the more refractory materials, and trap the volatiles. This phenomenon, which has been observed in different experiments, is illustrated in Figure 4.35. Injected melt may extend as far as one or two cavity radii into the rock, and then progress no farther. On the other hand, if an expanding cavity is coupled into a poorly stemmed emplacement hole or instrument hole, then the large-diameter hole may offer no resistance to the expanding cavity and may indeed permit venting to occur. In particular, if a hole is only partially stemmed and is intersected some distance above the working point by a joint or fault, then the combination of poor stemming and the presence of a fault or crack can afford a venting path to the material coming from the expanding cavity.

Our policy is to stem all emplacement holes and satellite holes adequately and carefully. Further, it is our policy to avoid emplacement on or immediately adjacent to known faults. We feel, however, that faults adjacent to the device are not important vent paths. Faults intersecting poorly stemmed holes may act as vent paths.

ACKNOWLEDGMENTS

REFERENCES

1. J. T. Cherry and W. R. Hurdlow, "Numerical Simulation of Seismic Disturbances," Geophysics 31, 33, 1966

2. G. Maenchen and S. Sack, "The TENSOR Code," Lawrence Radiation Laboratory, Livermore, Report UCRL-7316, 1963

3. J. T. Cherry, "Computer Calculations of Explosion-Produced Craters," Int. J. Rock Mech. Min. Sci. 4, 1, 1967

4. T. R. Butkovich, "The Gas Equation of State for Natural Materials," Lawrence Radiation Laboratory, Livermore, Report UCRL-14729, 1967

5. E. G. Rapp, Lawrence Radiation Laboratory, Livermore, Personal Communication

6. J. T. Cherry, D. B. Larson, and E. G. Rapp, "A Unique Description of the Failure of a Brittle Material," Lawrence Radiation Laboratory, Livermore, Report UCRL-70617, 1967

7. J. G. Ramsay, "Folding and Fracturing of Rocks," McGraw-Hill, New York, 1967

8. J. T. Cherry and E. G. Rapp, "Calculation of Free-Field Motion for the Piledriver Event," Lawrence Radiation Laboratory, Livermore, Report UCRL-50373, 1968

9. C. R. Boardman, "Results of an Exploration into the Top of the Piledriver Chimney," Lawrence Radiation Laboratory, Livermore, Report UCRL-50385, 1967

10. J. Schlocker, "Petrology and Minerology of Tatum Salt Dome, Lamar County, Mississippi," U. S. Department of the Interior, Tech. Letter: Dribble-28, 1963

11. L. A. Rogers, "Free-Field Motion Near a Nuclear Explosion in Salt: Project Salmon," J. Geophys. Res. 71, 3415, 1966

12. R. L. Braun, J. S. Kahn, and S. Weissmann, "X-Ray Diffraction Analysis of Plastic Deformation in the Salmon Event," Lawrence Radiation Laboratory, Livermore, Report UCRL-71249, 1968

13. J. T. Cherry, D. B. Larson, and E. G. Rapp, "Computer Calculations of the Gasbuggy Event," Lawrence Radiation Laboratory, Livermore, Report UCRL-50419, 1968

14. J. A. Korver and D. E. Rawson, "Gasbuggy Post-shot Investigations in GB-ER," Lawrence Radiation Laboratory, Livermore, Report UCRL-50425, 1968

15. C. E. Chapin, Lawrence Radiation Laboratory, Livermore, Personal Communication, 1968

16. A. L. Edwards, "TRUMP: A Computer Program for Transient and Steady State Temperature Distributions in Multidimensional Systems," Lawrence Radiation Laboratory, Livermore, Report UCRL-14754 Rev. 1, 1968

17. C. W. Olsen, "Time History of the Cavity Pressure and Temperature Following a Nuclear Detonation in Alluvium," J. Geophys. Res. 72, 5037, 1967

18. H. Rodean, Lawrence Radiation Laboratory, Livermore, Personal Communication

19. F. W. Aron, Lawrence Radiation Laboratory, Livermore, Personal Communication

20. D. D. Dickey and W. L. Ellis, "Principle Linear Fractures Resulting from Nuclear Explosions in Pahute Mesa," U. S. Geological Survey, Tech. Letter: Special Studies 67, 1968

21. D. D. Dickey, U. S. Geological Survey, 1968, Fault Displacement as a Result of Underground Nuclear Explosions; GSA Memoir 110

22. P. J. Barosh, "Preliminary Geologic Section from Pahute Mesa, Nevada Test Site, to Enterprise, Utah," U. S. Geological Survey, Tech. Letter: Interagency Report NTS-1, 1967

Chapter 5

GEOLOGIC CONSIDERATIONS

Frank W. Stead, *Research Geologist*
U.S. Geological Survey, Denver, Colorado

INTRODUCTION

The Geological Survey is the principal geological organization in the Federal Government with broad responsibilities for the protection and development of the mineral and water resources of Federal and Indian lands. The Survey is primarily a scientific investigative agency, and is only in minor part a regulatory agency.

On behalf of the Atomic Energy Commission, it is the responsibility of the Geological Survey to provide and to recommend the types and kinds of geologic, geophysical, and hydrologic information needed to evaluate the safety aspects of nuclear test explosions. As all present testing of nuclear devices is conducted underground in a particular geologic environment, it is imperative that we have, prior to testing, a reasonably complete understanding of each particular geologic environment.

Most of the geologic information that must be provided falls in the category of background information which is needed by other safety contractors for interpretation and evaluation in terms of specific safety criteria established by the Atomic Energy Commission. Only occasionally does geologic information bear directly on safety criteria; for example, a major fault or joint system, connecting the proposed point of an underground nuclear explosion with the surface, would suggest the possibility of undesirable release of radioactivity to the atmosphere.

Uses of Geologic Information

In considerations of the safety of detonating nuclear explosives, geologic information is essentially restricted in use: first, to potential contamination by radionuclides of ground and surface water resources and other natural resources; second, to potential damage by ground motion to man-made and natural structures and to natural resources, particularly water supplies; and third, to the proposed degree of containment of a nuclear explosion. Geologic information, in general, is not directly applicable to considerations of radioactive fallout and air blast from cratering explosions, except insofar as the degree of containment of nuclear explosion might vary beyond acceptable limits where an unfavorable geologic setting has been overlooked.

Types of Information

The four scientific divisions of the Geological Survey conduct specialized research as briefly outlined by the following chart to provide various types of information for the technical divisions of the Atomic Energy Commission. Much of this work is interrelated and contributes to public health and safety.

TOPOGRAPHIC DIVISION	GEOLOGIC DIVISION	WATER RESOURCES DIVISION	CONSERVATION DIVISION
Maps the physical features of the nation.	Maps the geology of the nation and appraises its mineral, mineral fuel, and land resources.	Appraises the nation's water resources and does related research.	Classifies Federal lands as to water power and mineral values, supervises development and production of such minerals under appropriate leases

AEC ORGANIZATION

TYPES OF SPECIALIZED RESEARCH CONDUCTED BY GEOLOGICAL SURVEY

DIVISION OF REACTOR DEVELOPMENT ———————— RADIOACTIVE WASTE DISPOSAL STUDIES

DIVISION OF RESEARCH ——————————— GEOCHEMICAL AND GEOPHYSICAL RESEARCH

DIVISION OF BIOLOGY AND MEDICINE ———————— BIOENVIRONMENTAL STUDIES

DIVISION OF RAW MATERIALS ————————————— URANIUM & THORIUM RESOURCES

DIVISION OF MILITARY APPLICATIONS (NVOO) ——— PROVISION AND EVALUATION OF DATA

DIVISION OF PEACEFUL NUCLEAR EXPLOSIONS (SAN) —————————— SPECIAL STUDIES

The Topographic Division provides 90 percent of the general purpose topographic maps of the United States. Presently, only two-thirds of the country is covered by adequate 1 mile to the inch or larger scale maps.

The Geologic Division provides both general purpose geologic maps and specialized geologic maps. Presently less than 20 percent of the United States has adequate geologic map coverage at a scale of 1 mile to the inch, and less than 40 percent has coverage at a scale of 4 miles to the inch. Quite obviously, we do not always have adequate topographic and geologic maps of areas of interest to the Atomic Energy Commission.
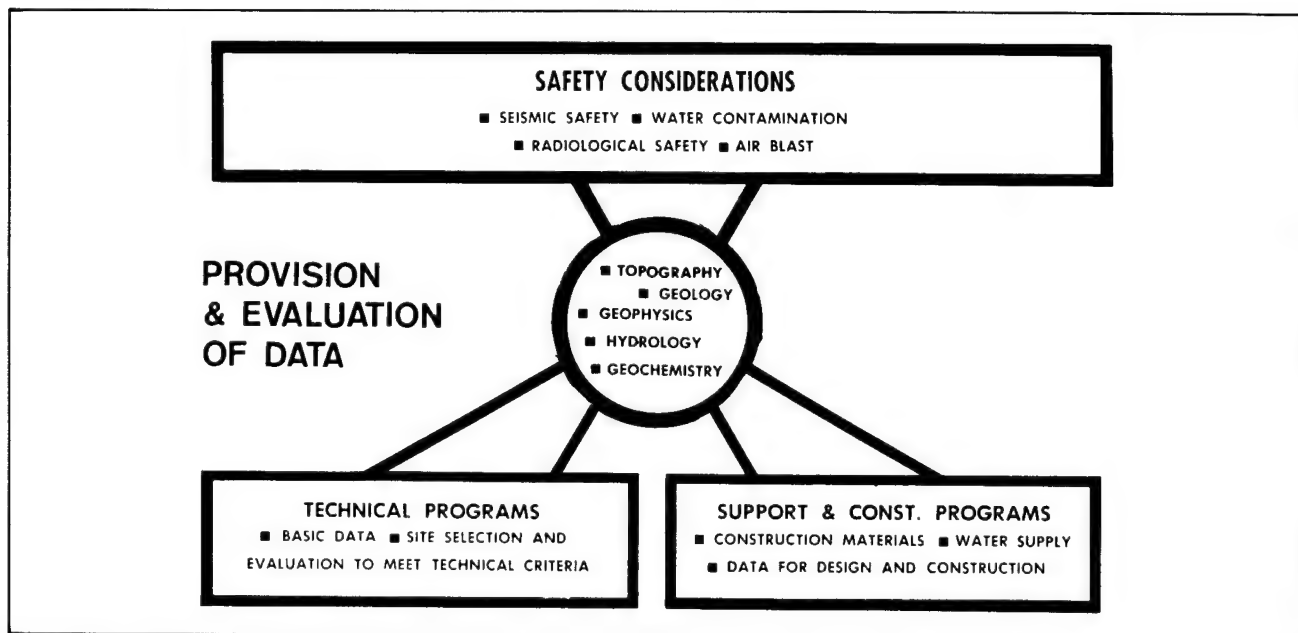
The Water Resources Division provides data on the occurrence, quality, and quantity of ground and surface waters, again with the better and adequate coverage in the more populated and industrialized areas, and with scanty coverage in the less populated and desert areas of the western states.

The Conservation Division provides considerable geologic data on federal lands. By law, agencies conducting mineral, oil, and gas operations on leased public lands must provide to the Geological Survey any requested geologic information.

Applications of Geologic Information

The information provided by the Geological Survey is fitted to the needs of the Atomic Energy Commission programs related both to the testing of nuclear weapon devices and to the peaceful use of nuclear explosives. As shown by the following chart, the provision and evaluation of topographic, geologic, and hydrologic data have multiple uses.

SAFETY CONSIDERATIONS
■ SEISMIC SAFETY ■ WATER CONTAMINATION
■ RADIOLOGICAL SAFETY ■ AIR BLAST

PROVISION & EVALUATION OF DATA

■ TOPOGRAPHY
■ GEOLOGY
■ GEOPHYSICS
■ HYDROLOGY
■ GEOCHEMISTRY

TECHNICAL PROGRAMS
■ BASIC DATA ■ SITE SELECTION AND EVALUATION TO MEET TECHNICAL CRITERIA

SUPPORT & CONST. PROGRAMS
■ CONSTRUCTION MATERIALS ■ WATER SUPPLY
■ DATA FOR DESIGN AND CONSTRUCTION

For example, under technical programs conducted by Los Alamos Scientific Laboratory, the Lawrence Radiation Laboratory, the Defense Atomic Support Agency, and other groups, the water content of the rock in the immediate vicinity of the nuclear explosion is needed to calculate the interactions between the explosion and the surrounding medium. Under support and construction programs, the volume and chemical quality of water available for domestic and construction activities are needed; also required would be the volume of water to be handled in design and construction of holes and shafts for deep device-emplacement. For safety considerations, the volume of water likely to be initially contaminated, and the probable rate and direction of movement of such contaminated water must be assessed. Thus, knowledge of the volume of water, and its mobility at the site of any proposed underground nuclear explosion is required for a variety of purposes.

SAFETY CONSIDERATIONS

Safety considerations require detailed geologic information for studies involving seismic safety and water contamination; less detailed geologic data are needed in radiological and air blast safety studies.

Geologic Environment, Nevada Test Site

A block diagram of Yucca Flat as shown in Figure 5.1 illustrates some of the regional geologic data needed. Rainier Mesa, where the first nuclear explosions in tunnels were detonated, is at the northwest corner of the block. The small granite mass in which two
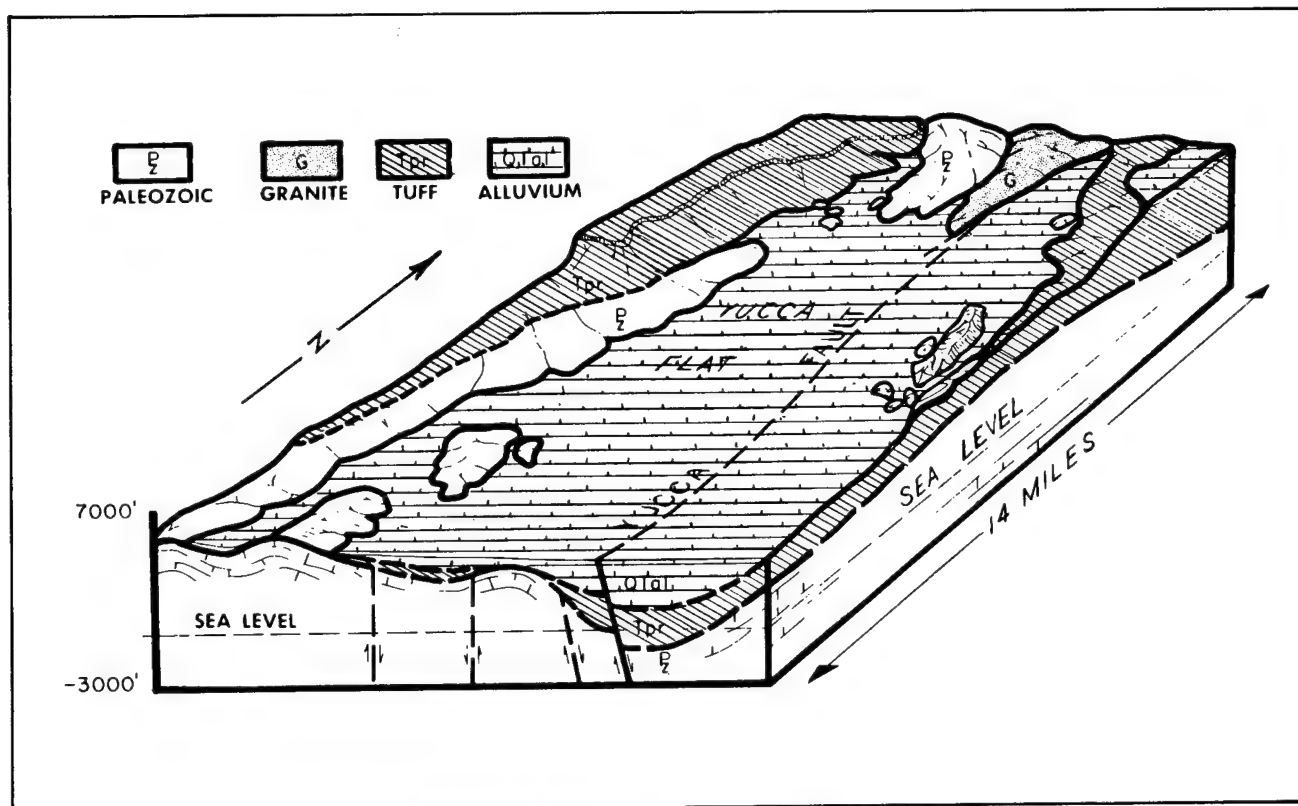
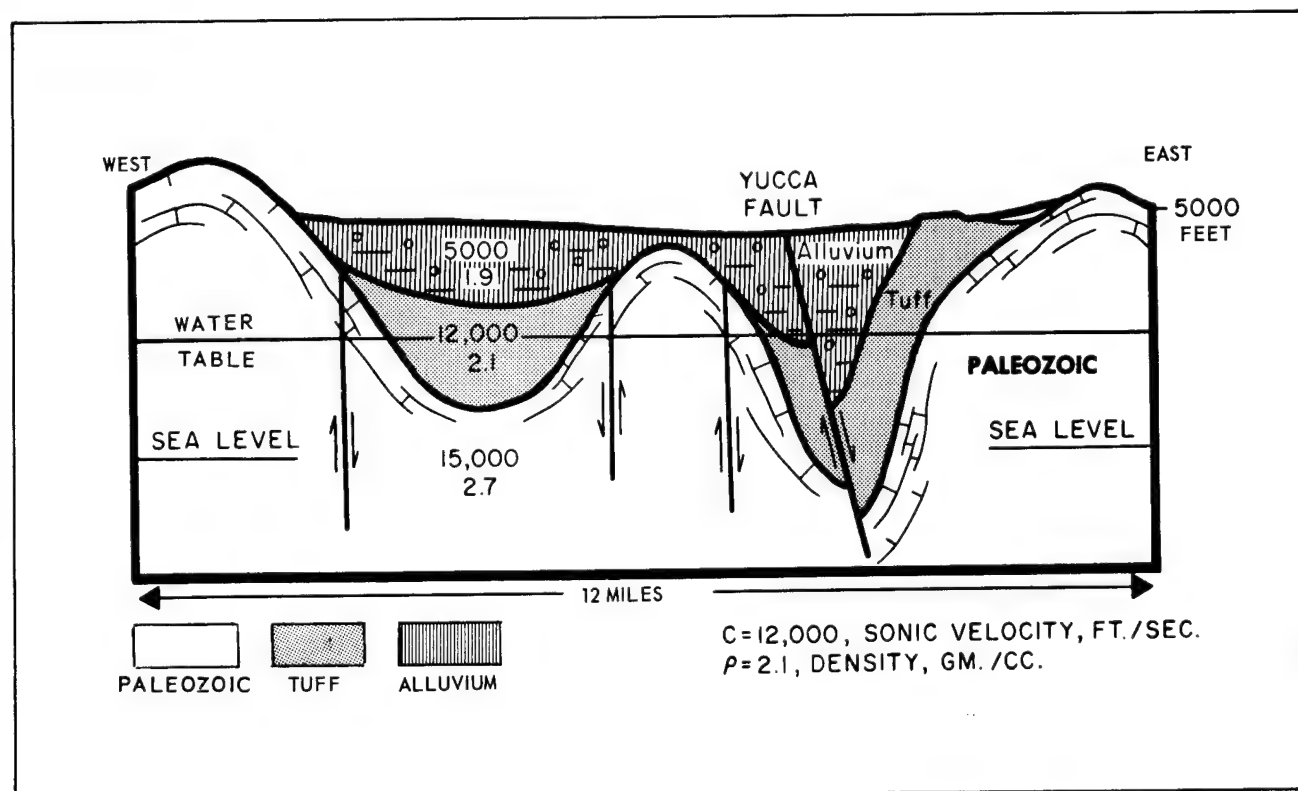Figure 5.1.   Block Diagram of Yucca Flat, Nevada Test Site.

Figure 5.2.   Diagrammatic Section Through Central Yucca Flat, Nevada Test Site.

53

nuclear devices have been detonated at a depth of about 1,000 feet is shown in the north-central part of the block. Many of the recent underground nuclear explosions have been detonated in deep drill holes in Yucca Flat proper.

The three major rock types — alluvium, volcanic tuff, and basement rocks of Paleozoic age — are shown. Most of the area of Yucca Flat is blanketed by a variable thickness of alluvium, that is, recent sands and gravels up to 2,000 feet thick. This alluvium effectively conceals the underlying volcanic tuffs and lava flows; it also conceals the still older Paleozoic rocks such as dolomites, shales, and quartzites.

In addition to adequate topographic maps — which tell us where we are — and accompanying geologic maps — which tell us what's there — hydrologic safety and other technical considerations require more specific information, such as, first, the configuration of the rocks to considerable depth, including the thickness of the rock units, their depth below the surface, and their structural attitude; second, the planes of weakness in the rocks such as faults, joints, and cooling cracks; third, the detailed physical and chemical properties of the rocks, such as porosity, permeability, and mineralogy, and more importantly the spatial variation of these properties; and fourth, the amount and location of water in the rocks, particularly the position of the water table below which rocks are water saturated.

Bearing on seismic safety considerations, we are particularly interested in the spatial distribution of the rock types and the variations in the physical properties of these rocks. In particular, the location and orientation of faults or breakage planes in the rocks are important.

For example, some of the faults shown on the front face of the block diagram break through and offset only the older Paleozoic rocks and have no effect on the overlying younger rocks. The major Yucca Fault, along which very recent movements have occurred, clearly breaks through and offsets all the rocks. At the north edge of the block, the Yucca Fault cuts through the small granite mass, in which two nuclear devices have been detonated at a depth of about 1,000 feet. To the east of the fault, the granite is concealed by the alluvium, and is naturally downdropped at least 1,000 feet, possibly several thousand feet. For an underground nuclear explosion such as the Hardhat event, detonated in the granite mass at about the Point "G," the seismic energy moving outward from the point of explosion would be distorted by the asymmetry of the geologic environment. To the east, the seismic energy would initially propagate outward through a considerable thickness of alluvium and tuff;

to the west, the energy would move through Paleozoic rocks with markedly different physical properties.

Data normally required for safety considerations are shown on the diagrammatic section through Yucca Flat in Figure 5.2. First, bearing on water contamination consideration, the water table is shown at about 2,400 feet above sea level and about 1,600 feet below the land surface, which is at 4,000 feet above sea level. The important fact is that the water table is essentially flat and does not tend to follow the ground surface, the normal behavior of the water table in most environments. We have enough deep test drilling at the Nevada Test Site to confirm this somewhat unusual behavior of the water table. You will note that under the ridges to the east and west of Yucca Flat the ground water table is in the Paleozoic rocks, where the ground water flow is through dolomite or limestone characterized by numerous fractures.

Second, bearing on seismic safety considerations, shown for each of the rock types are their sonic velocities and densities. These background data are required input for the U.S. Geological Survey and other safety contractors to calculate the transmission of seismic energy, the resultant ground motion, and the possibility of structural damage.

You will note that the densities of the alluvium and the tuff are about the same, and are in marked contrast to the much higher density of the underlying Paleozoic rocks. This density contrast permits us to interpret the depth to the older Paleozoic rocks from surface gravity data. For example, the buried ridge of Paleozoic rock immediately to the west of the Yucca Fault was predicted on the basis of a gravity survey, and was confirmed by a shallow drill hole which penetrated Paleozoic dolomite at a depth of 100 feet.

Dependent on the point of an underground explosion, the ground motion and the possibility of structural damage might be much different over such a buried ridge of dense, high velocity rock than it would be over a deep trough filled with alluvium and tuff. Thus, it follows that the geologic character of the site of any structure near a major explosion must be provided in reasonable detail, and not broadly generalized.

Although gravity and seismic survey methods can be used successfully in many areas, it is imperative that some knowledge of the density and velocity distribution with increasing depth is in hand; otherwise, the interpretation of the raw geophysical data must assume a density and velocity distribution. It follows that in new or complex areas, a few deep exploratory drill holes are needed.

Surface Fractures, Yucca Flat

Moving closer to the point of explosion, shown in Figure 5.3 are some of the postexplosion effects and their relation to geologic structure. The natural faults, with observable surface expression, are shown in solid black lines. Concealed faults, inferred from geophysical methods, are shown by dotted lines. Explosion-produced fractures, observable at the surface, are shown by dashed lines.

It will be noted that the explosion-produced fractures tend to coincide with the preexisting fractures, suggesting the possibility of renewed movement or differential compaction along the old fault planes.

Of more interest, the Bandicoot event, an underground explosion conducted on October 19, 1962, located almost on the subsurface fault inferred from geophysical data, vented to the atmosphere. This illustrates a major requirement in evaluating the possibility of venting, that is, the provision of the best possible three-dimensional interpretation of faults, joints, and other planes of structural weakness in the rocks around a proposed underground nuclear explosion. Such data are needed out to a radius of a few thousand feet from the explosion, and to a depth at least equivalent to the depth of burst.

Geologic Section, Areas 19 and 20, Nevada Test Site

Pahute Mesa, the northwest portion of the NTS, is the area in which tests have been conducted to a depth of about 4,600 feet. Two vertical sections as shown in Figure 5.4 illustrate the complexity of the volcanic rocks at depth and the numerous faults characteristic of basin and range structure. This interpretation is based on one deep small diameter, exploratory drill hole, in excess of 13,000 feet, and on several dozen other exploratory drill holes in excess of 5,000 feet.

Although some of the rock units can be projected into this area from adjacent areas where they can be observed and geologically mapped, volcanic rock units such as lava flows are not uniform in thickness or composition over any significant distance and are more difficult to map accurately. Additionally, the velocity and density contrast among the various rock units is small. This lack of contrast sharply reduces the effectiveness of present geophysical methods, such as gravity and seismic surveys for defining rock type and structure at depths from 1 to 2 miles.

All information, no matter how indirect, from each of the exploratory drill holes must be used in our interpretation of the geologic setting at depth.

Favorable Areas For Test, Areas 19 and 20, Nevada Test Site

Figure 5.5 is an example of an interpretive map of Areas 19 and 20, Pahute Mesa, showing favorable areas from which sites for underground testing of intermediate and low-megaton nuclear devices are selected; such maps are modified as new information at depth becomes available and as requirements change. This map combines and interprets data from surface geologic mapping, drill hole sample data, hydraulic pumping tests, the chemical composition and quantity of water at depth, and surface and in-hole geophysical surveys.

Two types of emplacement sites for nuclear tests are desired: (1) in chambers mined at or near the bottom of a large diameter drill hole, and (2) in cased and uncased large diameter drill holes. Areas are designated as: (1) favorable for chambered sites—where the rock types at depths between 2,000 and 5,000 feet below the surface have low transmissibility for water, which is a construction safety consideration; (2) favorable for cased and uncased sites—where the amount of ground water is not a limiting construction consideration; and (3) unfavorable for any site—where the topography is too rugged for construction. Also each proposed emplacement site is evaluated for its proximity to geologically recent faults and fractures.

As shown, approximately 90 percent of the Pahute Mesa is favorable for cased and uncased sites, but less is favorable for chambered sites. The actual acceptability of a proposed site is confirmed by data from one or more exploratory drill holes.

Project Dribble, Velocity Sections

Figure 5.6 is the Project Dribble site in southern Mississippi showing the location of velocity sections radiating out from the Tatum salt dome in which the two nuclear explosions have occurred. In this case, the velocity sections serve a twofold purpose: first, to provide data for seismic safety considerations, that is, for predicting ground motion; and second, to characterize the symmetry of the environment as needed input for the long-distance seismic detection studies under the Vela program.

Fortunately, this area of several thousand square miles has numerous deep oil-exploratory drill holes, shown by the black dots; these drill holes provided extensive data at depth on the structure, stratigraphy, the physical properties of the rock units, and the location and amount of fresh water, saline water, oil, and natural gas.
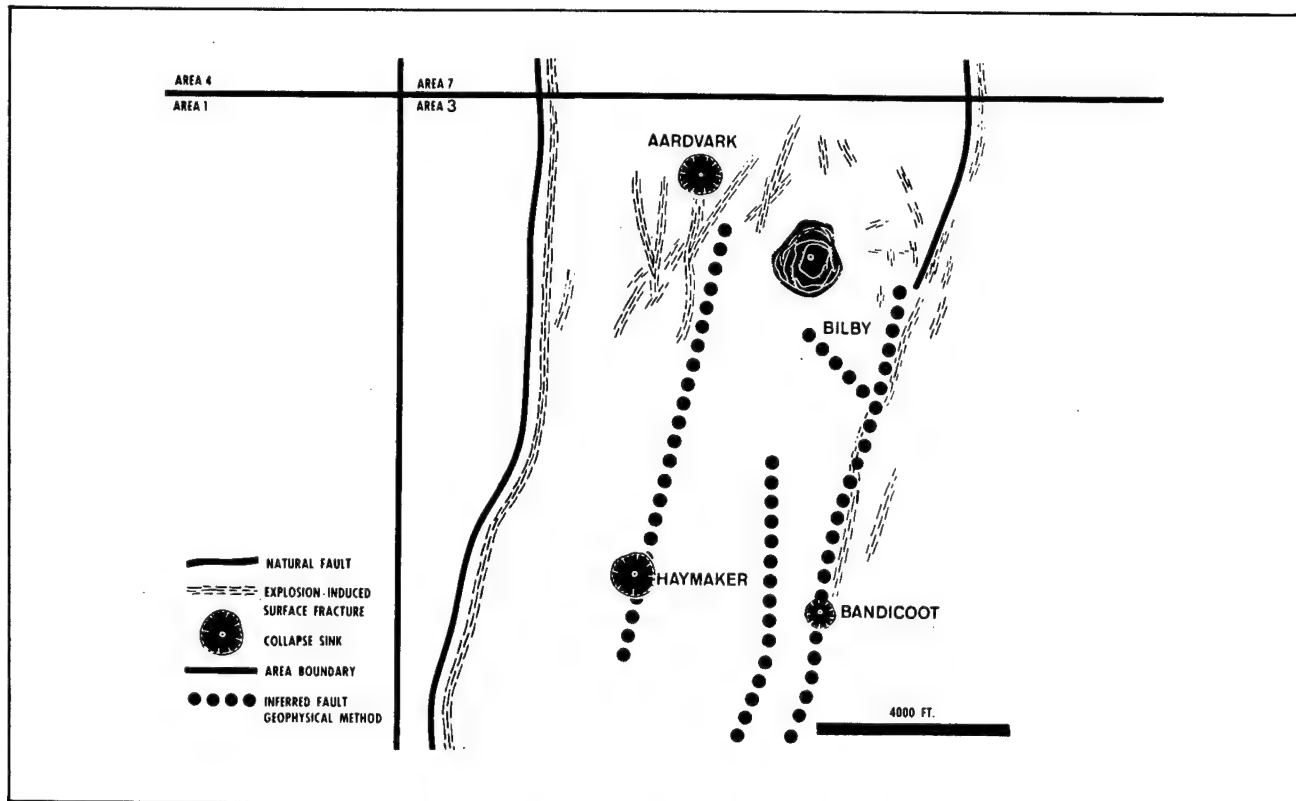
Figure 5.3. Surface Fractures in Yucca Flat Since Bilby Event.
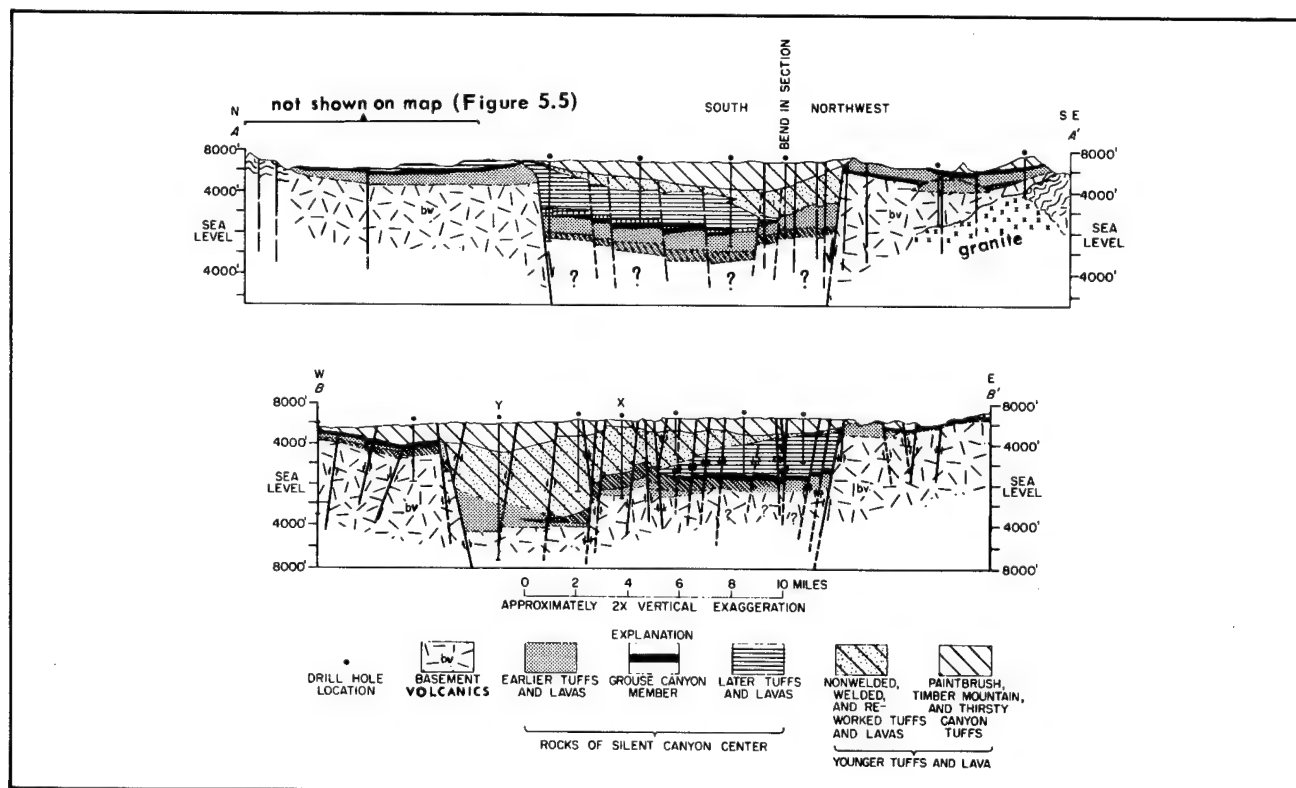

Figure 5.4.   Geologic Sections, Pahute Mesa, Nevada Test Site.
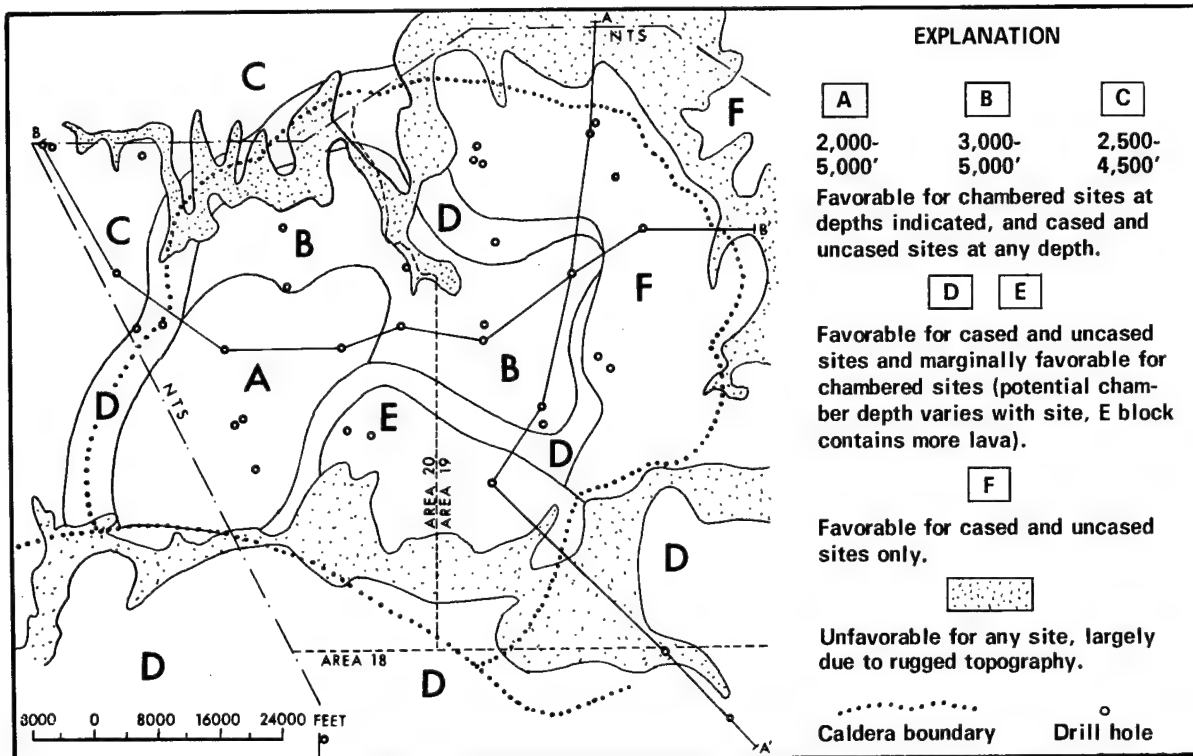
56

Figure 5.5. Favorable Areas for Test Sites in Areas 19 and 20, Pahute Mesa, Nevada Test Site.
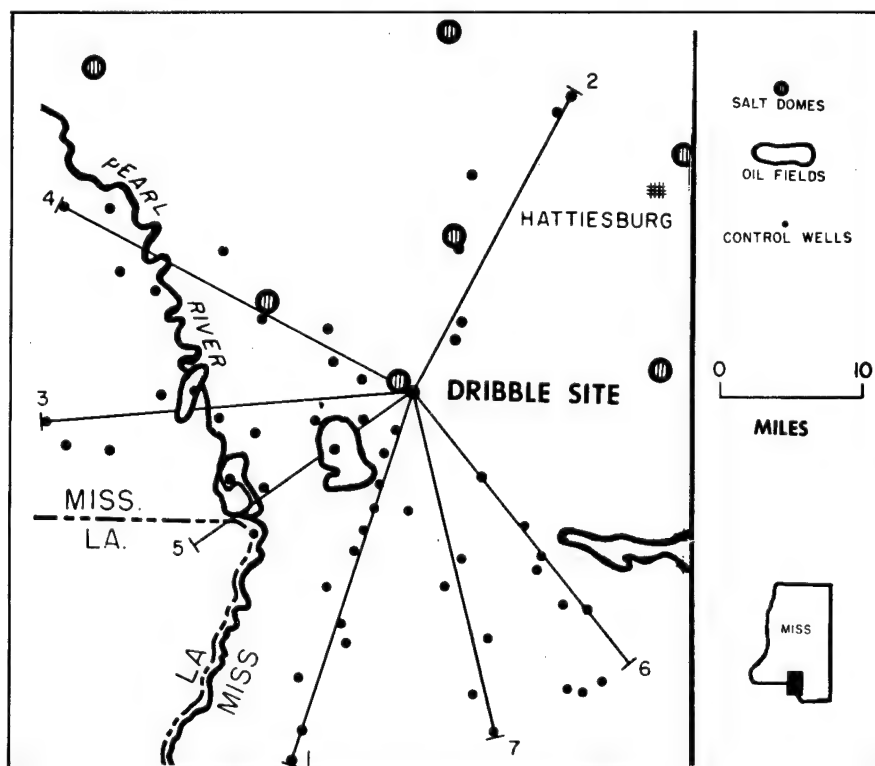

Figure 5.6. Project Dribble, Location of Velocity Sections.

Project Dribble, Section No. 7

Section No. 7 as shown in Figure 5.7 is 24 miles long and about 2 miles deep; it is typical of the eight velocity sections prepared for Project Dribble. The primary control data for this section came from the three exploratory drill holes whose location and total depth are indicated on the section; secondary data came from nine additional drill holes.

Geologically, this section shows part of a deep sedimentary basin, probably in excess of 30,000 feet to the underlying crystalline rocks. The sedimentary rocks in this basin are characterized by relative uniformity over long distances and by essentially no major faults, in marked contrast to the complex stratigraphy and structure of the volcanic rocks at the Nevada Test Site.

Only the continuous high-velocity zones, greater than 10,000 feet per second, and continuous low-velocity zones, less than 10,000 feet per second, are shown on the section. The zones not so indicated have variable sonic velocities and densities; that is, the velocity in a particular sedimentary bed or unit varies from high to low between adjacent drill holes.

Surface Water Safety Considerations

Illustrated in Figure 5.8 is a surface water problem, where fallout from a large nuclear cratering explosion might lead to contamination of surface water supplies.

In such a case, the fallout pattern and radionuclide concentration on the ground must be accepted as input data. The problem is then to select and to provide the geologic and hydrologic data needed to evaluate the potential contamination of surface water. As summarized in Figure 5.8, some of the data needed by other safety contractors over an area of several thousand square miles are: first, rainfall, runoff, and stream flow; second, the suspended sediments, dissolved solids, and chemical composition for the surface water; third, the variations in stream bed characteristics such as bare rock, mud, and sand; fourth, the character of the land surface; and last, the distribution coefficients for various radionuclides for the whole and parts of the system.

Here again, to confirm theoretical calculations, we have conducted extensive field tests, using fallout material from the Nevada Test Site and also known amounts of radioactive cesium, strontium, and iodine. Risking some broad generalizations, two distinct phases of potential water contamination can be discriminated; first, contaminating effects that are due to fallout directly on open-water surfaces with the radionuclides partitioned between the water and solid phases in accordance with the distribution coefficients for the system; this results in a wave of radionuclide concentration moving downstream with reasonably calculable attenuation and duration; second, after the initial wave, further potential contamination depends on actual movement of radioactive particulates to the streams; that is, on the rate of erosion of the surface on which the fallout is deposited.

Bearing on geologic data, we must provide a better characterization of the land surface than is provided by normal geologic mapping — that is — we must discriminate bare soil, bare rock, and vegetated areas together with their geochemical and physical properties. Bearing on hydrologic data we must provide more information on the stream bed than is normally obtained in conventional stream gauging and water sampling.

SUMMARY

In summary, we have reviewed the geologic and hydrologic information needed to evaluate specific safety criteria established by the Atomic Energy Commission. As demonstrated by the examples shown, the geologic and hydrologic environment of each proposed underground nuclear explosion tends to be quite different and must be determined on an individual basis. We cannot generalize with sufficient accuracy the properties of a new site environment where information at depth is lacking. In some areas, such as southern Mississippi, considerable geologic information at depth is already available because of previous petroleum and mining industry activities; in other areas, little, if any, information at depth is available, which would necessitate rather extensive geologic exploration at a proposed site.

The limitations on obtaining adequate geologic information at depths such as 1 or 2 miles are primarily economic rather than technical. Given sufficient funds for deep-hole exploration, the environment of any proposed site of an underground nuclear explosion can be determined within a predetermined accuracy.

Potential water contamination is long term and can extend over many years, while seismic effects are in essence immediate at the time of explosion. It follows that all geologic information, possibly useful to other safety contractors in evaluating and predicting seismic damage, must be acquired well in advance of a proposed explosion.
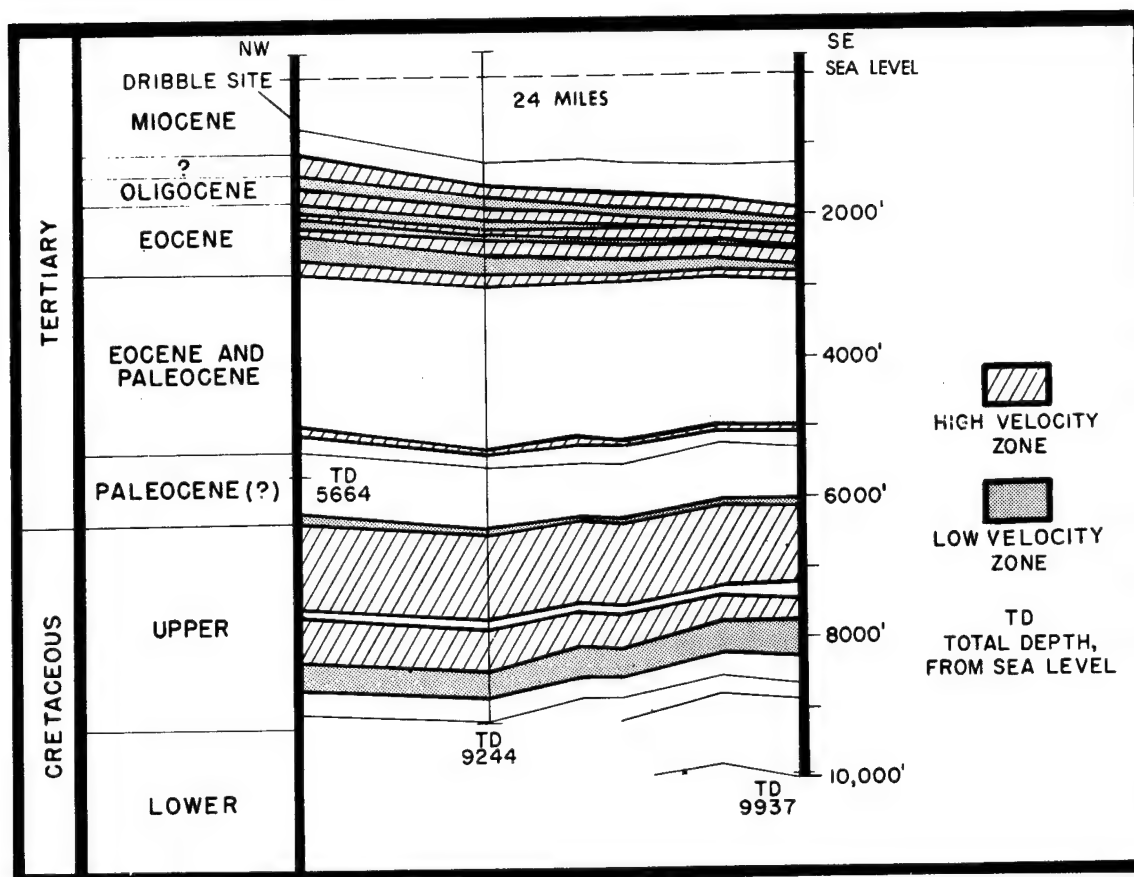
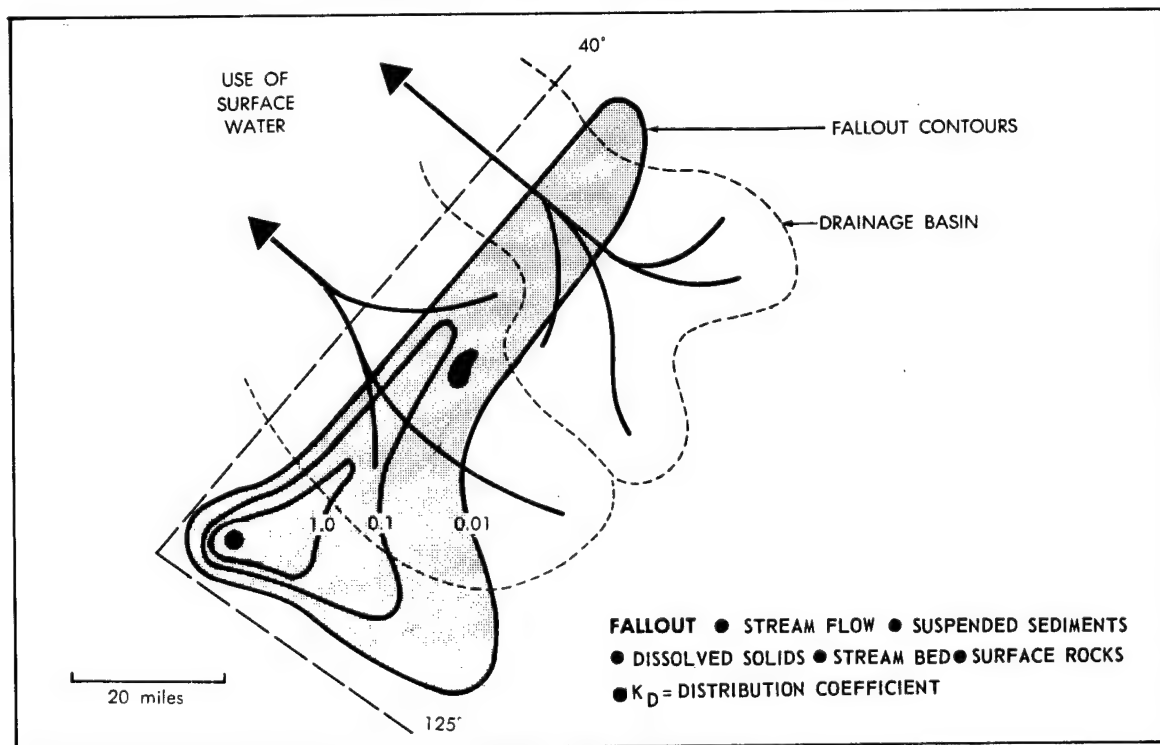Figure 5.7. Stratigraphic and Velocity Cross-Section No. 7. Project Dribble.

Figure 5.8. Surface Water Considerations.

Chapter 6

HYDROLOGIC CONSIDERATIONS

Samuel W. West, *Research Hydrologist* and David B. Grove, *Chemical Engineer*
U.S. Geological Survey, Denver, Colorado

INTRODUCTION

All underground nuclear explosions add some quantity of radioactive material to underground water, either directly by explosion in the zone of saturation or indirectly by water percolating downward through the zone of aeration. In either case, ground water is the transport vehicle in movement of radionuclides underground.

The purpose of hydrologic studies by the U. S. Geological Survey in support of underground nuclear testing is to provide data on the occurrence, quality, and quantity of ground and surface waters that might be affected by the testing. These types of data provide a basis for assuring the public that (1) radioactive pollution of water resources will be limited to a minimum area, (2) the areal distribution of radioactivity in water will be known at all times to prevent inadvertent use of polluted water, (3) adequate supplies of water for local needs will be available after nuclear testing, and (4) well and spring damage will be minimized.

In addition to data collection responsibility in the safety program, the Geological Survey supplies hydraulic engineering support to the construction program of the nuclear test program. Data from these studies supplement the data for safety evaluation.

METHODS AND RESULTS OF STUDIES

The hydrologic studies are divided into regional studies, site studies, and special studies. The regional studies are designed to provide definition of principle aquifers, ground water flow patterns from recharge areas to discharge areas, changes in quality of ground water as it moves through the geologic environment, and the relationship of ground water to surface flow.

The site studies are designed to define hydraulic properties of rocks in the immediate vicinity of nuclear emplacement sites in order to predict the rate of water inflow to the rubble chimney and the capacity of ground water to affect initial transport of radionuclides away from the rubble chimney. The special studies are designed to explore the mechanics of ground water flow by use of tracers in the natural environment and to study the effects of nuclear explosions on the hydrologic environment and the relationship of induced hydraulic pressures to ground motion.

Regional Hydrology

Available data, such as yields of wells, ground water levels, water temperatures, spring and stream discharge measurements, and chemical analyses of water are compiled. These data, obtained from published literature, the files of State and Federal agencies, and by canvass of individuals and corporations, are then evaluated for completeness. Gaps in the data are filled by field studies, including drilling of deep exploratory holes. Wells and springs within a few miles of a proposed nuclear test site are inspected for preshot condition and are sampled for chemical and radiochemical analyses of the water. The regional hydrologic setting is portrayed on suitable maps.

Nevada Test Site

Figure 5.1, a block diagram of Nevada Test Site, shows the distribution of rock types. Thick accumulations of alluvium of Quaternary and Tertiary age and volcanic rocks of Tertiary age are the principal rocks exposed at the surface. Both have wide variations in permeability, which tend to retard infiltration and deep percolation of water. Figure 5.2, a diagrammatic section through

61

central Yucca Flat, shows that limestone and dolomite underlie the alluvium and tuff beneath much of the test site. These rocks are highly permeable, and they function as a ground water drain beneath a large segment of the test site.

Precipitation at Nevada Test Site is 3 to 8 inches annually. The area is devoid of perennial streams. Only a small part of the precipitation infiltrates the rocks and reaches the zone of saturation. Downward movement of water through alluvium and tuff is extremely slow. As shown in Figure 5.2, the land surface in Yucca Flat is about 4,000 feet above sea level. The water table is approximately 1,600 feet below land surface, at an altitude of almost 2,400 feet above sea level.

Although the alluvium and the volcanic rocks beneath Yucca Flat contain some water, most of the lateral flow from Yucca Flat is in limestone and dolomite. Buried ridges of Paleozoic quartzite and shale having low permeability along the east and west sides of Yucca Flat greatly retard the movement of ground water in those directions.

The present interpretation of the hydrologic setting at the Nevada Test Site is shown on Figure 6.1. Such interpretive information, continually reevaluated as new data becomes available, is needed for evaluating the possibility of water contamination extending beyond the limits of the test site.

Shown on Figure 6.1 are the water level contours expressed in feet above sea level. The surface drainage basins, outlined by dashed lines, are mostly closed basins without surface outlets. Obviously, the position of the water table and the regional movement of ground water are not controlled by the surface drainage pattern. Ground water moves under the high ridges primarily through fractured limestones and dolomites. The direction of ground water movement is indicated by arrows. Ground water from deep below Yucca Flat flows downgradient in a southerly direction, passes under Mercury, and ultimately reaches discharge areas at springs in the Amargosa Desert south of the test site. The distance from Yucca Flat to the discharge areas is about 50 miles. Figure 6.1 in general shows the direction of ground water flow, the hydraulic gradients existing near the Nevada Test Site, and the ground water divide about halfway between Mercury and Las Vegas.

The calculated rate of ground water flow in the carbonate aquifers beneath Yucca Flat, based on transmissivity, hydraulic gradient, and porosity, is in the range of 0.02 to 2.0 feet per day or 7.3 to 730 feet per year, assuming a reasonable range in porosity. Using these calculated velocities as an average, the travel time of ground water from central Yucca Flat to the discharge areas is a minimum of 400 years. However, the velocity may be greater where fracture zones are extensive and where the aquifer narrows beneath the Specter Range just south of the test site.

The velocity of ground water in volcanic rocks of Pahute Mesa has been computed to be 5 to 250 feet per year, based on hydrologic parameters.

Samples of water have been taken for carbon-13 and carbon-14 analyses and age determinations of the water. Preliminary analysis of this data for Nevada Test Site indicates a ground water velocity beneath Yucca Flat of 7 feet per year. As our understanding of the applicability of these data increases, predictions of travel times of ground water will improve.

The velocity of ground water is the maximum rate at which radioactive contaminants can travel in the hydrologic system. Most contaminants move much more slowly than the transporting water.

Inferences on regional flow patterns can be drawn also from the chemical quality of water. Water in the carbonate rocks is a calcium and magnesium bicarbonate type, increasing in total hardness with distance from the recharge area. Water in the volcanic rocks is a sodium bicarbonate type with a high silica content. The dissolved-solids content of water in the volcanic rocks varies less with depth than does the dissolved-solids content of water associated with carbonate rocks. The dissolved-solids content and the chemical composition of water in the valley fill varies with distance from the recharge area and the source of the detritus with which it is reacting.

Figure 6.2 illustrates how these and other generalizations have been useful in determining limits of parts of the flow nets near the Nevada Test Site. This figure is the same base as Figure 6.1 with pie diagram symbols showing concentrations of common ions in ground water. The upper left quadrant of the diagrams portrays the concentration of calcium and magnesium ions in the water. The lower right represents sodium ions; the upper right, bicarbonate and carbonate; and the lower left, chloride and sulfate ions. The radius of the quarter circle is directly proportional to the quantity of the ion represented.
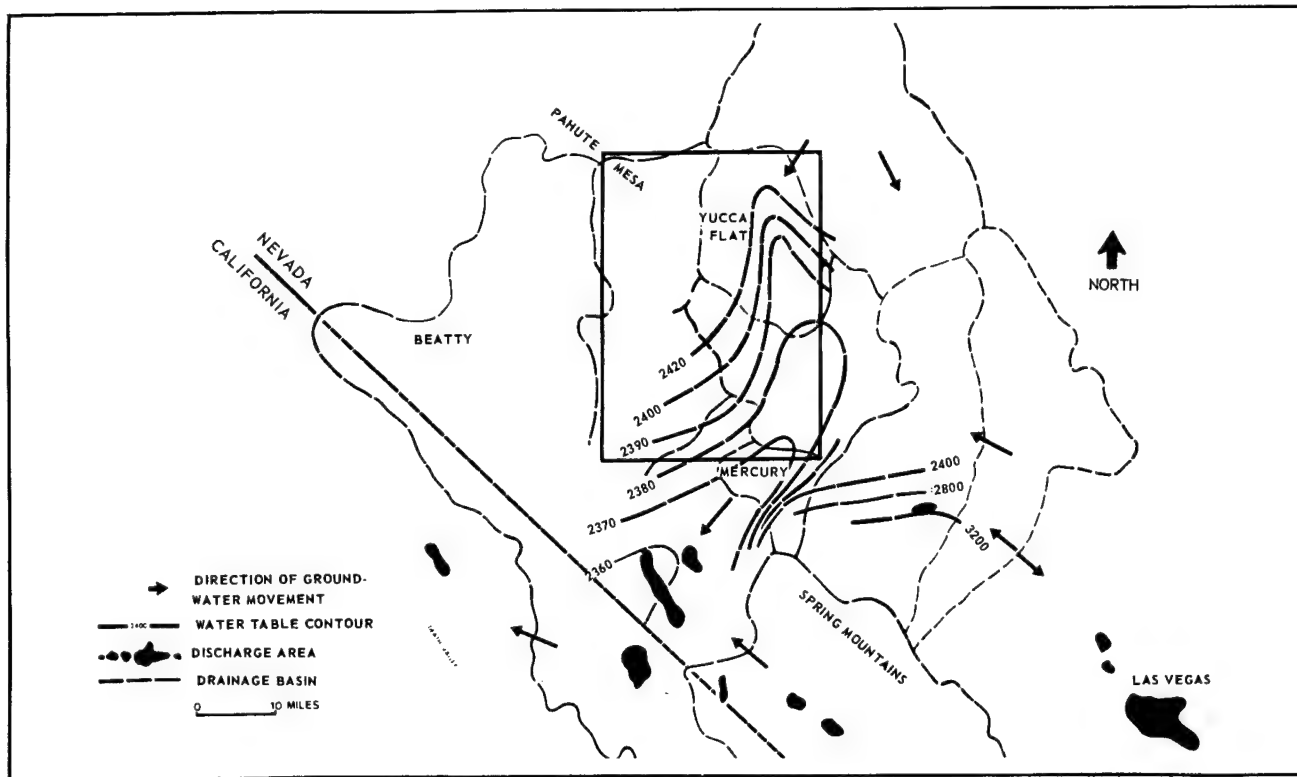
Figure 6.1.   Hydrologic Setting of Nevada Test Site and Vicinity.
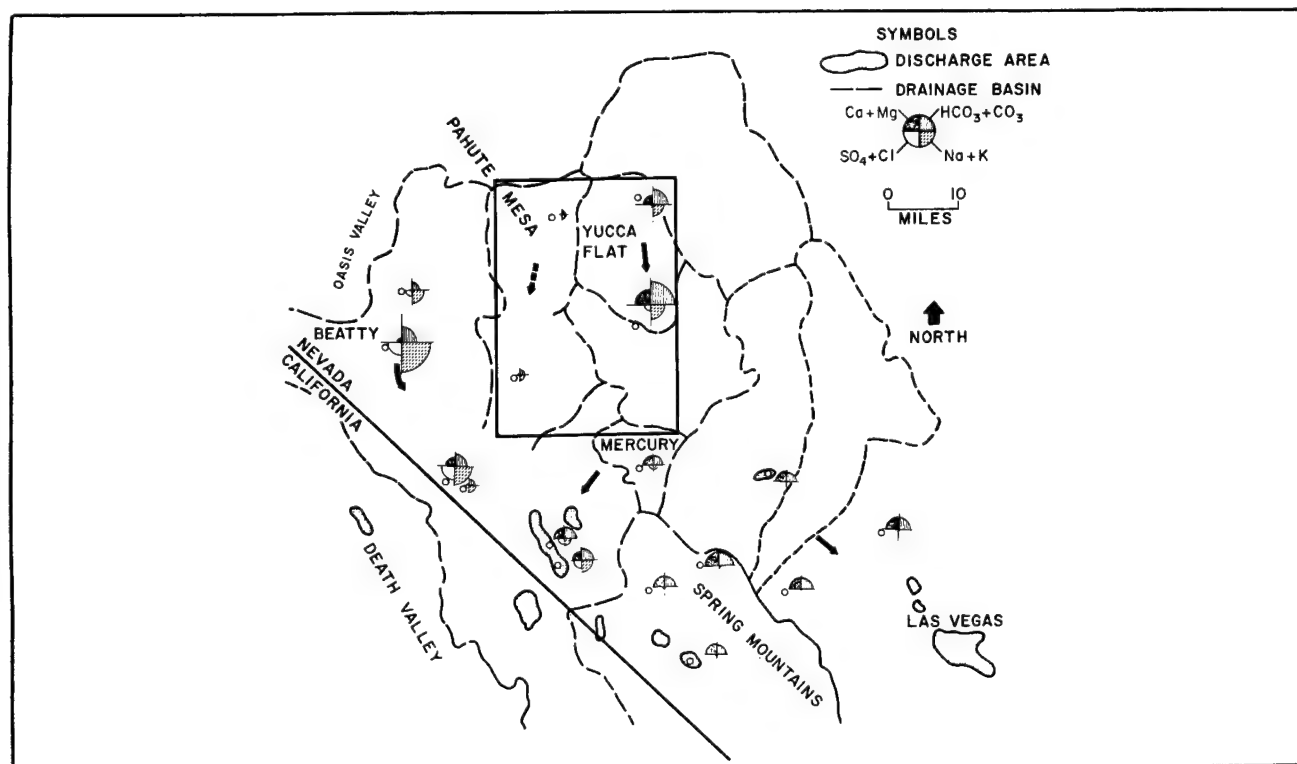

Figure 6.2.   Ground Water Chemistry and Hydrochemical Facies, Nevada Test Site and Vicinity.

Water from the Spring Mountains recharge area is a calcium and magnesium bicarbonate type derived from limestone and dolomite forming the mountain. On the other hand, water from Pahute Mesa is a sodium bicarbonate type of lower dissolved-solids content. Water in the vicinity of Beatty has, in addition to large proportions of sodium and bicarbonate ions, significant amounts of sulfate ions. Water in the discharge area is a mixture of all these types.

Central Nevada

New sites for individual underground nuclear tests in central Nevada are being investigated. Exploration has narrowed the search to a few hundred square miles northeast of Tonopah, Nevada, and centered in Hot Creek Valley and the Pancake Range. Figure 6.3, a diagrammatic geologic section, illustrates the gross geologic features in this area. Three major rock types are shown: valley fill of Quaternary and Tertiary age; volcanic rocks of Tertiary age; and carbonate rocks of Paleozoic age.

The sequence of volcanic and carbonate rocks has been disrupted by high-angle faults, which formed a series of nearly parallel mountain ranges and valleys. Valley fill has accumulated to a thickness of more than 4,000 feet in places. Carbonate rocks underlie virtually all the area at some depth.

The alluvium and volcanic tuff generally have low permeability, except for thin beds of sand and gravel in the alluvium and for zones of high-angle fractures associated with faults in the volcanic rocks. Of the three rock types, the carbonate rocks have the highest permeability because of their greater number of open fractures.

The mountains in the study area rise as high as 10,000 feet above sea level. The valley floors range generally between 5,000 and 6,500 feet. Precipitation ranges from 5 to 12 inches annually. Perennial streams rise in the highlands but sink into the alluvial fans at the foot of the mountains.

In central Nevada the water table generally is less than 600 feet below land surface. Most of the valleys are filled to the point of spilling in their lowest parts, where the water table intercepts the the land surface. The hydraulic potential may in-

crease or decrease with depth, depending on location within the geohydrologic system.

The tentative interpretation of the hydrologic setting of Hot Creek Valley is shown on Figure 6.4. Large parts of the area lack hydrologic control, so the interpretation will be revised periodically as new data becomes available.

The water level contours (in feet above sea level) on Figure 6.4 indicate a potential for ground water flow from Little Fish Lake Valley, Hot Creek Valley, Reveille Valley, and Little Smoky Valley into Railroad Valley. In general, the major topographic divides coincide with ground water divides. Thus, much of the ground water flow from one valley to another is limited to narrow, interconnecting canyons containing alluvium.

Ground water velocities in central Nevada computed from hydraulic tests of deep exploratory holes are less than 0.5 foot per day for intervals tested. However, the values were computed as averages in intervals of about 200 feet, so that velocities in some fracture zones probably are considerably more than 0.5 foot per day.

Chemical data for central Nevada are currently being analyzed to aid in analysis of regional ground water flow.

Site Hydrology

Studies of site hydrology include detailed hydraulic testing of exploratory drill holes by using straddle packers to isolate specific zones. The immediate objective of the hydraulic testing program is to determine the water yielding potential of the rock strata in each test hole and, in particular, those strata that have the lowest water yield and are favorable for construction of chambers in emplacement holes. These data are used also to predict rate of chimney filling and ground water velocities during initial movement of contaminated water away from the rubble chimney.

During the drilling and the hydraulic testing program, water and rock samples are collected and chemically analyzed for use in interpretation of ground water flow in the immediate vicinity of the emplacement hole. Work also includes collection and analysis of water samples for carbon-13, carbon-14, and tritium concentrations for use in dating the age of the water as a tool in determining regional velocities of ground water flow.
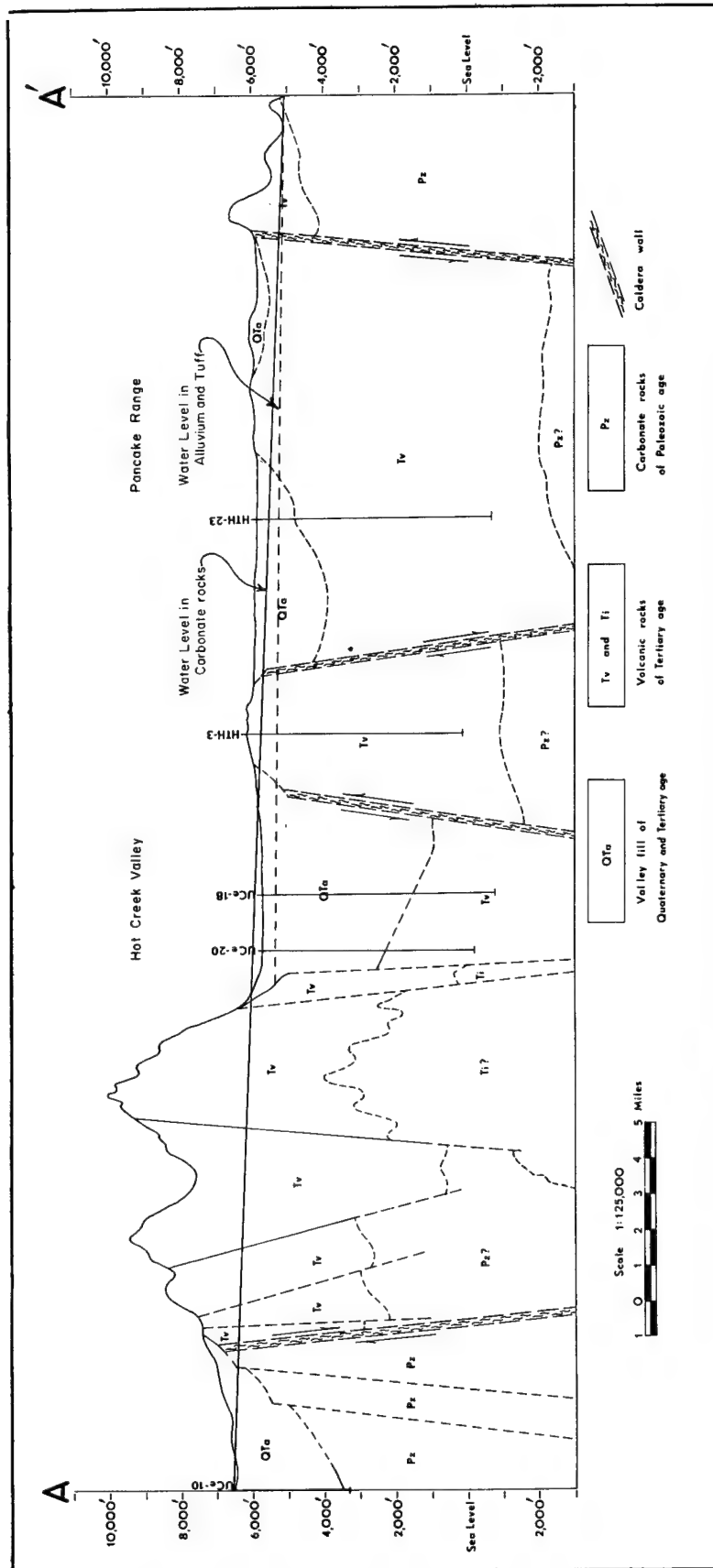
Figure 6.3. Diagrammatic Section Through Hot Creek Valley and Vicinity, Central Nevada.
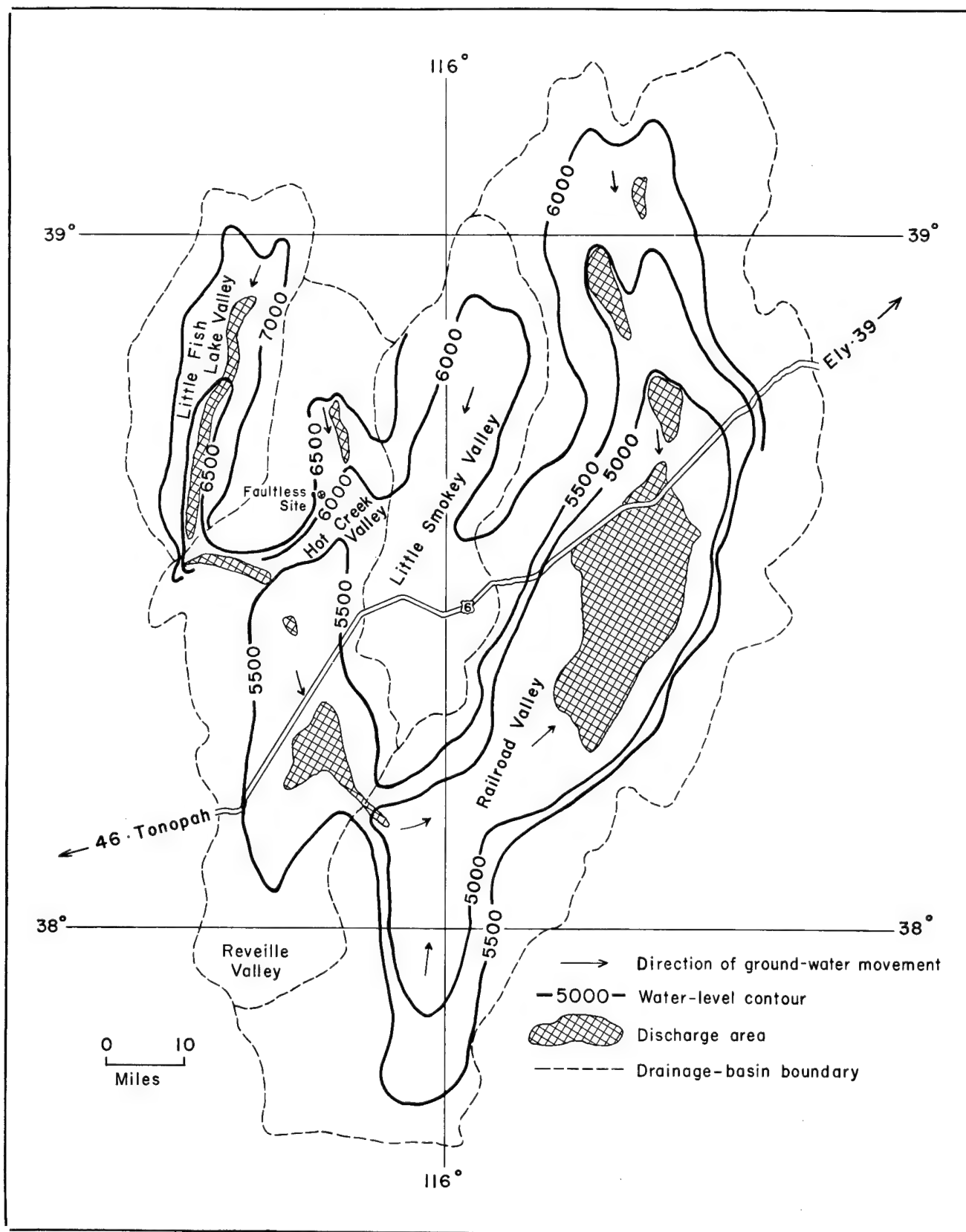
65

Figure 6.4.   Hydrologic Setting of Hot Creek Valley and Vicinity, Central Nevada.

66

Special Studies

Monitoring Response of Well Aquifer Systems to Nuclear Explosions

Underground nuclear explosions produce marked changes in surrounding rocks and in the fluid pressure distribution within aquifers. Currently under study are: (1) the effects of nuclear explosions on fluid pressures in aquifers; (2) the permanent effect of an explosion on the hydraulic characteristics of the surrounding media; (3) the relationship between explosion effects, such as ground motion, and resulting damage to wells and pumping equipment; and (4) the effect of hydrologic conditions, including disturbances in the natural environment as by pumping, on the ground motion resulting from an explosion.

Fluid pressure responses have been measured in wells at various distances from explosion points. Two distinct postshot effects have been noted—a short-term cyclic pressure fluctuation, which is probably related to surface motion, and a long-term elevation of pressure that dissipates gradually and that may indicate permanent changes in aquifer properties. In the future, these measurements will be closely coordinated with seismic instrumentation, particularly that measuring long-period surface waves. This should lead to an increased understanding of the relationships between hydrology and ground motion.

Tracer Study

The Geological Survey is making some tracer studies to better define the velocity of ground water movement in carbonate rocks that underlie valleys in southern and central Nevada.

The tracer site is underlain by lake deposits, alluvium, and basalt of Cenozoic age and at greater depth by carbonate rocks of Paleozoic age. The rocks of Cenozoic age at the site range from 580 to 650 feet thick. The rocks of Paleozoic age include brecciated dolomite and unbrecciated limestone.

The site is 15 miles southwest of Mercury, between the areas of nuclear testing and the ground water discharge points. Four wells that penetrate the carbonate rocks have been drilled, and a fifth was completed in the lower part of the alluvial material overlying the carbonate rocks. A high capacity turbine pump is installed in one well that penetrates the carbonate rocks.

The artesian head in the carbonate rocks is sufficient to give a static water level rise of about 600 feet above the top of the carbonate aquifer, or to 44 feet below land surface. This head is about 2 feet higher than the head at Ash Meadows discharge area, 7 miles to the southwest.

In late 1967, a 51-hour pumping test was made to obtain hydraulic data. While the pump was operating, potassium chloride was injected into one of the observation wells to obtain data on porosity of the aquifer and dilution of the salt. However, dilution was so great, the salt was not detected. Transmissivity was computed to be 720,000 gpd (gallons per day) per foot and storage coefficient as 0.00016. Similar tests using rhodamine dye and tritium will be made to further develop knowledge about the character and extent of openings in the carbonate rocks at the tracer site.

Chapter 7

PREDICTION OF RADIONUCLIDE MIGRATION IN GROUND WATER

Paul R. Fenske, *Project Manager*
Palo Alto Laboratories of Isotopes, Inc., Palo Alto, California

INTRODUCTION

All nuclear explosions add some radioactivity to the natural radioactivity of the immediate environment. Moving ground water may redistribute the radioactivity. A hazard exists if water carrying excessive concentrations of radioactivity enters the bioenvironment. Isotopes is under contract to AEC/NVOO to predict the migration of radioisotopes in ground water. Water containing excessive concentration of radioactivity, as used here, is water containing concentrations of explosion produced radionuclides above the maximum permissible concentrations (MPC).* This is a baseline concentration, a warning flag.

Prediction of the migration of water containing excessive concentrations of radioactivity includes prediction of the location of the volume of this water and description of it (size, shape, concentration). The first aspect of the prediction, location, depends upon analysis of the hydrologic system and its relationship to the explosion zone. In addition, the rate of movement of the radioactivity relative to water velocity must be known. The second aspect of the prediction, description, requires assessment of radionuclide production, sorption, and dispersion. A detailed analysis of the movement of ground water is a fundamental requirement for migration prediction. We must know the path of the water through the explosion zone, where the water enters the hydrologic system, and the water's velocity.

Basic data required for the prediction of migration of radionuclides include radionuclide production, provided by the nuclear device designers, explosion zone parameters, provided by Environmental Research Corporation, and velocity and direction of water, provided by United States Geological Survey. All other measurements, analyses and calculations are made by Isotopes.

HYDROLOGY

The movement of ground water through the explosion zone depends upon the position of the explosion zone relative to the potentiometric surface. The potentiometric

---

*MPC values are based upon concentrations given in AEC Manual, Chapter 0524, and reduced by a factor of three to be consistent with guidelines for uncontrolled areas.

surface is the height to which water will rise in a well under hydrostatic pressure. This surface is located at any point from above the ground surface to below any explosion effects. If the potentiometric surface is near or above the ground surface and surface effects are present, both ground water and surface water may be contaminated. If the potentiometric surface is below any subsidence craters, only the ground water may be contaminated. The greatest ground water contamination potential exists when the potentiometric surface approximately coincides with the top of the explosion cavity. The least ground water contamination potential exists when the potentiometric surface is below the detonation cavity and associated fractures. When large, deeply buried devices are detonated, a considerable thickness of aquifer may be intersected by the rubble chimney. There is high probability that this section of rock will consist of zones with varying hydraulic potentials. Ground water may flow into the explosion zone at one point and out through another. The hydrologic system will be complex.

For the sake of clarity, I will consider only the simplest case. In many instances obvious ramifications lead to greater complexity. Detonation of a nuclear device below the potentiometric surface causes the formation of a potential sink. Ground water flow will be initially toward the sink until the potentiometric surface reaches equilibrium (Figure 7.1); at this time outflow from the rubble in the explosion zone begins (Figure 7.2).

During outflow from the explosion zone, water adjacent to the downstream side of the explosion zone will immediately enter the hydrologic system. In the hydrologic system the radioactivity concentration will be reduced as a result of sorption and dispersion. Radioactive water within the explosion zone will also be subject to processes that will change the concentration of the radioactivity with time. This includes the dissolution of radionuclides from explosion debris and sorption or desorption of radionuclides upon the surfaces produced by the explosion and by postexplosion chemical processes. Most of the radioactive water will also be transported through the explosion zone. The explosion zone
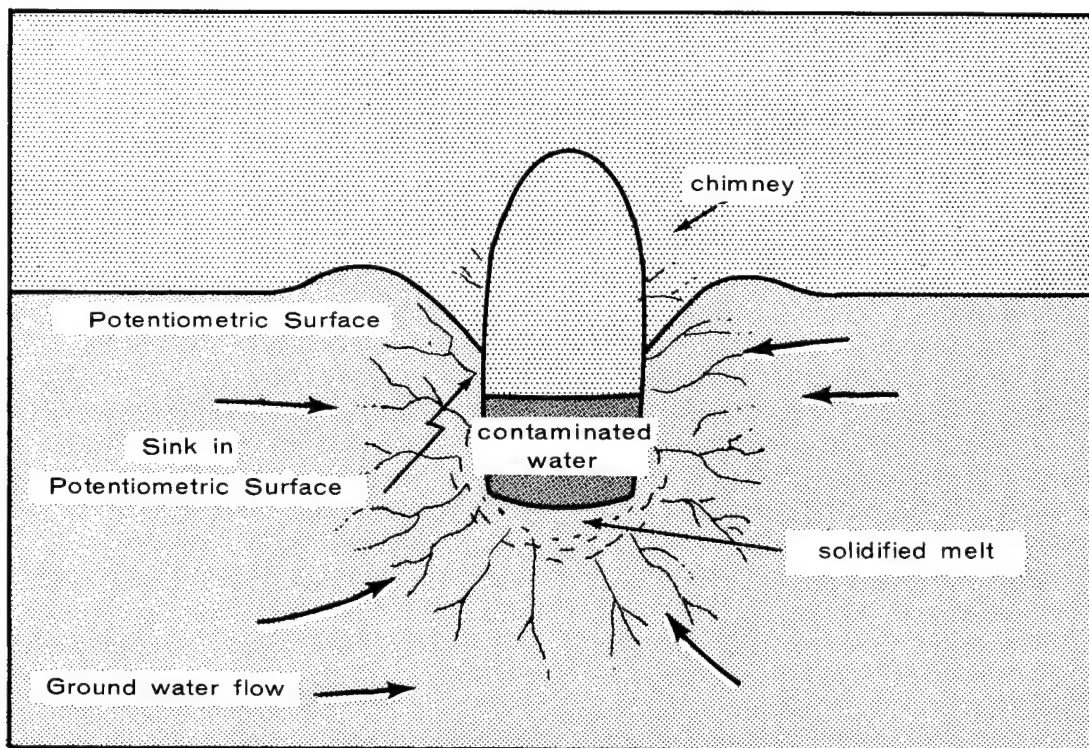
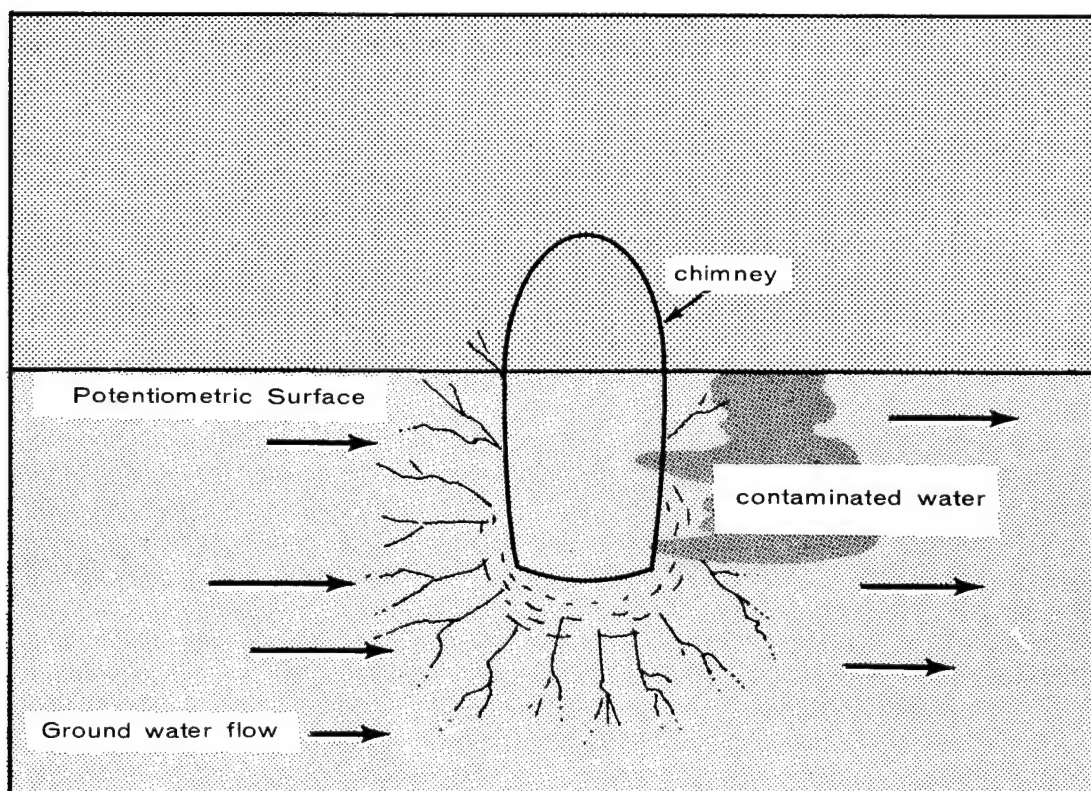Figure 7.1.   Readjustment of Potentiometric Surface.

Figure 7.2.   Outflow of Contaminated Water.

will have properties substantially different than the unperturbed hydrologic system. Uncontaminated water entering the upstream side of the explosion zone will similarly become radioactive, because of desorption and dissolution of radionuclides from rock surfaces, as it moves through the explosion zone.

For most underground nuclear detonations the porosity and permeability of the explosion zone will be higher than the porosity and permeability of the surrounding undisturbed rock. Porosity and permeability also vary from place to place along the flow path. This variation of porosity and permeability causes distortion of the volume of radioactive water during flow. As the volume of radioactive water flows into the ground water system it will occupy a larger volume of rock, since there is less pore volume available than in the explosion zone. It will be lengthened in the longitudinal direction and become wider because of the lower permeability and porosity of the aquifer. The area underlain by contaminated water in the ground water system will be larger and a different shape than the area underlain by contaminated water in the explosion zone. This area will also change shape along the flow path.

Skibitzke (1958) analyzed the distortion of flow lines caused by an infinite permeability contrast. Nork (1968) investigated the same problem for series of permeability ratios with electrical analog models. This latter study is still continuing. These studies show that the width of the contaminant stream exiting the explosion zone will probably be twice the width of the explosion zone (Figure 7.3).

SIMPLE MIGRATION PREDICTION

If sorption or dispersion are neglected, a simple approximate prediction of radioactivity migration is possible. All that is required is an inital concentration, decay constant, size of the initially contaminated volume, and the velocity and direction of ground water. For further simplification we shall also assume that the initial concentration of radioactivity in the explosion zone water is not more than 1024 MPC for any radionuclide of interest. Ten half-lives of decay will reduce the concentration of radioactivity to MPC.

I should point out that concentrations of radionuclides will not change substantially with yield of the device, other conditions being somewhat similar. Since the volume of explosion zone is approximately proportional to yield of the device, the volume of water available for contamination is approximately proportional to the quantity of radioactivity produced. Radionuclide migration predictions will remain substantially the same. The
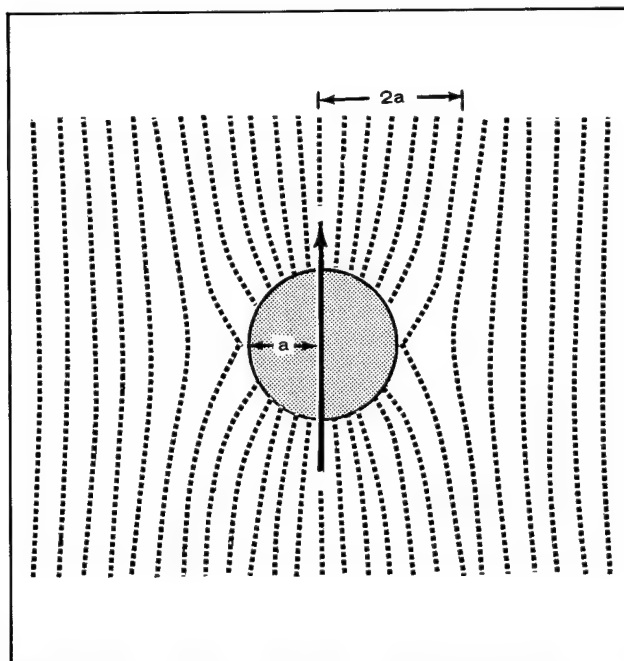

Figure 7.3. Flow Through a Circular Area of High Permeability.

area of ground underlain by above MPC water will increase slightly because of the larger volume of water involved.

Let us assume that a 1 megaton device is detonated somewhere along the west side of Area 20 on the Nevada Test Site. In this area the water moves at about 100 meters per year. In general, it flows southwest. This device would be buried at a depth of 1300 meters below the surface. It would be 650 meters below the water table. The radius of the resulting cavity and chimney would be 130 meters. The rubble chimney would fill with water to the water table in 2 or 3 years. The initial volume of contaminated water and rock would be roughly cylindrical. It would have a diameter of 260 meters and a height of 650 meters. The volume would be 34.5×10^{12} cm^3. These rounded numbers, of course, are only approximate, though representative. In practice we obtain these dimensions from Environmental Research Corporation. Only the velocity of the ground water and the size of the explosion zone are considered. A circular area at ground zero, twice the diameter of the explosion zone, is initially assumed underlain by above MPC water. We select a diameter twice the diameter of the rubble chimney to allow for the distortion of flow lines described by Skibitzke and Nork. This area is moved in the direction of ground water flow at the average water velocity. The velocity used in this example is 100 meters per year. The above MPC radioactivity is assumed to disappear after 10 or 11 half-lives of radioactive decay. For tritium,

71

which moves near the average water velocity, the above MPC water will probably underlie this moving area at any time (Figure 7.4). Most of the other radionuclides, which probably are retarded relative to the water velocity, will probably not be found at any time outside the zone swept out by the moving area. This approximate prediction illustrates the worst believable situation. It is similar in many respects to some of the predictions made during the early days of underground nuclear testing.

Present appraisals of migration of above MPC water start with this approximate calculation, and add consideration of sorption, dispersion, radionuclide production, and detailed hydrologic analysis.

In the remainder of this chapter I will calculate initial concentrations for tritium and strontium-90. These two radionuclides adequately represent both the long-lived and biologically significant radionuclides. Dispersion and sorption, two phenomena that act in a way to reduce concentrations of radioactivity will be investigated in detail. Finally, I will describe a migration prediction for an impossible conservative device that is 100 percent fission and 100 percent fusion. When I predict the migration of tritium, it will be as though the nuclear explosive energy were all derived from fusion. When I predict the migration of strontium-90, it will be as though the nuclear explosive energy were all derived from fission. This, of course, represents extremes. An actual device, for example, might be 90 percent fusion and 10 percent fission.

SORPTION AND DISPERSION

Now, let us investigate the phenomena that decrease the activity of the explosion produced radionuclides in water. These are sorption, dispersion, and radioactive decay. The effect of radioactive decay is well known and will not be discussed.

Radionuclides produced in underground nuclear experiments are dissolved in ground water which fills the rubble chimney. Dissolved radionuclides then exit the rubble chimney with the water as it starts to flow out. The amount of radionuclide remaining soluble and the rate with which it moves from the zone of production is governed in part by the chemical interactions of the radionuclide with the surfaces of the material through which the radionuclide contaminated water flows.

The amount of radionuclides available for migration and the rate of migration in ground water are governed by the degree of chemical exchange (sorption) which takes place after the radionuclides are dissolved. Radionuclide sorption is a term which represents the effect of all chemi-

cal reactions which might alter the concentration of the radionuclides in water. The net radionuclide sorption is represented by the parameter, distribution coefficient, which is unique for each combination of geologic medium, water quality, radionuclide, and chemical form of the radioactive material. The distribution coefficient (K_d) is a number which represents the ratio of the amount of radioactive material held on the solid phase to that in solution. In equation form:

$$K_d = \frac{V}{M} \cdot \frac{A_s}{A_w} \qquad (1)$$

where A_s = amount of radioactive material taken out of solution by the solid phase

A_w = amount of radioactive material left in solution

V = volume of solution (ml)

M = mass of solid (g)

A reasonable value for K_d may be difficult to obtain because of the many phenomena which affect the degree of radionuclide sorption. K_d's ideally should be measured in the geologic formations (aquifers) in which the radionuclide is expected to migrate. Since it is quite expensive and time consuming to gain access to most aquifers, other means of estimating K_d's are used. Presently K_d's are measured in the laboratory using rock material and water collected from the zone of concern. Temperature, time of contact, and liquid-solid volume ratio are set to represent natural conditions and are controlled during the course of K_d measurements. Laboratory induced variability is thereby minimized.

We believe that laboratory derived K_d's are valid for field conditions in the case of aquifers: 1) K_d's measured on samples of various particle diameters were found to be nearly constant for a wide range of particle diameters, 2) associated rock-water chemical interactions were also found to be constant for the same range of particle diameters. These observations suggest that K_d values derived from specific particle diameters may be extrapolated to field conditions.'

There are two methods of measuring K_d's in the laboratory — batch and column leach method. In the batch method we suspend crushed and size-graded rock material in water dosed with the desired radionuclide. After equilibrium is reached we separate the solution from the rock material and measure the amount of radionuclide remaining in solution. We then calculate K_d values with equation (1). In the column leach method we leach columns of the crushed and size-graded material with radionuclide-dosed water. We analyze samples of the

Explosion Zone

Ground-water

Flow Direction

12.5 Kilometers

Envelope enclosing area expected to be contaminated at some time following the detonation

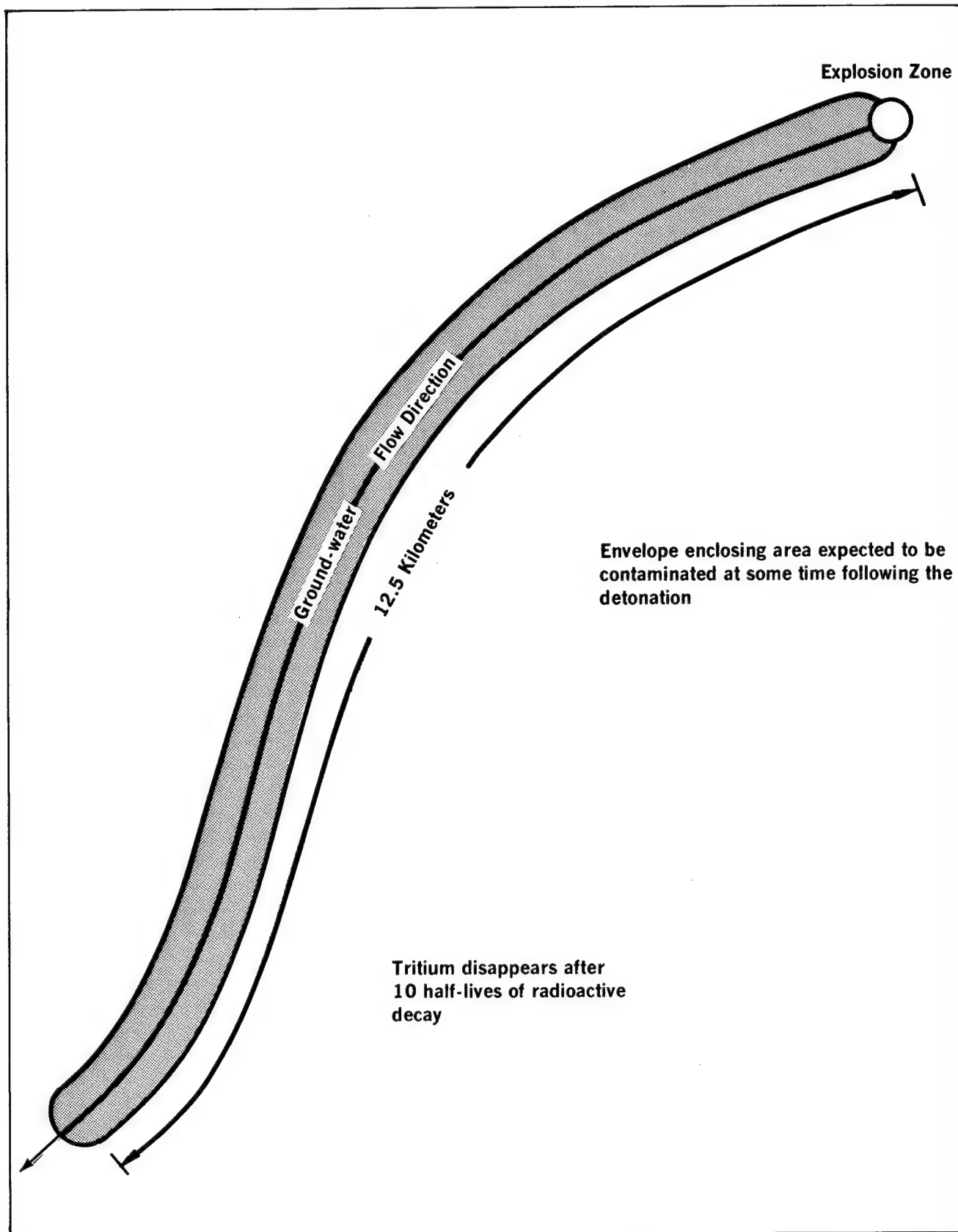**Tritium disappears after 10 half-lives of radioactive decay**

Figure 7.4. Simplified Hydrologic Contamination Prediction for Tritium.

leachate periodically to determine the shape of the radionuclide breakthrough curve. K_d's are then calculated using the following equation (2):

$$K_d = \frac{(Cv-1)\,\theta}{\rho\,(1-\theta)} \qquad (2)$$

where

$C_v =$ number of column volumes of effluent necessary to attain maximum radionuclide concentration

$\theta \quad =$ porosity

$\rho \quad =$ grain density

Neither method is completely satisfactory for all radionuclides. The batch method is used to measure only the equilibrium concentrations of radionuclides whereas the column leach method is used to represent radionuclide concentration in dynamic flow conditions. Those radionuclides which change chemical form during the course of the measurement will not yield a reasonable K_d by either method. Those radionuclides which are highly sorbed or retarded in flow will take very long times to yield K_d's by the column method but are easily evaluated by the batch method. If a K_d is to be representative of flow conditions, where equilibrium cannot be attained, column leaching must be used with flow velocities representative of the aquifer in question.

We and others have measured distribution coefficients for various geologic materials and associated waters. Values for radioisotopes such as strontium-90 range from less than 1 for clean quartz sand to more than 5000 ml/g. In many cases of underground nuclear testing the rate of ground water movement is low. The combined effects of radioactive decay and radionuclide retardation are sufficient to reduce the concentration of the radionuclide to below MPC within short distances of migration.

Figure 7.5 shows the effect of sorption on the initial radionuclide concentration as determined by K_d. For K_d's above 0.4 ml/g in systems of 5 percent porosity, the proportion of radionuclide remaining in solution is less than 5 percent of the original. This is a considerable reduction in radionuclide concentration, and upon migration of the radionuclide-laden water through aquifer material the portion of radionuclide remaining in solution will approach 5 percent of the total present in each successive increment of aquifer material. In a very short distance there will be a much greater reduction in concentration of the radionuclide. This also means that the mass of the radionuclide will migrate only 5 percent the distance of water migration. A small amount of the radionuclide, however, will migrate the same distance and as fast as the ground water. Laboratory measurements of K_d's are often more than 4 orders-of-magnitude higher than this value for all radionuclides of interest except tritium.

For K_d values less than 10, significant migration of the radionuclides may occur. We are presently evaluating the basic parameters of ground water aquifers which most affect radionuclide migration and K_d. One basic objection to the use of K_d, as defined earlier, is that radionuclide sorption is a function of surface area exposed to the radionuclides. It is not a direct function of the mass of materials involved. Deviations in pore size distribution and types of pores, whether open or closed, result in discrepancies in the predicted radionuclide migration rate. For this reason we are considering a redefinition of radionuclide distribution on the basis of measured surface areas.

Dispersion is the mixing that occurs between the radioactive water and nonradioactive water at their mutual boundary. Radioactive water is diluted. Substantial reduction in the concentration may occur if the dispersion coefficient is great enough. Early warning of contaminant arrival is also possible due to dispersion. The effect of dispersion is illustrated in Figure 7.6. A hypothetical MPC concentration is indicated. Note the toe that is below MPC. This toe, caused by dispersion, makes it possible to identify increases in radioactivity before MPC is reached. Also shown for comparison is the undispersed slug of contaminant. The trailing edge is shown as more dispersed than the leading edge because the trailing edge, in addition, must pass through the rubble chimney. The higher porosity and permeability of the rubble chimney may cause greater dispersion. In the example dispersion is great enough not only to cause dilution of the edges of the slug, but also to reduce the concentration at the center of the slug. It is relatively simple to calculate the minimum dispersion coefficient required to be effective in decreasing the peak concentration of contaminant in this manner. We already know that in approximately 10 half-lives most contaminant concentrations will be reduced to MPC by radioactive decay alone. Dispersive mixing to be effective in reducing peak concentrations must then affect the entire contaminant slug in less than 10 half-lives of transport. Since the dispersive portion of the transport equation is Gaussian, we take one-half the length of the contaminant slug and consider it to be 3σ.

$$\sigma^2 = 2Dt \qquad (3)$$

$\sigma^2 =$ variance of dispersion of contaminant slug

$D =$ coefficient of dispersion

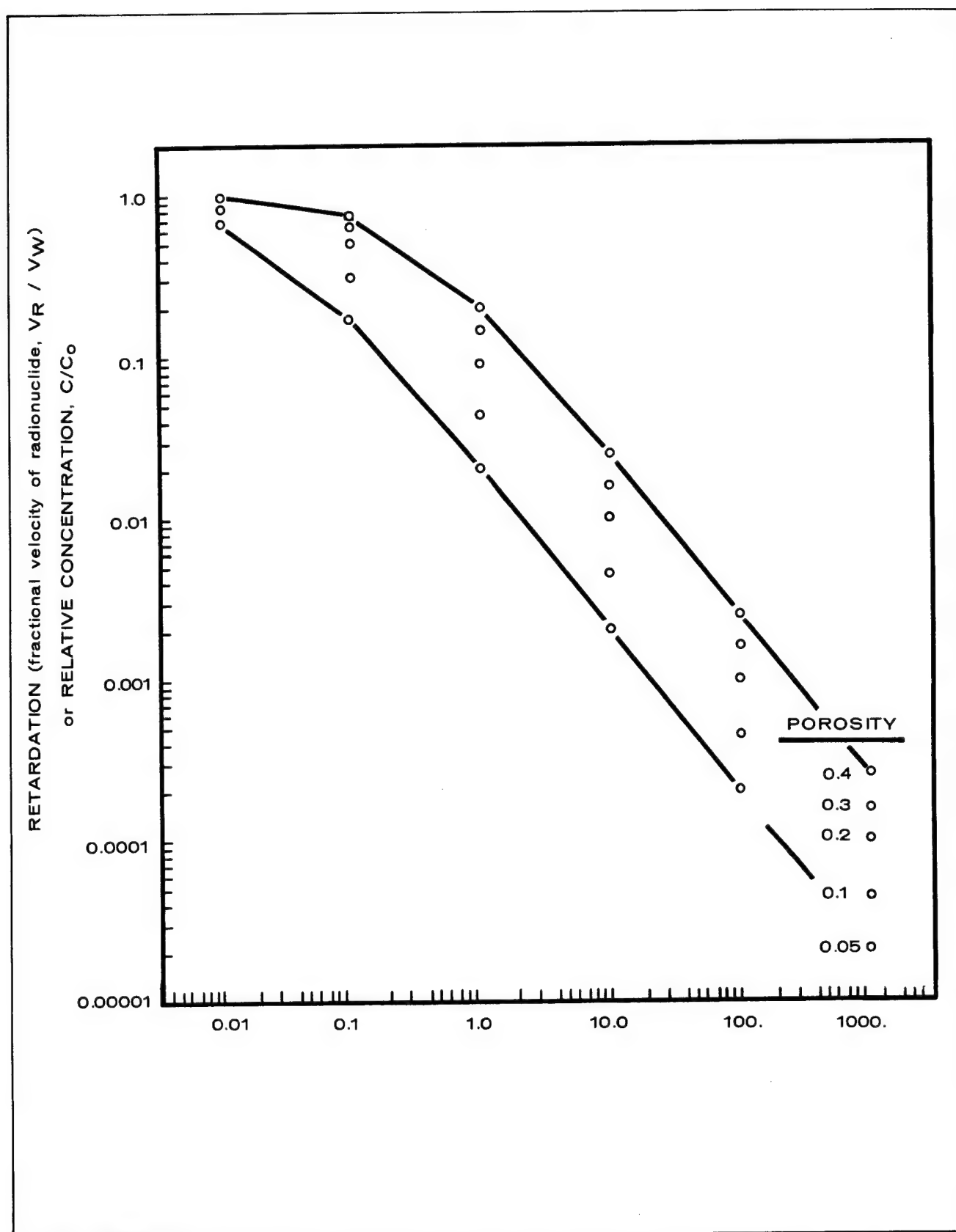$t \quad =$ time $= 10$ half-lives

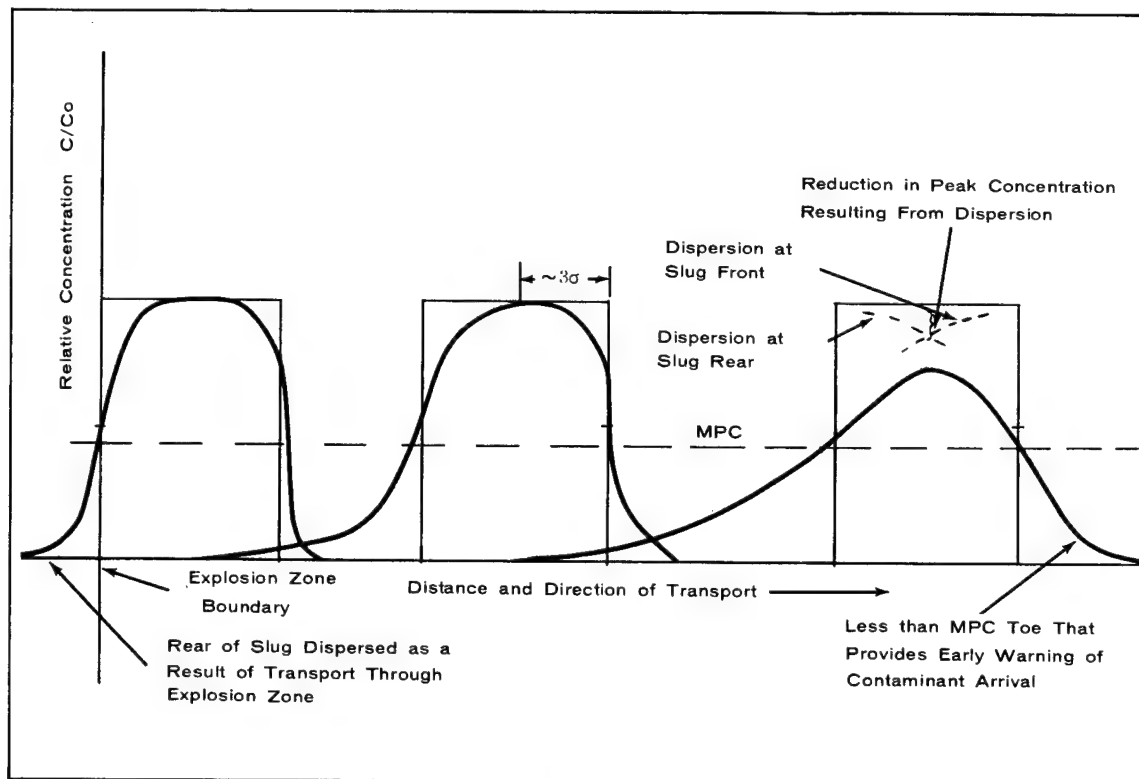74

Figure 7.5. Distribution Coefficient, K_d (ml/g).

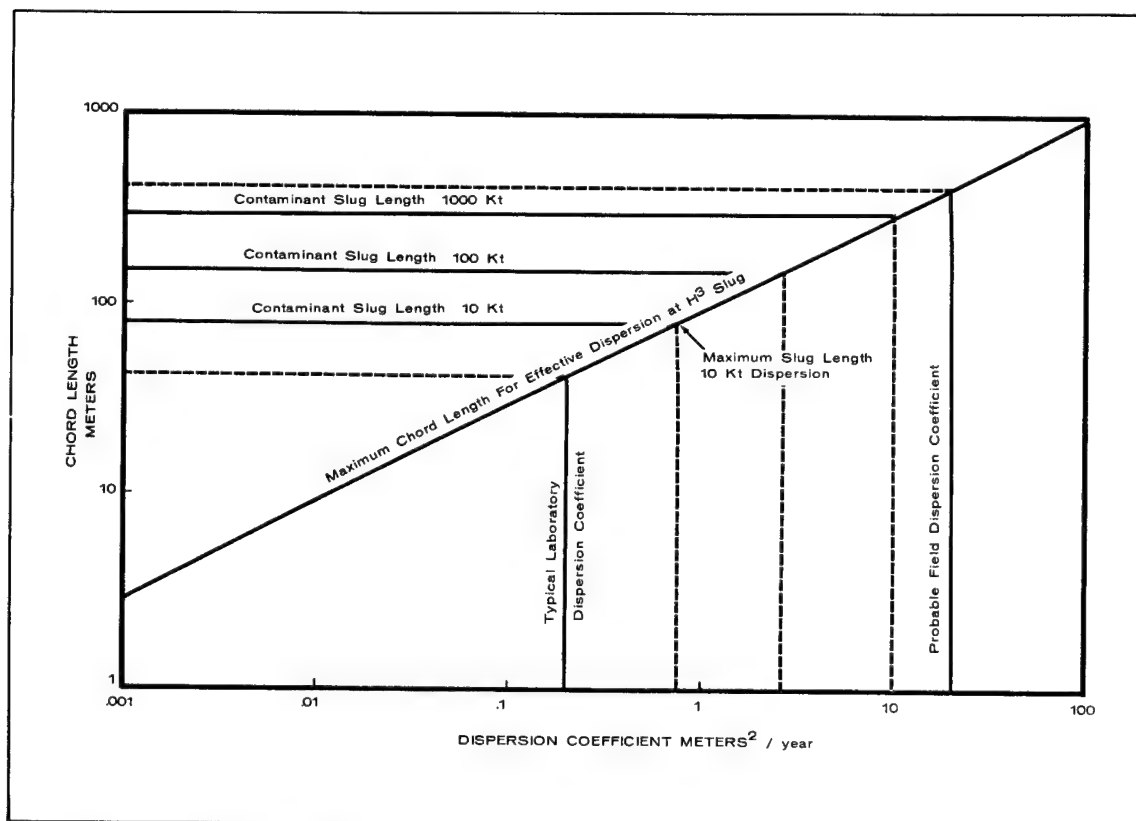Figure 7.6. The Effect of Dispersion on Contaminant Slug.

Figure 7.7. Minimum Dispersion Coefficient for Reduction of Peak Concentration Along Any Chord in 122.6 Years (10 Half-Lives).

76

Figure 7.7 shows the result of this calculation for a range of contaminant slug lengths. Laboratory dispersion coefficients are around 0.2 meters^2 per year. Reasonable values for heterogeneous rocks in the field are at least 2 orders-of-magnitude greater. Theoretical investigations of dispersion indicate that the coefficient of dispersion for heterogeneous material may be 2 or 3 orders-of-magnitude higher. In Figure 7.7, dispersive mixing is indeed significant. I should point out that D is dependent upon both the medium and ground water velocity. Figure 7.7 was calculated for an approximate velocity of 100 meters per year.

We have been considering only the slug length represented by the diameter of the explosion zone. Chords parallel to the maximum length are shorter and become zero in length at the sides of the contaminant slug. Dispersion will also reduce the peak concentration of contaminant along these chords. This reduction will be effective at the sides of the contaminant slug first (Figure 7.8).

I have discussed the effect of dispersion on the migration of radiocontaminants. Before moving on I want to discuss dispersion theory and provide some basis for estimating that dispersion coefficients for heterogeneous media are several orders-of-magnitude higher than dispersion coefficients for homogeneous granular materials.
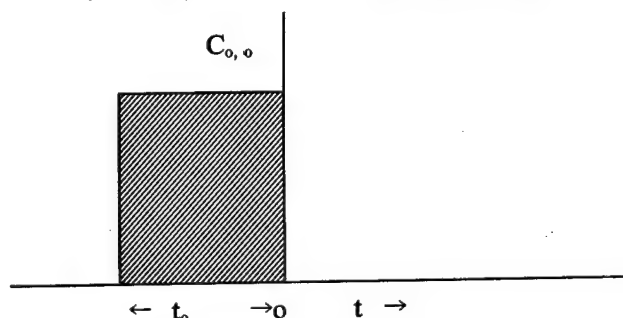
Dispersion is caused by velocity variations about the mean velocity of flow of the ground water. These velocity variations are the result of parabolic velocity distribution through pores, pore size variations, local differences in permeability between strata or lenses of rock of the same lithology, differences in permeability of closely associated rocks of different lithologies, and so forth as far as one desires to extend the hierarchy. It can be shown on probabilistic basis that the dispersion coefficient for homogeneous granular material is proportional to the product of the mean pore radius and the mean velocity of ground water. This is also confirmed by laboratory measurement. Similarly, it can be shown that the dispersion coefficient for heterogeneous rocks is proportional to the product of the mean ground water velocity and the mean length of the heterogenieties. In the first instance, homogeneous granular media, we are talking about tenths of millimeters as a characteristic dispersive length. In the second case, heterogeneous rocks of similar lithology, we are perhaps speaking of several meters as a characteristic dispersive length. Dispersion in homogeneous granular media becomes a second order effect. The dispersion coefficient in heterogeneous rocks is several orders-of-magnitude higher. As we move up the hierarchy and include larger samples of rock, the dispersion coefficient probably increases by several additional orders-of-magnitude. Dispersion under field conditions may be high. Dispersion can conceivably be great enough to significantly reduce contaminant concentrations by dilution.

RADIOACTIVE CONTAMINANT TRANSPORT EQUATION

We calculate the location and concentration of the radioactive contaminant with this equation:

$$C(x, t) = \tfrac{1}{2} C_{o,o} \exp(-\lambda t) \cdot$$
$$\left[\operatorname{erfc} \frac{x - vt/B}{2\sqrt{Dt/B}} - \operatorname{erfc} \frac{x - v(t - t_o)/B}{2\sqrt{D(t - t_o)/B}} \right] \quad (4)$$

This equation was obtained by setting up the differential equation for transport of contaminants. The transport differential equation was then reduced to the form of a heat-flow differential equation. Solutions to heat-flow equations for many combinations of geometries and boundary conditions are known and reported in Carslaw and Jaeger (1959) and other standard references. The method of reducing the contaminant transport differential equation to a heat-flow differential equation was discussed in detail by Holly and Fenske (1968). The solution presented above is not a complete solution. Several terms have been neglected because the simplification obtained was great. The error caused by the neglect of these terms is small.

The equation describes the transport of a slug of contaminated water that was originally rectangular. The first term in the brackets represents the effect of transport on the front of the slug. The second term in the brackets represents the effect of transport on the rear of the slug. The exponential modifier preceding the bracketed expression corrects for radioactive decay.

We define the terms in the equation in the following manner:

t   = time measured from when the explosion zone outflows

t_o = the original length of the slug in terms of time of transit

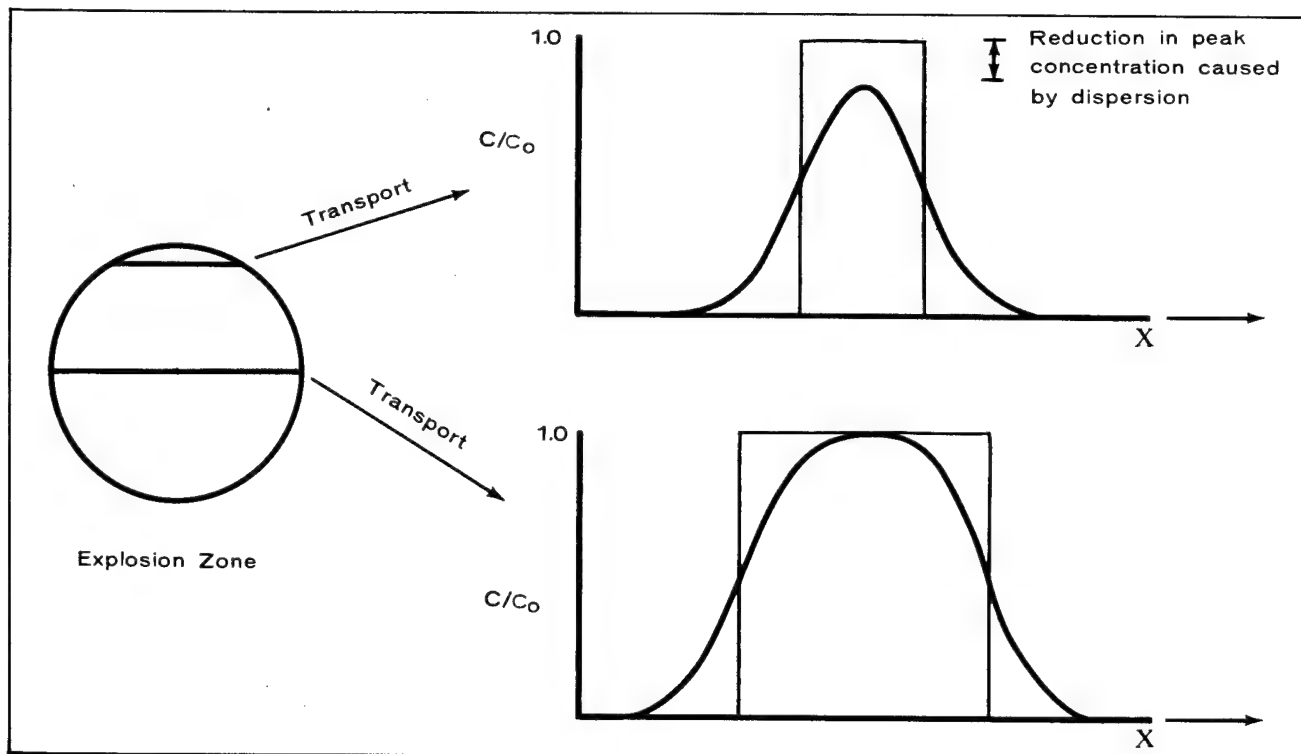x   = distance from explosion point measured along a streamline
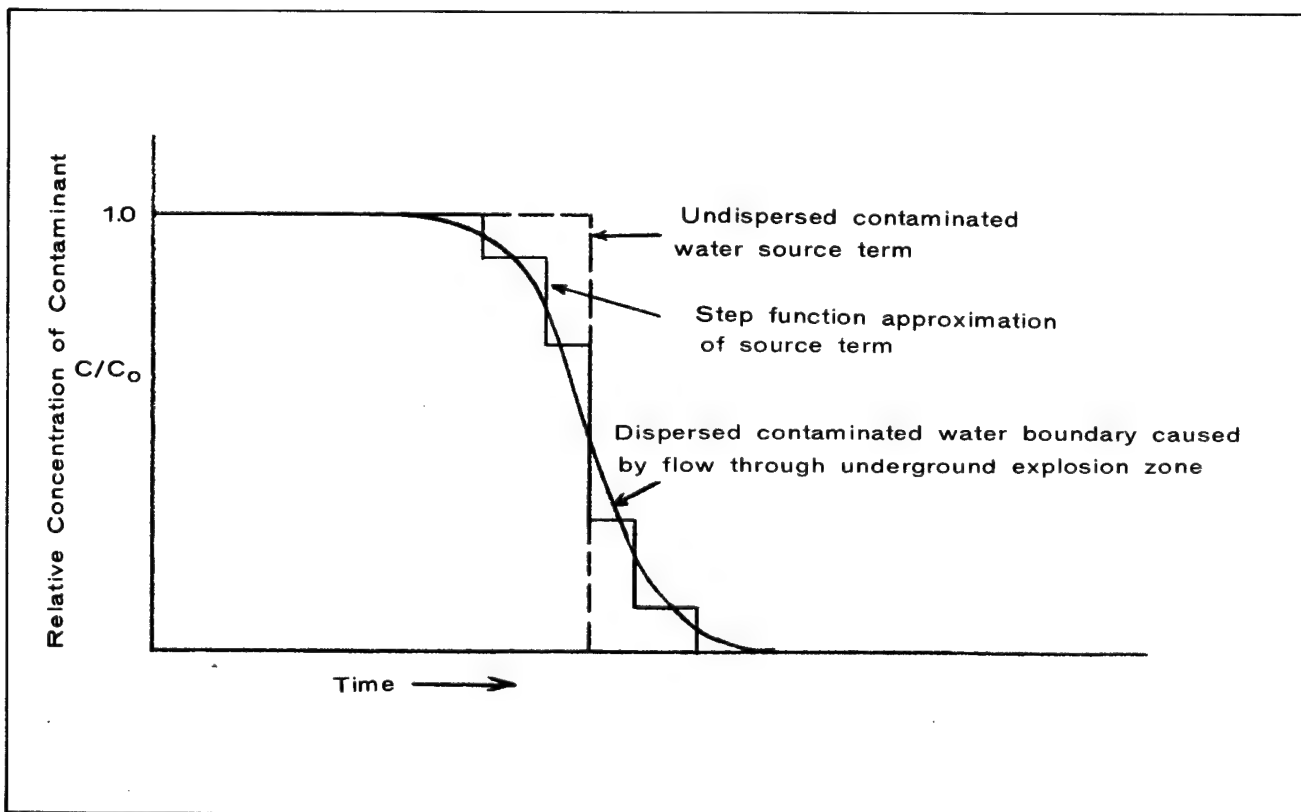
Figure 7.8.   Effect of Dispersion on Contaminant Slug.

Figure 7.9.   Source Term for Flow from Underground Explosion Zone Into Ground Water System.

λ = radioactive decay constant of the radionuclide

v = the average seepage velocity of ground water

B = $1 + \dfrac{1-\theta}{\theta} K_d$ = retardation factor

θ = porosity of the aquifer

K_d = distribution coefficient of the radionuclide between the solid and aqueous phase of the hydrologic system

D = dispersion coefficient

$C_{o,o}$ = initial concentration of radioactive contaminants

$\dfrac{Dt}{B}$ = one-half the variance of the radioactivity concentration curve

The variables, t and x, are determined by the requirements of the hydrologic safety program. The velocity of the water and the porosity of the aquifer are obtained through hydrologic system analysis. The variable, D, describes the physical dispersive process. The variable, K_d, describes sorption of the radionuclide and retardation relative to ground water movement.

Our present contaminant transport equation (4) permits input of only a constant initial concentration, $C_{o,o}$. It is solved for a rectangular slug of contaminant. The origin for the transport calculation is the downstream edge of the explosion zone. All but an infinitesimal quantity of the contaminated water is also subject to sorption and dispersion within the explosion zone. The initial concentration is time-variant. In addition, the transport equation is one-dimensional. We do not feel that this is a serious restriction. The two-dimensional distribution in a horizontal plane may be closely approximated by including an equation to estimate the effect of lateral dispersion. Concentrations may also vary vertically in the explosion zone. We correct for these variations, when we know they exist, by approximating any source term with a series of rectangular slug inputs of different lengths (Figure 7.9).

The concentration of contaminant in the system is calculated in terms of a concentration distribution in space at selected times. A large number of repetitive calculations are required. For this reason we have programmed the equation for solution by a digital computer. Output from this program is a series of matrices. Each matrix represents the longitudinal and lateral distribution of concentrations at an instant of time. As I mentioned earlier, the lateral distribution is approximated by a lateral dispersion program. The matrices can be converted into concentration isopleths. We are confident that the calculated concentrations are equal to or greater than the real concentrations. At the present time we bound an area on the map that includes, with a high level of confidence, all surface area underlain by water containing concentrations of explosion produced radioactivity above MPC.

RADIONUCLIDE CONCENTRATION

The device designers, Lawrence Radiation Laboratory and Los Alamos Scientific Laboratory, provide us with radionuclide production data for nuclear devices.

Tritium production for a pure fusion explosion is reported in the open literature in the range of 7×10^3 to 5×10^4 curies per kiloton (Miskel, 1964). The lower figure is one reported in the Russian literature by Leipunsky (1959). Since the distance of radionuclide movement in ground water is time-dependent, I will point out that the difference between the high value and the lower value represents less than 3 half-lives of radioactive decay. For our purposes we might as well use a half-life mean value, a value about 1.5 half-lives above 7×10^3 curies per kiloton. The mean value calculated on this basis is 2×10^4 curies per kiloton in round numbers. I will use this value as being probable; however, we will examine the error involved if the larger value 5×10^4 curies were the real value.

Quantities of fission products are relatively simple to calculate if the device fissionable material is known. Assuming that plutonium is the fissionable material the fission yield of strontium-90 would be 1×10^2 curies per kiloton. An impossible megaton device would then produce 2×10^7 curies of tritium and 1×10^5 curies of strontium. These two radionuclides were chosen to represent the biologically significant and long-lived radionuclides.

The volume beneath the potentiometric surface in the explosion zone was already shown to be 34.5×10^{12} cm^3. We must know the porosity of the rubble to calculate the total volume of contaminated water. The porosity of the rubble depends upon the kind of rock in the explosion zone. If the original rock is porous, the explosion created porosity must be added to the original porosity. In Area 20 of the Nevada Test Site I have estimated the average rubble porosity as 15 percent. The volume of water that will be initially contaminated then is 5.2×10^{12} ml. We will conservatively assume that all of the radionuclides are dissolved. MPC values will be calculated using AEC radiation protection standards for average exposure of populations in uncontrolled areas. The activity of tritium will be 384×10^{-8} curies/ml or 3840 MPC. The tritium will decay to below MPC in 11.91 half-lives or 146 years. The activity of strontium-90 will be 1.92×10^{-8} curies/ml or 1.92×10^5 MPC. Strontium-90 will decay to below MPC in 17.55 half-lives or 491 years. Earlier we said that 10 or 11 half-lives of radioactive decay would be sufficient for reduction of concentrations in water of any

radionuclide of interest to below MPC. Sorption and dispersion will significantly reduce the concentrations of radionuclides in water during transport. I will show that there is a high probability that strontium will not be found above MPC outside of the explosion zone.

HYPOTHETICAL CONTAMINATION PREDICTION

Our problem is to predict the migration of 5.2×10^{12} ml of contaminated water. The tritium concentration could be as high as 3840 MPC. The strontium-90 concentration could be as high as 1.92×10^5 MPC.

Next we select a value for the dispersion coefficient. I have shown that the dispersion coefficient is proportional to a characteristic length, the length of heterogenieties in the rocks. We are not being unreasonable to use the higher coefficient from Figure 7.7, 20 meters^2 per year. Dispersive mixing will affect the entire slug of tritium in somewhat less than 123 years, 10 half-lives, of transport. Because of sorption and resulting retardation of strontium-90, dispersive mixing may have little effect upon the concentration of this contaminant.

In our discussion of the K_d, I have a range for the K_d for strontium-90 of less that 1 to more than 5000 ml/g. Measurements at NTS and in central Nevada indicate that 200 ml/g is a reasonable value. I will assume that tritium is not significantly sorbed. There is considerable doubt about this. We are working on this problem currently. Assuming nonsorption for tritium as with the other assumptions I have made, leads to predictions that indicate worse contamination conditions than actually will exist. No explosion-produced radioactivity has been found in ground water outside of explosion zones. Less than anticipated has been found in explosion zone waters. However, checks of this type are too few to permit statistically valid inferences.

The ground water velocity in Area 20 of the Nevada Test Site is 100 meters per year. We derived this ground water velocity from data on the Area 20 hydrologic system supplied by the U.S. Geological Survey. Errors in this number have significant effect on predictions of the location of above MPC water. This is perhaps the greatest single source of error in predicting migration of radioactivity. Water in central Nevada moves at about half that velocity, 50 meters per year.

The original length of the slug in terms of transit time is readily calculated. We use the studies of Skibitzke and Nork as basis for assuming a water velocity across the explosion zone of 80 meters per year. The time length of the slug would then be 3 years.

The initial concentration of tritium that enters the hydrologic system is 3840 MPC. The initial concentration of strontium-90 must be reduced in the explosion zone as a result of sorption on rubble. Referring back to Figure 7.5, we see that for explosion zone porosity of 15 percent, the relative concentration in the water will be about 4×10^{-4}. The concentration originally calculated for the water was 1.92×10^5 MPC. The initial concentration of strontium-90 in water exiting the explosion zone will be about 80 MPC. This water is coming into contact with rock surfaces that do not contain sorbed strontium. The relative concentration in water here will be 2×10^{-4}. Strontium-90 in water outside the explosion zone will be approximately 2×10^{-2} MPC. We will not consider strontium-90 further. Other sorbed radionuclides, cesium-137 and calcium-45 for example, will have a similar migration history.

In our hypothetical migration prediction for tritium, I will assume a rectangular source term.

Let us now briefly review our data for tritium:

t and x	= any time and place of interest
t_o	= 3 years (time length of contaminant slug)
λ for tritium	= .0565 (half-life = 12.26)
v	= 100 meters per year
K_d	= 0
D	= 20 meters^2 per year
$C_{o,o}$	= 3840 MPC

Figure 7.10 is a map predicting the migration, decay, and diffusion of tritium. The tritium disappears in approximately 145 years as a result of radioactive decay and dispersion. The elliptical shaded areas represent the location of the above MPC water at selected times. The area enclosed in dashed lines encloses all area ever underlain by above MPC water. The total distance of transport will be not more than 14.5 kilometers. The longest time of transit of above MPC water past any point is less than 6 years. The largest above MPC area will be about 2×10^5 meters^2, 20 hectares less than 50 acres. This area will shrink during transport until it disappears near the end of 14.5 kilometers of transport.

SUMMARY

Hydrologic safety involving the detonation of nuclear devices requires predicting the location of radioactively contaminated water and describing it. As time passes the volume of contaminated water will increase and then decrease. The concentration of the radioactivity will also decrease. Shrinkage of the volume of contaminated water and reduction of its concentration are caused by radioactive decay, sorption, and dispersion. Variations in porosity and permeability between the
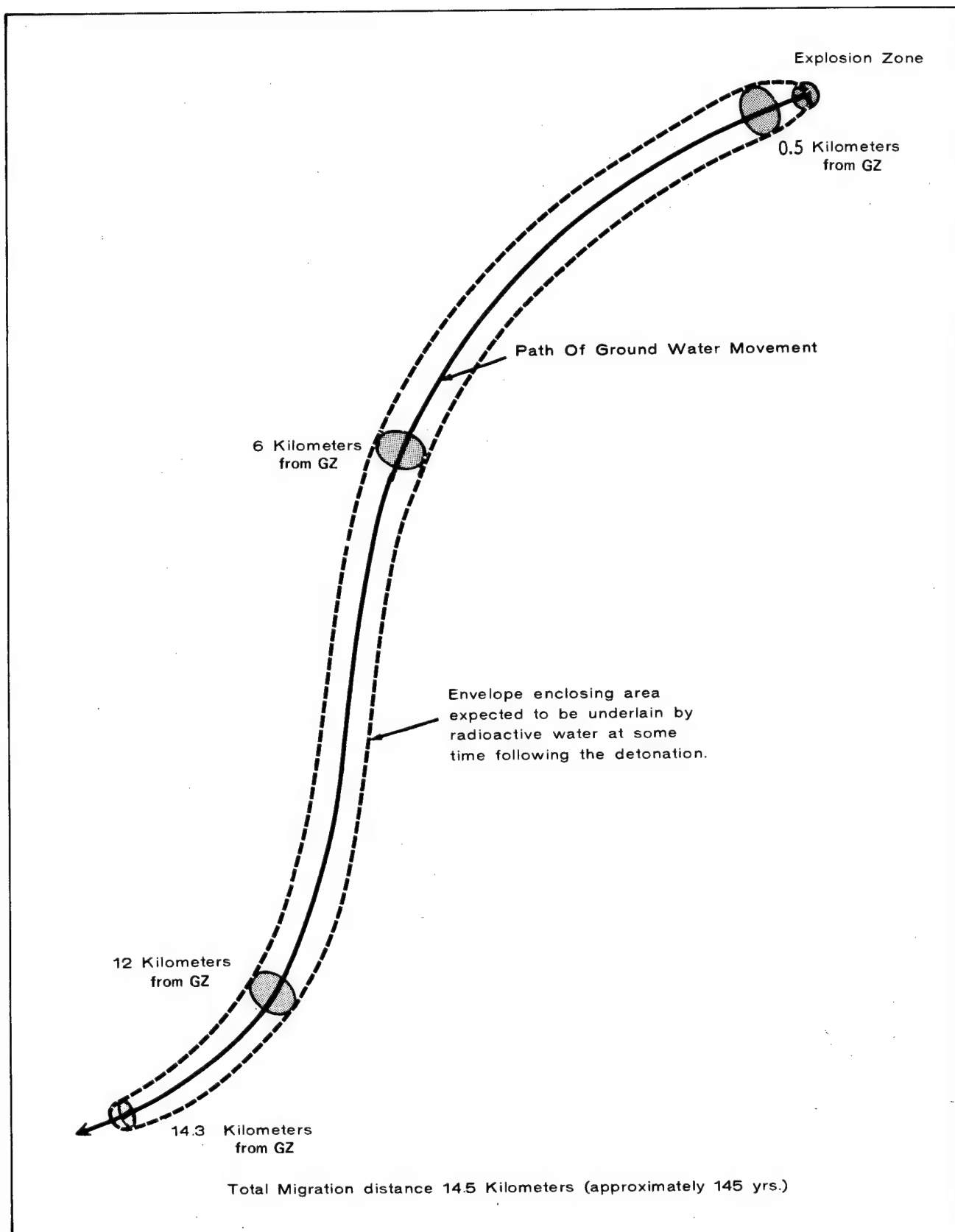
Figure 7.10. Hypothetical Contamination Prediction for Tritium.

explosion zone and aquifer and within the aquifer distort the contaminated volume. The area of the ground surface underlain by above MPC water is the vertical projection of the above MPC water volume. At present all concentrations are referred to MPC as a standard. Radioactive decay, sorption, and dispersion ultimately reduce all radioactivity concentrations to below MPC. If only radioactive decay and ground water velocity are considered, a crude migration prediction is possible. A circular above MPC area twice the diameter of the explosion zone is moved downgradient at the ground water seepage velocity for 10 or 11 half-lives. At the end of this time the contaminant concentration will probably be close to or below MPC. This prediction has a high probability of representing the worse conceivable case.

We can carry out a more detailed and realistic prediction of contaminant migration if we consider radionuclide production, sorption, and dispersion. I discussed radionuclide production briefly. I calculated the level of contamination of the explosion zone water by strontium-90 and tritium for an impossible conservative device that was 100 percent fission and 100 percent fusion. Actual nuclear devices lie between these extremes. Sorption and dispersion were discussed in detail.

Finally I predicted the migration of strontium-90 and tritium from the explosion zone through the hydrologic system. I demonstrated that strontium-90 produced by 1 megaton of fission would not represent a contamination problem under the worst believable conditions. Tritium will migrate from the explosion zone. It will move about 14.5 kilometers in 145 years before decaying to below MPC. Largest above MPC area will be less than 50 acres. The time of transit of the slug past any point will be less than 6 years.

A long-range study program is financed by the AEC and managed by the Effects Evaluation Division, AEC/ NVOO. This program provides for studies of sorption, dispersion, and other phenomena relevant to the prediction of migration of radionuclides in water. The results of these studies have provided improvements to our predictive capability. These improvements have always been in a direction indicating less ground water contamination than previously predicted.

BIBLIOGRAPHY

1. Carslaw, H. S. and J. L. Jaeger, "Conduction of Heat in Solids," London, Oxford at the Claredon Press, 110 p. 1959

2. Holly, D. E. and P. R. Fenske, "Transport of Dissolved Chemical Contaminants in Ground Water Systems, " Geol. Soc. Am. Memoir 110, pp. 171-183, 1968

3. Leipunsky, O. I., "Radiation Hazards from Clean Hydrogen Bomb and Fission Atomic Bomb Explosions," Atomic Energy (USSR) 3, p. 530, 1957; Translated in U. S. Congressional Hearings on Fallout from Nuclear Weapons Tests, pp. 2423-2447, May 5-8, 1959

4. Miskel, J. A., "Characteristics of Radioactivity Produced by Nuclear Explosives," in Engineering with Nuclear Explosives, Proc. Third Plowshare Symposium, Davis, Calif., April 21-23, 1964, TID-7695, pp. 153-158

5. Nork, W. E., Personal Communication, 1968

6. Skibitzke, H. E., "The Use of Radioactive Tracers in Hydrologic Field Studies of Ground Water Motion, "Extrait des Comptes Rendus et Rapports — Assemblee General de Toronto, 1957 (Gentbrugge, 1958) Tome II, pp. 243-252

Chapter 8

GROUND MOTION AND STRUCTURAL RESPONSE INSTRUMENTATION

Kenneth W. King, *Chief of Party*
U.S. Coast and Geodetic Survey, Las Vegas, Nevada

INTRODUCTION

The U.S. Coast and Geodetic Survey (USC&GS) has measured ground motion from nuclear events beginning with the Bikini Atoll testing in 1946. Since that time a special field party has been assigned from the Coast and Geodetic Survey Albuquerque Research Laboratory and the West Coast district office to measure ground motion and structural response from energy generated by underground nuclear explosions.

The field party generally consists of 20 to 25 personnel who are qualified electronic technicians and have 1 to 8 years of training and experience in seismology. The party's staff consists of a geophysicist, a physicist, an engineering geologist, and a seismological engineer. Technical assistance is furnished by the C&GS Albuquerque Research Group and a Rockville, Maryland, analytical section.

The Special Projects Party was permanently assigned to the Las Vegas area in 1961 to support the Atomic Energy Commission under the direction of the Effects Evaluation Division, Nevada Operations Office (NVOO). This support includes:

1. Measurement of the various parameters of ground and structural motion. Specifically, particle displacement, velocity, and acceleration at selected stations on and around the Nevada Test Site, supplementary test sites, and Plowshare sites.
2. Instrumentation of seismic anomalies and ambient conditions.
3. Operation of continuously recording seismic instrumentation at Mercury, Las Vegas, and Tonopah, Nevada. Data obtained from these instruments are integrated into the national C&GS seismic net.
4. Dispersion of high quality data to AEC contractors and supporting agencies for information and analysis.
5. The responsibility of acting in an advisory capacity to the Manager, NVOO, on various aspects of seismic phenomena.

DESCRIPTION OF INSTRUMENTATION AND CALIBRATION METHODS

The Coast and Geodetic Survey Special Projects Party presently utilizes four major and four minor seismic systems in fulfilling their program objectives of measuring nuclear event caused ground motion, structural response, structural vibration, and seismic wave propagation studies. Major seismic instrumentation systems are: the strain gauge accelerometer, the C&GS strong motion accelerograph, the NGC-21 velocity seismometer, and the L-7 velocity seismometer. The minor systems are: the Wood Anderson displacement gauge, the EV-300 and 301 displacement gauge, the long and short period Benioff velocity seismometer, and the Sprengnether portable blastmeter.

The Wood Anderson, Benioff, EV-300 and 301, and Sprengnether seismographs were systems used in the early stages of subsurface testing at the NTS. Since that time, advances in electronics and magnetic circuitry technique have been responsible for development of seismic instrumentation systems with higher reliability, more precise field calibration, and wider dynamic ranges of sensitivity and frequency response. These improvements allow a more complete analysis of ground motion and response measurements for the AEC Safety Program.

Development of new field seismic systems require the consideration of two basic objectives. These are: (1) an attempt to fulfill the required data acquisition parameters; and (2) to be operational under all field conditions. The definition of these objectives is established and continually reevaluated by a Panel of Consultants to the AEC.

Continued improvement in field operations and instrumentation are the goals of the AEC through the USC&GS. The acquisition of new field seismic systems have resulted in less man-hours per station, more precise calibration, higher reliability of data, and an expanded data spectrum.

Figure 8.1 shows response curves of four different types of seismic instruments. Note that no single instrument
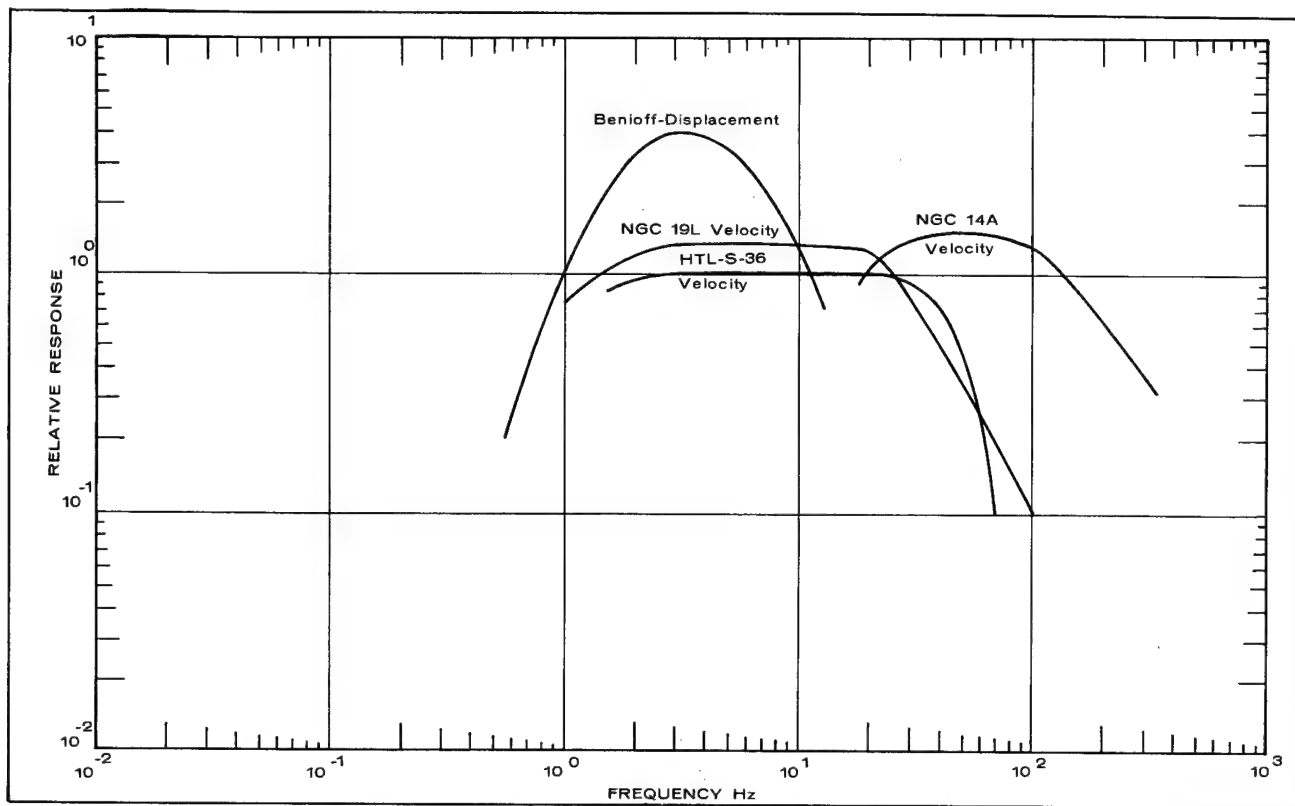
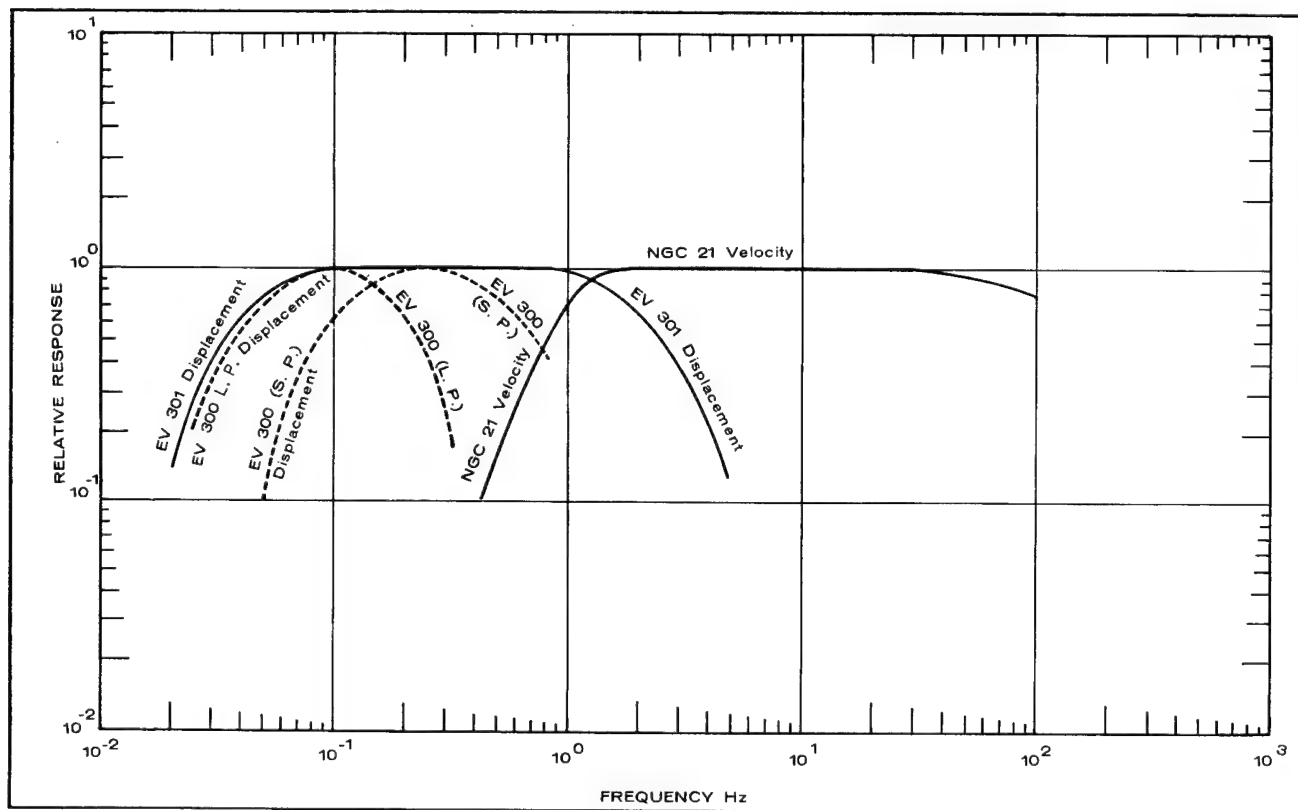Figure 8.1. Frequency Response Curves for Various Seismograph Systems.

Figure 8.2. Frequency Response Curves Showing Extension of Response for Various Seismograph Systems.

84

covers the desired frequency range of 0.1 to 100 Hz without deviation in signal output. The NGC-21 velocity seismometer and other seismic instruments were developed to extend the frequency response. The NGC-21 seismometer response curve as shown in Figure 8.2 covers a frequency range of 1.0 to 100 Hz with almost no deviation in signal output. This is the frequency range previously covered by all of the instruments indicated in Figure 8.1. While the NGC-21 was in use exclusively, frequencies between 0.1 and 1.0 Hz were being covered by the EV-300 and -301 displacement meters. Finally, the L-7 velocity seismometer was developed, having a frequency response of 0.1 to 100 Hz with little signal output deviation, as shown in Figure 8.3.

Strain Gauge Accelerometer System

The strain gauge accelerometer is a linear response, demountable transducer. The conditioned signals from this gauge are recorded directly as acceleration in analog form on magnetic tape. This instrument has a dynamic range of approximately 0.02g to 5g, the lower limit being governed by the system's signal to noise ratio. Briefly, the accelerometer utilizes a nonpendulous type

mass suspension for very low cross axis sensitivity and is 70 percent critically damped by viscous oil shearing. Generally, 12 channels of data are recorded on a 14-channel magnetic tape recorder. This accelerometer will measure g with little signal deviation due to frequency in the range of 0.5 to 300 Hz.

The strain gauge accelerometer has two general applications: (1) the gauges are used to measure particle ground motion at close-in areas which are defined as receiving 1.0g or more acceleration, and (2) to measure the response of experimental structures on the test site. The 1- x 2- x 1-inch size of the gauge lends itself to convenient mounting and proper coupling with most structural members.

Calibration of the strain gauge accelerometer is performed in place, and can be accomplished either electrically or mechanically. The electrical method is more accurate for most purposes. All calibration resistors are within tolerances that enable instruments to be calibrated to plus or minus 1 percent of the desired value. Our experience indicates that accuracy of data produced by this instrument under field conditions is 90 to 97 percent dependent primarily on signal to noise ratios.
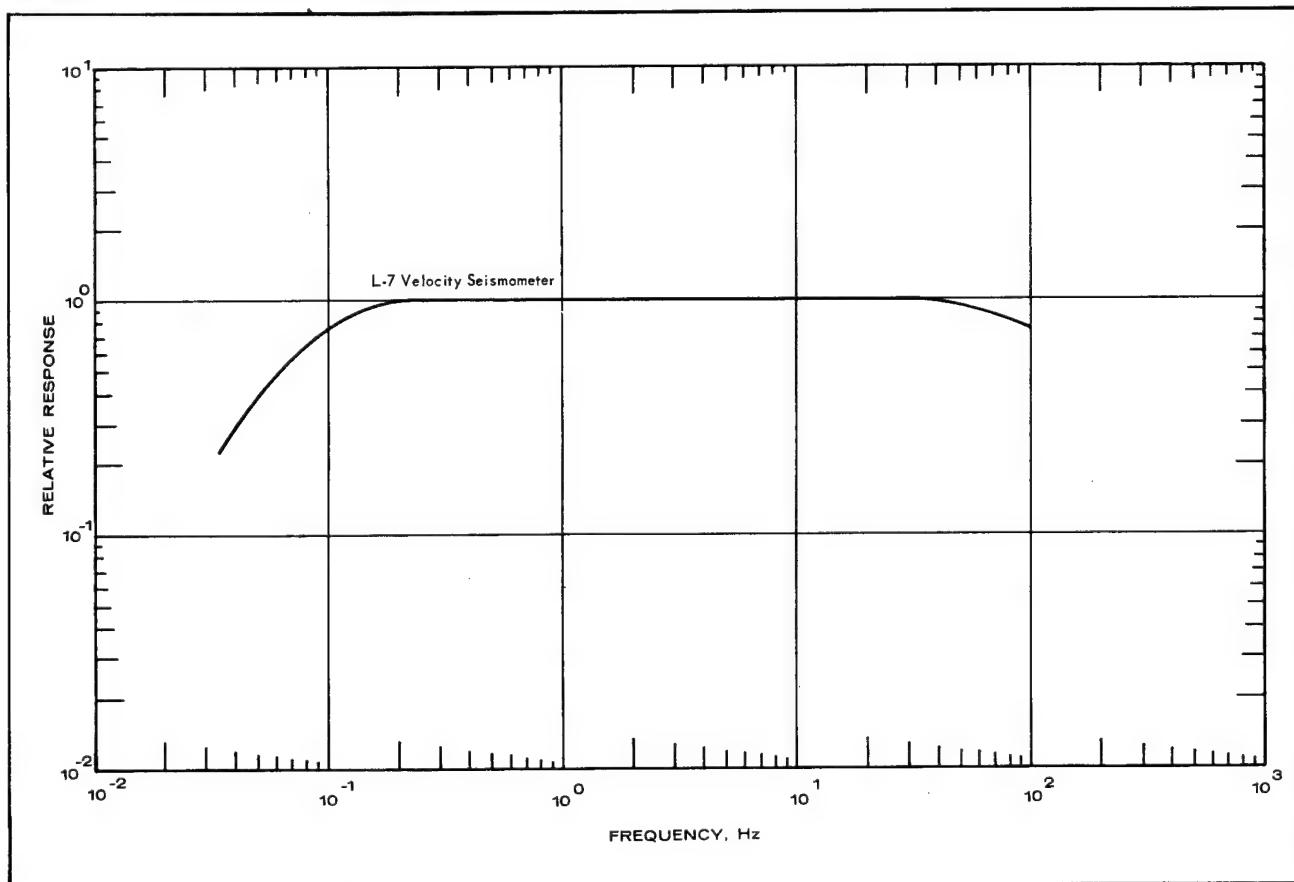

Figure 8.3. Frequency Response Curve for L-7 Seismograph System.

85

Strong Motion Accelerograph

The standard C&GS strong motion accelerograph is a combination of six optical-mechanical instruments all packaged in one container, which records earth or structural motions directly in parameters of particle acceleration and displacement on 12-inch photographic paper. The six instruments that comprise the accelerograph are: three C&GS accelerometers mounted orthogonally, and three Carder displacement meters also mounted orthogonally. The instrument can be started manually, by remote radio signals, or by a motion activated pendulum starting mechanism. This starting device is a damped pendulum, preset at a calibrated swing distance. When the pendulum exceeds this swing distance, a contact will close that activates the system. Therefore, a moderate earthquake will start the unit. Usually this start system is used to activate the accelerograph between nuclear events for recording earthquakes and structural motion caused by high winds. Figure 8.4 shows a complete accelerograph unit.

Accelerometer

Figure 8.5 suggests a closer look at a C&GS horizontal accelerometer will show that it is a torsion instrument with an inertial mass suspended eccentrically on a vertical unifilar suspension so that it acts as a horizontal pendulum. The pendulum period is controlled by torsional reaction in the fiber and a small gravity component that can be varied for the desired sensitivity. The vertical accelerometer in Figure 8.6 has a horizontal unifilar element whose period can be varied according to the desired sensitivity. A small concave mirror is attached to the loop-vane mass of the accelerometers. This mirror, by an incandescent light reflection method, allows optical lever magnification and affords direct recording on photographic paper. The accelerometers have a static magnification of approximately 120, damping of 57 percent critical, and instrument periods from 0.02 to 0.18 of a second which corresponds to a sensitivity range of 1.0 to 70.0 centimeters per unit of gravity on the recording paper. The accuracy of data from the accelerometer is generally between 90 to 98 percent depending on the optics of the optical-mechanical lever and signal to noise level. The frequency response of this instrument is acceptable from about 1 to 20 Hz depending on the instrument period.

Carder Displacement Meter (CDM)

The horizontal CDM in Figure 8.7 utilizes a compound inverted pendulum. A small concave mirror located on the axis of rotation of the pendulum permits optical-mechanical magnification of the pendulum motion, and provides a means of recording on photographic paper. The vertical displacement meter consists of a small disk mounted on pivot and jewel spindles. The effective pendulum length is governed by offset weights on the rim of the disk with coiled springs supplying the balance-restoring force. Magnification of the displacement meter is near unity with a normal instrument period of approximately 2.5 seconds. The CDM has an acceptable frequency response between 0.3 and 100 Hz. Accuracy of data from this instrument is from 90 to 98 percent depending on the signal to noise ratio.

The C&GS accelerographs have been used for earthquake recording since the 1930's. Many of the basic earthquake zoning laws and building criteria were developed from data obtained by these units. For earthquake purposes, the instruments are usually installed at the top and at the bottom of a structure. On underground nuclear events, the equipment is installed in structures, measuring from as low as 0.005g to beyond the 1.0g range on the ground.

Calibration

The C&GS accelerometers have been calibrated mechanically by the Bureau of Standards and the Coast and Geodetic Survey on shake tables which are driven with a calibrated frequency and amplitude. The accelerometers are also tuned and calibrated to predicted sensitivities in the shop before field installation. After installation in the field final calibrations are made and sensitivities are compared with shake table and shop data. Should there be a discrepancy between the field calibration and other various calibrations, the instrument is replaced.

The CDM magnifications are varied by changing the size of the pendulum and the weight of the mass on the pendulum. A gravity test is made of each displacement meter before installation. The gravity test consists of preswinging the pendulum and setting the period to the desired magnification. After the instrument is installed in the field, the period, damping, and optical distances are remeasured. Any discrepancy between the field calibration data and the shop data would result in replacement of the equipment.

NGC-21 Velocity Seismic System

As shown in Figure 8.8, the basic NGC-21 seismic system consists of three orthogonally oriented seismometers, a five-stage amplifier, and a recorder (either a magnetic tape recorder or a photographic recorder, NGC-4-D oscillograph). The NGC-21 seismometer is a versatile instrument with a period of 1.0 second, plus or minus 0.5 percent, and a basic sensitivity of 2.89 volts per cen-
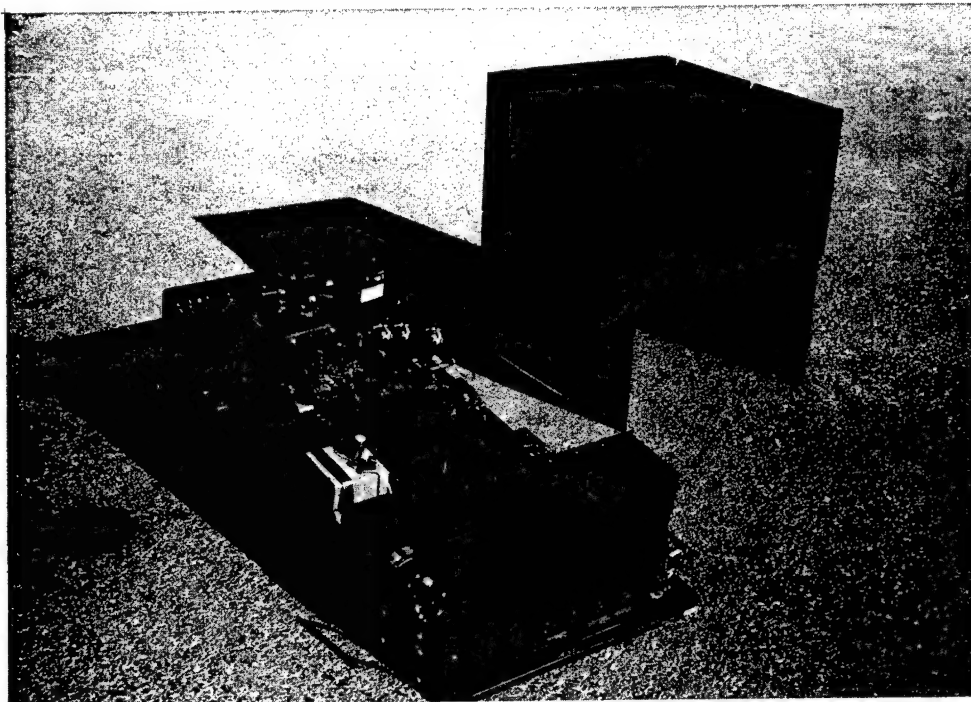
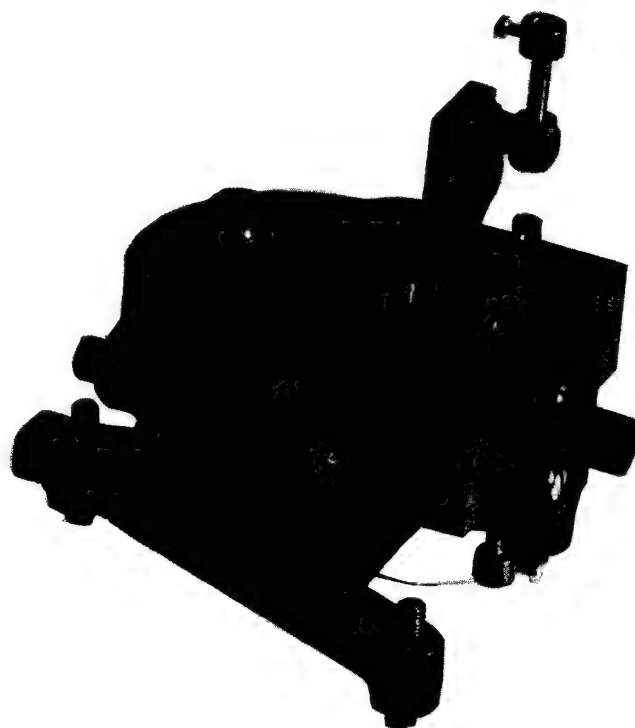Figure 8.4. Strong Motion Accelerograph.
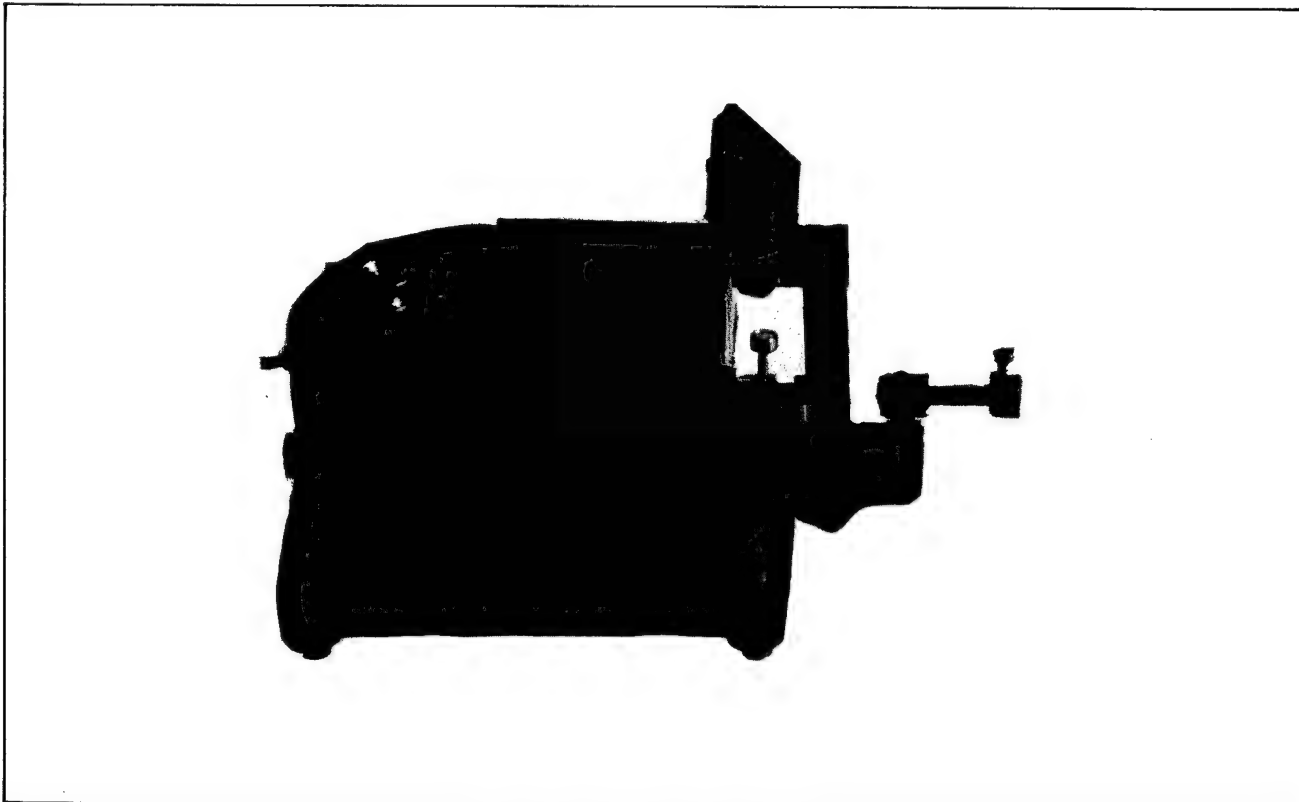

Figure 8.5. Horizontal Accelerometer.

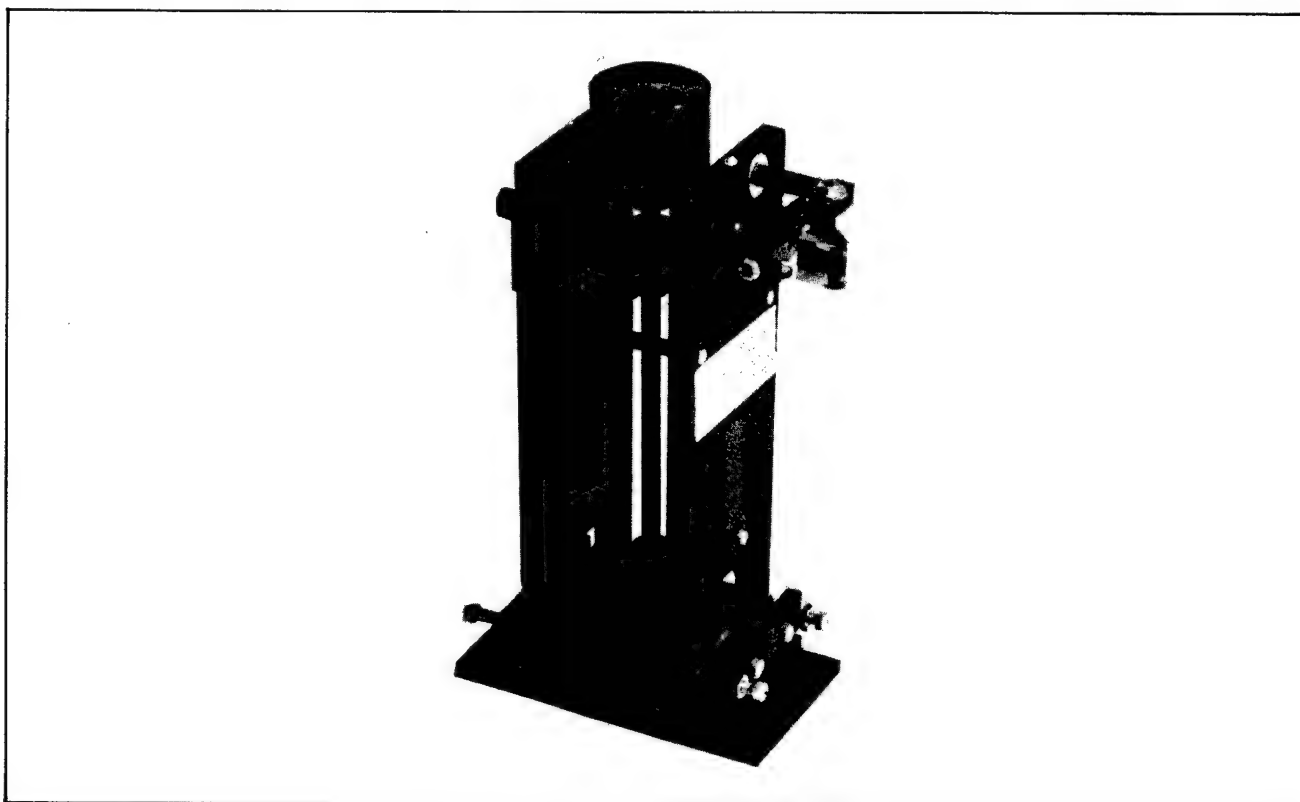Figure 8.6. Vertical Accelerometer.

Figure 8.7. Carter Displacement Meter.
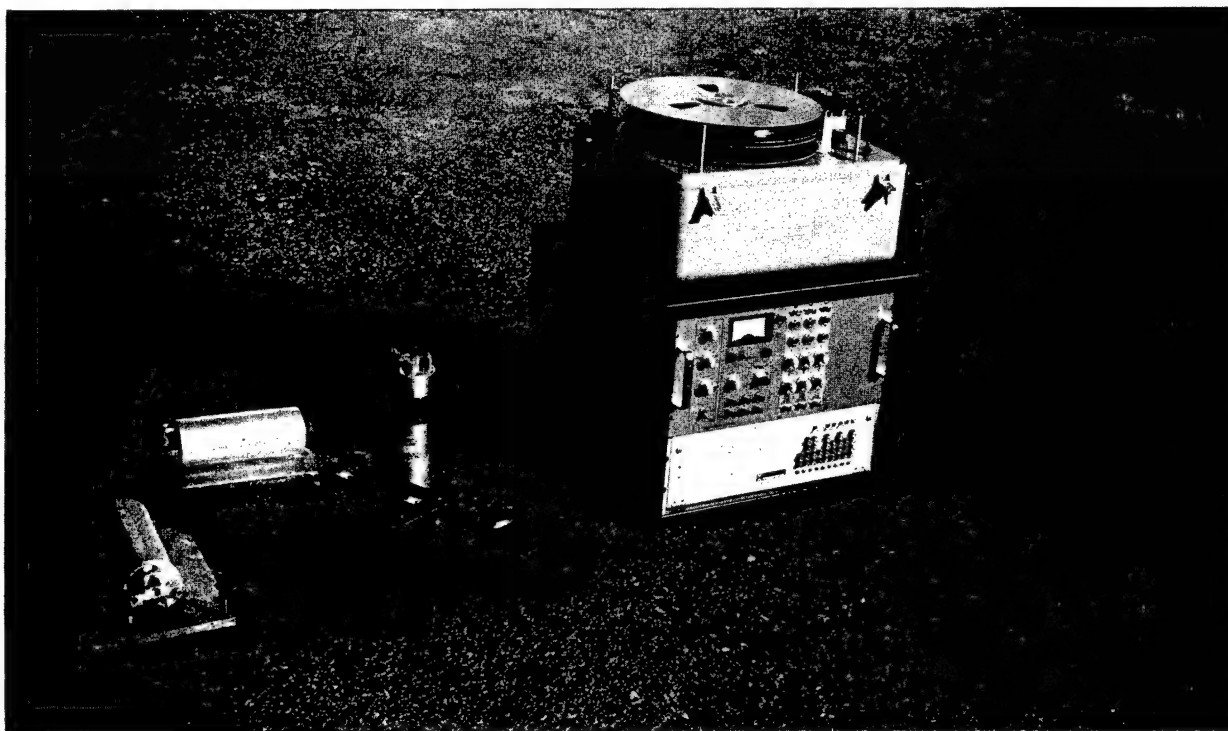
Figure 8.8.　NGC-21 Velocity Seismic System.

Figure 8.9.　L-7 Seismograph System.

89

timeter per second. The 12.7 millimeter peak-to-peak travel of the 12.0 kilogram seismic mass allows the instrument to handle a variety of ground motion levels.

A five-stage amplifier is used in the system which has a noise level sufficiently low to permit the recording of motions with a displacement as small as 1.0 angstrom. The high frequency response of the five-stage amplifier is controlled by a variable filter which has 11 positions of high frequency cutoffs from 16 to 100 Hz.

The NGC-21 was designed for the Coast and Geodetic Survey to record velocities as low as 10^{-8} centimeters per second and as high as 17 centimeters per second with flat response in the period range of from 0.01 to 1.0 second. The system is used for both structural response and ground motions from earthquakes and underground nuclear detonations.

This instrument is calibrated on the shake table yearly at the C&GS Albuquerque Research Laboratory. Tests confirm system characteristics and can be combined with a standard sine-wave calibration made in the field, resulting in a reliable calibration. The normal accepted accuracy of the instrument under field conditions is plus or minus 5 percent, which is dependent on signal to noise ratios.

L-7 Seismograph System

The L-7 seismograph system as shown in Figure 8.9 is the latest and most up-to-date system used in the AEC/NVOO Ground Motion and Structural Response Safety Program. The seismic system consists of L-7 seismometers, integrating amplifiers, time code generator, and frequency modulated (FM) magnetic tape recorder.

By a method of overdamping, the L-7 has an output voltage proportional to acceleration instead of velocity. Figure 8.10 illustrates several arbitrary frequency response curves for various damping ratios. It is shown that a typical velocity seismometer of the L-7 type when undamped has a natural resonant frequency of about 1.875 Hz, cycles per second. As electrical damping is applied, the curve smooths out until a point is reached that is known as critical damping. The critically damped condition occurs when the number 5 curve in Figure 8.10 exhibits a flattened out condition. This output is proportional to velocity and may be measured in volts per centimeter per second.

Seismometer engineers have expanded the seismometer damping and response phenomenon by damping in ex-

cess of the critical damping. When an L-7 transducer is damped in excess of 10 times critical, the voltage output is proportional to acceleration rather than velocity over a portion of the frequency spectrum. Figure 8.10 shows the curve continuing up as an acceleration curve instead of leveling off as a velocity curve.

Before the signal output of the seismometer is recorded, it must be conditioned. In this case, an integrating amplifier is used to amplify and integrate the incoming signal. Electronic integration of an acceleration signal transforms it into a signal representing velocity which is then recorded on magnetic tape. The reason for changing the output mode of the L-7 velocity meter to acceleration and back to velocity is for the effect this process has on the dynamic range of the transducer. Damping restricts the movement of the coil relative to the fixed magnets in the instrument case. This allows the transducer to measure stronger motions. An undamped seismometer coil has a tendency to exceed its range of travel and therefore to hit the stops above and below its spring suspension, thereby distorting the signal.

As we know, the integral and differential of velocity is displacement and acceleration, respectively. If acceleration and displacement data are desired, they may be derived from the velocity data, minimizing possible error involved in a double integration from acceleration.

Perhaps the most important component of the L-7 seismic system is the magnetic tape recorder. This machine can record 14 channels of data simultaneously through its frequency modulated record amplifiers. Two additional channels are also available for recording time code signals and any other information that may be necessary. Most advantageous is the ability of this unit to record continuously and unattended in the field for 5.3 days. This extended recording capability is made possible by the very low tape speed of 3/16 inches per second and 7,200 feet of magnetic tape on a 14-inch diameter reel.

Many advantages are derived from using a magnetic tape machine with an extended recording capability. For example, this system completely eliminates the necessity for remote starting procedures at zero time (the time of nuclear detonation) such as radio tone signals, relay closures sent via long runs of field wire or personnel standing by to turn the machines on manually. The recording systems are turned on approximately 24 hours before a scheduled underground nuclear detonation and left running through the event. If the event is delayed 24 to 96 hours the recording capability is unimpaired and there is no need to check the equipment. With delays of over 4 days (which rarely occur) the machinery would have to be reset.

Since the zero time signal is not recorded on the tape, a time code generator is incorporated in the system. The generator encodes the year, day, hour, minute, and second in a 10-second time frame on the tape. This time code syncronizes with the time signal as broadcast by radio station WWV near Fort Collins, Colorado.

Complete electronic test circuitry is built into the L-7 seismic system. This circuitry enables the system to be fully calibrated in the field. Calibration includes dynamic range settings for seismometers, amplifiers, tape recorder, and time code generator with reference to distance and nuclear device yield.

APPLICATION OF EVENT INSTRUMENTATION

Seismic instrumentation is used for both nuclear event and non-nuclear related applications. Structural response instrumentation represents one of the two primary efforts being expanded by the C&GS in support of the Atomic Energy Commission's Safety Program. Because some underground explosions at the Nevada Test Site and various other test sites release enough energy into the ground to cause some ground and structural motion in nearby communities, the AEC feels this motion should

be recorded and documented. The reasons for documentation will be given by the AEC's Structural Response Analysis Contractor in Chapter 10.

Some seismic instruments are semipermanently installed in high rise buildings in Las Vegas to measure the effects of motion from natural earthquakes and high winds as well as underground nuclear explosions. Structural response records from underground nuclear explosions, natural earthquakes, and high winds are compared and conclusions reached, many of which are pertinent to the AEC's testing program at the Nevada Test Site.

Many high-rise structures have been instrumented in Las Vegas. These buildings include the Sahara, Mint, Horseshoe, Sands, Landmark, Riviera, Caesars Palace, Stardust, Desert Inn, Fremont, and Dunes Hotels and the Bank of Nevada, First National Bank, and Clark County Court House. Instruments have also been placed in the Exchange Club in Beatty, the Belvada, Ramona, and Mizpah Hotels in Tonopah, and the Court House in Goldfield.

Although not specifically for the AEC, seismic instruments are also operated in and around Hoover Dam. Instrumentation in these structures includes the C&GS
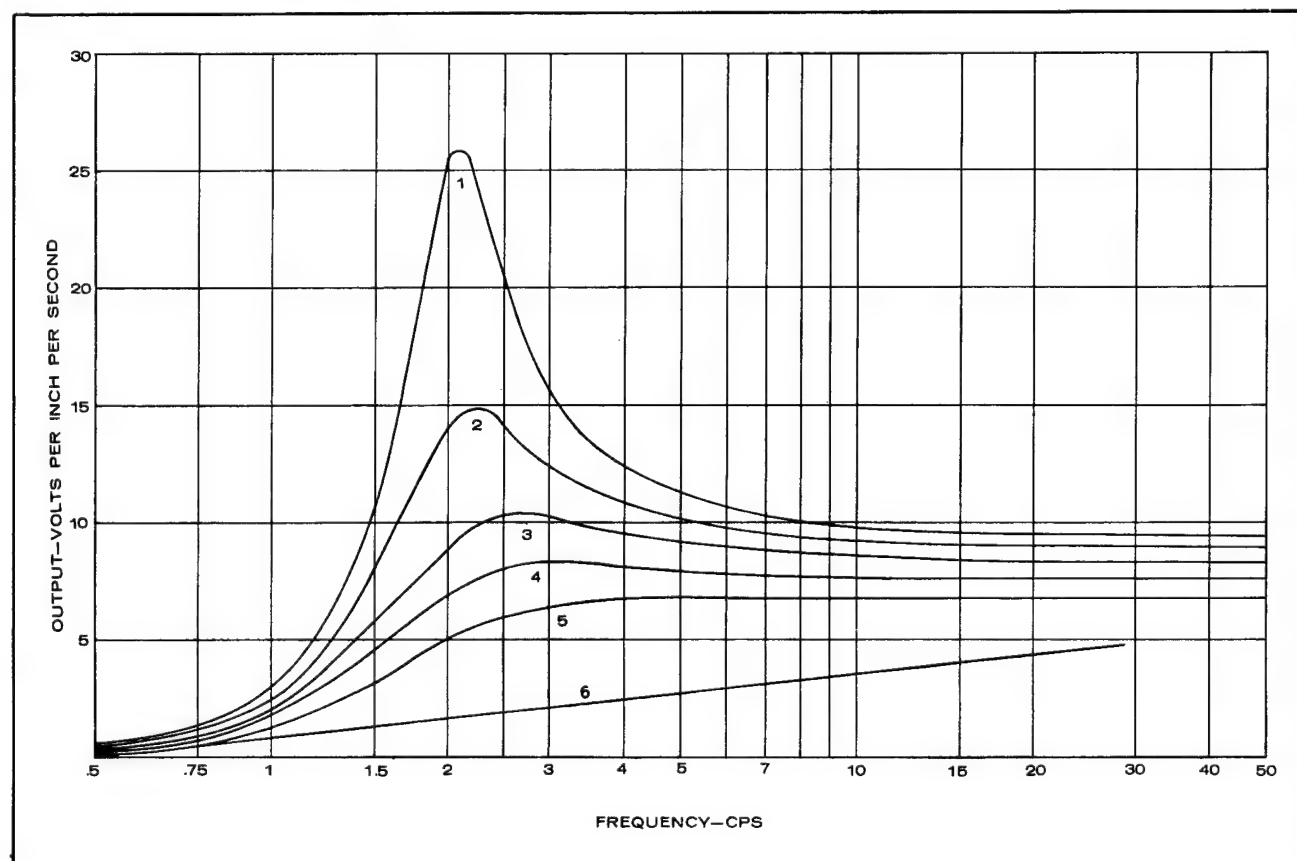

Figure 8.10. Variance in Sensitivity With Frequency Response Due to Damping.

91

accelerograph and on special occasions, the L-7 velocity system. It may be interesting to note that approximately 650 records have been made in these high-rise structures in order to systematically document their motions.

The second most important effort of the C&GS Special Projects Party is the seismic instrumentation of various ground stations within and surrounding the NTS (and other test sites) for ground motion generated by energy released from underground nuclear explosions. The AEC's Ground Motion Analysis Contractor utilizes these data for theoretical and empirical studies which compare actual and predicted motions. As a result, predictions of motion at these and other stations can be made for various and increasing yields. The Structural Response and Ground Motion Contractors explain in Chapters 9 and 10 to what degree the ground motion must be known if structural response is to be predicted.

Ground motion for events at the Nevada Test Site and the central Nevada test site is usually recorded at stations on the Nevada Test Site, Las Vegas, Alamo, Tonopah, Beatty, and Goldfield. Some of these stations record ground motion from both nuclear events and natural earthquakes. C&GS accelerographs, NGC-21 velocity systems, and L-7 velocity systems are primarily used to accomplish these objectives. The stations mentioned here are not the only ones instrumented. If a need to fill data gaps or document perceptible motion arises, seismographs are installed in other areas of interest.

When a nuclear event has been scheduled, instrumentation plans are submitted to the Effects Evaluation Division, Nevada Operations Office. These plans which contain requests for ground motion and structural response instrumentation are evaluated, coordinated and altered as necessary. When finally approved, they are turned over to the C&GS for implementation. Instruments are thoroughly checked and carefully calibrated before installation in the field. A final calibration is made as close to event time as possible. After an event the seismic records are promptly recovered and processed. Records from some selected stations are analyzed within hours after an event by the NVOO Effects Evaluation Division.

A unique nuclear detonation was event Faultless for which the C&GS deployed seismic instruments at ranges from 4 to over 500 kilometers from surface zero. The Faultless seismic program called for the use and operation of about 130 seismic stations. Instrumentation was loosely divided into three areas of interest: short, intermediate and long range. The short range area from 4 to 15 kilometers was instrumented with strain gauge accelerometers and C&GS accelerographs, capable of re-

cording strong ground motions of 1.0g and above. The intermediate range, 15 to 85 kilometers, was instrumented with accelerographs, L-7 velocity systems, and NGC-21 velocity systems. Long range, 85 to 500 kilometer stations were also instrumented with NGC-21 and L-7 velocity seismic systems. Figure 8.11 is a map of the area covered by the instrumentation plan. The indicated seismic stations measure velocity, utilizing the NGC-21 velocity systems relatively close-in where C&GS personnel were situated. The L-7 velocity systems with 5-day tape recorders were used at longer distances and in more remote areas. Velocity seismometers are normally used at greater distances than strain gauges or accelerographs because they have high sensitivity and are easily operated making them ideal for extended range locations. Besides those seismic stations shown in Figure 8.11, there were a number of semipermanently installed accelerographs operated for Faultless in Las Vegas, Tonopah, Alamo, Beatty, and on the Nevada Test Site.

The close-in Faultless instrumentation is shown in Figure 8.12. The seismic stations shown here utilized strong motion type instruments; strain gauge accelerometers comprise the "Y" array, and the rest of the stations are C&GS accelerographs.

One example of instrumentation for an event on Pahute Mesa was that of Boxcar. Over 90 seismic stations were operated, from a distance of 4 to 550 kilometers. Figure 8.13 again gives an overall view of the area instrumented, showing Boxcar surface zero and the seismic stations at intermediate and long ranges. Note that a number of the cities (Salt Lake City, San Francisco, etc.) instrumented for event Faultless were also instrumented for Boxcar. Also more stations were operated in and toward Las Vegas. Figure 8.14 shows additional detail of the seismic stations in Nevada.

NONEVENT RELATED APPLICATIONS

The C&GS pursues several other projects that are not directly event related but whose results have effects upon event related work. The accelerograph is frequently used as a continuously recording seismograph. This does not mean that the instrument is running all the time, but is in a continuous state of readiness. It can be activated by its pendulum start mechanism any time a detectable motion occurs, as may happen during a high wind or in the event of an earthquake. Such data may provide insight into how a structure responds to other forcing functions, and is thus of interest to the Structural Response Contractor. The L-7 velocity system is also used for the measurement of forcing functions in structures but it is started manually.
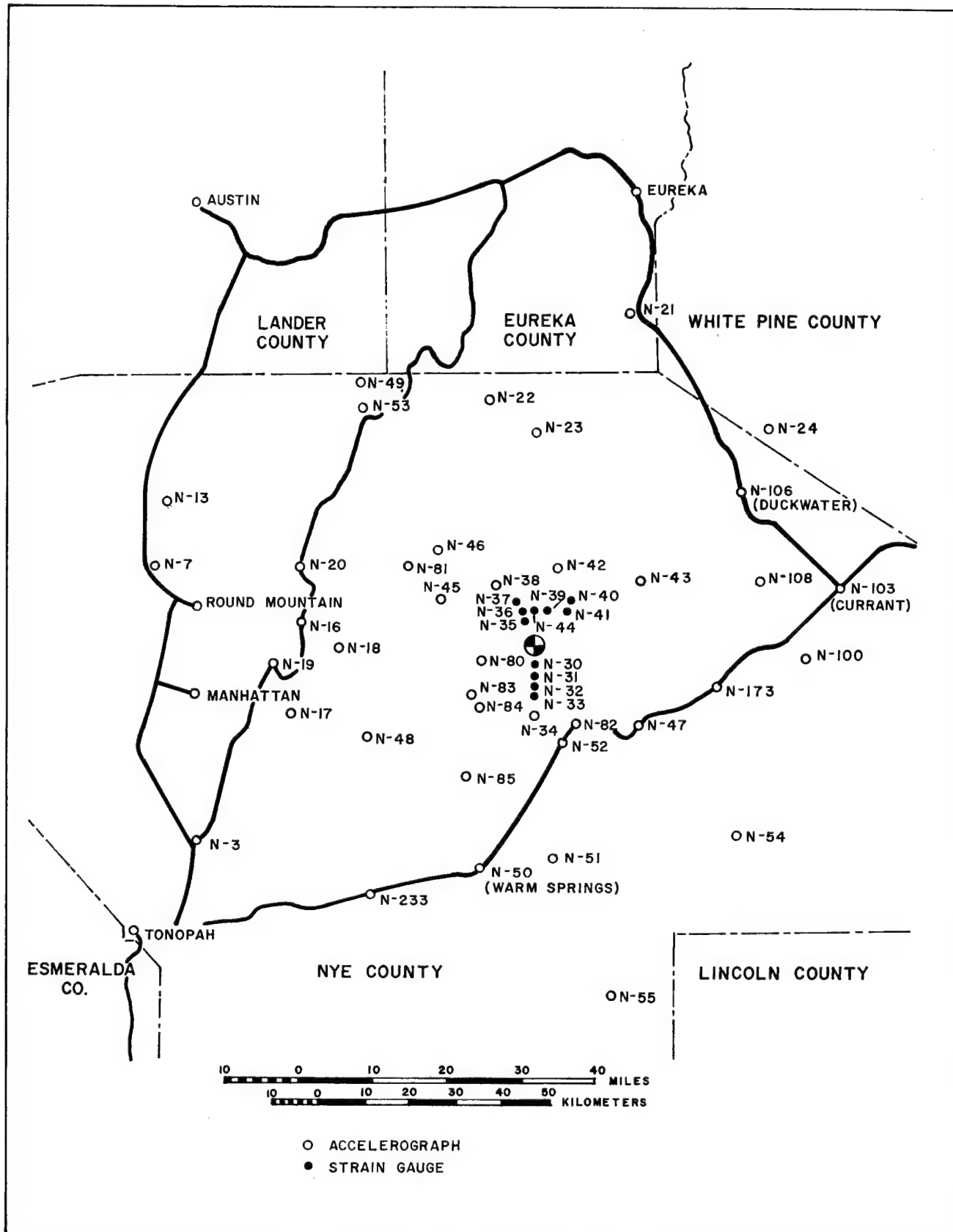
Figure 8.11. Faultless Event Velocity Instrument Locations.

93

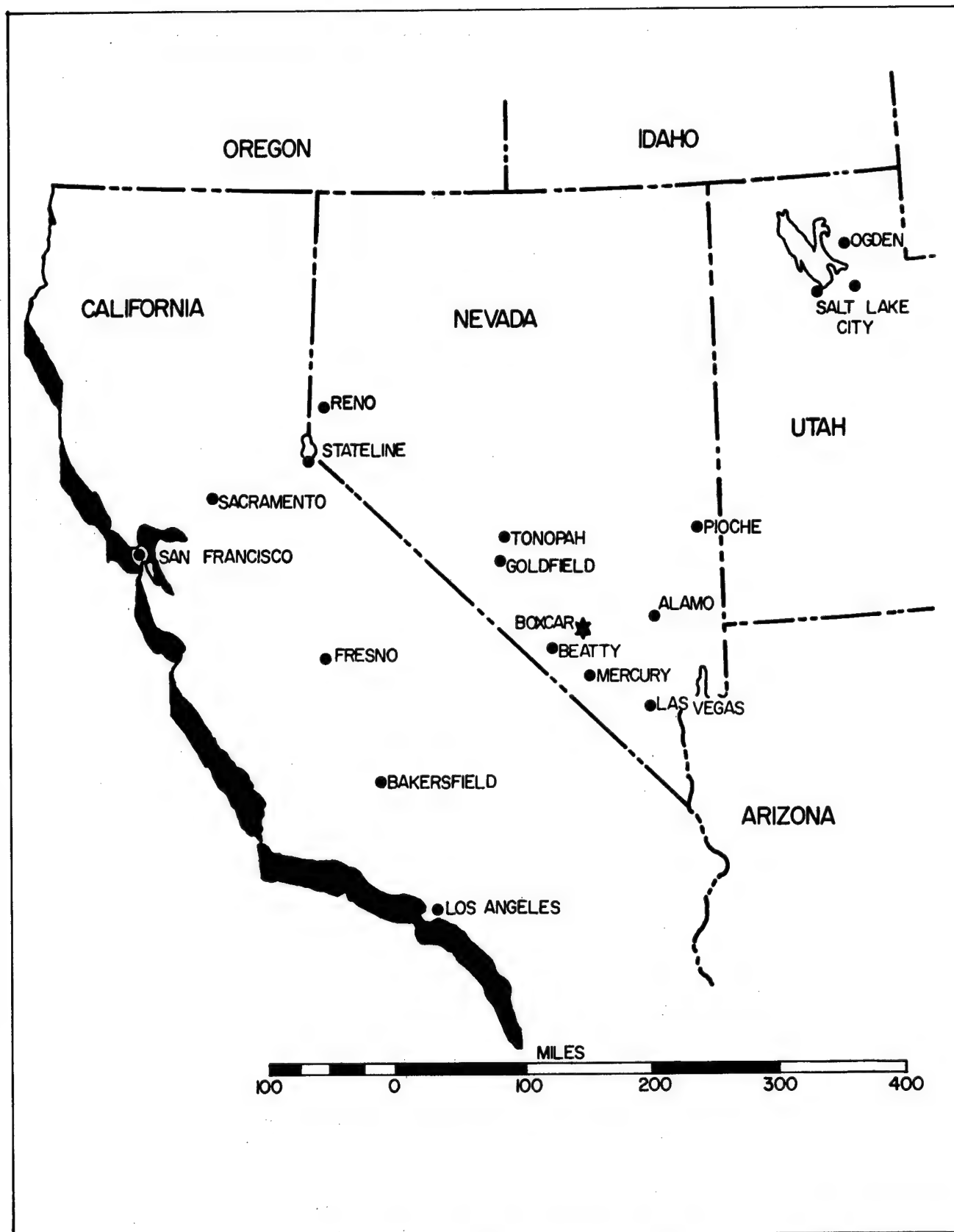Figure 8.12.   Faultless Event Close-In Instrumentation.

94

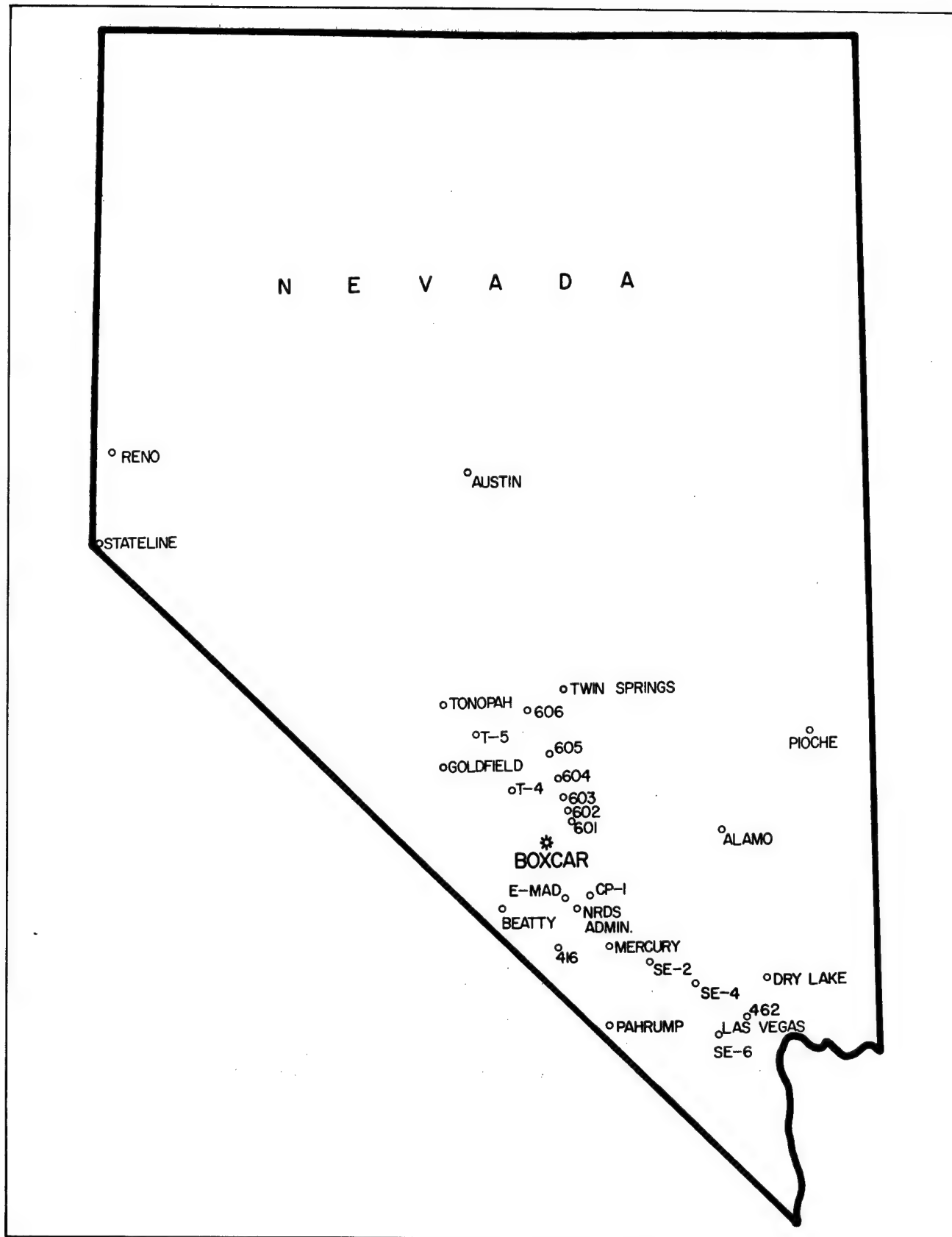Figure 8.13. Boxcar Event Velocity Instrument Locations.

Figure 8.14. Boxcar Event Close-In Instrumentation.

Other structural response measurements include the instrumentation of several sets of experimental structures on the NTS in the forward areas. These structures are built in locations where damage from ground motion associated with underground nuclear explosions is probable. The instrumentation requirements for these structures are, of course, designed by the AEC's Structural Response Contractor to suit his theoretical and analytical analysis methods. Instrumentation and vibration of high-rise buildings are also responsibilities of the C&GS. Structures are excited into motion by human vibration techniques, the force of wind, or by mechanical vibration devices and these vibrations are recorded for calculation of the building's fundamental and, if possible, higher modes of vibration.

Other activities include research into amplification of ground motion, as related to the depth of alluvium and frequency. This project is being conducted on a dry lake northeast of Las Vegas.

A definition of ground motion station near surface lithology is being pursued by running short seismic refraction profiles in close proximity to these stations. Compressional wave propagation velocity is measured through the near surface medium. The velocities of the medium can then be used to quantitatively define the thickness of the medium on which the ground motion measurements (from nuclear detonations, or natural earthquakes) are to be made.

DATA PROCESSING

The C&GS maintains a magnetic tape playback and dubbing facility in Las Vegas, Figure 8.15. This system consists of several magnetic tape machines, galvanometric oscillographs, time code display units, and a time code tape search system.

The time code tape search system is particularly important. After a nuclear event, the actual data are recorded on probably less than 2 feet of a 7,200-foot reel of magnetic tape. To look for these data manually would be an arduous task at best, considering there are in excess of 40 tapes. However, with the time of the event known, and the time code recorded on the tape, the automatic search system can find these data on the tape very rapidly. Data from many velocity units can be found this way and dubbed onto a single tape with all of their calibrations for ease in handling. These tapes are then sent to the NVOO Data Anaylsis Contractors for processing and interpretation.

The playback facility also plays back data from tape onto paper records for rapid initial evaluation. The seismic records recorded on photographic paper are labeled with the appropriate station name, event name, and any other pertinent constants before being reproduced. The reproductions are then made available to the Data Analysis Contractors for their study.

Figure 8.15. Coast and Geodetic Survey Playback Facility in Las Vegas.

Chapter 9
GROUND MOTION

Environmental Research Corporation, Alexandria, Virginia

Part A — General

Lawrence L. Davis; *Executive Member, Technical Staff*

The Environmental Research Corporation (ERC) is the Ground Motion Safety Contractor to the Atomic Energy Commission. The final responsibility for safety of every underground nuclear detonation at the Nevada Test Site rests with the AEC. ERC is responsible for providing predictions of ground motions and their effects on subsurface facilities. Together with consideration of other aspects of safety, this information enables the AEC to evaluate all safety aspects of each detonation.

In seven years of study on this subject, ERC has developed capabilities to provide accurate preshot predictions of ground motion generated by detonations at the Nevada Test Site. Additional studies are continuously being pursued to refine procedures and improve the accuracy and scope of preshot predictions.

To introduce various technical aspects of ground motion safety studies conducted at ERC, let us consider technical objectives, scientific technique available for achieving these objectives, and other resources being applied to the problem. The major objective is to predict quantitatively the ground motion at Las Vegas and other points of interest. These predictions are given to the Structural Response Contractor who evaluates their effect on structures. First, let us consider some of the aspects of this problem.

The ground motion recorded at a seismograph station from an underground nuclear explosion is the net result of a number of complex physical and mechanical processes (Figure 9.1). Physical processes take place mainly in the crust of the earth and the upper mantle when the source-receiver distance is small; i.e., less than 1,000 km. Mechanical processes involve seismometer coupling and instrumentation. Although difficult to generalize, these processes may be classified as occurring in three main areas: (1) the sources and hydrodynamic area, (2) the seismic or elastic wave transmission region, and (3) the receiver and near surface area. Physical proc-

esses which occur in these three areas are illustrated schematically in Figure 9.2, and may be described in a general way as individual parameters of a complex transmission system. The parameters may be listed as follows:

1. *The Source* — the nuclear explosion produces a signal which is close to the ideal shape of a Dirac delta function; i.e., a sharp impulsive disturbance with enormous amplitude. A perfect delta function has a white amplitude spectrum; i.e., all frequencies are present with the same amplitude.

2. *The Inelastic Region About the Source* — Immediately surrounding the explosion and extending radially outward for a distance, the rock behavior is extremely nonlinear and complex. Approximately 50 percent of the available energy immediately feeds a shock wave which propagates radially outward from the wall of the shot cavity. The general characteristics of the intense shock wave are a function of the explosive as well as the cavity geometry and the properties of the medium in which wave propagation takes place. These characteristics are known to be complex and are the subject of continuing research by many scientists such as Bishop (1963), Holzer (1965), Cassity (1966), Cherry (1966), and Reily (1967). As the shock wave propagates to still greater radial distances, the dissipative characteristics of the rock reduce the loading intensity to the point where the elastic properties of the medium begin to play a significant role.

3. *Normal Earth Filtering* — As the wave propagates into the seismic or elastic region, less than 5 percent of the original energy is generally available to propagate as elastic waves. As the signal propagates over a distance of a few km, the pulse changes shape, broadens in time, and decays in amplitude as a consequence of the earth's transmission

characteristics. Although the explosion generated a very wide band of frequencies, differential frequency attenuation and absorption by the earth reduces the transmitted disturbance to a rather limited frequency band. As a result, the signal is transformed into a spreadout oscillating wavelet. As the disturbance propagates through the earth, it encounters many major and minor geological boundaries. At each boundary, the energy is in part reflected and in part refracted; hence, a great variety of different transmission paths are generated. Other physical phenomena such as wave mode conversion, ghosting, reverberation within and between layers, scattering, and diffraction occur along each transmission path and compound the complexity of the total process. Processes such as ghosting and reverberation tend to introduce notches and resonant frequencies in the amplitude spectrum. Scattering causes attenuation which increases rapidly with decrease in wavelength of the pulse. This action causes the earth to tend to act as a high-cut filter to seismic signals.

4. *Geophone-Earth Coupling*—In the emplacements of seismometers, every effort is made by the USC&GS to insure a very high quality coupling of the instrument with the earth. Good coupling is difficult to achieve, but it is important in reducing the number of distorting effects acting on the propagating signal.

5. *Instrument Response*—The movement of the free surface of the earth is measured with a seismograph having a restricted bandwidth. This means that the output of a seismometer is a distorted version of the actual movement of the free surface. Noise, (defined as all the disturbances which appear on the seismogram, unrelated to the desired signals) also tends to complicate instrument response. Noise can consist of disturbances which are random in both amplitude and phase as well as disturbances having identifiable coherent properties. Random noise is made up of wind noise and noise related to cultural activities. Coherent noise is introduced by the recording and the data processing systems.

A little later we will outline some of ERC's studies on all these aspects of the problem. For now, let us look at a sample of nuclear generated seismic motion (Figure 9.3). The signal received at a seismometer is not a single
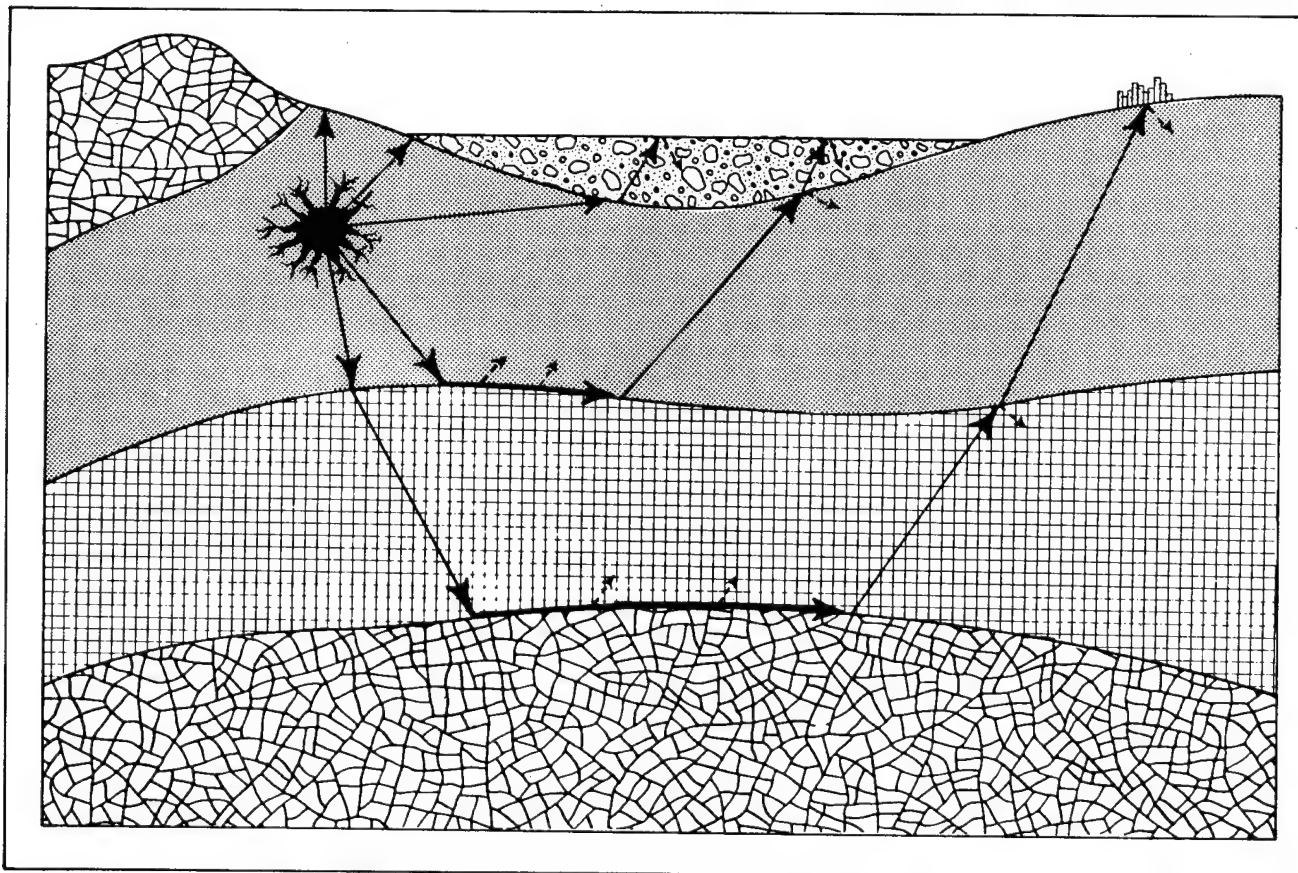

Figure 9.1. Transmission Model of the Earth for Seismic Waves from an Underground Nuclear Explosion.
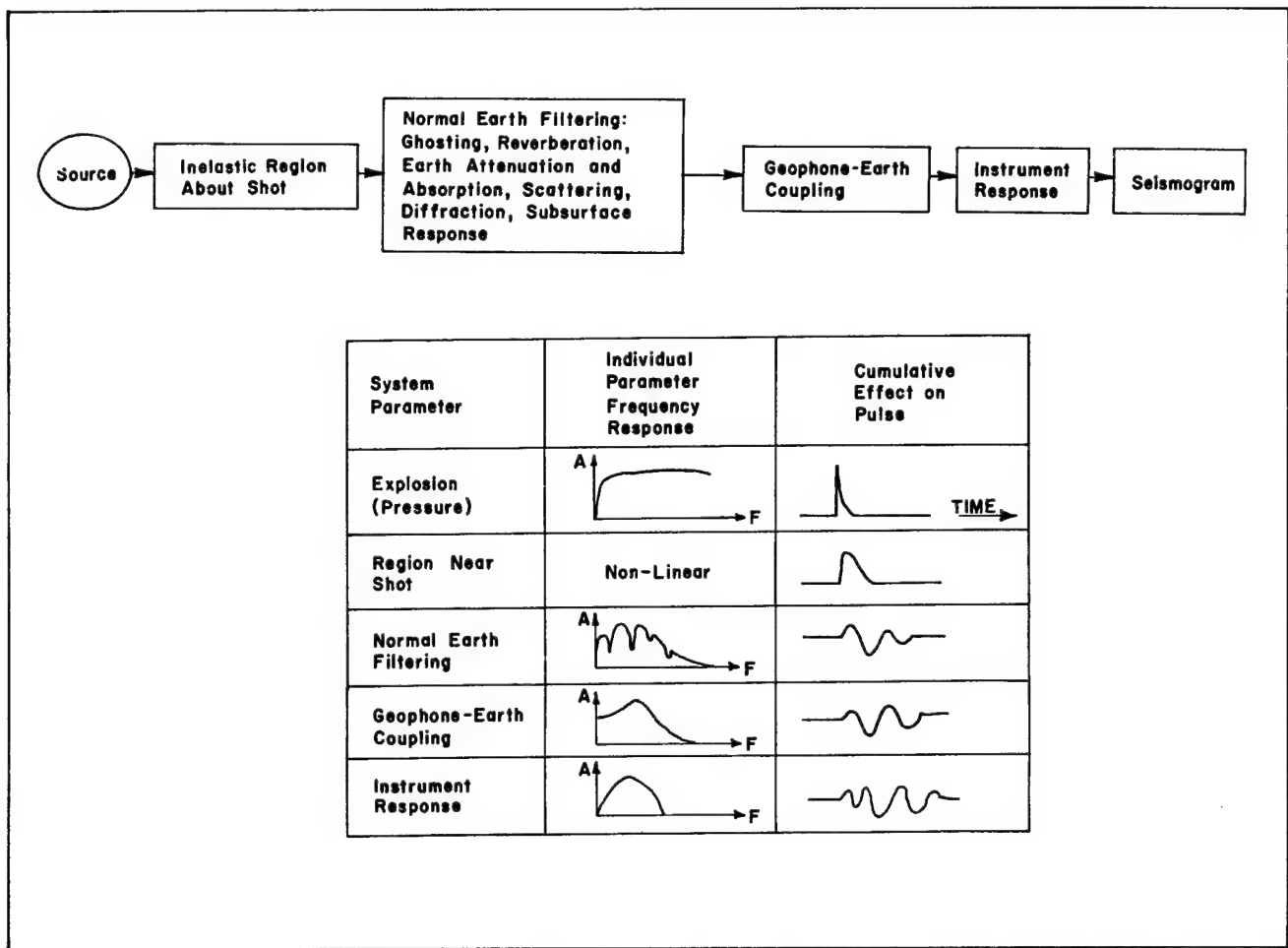
Figure 9.2. Schematic Diagram of Parameters of the Transmission Model of the Earth and the Effect of Each Parameter on a Propagating Pulse.
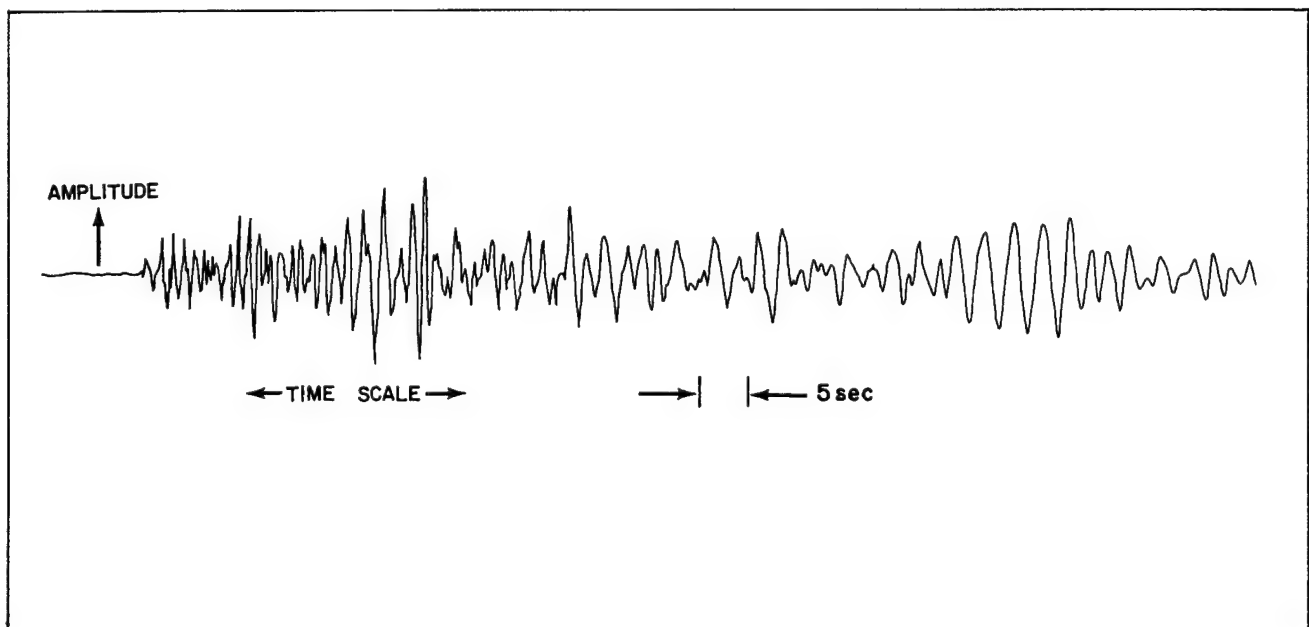

Figure 9.3. Example Seismogram from an Event at the Nevada Test Site.

101

wave. It represents the combined effect of waves from all the different transmission paths possible within the crust of the earth. In addition, spurious signals related to wave groups arriving from random directions, such as near-surface waves impinging upon randomly-located inhomogeneities, are present. The seismogram, therefore, may be thought of as representing the totality of response to impulses, each impulse being associated with a disturbance that has traveled a certain path in the crust and upper mantle by reflections and refractions.

This particular seismogram represents the vertical component of velocity measured at the base of the Dunes Hotel. The seismogram is corrected at ERC for the response of the recording instrument, in particular at those frequencies to which various structures respond.

Because of the complexities involved in elastic wave propagation and the inherent inaccuracy of the instrumentation, it is unlikely that all of the detail in a seismogram as shown in Figure 9.3 can be predicted with an accuracy of two significant figures. Even if the elastic region input wave function and all intervening geologic and physical parameters were known exactly, a completely deterministic solution would still be difficult.

The questions then arise, for what features or characteristics and in what sense should solutions to the ground motion prediction problem be sought. With the primary consideration that each study should relate to the structural response prediction problem, the following major characteristics have been investigated:

1. Peak Motion
2. Amplitude-Frequency Content
3. Wave Modes

Investigations in each of these broad categories were initiated in the order given although studies of each are continually being pursued. Peak motions were looked at first because they provide a rapid means of quantitatively describing the amount of motion generated. Relationships between amplitude, yield, and distances were developed and a reliable capability established. While this was in progress, equipment, programs, and methods for studying frequency were developed. The amplitude-frequency studies led to the present capability, which includes the prediction of frequency content and the response of a building model to the predicted motion. A further refinement in the analysis of seismic data is the identification and study of the behavior of the individual wave arrivals such as the P wave, S wave, and surface wave.

The viewpoints from which we investigate the behavior of the ground motion characteristics are:

1. Empirical, Theoretical-Empirical, and Theoretical
2. Source Region, Transmission Path, Surface Point of Interest (i.e., Receiver)
3. Deterministic and Statistical

Before discussing ERC's methods in detail, let us first consider the measurements program being conducted at NTS. A large effort has been expended in comprehensive programs for collection of seismic data. These data are required for studies of variations in ground motions and their causes, to complement the studies which have been conducted and those now in progress and to verify the validity of the prediction methods.

The installation and operation of measurement instruments is a primary responsibility of the USC&GS. ERC as the Ground Motion Contractor and J. A. Blume & Associates as the Structural Response Contractor provide plans designating the location and types of instruments required at each station. These plans are designed so that all centers of population in the vicinity of the Nevada Test Site are instrumented, often with several locations in each city. The plans are also designed to collect data used to support theoretical studies and to provide understanding of ground motions for selected geologic conditions. A large detonation is usually monitored by about 100 recording stations. Typical plans are shown in Figures 9.4 through 9.6. (See also Figures 8.11 through 8.14.)

The instruments used by USC&GS were selected because of their suitability for recording the essential information. They have a wide dynamic range and a broad band response to frequency. However, each type of instrument has its own performance characteristics. One of the most important is the response to frequency. If the instrument does not respond as well to some frequencies as to others, the resulting measurements (seismograms) will be distorted at some frequencies. Knowing the response to frequency of the various instruments, ERC has developed programs which remove (within given limits) any distortions produced by the instruments. An example of this is shown in Figure 9.7. The data from some instruments do not need corrections (L-7 and CEC accelerometers) because they respond uniformly to all frequencies of interest. Additional programs have been developed which produce seismograms of other kinds of motion. For example, from a velocity seismogram corrected for instrument response, acceleration and displacement seismograms can be derived. Figure 9.8 shows a velocity seismogram and the acceleration and displacement seismogram derived from it.

Although ERC has many studies (both empirical and theoretical) in progress, the following discussions will be directed toward ERC's current prediction methods—what we predict and how we do it. In the early days of

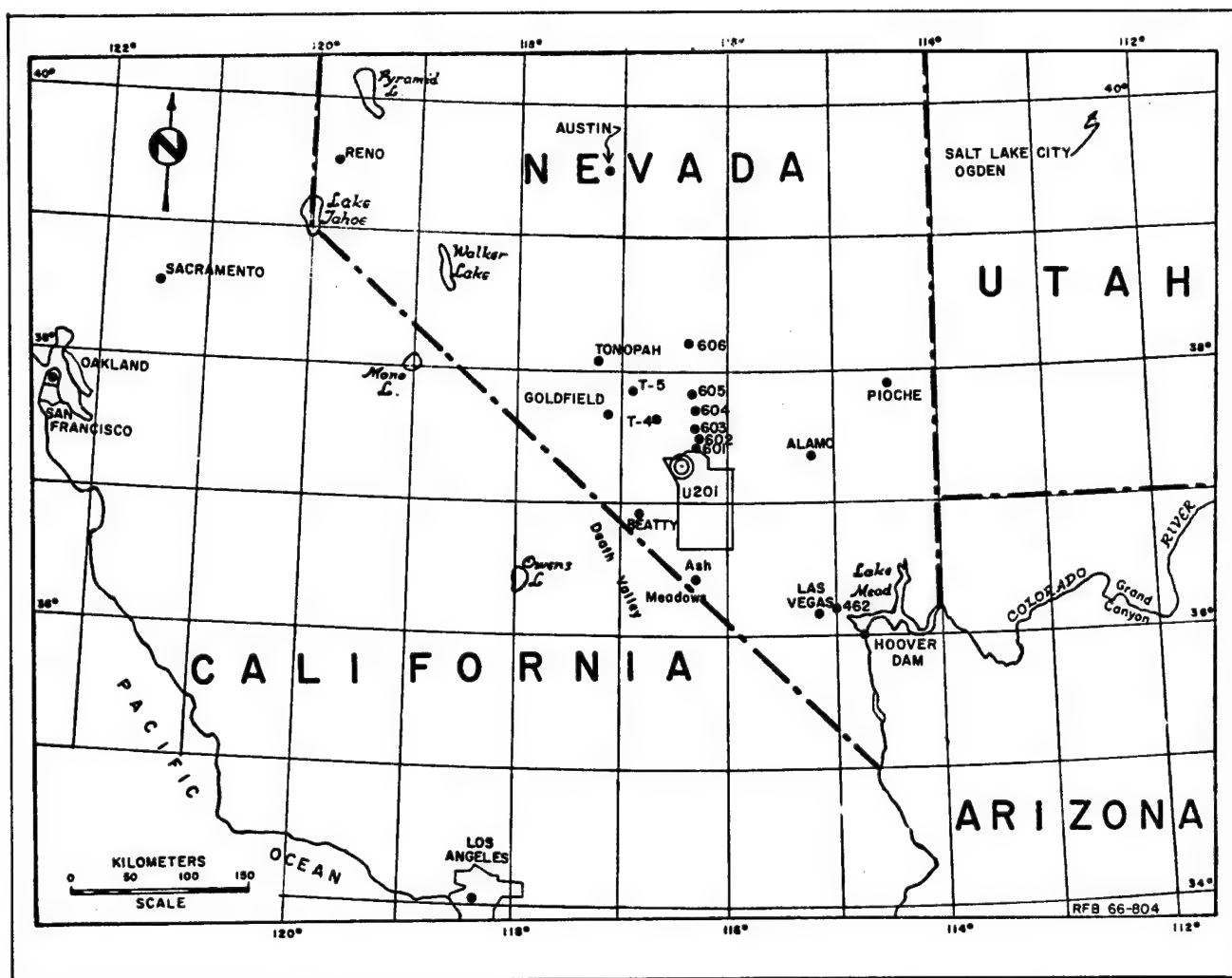Figure 9.4. Recording Stations Located Off the Nevada Test Site.
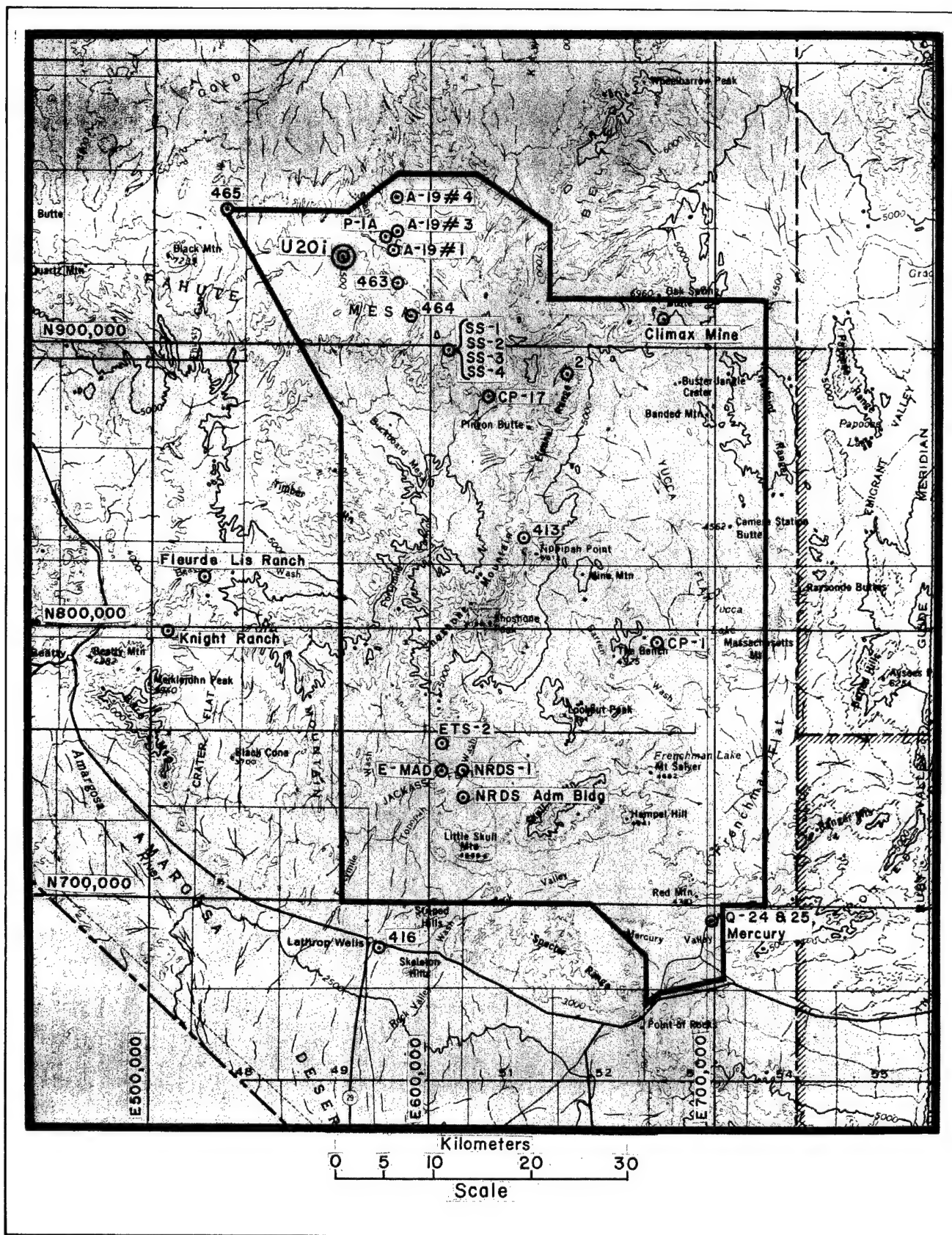
Figure 9.5. Recording Stations Located on the Nevada Test Site.
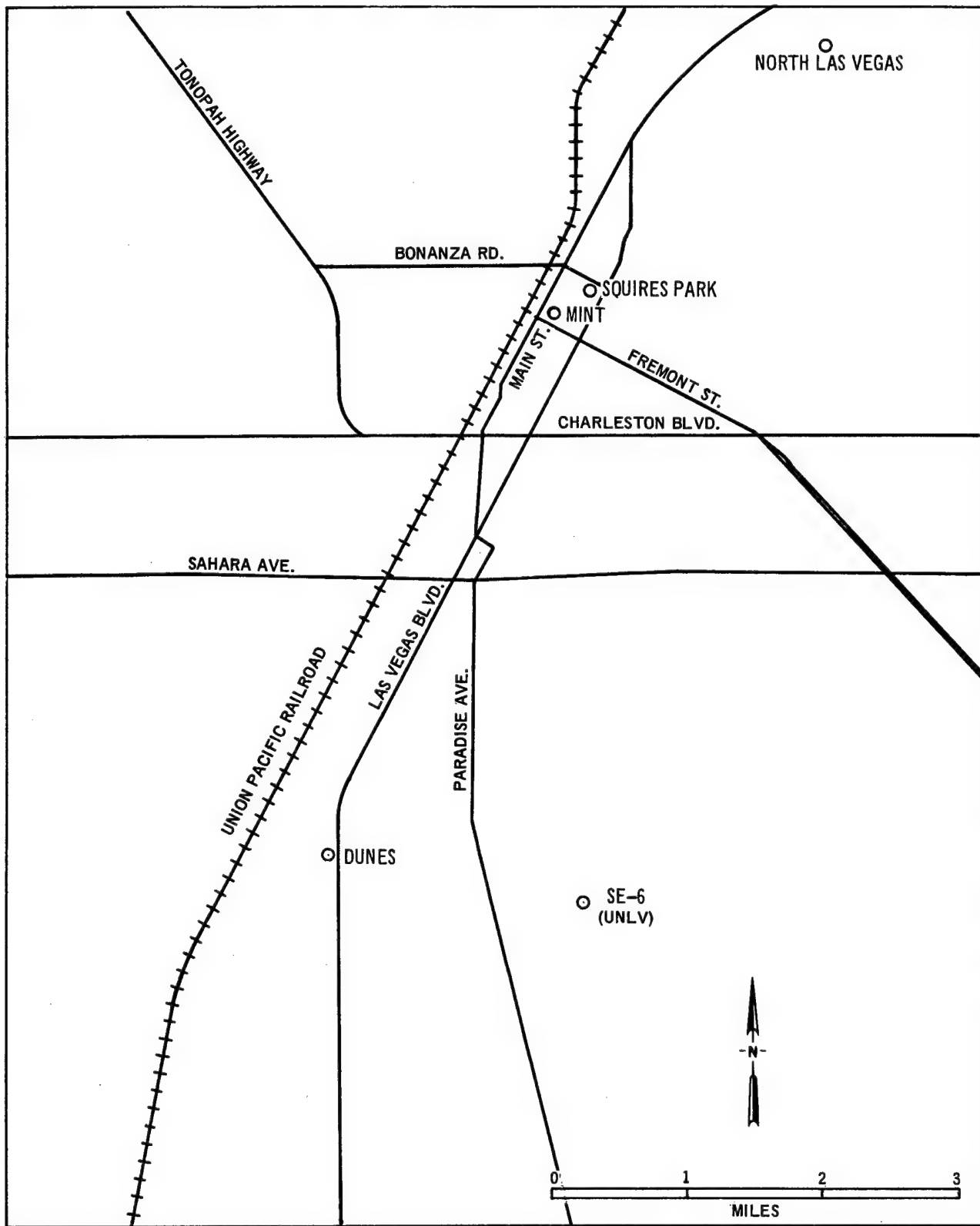
Figure 9.6. Map Showing Instrument Stations in Las Vegas.
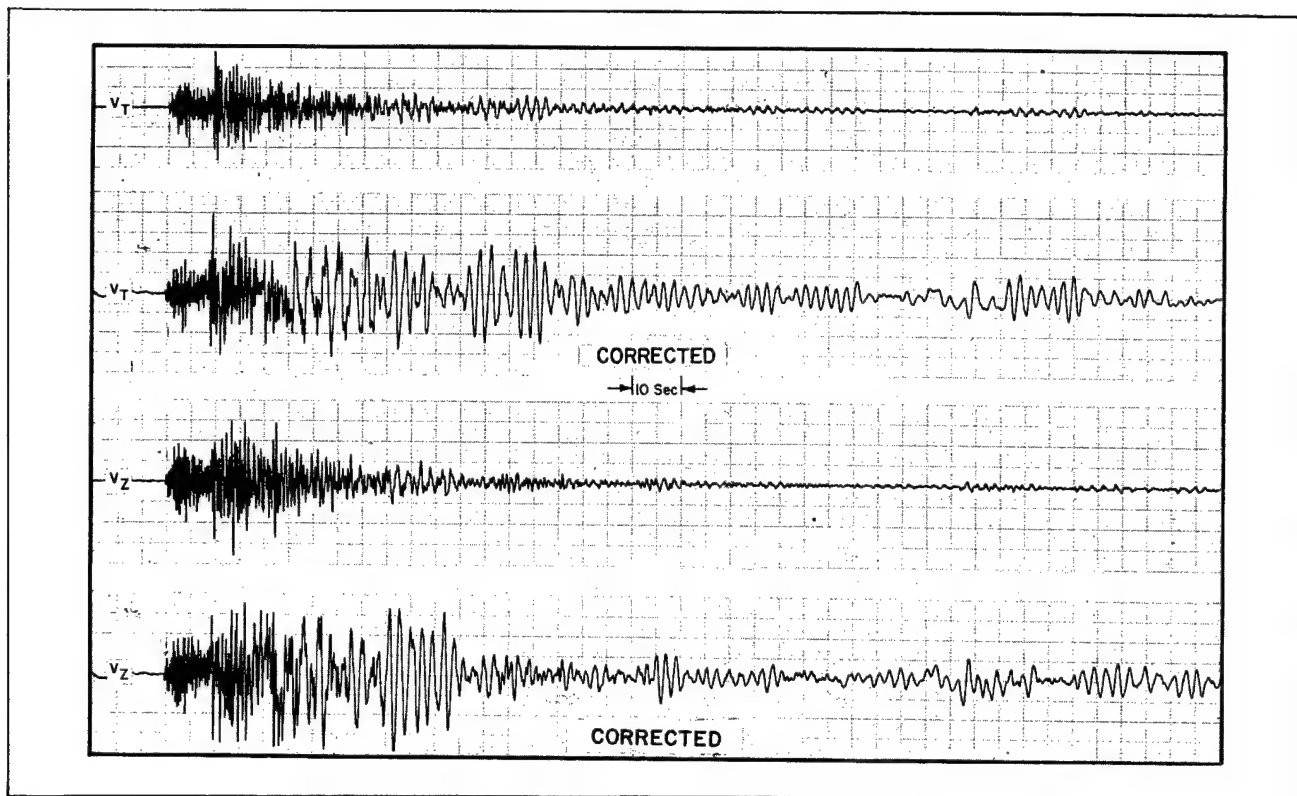
Figure 9.7.   Seismic Signals Before and After Correction.
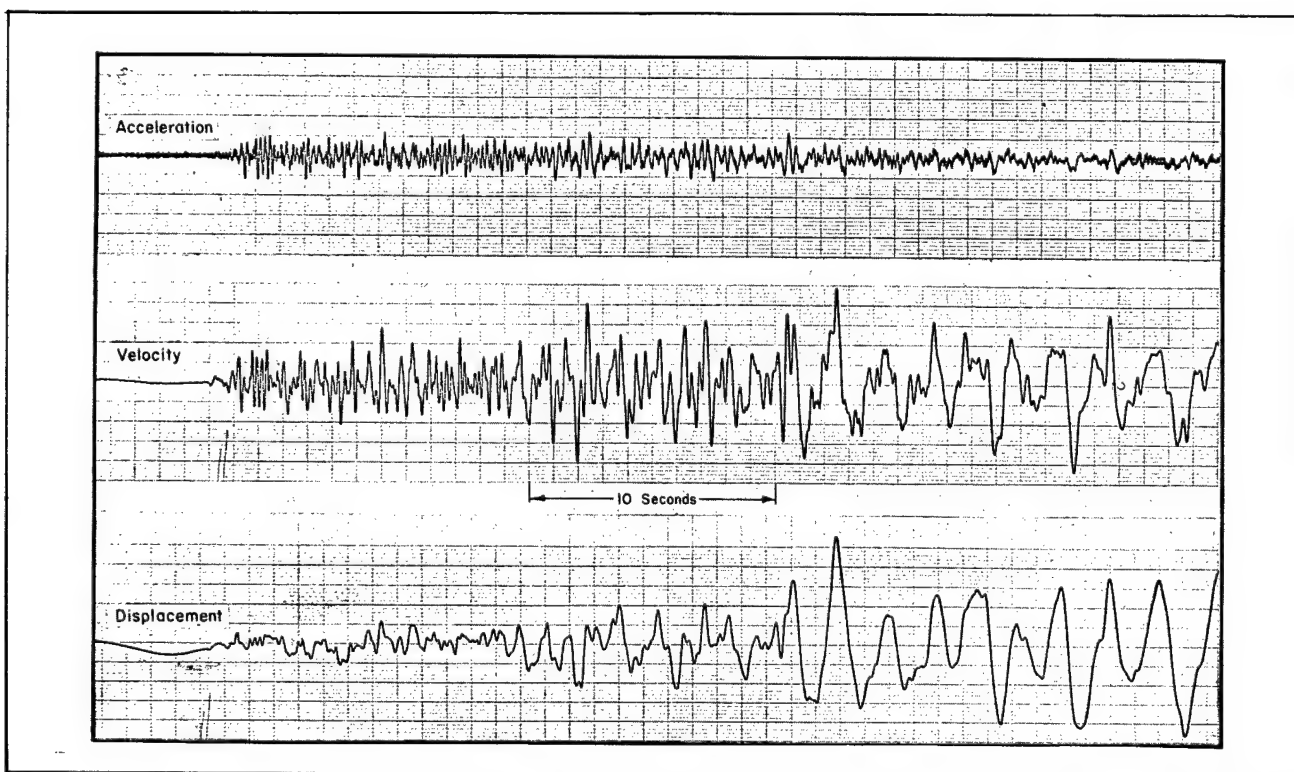
Figure 9.8.   Acceleration and Displacement Derived from Corrected Velocity.

106
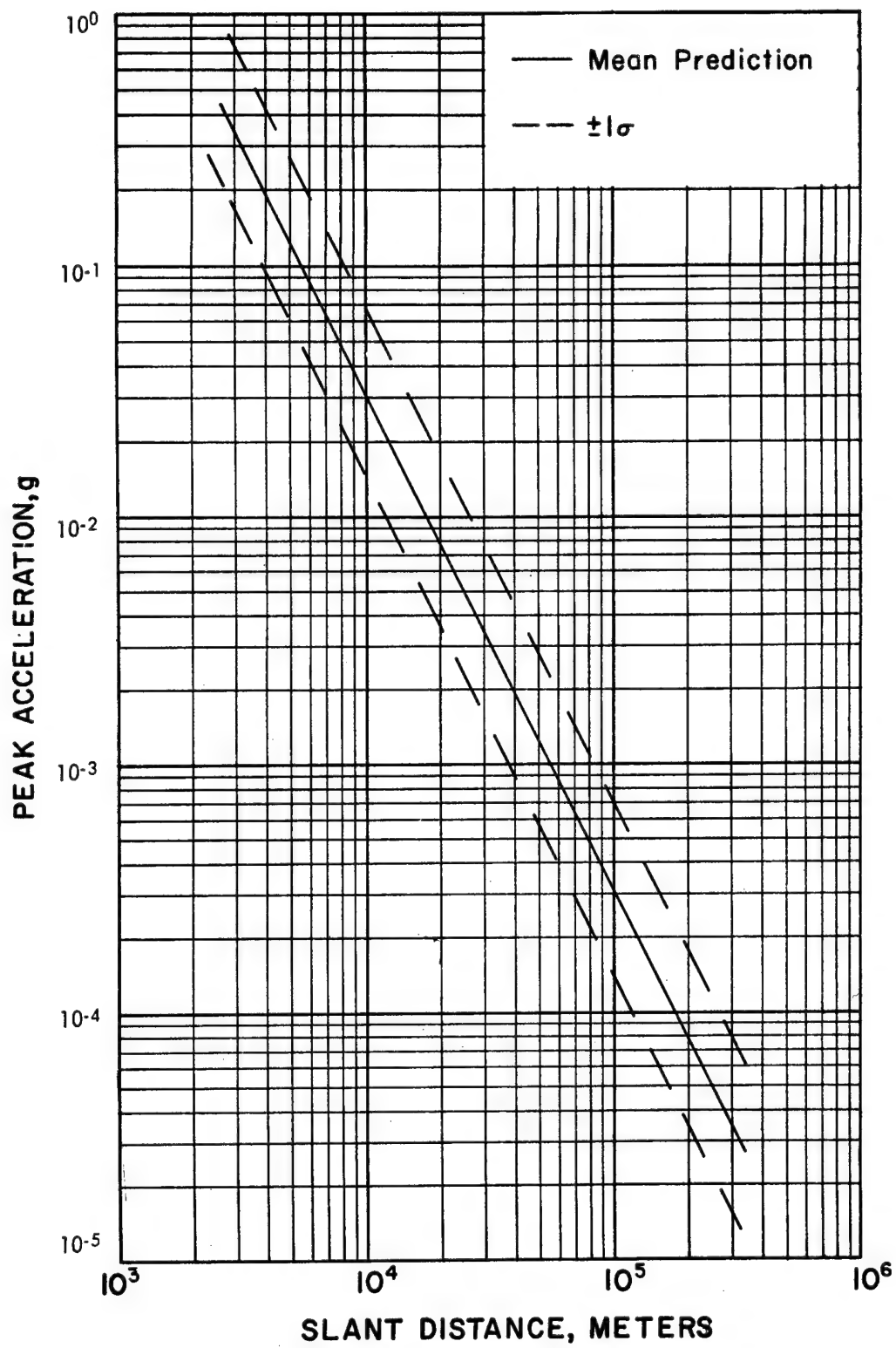
Figure 9.9.   Prediction of Peak Acceleration for a Hypothetical Event.

107

Figure 9.10. Comparison of Peak Acceleration Predictions with Observed Data from the Boxcar Event on Pahute Mesa — Stations on Hard Rock.

108
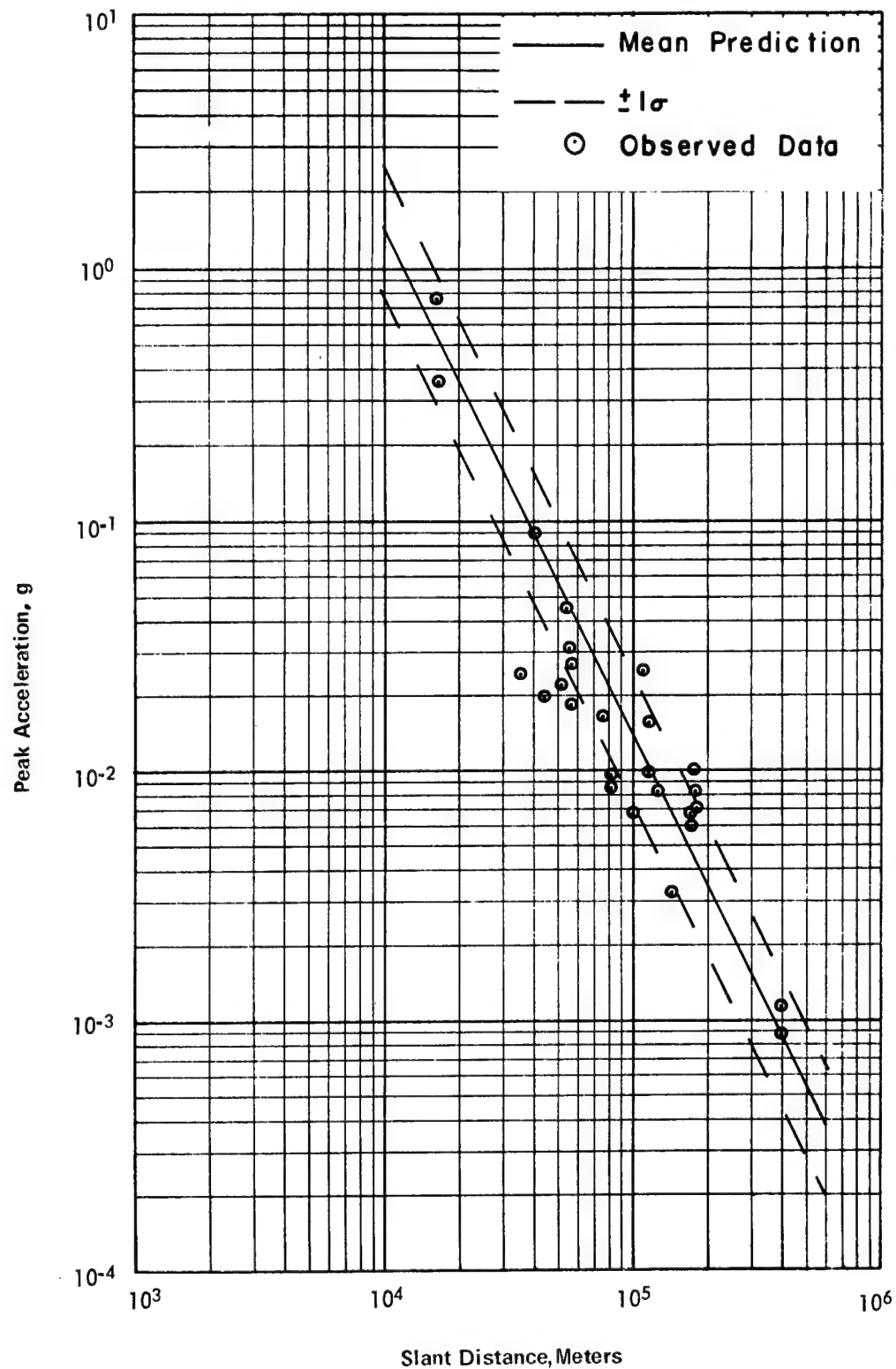
Figure 9.11. Comparison of Peak Acceleration Predictions with Observed Data from the Boxcar Event on Pahute Mesa —
Stations on Alluvium.

109
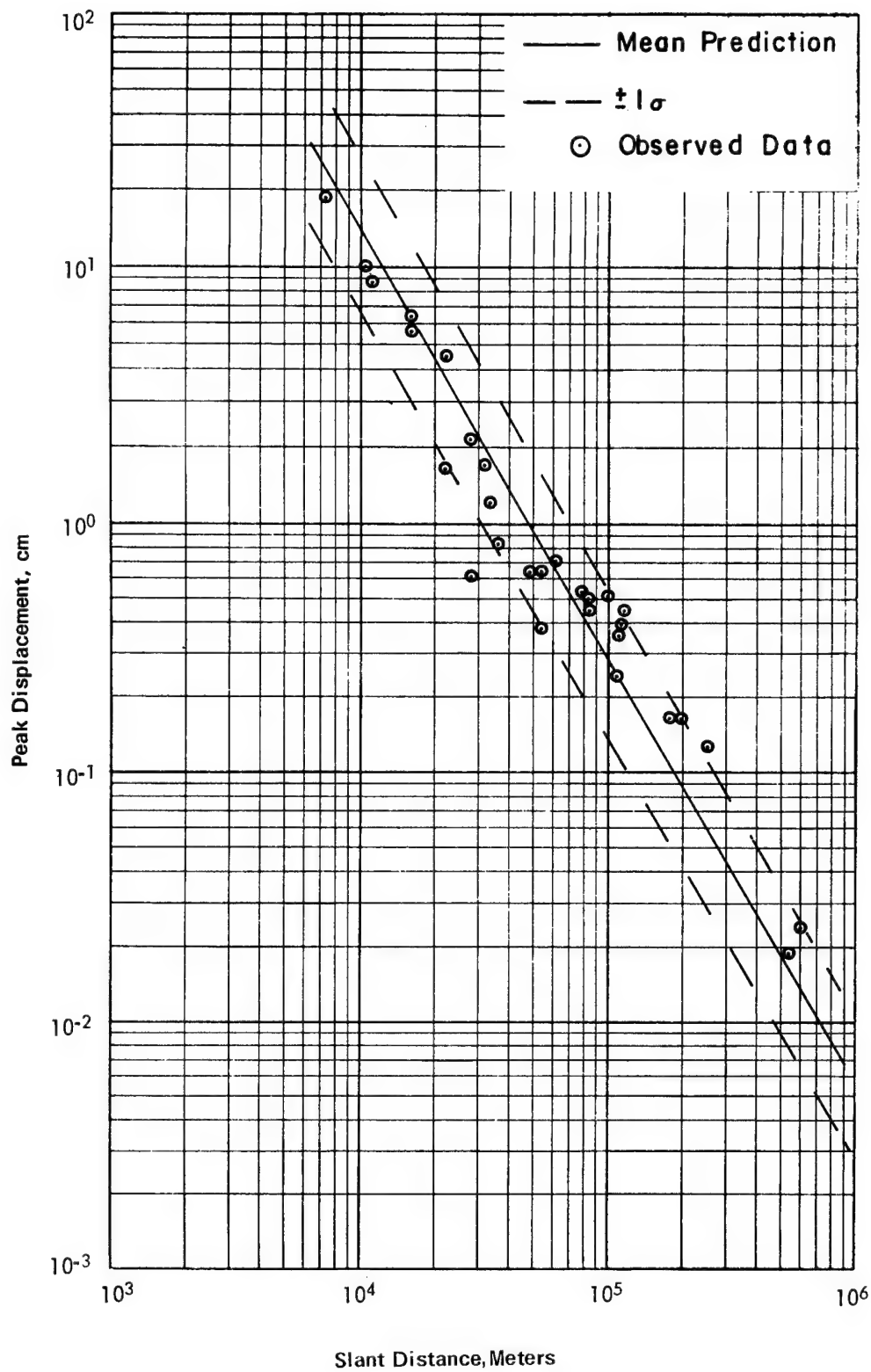
Figure 9.12. Comparison of Peak Displacement Predictions with Observed Data from the Boxcar Event on Pahute Mesa —
Stations on Hard Rock.
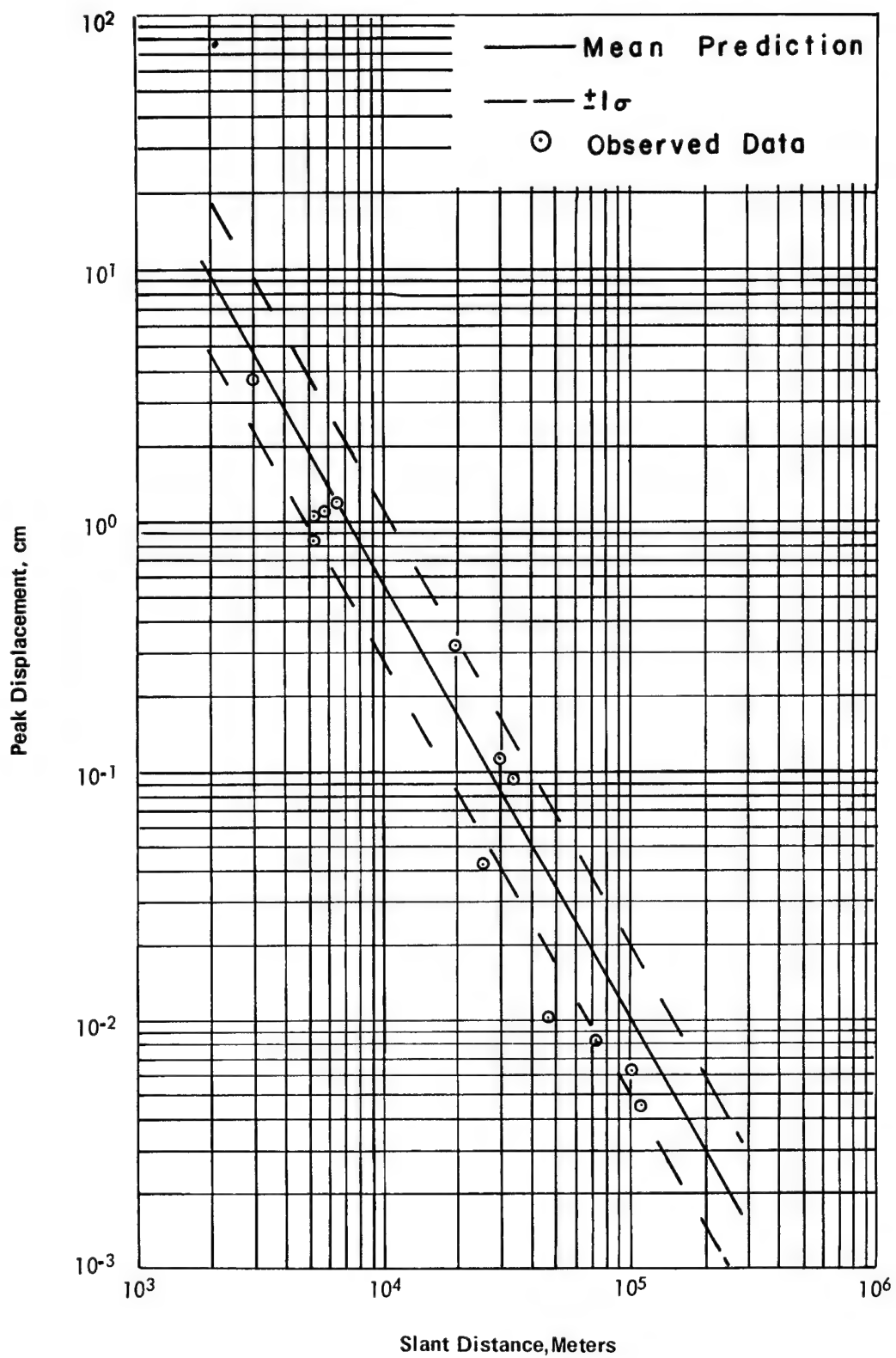
Figure 9.13. Comparison of Peak Displacement Predictions with Observed Data from the Rex Event on Pahute Mesa —
Stations on Hard Rock.

111

Figure 9.14. Comparison of Peak Velocity Predictions with Observed Data from the Boxcar Event on Pahute Mesa – Stations on Hard Rock.

Figure 9.15.   Peak Accelerations in Las Vegas from the Nevada Test Site (Pahute Mesa) Events.

113

Figure 9.16. Peak Displacements in Las Vegas from Nevada Test Site (Pahute Mesa) Events.

Figure 9.17.   Peak Velocities in Las Vegas from Nevada Test Site (Pahute Mesa) Events.

115

the Safety Program, peak motions were predicted usually with very limited past data in conjunction, say, with a cube root scaling law. Slow esc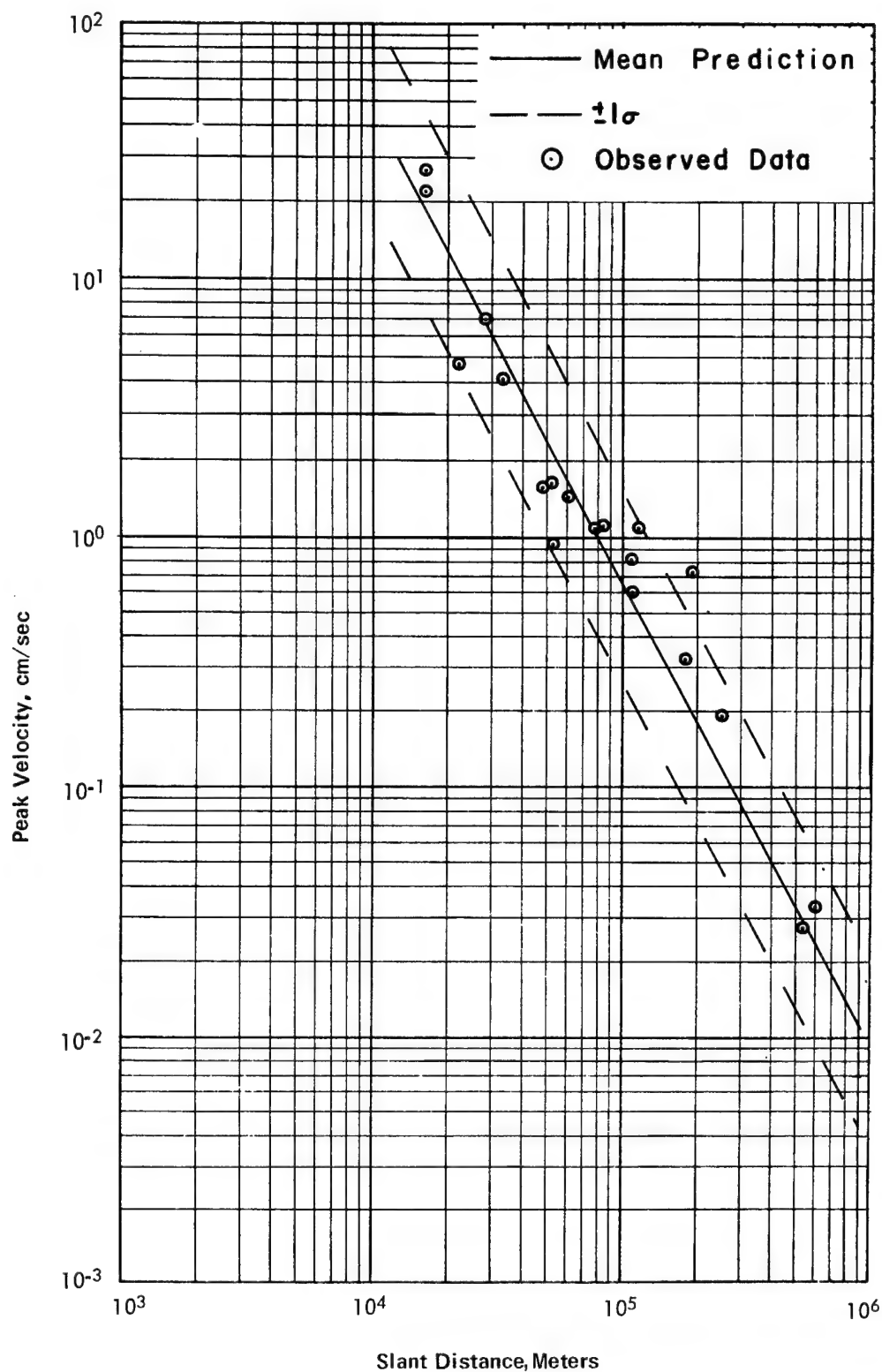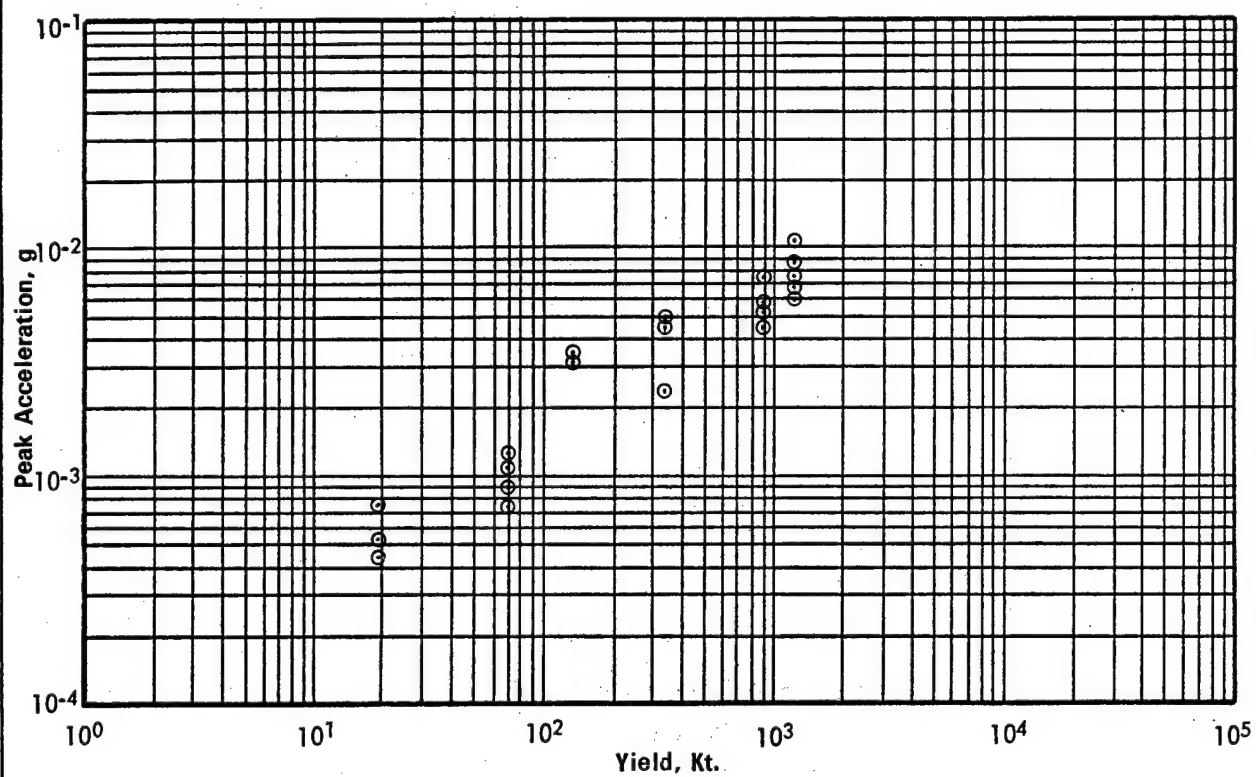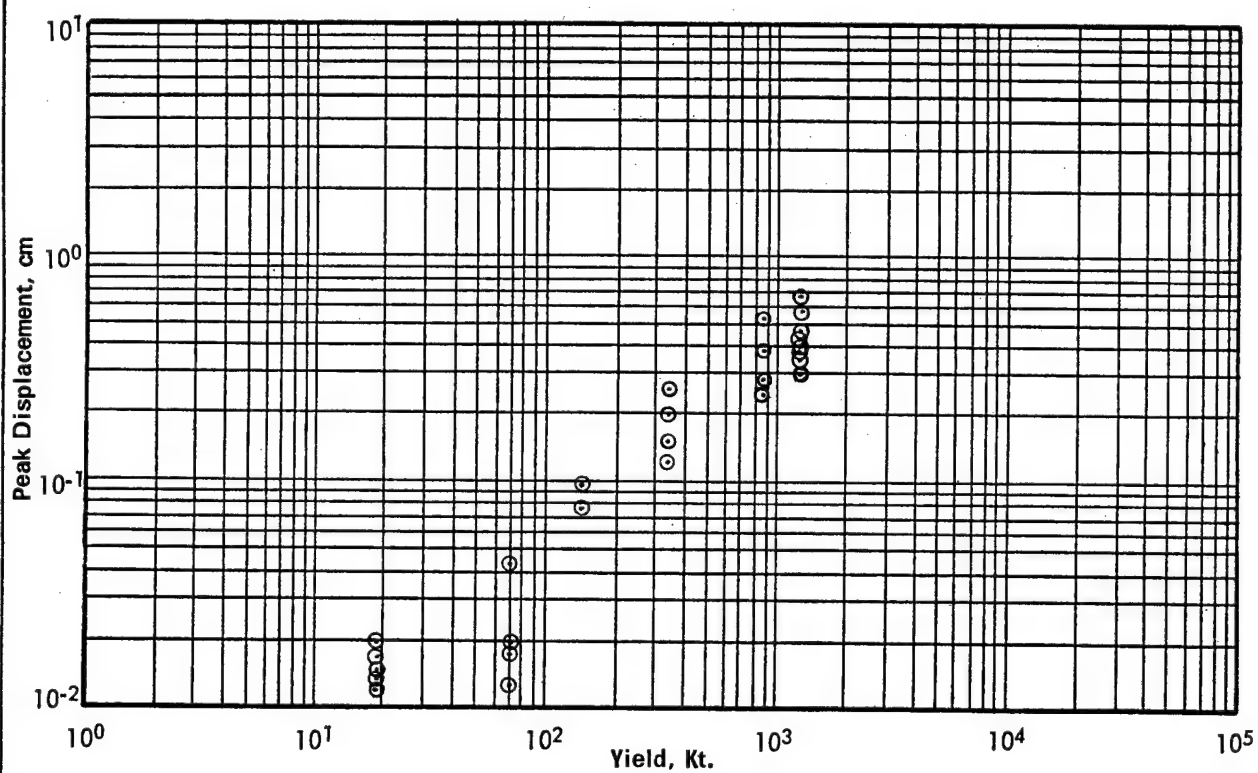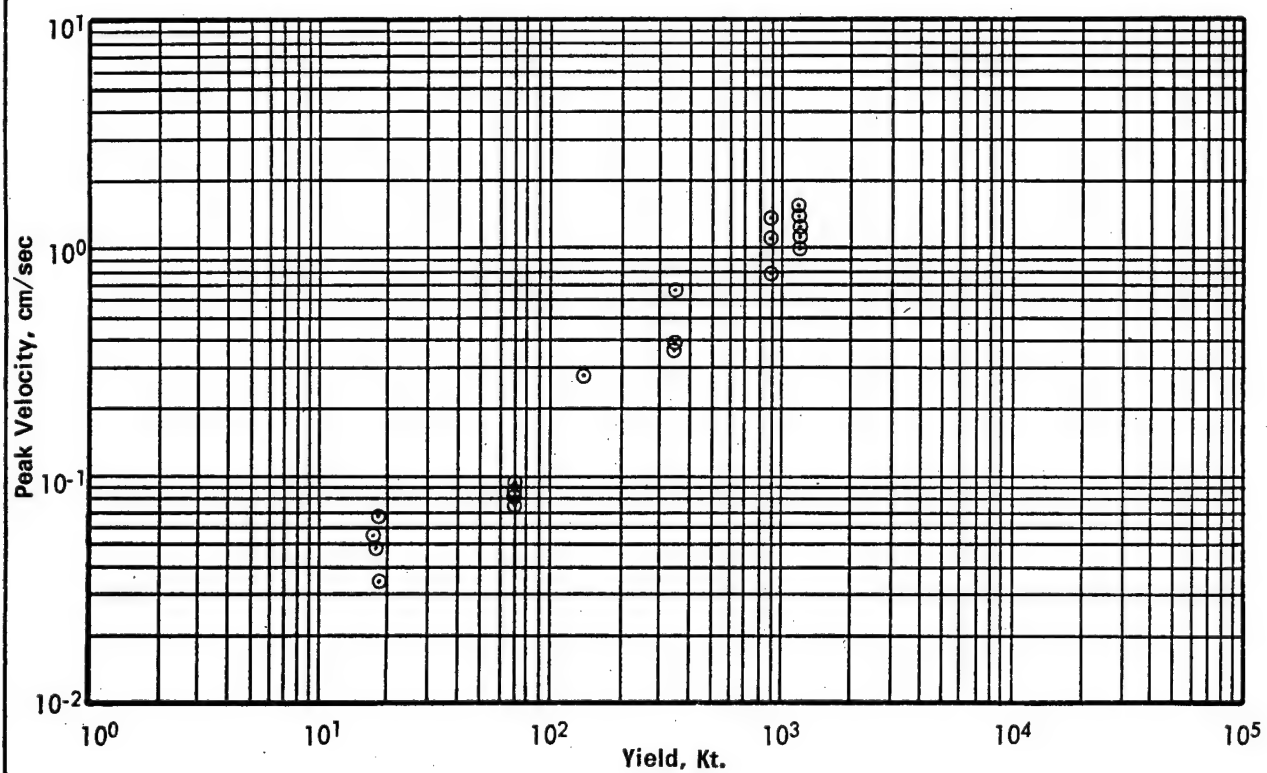alation in yields for several events, however, has permitted a steady accumulation of a large number of nuclear generated seismograms. The seismograms recorded by USC&GS typically are measured at distances of from 1 km to about 200 km, at populated areas around the Nevada Test Site. The data are then transmitted to ERC for analysis.

The most unambiguous parameter which can be obtained from seismograms, such as those shown earlier, is the peak value of the recorded ground motion. Since some structural damage criteria are based on a correlation of damage with peak ground motion, ERC has developed a prediction capability with regard to this parameter. Experience gained since the initiation of the testing program has indicated that this parameter varies in a predictable manner as a function of yield and distance. Thus, an equation of the form:

$$A = KW^m R^{-n} \qquad (1)$$

can be used to describe peak acceleration, velocity, and displacement where

A = peak surface particle motion

W = yield in kilotons

R = slant distance in meters

$K,m,n,$ = constants

K, m, and n constants are obtained by grouping the available data in homogenous subgroups to minimize the effects of the parameters.

The above functional relationship ignores a number of independent variables which are known to be significant. One such variable is the geologic medium on which the recording instrument is placed. The appropriate functional form for such a variable is not completely clear at this time and for this reason its effect is minimized by grouping the data into homogenous subsets containing hard rock and alluvium, respectively. Other variables which are needed to completely describe the system such as shot media and transmission path are treated in a similar fashion whenever statistically adequate subsamples are available.

When an underground detonation is planned, ERC makes predictions of the peak values of displacement, velocity, and acceleration at all known points of possible concern. Based on the location of the proposed shot and the locations of points of interest, appropriate prediction equations with associated standard errors of estimate based on the data from previous detonations in similar environments are used to estimate these peak motions. At a given yield the predictions can be shown against distance as illustrated in Figure 9.9. Where re-

quired, station correction factors are applied to account for consistent deviations which have been noted in the past data at a few particular stations. (A discussion of these factors and an example of their application may be found in ERC Report 1163-133.)

These predictions are then provided to the Structural Response Contractor and AEC so that they can be incorporated into the total Safety Evaluation Program. The peak amplitudes of the ground motion have been predicted for a large number of past NTS events. The comparison between these predictions and the measurements has been very good. Examples of peak amplitude predictions compared with observed data from a few recent events are shown in Figures 9.10 through 9.14. At selected locations such as Las Vegas the observed data can be related directly to yield with graphs similar to that shown on Figures 9.15 through 9.17. These provide additional checks on the accuracy of the predictions at specific locations and confirm the yield scaling exponents used in the prediction equations.

Frequency content of the ground motion is an important consideration in evaluating effects of the motions on structures because structures respond differently to different frequencies. Some buildings in Las Vegas have response curves which look like that shown in Figure 9.18. Thus, the response of a building to a given amplitude at one frequency can be seen to be entirely different from its response to the same amplitude at another frequency. To provide frequency content predictions which can be used by the Structural Response Contractor, ERC has developed a method called the Band-Pass Filter (BPF).
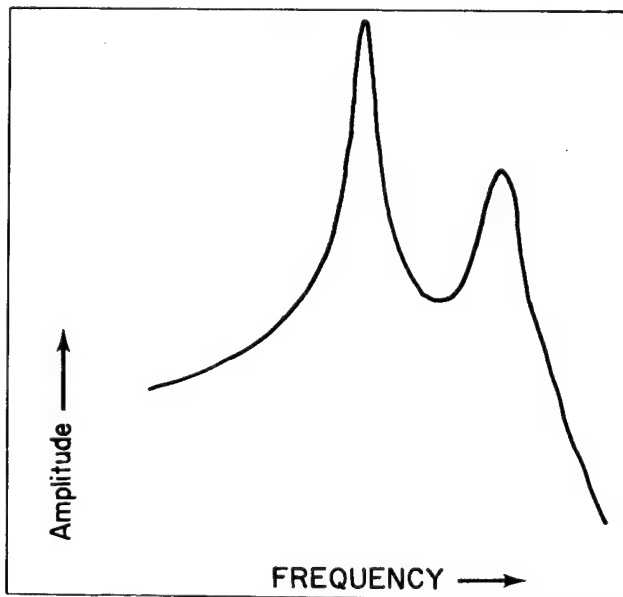
Figure 9.18. Amplitude Response of a Two-Degree-of-Freedom System.

The BPF may be considered roughly as a sampling of several seismogram amplitudes, measured across the frequency range of interest. Due to the nature of seismograms, these amplitudes typically are sampled from the beginning to the end of the seismogram. Further description of this concept follows.

Given a seismic trace, f (t), containing a broad spectrum of frequencies, one can transform that trace to another time trace containing a restricted range of frequencies by utilizing a narrow band-pass filter centered at a selected frequency. The resulting time-history, f_b (t), will be a trace retaining that portion of the input trace having frequencies comparable with that of the selected center frequency. The amplitude is representative of the amplitude of waves seen in f (t) having that frequency. A set of 12 such filters with logarithmically-spaced center frequencies is routinely used to cover the frequency range of 0.4 to 11 Hz. This is illustrated in Figure 9.19. Using the peak amplitude of the output of each filter, a peak amplitude versus center frequency curve can be constructed. We call this a BPF curve. An example is shown in Figure 9.20.

Least-squares analyses (both yield, and yield and distance as independent variables) have been performed on these BPF amplitudes obtained from stations between 40 km and 200 km. These form the basis of the capability to predict BPF spectra at selected locations. BPF predictions have agreed well with the observed data. Examples of these predictions compared with measured data are shown in Figures 9.21 through 9.24.

In addition to the Band-Pass Filter curve, the frequency content is described for use by the Structural Response Contractor, by the Pseudo Relative Velocity (PSRV) response spectra. In general, the PSRV approximates the velocity at the top of a building relative to that at the bottom as a function of frequency. The PSRV is defined as the peak response to ground motion of a single-degree-of-freedom system (mass-spring system with velocity damping). Two parameters, resonant period $P_0 = 2\pi/\omega_0$ and damping factor H, characterize this system. Typical values of damping are 0.02, 0.05 and 0.10. For velocity seismograms recorded between 50 and 200 km, PSRV and BPF spectra have been obtained at a sufficient number of frequencies to define continuous spectra over the frequency range from 0.41 to 11.3 Hz. In this frequency band the BPF spectra are defined by peak velocities at each of 12 center frequencies, and PSRV spectra by peak velocities at about 200 center frequencies. A typical example is given in Figure 9.25. It can be seen that the two spectral curves are approximately parallel over the entire period range. It

has been found that multiplication of the BPF curve by a constant factor represents a smoothed PSRV curve. Thus PSRV curves are predicted from the BPF curves. Examples of the accuracy with which the PSRV curves can be predicted are shown in Figures 9.26 through 9.29.

Both the BPF and PSRV spectra are used at ERC to study amplitude-frequency information about nuclear generated seismograms; BPF spectra are a direct characterization of the ground motion, whereas PSRV spectra characterize both the ground motion and its effect on certain mechanical systems.

Application of ERC's safety studies can best be summarized by citing the activities which are conducted for a typical detonation at the Nevada Test Site. Upon receipt of the plans for a proposed test, the safety studies begin. A review of the geologic and geophysical factors at the proposed location is made and the appropriate prediction procedures are selected. A plan of instrumentation is designed for collecting data at specific locations. These locations are selected by consideration of the planned yield and location of the test and its relation to population areas surrounding the Nevada Test Site. Approximately 2 months prior to the readiness date, a summary report of predictions is submitted to AEC. This report includes predictions of the peak displacements, velocities, and accelerations at all towns and cities where motions might be felt. At selected locations such as Las Vegas, Beatty, and Tonopah, predictions of the frequency content are given. These are used by the Structural Response Contractor to evaluate the possible effects of the predicted motions of buildings in these cities. The preshot report also explains the methods used, their basis, and the degree of confidence associated with the predictions. Where appropriate, effects of the predicted ground motions on tunnels, mines, wells, and slopes are given. The effects of the predicted ground motions on such facilities are evaluated by considering the magnitude of the motion, the physical condition of particular structures, and experience with similar motions at similar structures. General criteria have been developed which indicate that ground motions below certain levels will produce no damage. However, it must be pointed out that each individual case must be evaluated separately. Similarly, the effects of ground motion on steep slopes must be evaluated on an individual basis considering not only the predicted ground motions but the type and condition of the slope in question. General criteria are useful and have been developed but the final evaluation must be based on experience gained from the effects of previous motions on similar slopes.

In general, subsurface facilities and slopes are relatively
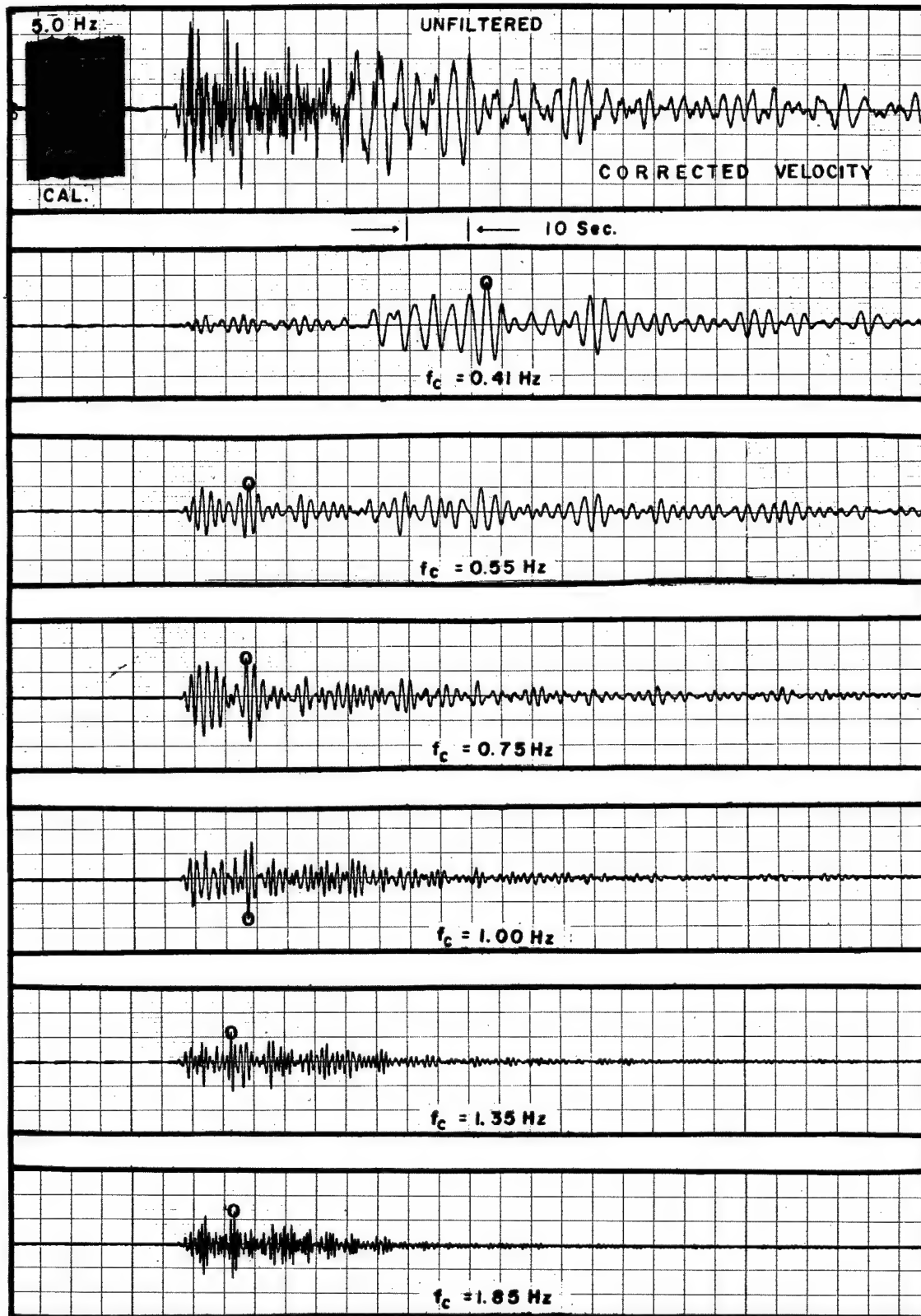
Figure 9.19. Band-Pass Filtering of a Seismogram. Event: Greeley. Station: SE-2.

118
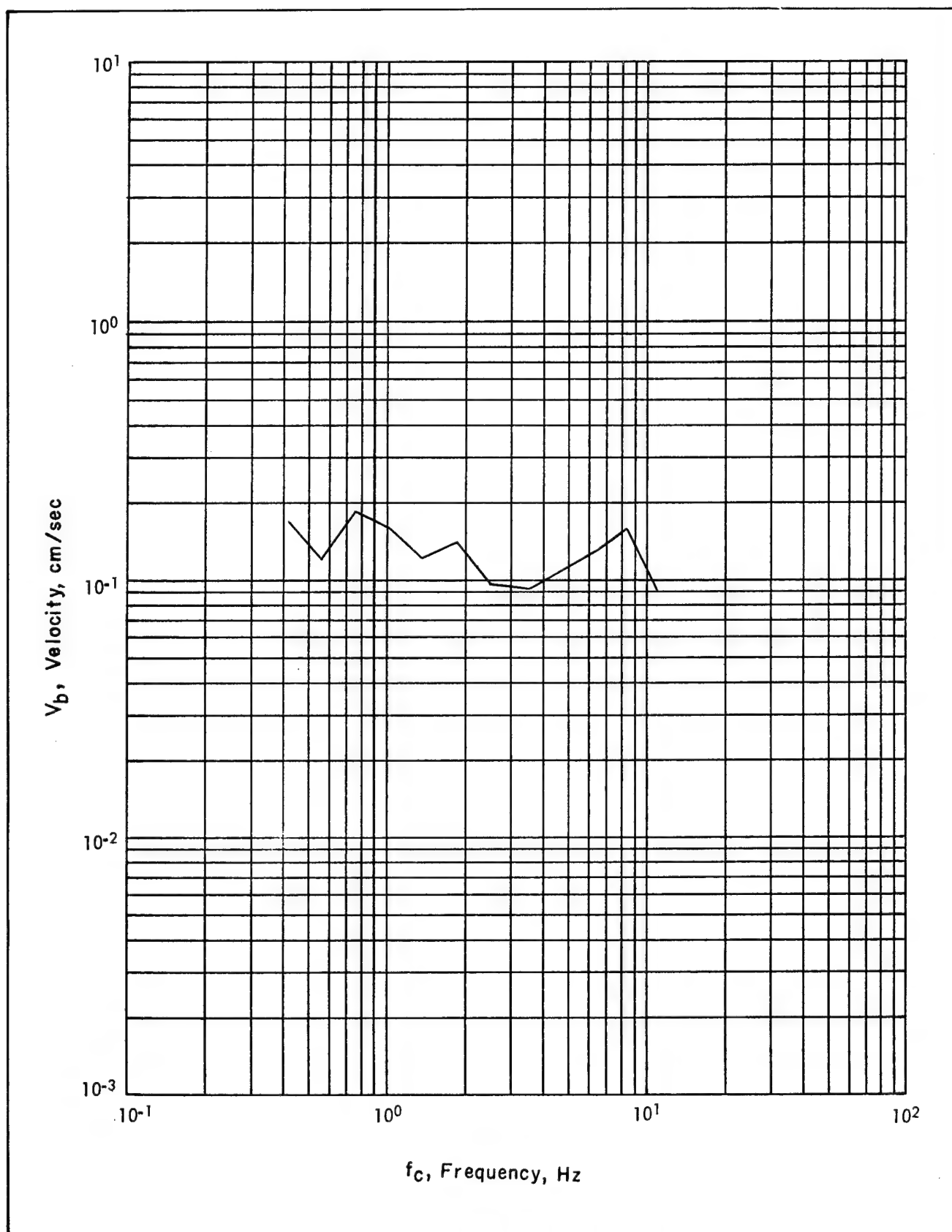
Figure 9.20.   Band-Pass Filter Curve from the Greeley Event.

119
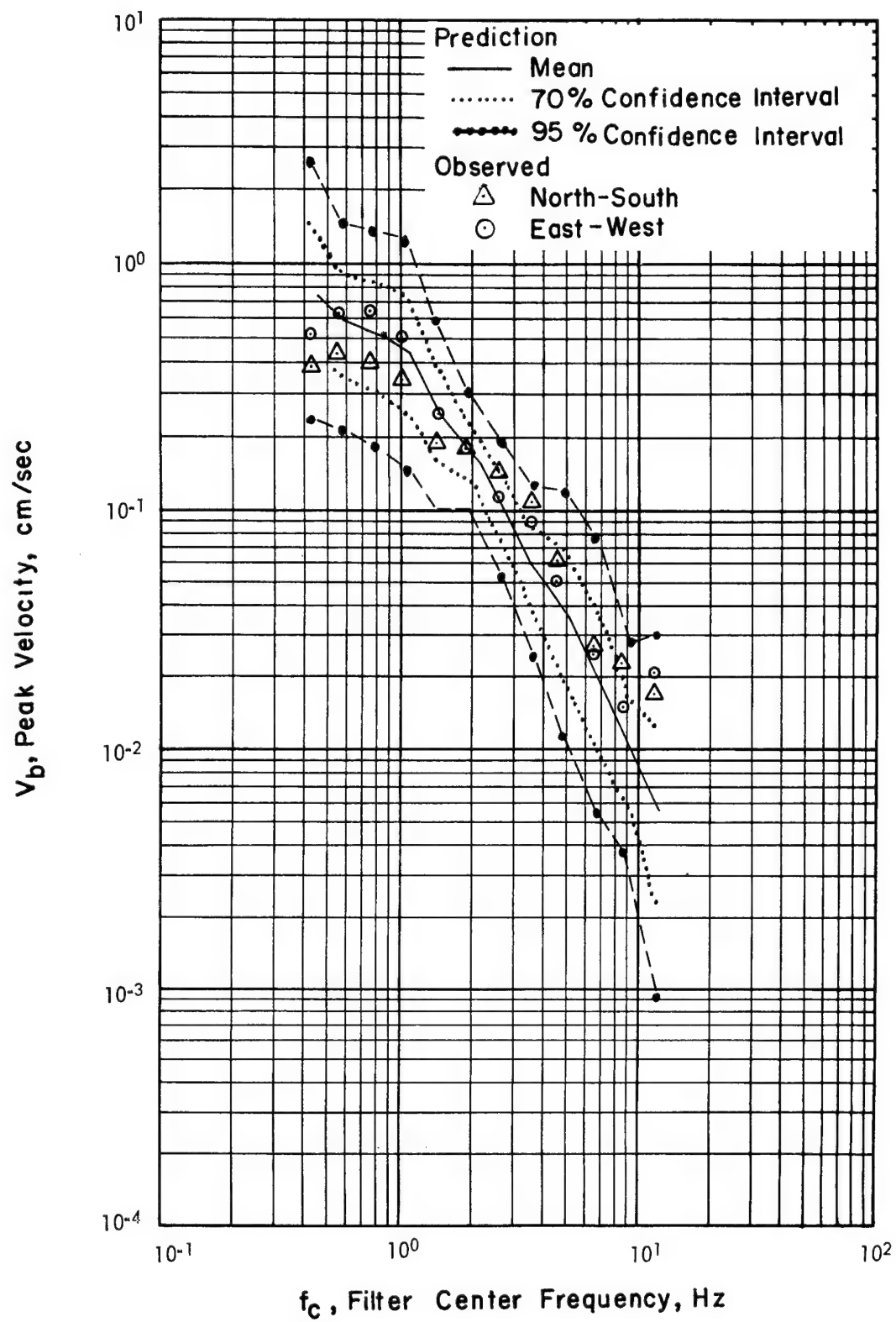
Figure 9.21.   Comparison of BPF Prediction with Observed Data from the Boxcar Event, Pahute Mesa.
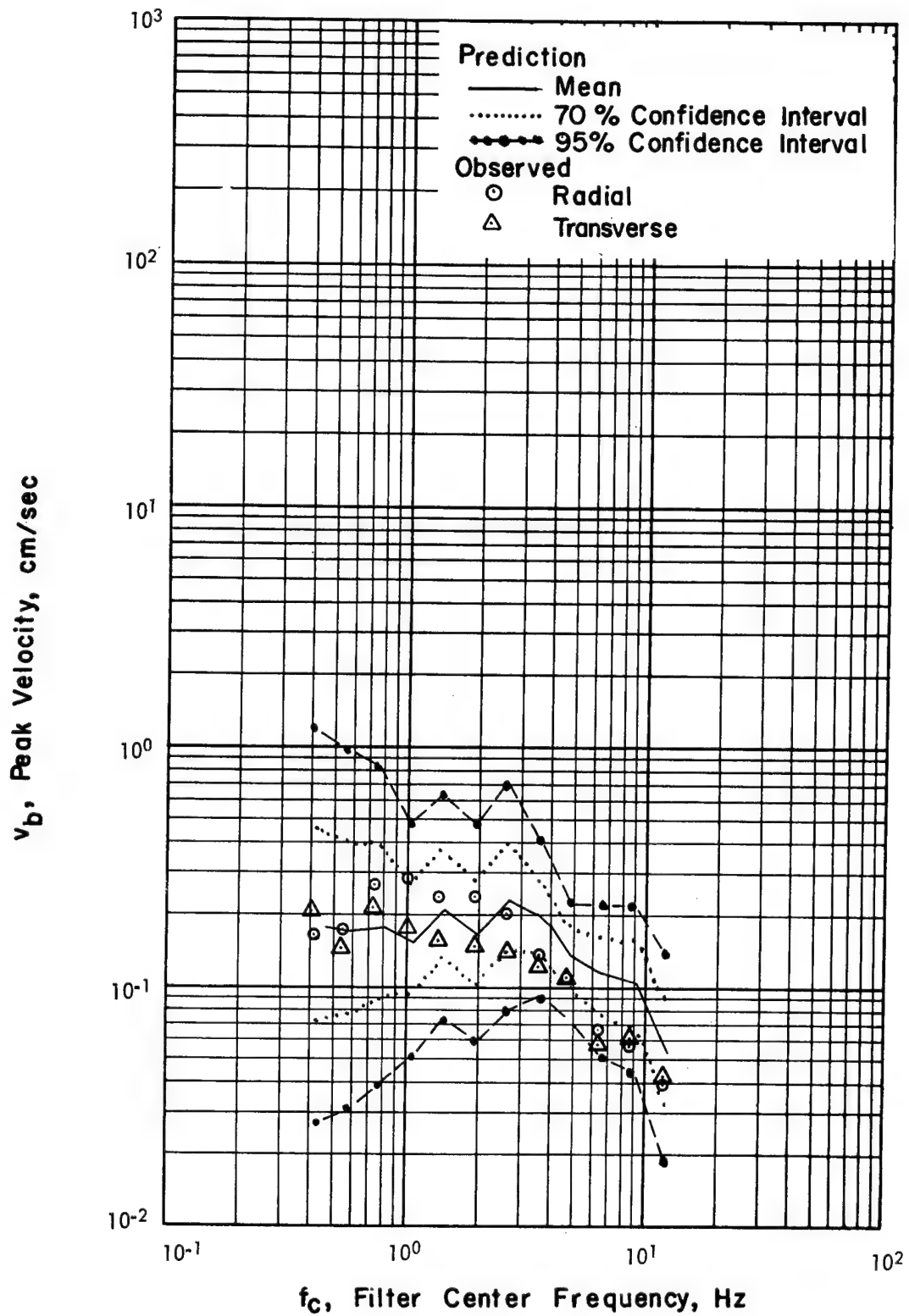
Figure 9.22.   Comparison of BPF Prediction with Observed Data from the Boxcar Event, Pahute Mesa.
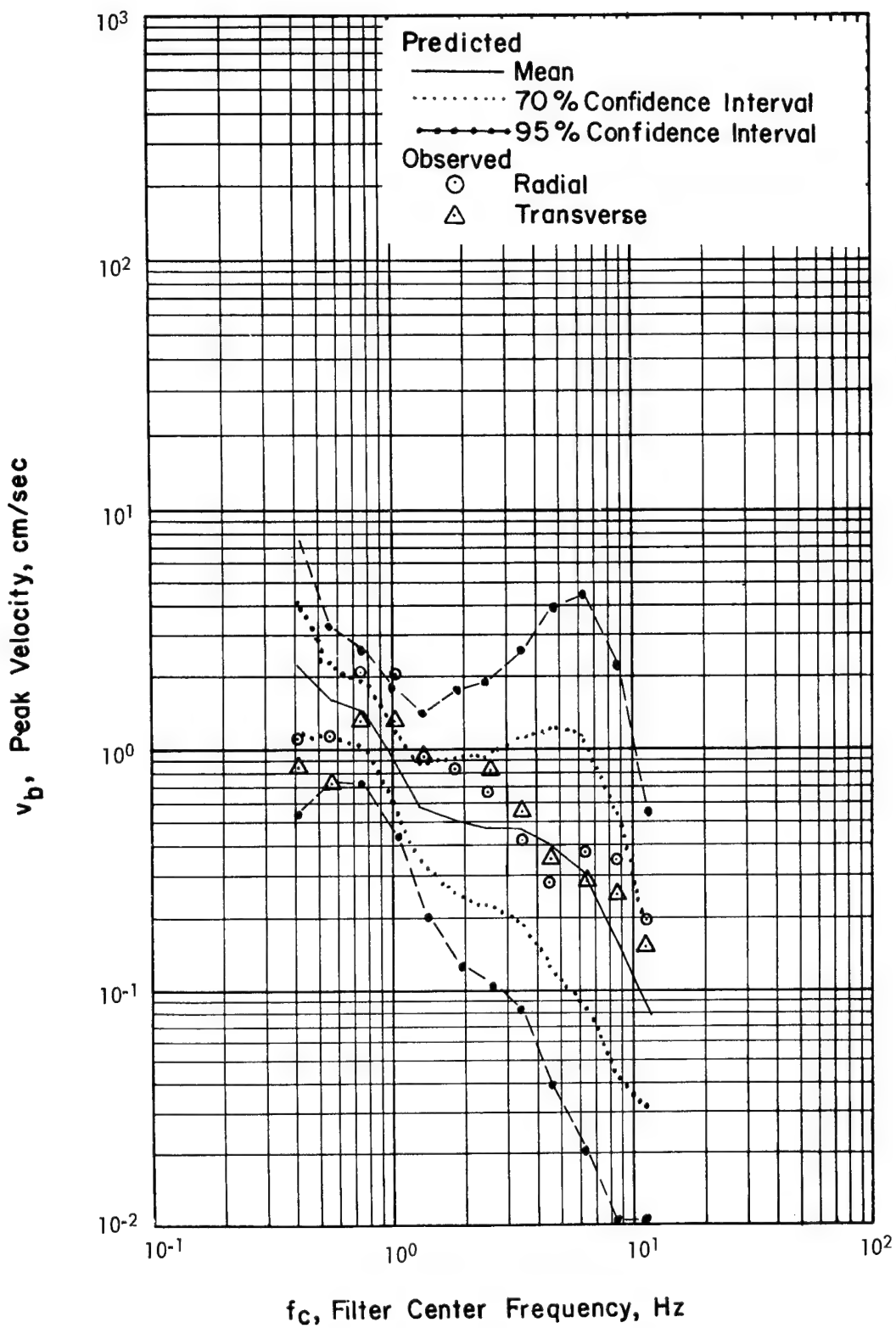
Figure 9.23. Comparison of BPF Prediction with Observed Data from the Boxcar Event, Pahute Mesa.

122
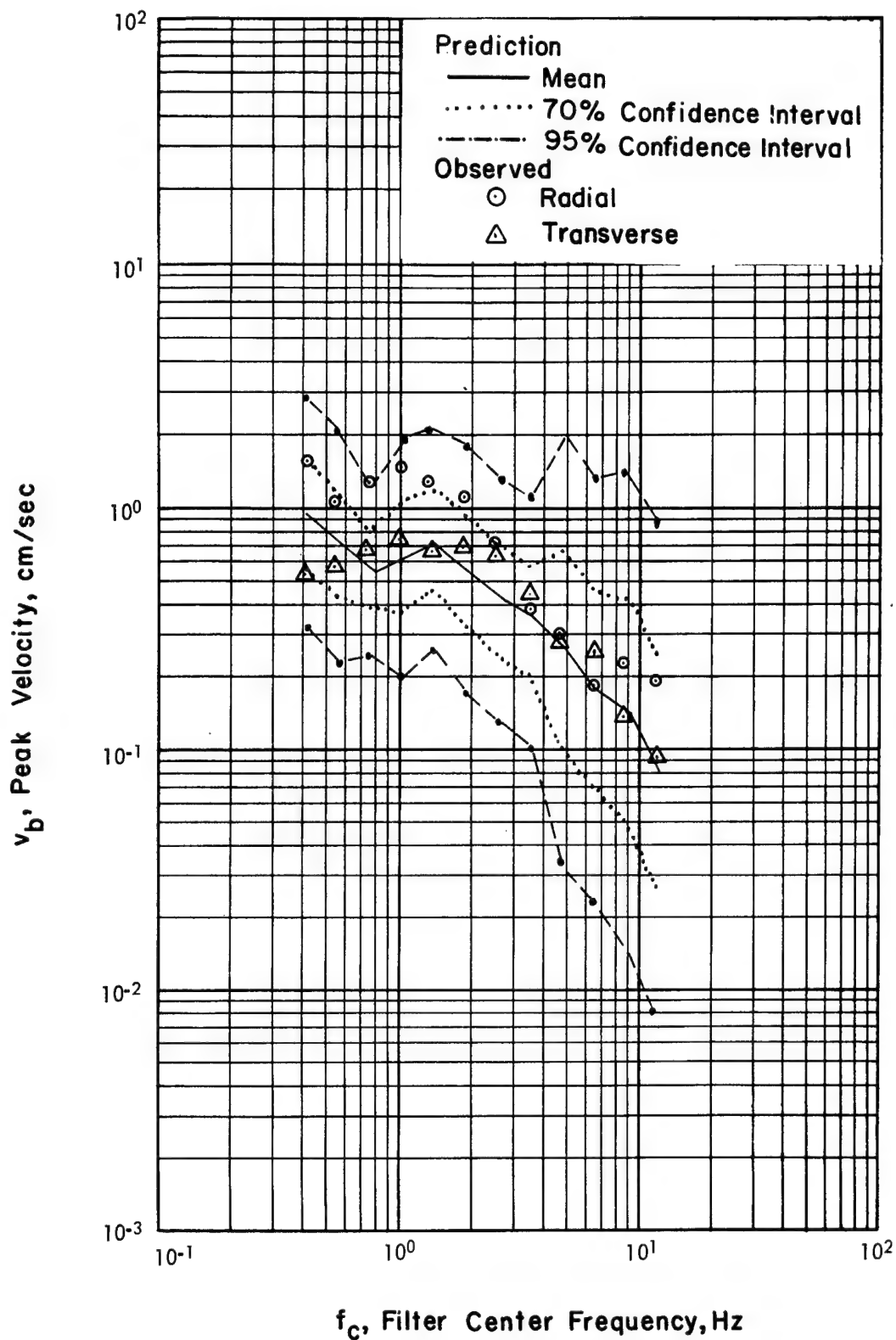
Figure 9.24. Comparison of BPF Prediction with Observed Data from the Boxcar Event, Pahute Mesa.

123
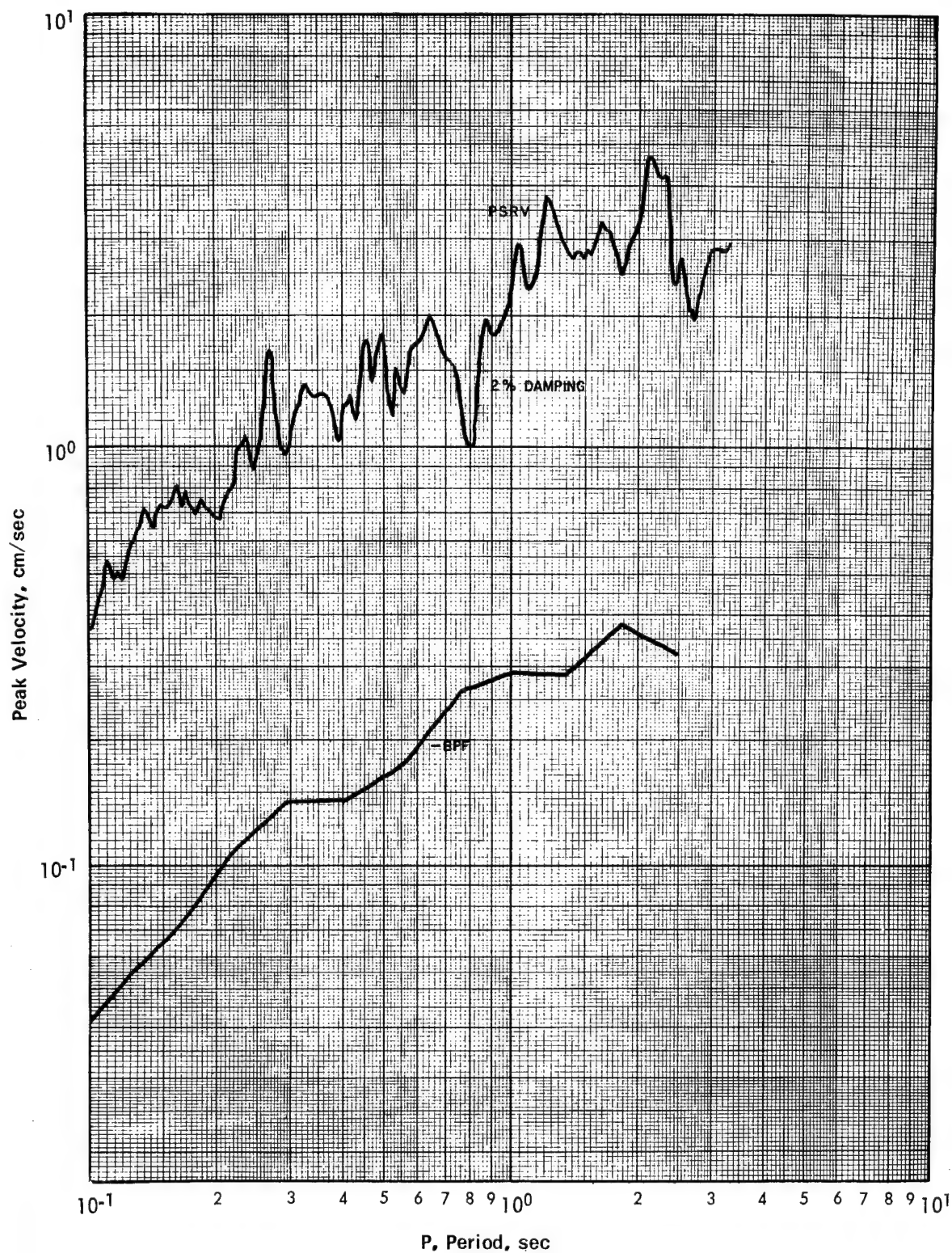
Figure 9.25.   Pseudo Relative Velocity and Band-Pass Filter Spectra — Halfbeak Event, Pahute Mesa.
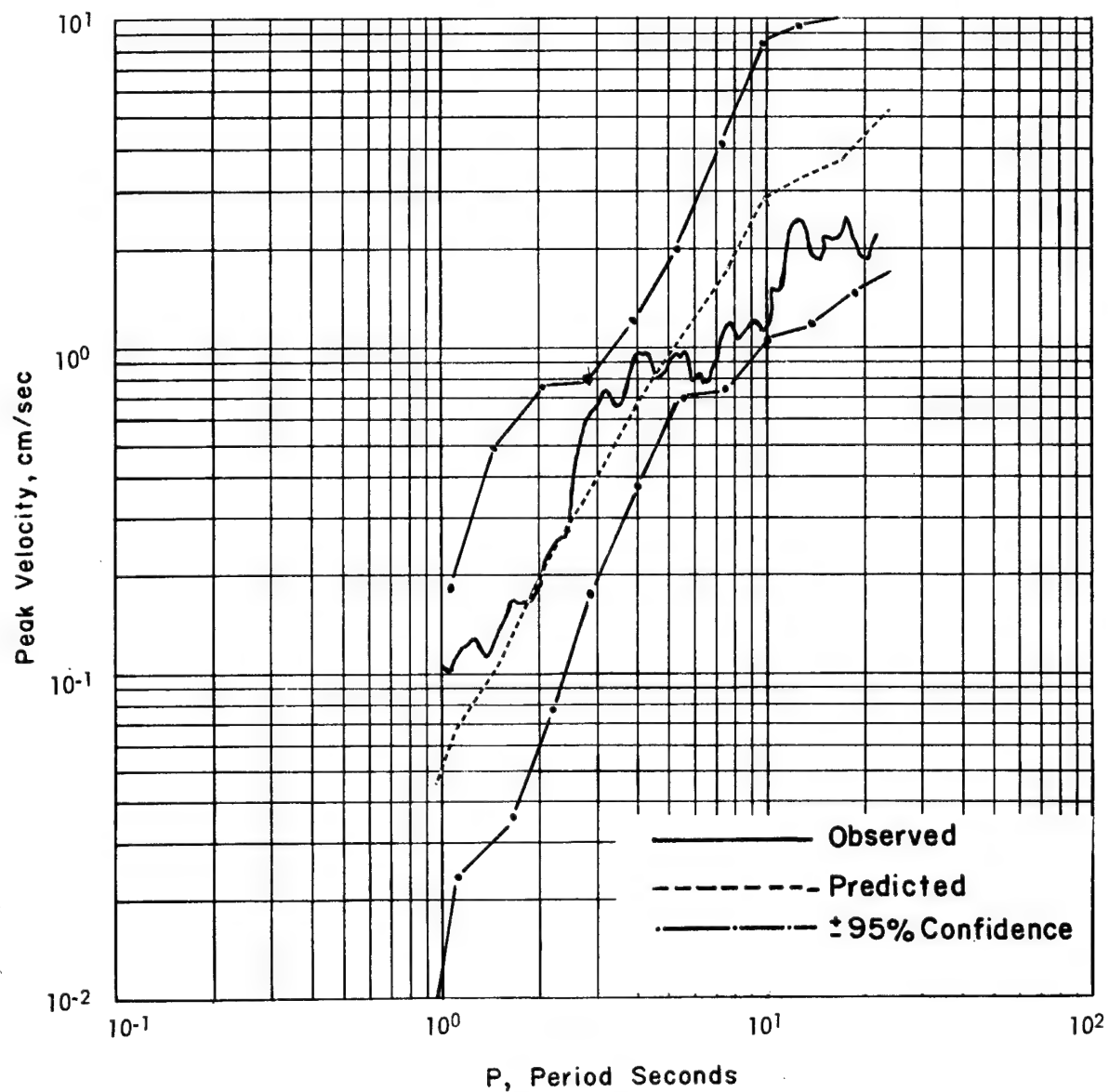
Figure 9.26. Pseudo Relative Velocity Spectra for 5% Damping from the Boxcar Event, Pahute Mesa.

125
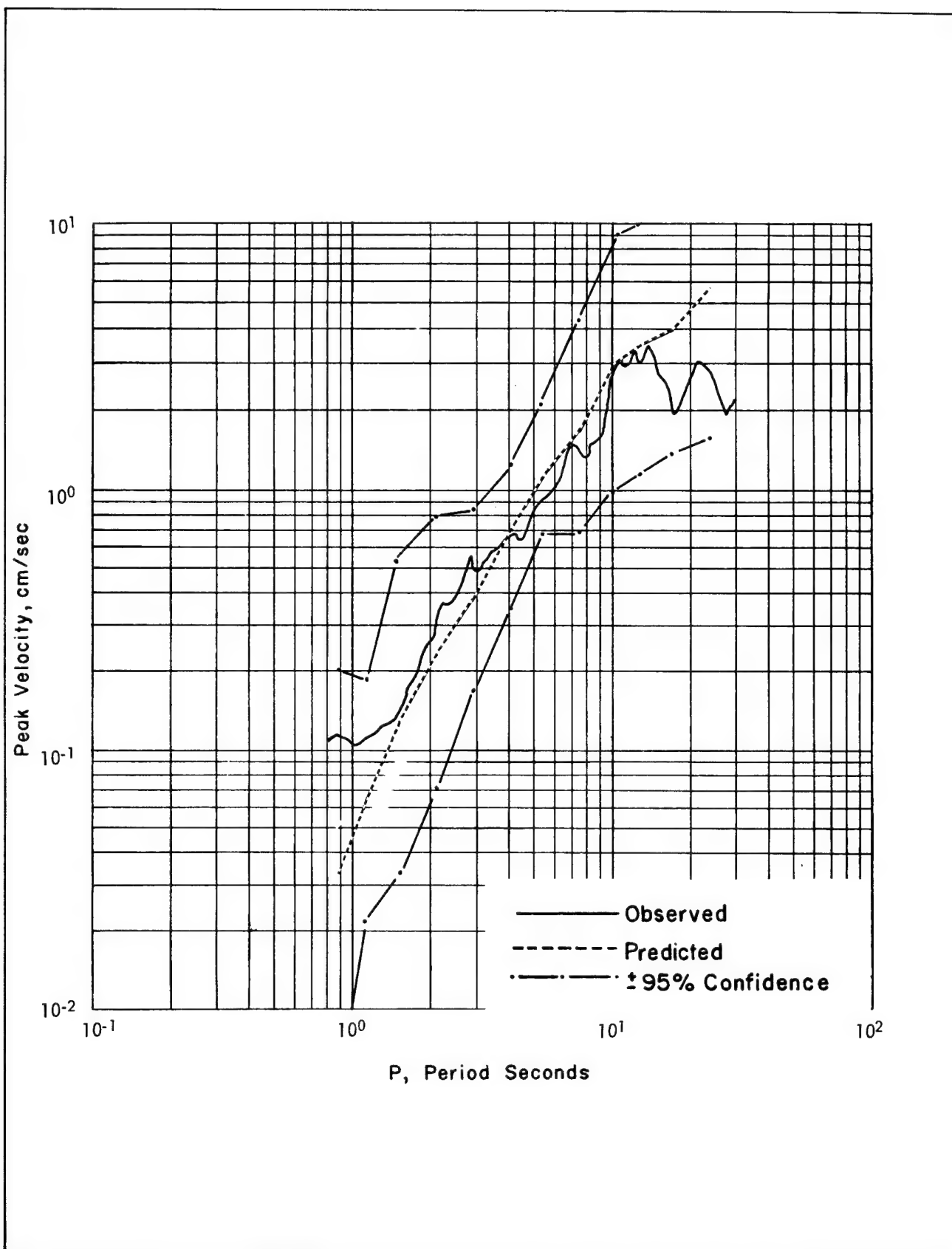
Figure 9.27. Pseudo Relative Velocity Spectra for 5% Damping, Boxcar Event, Pahute Mesa.

126
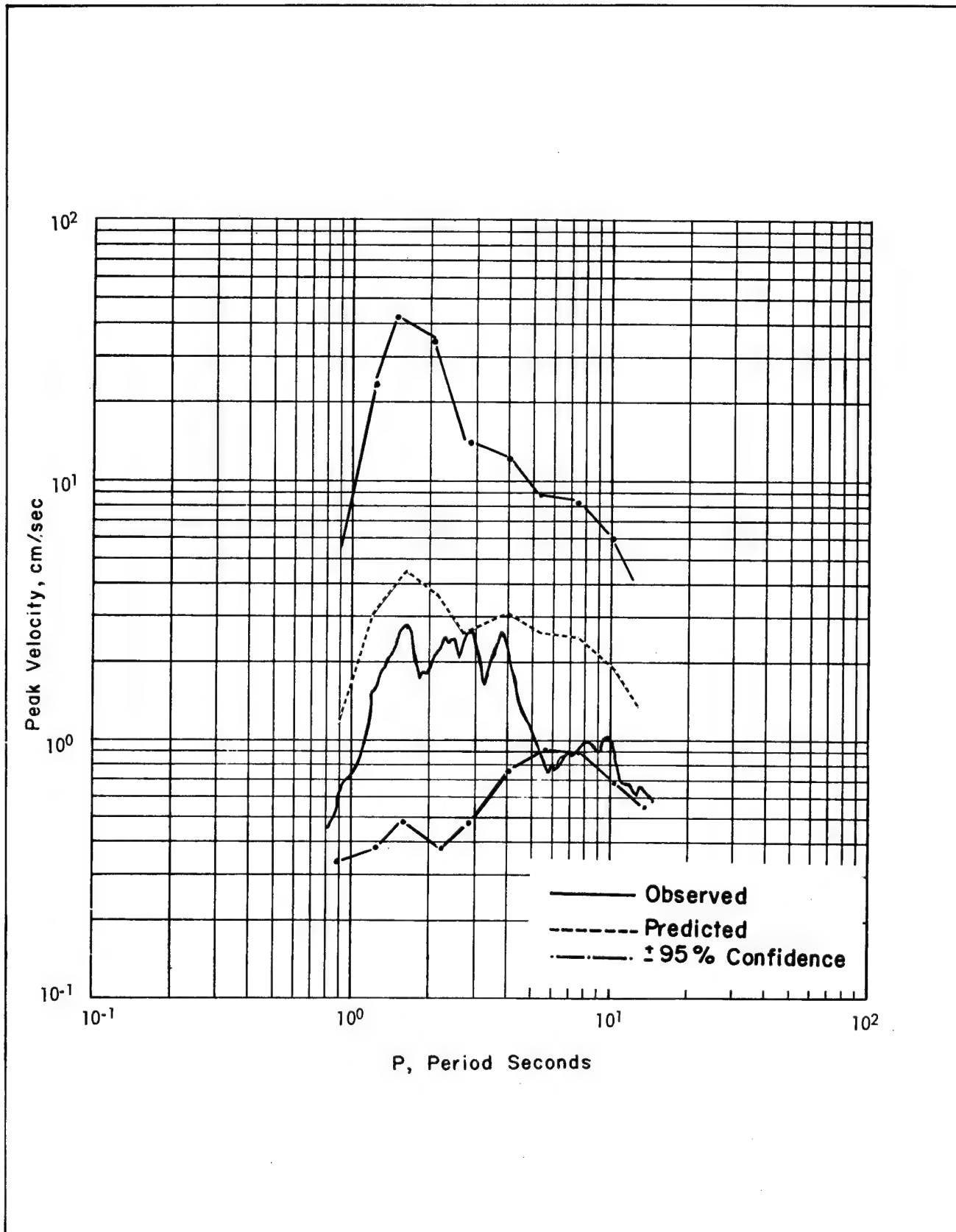
Figure 9.28. Pseudo Relative Velocity Spectra for 5% Damping, Boxcar Event, Pahute Mesa.

127
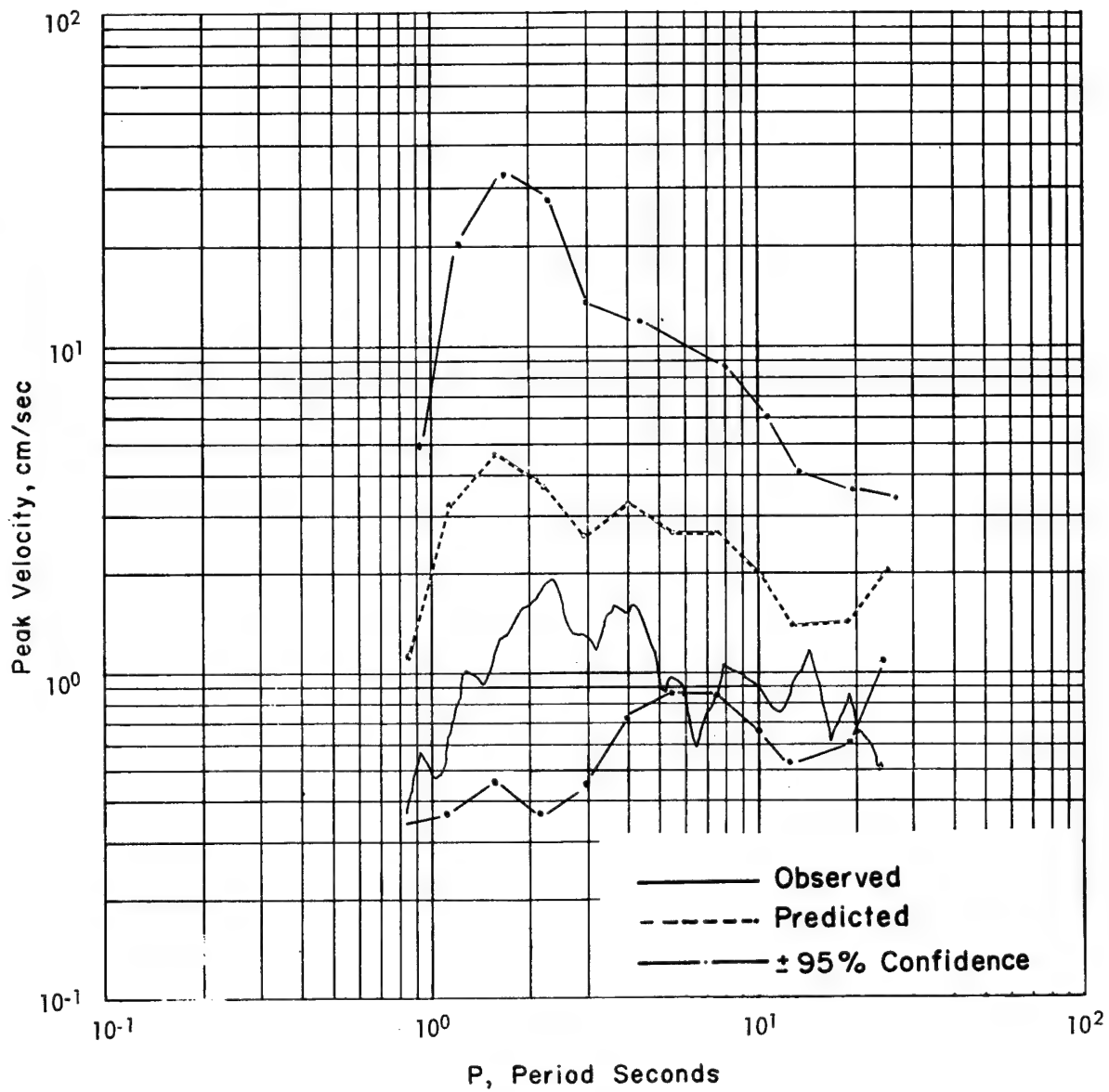
Figure 9.29.   Pseudo Relative Velocity Spectra for 5% Damping, Boxcar Event, Pahute Mesa.

128

more resistant to damage than surface structures, particularly if in good condition. Therefore, unless very precarious conditions are known to exist, concern over safety of these structures is limited to close to the detonation. The area of concern does not normally extend off the Nevada Test Site.

Following the explosion, the seismic data recorded by USC&GS are compiled, processed, and analyzed. The ground motions (both the peak values and the frequency content) are extracted from the seismograms and compared with preshot predictions. A postshot report is submitted in which the measured motions are documented in comparison with the predictions and the significance of the results in relation to current prediction methods

is discussed. The data are added to the existing fund of data so as to be available for predicting the ground motions for the next forthcoming event. This cycle is repeated on every significant underground detonation at the Nevada Test Site, and provides a thorough and constantly up-to-date evaluation of the safety aspects of the ground motions generated by underground testing at the Nevada Test Site.

Before and after each large detonation, the predictions and the results are reviewed by the NVOO Safety Panel of Consultants and by the Ground Shock Subcommittee of the NTS Planning Board. Both committees evaluate the results and make recommendations concerning the safety of each proposed new test.

Part B — Technical

Peter C. Loux; *Director, Geophysics Division*

INTRODUCTION

In Part A of our discussion, ERC's ground motion prediction problem was surveyed, current prediction parameters were described, and the purpose for these predictions was given. Let us keep this purpose firmly in mind as we continue in Part B. We are in the business of *predicting* those characteristics of ground motion that affect structures.

What are the ground motion characteristics that affect structures? One possible answer is *all of them;* that is, the complete, time-dependent ground motion vector. After much thought and study one suspects that eventually it would be possible to predict the complete seismogram, probably in some statistical sense. However, the Safety Program demands more immediate results.

Consequently, attention at ERC was first focused on the peak ground motion, amplitude-frequency content of the ground motion (BPF), and the response spectrum (PSRV). For these quantities accurate prediction techniques have been in use for approximately 5, 2, and 1½ years, respectively. The remainder of our discussion will center on these quantities as they relate to current prediction capability and also, on additional studies designed to improve our prediction capability primarily at new locations outside of Nevada.

CURRENT PREDICTION TECHNIQUE

Before discussing the ground motion analysis technique and prediction capability it is appropriate to briefly discuss the data processing effort that precedes any of the analysis. Typical velocity measurements are recorded in the field on analog magnetic tape at two or three recording levels by the USC&GS. Several field tapes are dubbed onto the tape processed at ERC. This tape is previewed,

the best data channels are selected, compensation is made for variable instrument gain, calibration is performed, appropriate seismometer response correction is made, and finally a master tape containing only useable, corrected data is generated. Velocity seismograms on the master tape are routinely processed to obtain peak amplitudes, ground motion amplitude-frequency content, response spectra, acceleration and displacement seismograms, Fourier transforms, wave mode information, and other selected parameters. This processing may be performed on the analog computer; or, the analog velocity traces are digitized automatically and the processing done on a CDC 160A or 3600 digital computer.

For those interested in the response characteristics of the velocity meters typically employed for the Safety Program, Figures 9.30 and 9.31 give the transfer functions of the NGC-21 and L-7 seismic systems currently used by the USC&GS as described in Chapter 8. It is noted that in the processing of data from these systems, the response of the NGC-21 is corrected to about 0.3 Hz and that instrument response correction is not required for the L-7 system.

Processing of the strong motion acceleration and displacement photographically recorded paper traces follows another course. These traces are digitized, semi-automatically, and run through an edit, calibration, and plot routine. The plotted, digitized trace provides an overlay trace to verify the correctness of the digitized trace. Peak amplitudes, BPF, PSRV, etc., may then be obtained via digital programs. In each large test, the processing described above for seismograms recorded on magnetic tape and on paper usually result in about 30 to 40, three component, digitized seismograms being available for analysis.
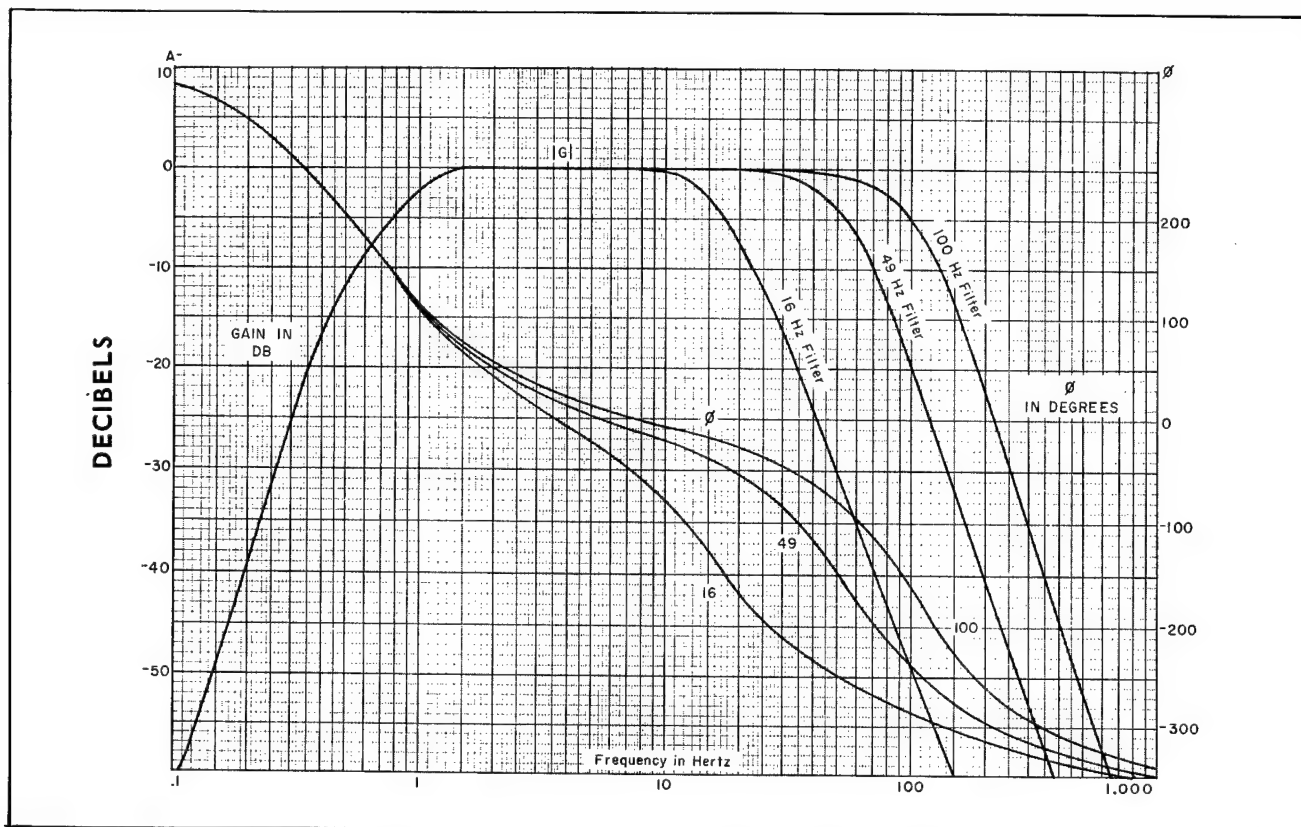
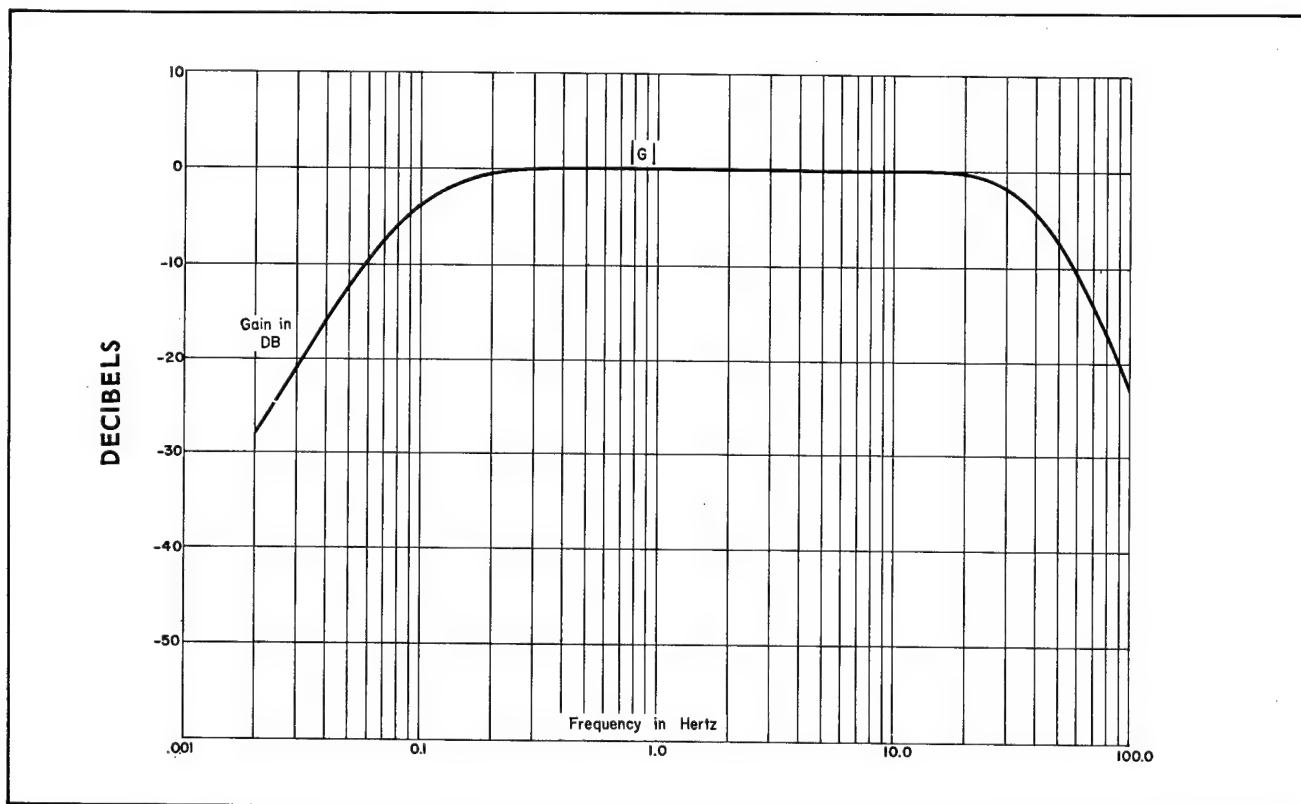Figure 9.30. Response Curve of the NGC-21 Seismic System.

Figure 9.31. Amplitude Response Curve of the L-7 Seismic System.

130

Peak Motion

As a first attempt at establishing a relationship (significant from the structural response point of view) between underground nuclear explosions and resulting seismic motion, analyses were made of nuclear generated seismic peak amplitudes recorded in and around the Nevada Test Site. It is noted that although the peak amplitude represents only one characteristic of a complicated ground motion, it is a good measure of the overall seismic signal strength.

ERC has developed appropriate prediction equations based on the data from previous detonations in similar environments to estimate the peak motions. For an example of such equations:

$$a = 5.03 \times 10^5 \, W^{.70} \, R^{-2.00}$$
$$u = 8.64 \times 10^6 \, W^{.73} \, R^{-1.87} \qquad (2)$$

where a = peak surface particle acceleration - g

u = peak surface particle velocity - cm/sec

W = yield - Kt

R = distance - meters

These equations are derived empirically; their increased accuracy being proportional to the quantity of new data available. For this reason the exponents of W and R and the constant K is subject to change from time to time. The period of change is also dependent on the quantity of new data available. Data collected by USC&GS in Las Vegas and elsewhere around NTS provide the best basis for ground motion predictions.

Ground Motion Frequency Content

We now know that we can predict peak motions within acceptable limits. But what about the frequency content of the seismic motion? Surely, for example, the high-rise buildings in Las Vegas possess certain resonant frequencies. The validity of that statement can be seen from the following experiment where the response of a few Las Vegas buildings was simulated on an analog computer, each with just two, coupled, single-degree-of-freedom systems each, by definition, possessing a single resonant frequency (Figures 9.32 through 9.34). At the top of Figure 9.33 is shown the transverse velocity caused by event Halfbeak and recorded at the base of the Dunes Hotel. The center seismogram is the measured top velocity, and the bottom seismogram is the output of the simulation circuit. Thus, this rather accurate simulation makes it appear quite obvious that these high-rise buildings are characterized by at least two dominant frequencies.

The point here is that the *frequency content* of the seismic motion that drives the structures must be predicted; otherwise, only a rough estimate can be given for the associated structural response. What kind of frequency information can and should be predicted? Visual seismic frequencies are rather tenuous in that the wave form is very often superpositions of several frequencies. Fourier amplitude spectra of these seismic motions are useful for selected studies. However, Fourier spectra exhibit extremely detailed oscillations due to ringing caused by the several arrivals. In addition, the corresponding phase spectra are complex and cannot be conveniently used. Because of these and economic factors we decided to study the peak output of narrow analog band-pass filters, with actual seismograms as input.

Band-Pass Filtering (BPF) is a fundamental operation in many well known analog data processing schemes. The basic operation is simply to filter a signal in the frequency domain with a narrow band-pass filter having a tuneable bandwidth. Two familiar analog operations which utilize BPF are power spectral density measurements and cross spectral density measurements. Figure 9.35 illustrates the power spectral density operation.

The power spectral density function, as an analog operation, can be described as follows:

1. Frequency filtering of the signal by a narrow band-pass filter having a bandwidth of B_e Hz.

2. Squaring of the instantaneous value of the filtered signal.

3. Averaging the squared instantaneous value of the filtered signal.

4. Division of the mean square output by the bandwidth B_e.

The cross spectral density function is estimated by the following analog operations, as indicated in Figure 9.36:

1. Individual frequency filtering of the two signals $x(t)$ and $y(t)$ by narrow band-pass filters having identical bandwidths of B_e Hz and the same center frequency.

2. Multiplying the instantaneous values of the two filtered signals with no phase shifts.

3. Multiplying the instantaneous values of the two filtered signals with one shifted 90 degrees out of phase with the other.

4. Averaging each of the two instantaneous product values over the sampling time.

5. Division of each of the two mean products by the bandwidth B_e.

The important point is that the BPF principle is the key step in spectral density operations which many people in oil exploration, earthquake seismology, and other disciplines use routinely. Many articles have been pub-

131
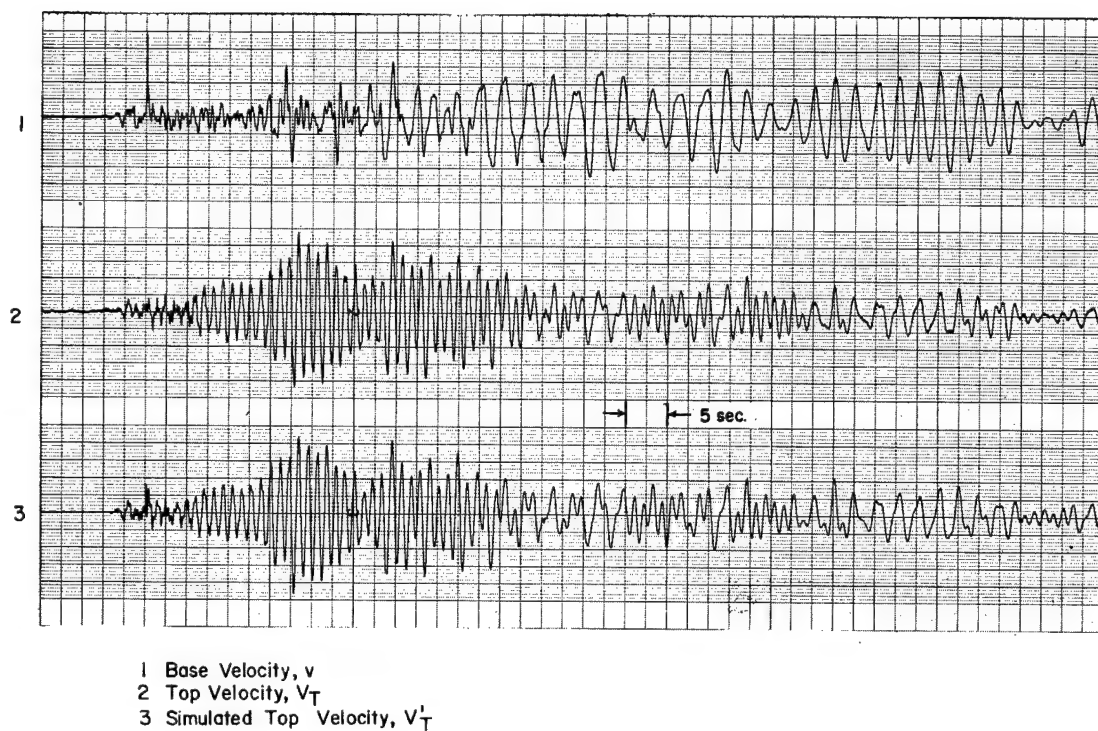
Figure 9.32. Example of Simulation. Event: Corduroy. Building: First National Bank. Component: T.

1   Base Velocity, v
2   Top Velocity, V_T
3   Simulated Top Velocity, V_T'
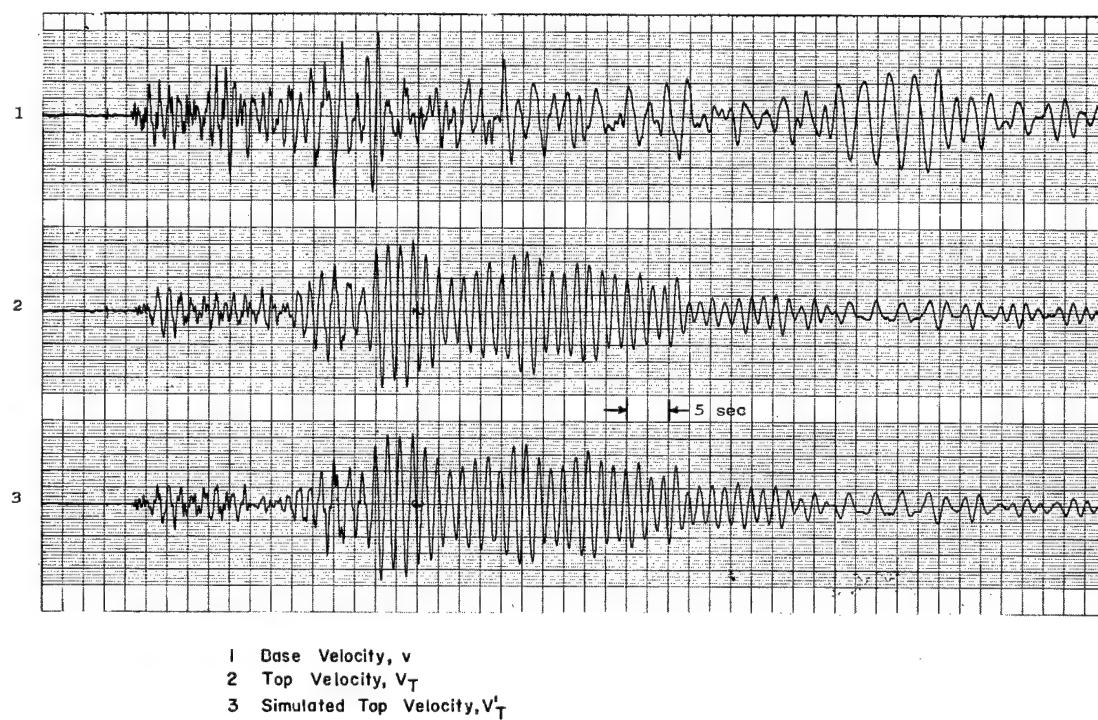
Figure 9.33. Example of Simulation. Event: Halfbeak. Building: Dunes Hotel. Component: T.

1   Base Velocity, v
2   Top Velocity, V_T
3   Simulated Top Velocity, V_T'

132
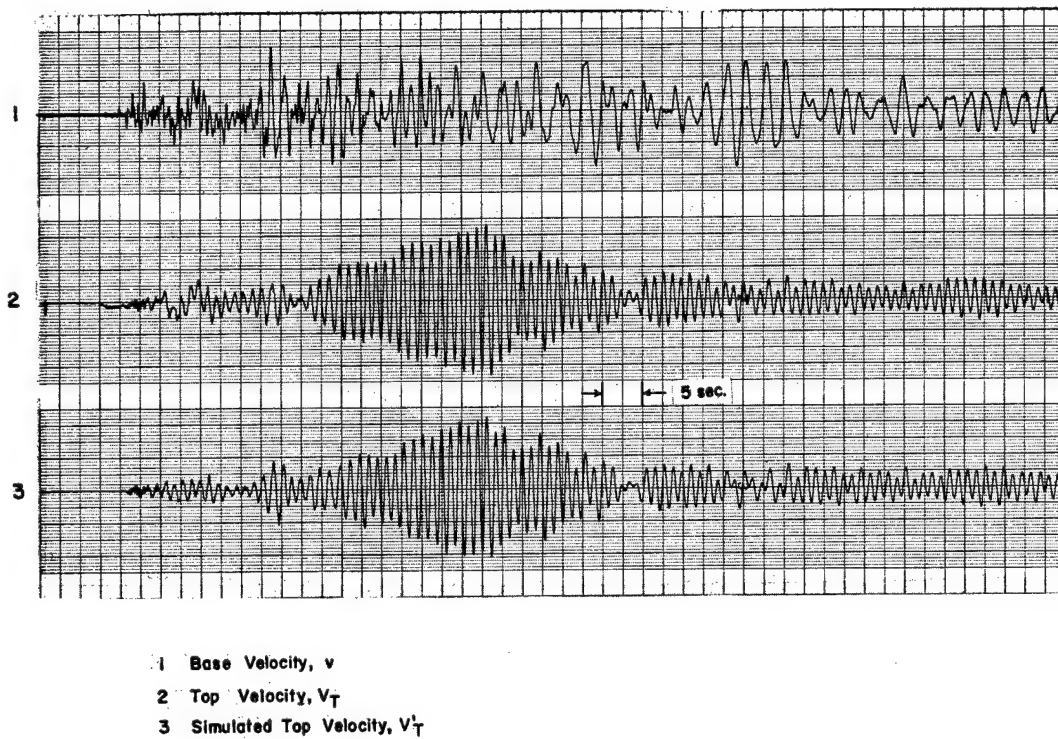
Figure 9.34.   Example of Simulation. Event: Tan. Building: Sahara 400. Component: T.

1   Base Velocity, v
2   Top Velocity, V_T
3   Simulated Top Velocity, V_T'

Figure 9.35.   Functional Block Diagram for Power Spectral Density Analyzer.

133
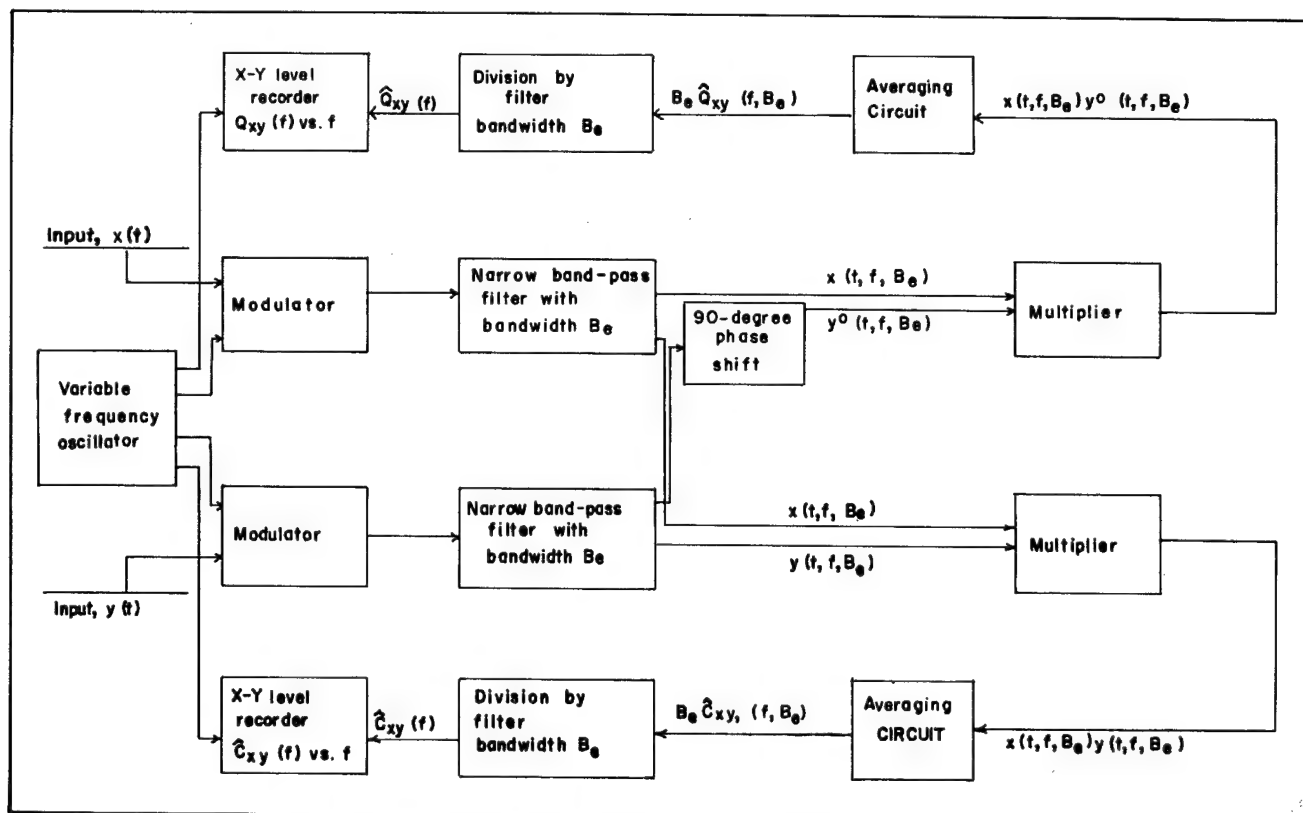
Figure 9.36. Functional Block Diagram for Cross Spectral Density Analyzer.
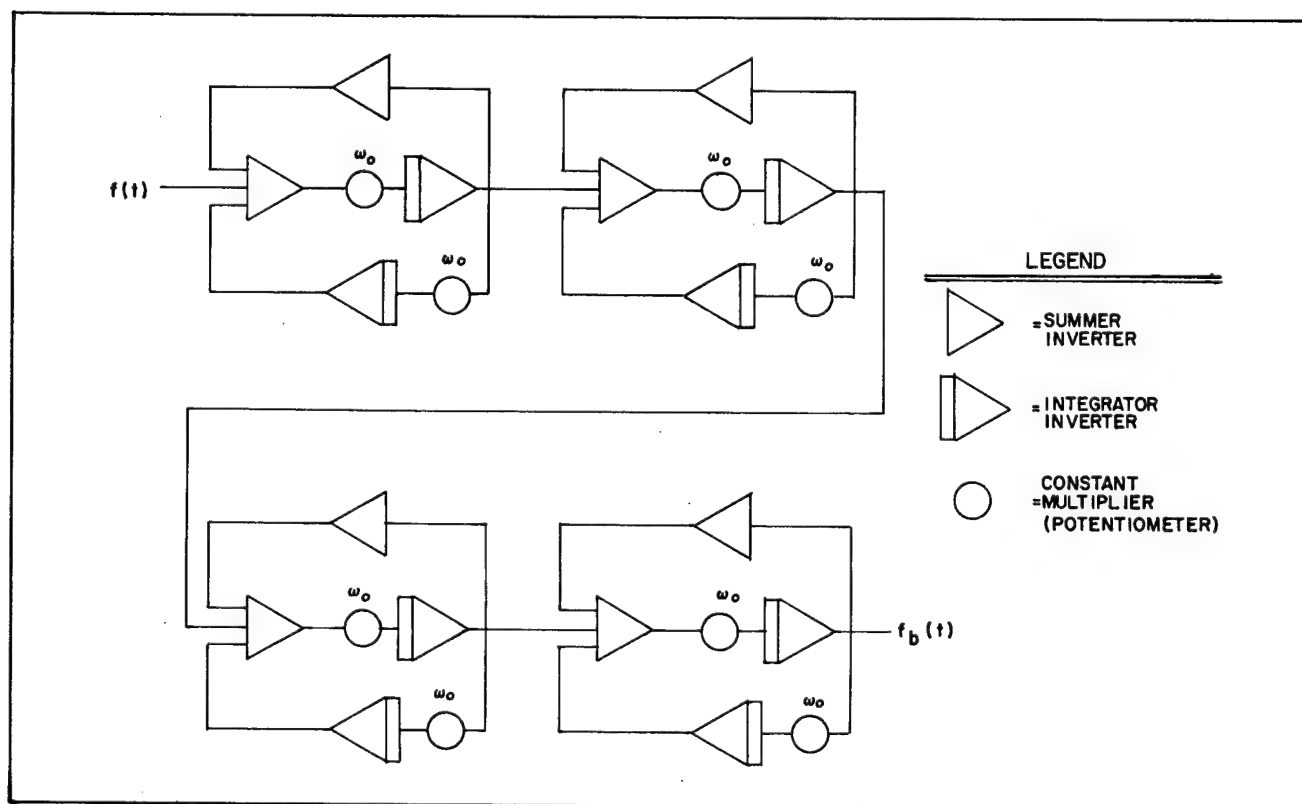
Figure 9.37. Band-Pass Filter Analog Computer Diagram.

134

lished in Geophysics, Bulletin of the Seismological Society of America (BSSA), and Journal of Geophysical Research (JGR) which describe specific application of BPF to problems in these professions. For example, Willis, DeNoyer, and J. T. Willson employ the band-pass filtering technique in the study of high frequency energy in seismic recordings from high explosive, underground nuclear, and earthquake sources (VESIAC 4410-52-x). Sutton and Pomeroy of Lamont Geological Observatory described the use of BPF and other techniques (JGR, vol. 68, p. 2791, 1963) for routine processing of earthquake records. Oil companies have used band-pass filtered seismic data for many years to obtain greater time resolution in subsurface mapping. Some specific references to this work in the broadest sense are the MIT Geophysical Analysis Group reports and various reports such as, "A Review of Methods of Filtering Seismic Data," (Geophysics, vol. 23, p. 44, 1968) by Mark Smith. Other oil company uses include special BPF applications to remove the effect of ghosting and reverberation by shallow surface and water layers, to whiten the amplitude spectrum, for power spectral density determinations, and recently for analysis filtering. Many of these uses have not been published explicitly and are in the category of company confidential information. Others are not published except in the brochures of contract geophysical crews.

Earlier you saw typical band-pass outputs and the Band-Pass Filter, or BPF curve, representing a plot of the peak filter outputs as a function of filter center frequency. Realization of the BPF filter on ERC's analog processor is shown by the circuit in Figure 9.37.

Let us now consider ways this indicator of ground motion frequency content is routinely predicted at ERC. Three methods are employed. The first, employing data from over 20 nuclear events and a dozen stations in the Las Vegas — NTS area, is a linear regression on the seismic BPF peaks processed at ERC. Yield and distance are the independent variables and BPF center frequency is the parameter. Thus, 12 BPF prediction equations, one for each filter center frequency of interest, were developed from the entire BPF data sample which is composed of over 200 samples at each frequency. Figures 9.38 through 9.40 show the BPF predictions with yield as parameter, for three distances, 40 km, 100 km, and 160 km. In all cases a shift toward lower frequencies is observed as the yield increases. Also, the low pass filter action of the earth is evident in that the higher frequencies are more attenuated with distance.

Figure 9.41 provides a comparison of predicted and measured BPF seismic frequency content at a Las Vegas station, for one of the larger detonations. The solid line
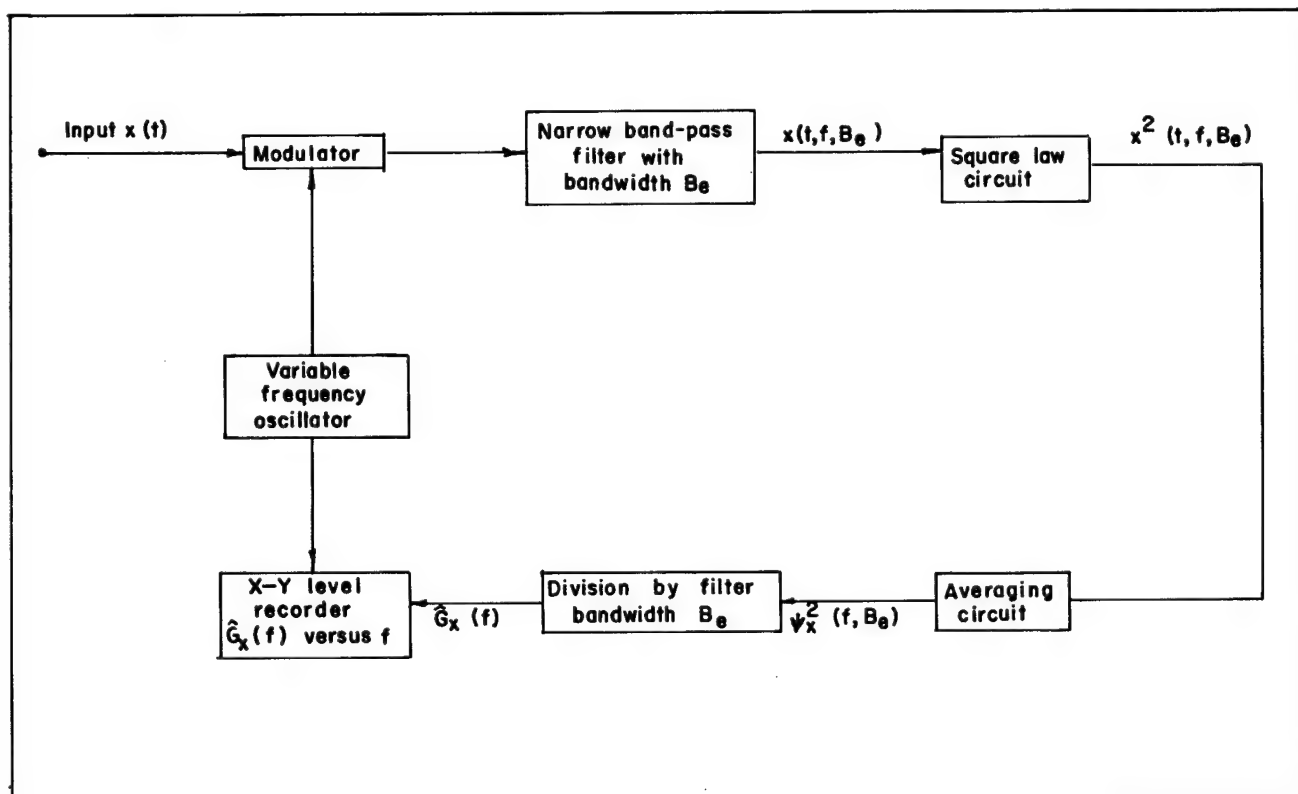
is the predicted mean, the inner dashed lines enclose the 50 percent confidence interval on the prediction, and the outer dashed lines enclose the 90 percent confidence interval.

A second method, feasible where sufficient data have been accumulated, effectively removes the data scatter associated with the distance variable. The technique in this case is to run the regression on BPF peaks with only one independent variable, namely yield. This is done particularly at stations of interest. For example, Figure 9.42 provides comparison of this single-station and the aforementioned (total sample) technique versus measured BPF values at a station in Las Vegas, and for one of the larger events. The dashed line gives the total sample prediction and the solid line gives the single-station prediction. As anticipated, the single-station prediction is more accurate.

Another seismic frequency prediction technique is based on an extrapolation method. The BPF amplitude variation with yield at each frequency is assumed to be independent of distance, transmission path, station factor, and other indeterminates. Variation with yield is taken to be the same as was derived from the regression analysis on the total BPF data sample. Finally, given a BPF curve from a low yield event, the assumed variations with yield are applied to this curve appropriately at each BPF frequency. Thus, a BPF prediction can be generated fairly accurately for a larger yield. Figures 9.43 and 9.44 provide examples of this technique. The first, an extrapolation in yield of 1.5 orders-of-magnitude at a station in the town of Tonopah, is seen to agree well with the measured values. The second is an extrapolation of 3 orders-of-magnitude. Note that the seismic amplitude-frequency content is different at these two stations. In spite of this, we see that the seismic frequency content of both can be predicted quite well.

Response Spectrum (PSRV)

If a simple single-degree-of-freedom system such as that shown in Figure 9.45 is subjected to ground motion caused by a nuclear explosion or an earthquake, it will be excited into motion and will respond in a vibratory fashion. The equation of motion for the system can be written as

$$m \ddot{u} + \eta \dot{u} + \lambda u = -m \ddot{x} \qquad (3)$$

This equation can be solved in various well-known ways. It turns out that for a given transient ground motion X as a function of time, the resistance of an elastic system
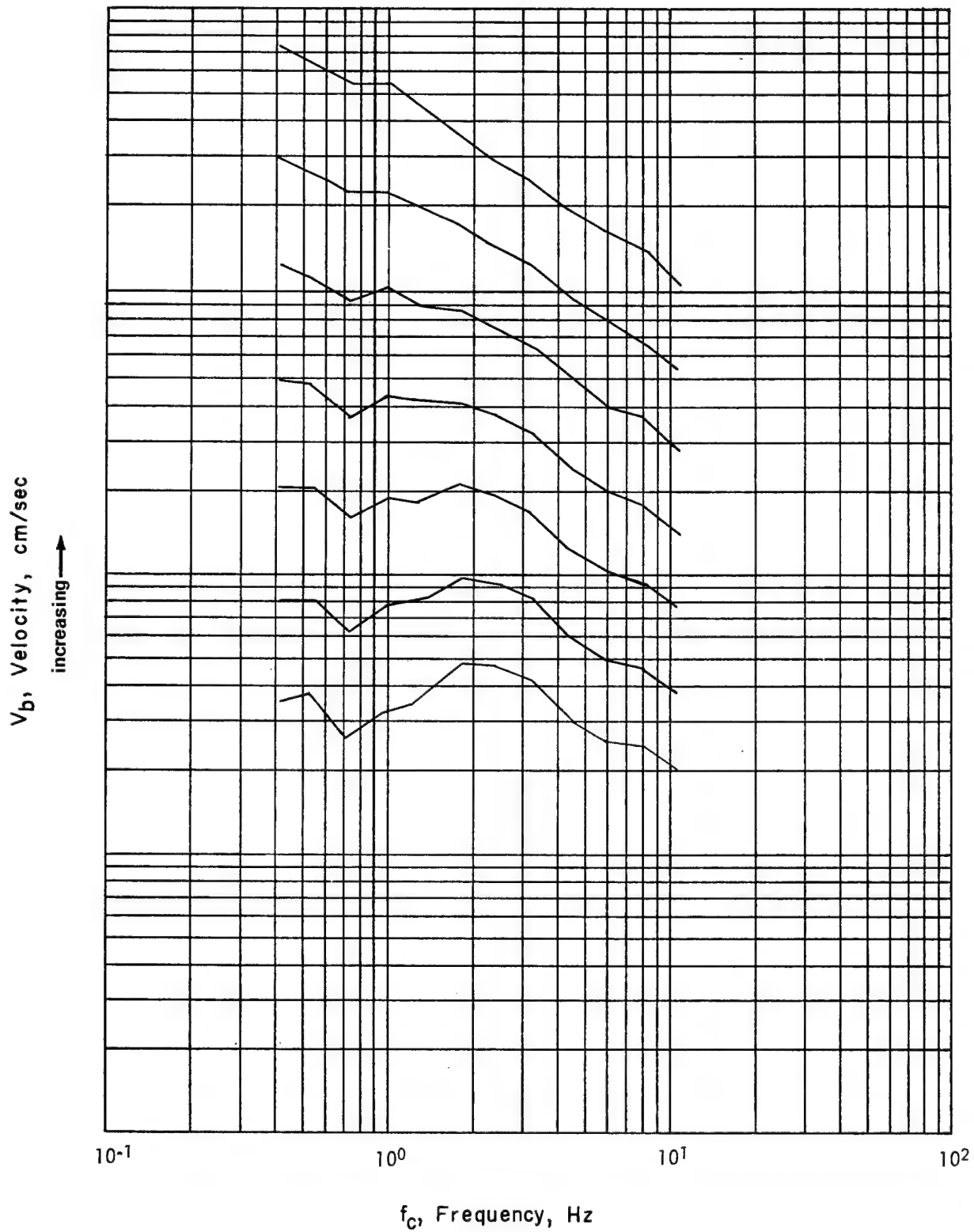
Figure 9.38.   Family of Mean BPF Curves, V_b Versus f_c, for Seven Yields. Distance Equals 40 km.
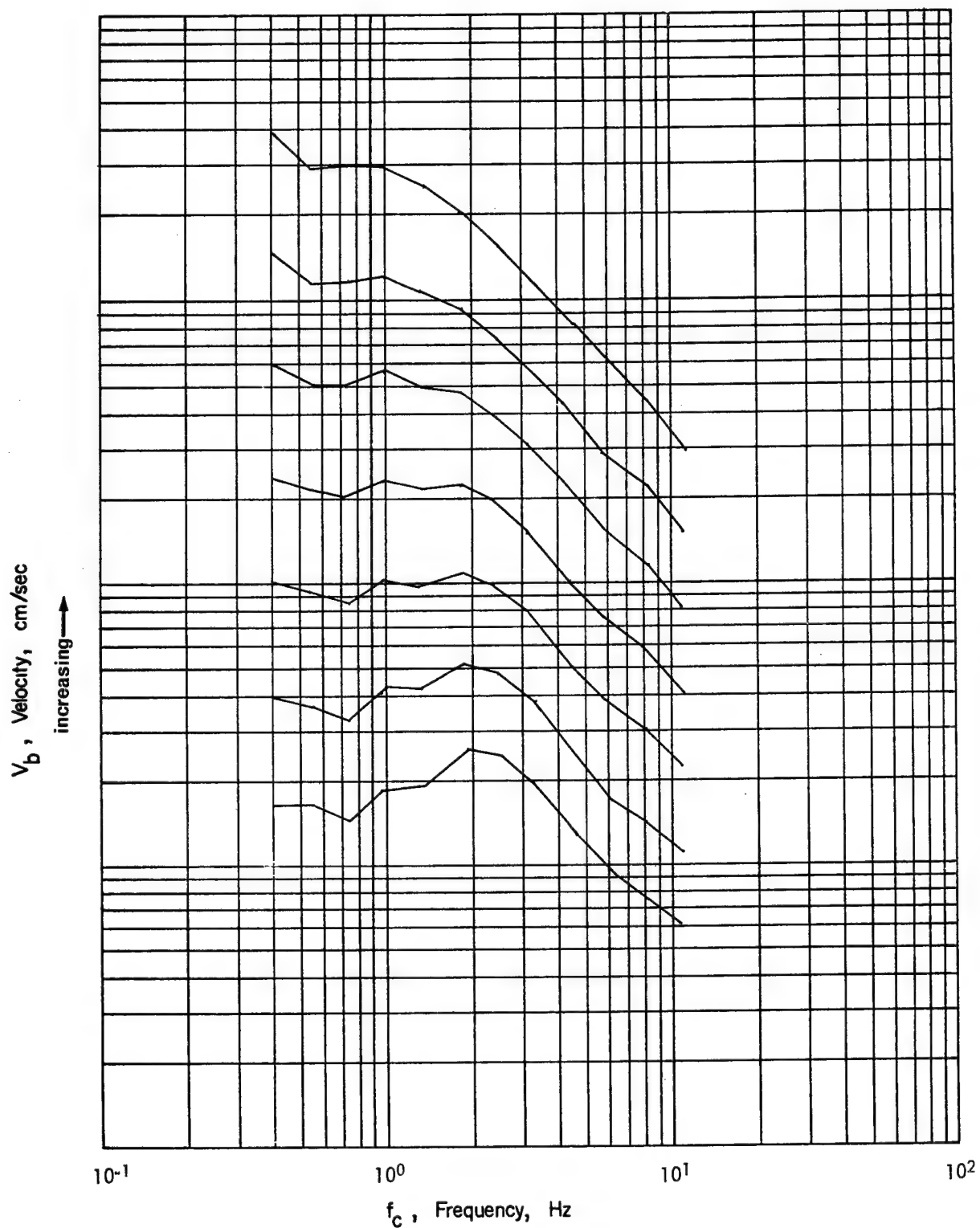
Figure 9.39.   Family of Mean BPF Curves, V_b Versus f_c, for Seven Yields. Distance Equals 100 km.
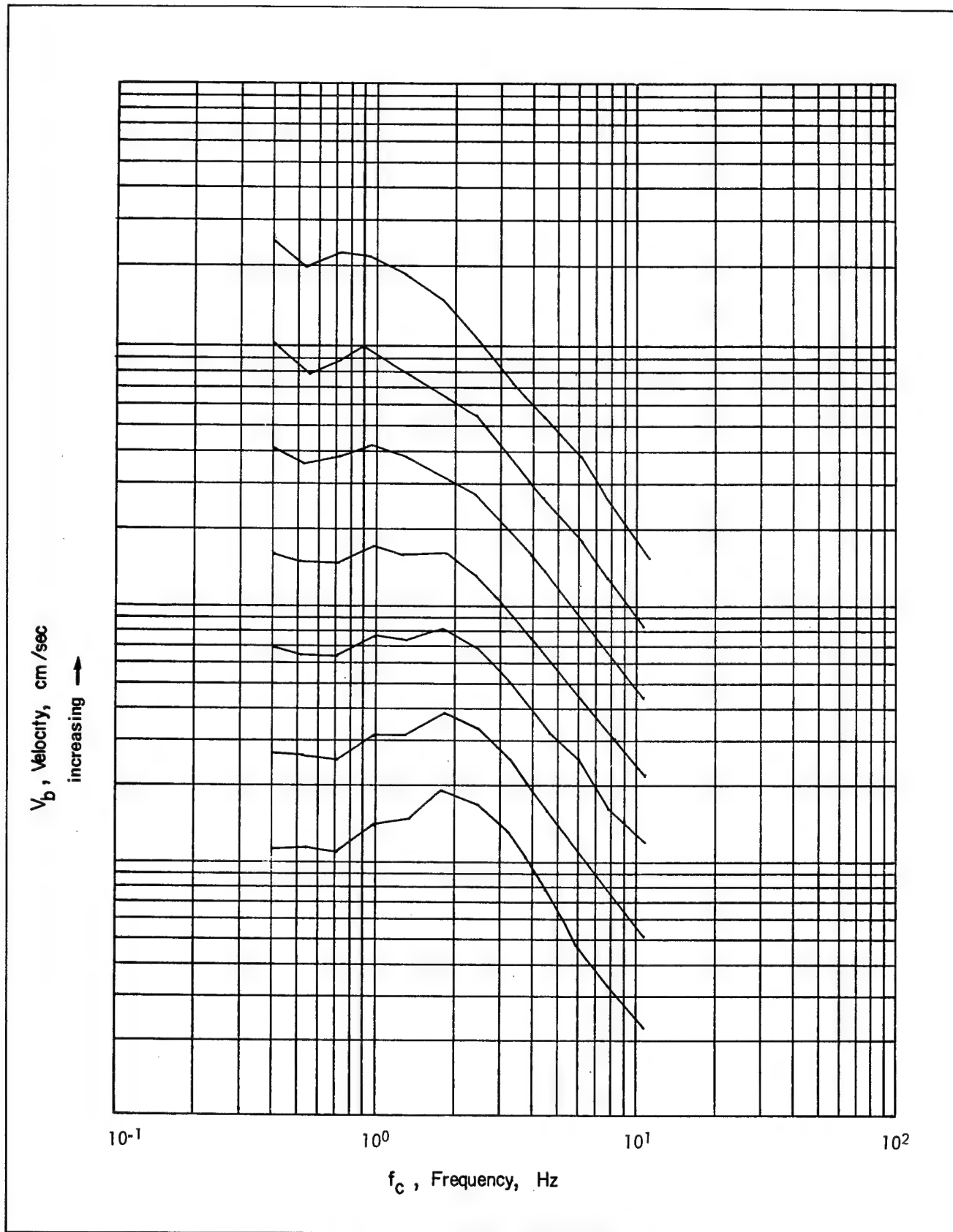
Figure 9.40. Family of Mean BPF Curves, V_b Versus f_c, for Seven Yields. Distance Equals 160 km.

138
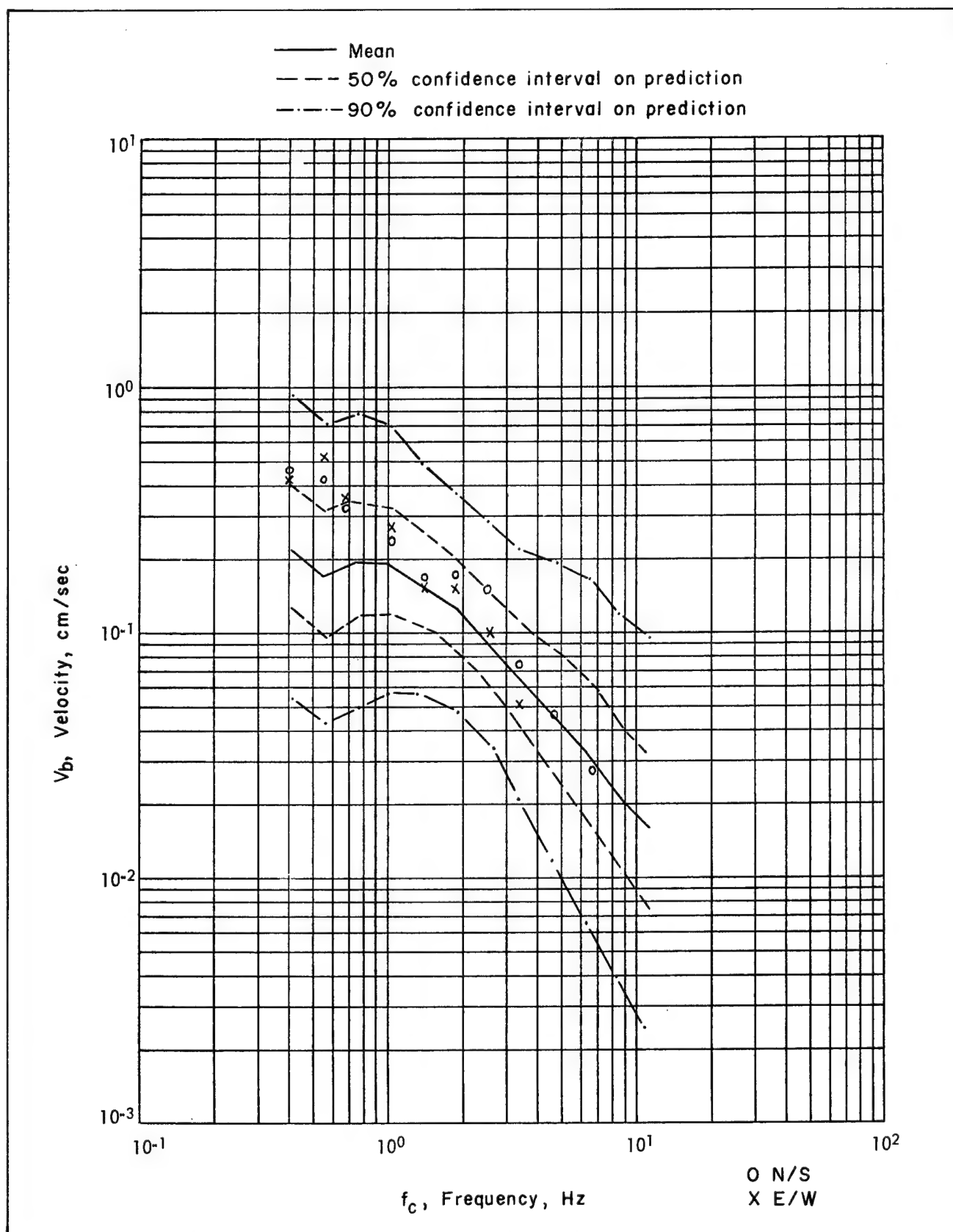
Figure 9.41. Predicted (From Total Sample) and Observed BPF Data at Station SE-6, Las Vegas, for the Greeley Event, Pahute Mesa.

139
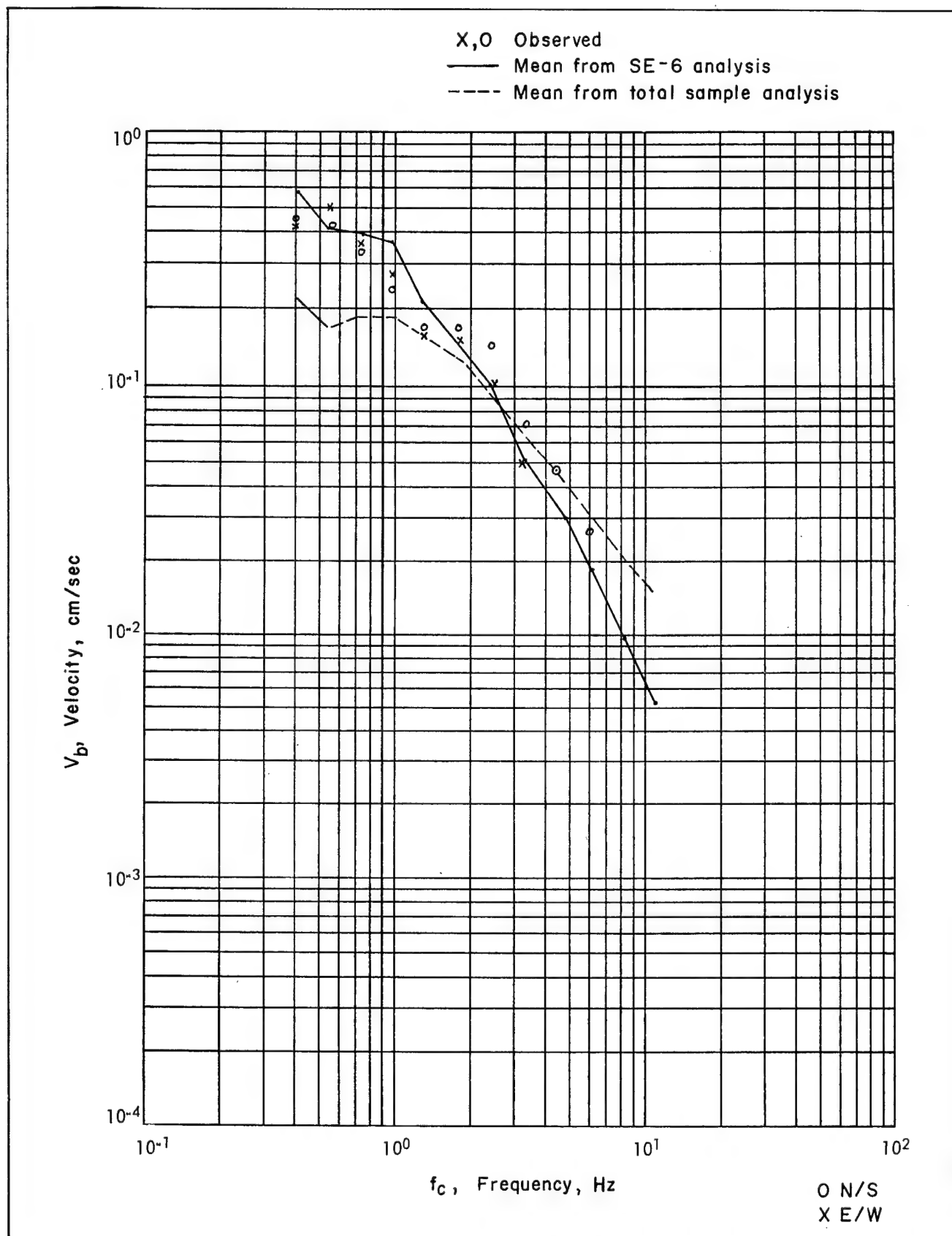
Figure 9.42. Observed BPF Data at Station SE-6, Las Vegas, for the Greeley Event, Pahute Mesa, With Predictions from the Total Sample and SE-6 Analysis.
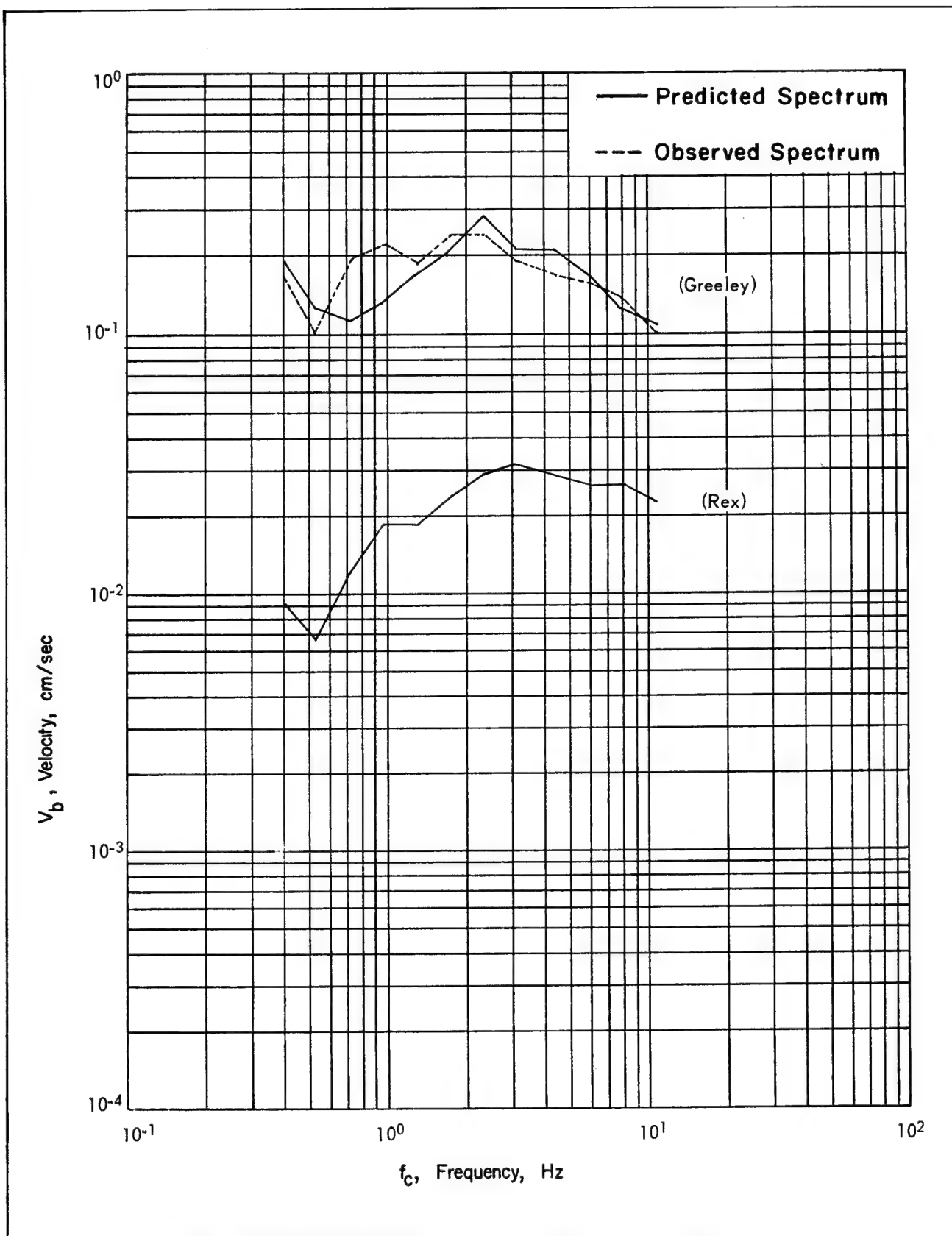
Figure 9.43. Extrapolation (Dashed Line) of a Low Yield BPF Curve to a Higher Yield Curve. Station: Tonopah Motel. Yield Ratio: 44 from Events Greeley and Rex, Pahute Mesa.
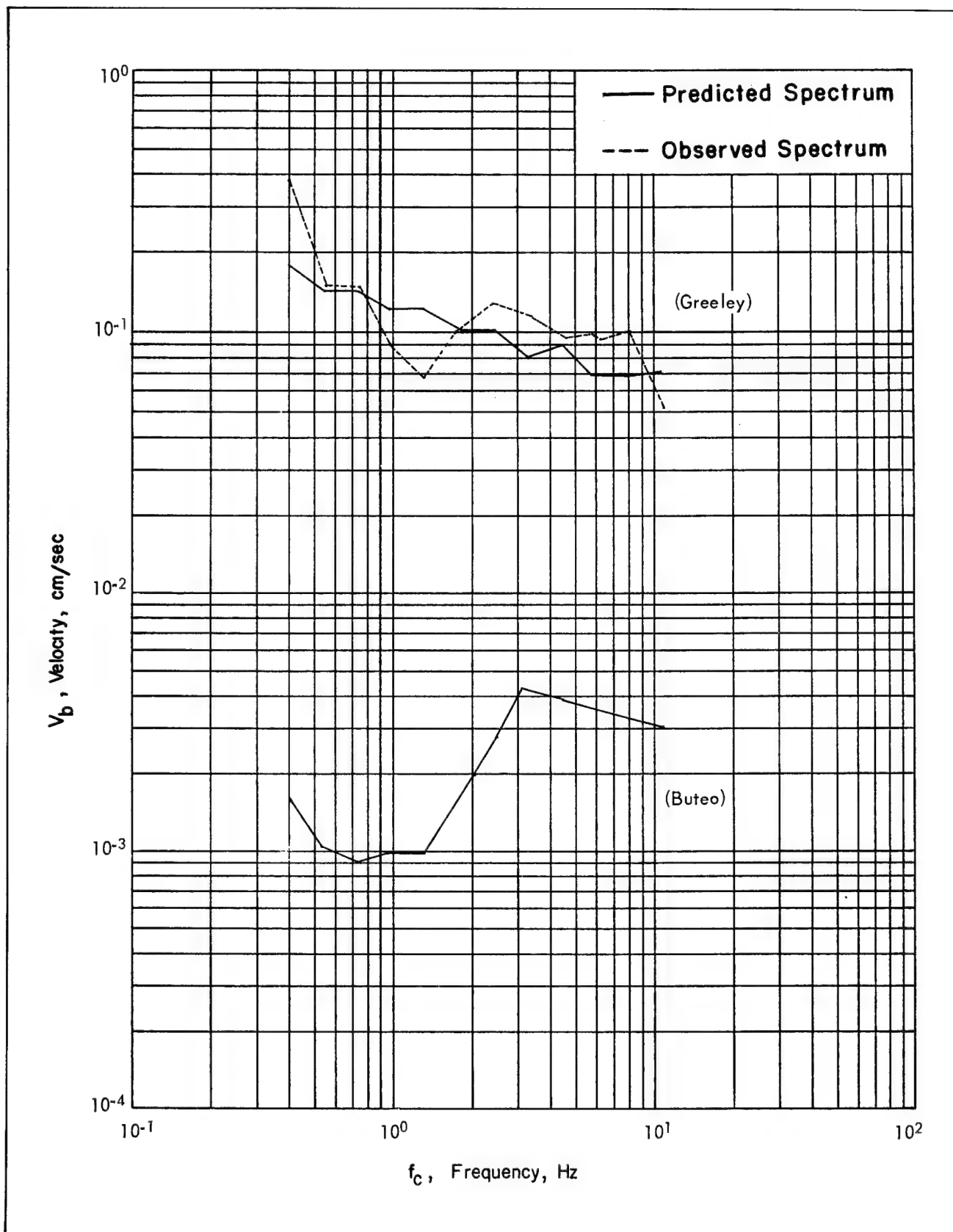
Figure 9.44. Extrapolation (Dashed Line) of a Low Yield BPF Curve to a Higher Yield Curve. Station: SE-2. Yield Ratio: 1200 from Events Greeley and Buteo.

$$M\ddot{U} + \eta\,\dot{U} + \lambda\,U = -M\ddot{X}$$
$$(\lambda = \text{stiffness coefficient})$$

Y

U

MASS M

POSITIVE DIRECTION OF
MASS DISPLACEMENT

Y ⟶

X

ORIGINAL
POSITION

DAMPER

η

COLUMN DEFORMATION

U = Y − X

Positive Direction of Ground
Displacement X ⟶

Figure 9.45.   Single-Degree-of-Freedom Structure.

143

depends only on the magnitude of the damping η and on the circular frequency of vibration of the system or, what amounts to the same thing, on the percentage of critical damping and the natural period of the system. In other words, the magnitudes of the mass and of the spring stiffness of the system do not independently affect the response to a ground motion.

For a specific excitation of a simple system having a particular percentage of critical damping, the maximum response is a function of the natural period of the system. A plot of the *maximum* response (relative displacement u, absolute displacement y, relative velocity $\dot{u}$, absolute acceleration $\ddot{y}$, or spring force V) against the period of vibration is called a response spectrum. The most useful response spectra are those for absolute acceleration $\ddot{y}$, relative velocity $\dot{u}$, and relative displacement u. The maximum values of velocity and acceleration are not actually plotted as the spectral values, because it is more convenient in practice and sufficiently accurate to use something that approximates the maximum velocities and accelerations and which is more simply related to the displacements. The quantity used for velocity is

$$S_v = 2\pi f s \qquad (4)$$

where s is the spectral value of the displacement and is relative to the ground, and f is the frequency of the vibration. The quantity used instead of the actual relative velocity spectra is called PSRV, and is very nearly equal to the maximum relative velocity except for very low frequency systems. It is precisely equal to the maximum velocity if the maximum velocity occurs after the ground motion ceases. It is a measure of the elastic energy in the spring elements of the system.

Although there are minor differences among spectra plotted for different input data, they all show roughly the same general characteristics:

1. The spectra for zero damping show rather marked oscillations with very irregular sharp peaks.

2. The oscillations generally decrease as the damping increases.

3. For intermediate frequencies, the maximum spectral velocity has a magnitude of several times the input velocity for no damping — ranging down to values about equal to the input maximum ground velocity for about 20 percent critical damping.

The Pseudo Relative Velocity (PSRV) curve, the peak response to ground motion of a single-degree-of-freedom system, operationally is obtained in much the same manner as the BPF curve. A basic difference is that the PSRV response spectrum is derived from a second-order

versus eighth-order filter as shown in the following equations:

$$\text{PSRV: } F(S) = \frac{S\omega_0}{S^2 + 2h\,\omega_0 S + \omega^2_0} \qquad (5)$$

$$\text{BPF: } F(S) = \left[\frac{S\omega_0}{S^2 + \omega^2_0 + S\omega_0}\right]^4 \qquad (6)$$

ω_0 = filter center frequency
h = damping coefficient
S = laplace transform variable

Figures 9.25, 9.46, and 9.47 show examples of pairs of PSRV and BPF curves derived from the same input seismogram. Very apparent is the fact that the pairs all are approximately parallel over the entire period range. The ratio of several of these pairs, derived from seismograms recorded from 40 km to 200 km from NTS, was analyzed statistically and a relatively constant factor was derived from the analysis.

Data were taken by component, event, and combined events. From the entire sample of 1673 readings the amplitude ratio was found to have a mean value of 8.57 for 2 percent response spectrum damping, a standard deviation of 2.45, and a normal distribution about the mean. That is if we multiply the BPF curve by a factor of 8.57, a good approximation to the PSRV curve is obtained. This factor is presently used to predict an estimate of the response spectrum, which in turn is used by the AEC Structural Response Contractors in estimates of predicted structural response.

Now let us review programs related to the ground motion prediction problem and discuss a few of the related studies being conducted for the purpose of furthering prediction capability, primarily in new areas outside of Nevada.
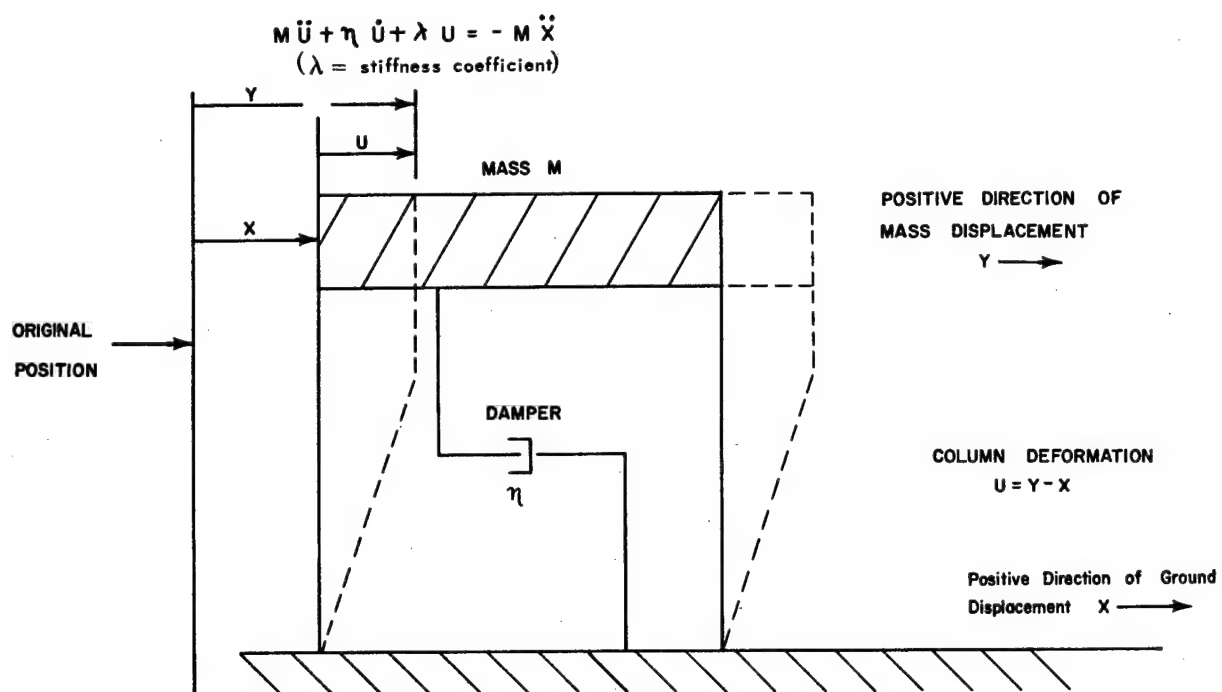
RELATED STUDIES

Part A — Theoretical-Empirical

Shock Wave Studies (Source)

A method for calculating nonlinear earth motions from an underground nuclear detonation has been developed. The calculation begins with a thermodynamic description of material in some initial cavity and proceeds to calculate the dynamic response of material both within and without the expanding cavity by utilizing adiabatic equations of state for cavity material; a one-dimensional mass-spring system for material near, but outside, the cavity and a two-dimensional mass-spring system for material beyond the distance at which motions are effectively radial. The two-dimensional model is suffi-
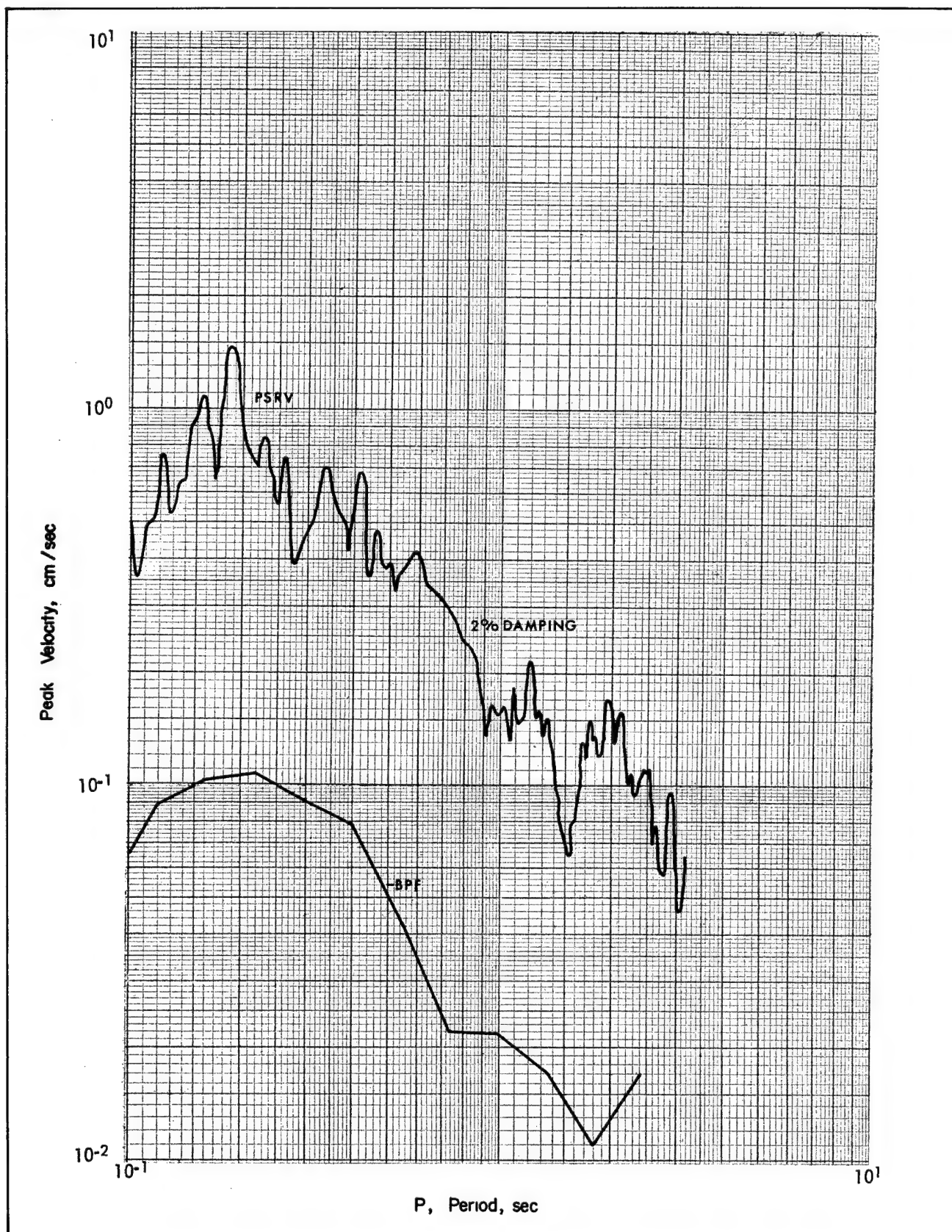
Figure 9.46. Pseudo Relative Velocity and Band-Pass Filter Spectra — Chartreuse Event, Pahute Mesa.
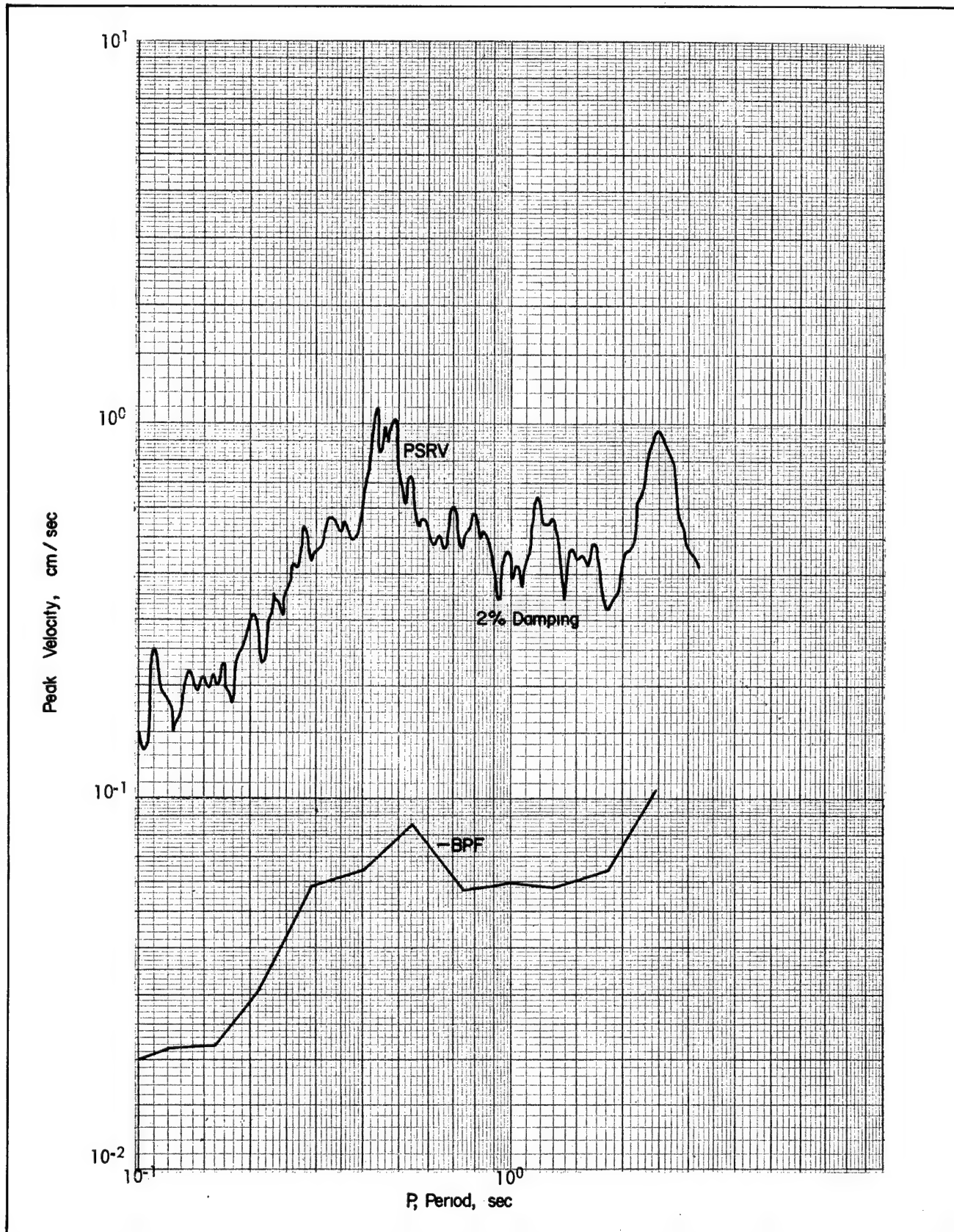
145

Figure 9.47. Pseudo Relative Velocity and Band-Pass Filter Spectra – Duryea Event, Pahute Mesa.

ciently versatile to permit incorporation of permanent distortions, spalling, and cracking. The calculation is intended to provide an input to the elastic (seismic) region as well as a description of events within the non-elastic region.

The equation of state used for the cavity material was derived from an equation developed from statistical mechanics considerations by Lewi Tonks (Physical Review, vol. 50, 1936). The adiabatic form of the equation is:

$$P^{\Omega} = Constant$$

where

$$\Omega = V\left[\frac{1 - 0.85\Theta^3 - 0.15\,\Theta^4}{1 + 2.96\Theta + 5.48\,\Theta^2}\right] \qquad (7)$$

$$\Theta = \frac{V_{min}}{V}$$

Thus, $V = V_{min}$ makes $p = \infty$, and $V >> V_{min}$, $\theta \simeq 1$, $\Omega \simeq V$ and the results approach those of the ideal gas. V_{min} is taken as the smallest volume, corresponding to $p = \infty$, from the Hugoniot equations of state.

Material outside the cavity is subjected to shock compression, the mathematical expression for which is the Rankine-Hugoniot equation:

$$p = \frac{A\,\zeta}{(1 - B\zeta)^2} \qquad (8)$$

where

$$\zeta = \frac{V_o - V}{V_o}$$

Experimental data collected under shock compression usually relate particle velocity to shock velocity. The relation is usually linear (or multilinear if there are phase changes) and, via the Rankine-Hugoniot equations, gives rise to a pressure, volume relation of the form shown. Figures 9.48 through 9.52 indicate a comparison of results of this model with measured pressures.

Wave Modes (Transmission Path)

The objective of the wave mode study is to correlate the observed ground motion recorded at various stations with individual elastic wave modes having a specific travel path. Wave mode identification is based primarily on the large body of theoretical and observational knowledge which seismologists have acquired through many years research. Fundamental physical properties such as wave propagation velocity, relative frequency content, and particle motion are used to divide a ground motion record into three time windows: (1) a P (compressional) wave window, (2) an S (shear) wave window, and (3) a surface wave window. Additional subgroups are made within each window on the basis of assumed direct, re-

fracted, and reflected travel paths in the crustal and upper mantle of the earth. Figures 9.53 through 9.57 show a good example of mode identification, taken from the Faultless and Boxcar events.

Figure 9.58 shows a simplified model developed at ERC of the earth's crust in the NTS area and the relative travel times for three elastic wave modes (a direct P wave, refracted P wave, and a reflected P wave) generated by a nuclear detonation. The model has parameters of velocity and crustal thickness similar to those observed and derived at NTS by others. The major point of interest is the fact that different wave modes arrive at a surface location with varying but predictable relative times in direct relationship to the physical properties of the earth, the depth and physical characteristics of the Mohorovicic discontinuity, and the distance of the recording site from the nuclear detonation.

Station Factors (Receiving Location)

The presence of a layer of alluvium can have a substantial influence on the magnitude of observed seismic signals. This effect, however, is a complex function of both the wave mode and the frequency, so that a simple statistical correlation of observed effects can be of only limited usefulness, especially if predictions are required at new locations. Therefore, a fundamental investigation of the propagation of different wave modes in an alluvial layer was undertaken; the aim is to predict the effect of the layer on the Fourier amplitude spectrum of the observed surface motion. The first attempt at ERC was a model of the variation of Love wave amplitudes on the line from the NTS toward Las Vegas which gave reasonable agreement with observation. Figure 9.59 shows the geological model used in computing the magnification factors: Figures 9.60 through 9.62 show the experimental versus measured amplification pairs. Then the case of body waves (both P and S) was considered and compared with data from pairs of stations at Beatty and Tonopah, where the general features of the resonant behavior of the alluvial layers were confirmed. Figures 9.63 through 9.67 indicate comparisons of theory with experiment for the radial components measured at Tonapah and Beatty. Further instrumentation to provide a better check of this theory is part of present planning. Finally, the case of Rayleigh waves in a surface layer, which is considerably more complex than the corresponding Love wave problem, has been formulated and programmed at ERC, and will soon be applied to a geologic model of the Las Vegas Line.

These studies should provide the best means for improving the predictions of frequency dependent phenomena (e.g., PSRV response spectra) at sites located on alluvium.
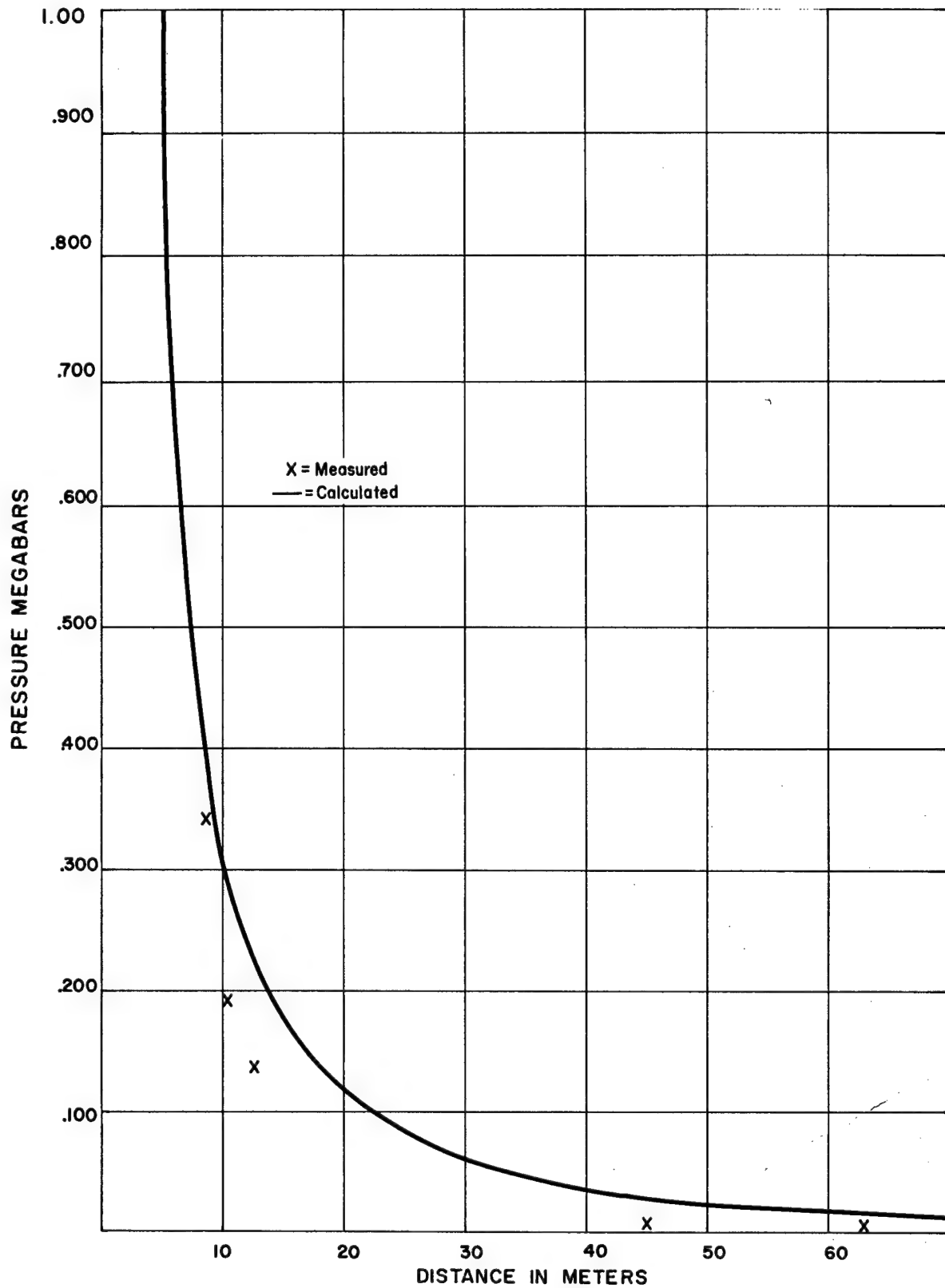
Figure 9.48.   Calculated Peak Pressure Versus Distance from the Handcar Event in Dolomite, Yucca Flat.
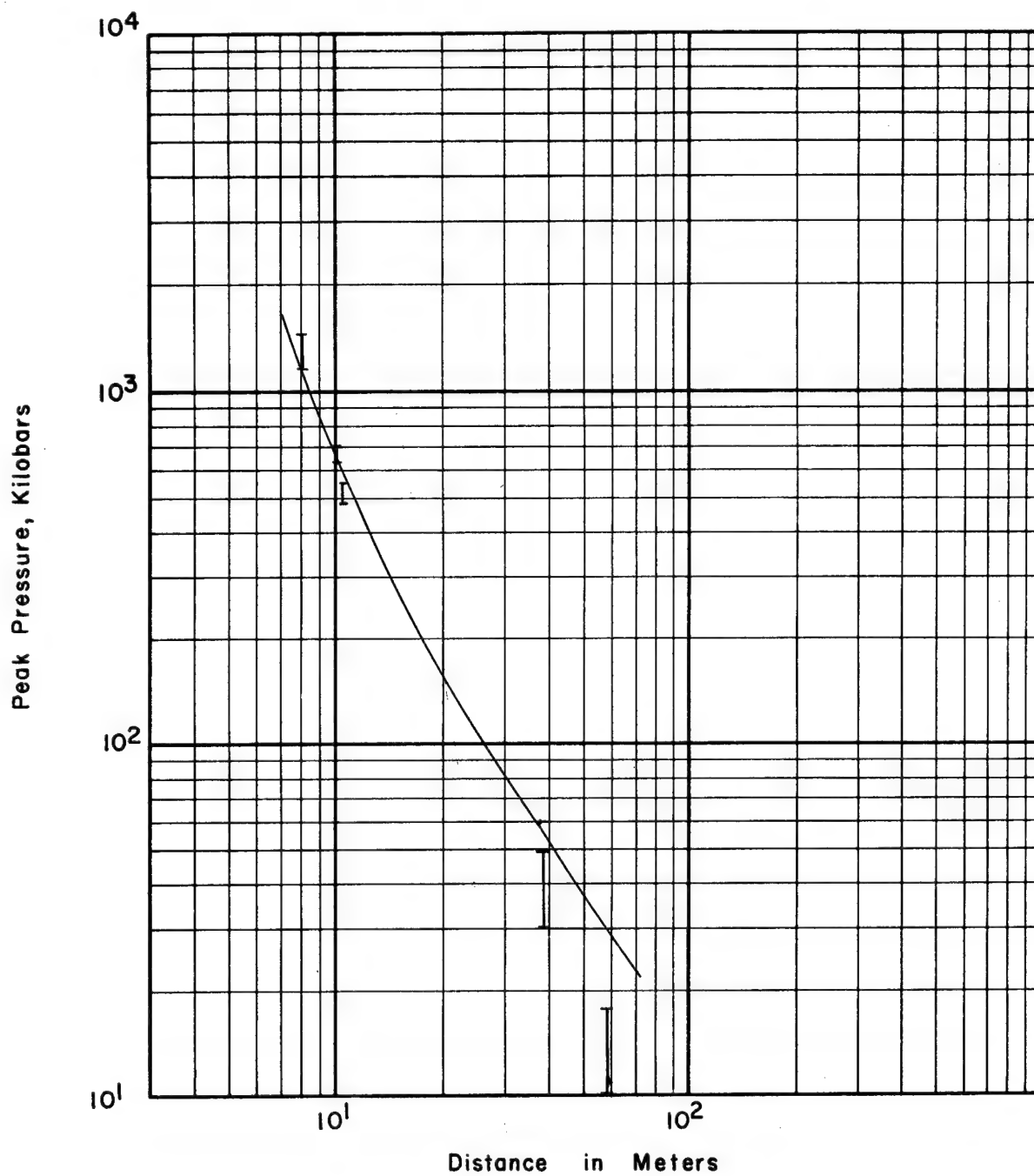
Figure 9.49. Calculated Peak Pressure Versus Distance from the Piledriver Event, in Granite, North of Yucca Flat.

149
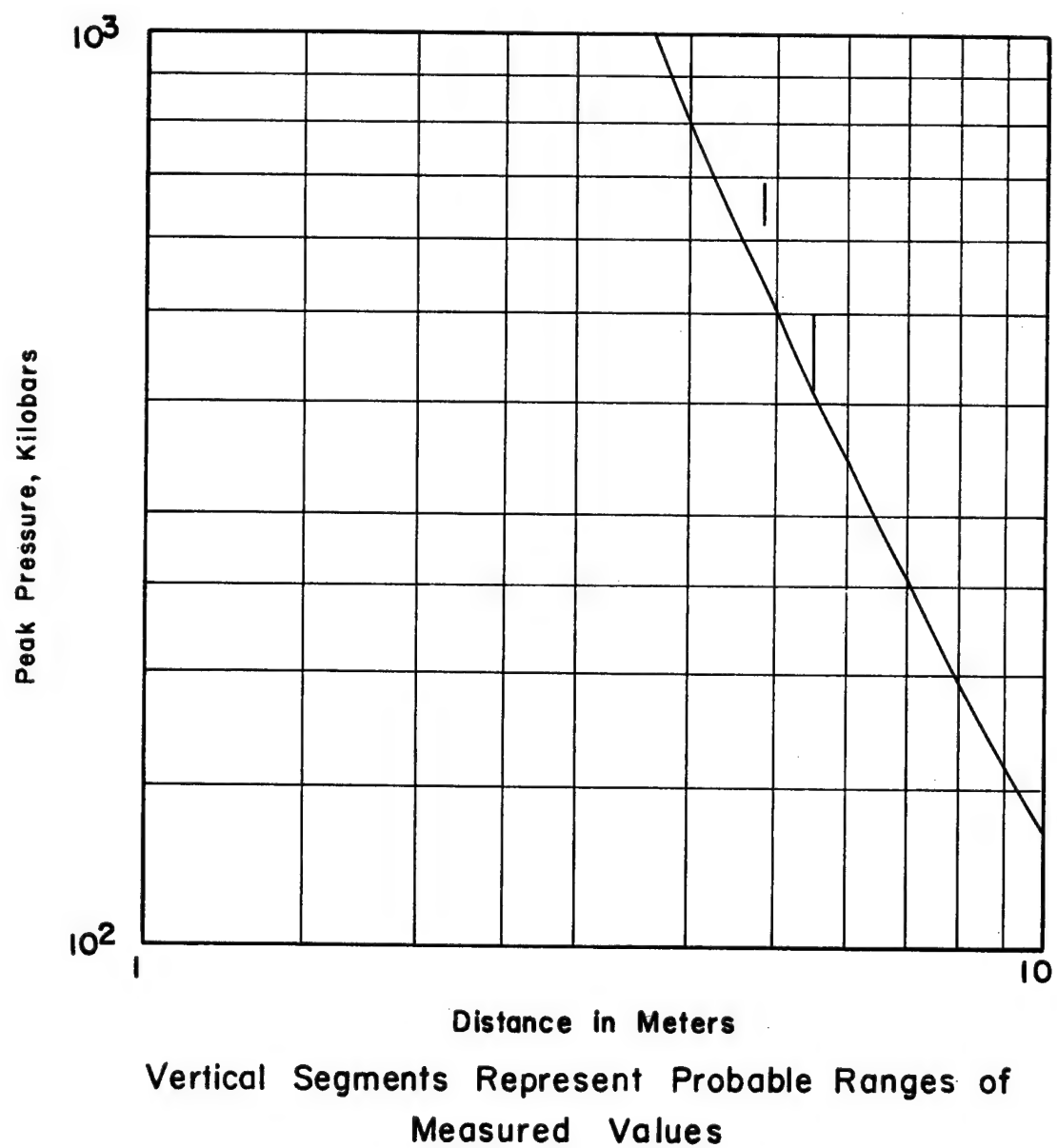
Figure 9.50. Calculated Peak Pressure Versus Distance from the Hardhat Event, in Granite, North of Yucca Flat.
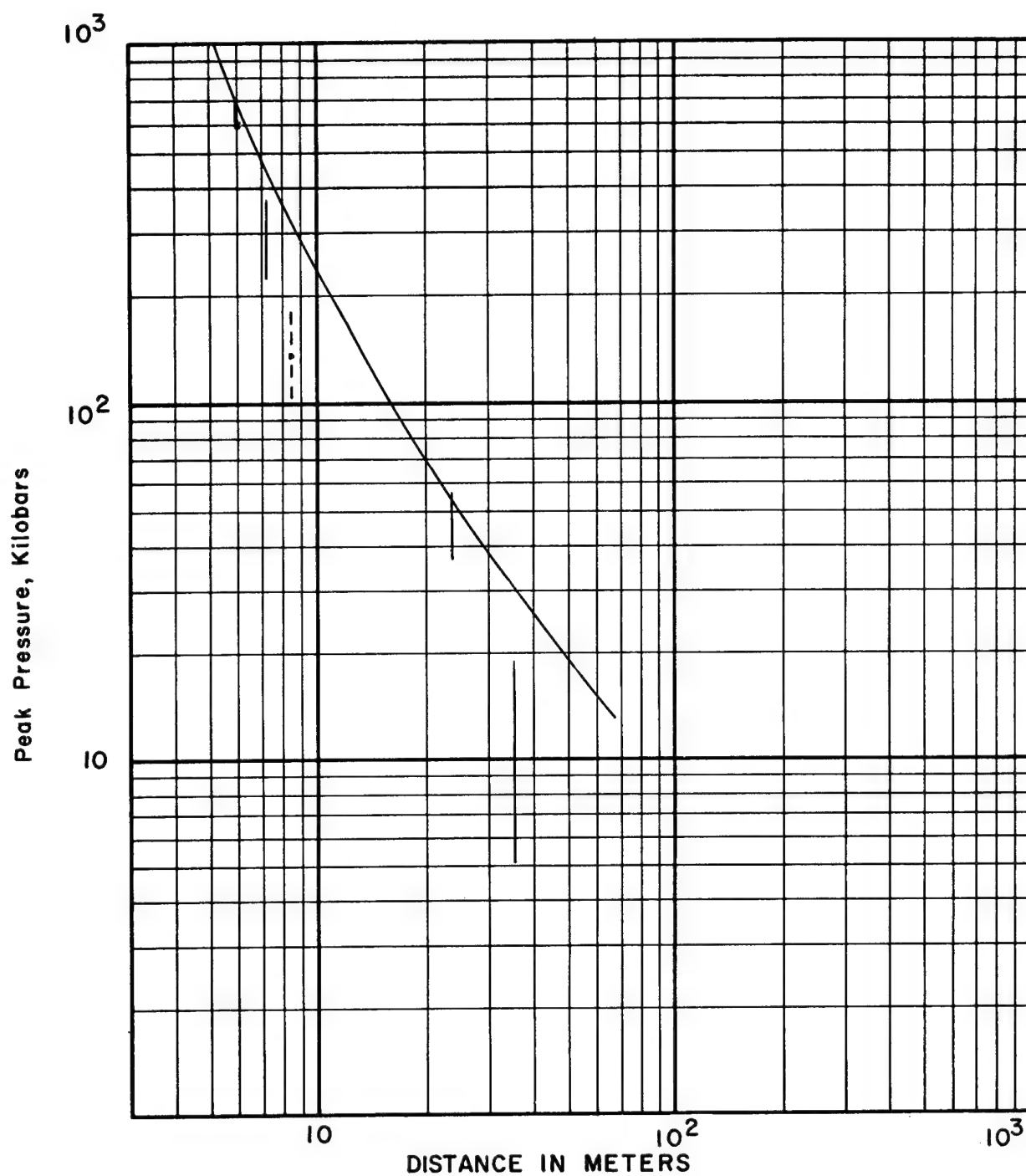
Figure 9.51. Calculated Peak Pressure Versus Distance, from the Shoal Event, in Granite, near Fallon, Nevada.

151
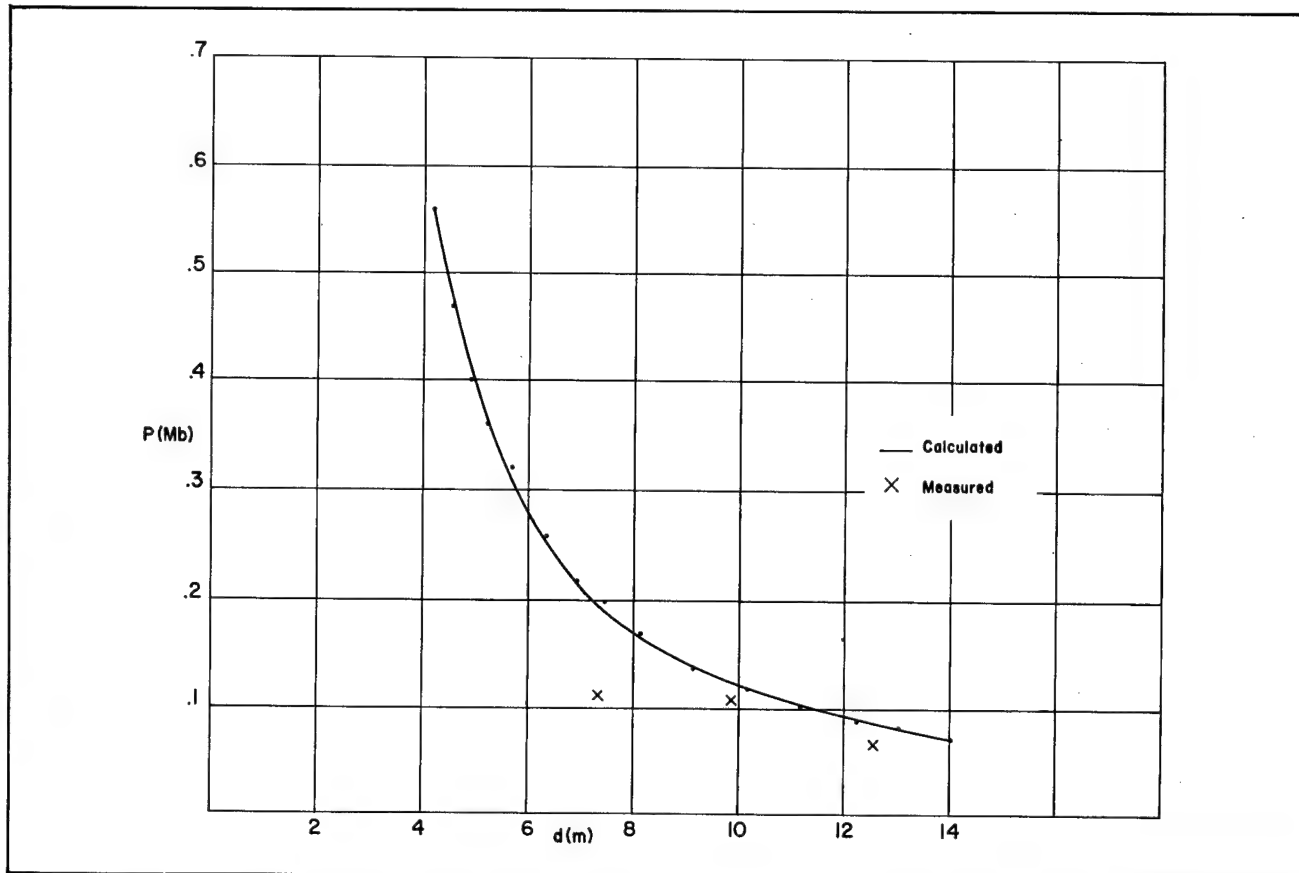
Figure 9.52. Calculated Peak Pressure Versus Distance from the Salmon Event, in Salt, near Hattiesburg, Mississippi.
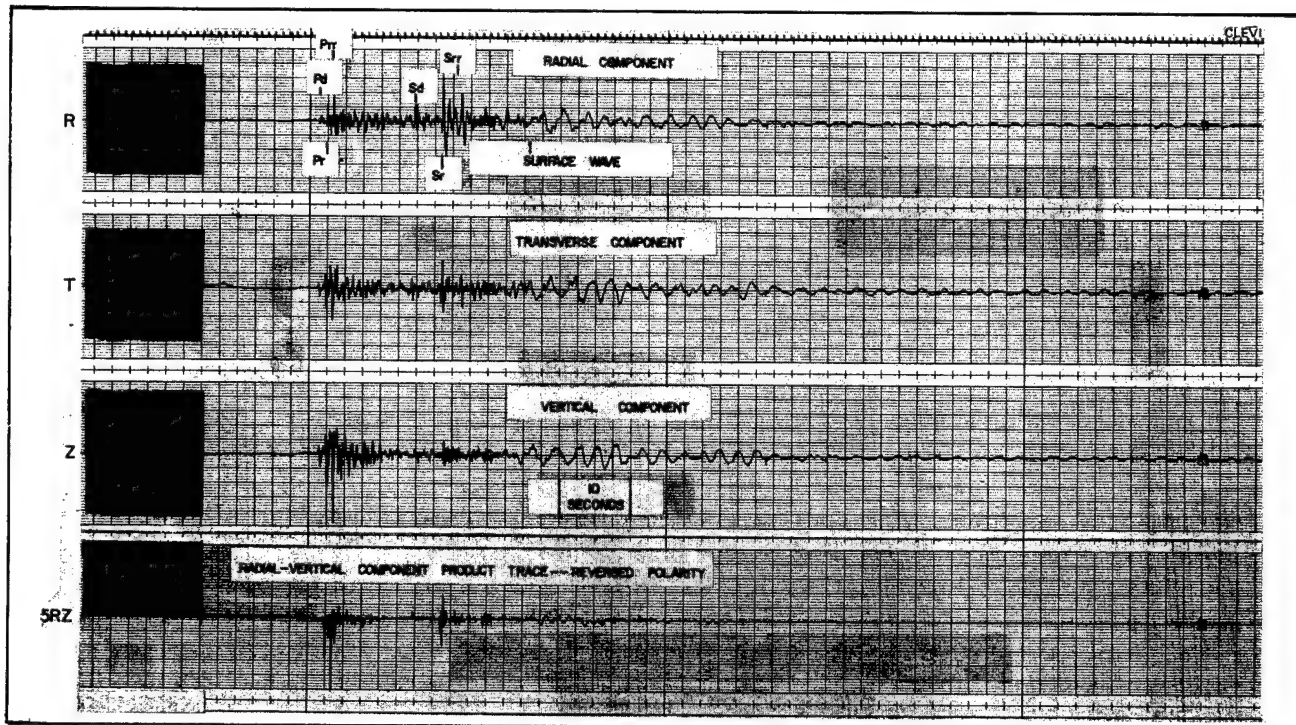
Figure 9.53. Particle Velocity Seismogram and Radial-Vertical Component Product Wave form. Station: Tonopah Church. Distance Equals 108.7 km. Faultless Event.

152
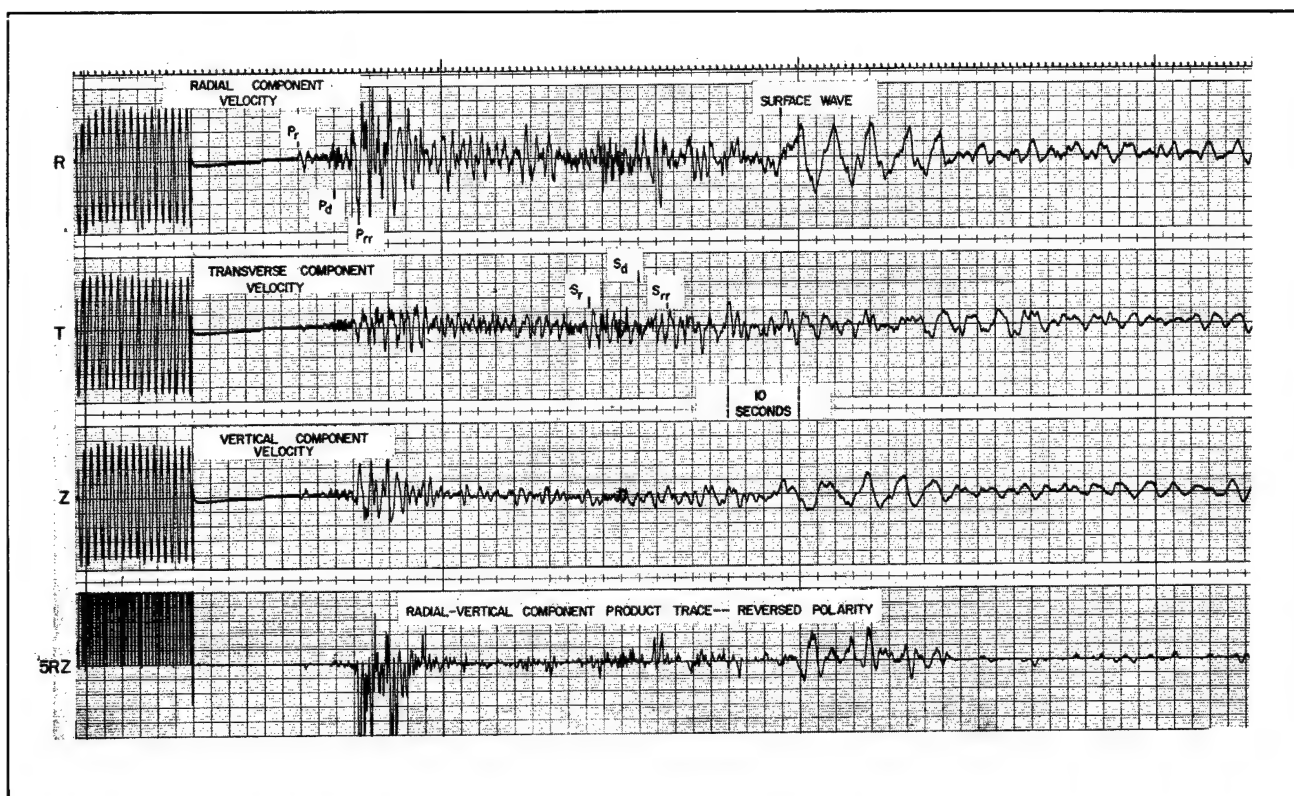
Figure 9.54. Particle Velocity Seismogram and Radial-Vertical Component Product Waveform. Station: Stateline (Hard Rock). Distance Equals 325.5 km. Faultless Event.
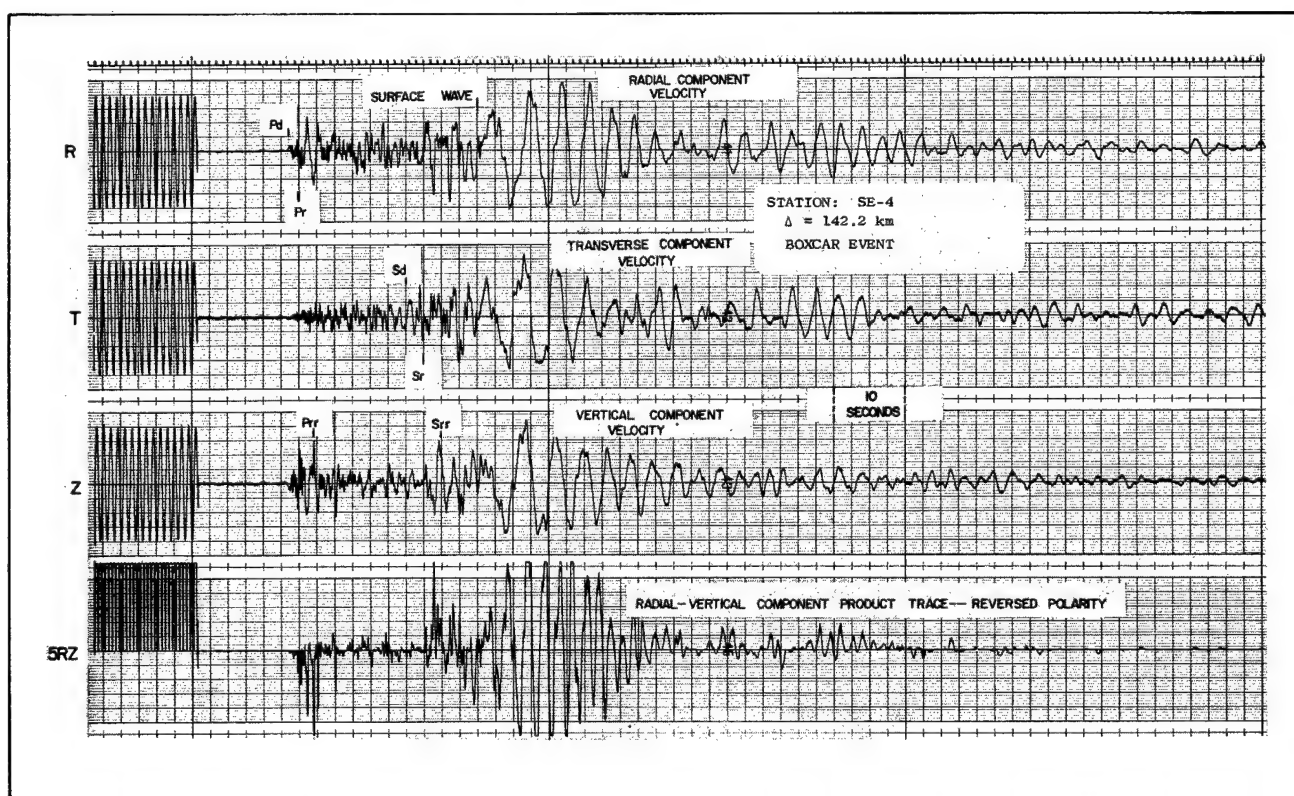
Figure 9.55. Particle Velocity Seismogram and Radial-Vertical Component Product Waveform. Station: SE-4. Distance Equals 142.2 km. Boxcar Event.
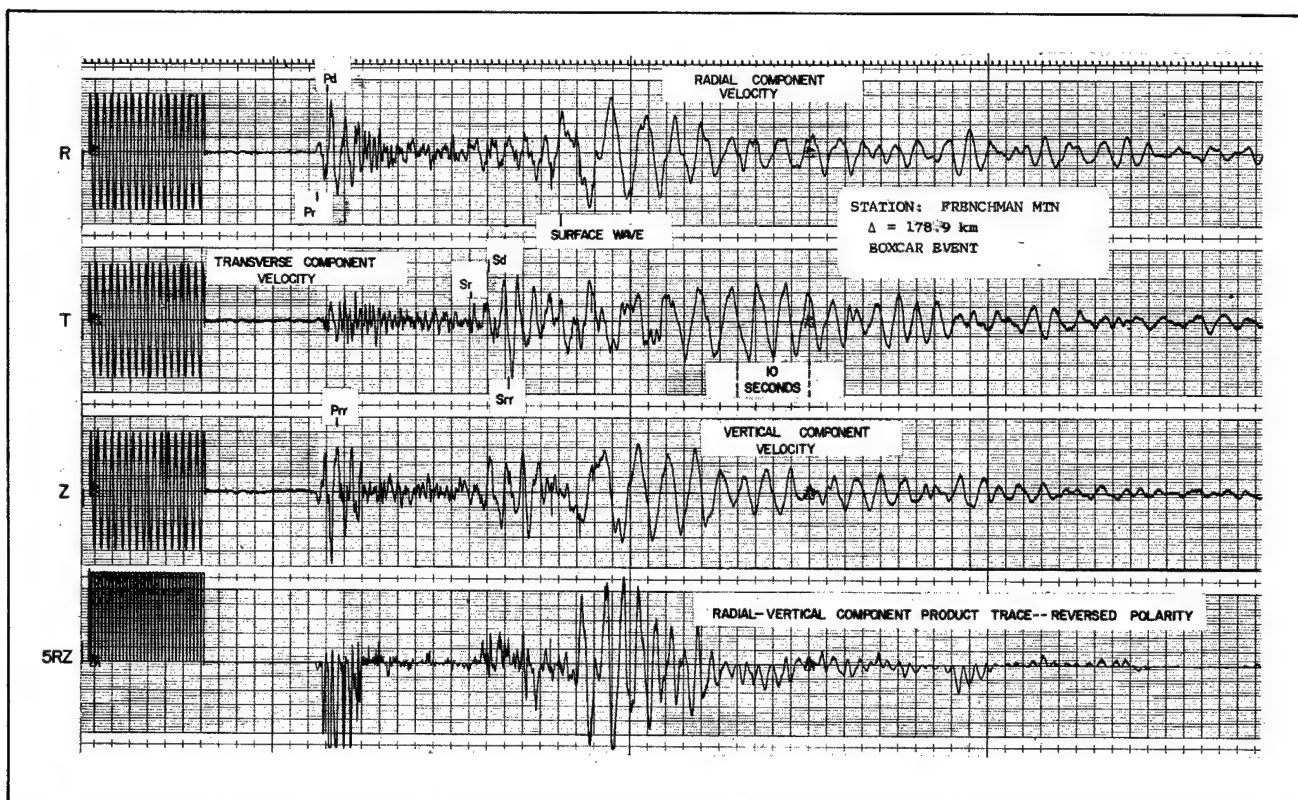
Figure 9.56. Particle Velocity Seismogram and Radial-Vertical Component Product Waveform. Station: Frenchman Mountain. Distance Equals 178.9 km. Boxcar Event.
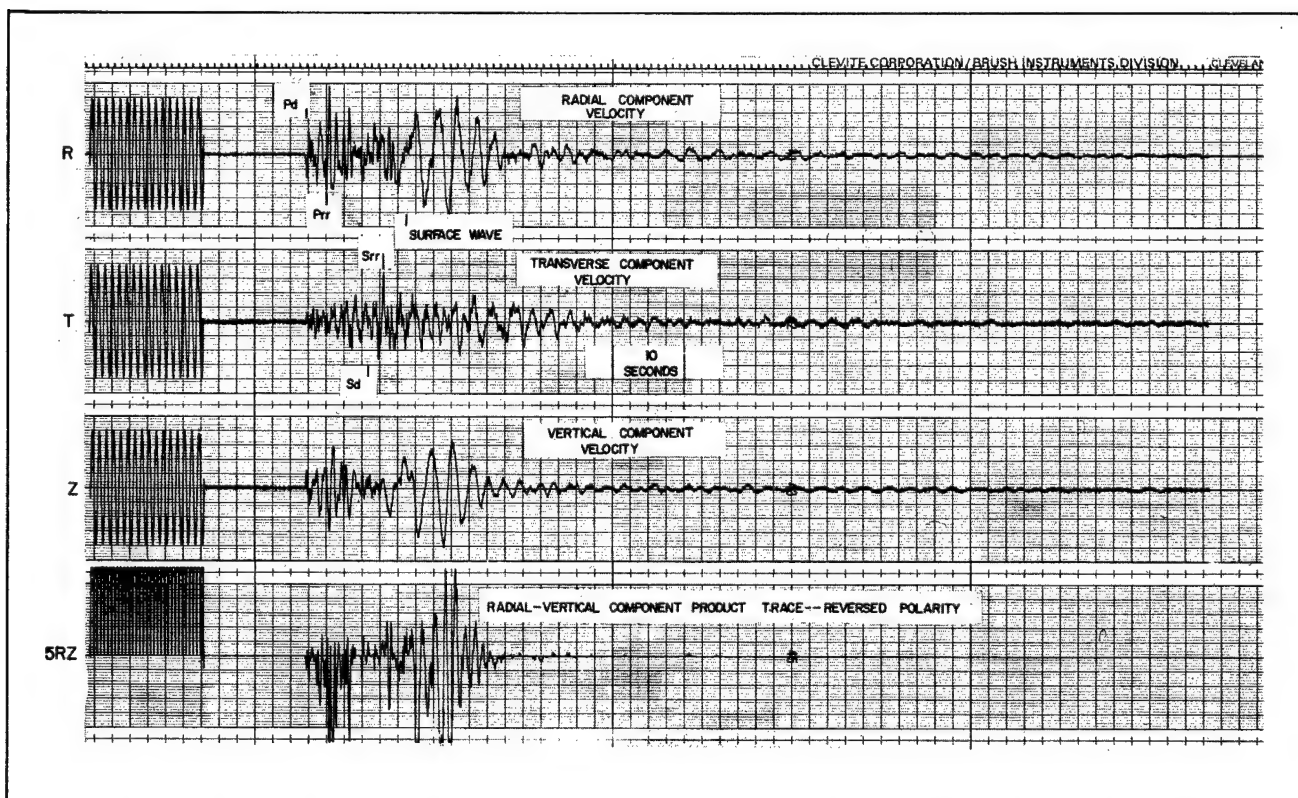
Figure 9.57. Particle Velocity Seismogram and Radial-Vertical Component Product Waveform. Station: Beatty (Alluvium). Distance Equals 50.6 km. Boxcar Event.
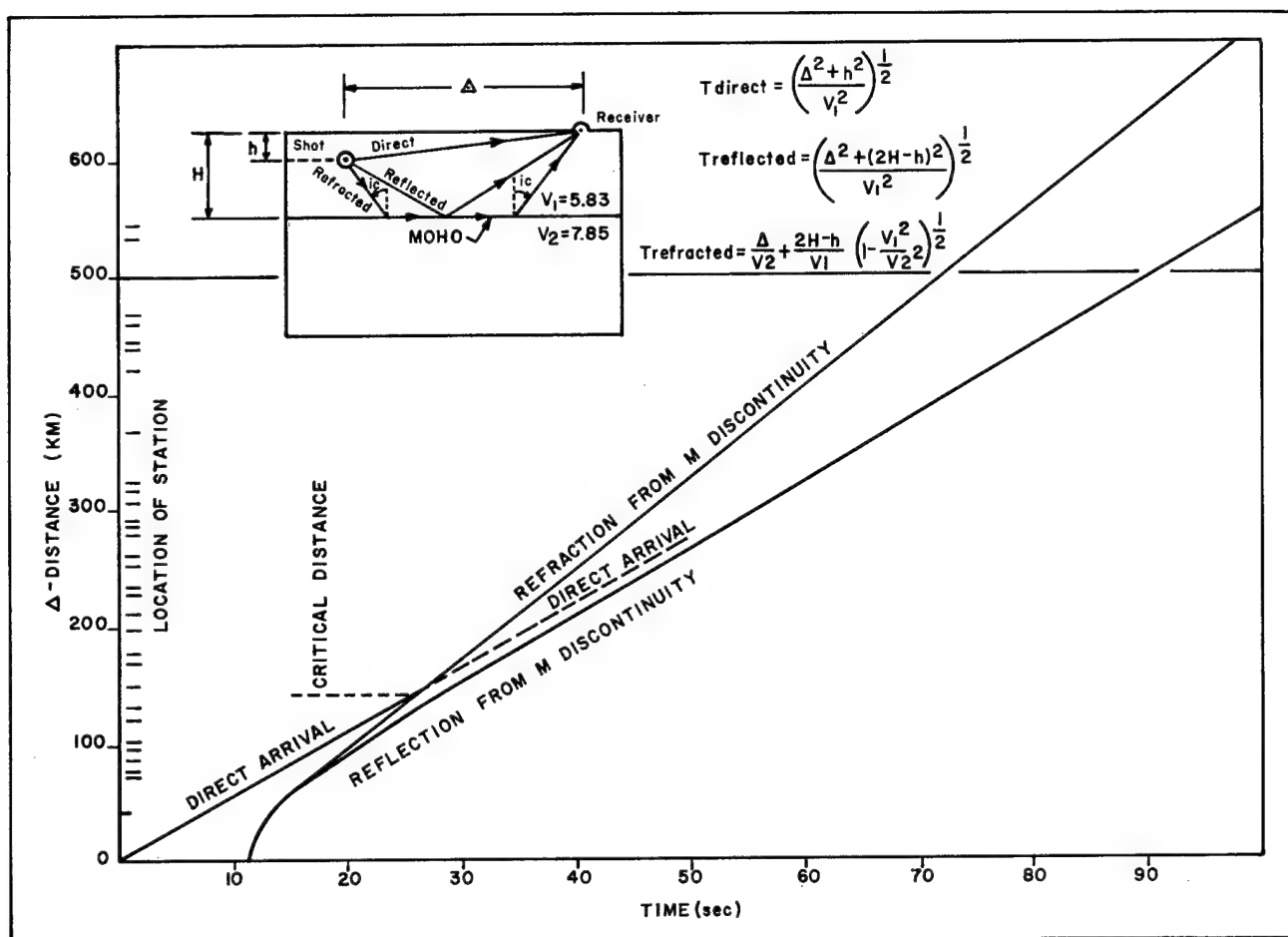
Figure 9.58. Determination of Depth of Moho and Propagation Velocity From Time Intercept and Time Distance Curve.
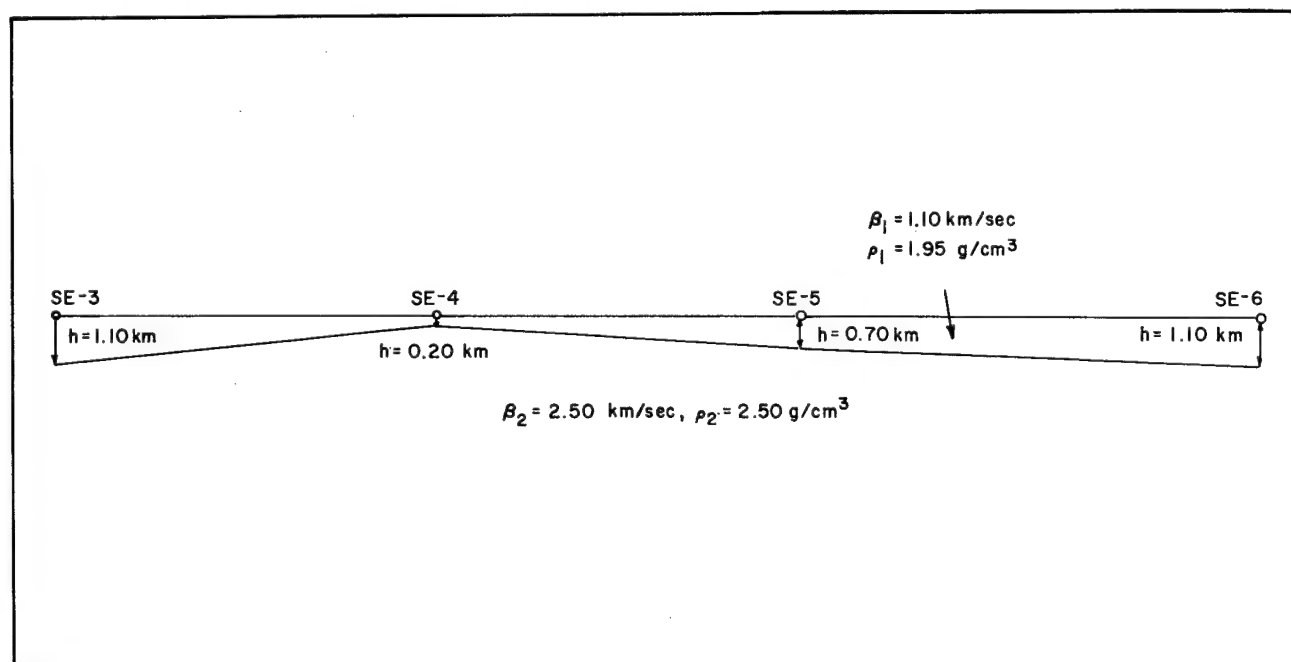
Figure 9.59. Geological Model Used in Computing the Magnification Factors Where β is the Shear Wave Velocity and ρ is the Density.

155
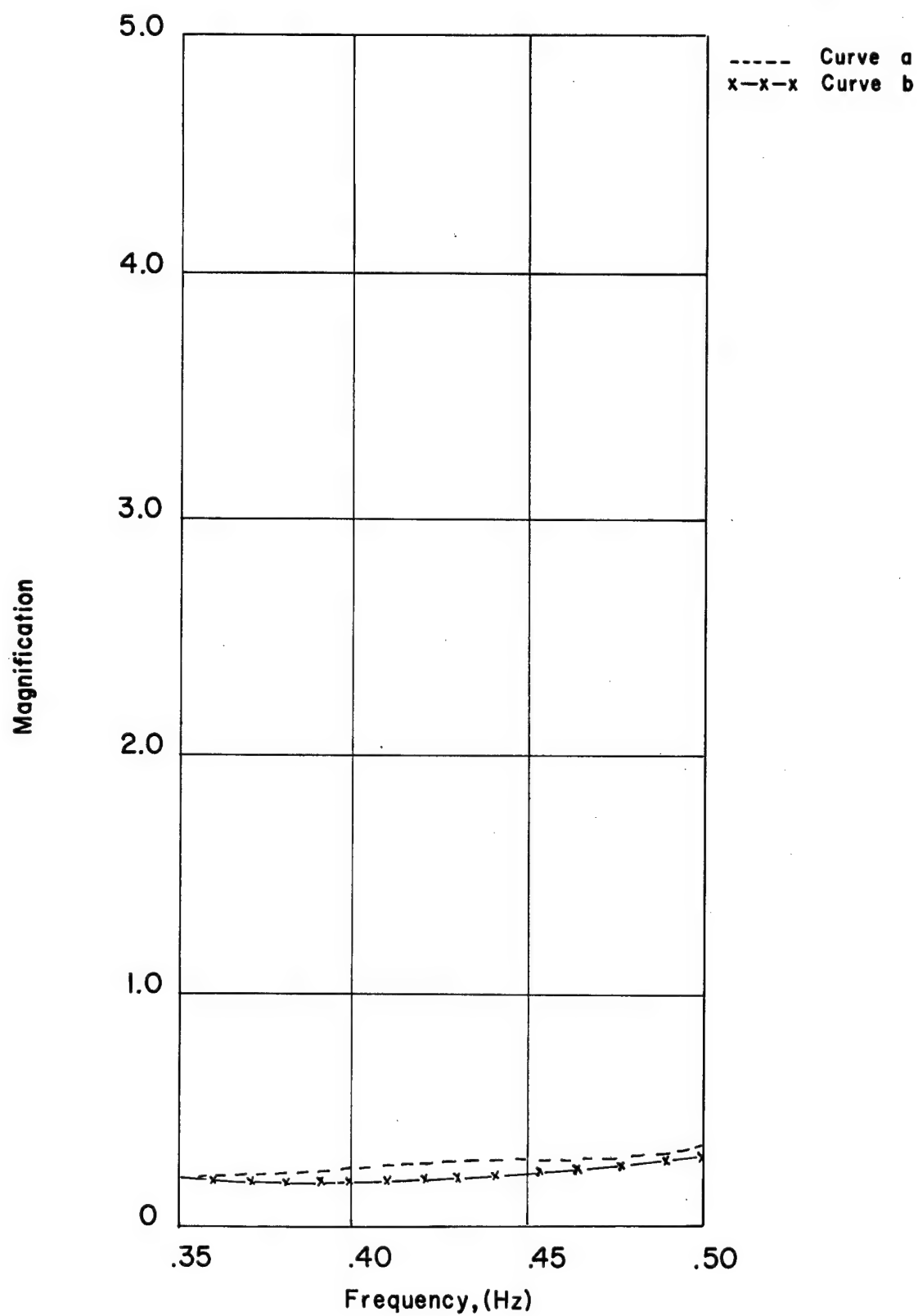
Figure 9.60. Amplitude at SE-4 Relative to Amplitude at SE-3. Curve "a" Is the Theoretical Amplification Factor; Curve "b" the Observed.
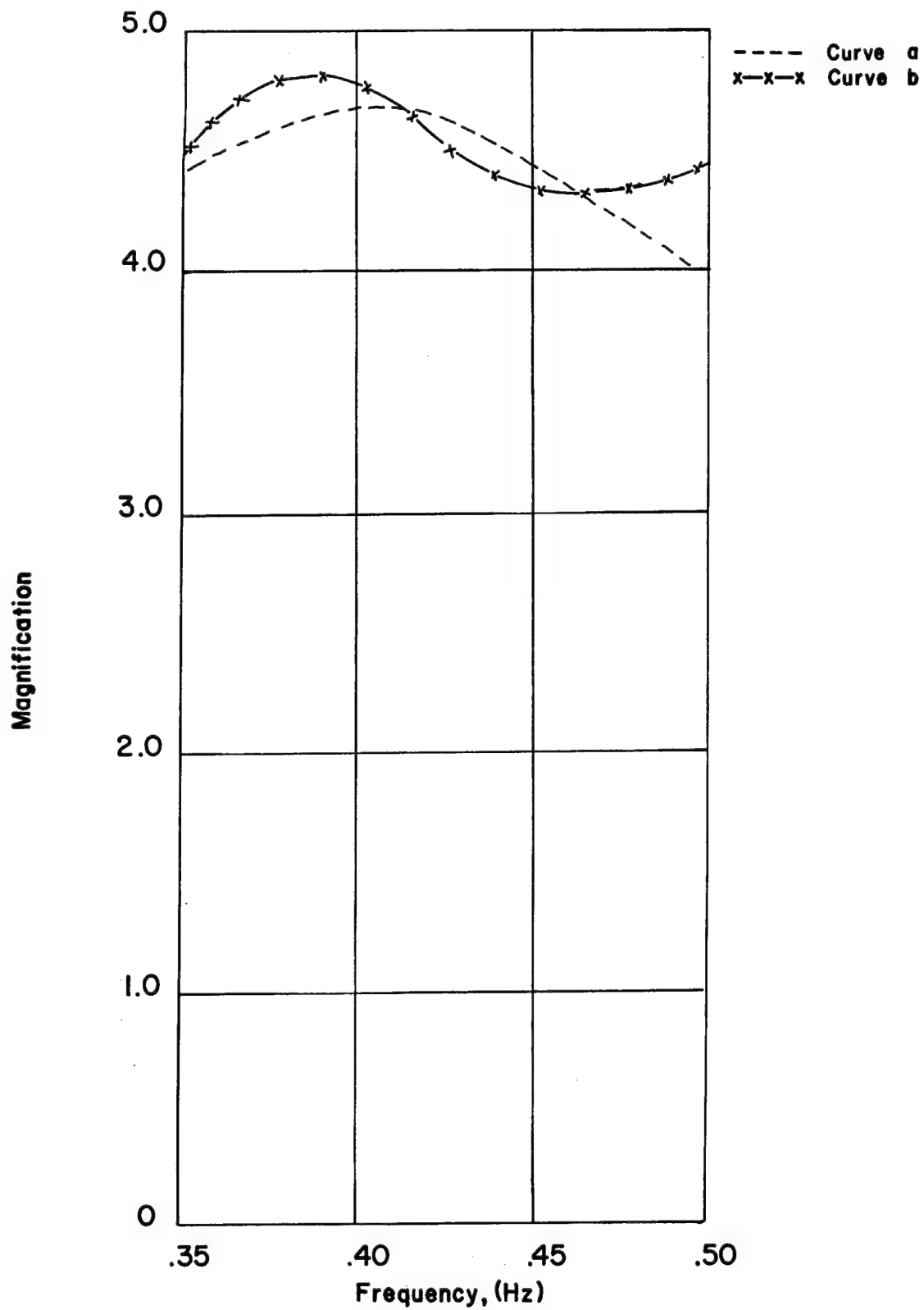
Figure 9.61. Amplitude at SE-5 Relative to Amplitude at SE-4. Curve "a" Is the Theoretical Amplification Factor; Curve "b" the Observed.

157
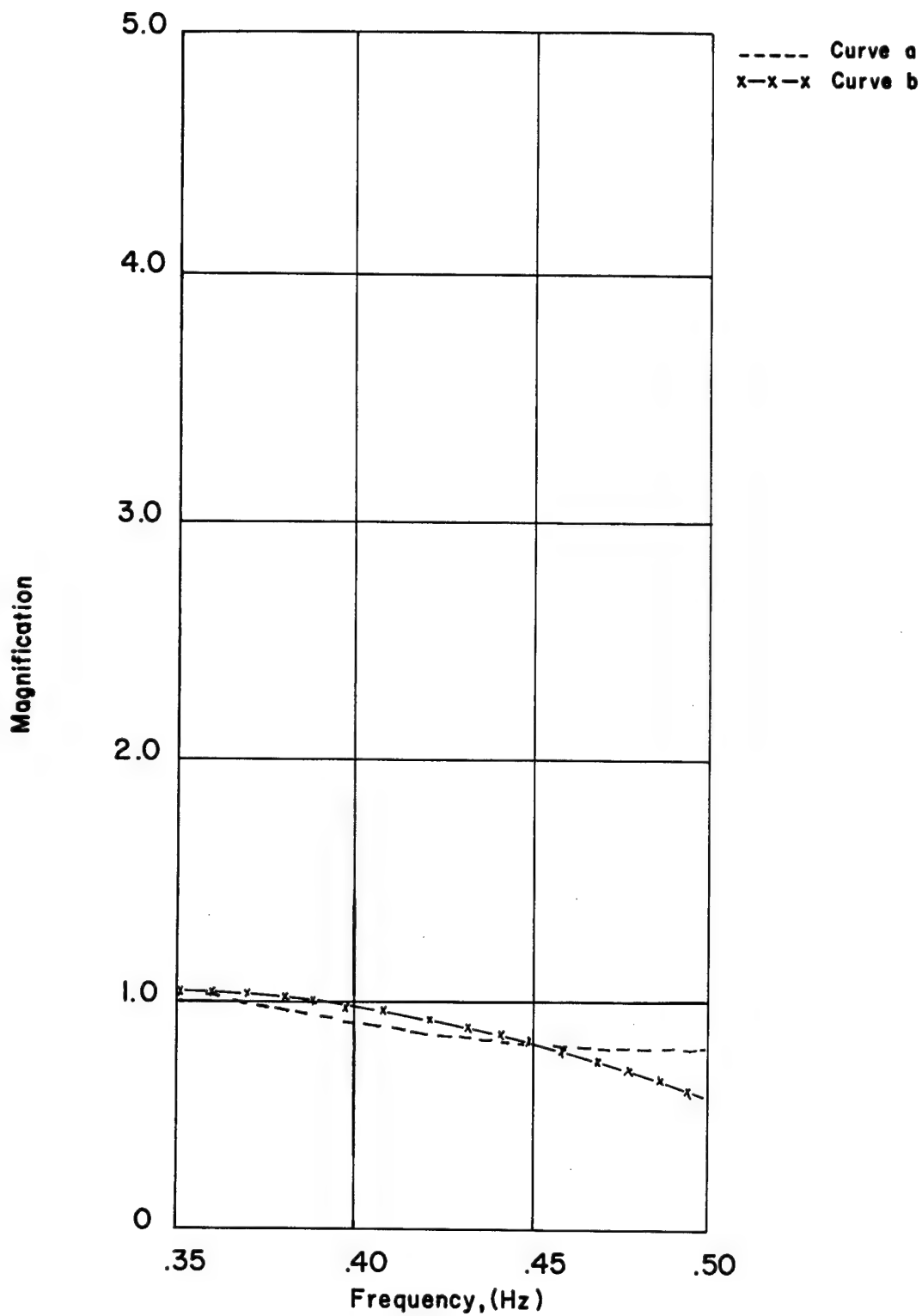
Figure 9.62. Amplitude at SE-6 Relative to Amplitude at SE-5. Curve "a" Is the Theoretical Amplification Factor; Curve "b" the Observed.
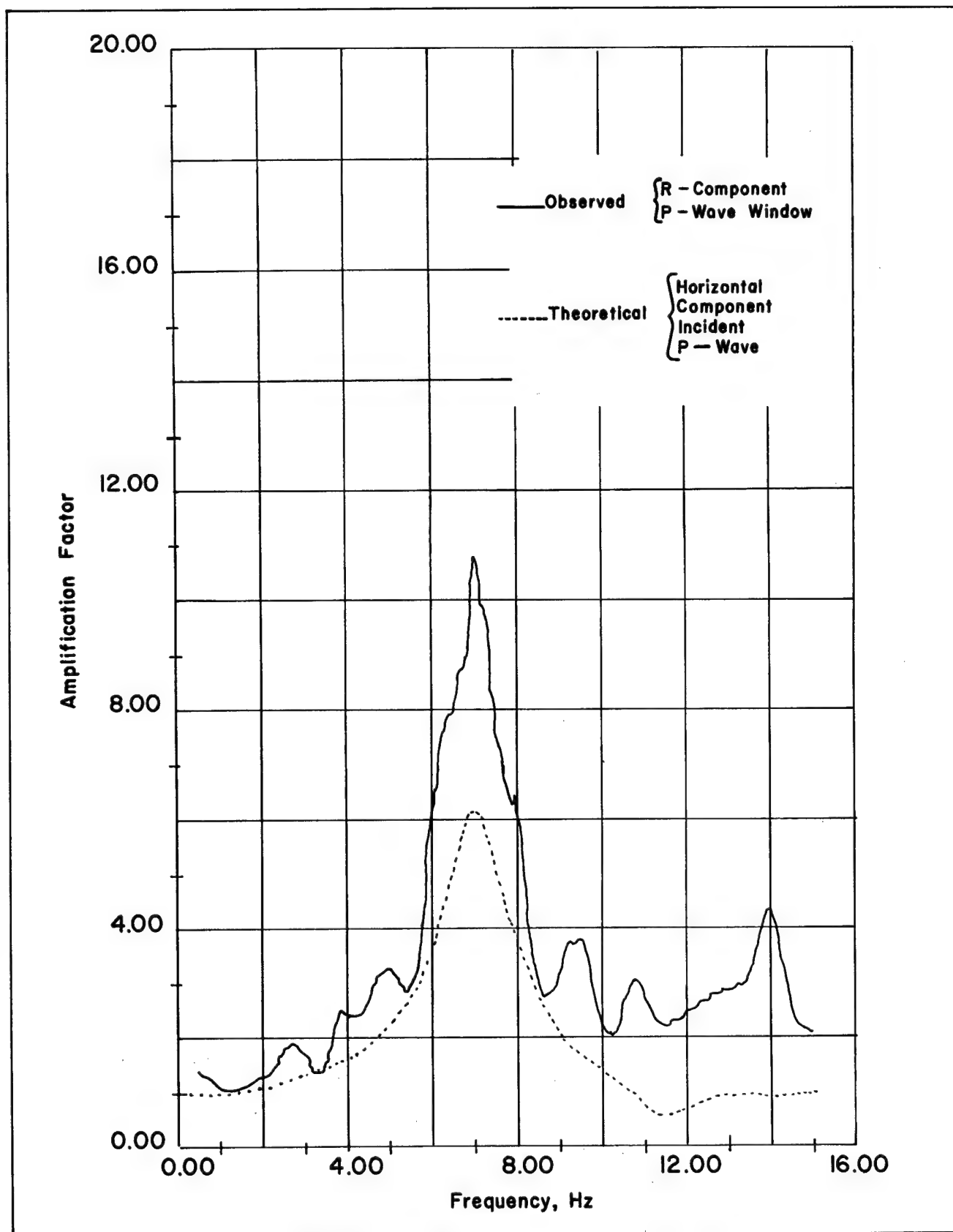
Figure 9.63. Tonopah Amplification Factor (R Component, P-Wave Window).

159
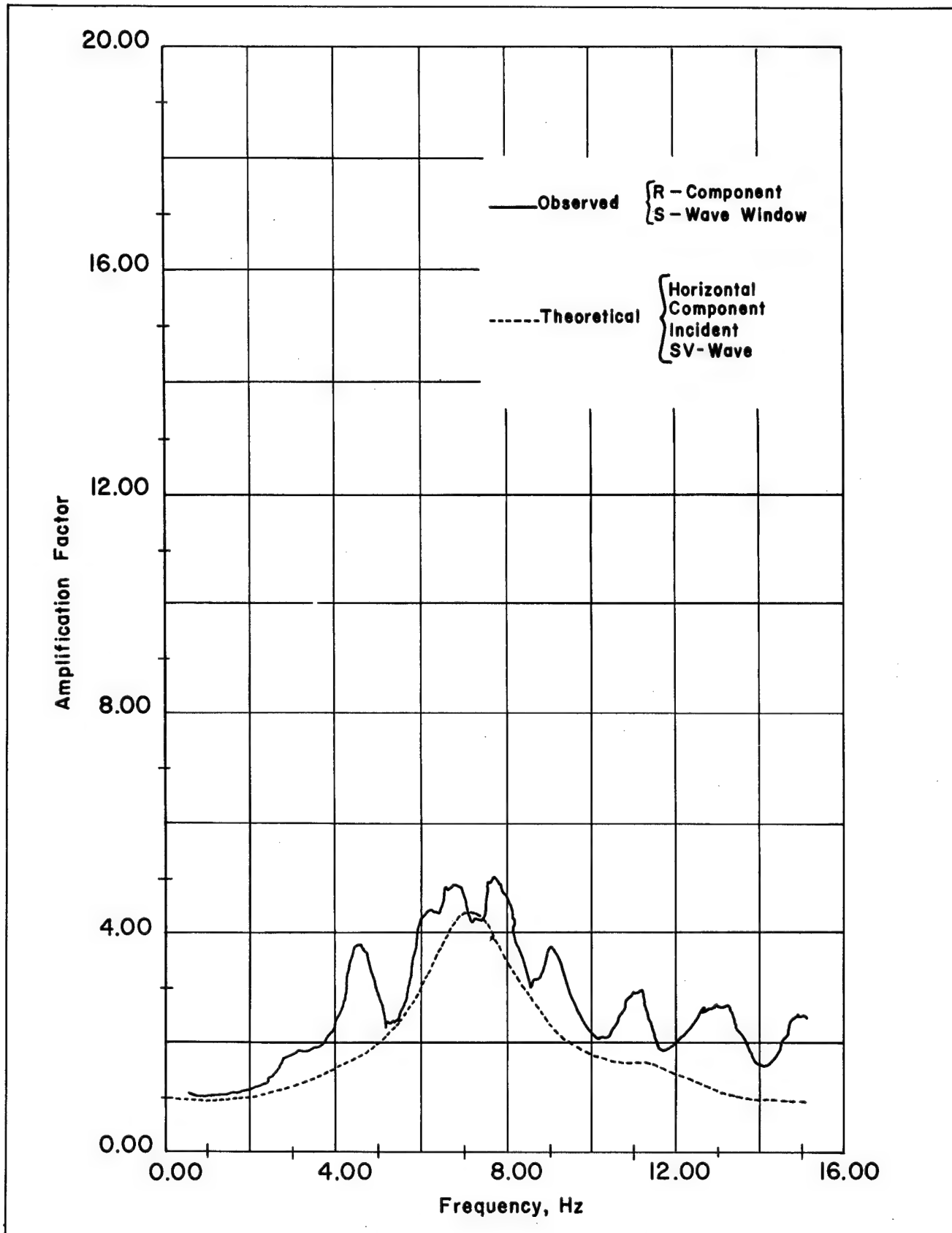
Figure 9.64. Tonopah Amplification Factor (R Component, S-Wave Window).

160
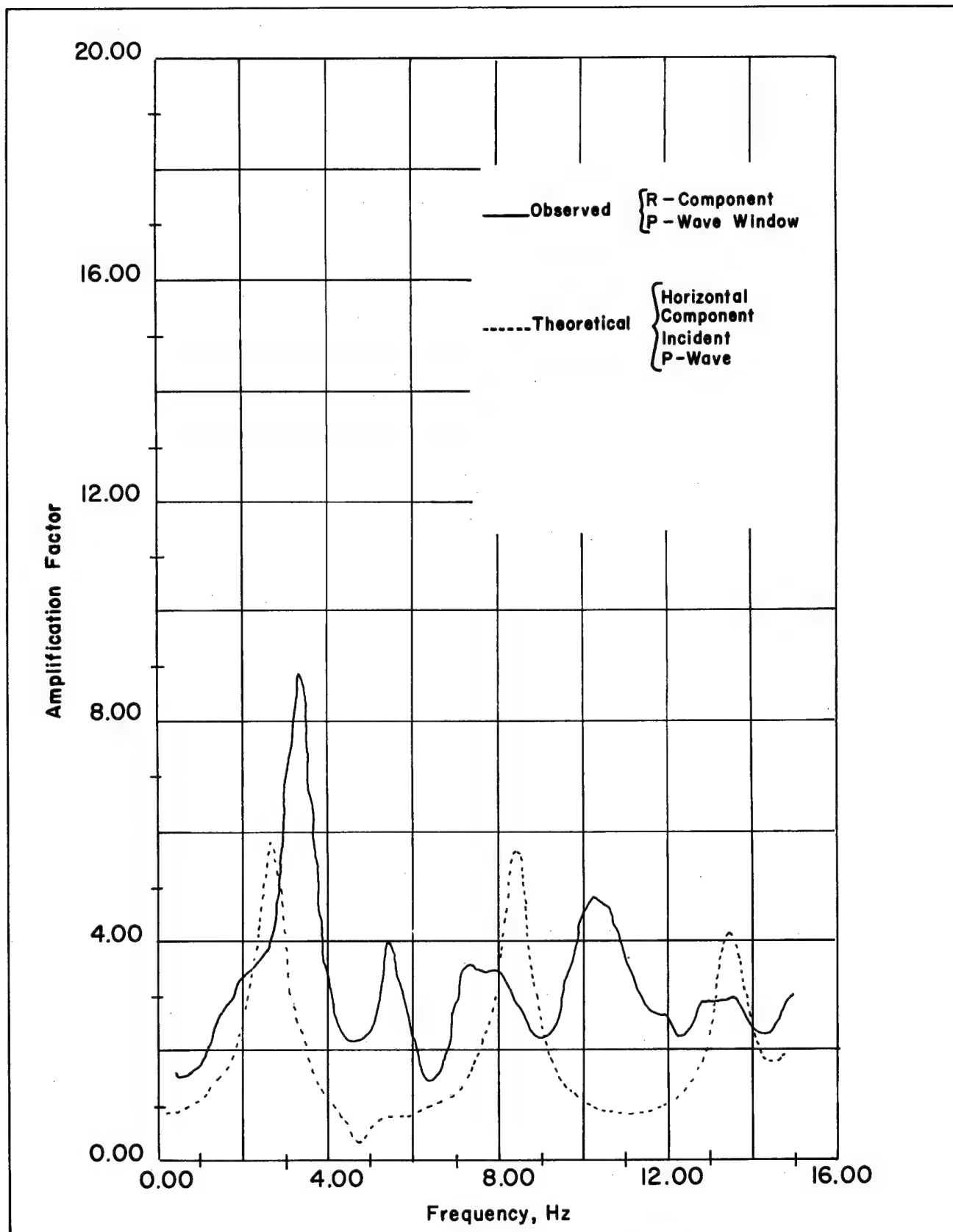
Figure 9.65.   Beatty Amplification Factor (R Component, P-Wave Window).
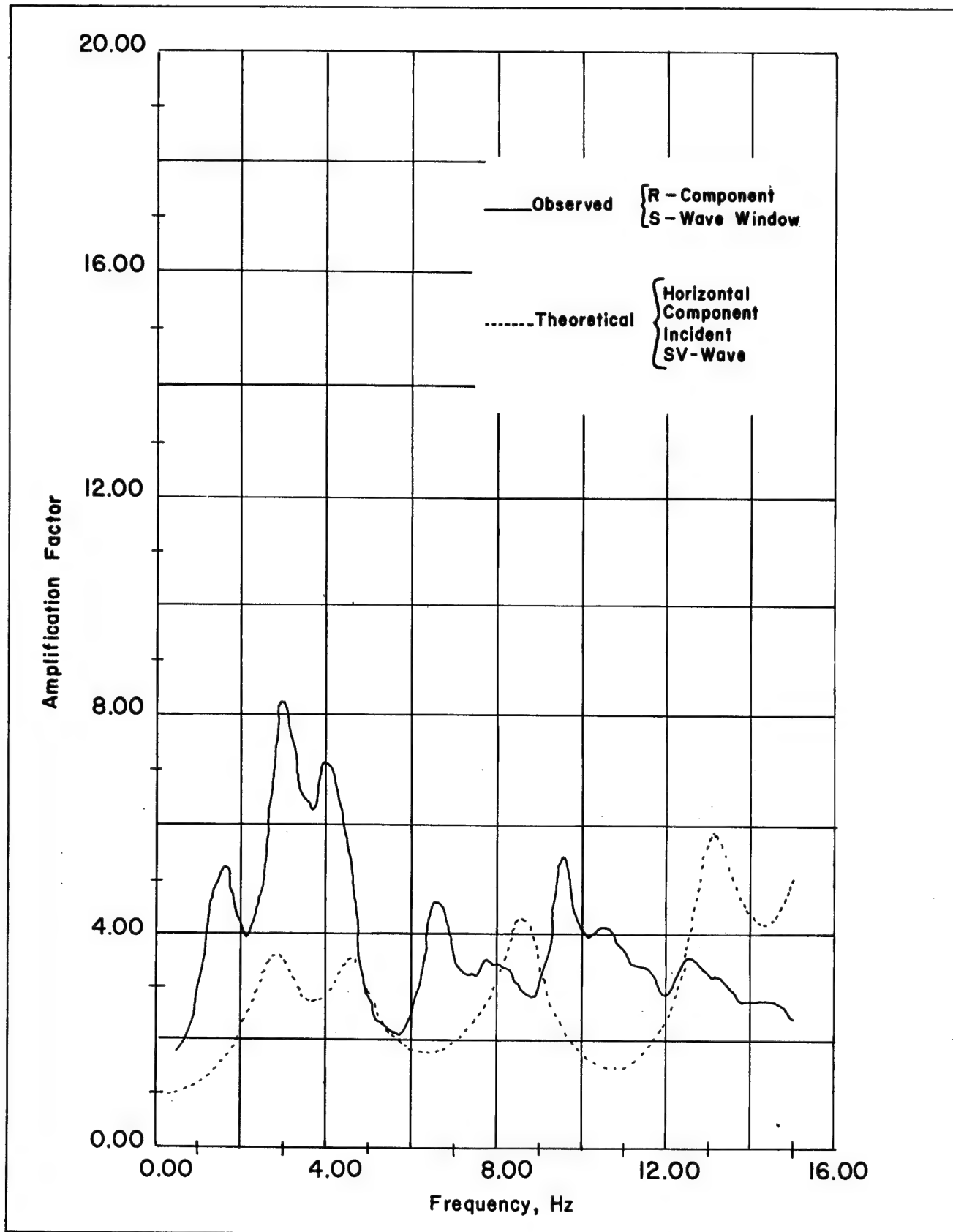
Figure 9.66.   Beatty Amplification Factor (R Component, S-Wave Window).

162

Part B — Theoretical Models

Wave Propagation in Homogeneous Media

The problem of propagation of a compressional pulse in a solid half-space overlain by a solid layer of different properties has been treated. Both the layer and half-space are homogeneous and isotropic. A source function which can be made to approach the unit step function is assumed, and the resulting exact analytic solutions for the time-histories of the vertical and radial components of displacement (i.e., the vertical and radial displacement seismograms) are derived. The results of an analysis by Pekeris were extended to include: (1) the radial displacement, (2) an arbitrary point of observation on, or within, the layer, (3) arbitrary medium constants in both the layer and the half-space, and (4) an arbitrary source depth within the layer. The model and mathematical approach are:

$z = 0$ $\longrightarrow$ r

     R $\circ$ P(r,z)

$z = d$ Source

     ρ_1, λ_1, μ_1 (Solid Layer)

$z = H$

     ρ_2, λ_2, μ_2 (Solid Half-space)

z   (9)
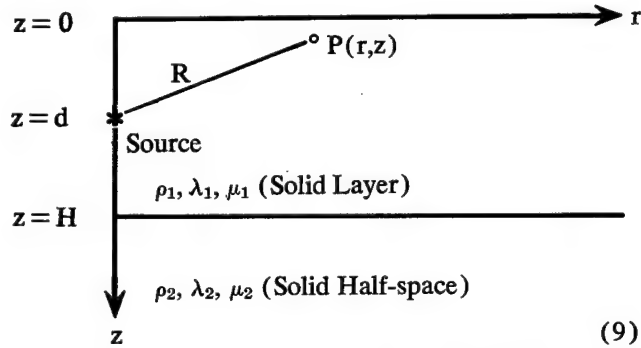
$q(r,z,t) = $ *horizontal* particle displacement as a function of time at the point P(r,z).

$w(r,z,t) = $ *vertical* particle displacement as a function of time at point P(r,z).

Constraints: $0 < d < H$ i.e., the source must be within the layer,

P(r,z) such that $\begin{array}{l} r > 0 \\ 0 \leq z < H \end{array}$

$(\nabla^2 - h^2)\,\Phi = 0$; and

$(\nabla^2 - k^2)\,\psi = 0$

where $h^2 = \dfrac{p^2}{c_p^2}$; $k^2 = \dfrac{p^2}{c^2}$; $p = \dfrac{\partial}{\partial t}$;

$\nabla^2 = \dfrac{\partial^2}{\partial r^2} + \dfrac{1}{r}\dfrac{\partial}{\partial r} + \dfrac{\partial^2}{\partial z^2}$

The operational solution for the vertical displacement is:

$$W_1(p,r,z) = \frac{V_0}{4\pi(\Delta)^2 c_1^2} \int_0^\infty x\, J_0(k_1\, x\, r)\, \frac{\overline{w_1}}{V}\, dx \quad (10)$$

where Δ is related to the source function and $\dfrac{\overline{w_1}}{V}$

is a series of terms each of which represents a different (plane wave) ray arrival. For times after the direct arrival, for example, the time domain solution of each complex integral in the series is of the form:

$$U(\tau,r,z) = \frac{2}{\pi H}\, i\, \left[\int_0^{x_1(\tau)} \frac{x f(x)\, dx}{\sqrt{K(x,\tau)}} \right] \quad (11)$$

This model provides computed theoretical seismograms which exhibit features of measured ground motion; namely, early body wave arrivals characterized by higher frequency content, followed by surface wave modes characterized by lower frequency content (Figure 9.67). It contains a precisely specified compressional source which approximates experimentally determined source functions. It also includes the ubiquitous surface layer and, most important, the solution is in terms of a superposition of individual reflected and refracted P and S wave arrivals. The latter feature is enabling separate study of the effects on the seismogram of each arrival as source depth, medium constants, and layer thickness are varied.

Wave Propagation in Heterogeneous Media

In this model Sharp's problem is extended to include a treatment of the elastic constants and the density as random variables. Figure 9.68 shows the input function and the characteristic features of Sharp's solution. At time $t = 0$, there is a sudden initial pressure P_0 which decays with an infinitesimal decay constant α. At large distances, the displacement as a function of time is a damped sinusoid which has a characteristic wavelength proportional to the cavity radius.

In the heterogeneous case, a different length, the correlation length, appears. This is defined as the distance over which the density and elastic properties of the medium change substantially.

For wavelengths less than the correlation length, there is an exponential selective frequency decay (due to scattering) with distance; for wavelengths greater than the correlation length, the medium appears homogeneous.

CONCLUSIONS

The purpose of discussing these related studies which are supported by the Effects Evaluation Division of NVOO is to indicate and assure the general and scientific public that applicable techniques are being exploited and developed to improve ground motion prediction reliability. Current accuracy of prediction is perhaps best indicated by comparison of predictions with measured values.

Plowshare/Gasbuggy

Peak amplitude predictions versus measured values are shown in Figure 9.69 for the recent Gasbuggy event

163
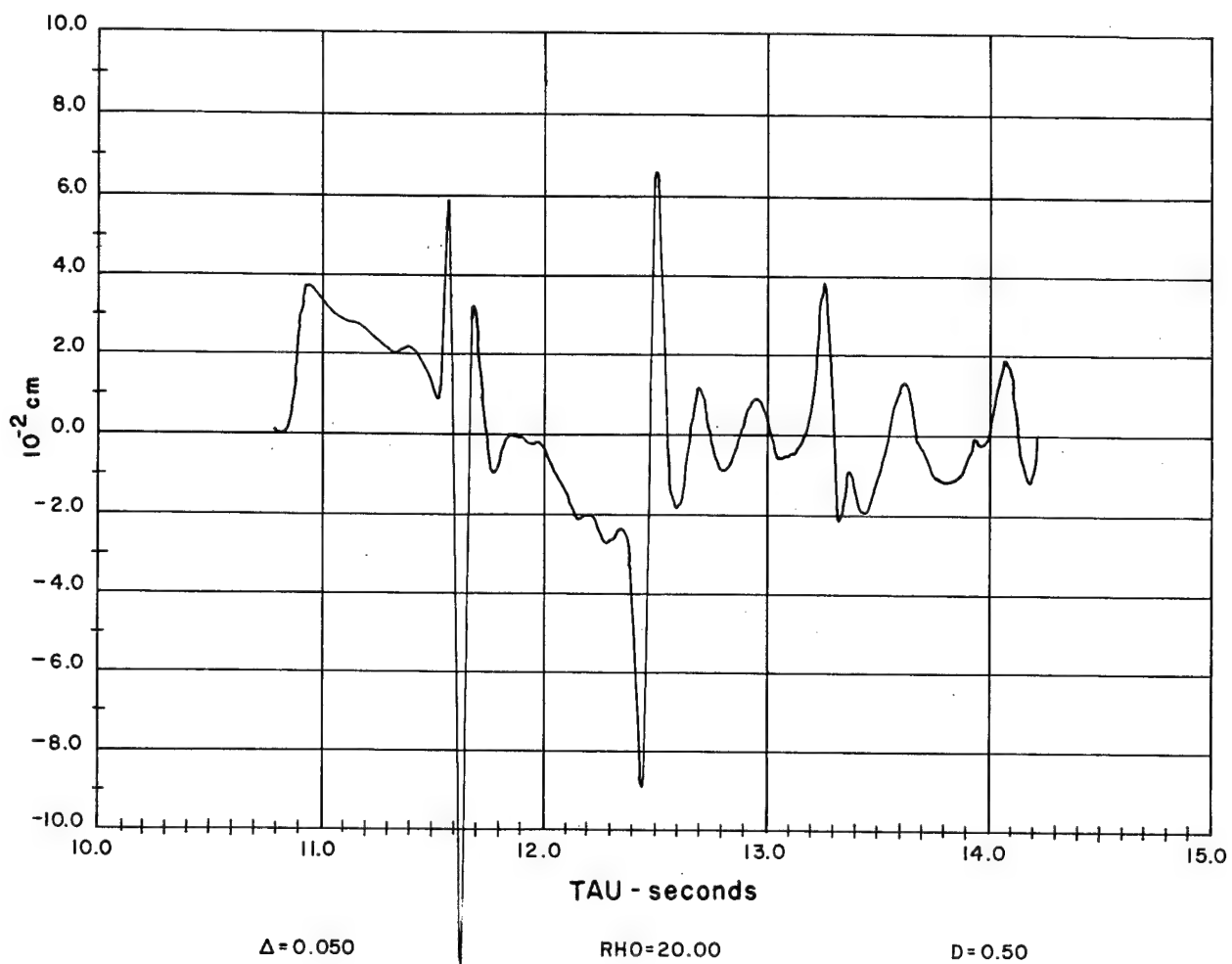
Figure 9.67.   Computed Vertical Displacement Seismogram.

164

Over-Pressure in a Spherical Cavity
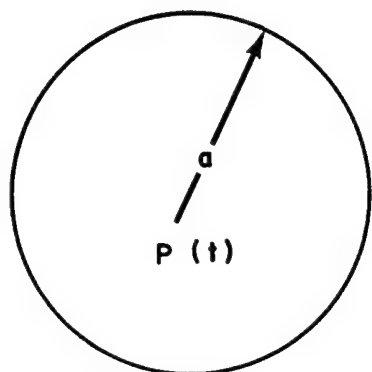
$$P(t) = \lim_{\alpha \to 0} \begin{cases} P_0 e^{-\alpha t} & t \geq 0 \\ 0 & t < 0 \end{cases}$$

SHARP'S PARTICLE DISPLACEMENT
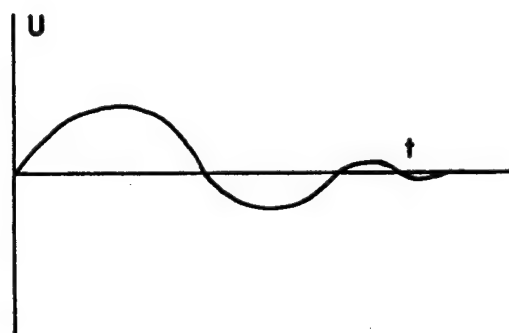
For Large Distances, The Wave Shape is a Damped Sine Wave With a Frequency Dependent on The Cavity Radius, a.

Figure 9.68. Sharp's Particle Displacement.

165
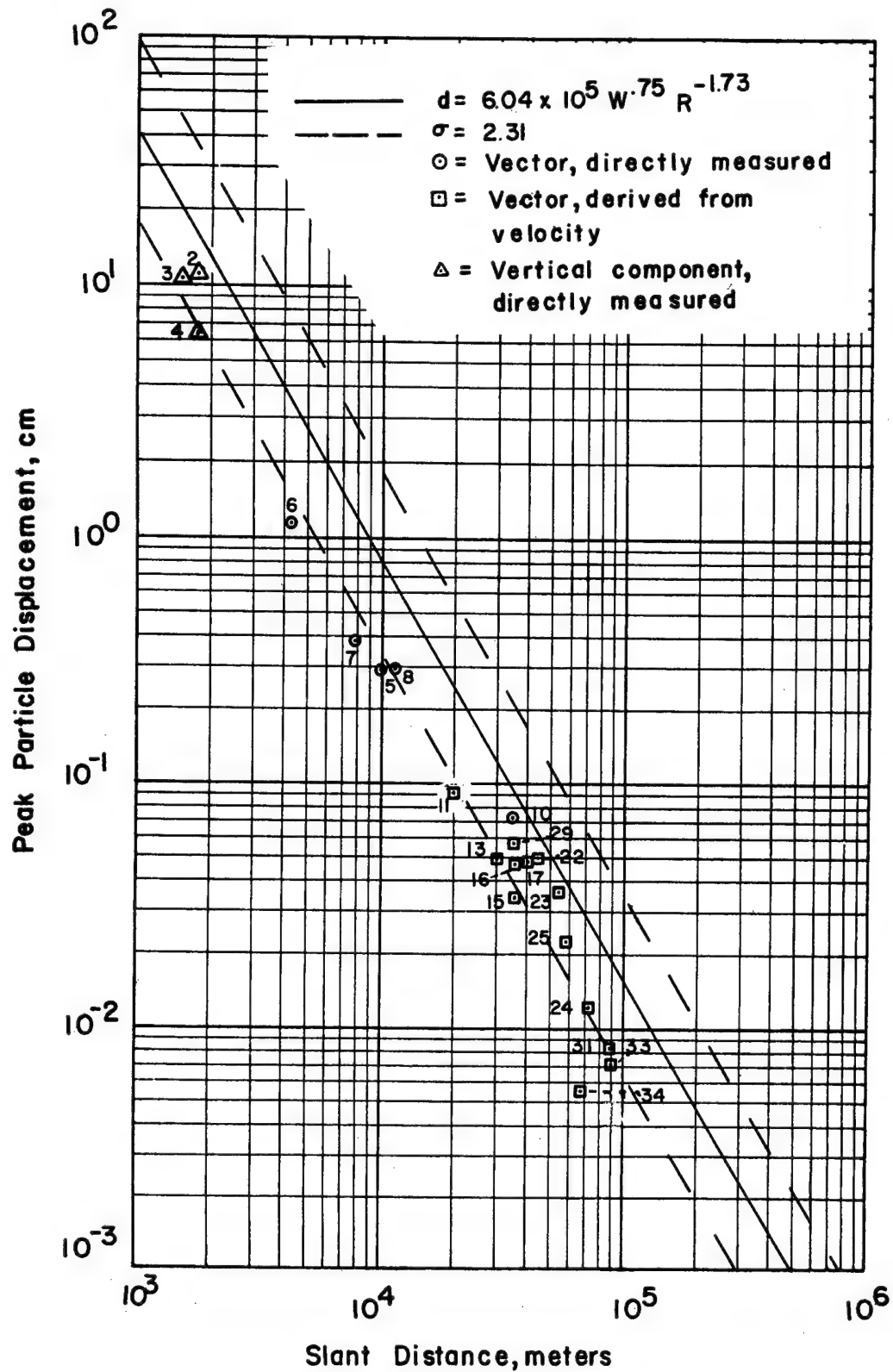
Figure 9.69. Peak Surface Particle Displacement Versus Slant Distance, Hard Rock Stations from the Gasbuggy Event, New Mexico.

(natural gas experiment) detonated in New Mexico. Amplitude-frequency predictions for a station in Farmington, New Mexico are shown versus measured values in Figure 9.70.

Nevada Test Site

Peak amplitude predictions versus measured values are shown in Figures 9.11, 9.12, and 9.14 for the recent, large yield event detonated at NTS.

At specific locations, for example Las Vegas, extra attention is devoted to the ground motion prediction capability. Special studies of the amplitude-frequency content have resulted in particularly accurate predictions, some of which you saw earlier. Amplitude-frequency variation with yield at a station in Las Vegas, with frequency as a parameter, is shown in Figures 9.71 through 9.74. Utilizing this measured amplitude-yield dependence, amplitude-frequency predictions were made for the recent, large yield event, and are shown versus measured values in Figure 9.21. Additionally, Las Vegas response spectra predictions versus measured values are given in Figures 9.26 and 9.27.

These typical comparisons indicate the high degree of ground motion accuracy associated with the ground motion predictions, especially at Las Vegas and from events detonated at the Nevada Test Site.
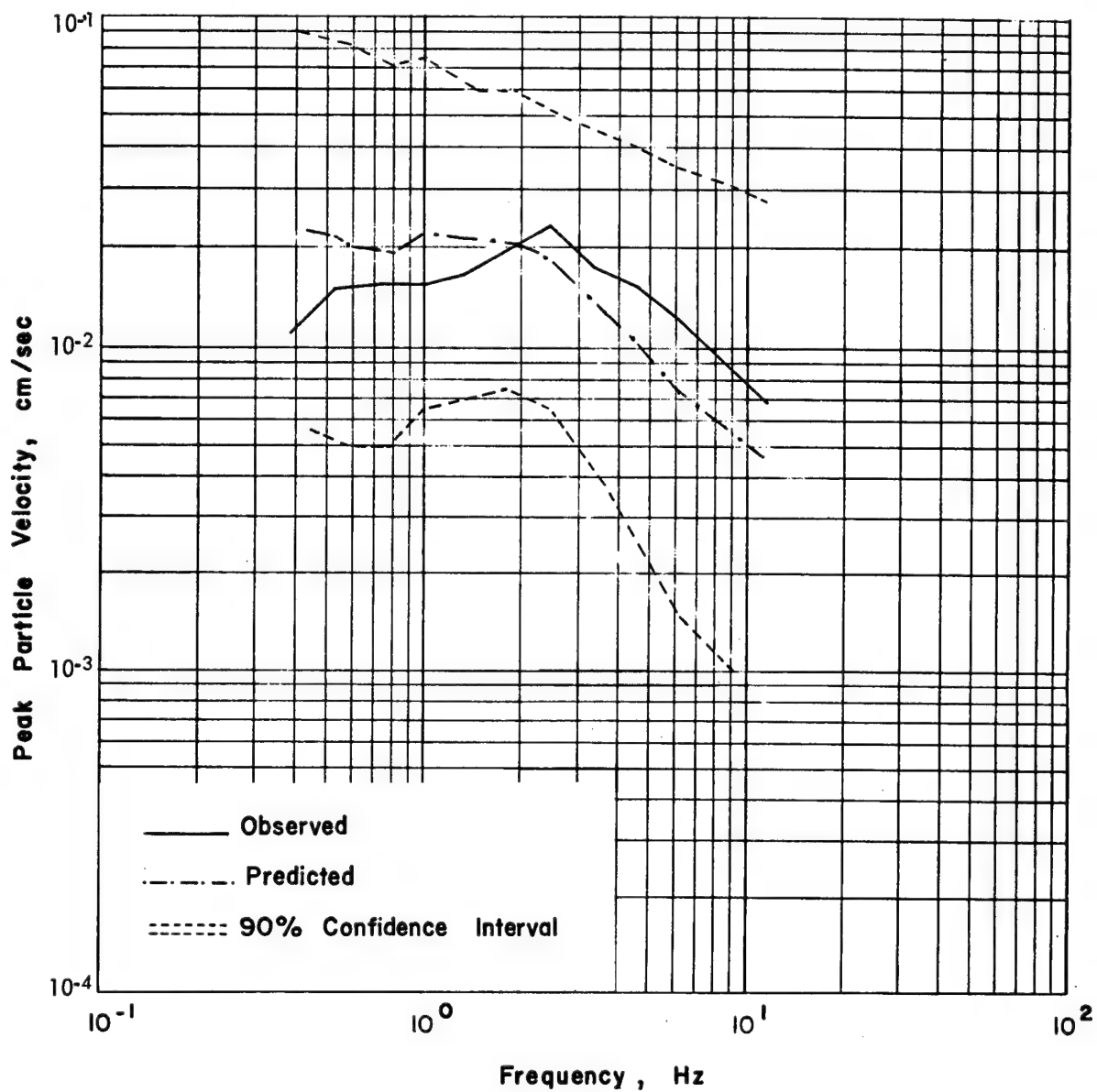
Figure 9.70. Predicted and Observed Band-Pass Filter Velocity from the Gasbuggy Event, New Mexico.

168
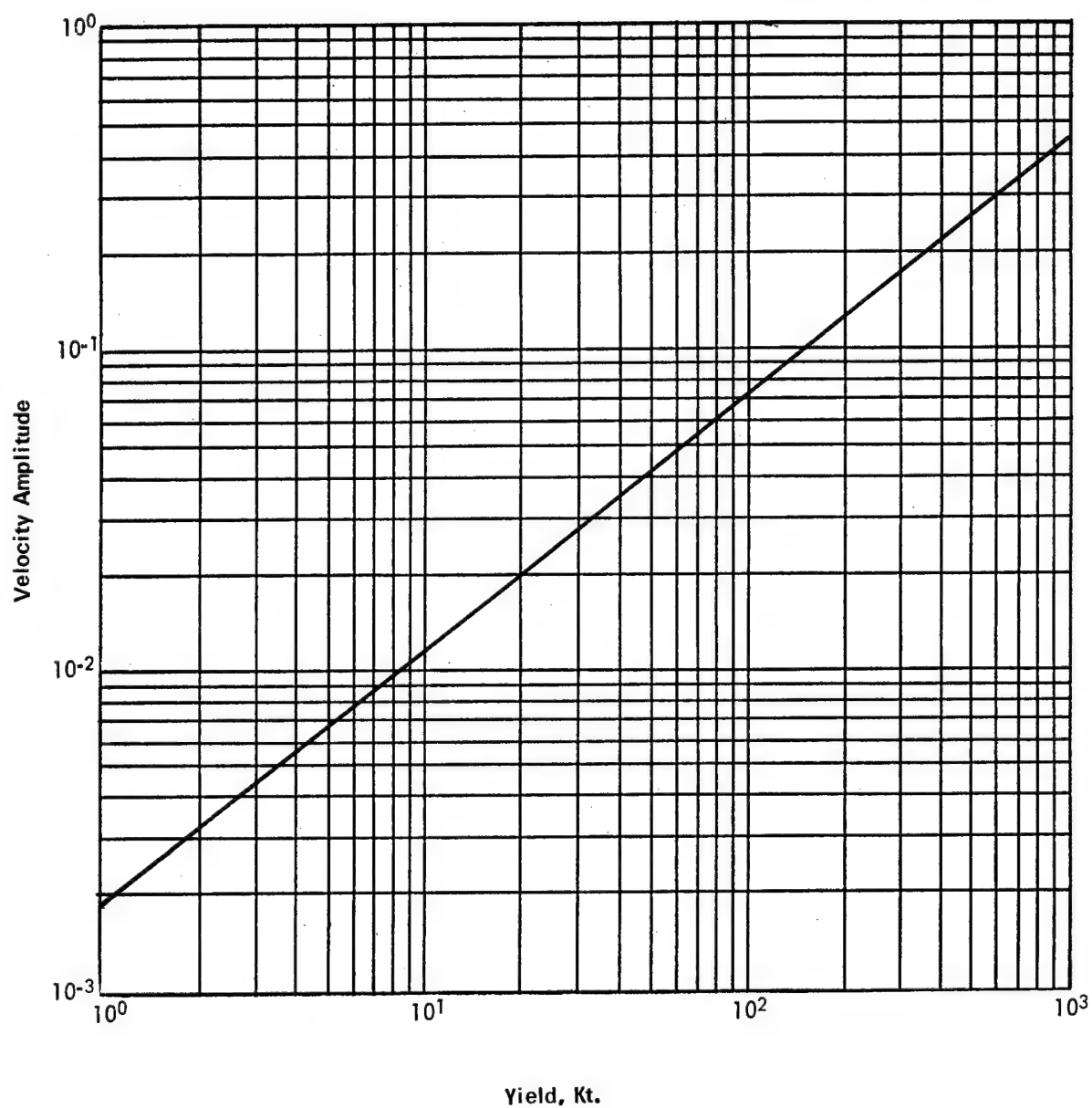
Figure 9.71.   Amplitude Versus Yield, 0.41 Hz from Selected Pahute Mesa and Yucca Flat Events.

169
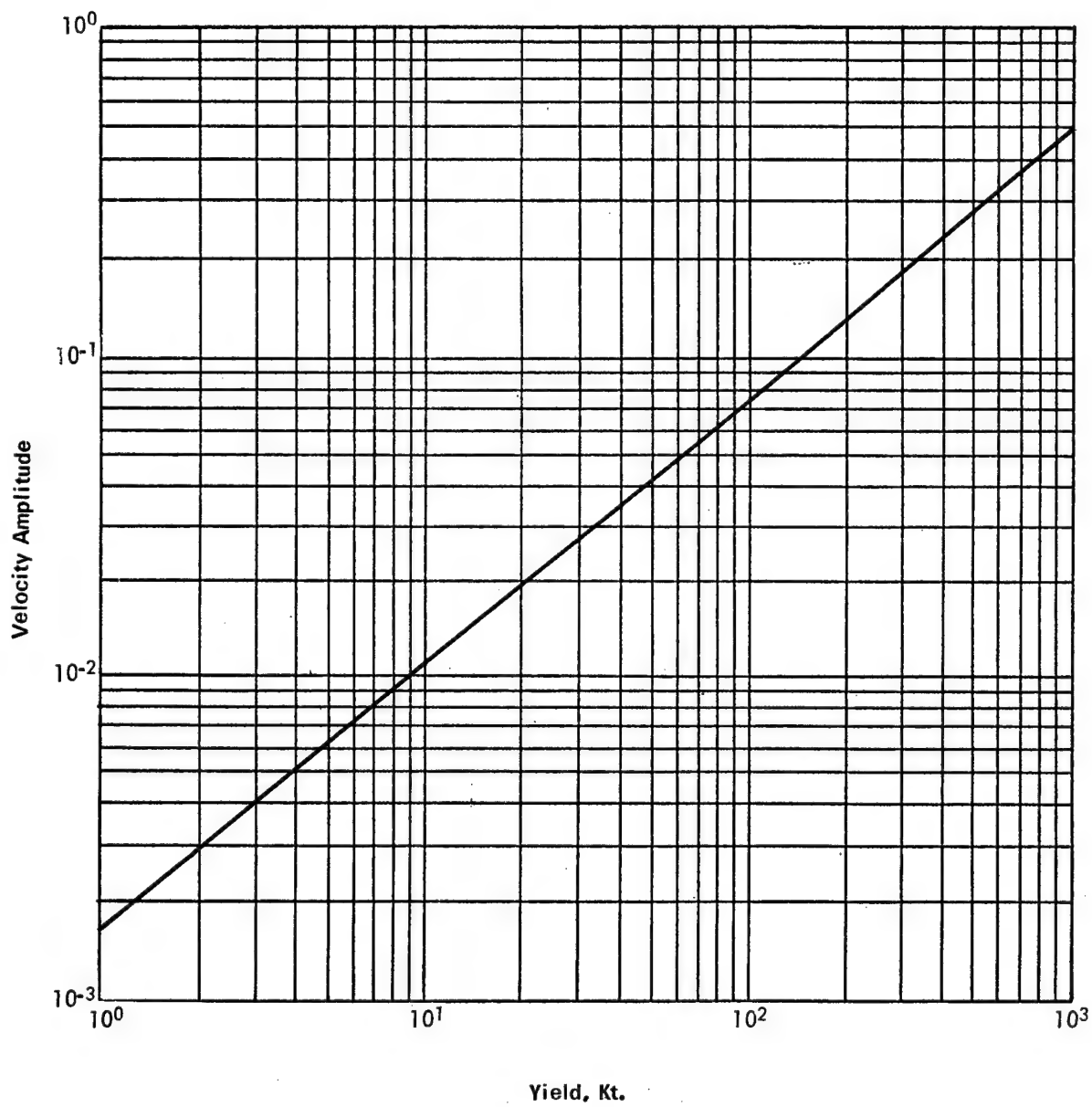
Figure 9.72. Amplitude Versus Yield, 0.55 Hz from Selected Pahute Mesa and Yucca Flat Events.
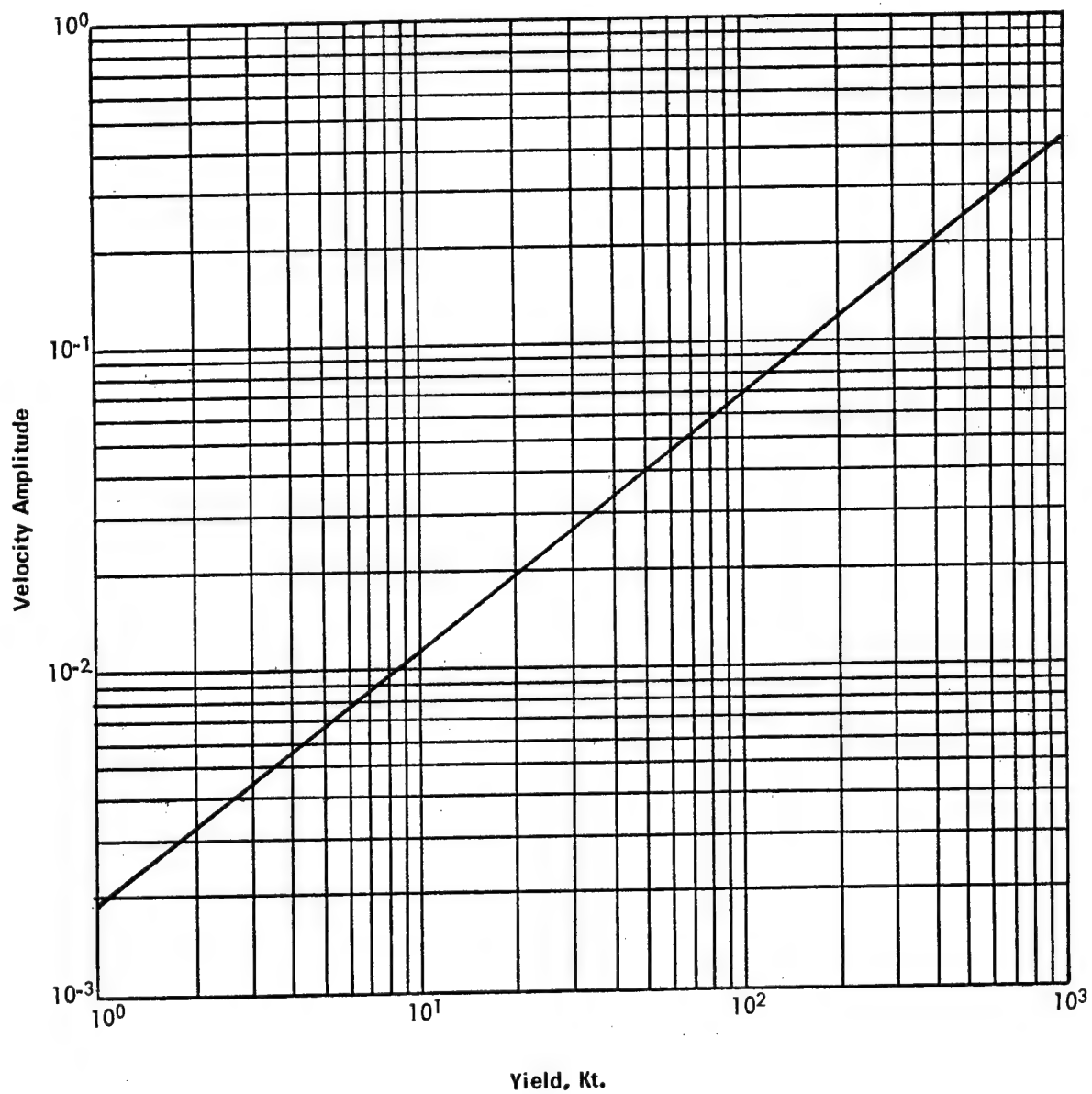
Figure 9.73. Amplitude Versus Yield, 0.75 Hz from Selected Pahute Mesa and Yucca Flat Events.

171
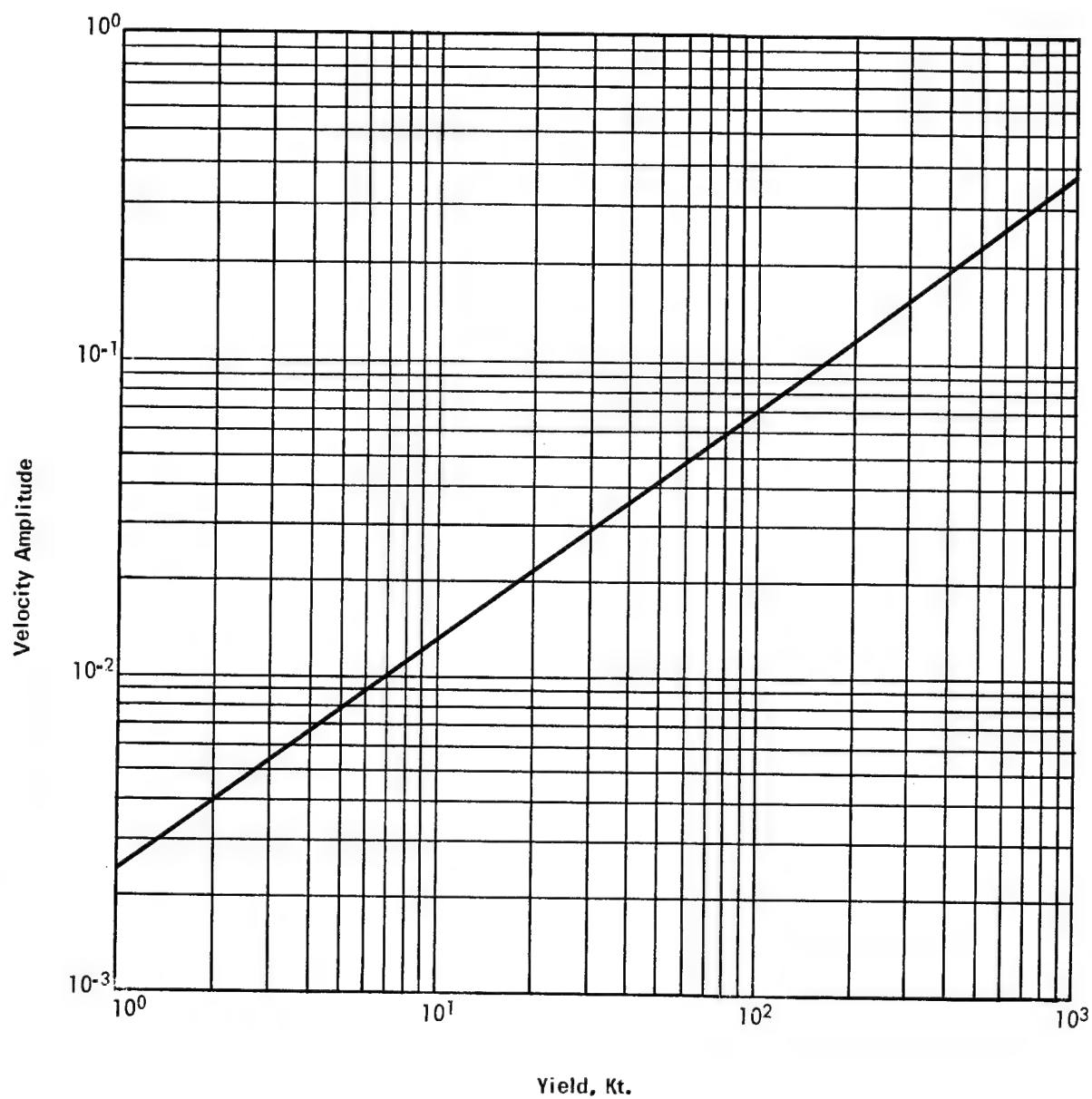
Figure 9.74. Amplitude Versus Yield, 1.00 Hz from Selected Pahute Mesa and Yucca Flat Events.

172

Chapter 10

STRUCTURAL RESPONSE TO NUCLEAR INDUCED GROUND MOTION

John A. Blume, *President*
John A. Blume & Associates Research Division, San Francisco, California

Part A — General Considerations

INTRODUCTION

The subject of this presentation is structural response to ground motion induced by underground nuclear explosions. A related matter to be discussed is safety of persons if there should be any risk of property damage. The material will be covered in two parts — general considerations including important theoretical aspects, and then specific discussion on selected major topics of what is being done and learned in the structural response program.

Responsibilities and Objectives

John A. Blume & Associates Research Division is assigned by contract the responsibility of providing AEC/NVOO with predicted effects of expected ground motion on structures and facilities. A basic long-range objective of the effort is to conduct studies and to compile and document data leading to the development of a formal technology dealing with the response to ground motion resulting from underground nuclear and chemical explosions. Other phases of our work include study of the structural dynamic properties of building elements, and also on soil-structure interaction; studies on how to minimize damage; investigation of natural earthquakes for pertinent data; and technical investigation of complaints of damage. We also make specific recommendations regarding the safety of persons as related to possible hazard to offsite buildings and other structures on or above the ground surface. The prediction of ground motion and effects to underground installations such as mines are done by the AEC's Ground Motion Contractor, the Environmental Research Corporation (ERC).

Qualifications and Background

It may be helpful, before proceeding, especially since we are not a federal agency but a private firm, to outline some of our qualifications and background for this im-

portant assignment in which we have been engaged since 1964. With our companion firm that engages in the design of structures and buildings of all types, John A. Blume & Associates Research Division brings the several necessary disciplines to the response problem. These include structural engineering, architectural engineering, civil engineering, engineering geology, soil and rock mechanics, earthquake engineering, dynamics, mathematics, computer technology, statistics, and probability theory. We have 35 years background of intensive work in the problems and effects of natural earthquakes and have conducted much original research in this allied field. The underlying specialty of the firm is in the effects of energy demands on so-called fixed structures; these demands may be from ground motion of natural or manmade sources, windstorm, airblast, sonic boom, ocean swell and waves, or from vibration of mechanical origin. This unwanted or excessive energy may be delivered to the structure through the soil or rock, through the atmosphere, through water, or through the structure itself. Much of our background experience has been, and will be, very useful in the NVOO Safety Program. We are pleased to be engaged in this very important assignment.

FUNDAMENTALS OF STRUCTURAL RESPONSE

Buildings respond to ground motion. Depending upon the vibrational characteristics of the structures, the response amplitude may be several times the amplitude of the ground. That is why motion is often felt by persons near the top of tall buildings while others are completely unaware of the disturbance. The ground motion may be caused by an earthquake, by an explosion, or even by a truck rolling over a bumpy street. The amplitude, duration, and the characteristics of the ground motion can vary over a wide spectrum depending upon many factors, the most important of which include the amount of energy at the source, the distance from the source, and the local soil characteristics. The dynamic response of build-

ings also depends upon the ratios between the natural periods of vibration of the buildings and the periods of ground motion that contain the maximum amount of energy. In other words, there is a tuning process. Tall buildings have long periods of vibration. In addition, ground motion at considerable distances from the energy source tends to contain a considerable portion of its energy in the long period range. We thus have a situation in Las Vegas where the tall buildings are subject to response to ground motion from distant sources of energy. This is true whether the energy is from underground nuclear detonations or from natural earthquakes.

Figure 10.1 shows ground motion traces recorded for a major earthquake. The acceleration was recorded by an instrument and the velocity and displacement were obtained by the integration process. The maximum acceleration of this earthquake, where recorded, was 0.33g. The maximum ground acceleration from a nuclear detonation recorded thus far in Las Vegas is less than 0.01g.

It must be kept in mind that ground motion is oscillatory. There is no continuity of motion in one direction. Instead the motion is back and forth, with changing acceleration, velocity, and displacement. In fact, the particle motion is three-dimensional — up and down, and sideways in both directions.

Motion of a Structure

The motion of real soil and real structures is quite complex. In order to simplify the problem, idealized models are often used to represent elements or structures and to enable response calculations to be made. The ability to model realistically is a key part of the analysis procedure and is an art more than a science.

Every structure and every element of a structure has one or more natural periods of vibration. Unless damage occurs these periods generally remain nearly the same no matter what causes the element to move or for how many times. The structural-dynamicist is as concerned with the periods of vibration, their possible changes and ratios, the damping (internal friction characteristics), and the amounts of motion, as the physician is with pulse rate, blood pressure, chemical analyses, and other indicators.

In Figure 10.2 the simple pendulum (No. 1) will move as shown if its support above moves or if the pendulum bob is initially displaced. The jack-in-the-box (No. 2) will vibrate up and down after release from its captivity, and later when its base is moved in the vertical direction. The inverted pendulum (No. 3) is sometimes seen in the form of a modern elevated water storage tank. Many buildings have the appearance of a slender rod (No. 4).

An idealized simple building (No. 5) vibrates back and forth as indicated. One of the more complex of the idealized systems is the rocking block (No. 6). This can represent a very rigid building rocking on hard ground. In all of these examples, except the rocking block (No. 6), the time required for free motion from one side to the other and back again, or the period of vibration, is constant (unless motion is otherwise forced by an outside agency such as the ground). However, the period of vibration decreases for the rocking block (No. 6), that is, the frequency increases rapidly as the rocking amplitude decreases.

The idealized vibrating motions illustrated in Figure 10.2 are very simple systems. Most actual structures such as buildings and bridges are much more complex, both structurally and dynamically. For example, in a typical high-rise building there are not only a great many natural modes of vibration between the structure and ground upon which it bears, but also other complications resulting from the interaction of nonstructural elements such as partitions, plaster, etc., with the structural frame, and from the interaction of the vibrating structure with the ground on which it rests. It could be said that the relationship between a simple pendulum and a modern tall building is analogous to but less complex than the relationship between an amoeba and the human body.

Figure 10.3 indicates the first three natural modes of vibration of a 15-story building. Any or all of these modes (and more) can vibrate at the same time. The nodes or loops of each mode oscillate back and forth, each mode in its own period of vibration. A vibration record taken in a building undergoing all three of these modes simultaneously would show complex wave forms. Different types of ground motion can induce different combinations of mode responses. The circular symbols in the figure indicate ideal positions for recording instruments to provide dynamic data on this building. The particular curves shown are for an actual San Francisco office building[1].

Dynamic Amplification

Figure 10.4 indicates how the relative response is greatly amplified when a period of the structure is approximately the same as the period of the ground motion, or the forcing function. This phenomenon is called resonance, and it is one of the most important considerations in structural dynamics. It also tends to explain why peak particle motion without reference to its period of vibration is generally meaningless in the response problem. In Figure 10.4 there are three damping values shown. Motion records show that most buildings, when under-

174
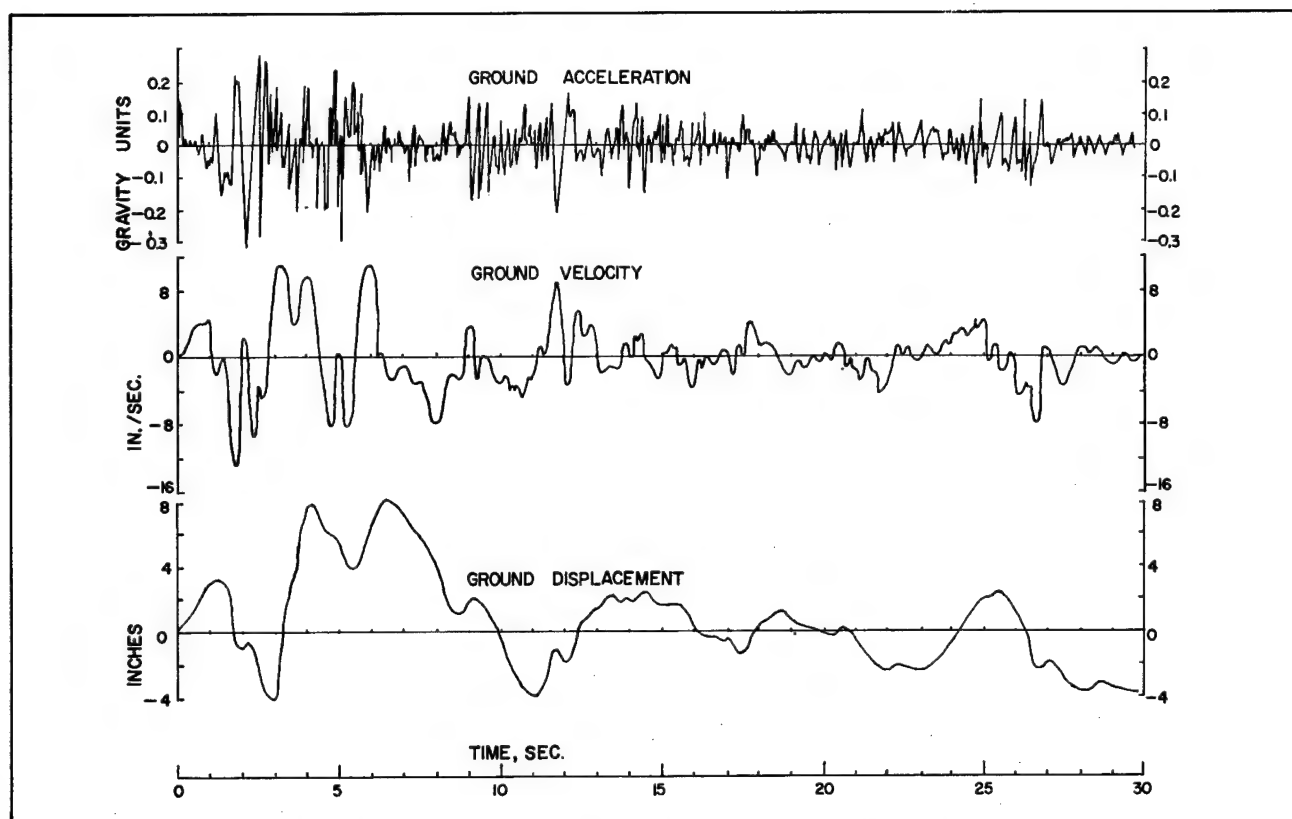
Figure 10.1.   1940 Earthquake at El Centro, California; North to South Component.
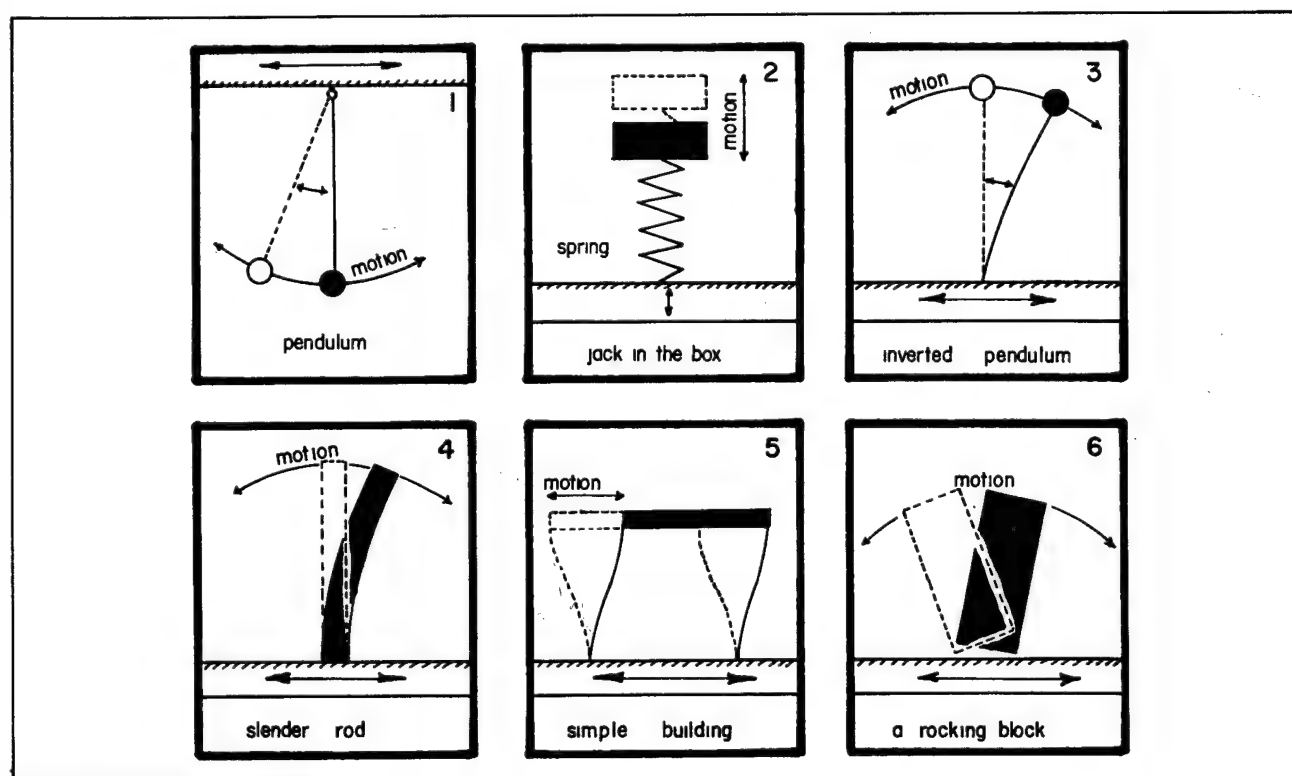
Figure 10.2.   Idealized Vibrating Systems.

175
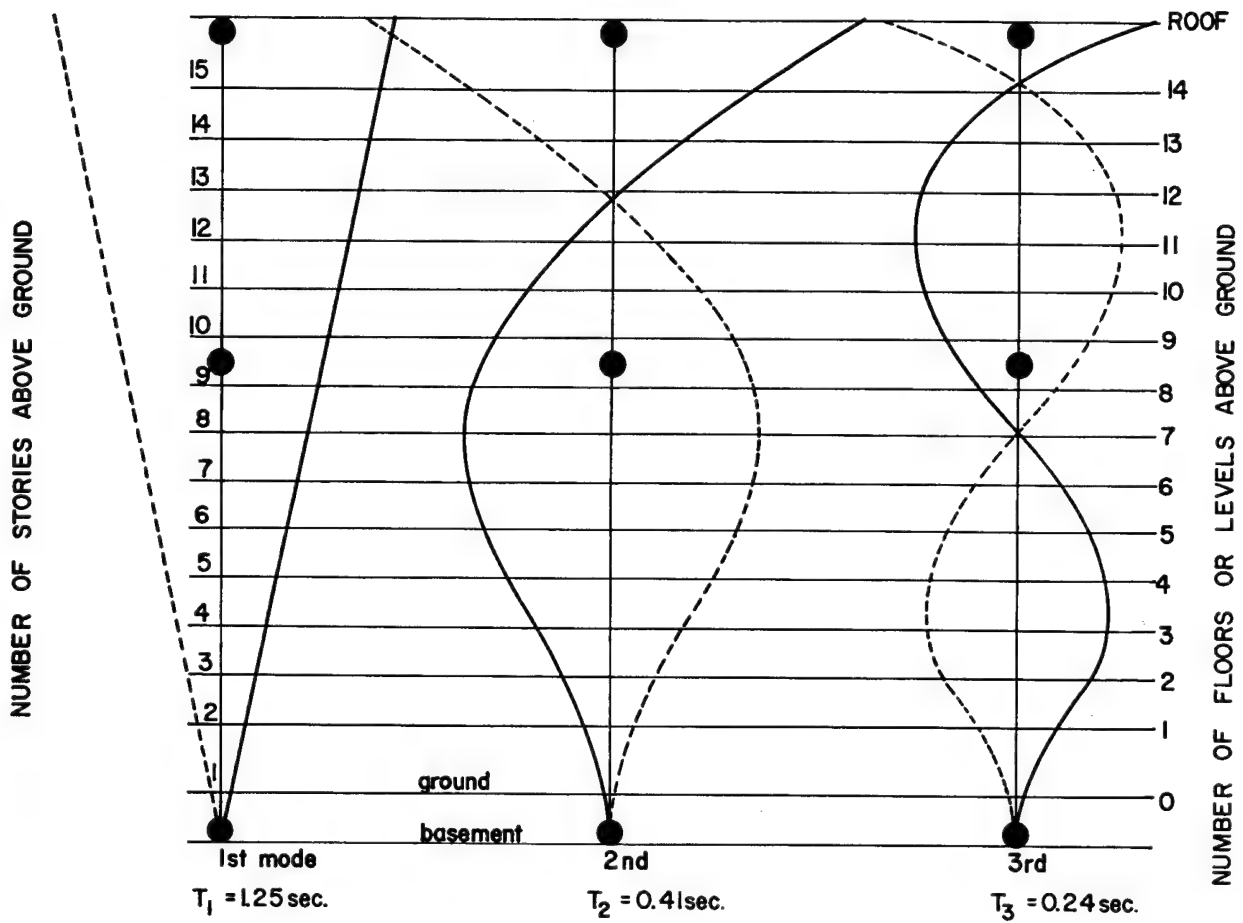
Figure 10.3. Mode Shapes of a 15-story Building.

going severe motion, have a damping value in the order of 5 percent of critical damping. Critical damping implies an amount under which a structure would not vibrate past its equilibrium position when released from an initial displacement.

Everyone has heard of the troop of marching soldiers breaking stride, or cadence, when crossing a bridge. The sergeant may not have studied dynamics, but for one reason or another he was ordering a random disturbance rather than a unified repeating rhythm that might have been close to a natural mode of vibration of the bridge, or close to the ratio of 1.0 in Figure 10.4. Another example would be the violinist breaking a glass situated across the room from where he was playing. In this case, the violinist deliberately sought the tuning ratio of 1.0, so that the air waves resulting from the violin string vibrations coincided with a natural mode of the brittle glass.

Although perfect tuning or a resonance ratio of 1.0 is not probable in structural response, there have been many examples to show that structures can and do respond according to Figure 10.4, and at times in a very few cycles of motion that are not necessarily closely tuned. This problem needs more reliable numerical values for structural response operations.

COMPLEXITIES OF RESPONSE PREDICTION

If we knew the precise history of the ground motion and how it varies with time, and if we knew the exact characteristics of the structures, we could make accurate calculations of the response. Because both the ground motion and the characteristics of real buildings are complex and as yet not entirely understood, it is necessary to approach the problem from two major directions. One is empirical where actual motion is measured and the other is theoretical where techniques are developed to model both the ground motion and the buildings. Basic to this whole operation is the concept that the measured data and the theory must be reconciled, particularly with consideration of the probability aspects of the many variables in the problem.

There are thus three basic elements in the response problem — the disturbance which in this case is ground motion, the structure which is really the combined soil-structure system, and the response or the results with respect to time-history of the disturbance acting upon the structure.

The response problem is further complicated by latent conditions existing in many buildings, especially residential type buildings. The capacity of a structure to resist response motion without damage varies greatly with any existing stress problems in the structure or in the soil below the structure. For example, a building which is founded upon unstable soil or soil that is subject to shrinking or swelling from moisture variations is subject to internal stresses. These stresses may reach the point where there may be cracking or other minor damage without any ground motion whatsoever. On the other hand, these stresses may not quite reach the cracking point but may be so close to this level that even minor ground motion, as for example that caused by a heavy truck on bumpy paving, may constitute "the straw that breaks the camel's back."

In addition to soil conditions, there are a great many other problem areas including shrinkage stress in cementitious materials, variations in dimension due to temperature changes or moisture changes, and so forth[2]. It is a responsibility in structural response work, insofar as possible, to relate cause and effect. This cannot always be done in a black or white manner. There may be gray areas or there may be situations where two or more causes are responsible for the distress signals.

Another problem even without latent conditions is the great variation in not only the ground motion from time to time and from place to place, but in the capacity of structures. By no means are structures all alike in the resistance to lateral forces induced by ground motion, even though designed under the same building code or constructed by the same contractor. There are basic and inherent variations in materials, design, and workmanship and other conditions, all of which lead to variations in the resistance of structures to ground motion. All structures are not alike just as people are not alike. The probability of a strong ground motion getting together with a weak structure must be faced. We cannot deal in averages but must consider variations from these averages when estimating damage or lack of damage. We have various probability laws that are most useful in approaching this part of the response problem. The larger the population of structures and buildings, the more we must consider the effect of variations from the mean (or average) capacity values.

TREATMENT OF DATA

The basic data obtained from each major event include measured ground motion and measured building motion over a complete time-history, observational reports on whether or not any damage occurred, gauge and other measurements on any differential motion of existing cracks in monitored buildings, reports on human perception of motion, and data on the actual yield of the nuclear device. Most of the detonations covered to date have been conducted at the Nevada Test Site, with data
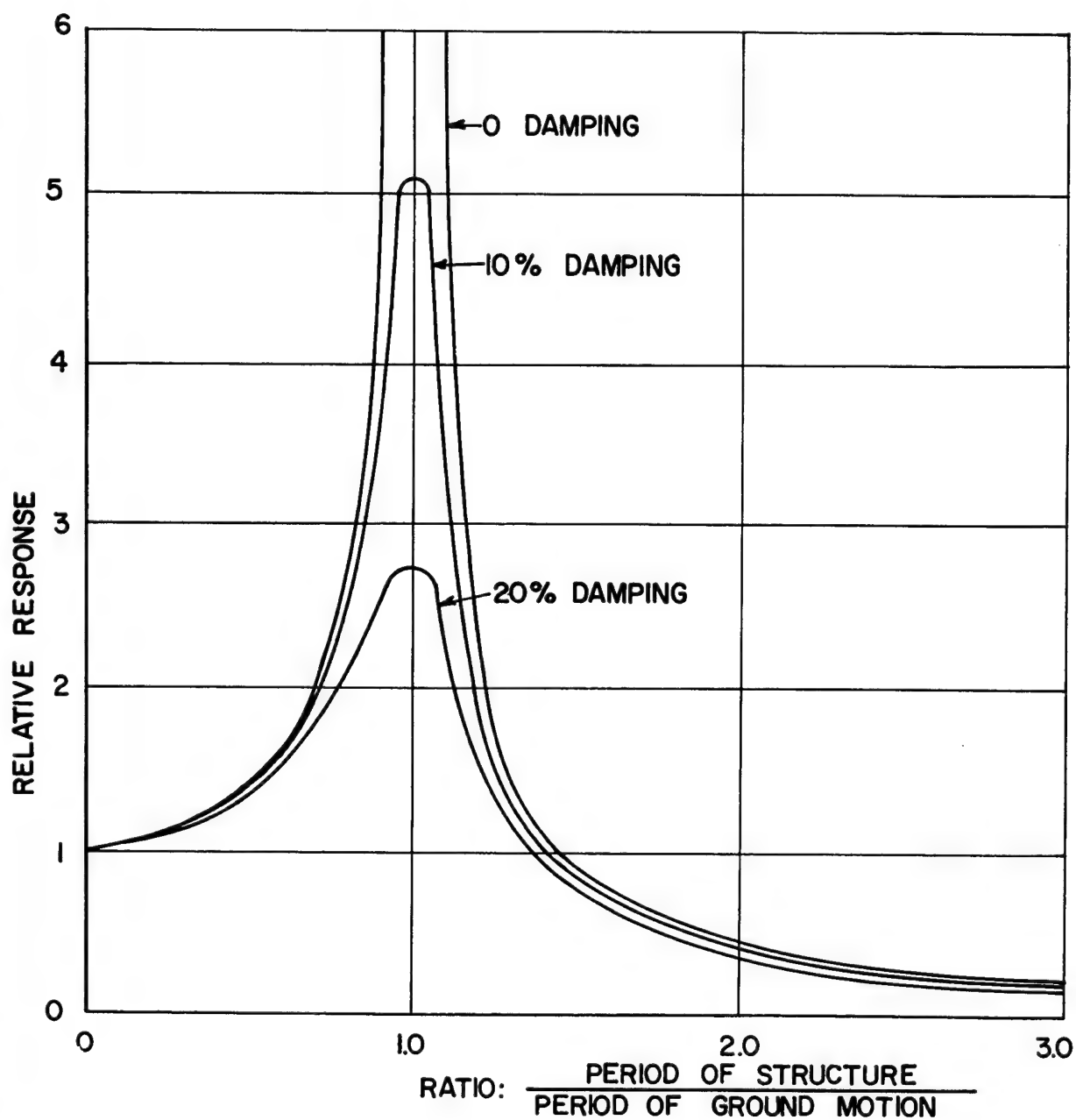
Figure 10.4. Response to Harmonic Motion.

178

generally obtained for all cities, towns, or areas where the motion was measurable. The number of instruments used and their deployment depends upon what data are considered most significant for each event, needed data points, and any budgetary or other problems. Providing this instrumentation is the responsibility of the Las Vegas Special Projects Party of the U.S. Coast and Geodetic Survey.

The processing of measured motion involves corrections and adjustments as necessary for all instrumental characteristics, calibrations, or errors and then the careful determination of peak responses by amplitude, frequency, and periodicity. Record processing, as well as ground motion prediction, is a responsibility assigned to the Environmental Research Corporation (ERC). For structural response studies we frequently require that records be obtained with simultaneous time scales, as for example simultaneous recordings at the top of a building, at two or more other stories, in its basement, and on the ground well away from the building. With these records we study modal and phase relationships and relative motions. This material can be very instructive in learning more about actual building response and the soil-structure interaction problem.

The data needed most are associated with real damage, which has been essentially unobserved in Nevada except for test structures at the Nevada Test Site. Because of this fact, and the fact that private buildings can never be subjected to much damage, test structures are used, and destructive testing is conducted in our dynamic laboratory in San Francisco[3,4,5].

Figures 10.5 and 10.6 show data points for relative top floor displacement of two Las Vegas hotel buildings. The names of the buildings are not identified. Each point represents a nuclear event. The lines are obtained by regression analysis and indicate the mean and the one-sigma variations from the mean. With more data, the linearity of the prediction lines would be challenged.

Figures 10.7 and 10.8 indicate peak top floor accelerations for two Las Vegas hotel buildings. It is to be noted that the top level motion is about 6 times greater than that of the ground in one building and about 7 times in the other. The scatter in the small values is no doubt due in large part to the relative instrumental and other errors inherent in very small measurements, as well as differences in ground motion for small events.

The peak top level displacements from nuclear events have been 0.5 cm at Beatty, 0.3 cm at Goldfield, 0.2 cm at Tonopah, and 1.5 cm in Las Vegas. Peak top level accelerations have been 0.07g at Beatty, 0.015g at Gold-

field and Tonopah, and about 0.05g in the Las Vegas high-rise buildings.

Data from Testing

As noted previously, one of the greatest problems is to model buildings properly for analysis. The participation of nonstructural elements such as partitions and filler walls, either alone or in conjunction with the structural frame, is not well understood. There are sparse data on such elements, and yet the indications are that they are very important in the response of buildings and in their damage potential. We are testing such elements in our laboratory and in test structures at NTS[3,4,5].

Figure 10.9 graphically represents the lateral force-deformation characteristics of 12 types of wall panels that are commonly found in high-rise and other buildings. The panels are constructed of various types of studs and various types of finishes, such as plaster, gypsum board, and plywood. Some panels have doors and some do not. The important thing here is to note the great variation in strength and stiffness, and the fact that at about 1/8-inch story displacement there is generally a considerable rounding off of the resistance curve, indicating a damage threshold. The stiffness is represented by the slope of the curve. We have found cases where the filler walls are so stiff as compared to the structural frame as to essentially dominate both the structural and the dynamic characteristics of the building. This means that the building can not function under lateral forces as the designer intended. It also means that building resistance and safety are highly variable and very difficult to evaluate without testing.

Figure 10.10 shows the energy capacity of wall panels plotted against story shear distortion. This energy capacity can be useful in resisting the demands of ground motion, but the high values are associated with damaging displacements as shown by the curve slopes in Figure 10.9.

We conduct tests in two 4-story reinforced concrete test structures at NTS. These structures have been damaged by ground motion from nuclear events in the general area. Sometimes the frames have been tested alone without partitions, whereas other tests have been made with various partition materials installed. The results have been very useful.

Figure 10.11 contains a plot of response velocity versus forcing frequency, where the forcing was being done by a special vibration-generating machine made in our NVO-sponsored laboratory. The first, second, and third mode resonant responses can be seen in the figure.
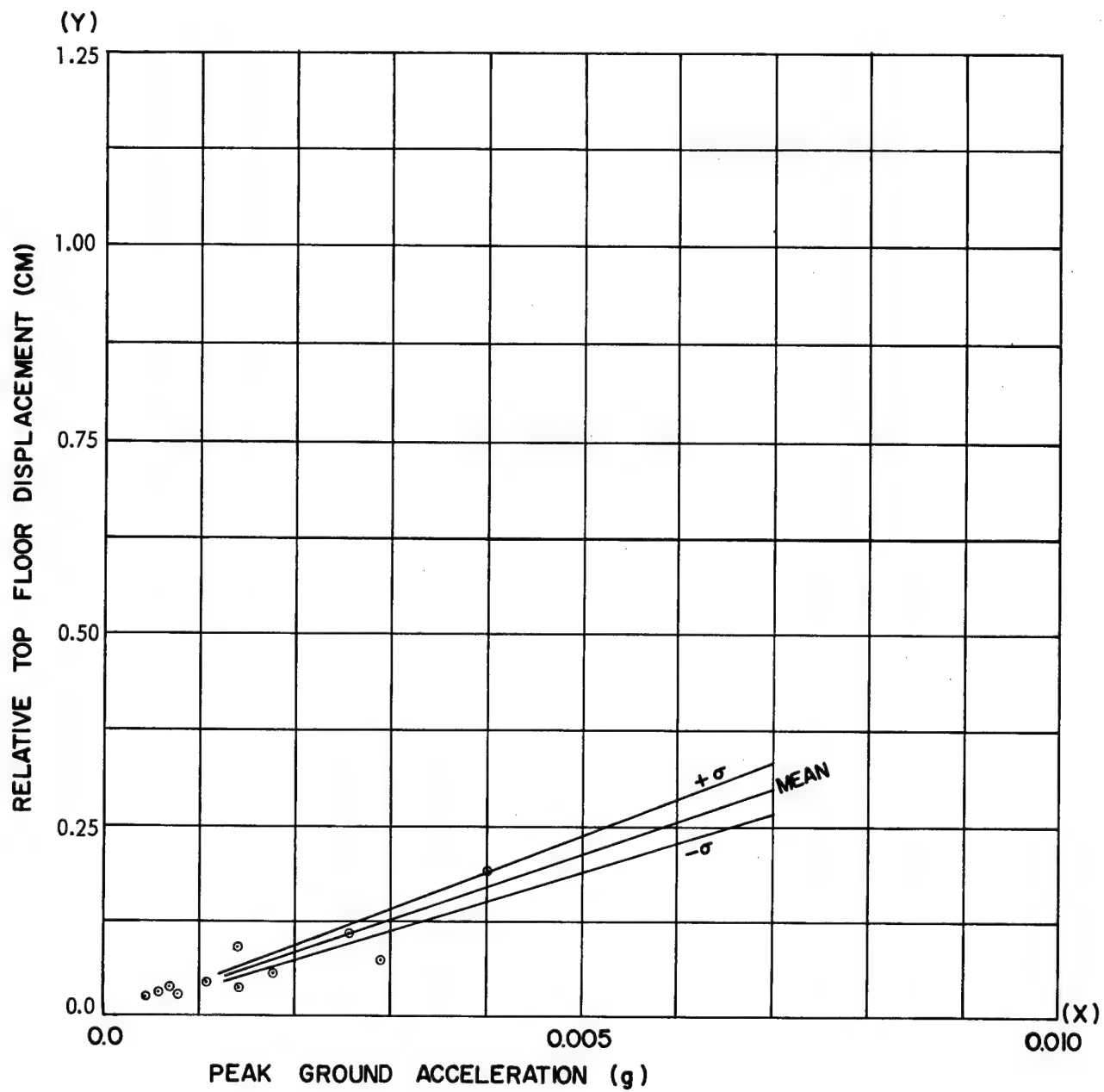
Figure 10.5. Relative Top Floor Displacement.
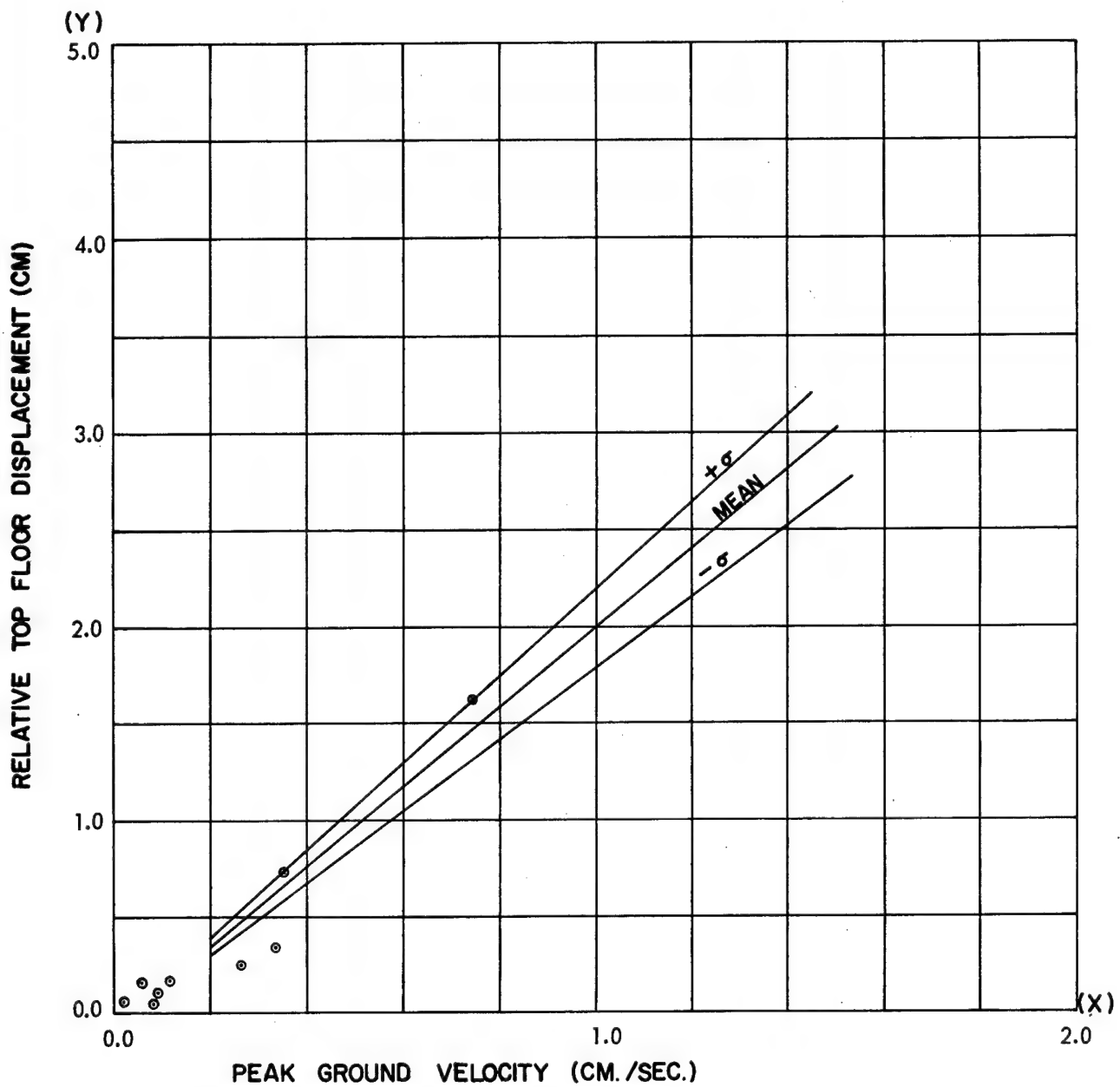
Figure 10.6. Relative Top Floor Displacement.
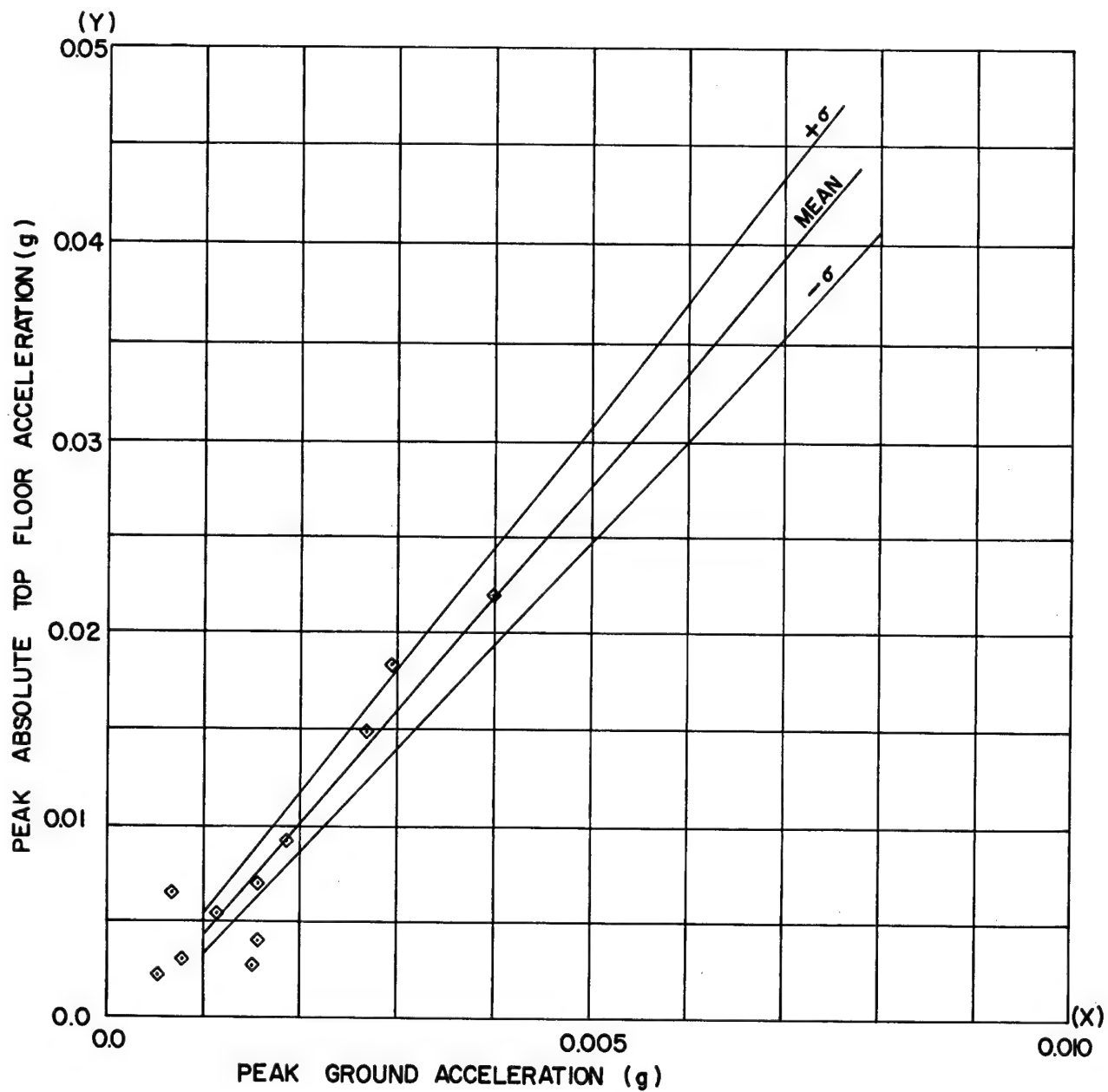
Figure 10.7. Peak Top Floor Accelerations.
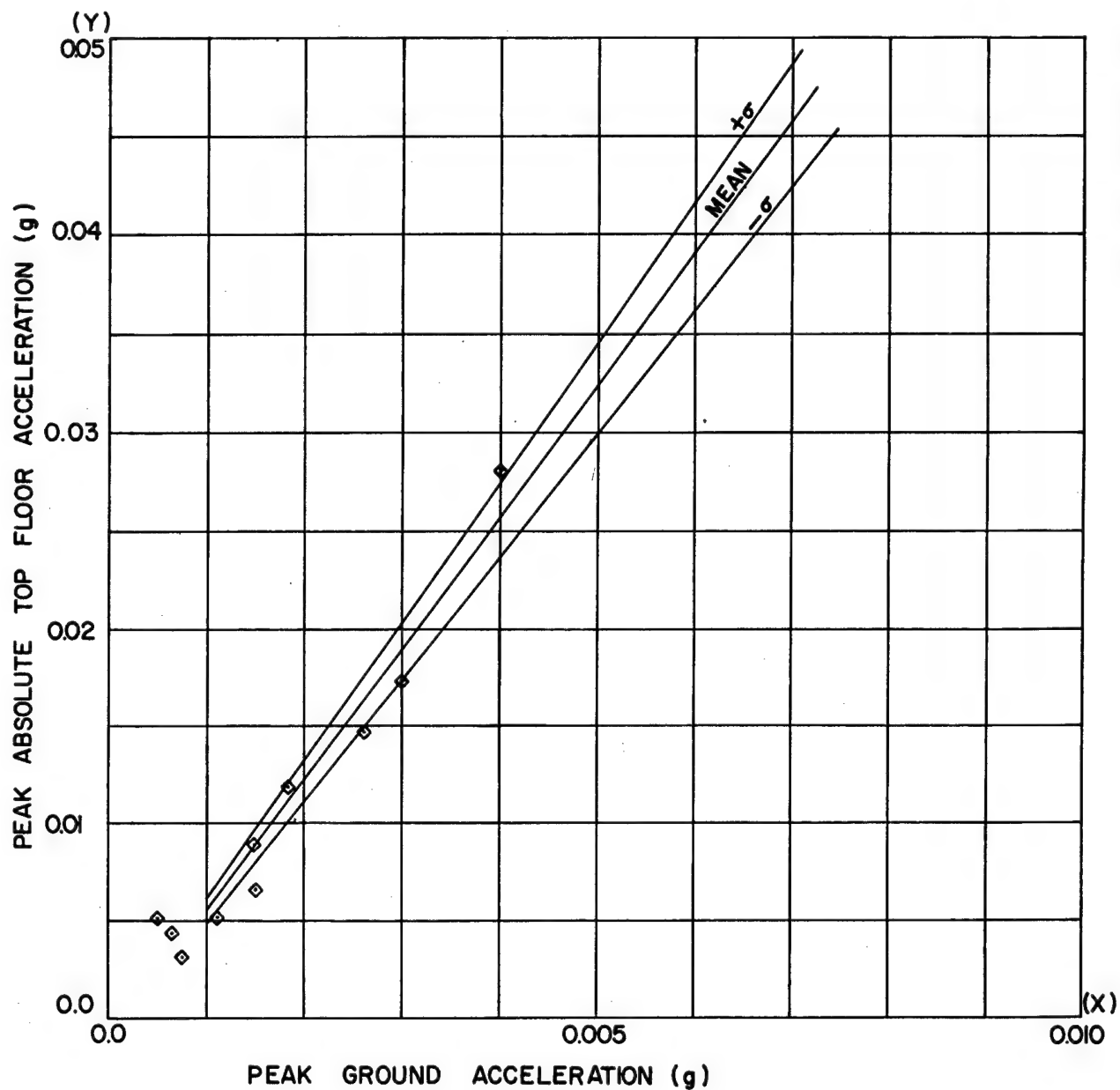
Figure 10.8. Peak Top Floor Accelerations.

183
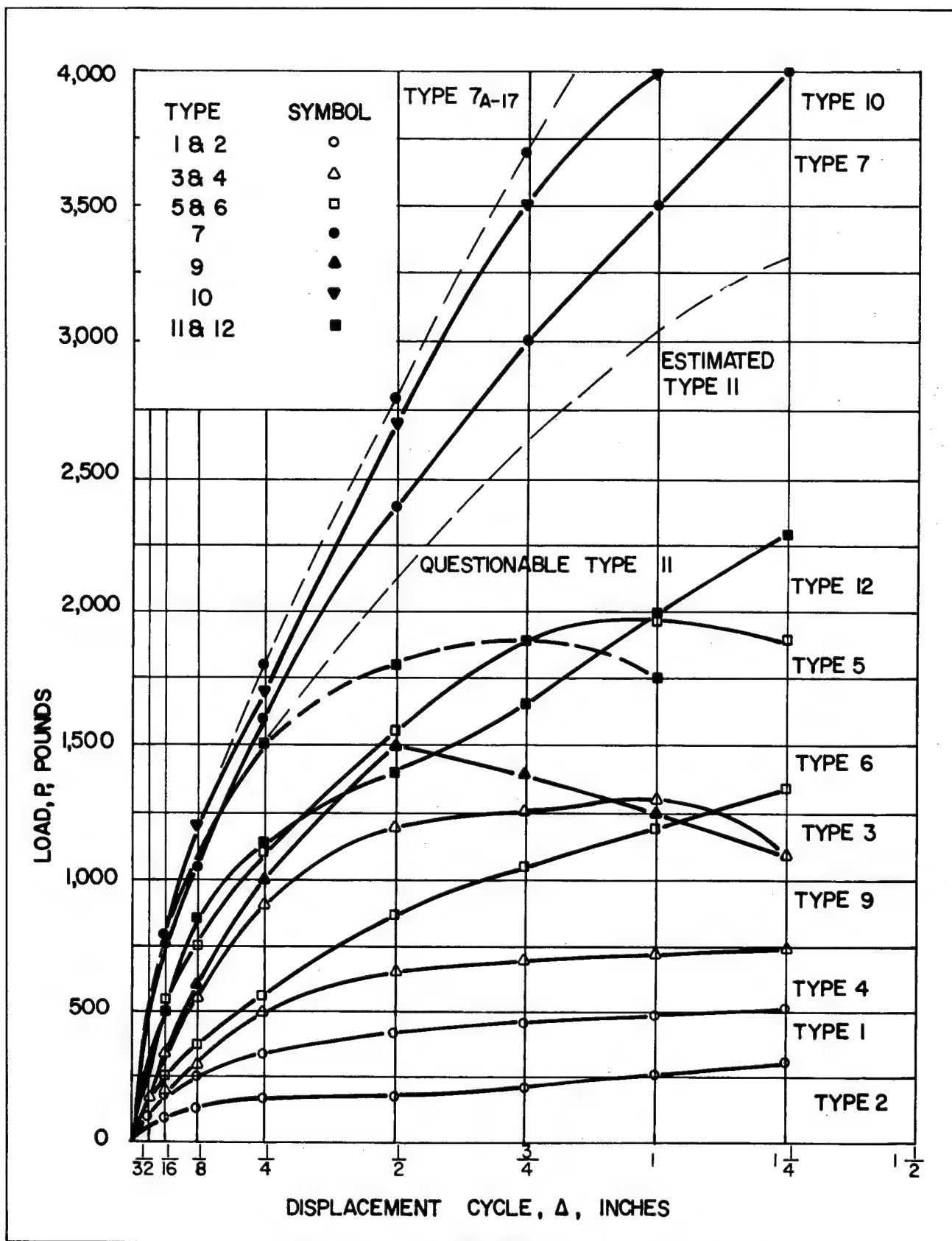
Figure 10.9.   Summary of Idealized Load Versus Displacement for All Types of Wall Panels.

184
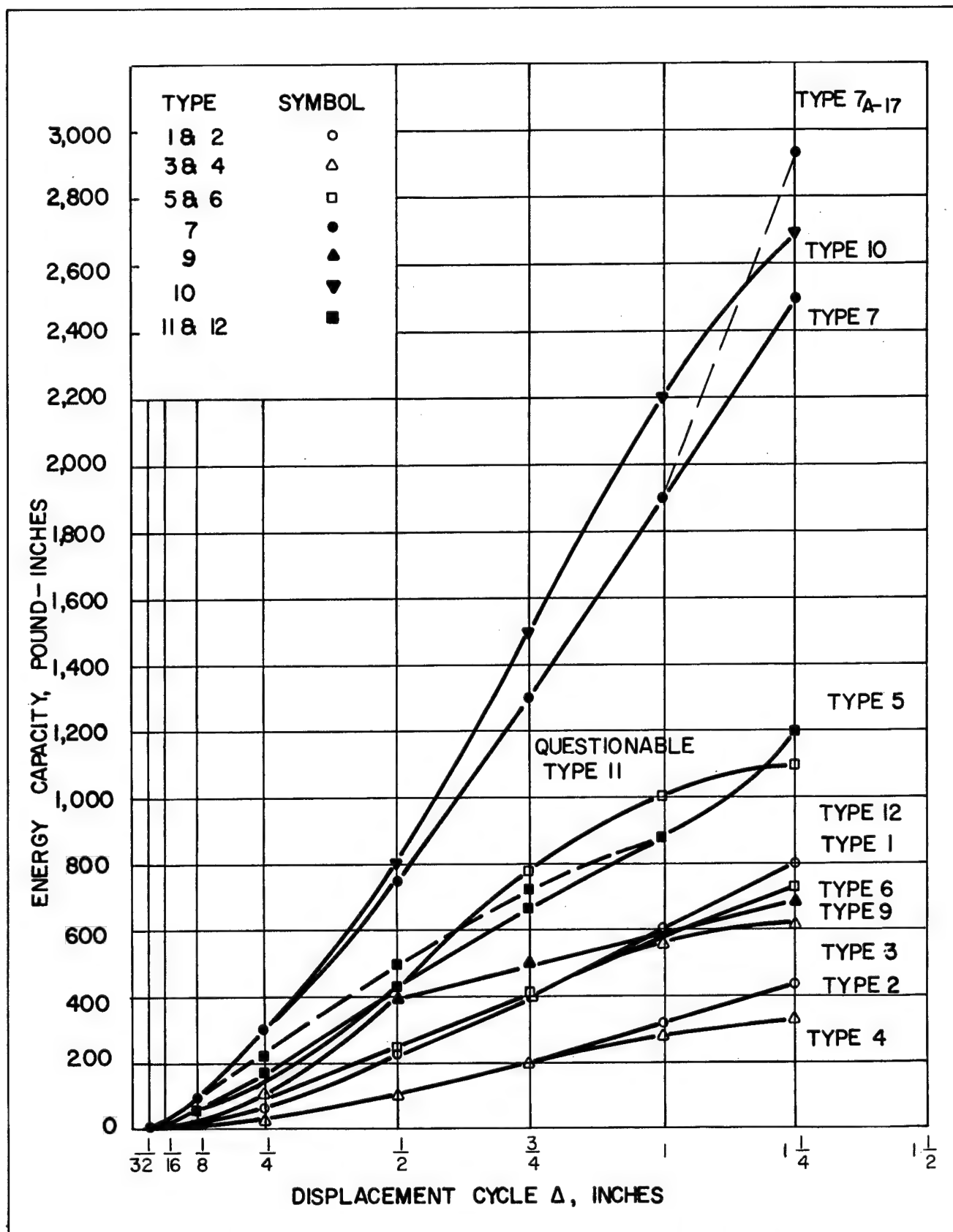
Figure 10.10.   Summary of Idealized Energy Capacity Versus Displacement for All Types of Wall Panels.
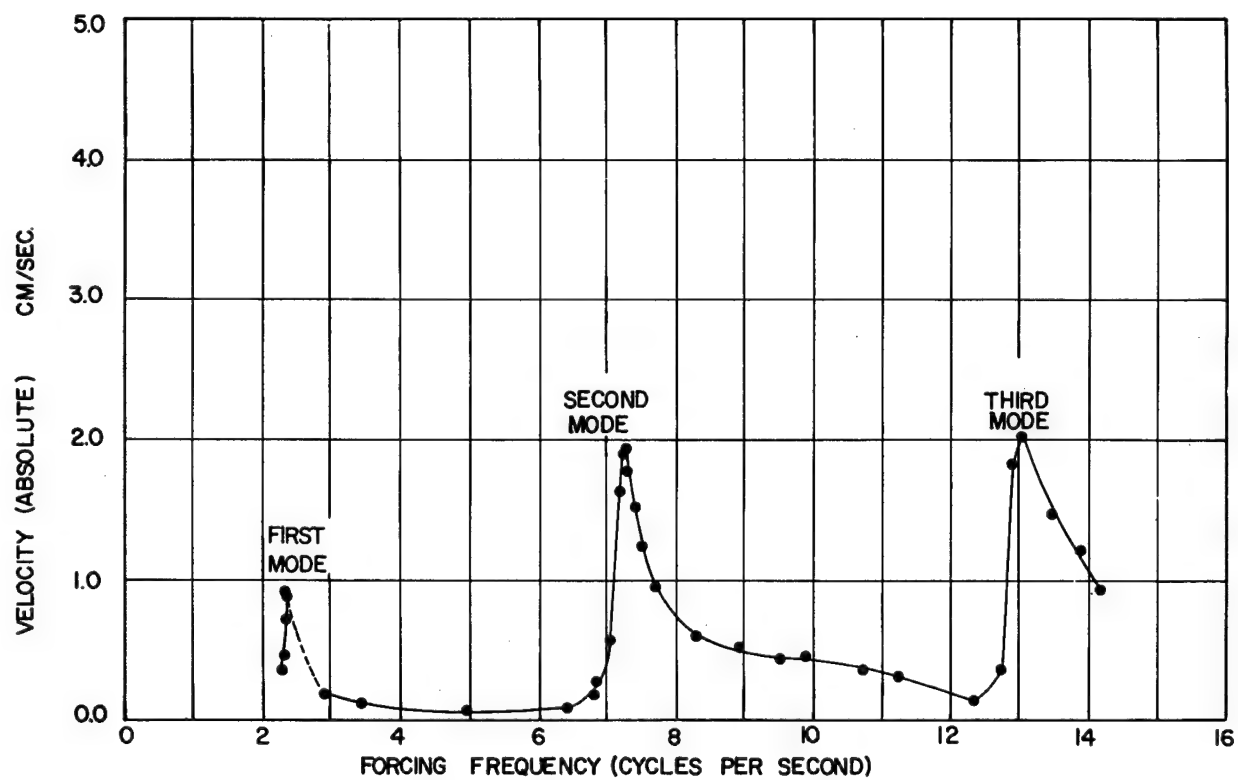
Figure 10.11. 4-Story Test Structures: South Structure, North to South Direction. Test Series D, Response Curve of Roof for Vibration Generator Located at Roof.

Figure 10.12 is a photograph of the machine. When in use this machine is bolted to a floor slab, and uni-axial horizontal forces are generated, parallel to a major building axis. The speed of the generator is slowly increased in steps, attempting to set a steady state condition at various forcing frequencies. First, second, and third mode responses are clearly perceptible as resonance occurs. Fourth mode response is not attempted. Each test normally lasts 3 to 5 minutes. This includes starting from 1 cps, increasing the speed in steps to about 14 cps, and then decreasing to approximately 1 cps.

Figure 10.13 is a graph of the top story displacement plotted against the fundamental period for 5 test series. The differences in natural period are due to three parameters: partition installation or removal, damage between tests from severe nuclear induced ground motion, and — as shown in the figure — from amplitude of the motion. All of these factors are being correlated and valuable data are being obtained.

Response induced in the structure by various nuclear events is presented in Figure 10.14. The test motions are also shown. This is the first such combination of experiments on any major structure.

One of the most important characteristics of a building aside from its natural periods is its damping, or energy absorption value in the nondamaging range of vibration. Figure 10.15 illustrates the relationships between the top story displacements and damping. Test Series A and B give roughly the same results, with damping values for Test B being slightly higher. Test Series C, D, and E results are about equal to each other, but vary in shape from Tests A and B. Damping is affected by partitions, damage, and amplitude of motion. The maximum damping shown here is about 3 percent of critical. In other test series we obtained values as high as 4 and 5 percent. The less damping, the more a building responds to a given ground motion. Damping data are very sparse, and beyond this testing program are essentially nonexistent for repeating vibration at high unit stress levels.

Other field data are being obtained on damage to single story residential-type buildings close to the detonations, and on the relative response of identical buildings on rock and on alluvium. The latter is expected to provide needed information on soil-structure interaction.

In addition, over 25 buildings in communities near the test site and in Las Vegas are being monitored for movement of existing cracks from any and all causes including temperature changes, moisture changes, soil conditions, wind, and ground motion[6].

TYPES OF PREDICTIONS AND TECHNIQUES
Response Spectra

A very useful device in the structural response program is the response spectrum[7]. An idealized single-degree-of-freedom system with an arbitrarily selected damping ratio is subjected mathematically to the entire time-history of recorded ground motion. Usually, the system is assumed to have elastic properties although inelastic properties may also be assumed. As a result of the response computation, the maximum response of the given structure to the given ground motion is obtained. This response may be in units of displacement, velocity, or acceleration, and it is plotted as a point on a diagram against natural period or frequency. By assuming a whole array of such simple vibrating systems having various natural periods, and repeating the computation process for each, other points are obtained and finally a curve is drawn giving the response for a structure of any period. The whole process can be repeated for other assumed damping values and thus spectral response curves are drawn for various damping values. Figure 10.16 indicates such a plot.

It is convenient to plot spectral diagrams on four-way logarithmic paper such as shown in Figure 10.17. Under the assumption of harmonic response motion, any point on such paper gives for the particular period value, the response in terms of relative displacement, pseudo relative velocity, and pseudo absolute acceleration. A great many such spectral curves have been constructed for both natural and man-made ground motion. Preparation of response spectra directly from magnetic tape records of ground motion is accomplished by ERC's analog computer. They also prepare digitized records of ground motion from which we construct response spectra using a digital computer.

The response spectrum is very meaningful in showing how an idealized simple structure would respond to a particular ground motion. The amount of the response, especially in the short and middle period range, is generally much greater than the ground motion because of dynamic amplification and the tuning-in phenomenon previously noted. The amount of the amplification depends upon a great many factors. It may be said that a response spectrum looks at a ground motion through the eyes of a structure.

Time-History Analysis

Procedures are available from the earthquake engineering field for making accurate dynamic analyses of response[8,9,10,11,12]. We have developed modifications of these procedures for use in the more complex structural
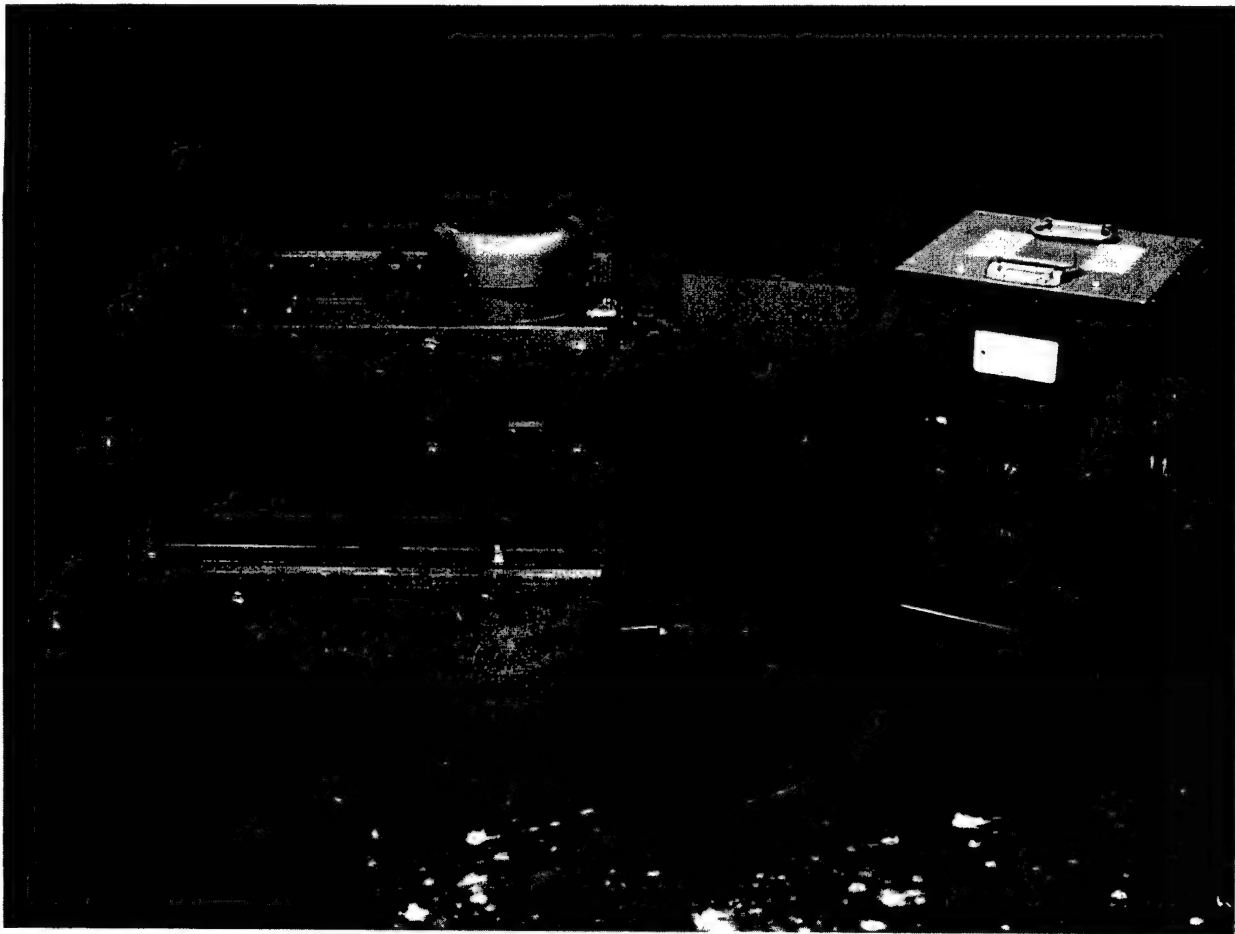
Figure 10.12. Forced-Vibration Generator.

188
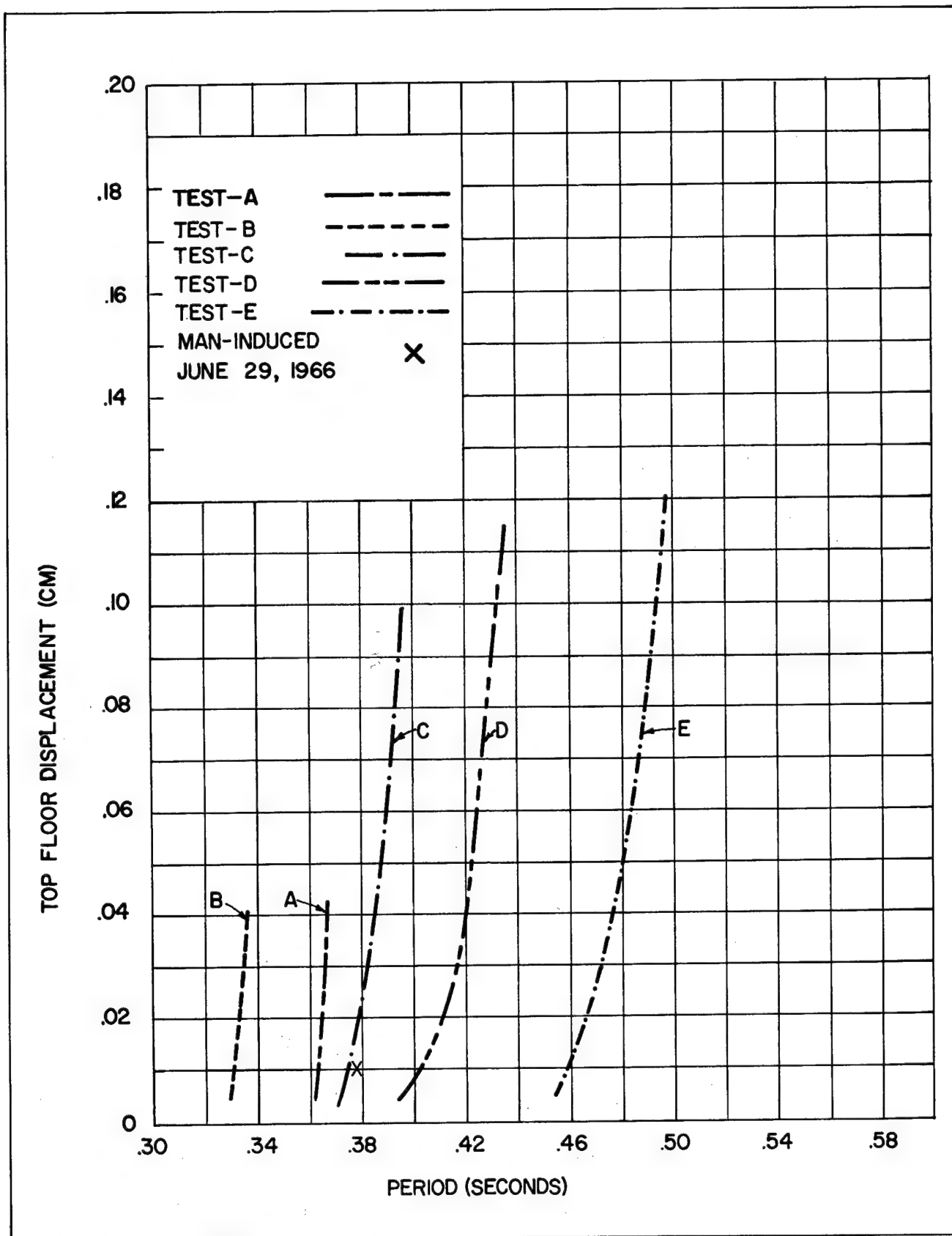
Figure 10.13. Summary of Displacement Versus Period for Test Series A through E. South Structure North to South Direction.
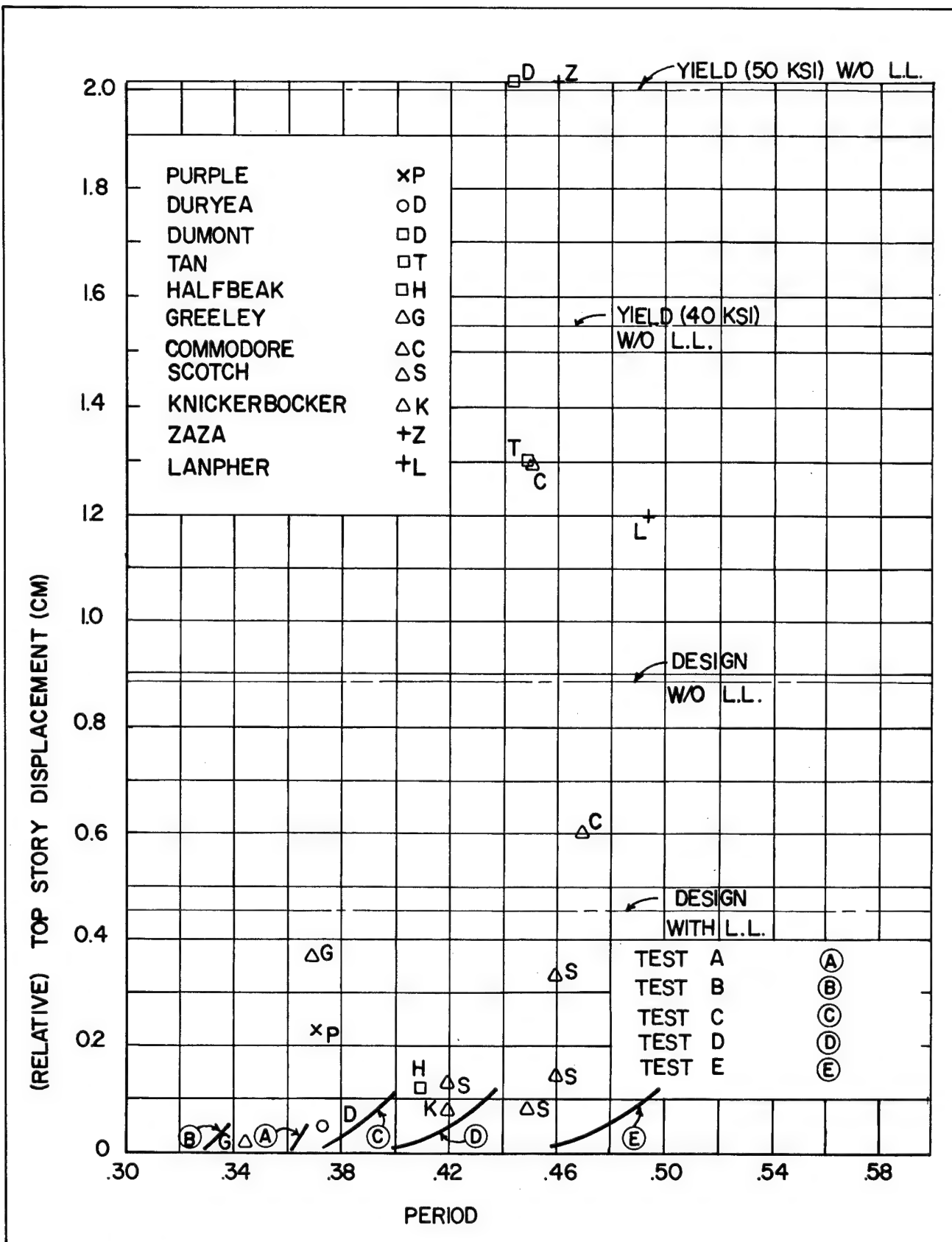
Figure 10.14. Displacement Versus Period from Event Records. South Structure, North to South Direction.
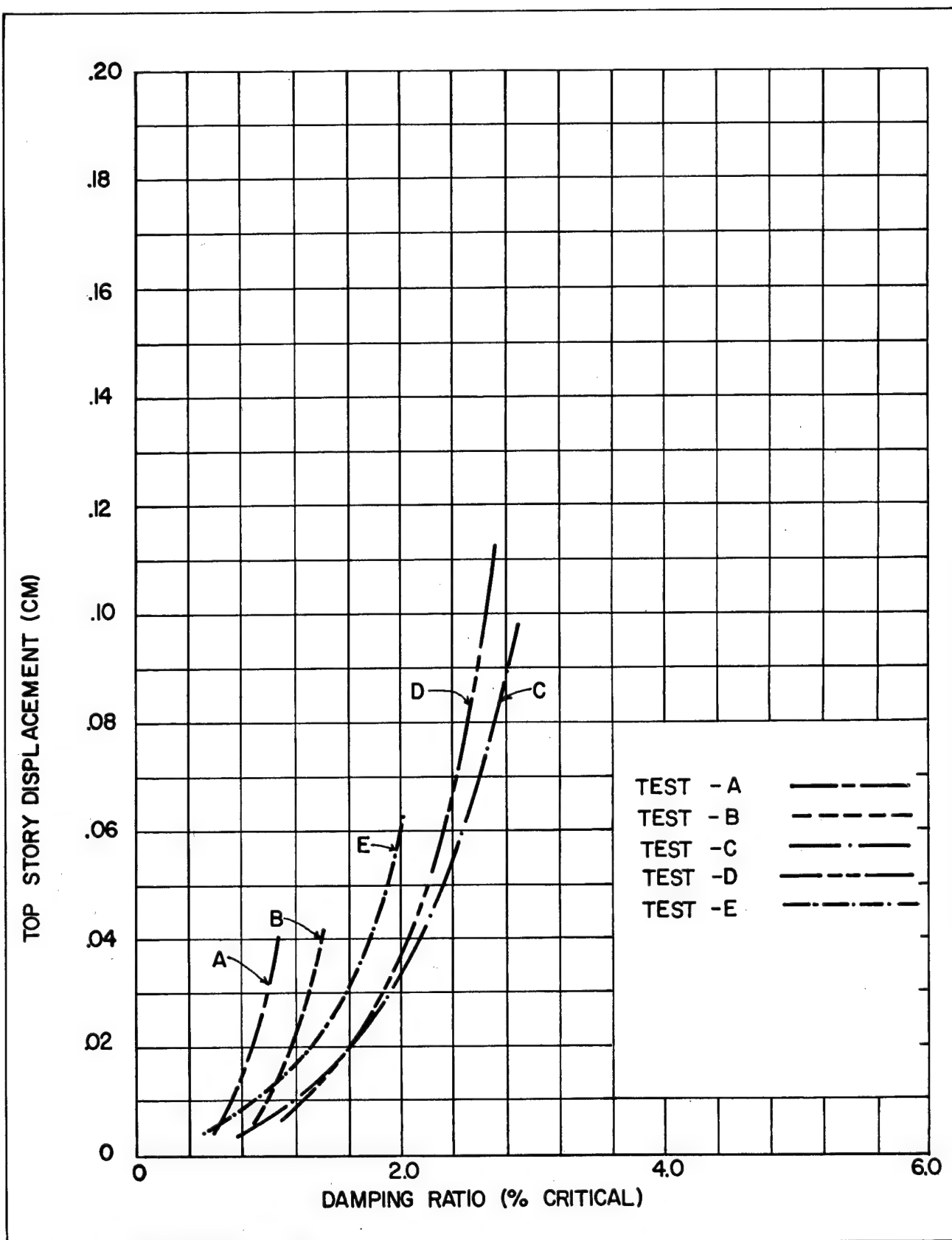
Figure 10.15. Summary of Displacement Versus Damping for Test Series A through E. South Structure, North to South Direction.
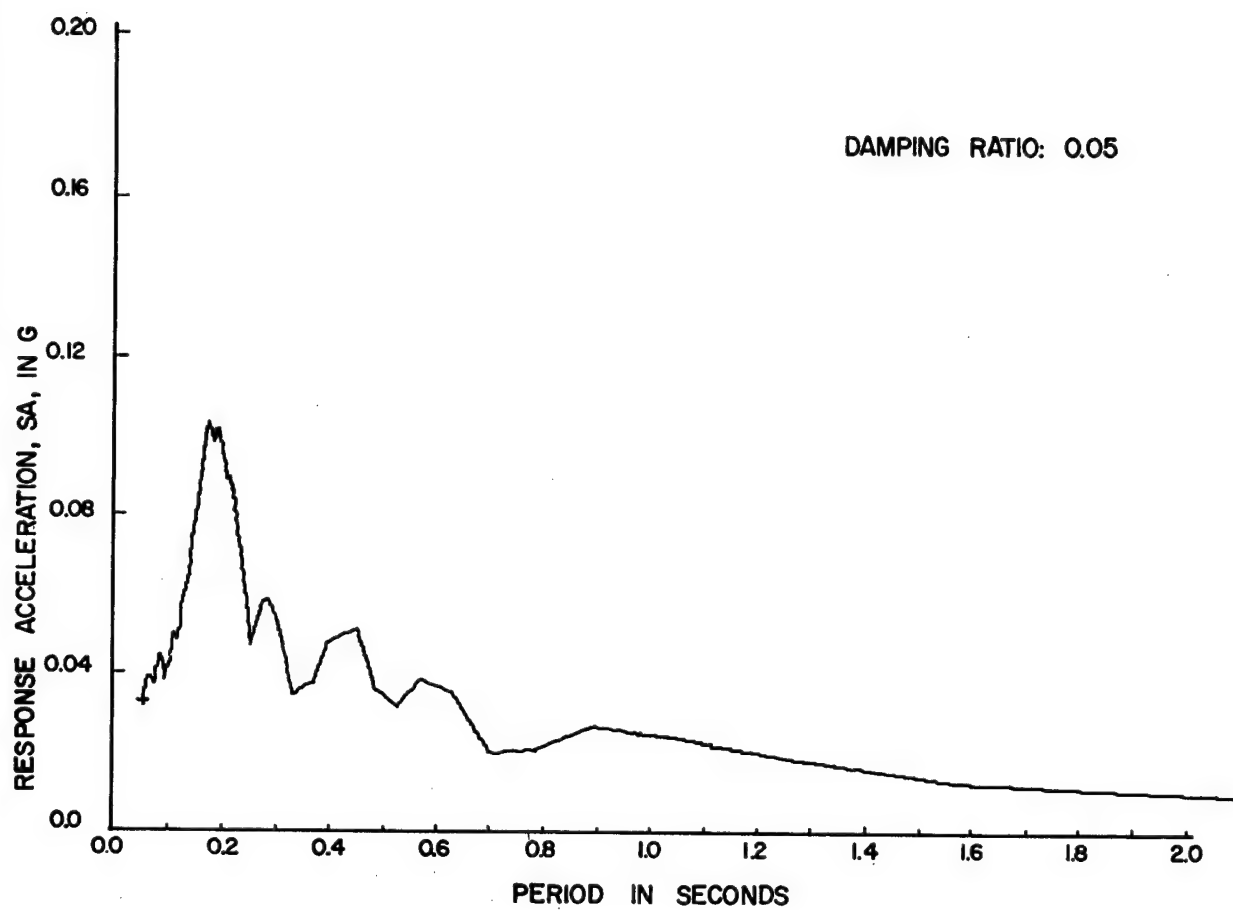
Figure 10.16. Response Acceleration Spectrum for NRDS/ETS 1 — Greeley.
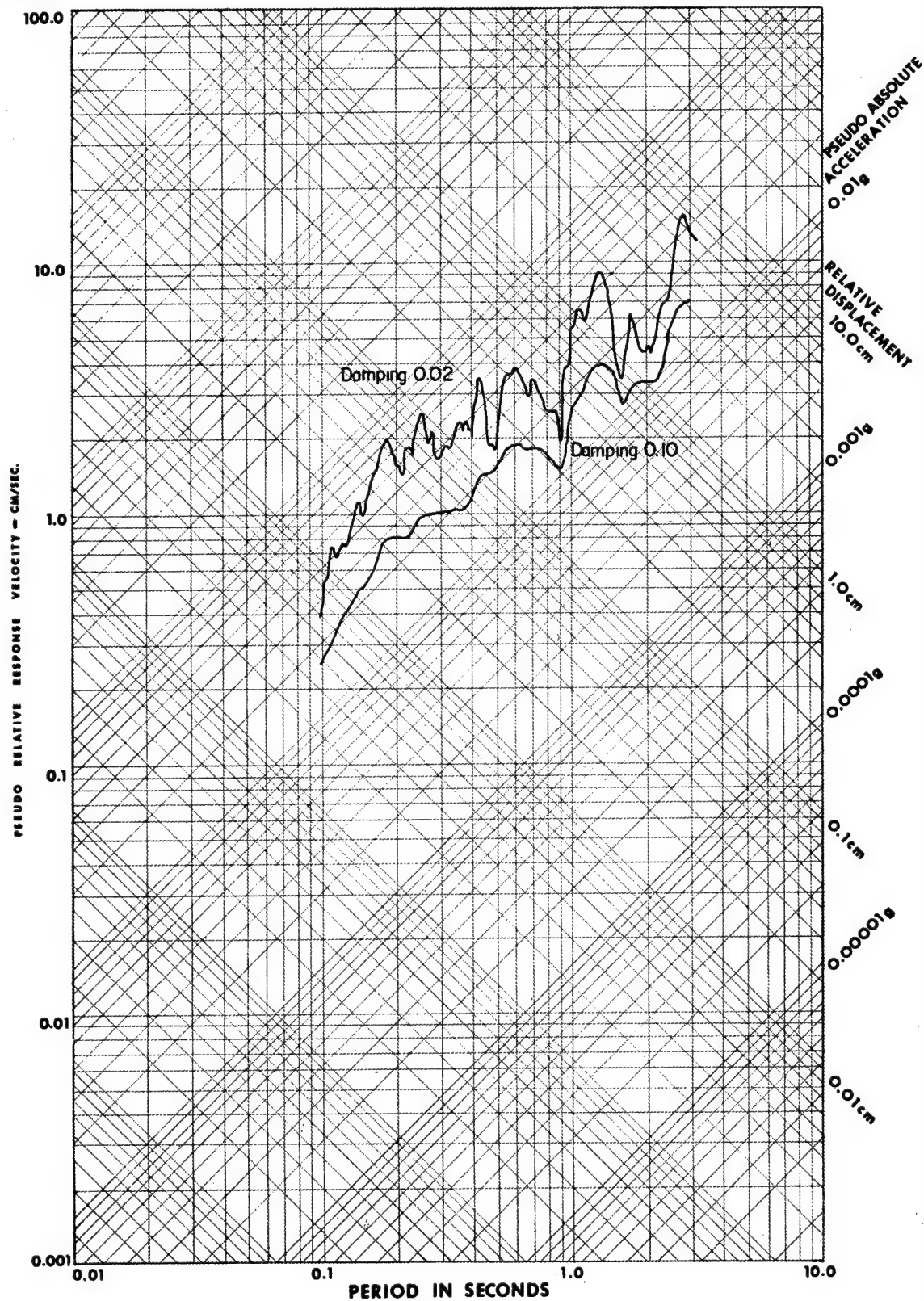
Figure 10.17.   Greeley Response, NRDS/E-MAD.

response problems presented by the AEC's testing programs. As an initial step, a particular building is modeled, very often as a series of lumped masses connected by weightless springs. The masses are computed from the drawings of the buildings and spring characteristics are computed from comprehensive structural analyses of the various members in the structure. Needless to say, this is a massive computation for a large building and is feasible, together with the resulting dynamic analyses, only with the aid of large computers.

From the mass and spring characteristics all of the natural periods of vibration of the structure are computed. This entire system with assigned damping characteristics is subjected to the entire time-history of the recorded ground motion, using either a single horizontal component of motion, or both components simultaneously. The output of the program consists of not only the natural periods of vibration and the mode shapes, but the desired response at any instant of time in terms of acceleration or displacement or of unit stress if required. In addition the computer can be instructed to scan the results for the maximum values and to print these on the output sheets. This is a highly exotic computation and the results are as good as the ability to model the structure. As previously noted, however, much more is to be learned about how best to model real buildings with a complexity of both structural and nonstructural elements and materials. This process cannot be followed for all buildings because of the time required to prepare the data cards for the computation. The procedure is followed mainly for analyses of special buildings such as high-rise structures, and in research operations.

Approximate Methods

Because of the time required to analyze complex buildings by rigorous methods, studies have been made as to the effects of various parameters on building periods, mode shapes, and other characteristics. From this work it has been found that the dynamic characteristics of many buildings can be determined within an acceptable range of error by developed approximate methods. It has also been found that some tall buildings have real characteristics considerably different than has been assumed by their designers and that certain approximate methods of structural design still being used can lead to structures having considerably less capacity for lateral forces than the designers contemplated [15, 18, 19]. These findings may be considered a byproduct of this structural response program. They are quite useful in the program in pinpointing possible trouble spots, in conserving time required for analysis, and in providing

data and methods for further developments in peaceful uses of nuclear energy.

Among other things it has been found that many contemporary tall buildings have been constructed with such thin floor framing as compared to the vertical members, such as columns or wall elements, that the buildings respond more as vertical cantilevers [18] than as conventional rigid frames. This type of response leads to different ratios of natural periods, different mode shapes, and different stress patterns than the more traditional buildings of other decades.

Figure 10.18 illustrates for a series of hypothetical 16-story frames how the moment varies with the height of the building for different ρ-factors which are defined as the ratios of the horizontal framing stiffness to the vertical framing stiffness [14,15]. We have thus brought to light a situation not previously recognized that contemporary buildings may have much different properties — both structural and dynamic — than the traditional type buildings which have been subjected to earthquake experience and have, implicitly at least, been a factor in determining building code requirements for earthquake resistance.

RESPONSE IMPLICATIONS

Figure 10.19 indicates the force-deformation characteristics of several hypothetical structures. The deformation of a structure under the force is linear as shown until the yield point is reached. In the range between the zero load and the yield point there would be no damage and the structure would be expected to return to its original equilibrium position when the load is released. The strength of a structure is indicated by the load required to reach yield point. The stiffness of the structure is represented by the slope of the line up to the yield point. A stiff structure has much less deformation than a flexible structure under the same loading. Although it is possible to calculate the yield point value of a structure, a great many buildings have redundant elements of a nonstructural nature such as partitions, filler walls, etc., that greatly complicate the situation and often make the determination of the effective yield point very difficult. We are conducting tests in our dynamics laboratory for the purpose of obtaining more reliable information on how nonstructural elements contribute to stiffness and strength and at what level they are apt to be damaged.

Another parameter about which there is much more to be learned, and one that becomes vitally important if and when the yield point should be reached, is the response behavior at deformations exceeding the yield point deformation. If the material is brittle such as glass,

194
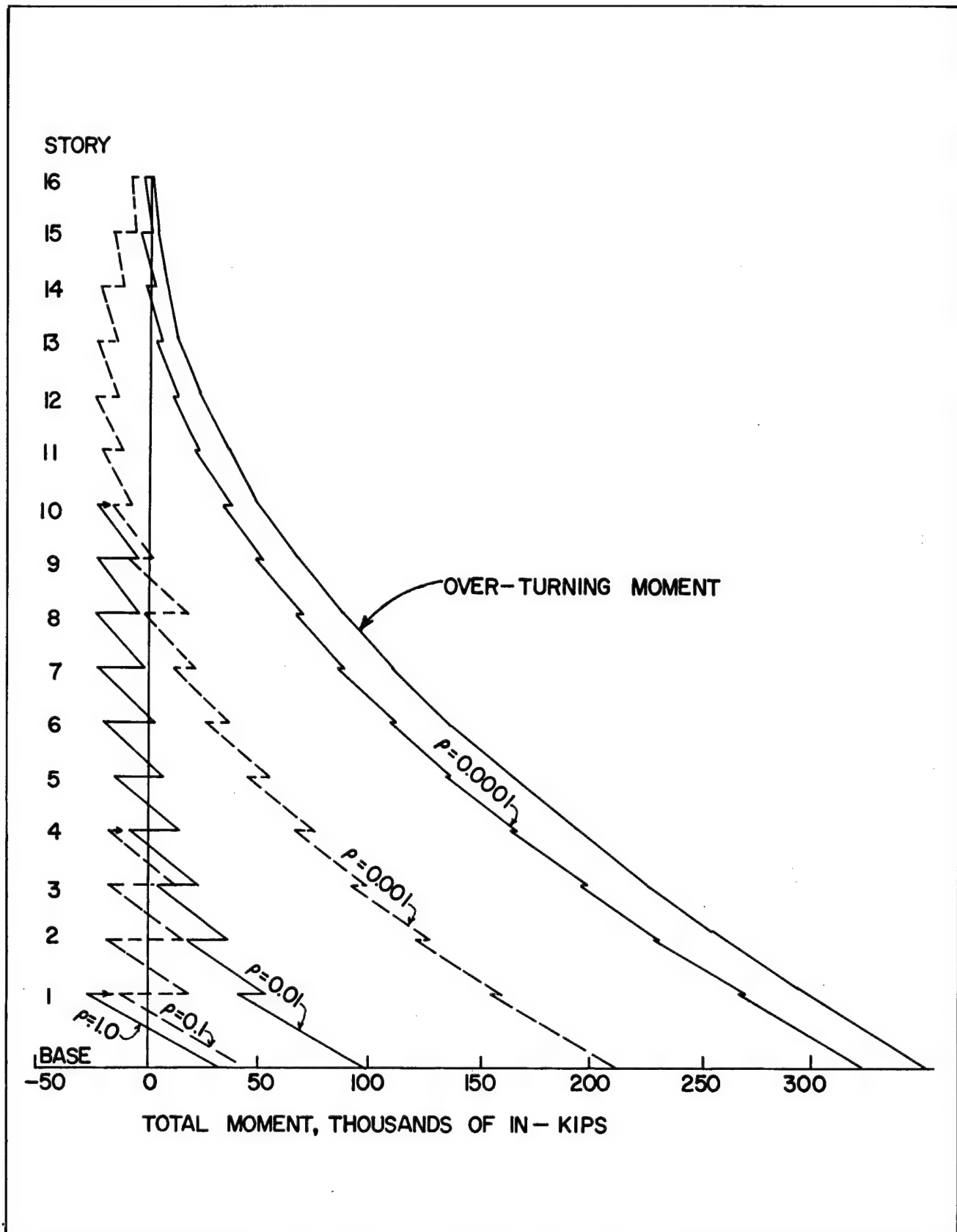
Figure 10.18. Total Moment Per Story, 16-story Frame.

195

(a) Non-linear, softening

(b) Elasto-plastic

(c) Bilinear, softening

(d) "Plateau" resistance
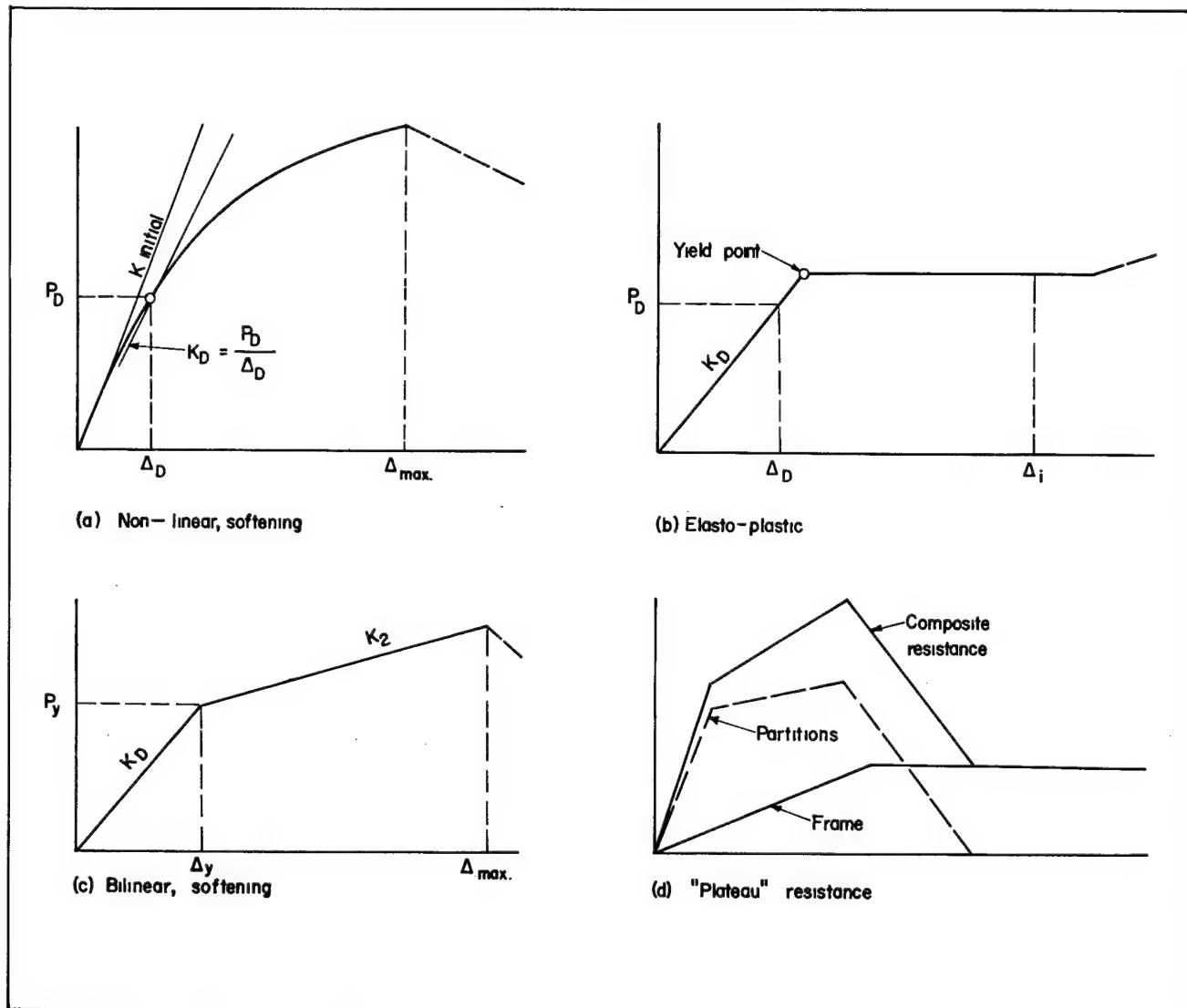
Figure 10.19.   Common Types of Inelasticity.

196

it will simply break at the yield point. However, if the material or the material combinations are ductile, there will be a yielding without actual failure beyond the yield point, at least until the ultimate capacity of the element is reached. Figure 10.20 shows two idealized structural elements. On the left side of the figure there is a ductile framework and its force-deformation characteristics are shown in Diagram (a) below the figure. Diagram (b) on the right side indicates a much stiffer and more brittle element. In this case, the ultimate value is reached at a deformation only slightly beyond that of the yield point. The work capacity of these two systems, that is the ability to mobilize resistance to the energy demands, is a function of the area of these force-deformation curves. Thus the ductile system shown has much greater capacity to resist complete failure than the more brittle element. The ductile system would show some permanent deformation after being loaded beyond its yield point but it would be in much less danger of collapse than the more brittle element, assuming of course that the two systems had essentially equal ultimate force capacities.

Most structural response computations are done under the assumption that the structure will remain elastic, that is its stress levels will not exceed the yield point. It is quite possible, however, to compute the response of inelastic systems or systems that are elastic until certain levels of stress are reached after which the response is inelastic. Figure 10.21 shows the computed response of two idealized systems subjected to the record ground motion of the 1940 El Centro, California, earthquake[16]. The upper part of the diagram shows the deflection in inches of a single-degree-of-freedom system that has enough strength not to have its yield point exceeded under this particular earthquake. It is noted that the maximum deformation from the equilibrium position is about 3 inches. The lower diagram is for a system of the same natural period and damping value that has less strength in the elastic range. There are five excursions into the plastic range occurring between 2 and 5 seconds after the start of the ground motion, and about 12 seconds after the start of the motion. In this case, the total deformation is still about 3 inches although a significant portion of this is in the inelastic range. Since, in this case, there were two inelastic excursions to one side of the equilibruim position and a total of three to the other side, and since these excursions were about equal, the structure has the residual deformation at the end of the motion, as shown. There is about 1 inch of permanent displacement or stretch. Putting this another way, the structure would be 1 inch out-of-plumb after the earthquake. There would thus be damage but not collapse.

Threshold Ladder

It is important to realize, whether dealing with man-made or natural earthquakes, that there are various thresholds and also that these thresholds measured in any convenient units such as acceleration, velocity, or displacement, are generally very widely separated. Another important point is that they vary considerably from place to place, or from person to person, or from building to building, as applicable.

Figure 10.22 is a schematic diagram of a threshold ladder. The lower rung indicates a level of motion which would be measurable by sensitive instruments. The second rung of the ladder indicates a level of motion that would just be perceptible to human beings. Well above that level is a point at which initial damage would occur to buildings in poor condition. It should be clarified that there is no vertical scale in this figure. If one were attempted, it would probably be of a logarithmic nature since the motion levels for these various ladder rungs are increasing exponentially. Above the point of initial damage there is a point where damage would begin occurring to buildings in good condition. Well above that level is a motion intensity at which there would be major damage, and to complete the scale, the top rung shows the point of collapse.

There is a very large range from the point at which people feel motion in buildings to the point at which damage would begin and there is even a greater range to the point at which damage would be substantial. In view of the fact, as previously noted, that buildings vary over a considerable range even though they may look alike, it is obvious that these ladder rungs should not be considered as fine lines but as very broad bands representing the variation of resistance levels for structures and the variation of human perception of motion.

The preceding discussion has attempted to present an overall view of the structural response problem associated with the AEC's testing program, and the procedures being followed and research being conducted to improve our solution to these problems. The second portion of the presentation will present in more detail and in more depth the complex nature of the problem and the matching complexities of the analyses and prediction procedures.

197
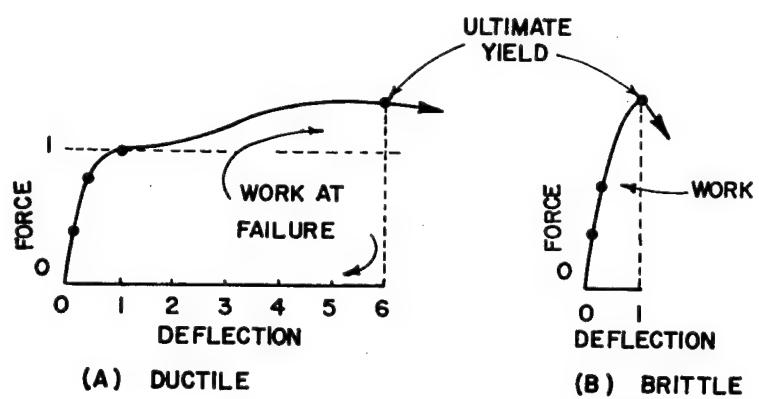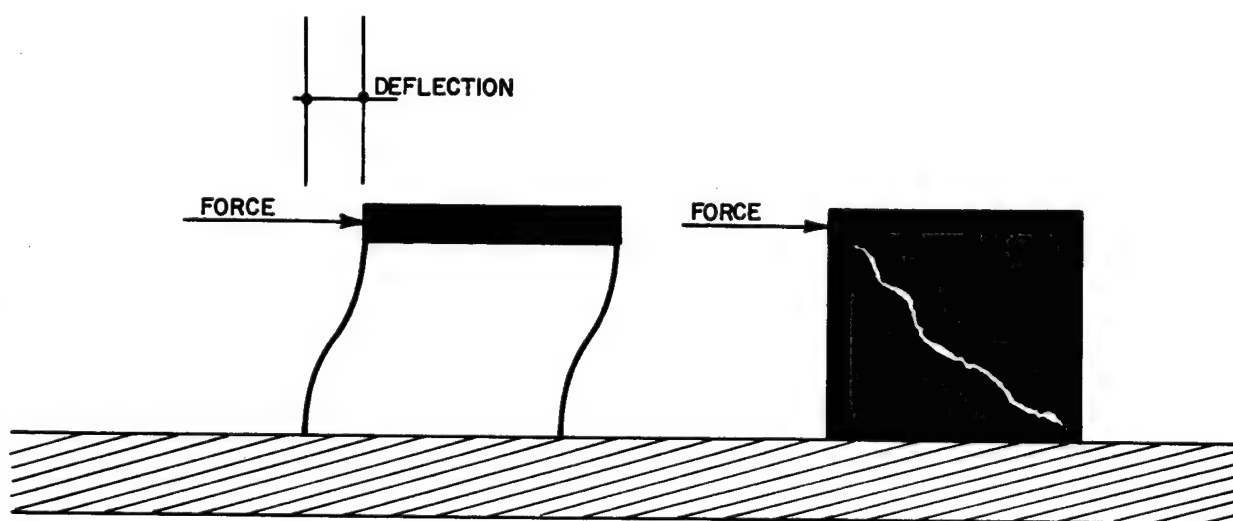
Figure 10.20. Building Material Characteristics.

198
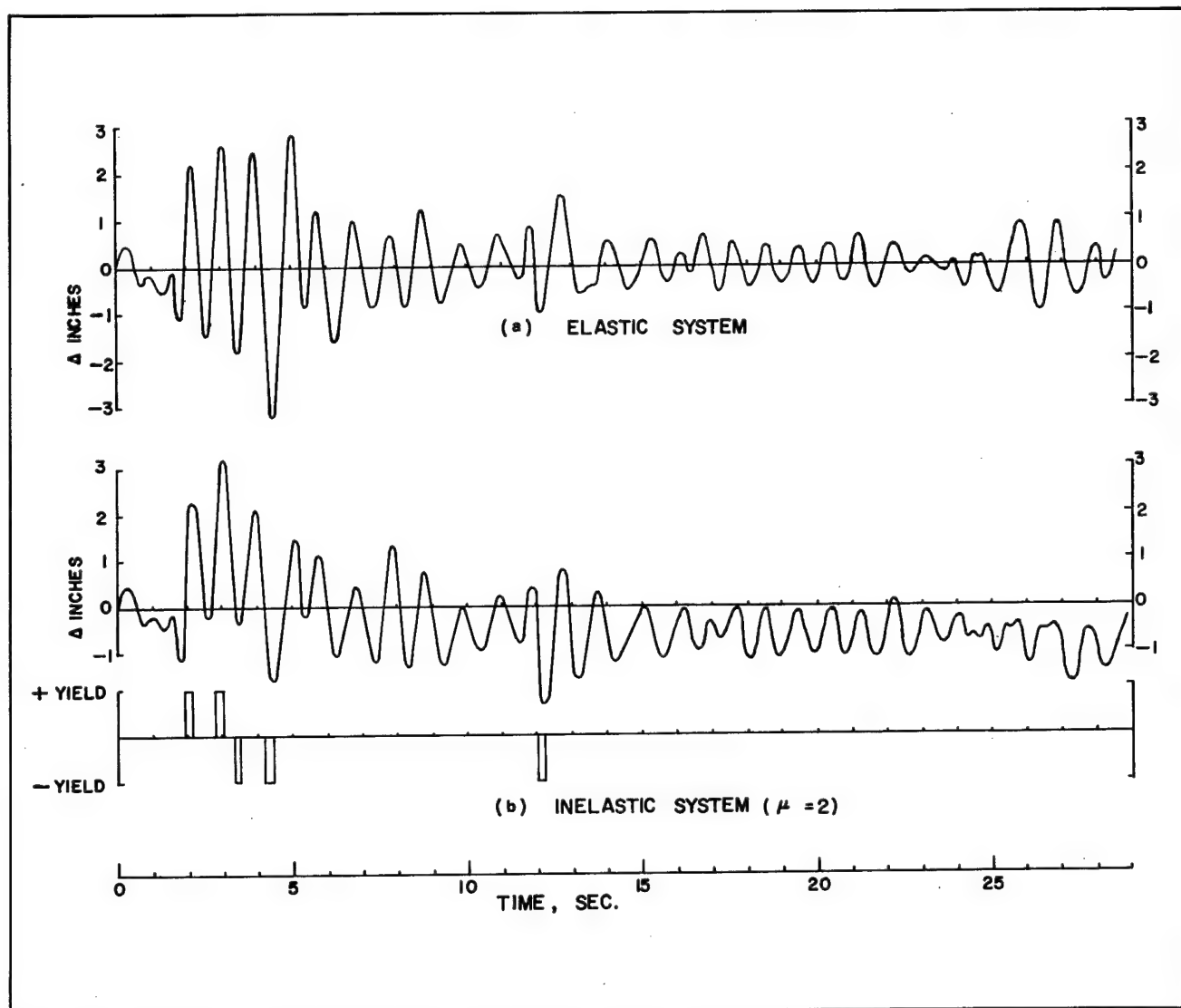
Figure 10.21. Deformation of Idealized Structure Under Ground Motion of 1940 Earthquake at El Centro, California; North to South Component.

COLLAPSE

MAJOR DAMAGE

INITIAL DAMAGE TO GOOD BUILDINGS

INITIAL DAMAGE TO BUILDINGS IN POOR
CONDITION

HUMAN PERCEPTION OF MOTION

INSTRUMENTAL RECORDING

No Scale

Figure 10.22. Threshold Ladder.

Part B — Technical Operations and Typical Data

INTRODUCTION

Structural response investigations have combined development of necessary theoretical techniques with concurrent participation in underground nuclear event operations. This event participation normally includes: (1) estimation of predicted ground motion effects on structures, (2) recommendations for control measures to prevent or minimize hazard to persons and damage to structures, (3) monitoring of selected buildings to observe effects of natural forces and event ground motion, and (4) analysis of motion records. Valuable data for further improvement of theoretical techniques are acquired from this participation as well as from analytical and laboratory studies, field test programs on test structures and other buildings, and earthquake damage investigations.

This second part of the presentation will cover some of these operations, especially the more technical phases, and present some of the results.

EARTHQUAKE HISTORY AND BUILDINGS

There are similarities and also differences between natural earthquakes and man-made ground motion. The similarities provide certain useful data to this structural response program, and full advantage is taken of this fact—not only with current earthquakes, but with available data from earthquakes of the past. The differences must also be kept in mind to avoid faulty conclusions.

In spite of any reports to the contrary it is still not possible to predict the specific time, place, or magnitude of a natural earthquake. This may not be possible for a long time, and even if it becomes possible, there would be no chance to save existing weak structures. Peak parameters of ground motion from underground nuclear explosions on the other hand, can be predicted quite accurately.

It is known where earthquakes have occurred in the past in man's short recorded history and also in recent times. Geology tells us much more about the great earthquakes that must have occurred in geologic times. Although California and Japan get the credit for most earthquake activity, these areas by no means have a monopoly. The most active areas are the entire rim of the Pacific Ocean (extending as far inland as Nevada) and a broad band through the Mediterranean Sea, across Asia Minor and India to the Pacific Ocean. But many earthquakes occur elsewhere. For example, in the winter of 1811-1812,

Missouri had three of the largest earthquakes ever experienced in North America.

Figure 10.23 is a map of the United States with the dots representing earthquake epicenters. The size of the dots represents the magnitude of the earthquakes. The numbered zones are arbitrary divisions of seismic risks[17]. These are in need of revision, especially to take into account the fact that modern tall buildings respond to very distant earthquakes.

Figure 10.24 illustrates some important earthquake terms. The earthquake energy is related to magnitude (M), whereas the local effect on structures is indicated by intensity scales such as the Modified Mercalli scale (MM).

Table I shows some recent and other earthquakes of interest. The list is by no means complete or up to date. It is to be noted that death and damage have little relationship to magnitude alone. The natural earthquake risk varies from place to place, but it is a fact — it exists. The only way to avoid costly or dangerous damage is to create buildings that have real earthquake resistance. This is not always done even in this technical society. It is our opinion that a repetition of the 1952 Kern County earthquake — which happened when Las Vegas had no high-rise buildings — would cause damage in Las Vegas today. Taking this thought a step further, there should be much more concern in modern cities about natural earthquakes than from the man-made explosions which are predictable in time, place and size, and are under the careful control of many knowledgeable persons and agencies.

In our opinion, the man-made energy releases may be useful and desirable if they make the public earthquake conscious so as to build better buildings for resistance to natural earthquakes.

Earthquake Provisions in Building Codes

The purpose of earthquake provisions in building codes is to provide sufficient resistance to ground motion to avoid collapse of buildings and other structures and hopefully to avoid damage of such degree as to cause loss of life. These provisions are by no means sufficient to prevent all damage in buildings subjected to very severe ground motion. In general, the building code provisions have been developed from consideration of previous earthquake damage and new findings from research in the earthquake problem. Although these seismic provisions provide for much better buildings than if there were no such provisions, they are admittedly far from
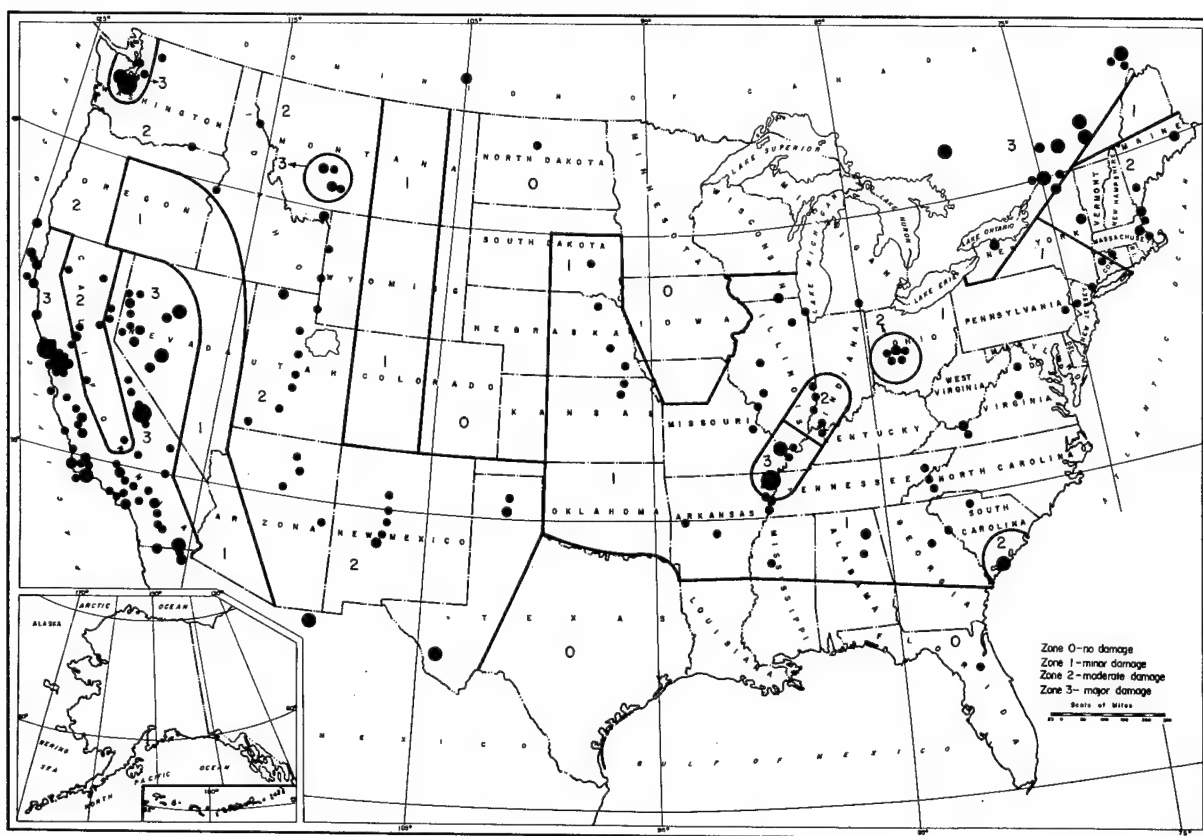
Figure 10.23. Map of United States Showing Epicenters and Zones of Approximately Equal Seimic Probability.

202
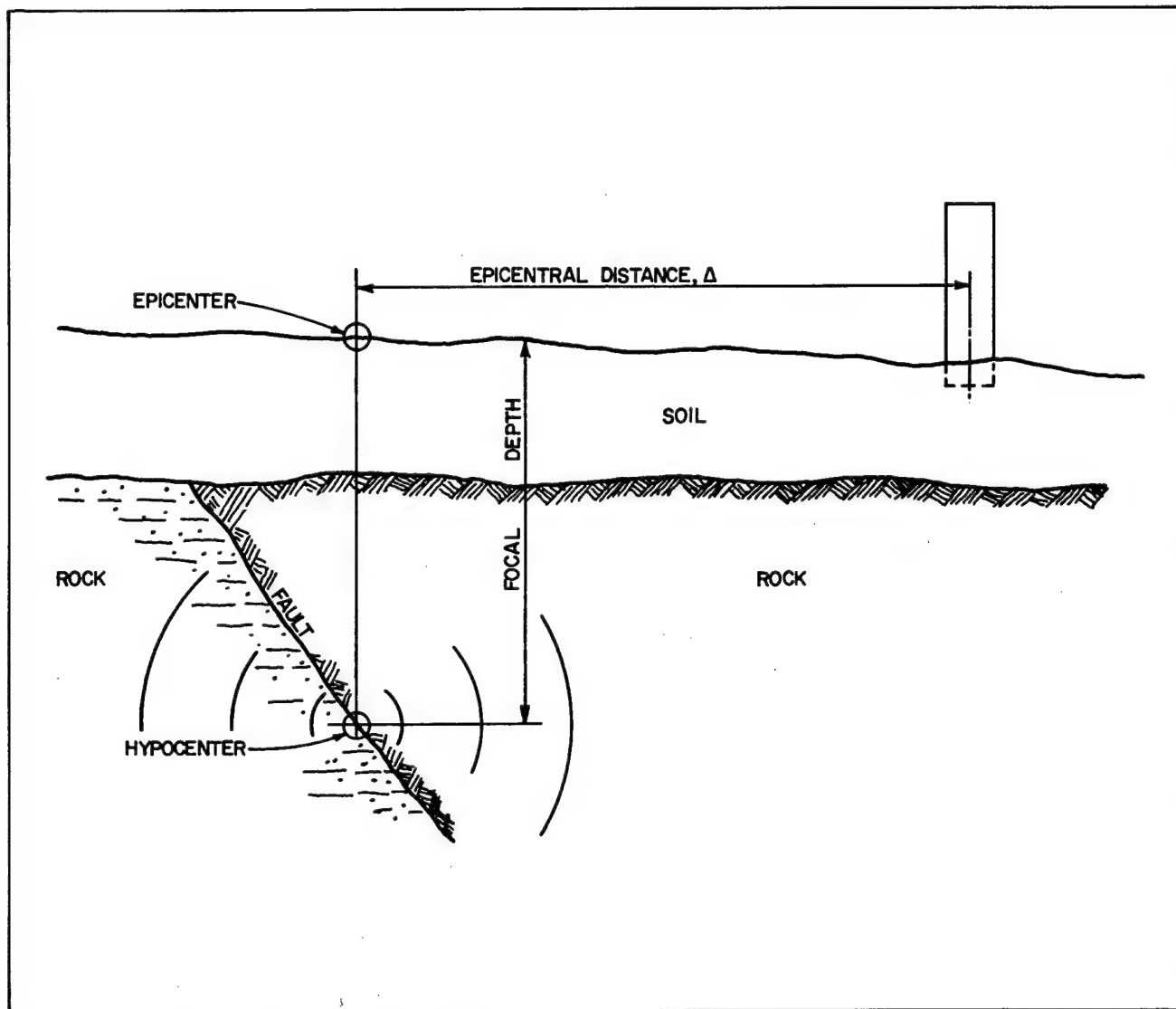
Figure 10.24. Definition of Earthquake Terms.

203

TABLE I SOME RECENT AND OTHER EARTHQUAKES OF INTEREST

DATE	PLACE	*M	EPICENTRAL DISTANCE TO MAIN CITY, MILES	DEPTH, MILES	ESTIMATED DEATHS	ESTIMATED PROPERTY DAMAGE $ x 10^6	HOUSES DESTROYED
1967	Colombia	6.75	185	**	98	18	**
1965	Seattle	5.75	13	35	6	0.8	**
1964	Niigata, Japan	7.5	25	24	25	800	1,000
1964	Alaska	8.4	75	12	125	311	**
1964	Skopje, Yugoslavia	5.4	9	8	1,000	**	37%
1962	Iran	7.5	**	12	12,000	**	21,300
1960	Agadir, Morocco	5.7	5	1-2	12,000	**	100% at Kasbah
1960	Chile	8.4	80-110	**	1,000	600	45,000
1957	Mexico City	7.5	220	**	125	150	Few
1957	San Francisco	5.3	10	7	0	1	0
1952	Kern County, California	7.7	27	15	15	50	**
1949	Seattle	7.1	38	45	8	40	**
1940	El Centro, California	7.1	20	15	9	6	**
1933	Long Beach	6.3	10	5-6	120	60	**
1925	Santa Barbara, California	6.3	10	**	Few	6	**
1923	Japan	8.3	60	**	>100,000	Vast	600,000
1920	Konsu, China	**	**	**	180,000	**	**
1906	San Francisco	8.3	30	**	700	800	Many
1755	Lisbon, Portugal	8.6	60	**	60,000	**	**
1737	Calcutta, India	**	**	**	300,000	**	**
1556	Shensi, China	**	**	**	830,000	**	**

*M = Magnitude
** = No data

perfect. They often contain compromise measures due to divergent views about matters which are not fully crystallized, and they usually lag a great many years behind new findings and developments. There is thus a situation where — even with modern codes — many of the structures that are still in use cannot really be considered as good earthquake risks.

In spite of these reservations about the building codes, it is strongly recommended that the most up-to-date code and the most applicable seismic zone be adopted and enforced in all cities and counties subject to earthquake motion. As previously noted and as shown on the map of earthquake zones[17], high-rise buildings should be recognized as responding to motion from distant sources. For this reason, and in view of the proximity of possible California earthquakes (not to mention Nevada earthquakes), it is believed that Zone 1 for the high-rise buildings in Las Vegas provides inadequate earthquake protection.

In considering possible damage from a large nuclear event in central Nevada, we are faced with the anomalous situation that Las Vegas buildings are designed for Zone 1, Salt Lake City buildings for Zone 2, and Reno buildings for Zone 3. The earthquake lateral force requirements for these zones are respectively in the ratios of 1, 2, and 4. This difference is not always as severe as it may seem, however, because the wind force may govern the design over low earthquake provisions, at least in one direction of the building.

Natural Causes of Damage

Materials used in building construction are subject to deterioration and damage from a variety of causes — both natural and man-induced. Wood, metal, masonry, and other construction materials are all affected to some extent by changes in moisture, temperature extremes, sun, and wind. Further, all materials can have defects unnoticed at use. Also they usually are used in various combinations — often without adequate consideration of the need for stress-relieving joints. The manner in which the materials are combined, the construction workmanship, and adjustment and settlement of the foundations after completion of construction all contribute to the nature and degree of deterioration or damage.

Deterioration is manifested, among other ways, in cracking. Cracks generally occur at locations of stress concentration; e.g., at the corners of doors and windows, at intersections of wall panels, or at other structure discontinuities. These areas are also the most likely locations of new or aggravated cracks that often result from dynamic loading of the structure by wind, earthquake, traffic, or ground motion from underground nuclear explosions.

Our study of cracks in structure elements is concerned principally with the effects of continuous temperature cycling, temperature differentials, and variations in wind, sun, and ground motion. Of these factors, ground motion and wind tend to subject the structure to abrupt motions; i.e., the building structure responds in a very short period of time. On the other hand, the structure and its elements are continuously moving as a result of changes in temperature and humidity, and of other forces such as those from differential settlement. The expansion or shrinkage due to temperature and humidity changes takes place over a much longer period of time than do the effects from wind or ground motion; e.g., diurnal or seasonal, rather than within seconds. The building structure and its materials are therefore better able to adjust to the effects of temperature and humidity than to ground motion and wind. Laboratory and field observations reveal that existing cracks in a structure are the first areas to be acted upon by ground motion and natural stimuli. The above reasoning summarizes the basis for our study of building element cracks.

STRUCTURAL DYNAMIC THEORY AND MODELS

Lumped Mass Models of Structures

One of the most popular methods of modeling a symmetric multi-story building is to develop a mass and a stiffness for each story and then to simply put these together to create a multi-mass system of n masses. The computation of the story weight (which is then divided by g to get mass) is not difficult. The stiffness determination may be straightforward, or extremely complicated depending upon the characteristics of the building, the accuracy desired, and the methods available. Rarely can a story stiffness properly be obtained as an independent unit. Some new concepts and data have been developed in the structural response program which have not only provided faster methods but have also revealed important new data on the characteristics of many contemporary high-rise buildings. First let us consider the idealized lumped mass model.

By Newton's second law and the balance of forces of the system vibrating freely without external force,

$$\left[M_{jk} \right] \{ \ddot{D}_k \} + [C_{jk}] \{ \dot{D}_k \} + [S_{jk}] \{ D_k \} = \{ 0 \} \qquad (1)$$

in which D = the displacement parallel to the x-axis; M = the story mass; S_{jk} = the stiffness-influence coefficient defined as the external force on the jth mass when the kth mass has a unit displacement and all other masses have zero displacement; j and k are subscripts referring to the story or lumped mass; and C = the damping coefficient defined as the force on the jth mass exerted by the damping dashpots when the kth mass has a unit velocity and all other masses have zero velocity.

It can be shown that in a principal mode of vibration, i, for the case where there is no damping (damping has a negligible effect on period for the damping values typical of buildings in the elastic range),

$$([S_{jk}] - p_i^2 [M_{jk}]) \{ D_{M_k} \}_i = 0 \qquad (2)$$

and, for nonzero displacements, from Cramer's rule,,

$$| [S_{jk}] - p_i^2 [M_{jk}] | = \{ 0 \} \qquad (3)$$

in which p_i = the natural angular frequency of the ith mode in radians per second; p_i^2 = the eigenvalue of the ith mode; and D_M = the modal displacement or mode shape displacement. Another form of equation (3) is

205

$$\begin{vmatrix} (S_{11} - p_i^2 M_i) & S_{13} & --- & S_{1n} \\ S_{21} & (S_{22} - p_i^2 M_2) & S_{23} & --- & S_{2n} \\ S_{31} & S_{32} & (S_{33} - p_i^2 M_3) & --- & S_{3n} \\ \hline S_{n1} & S_{n2} & S_{n3} & --- & (S_{nn} - p_i^2 M_n) \end{vmatrix} = 0 \quad (4)$$

The expansion of the determinant in equation (4) to obtain a polynomial in powers of the eigenvalues p_i^2, and the solution of the polynomial can be obtained directly or by iteration. The mode shapes $(D_M)_i$ can be found for each p_i^2 value by using equation (2). The natural period of vibration, T_1, in seconds is simply,

$$T_i = \frac{2\pi}{p_i} \quad (5)$$

The stiffness matrix and the damping coefficient matrix for a close-coupled or rigid-floor shear system, is tridiagonal and symmetrical, and there are relationships between the elements as may be seen in Figure 10.25. Thus, the stiffness matrix may be written directly from known story stiffnesses. This system is by far the simplest with which to work since there are only as many unknowns as there are stories. On the other hand, a far-coupled system, or one that includes joint rotation has a full matrix as shown in Figure 10.26. In this case there are $(n^2 + n)/2$ different elements, or unknowns, in which n is the number of stories. The far-coupled matrix is full, and thus general for various types of structural systems.

Characteristics of Multistory Buildings

In a special study employing many hypothetical and real buildings, the effects of story shear distortion, joint rotation, column axial deformations, and soil deformation under the foundations were considered in detail[18,19]. An index ρ was established as a measure of the relative stiffness of a building's floor framing and its vertical (column and wall) members.

$$\rho = \frac{\displaystyle\sum_{1}^{all} \frac{I_G}{L_G}}{\displaystyle\sum_{1}^{all} \frac{I_C}{L_C}} \quad (6)$$

wherein

I_G = the effective moment of inertia of a girder and its connected floor system, and I_C = the effective moment of inertia of a column together with any connected materials. Assume that the girder and the column are connected so as to retain the right angle between them under the imposed loading and that the values at the midheight

story are typical for the building. L_G and L_C refer to the length of the girder and column, respectively. Figure 10.27 shows the index ρ plotted against the ratio of the fundamental period with shear and joint rotation to the period with only shear distortion. The great effect of low ρ-values is obvious. Many contemporary buildings have such low values, although this has often been ignored. Figure 10.28 shows the average results for the first three modes.

Figure 10.29 is a similar plot but with an index Ω'(representing the column axial effect), plotted against the ratio of the period for mode i with shear, joint rotation, and column axial freedom to the period where only shear and joint rotation are considered. This effect, until recently, has been ignored in the technical literature.

$$\Omega' = \frac{(\overline{H})^3}{(E_r) \left(\displaystyle\sum_{k=1}^{all} A_k d_k^2 \right)^{1/3}} \quad (7)$$

in which Ω' is in units of feet $^{5/3}$; $\overline{H}$ = the height of the building from the base to the roof line, in feet; A_k = the gross area of a continuous vertical element or member k (such as columns, piers, pilasters, and walls) at the story closest to the midheight of the building, in square feet (if columns change at the midheight story, the average values of A from the adjacent stories are used); d_k = the normal distance in the direction of motion from the center of member k to the centerline of the floor plan, in feet; E_r = ratio of the modulus of elasticity divided by 30,000 kips per sq. in., dimensionless. (Example: If material is concrete with E_c = 3,000 kips per sq. in., E_r = 3,000/30,000 = 0.1.) The value of Ω' is to be calculated for only one story, that closest to the midheight of the building, as for the joint rotation index, ρ.

With the information shown in Figures 10.28 and 10.29 it is possible to compute a building period as though the building were a rigid-floor shear system as in Figure 10.25 – and this is a time saving procedure – and then to apply correction factors to obtain realistic approximations of the time periods with joint rotation and axial column deformation. The information is also valuable in determining what unit stresses occur from various response deformations.

Cantilever-Type Buildings

It has been found that many contemporary buildings are constructed with such long spans and/or shallow floor systems as to have very low ρ-value. We have found

$$[S] = \begin{bmatrix} S_1+S_2 & -S_2 & 0 & 0 \\ -S_2 & S_2+S_3 & -S_3 & 0 \\ 0 & -S_3 & S_3+S_4 & -S_4 \\ 0 & 0 & -S_4 & S_4 \end{bmatrix}$$

$$[C] = \begin{bmatrix} C_1+C_2 & -C_2 & 0 & 0 \\ -C_2 & C_2+C_3 & -C_3 & 0 \\ 0 & -C_3 & C_3+C_4 & -C_4 \\ 0 & 0 & -C_4 & C_4 \end{bmatrix}$$
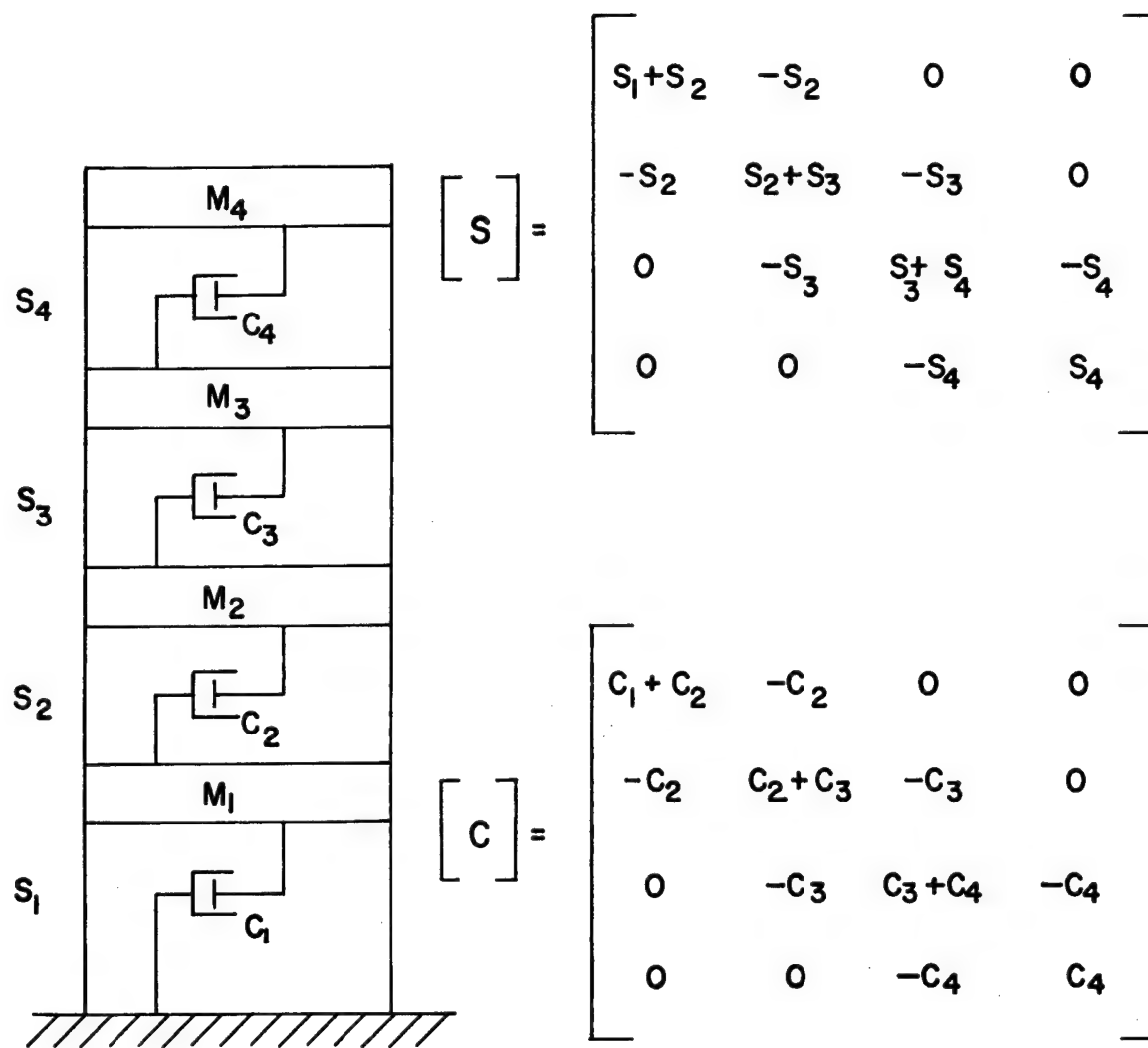
NOTE: S_j REFERS TO THE COMBINED STIFFNESS OF ALL VERTICAL ELEMENTS AT STORY j.

Figure 10.25. A Close Coupled Shear System.

207

$$
[S] = \begin{bmatrix} S_{11} & S_{12} & S_{13} & S_{14} \\ S_{12} & S_{22} & S_{23} & S_{24} \\ S_{13} & S_{23} & S_{33} & S_{34} \\ S_{14} & S_{24} & S_{34} & S_{44} \end{bmatrix}
$$

ELEVATION

MECHANICAL ANALOGY
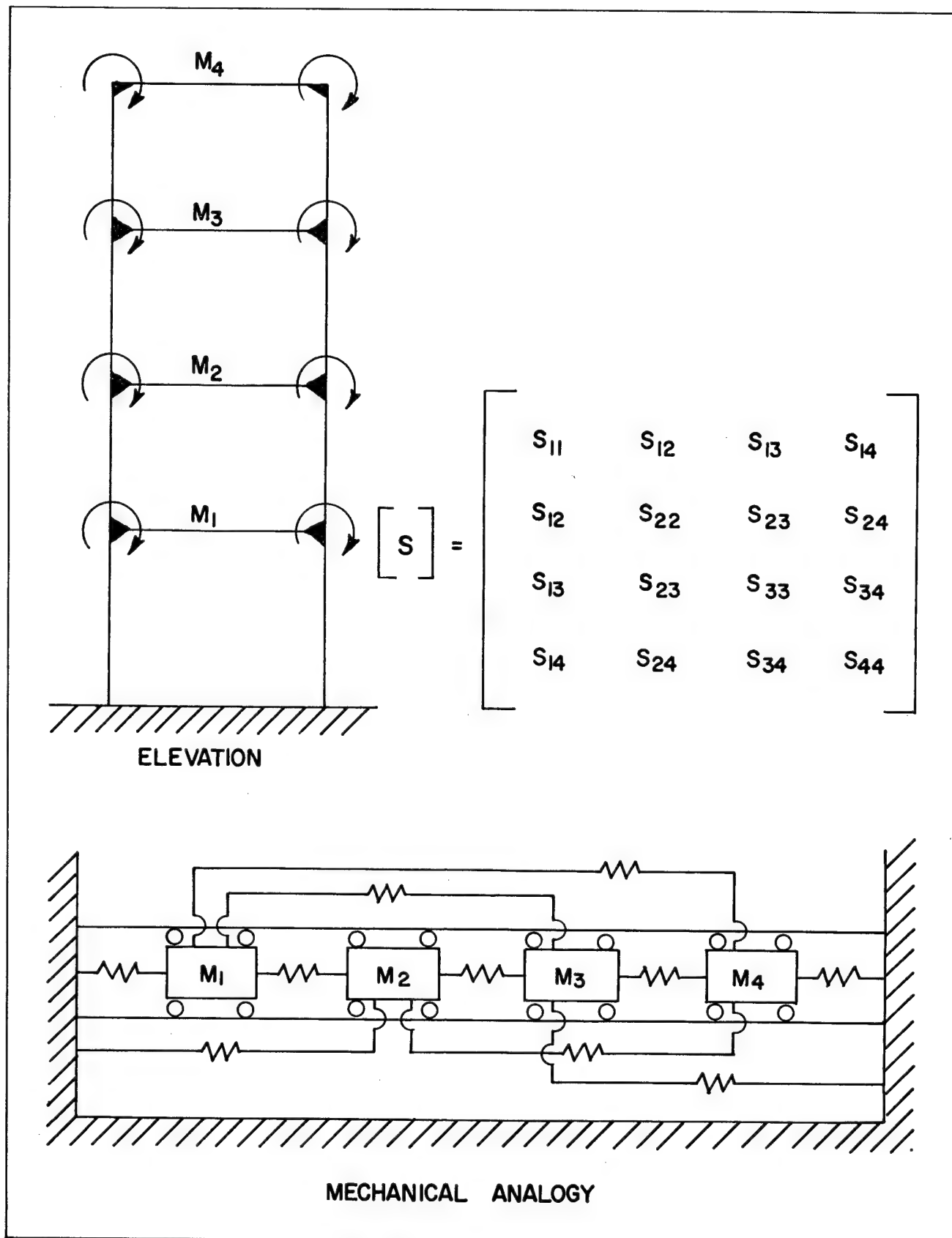
Figure 10.26.   A Far Coupled System.
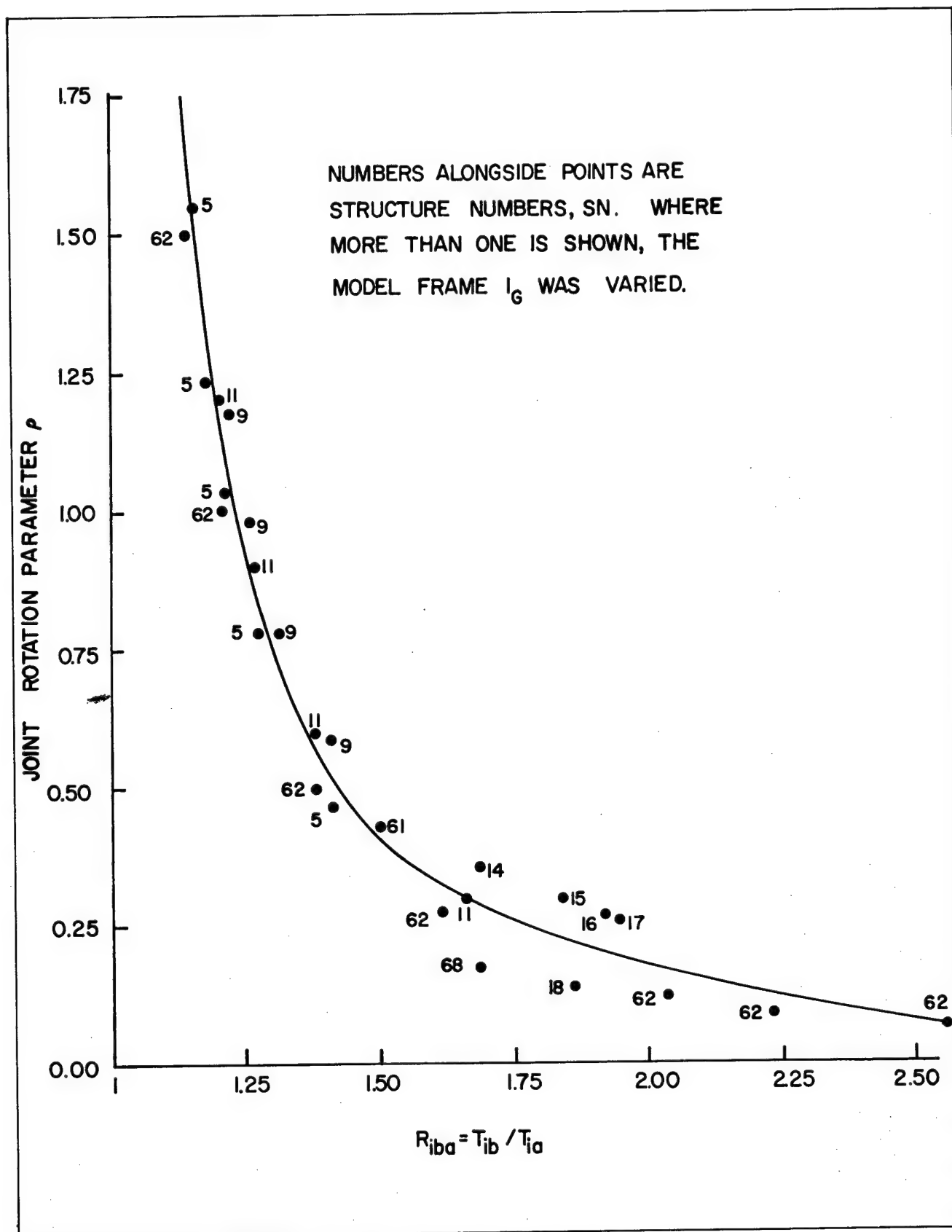
Figure 10.27. Effect of Joint Rotation on Fundamental Period.
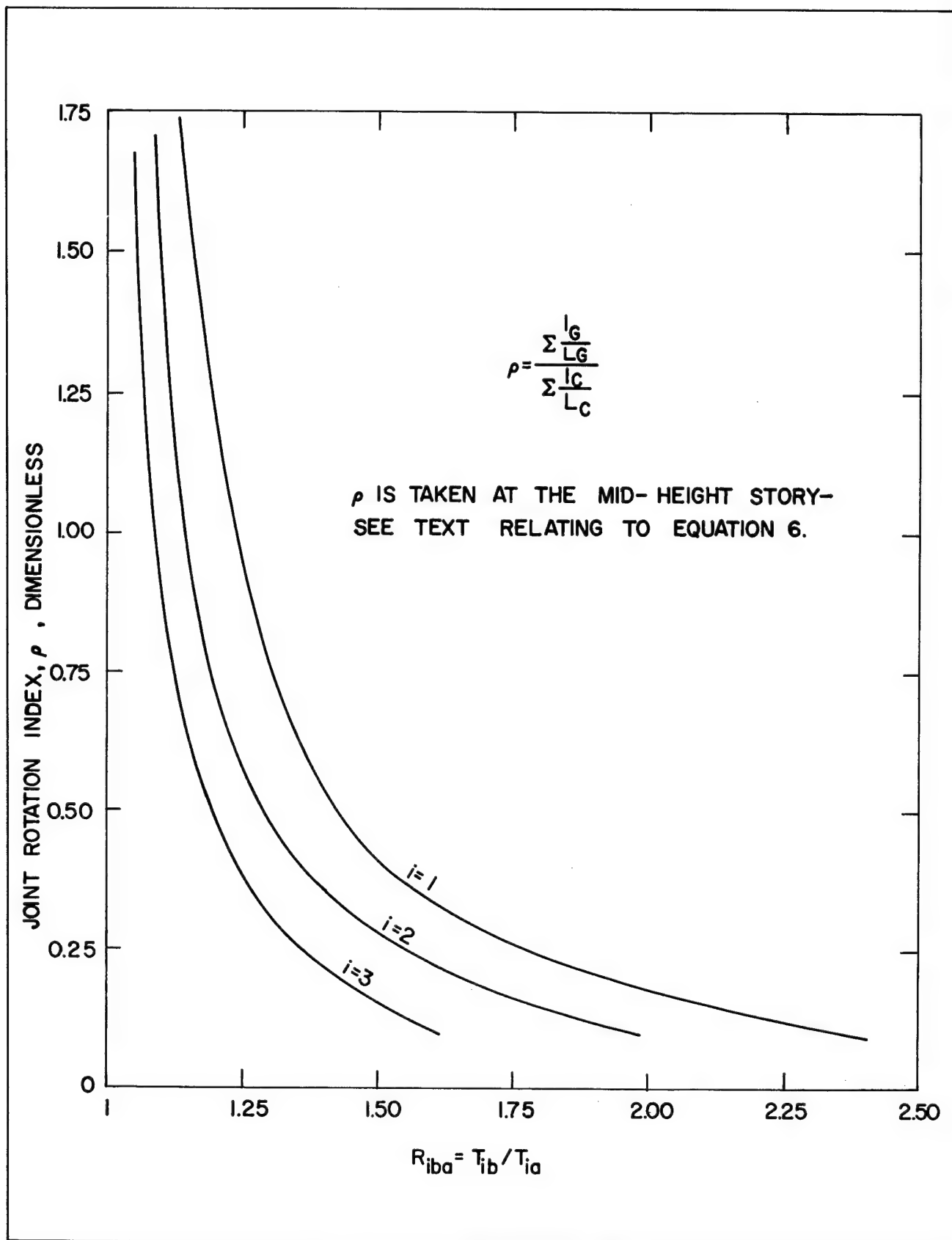
Figure 10.28.   Joint Rotation Index R_{Iba}

210
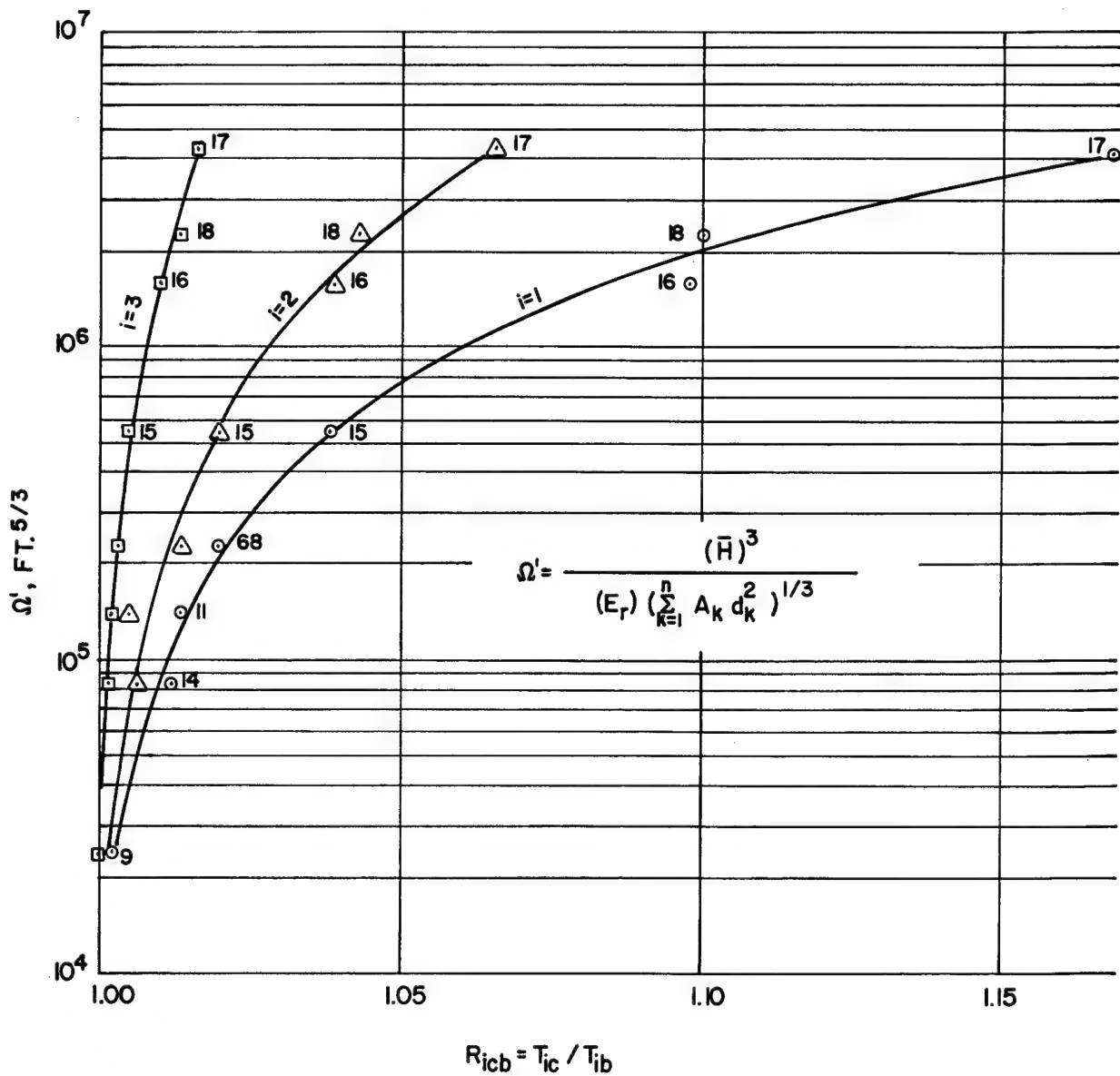
Figure 10.29.   Overall Flexure Index R_{icb}.

211

such buildings and such designs, and must allow for this in estimating any damage.

Figure 10.30 indicates ρ-values versus period ratios for an 8-story frame and for a 16-story frame. The top of the diagram has 2 curves approaching the values of 3 and 5, which are the classical corresponding period ratios for a bar in pure shear. The lower values are approaching the classical values of 6.27 and 17.6 for a bar in pure flexure. Between these limits there are various combinations of shear and flexure. Five building categories have been proposed as shown in the Figure 10.30 in order to recognize and to treat the various types of high-rise buildings that exist today. The cantilever types have different periods, period ratios, and response characteristics than their shear type predecessors that still tend to dominate the technical literature. In the structural response program it is essential to identify and to treat buildings as they exist. As seen by Figure 10.30, if we know the first, second, and third mode periods, we can now identify the type of building. We then also know best how to analyze for response to ground motion.

RESPONSE TECHNIQUES FOR ENGINEERED BUILDINGS

Response Spectrum

The concept of the reponse spectrum is attributed to Biot[7] who used a torsional pendulum to obtain dynamic response to a trace of actual ground motion. Today most spectra, which were described previously, are developed with the aid of large capacity, high speed computers. Response spectra are made for most horizontal ground motion records obtained in the NVOO Safety Program. These are then used for various purposes including computation of response, and in the Spectral Matrix Method of Damage Prediction.

The spectral response computation may be performed with the Duhamel Integral, which, using recorded ground acceleration $\ddot{y}(t)$, takes the form of equation

$$S = \left[\frac{1}{\omega\sqrt{1-\beta^2}} \int_0^t \ddot{y}(\tau) e^{-\omega\beta(t-\tau)} \cdot \sin \omega\sqrt{1-\beta^2}(t-\tau)d\tau \right]_{max} \quad (8)$$

wherein

S = the relative displacement response spectrum point for the particular set of values of ω and β, cm

ω = the natural undamped angular frequency of the idealized oscillator, rad/sec

β = the fraction of critical damping, dimensionless

$\ddot{y}(\tau)$ = the ground acceleration as a function of τ, cm/sec^2

t = time, seconds

τ = time to a pulse, d_τ, seconds

The above equation can be simplified if β is small by letting $\sqrt{1-\beta^2} \approx$ unity. It is to be noticed that the only structural characteristics involved are ω and β. These are varied over the entire range of interest in order to obtain the required points for the spectral curves. Since $y(\tau)$ is generally a long, complex function and d_τ must be taken in very small increments in numerical operations, the total computation is a massive effort. Simpson's numerical integration procedure is often employed. We generally have the results plotted directly on four-way log paper by the plotter. (See Figure 10.31.) The four-way log plot shows simultaneous values of spectral response motion (displacement, velocity, and acceleration) related according to the following equations. Since two of the three parameters are derived from measured values of the third, the two are termed pseudo values. However, the difference between the pseudo values and the actual values is negligible in almost all instances.

$$S_v = \omega S = \frac{2\pi S}{T}$$

and

$$S_a = \omega^2 S = \frac{4\pi^2 S}{T^2}$$

$\quad (9)$

wherein S_v = the spectral value of velocity relative to the ground, cm/sec

S_a = the spectral value of absolute acceleration of the oscillator mass, cm/sec^2

T = the natural period of the oscillator, sec

The response spectrum shows at a glance the maximum response of a simple oscillator of period T and damping β to the entire time-history of the ground motion under consideration. Using the four-way log plot one can enter the chart with the period T, go to the proper damping curve and read S, S_v, and S_a. For example, let us turn to Figure 10.31 that shows the response spectrum for event Boxcar in Las Vegas, and for event Salmon in Hattiesburg, Mississippi, both for 5 percent of critical damping. Entering the chart at periods of 0.20, 0.61, and 2.00 sec, one obtains the data shown in Table II.

TABLE II. SPECTRAL RELATIVE RESPONSE VELOCITY, S_v, CM/SEC

T. SEC	(1) EVENT SALMON HATTIES-BURG	(2) EVENT BOXCAR LAS VEGAS	(3) RATIO OF (1)/(2)	(4) ENERGY RATIO (1)/(2)
0.20	1.50	0.25	6.00	36
0.61	1.05	1.05	1.00	1
2.00	0.16	2.00	0.08	0.006

Column (3) gives the ratio of S_v at each period value, and column (4), the ratio of energy, which may be taken as the square of the column (3) values.

We thus not only have an example of using a spectral chart, but another lesson as well — peak response without reference to period or to frequency is meaningless. An 0.2 second period oscillator in Hattiesburg under Salmon would have 6 times the velocity response of the one in Las Vegas under Boxcar. The energy of vibration would be 36 times greater. And yet the peak S_v values as shown in Figure 10.31 are not much different — about 2.2 as compared to 3.0 cm/sec. At a period of 0.61 second, the values are equal. At a period of 2.00 seconds, closest to the fundamental period value of a tall building, the Las Vegas response is much greater than in Hattiesburg. The Salmon event was a small detonation fairly close to Hattiesburg while Boxcar was a large event at a considerable distance from Las Vegas. There was some very minor damage to low (short period) buildings in Hattiesburg. There was no damage in Las Vegas from Boxcar, although some complaints are still being processed.

Looking again at Figure 10.31, at the 2.00 seconds period the Las Vegas relative response S_v was 2 cm/sec. At the same point it can be seen that the response acceleration was 0.007g and the relative displacement was about 0.64 cm. Thus, a four-way log chart is very useful. Whether one uses acceleration, velocity, or displacement depends upon many conditions. There is usually less random variation in acceleration relative to period at short periods, in velocity at middle-range periods, and in displacement at long periods. The very short period spectral accelerations are asymptotic to the peak ground accelerations, regardless of damping. Acceleration is more meaningful in its effects on short period buildings, although if properly treated any unit may be used.

Applications of Response Spectra

It must be clearly recognized that the response of a real building is different from that of the simple oscillator assumed for the purpose of developing response spectra. Real buildings are complex, they have many degrees of freedom instead of one as for the oscillator; they do not have constant damping values and may not have constant periods, and they vary greatly one from another. Generally, the response of a real building is greater than indicated by the spectra. This is true even if only one mode should respond, and the relative response is even greater when two or more modes respond to the ground motion.

If a building is assumed to have elastic response and constant damping, and if its mode shapes and masses are known, the ratio of its response to that of the oscillator can be computed for each mode of interest, provided the mode shapes are normalized appropriately. These ratios, called modal participation factors, are greater than unity for the fundamental mode and less for the higher modes when the top level displacement is of interest. The equation is

$$\gamma_i = \frac{\sum\limits_1^n m_j \, \phi_{ji}}{\sum\limits_1^n m_j \, \phi^2_{ji}} \qquad (11)$$

wherein γ_i = the participation factor for top level deformation in mode i when ϕ_{jn} is normalized to unity

m_j = the mass story j

ϕ_{ji} = the modal deformation of story j in mode i

n = the total number of stories, with n at the top level

Modal participation factors may be computed for any point or unit of interest, as for example deformation, acceleration, shear, etc., at any story level.

If — for purposes of illustration — we assume a straight line mode shape in the fundamental mode, equal story heights, and equal masses for all stories, the equation would become

$$\gamma_1 = \frac{\sum\limits_1^n \phi_{j1}}{\sum\limits_1^n \phi^2_{j1}} \qquad (12)$$

wherein $\phi_j = j/n$ if the nth-level modal deformation is normalized to unity. Therefore, in this idealized special case, by arithmetic series,

213
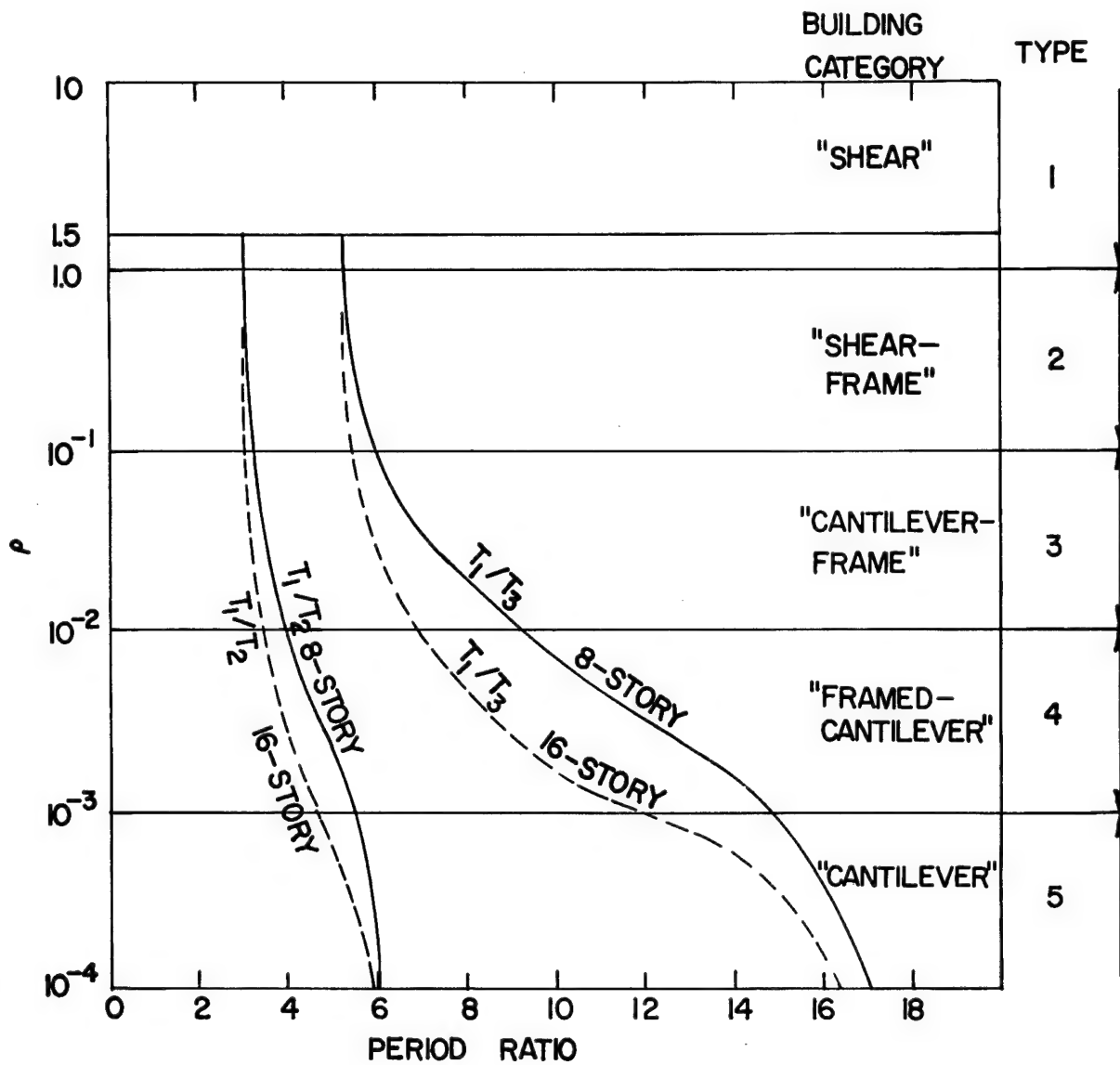
Figure 10.30.   Period Ratio Versus ρ.

214

$$\gamma_1 = \frac{\dfrac{1}{n}\displaystyle\sum_1^n j}{\dfrac{1}{n^2}\displaystyle\sum_1^n j^2} = \frac{3n}{2n+1} \qquad (13)$$

For a 20-story building of this special character γ_1 would be 60/41 or 1.46. This means that the top level fundamental mode deformation relative to the ground would be 1.46 S, or in the 2.00 sec Las Vegas-Boxcar example, $1.46 \times 0.64 = 0.93$ cm. Since there are 20 equal stories in this hypothetical case, the unit story deformation in this mode would be 0.93/20 or 0.046 cm = 0.018 in. This value is well below the partition test values of 1/8 in. previously discussed and shown in Figure 10.9.

But so far in our spectral analysis we have considered only the fundamental mode. According to the classical laws of multi-degree-of-freedom systems, vibration in the various modes—if excited—can occur simultaneously. If the modes are uncoupled, as is the case with most buildings, they are independent. If there is coupling, those modes involved are not independent; i.e., motion in one mode cannot exist without the coupled mode also being involved. Looking at the Las Vegas spectral response curve of Figure 10.31, it can be seen that even though the response is less in the short period range, there is some. The proper procedure would be to enter the curve with all modal periods greater than, say, 0.1 sec, to read the response for each mode, to compute the modal participation factors for each mode, level, and unit of interest and then to somehow combine these effects. Fortunately, the higher modes usually have lower participation factors. They are also suspected of having higher damping values[1]; this also reduces the response.

The combination of modes is a vexing problem in the spectral response method. Since we are dealing with maximum (peak) responses of independent motions that vary rapidly with time, it would seem unlikely that the absolute maxima would all occur at any one instant. On a probabilistic approach, the root-mean-square treatment seems reasonable wherein the peak response is considered to be the square root of the sum of the squares of the independent responses, properly corrected for normalization and participation. Some limited research, however, indicates that this may not be an adequate combination, especially for high-rise buildings. The average between the absolute sum and the root-mean-square may be more realistic in many cases. Regardless of how the modes are combined, the result is an approximation. Thus, the response spectrum method, even though useful, is an approximate dynamic analysis. However, it

is much more realistic than ordinary building code values and procedures. Where more accuracy is needed we employ the time-history method, for which sample results will be shown later.

Ground motion from nearby detonations, as in Hattiesburg, Mississippi, from the 1964 Salmon event (Figure 10.31), generally shows an energy concentration in the short period range.[20] In contrast, the Las Vegas ground motion caused by nuclear events at the distant Nevada Test Site contains a relatively large portion of its energy in the long period range. This comparison, which will be discussed further, is illustrated by response spectra for these two events, Figure 10.31. The response of the long-period Las Vegas high-rise buildings, therefore, is principally in the fundamental mode although higher mode participation must also be considered. One could take measured response at the top of Las Vegas high-rise buildings and divide by an arbitrary factor such as 1.5, which would be a crude allowance for the fundamental mode participation factor and also for a nominal amount of higher mode response, and then compare the results to a response spectrum curve generated from the ground motion in accordance with equation (8). This has been done for event Knickerbocker with results as shown in Figure 10.32. The circles in the figure represent the adjusted response of the tops of various Las Vegas high-rise buildings plotted against the fundamental mode period except for one case where the second mode response was obtained. Although the agreement is far from perfect (and this would be expected in view of the arbitrary factor employed, and other parameters), there is in general a definite correlation between the two independently obtained sources of data. This is an example of how data and theory are often reconciled in the course of the structural response program.

Time-History Response

The time-history response method of dynamic analysis subjects a mathematical model of a complete structure, no matter how complex, to the complete time-history of the ground disturbance, or at least to the complete portion of the strong ground motion which might be of interest. In other words, instead of subjecting a simple oscillator with one degree of freedom to the ground motion as is done in the spectral response procedure, the entire dynamic system is employed with variable masses, stiffness, degrees of freedom, and damping as may be appropriate. Either a single horizontal ground motion component, or both components simultaneously may be used as input. This is a highly complex operation involving massive matrices of numbers and the solution of as many simultaneous equations as there are degrees

215
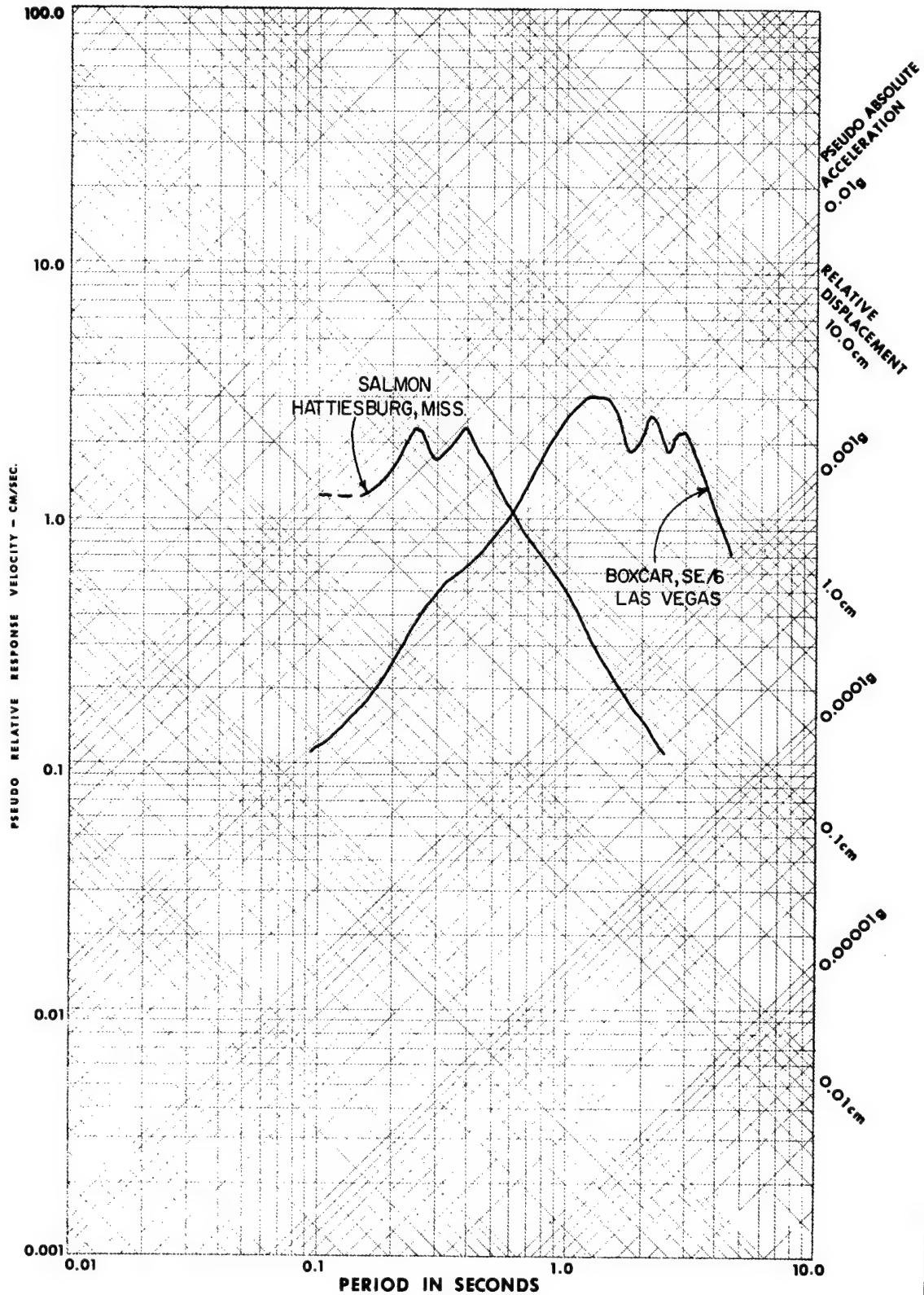
Figure 10.31. 5% Response Spectra.
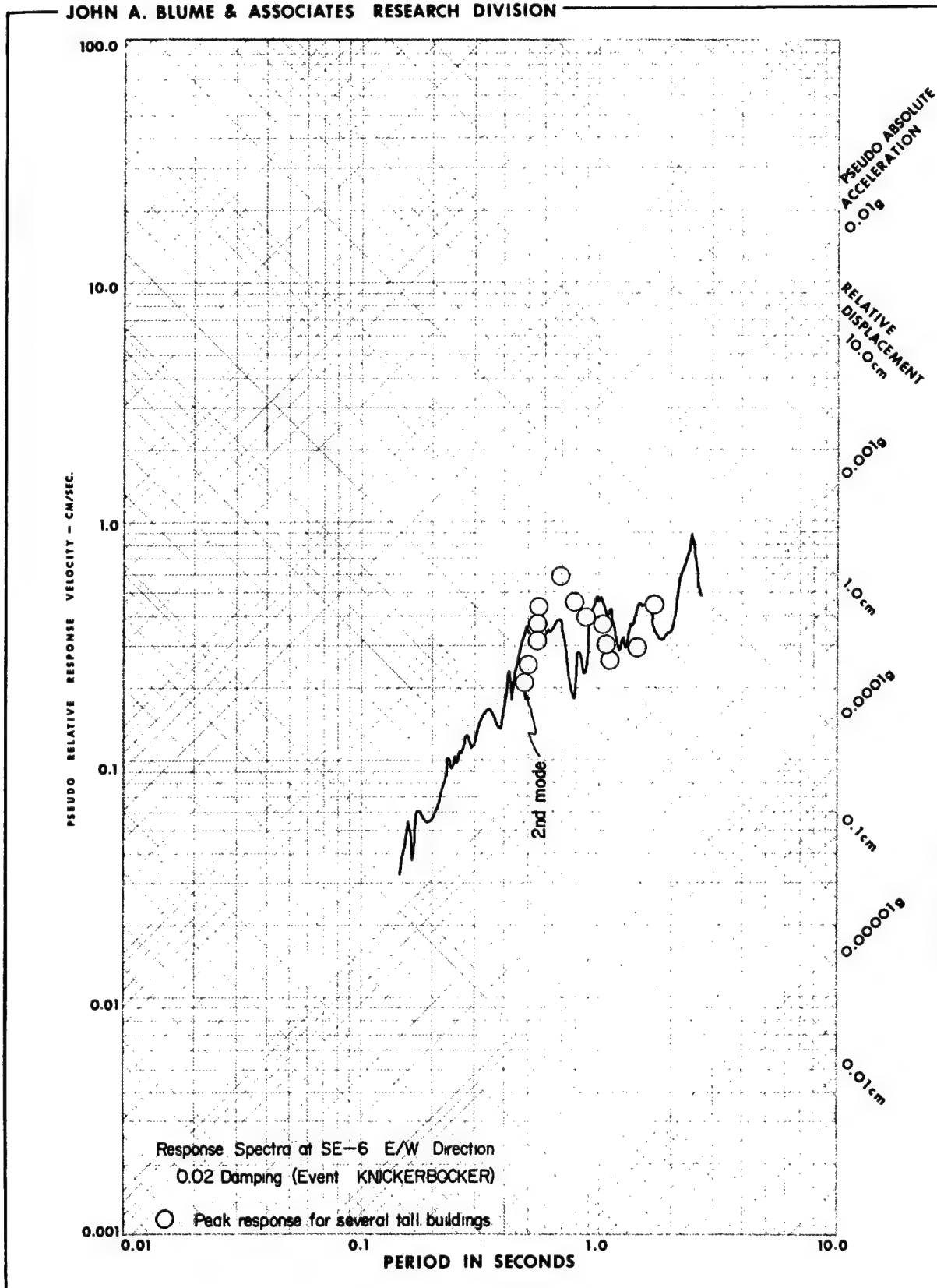
Figure 10.32. Recorded Maximum Structural Response Versus Period of Mode in Which Response Occurred. Knickerbocker Event (Fundamental Mode Unless Otherwise Noted).

of freedom in the system. Computations of this type are only possible with large capacity, high speed computers and the most advanced structural dynamics technology.

In spite of the complexity of the problem, solutions and accuracy are only limited by the ability to create representative models of the structures, and, of course, properly to correct and digitize reliable ground motion records.

Figure 10.33 shows on the upper curve the actual recorded relative displacement in a Las Vegas high-rise building during event Dumont. The lower figure indicates, for the same location in the same building, the computed displacement using a model of the building and ground motion time-history from a nearby seismic station on soil. The time scale is shown at the top of the diagram; each mark represents a half second. It can thus be seen that the measured and the computed response are almost identical across the entire time-history coverage of this figure. We would be very happy indeed if, in our present state-of-knowledge, we could obtain such close correlation all the time. Since we do not, we must challenge everything and even introduce the possibility that these very close results might have been due to a fortuitous combination of circumstances. We do not really feel this negative, but as scientists and objective engineers we must consider all the possibilities.

Figure 10.34 shows a similar comparison for another nuclear event and for another high-rise building in Las Vegas. In this case the correlation is not good. However, the maximum computed displacement is not much different than the maximum measured displacement. In spite of this circumstance it is obvious from the comparisons in Figure 10.34 that the particular building has not been adequately modeled.

DAMAGE ESTIMATION

One of the important operations in the structural response program is the estimation of damage, if any, for proposed nuclear detonation. A first step in this process is to survey the structures that might be subjected to significant ground motion. When events are conducted at the Nevada Test Site there is, of course, no necessity to resurvey the exposure that has been previously identified. However, for events in a new area, surveys are made to establish the types and the values of structures at various distances from the proposed detonation. In addition to the structural survey, the ground and surface geologic conditions are considered. This work is carried out to a radius where the estimated ground acceleration is 0.01g or less. Structures are identified by their type, height, age, condition, and dollar value. Following this,

a formalized procedure developed for the structural response program, and known as the Spectral Matrix Method of Damage Prediction, is followed.

Spectral Matrix Method

The Spectral Matrix Method (SMM) is an orderly procedure for the prediction of damage, or no damage, in structures subjected to ground motion[21]. It includes consideration of the frequency distribution of ground motion and corresponding structural response based upon the response spectrum technique, the distribution of natural frequencies for the various kinds of structures to be subjected to ground motion, foundation materials, structural conditions, and construction practices and standards. It also considers the probabilistic aspects of the problem in that it recognizes that there can be a significant variation of both the ground motion (demand) and the structural resistance (capacity). The method is suited to either computer or manual processing. With computer aid, however, it can readily be extended to large areas and a wide complexity of structure types.

The estimated ground motion for a particular detonation is provided in the structural response programs by Environmental Research Corporation. These values are then developed into spectral response velocities. Five percent of critical damping is used as a standard in this process. However, special structures or conditions with other damping values can readily be accommodated. We then apply corrections to the response spectral values in order to represent the type of structures under consideration. The result of this step is called demand. Another part of this phase of the work is to provide for the probabilistic variations from the demand values which are, up to this point, mean demand values. The distributions are highly skewed with a zero limiting value on the lower side and without limits on the upper side. These are generally modeled by the lognormal distribution.

The structures are divided into various classifications in each unit of exposure. A unit is defined as a city, town, or area that would not have a significant variation in its mean motion. If, however, a unit should have variations in its motion due to geologic or other local conditions it is subdivided into zones. For each unit and zone, corrections are introduced for any particular variations in the soil conditions or in the condition of the structures.

The structures are classified into not only applicable types but into natural period bands. A total of 8 period bands are usually considered covering the entire range of possible natural periods of vibration. For each unit, zone, and classification of structure there is a total dollar
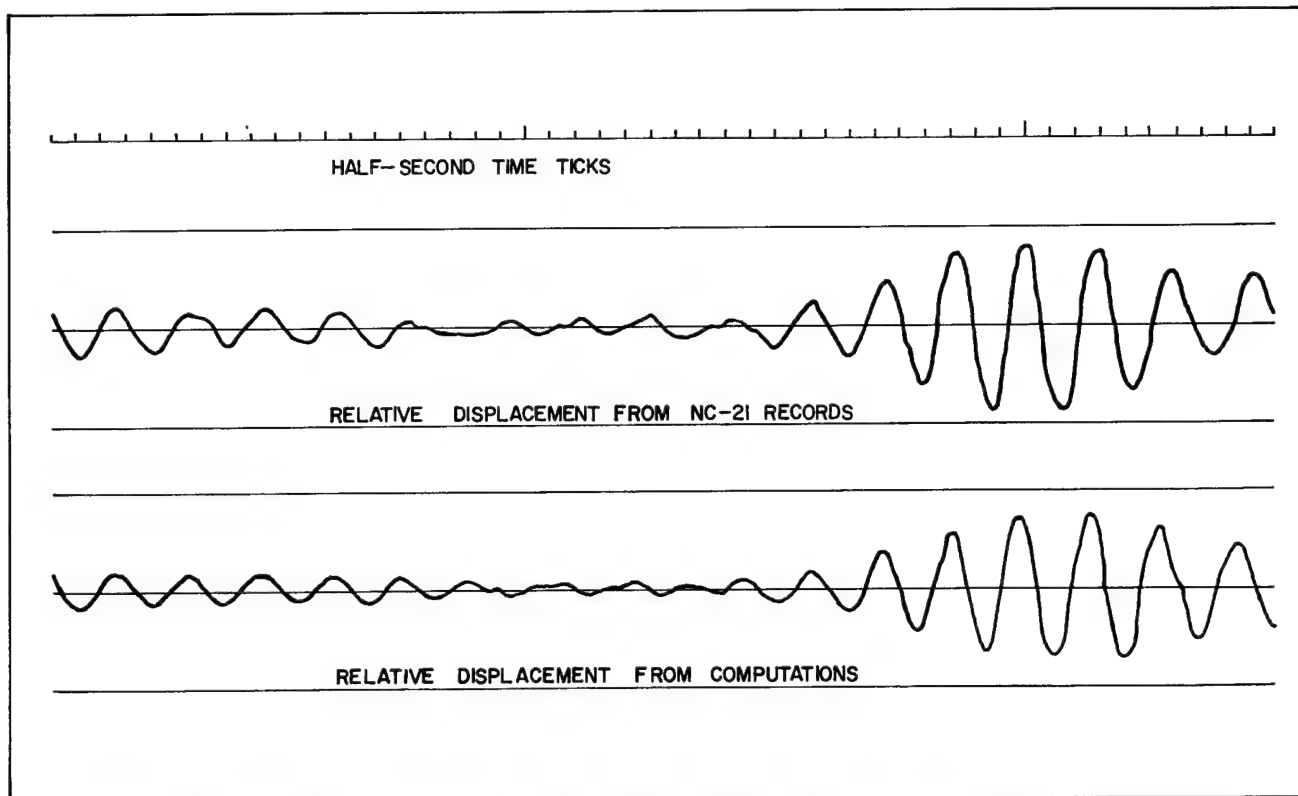
Figure 10.33. Comparison of Actual and Computed Relative Displacement, Top Floor, Building A, Dumont Event.
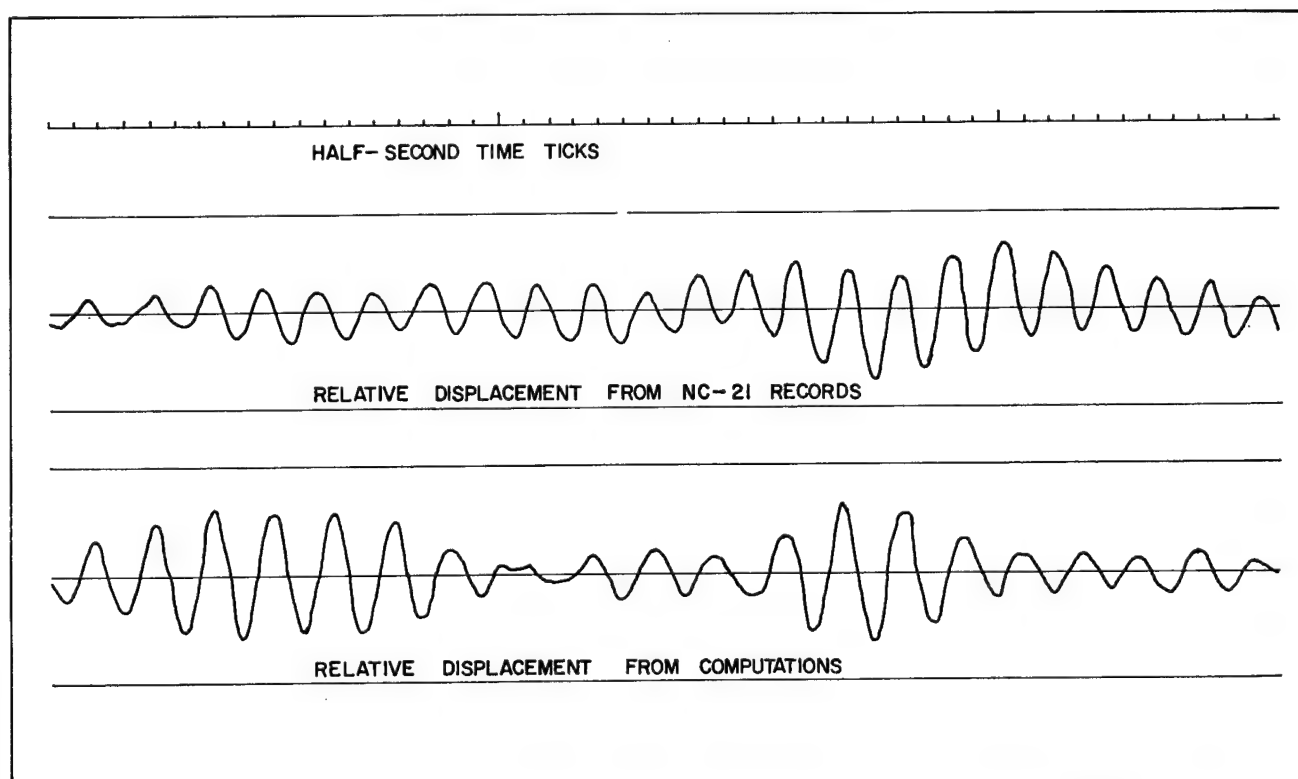
Figure 10.34. Comparison of Actual and Computed Relative Displacement, Top Floor, Building B, Halfbeak Event.

219

value of the structures. This is called the exposure. Usually, these values may be obtained from tax assessment data properly modified to allow for the difference between the tax values and real values and to allow for replacement costs. Figure 10.35 shows the Spectral Matrix System. A standard matrix of potential values is established with 12 rows of response velocity and 8 columns of period values superimposed on the four-way logarithmic spectral paper.

For each exposure we must determine or estimate the mean capacity in the same units as the demand, where capacity is defined as the yield point value of the structure. Various types of structures are then assigned various subclassifications which identify their inelastic characteristics as discussed previously. These characteristics may vary from brittle to elasto-plastic ductile, or they may involve bilinear or multilinear softening characteristics.

In estimating the mean capacity of the structures of various types, there are various approaches. The most straightforward perhaps is structural calculation of the yield point capacity. This, however, becomes highly complicated and often unsatisfactory because of the fact that real buildings have nonstructural elements such as partitions, filler walls, etc. Another approach is to utilize empirical data from earthquakes[12] or explosion-generated ground motion (but the latter provides very meager information on damage), and in terms of the estimated probabilistic variations to establish mean capacities. In most cases, a Gaussian or normal distribution is satisfactory for this purpose.

Damage occurs when the demand exceeds the capacity. As defined earlier, demand is ground motion, corrected for structural characteristics and participation, and capacity – in the same units – is the building's ability to resist the motion. The degree of damage varies, according to many factors, with the amount that demand exceeds capacity. Since both demand and capacity are random variables with probability distributions, we are thus dealing with a problem in joint probability, a problem in which there are various distribution functions such as lognormal and Gaussian. Since this becomes exceedingly complex mathematically, we have developed computer operations utilizing random numbers and the Monte Carlo technique in such a manner that we can rapidly process any combination of distribution functions. We normally use such a large number of random numbers (selected by the computer to fall within the narrow limits of each structure classification) that the results are essentially the same as would be obtained if direct integration were feasible.

Figure 10.36 is a schematic diagram of two sets of discrete probability distributions combined in a joint probability diagram. Capacity, shown at the upper left, is roughly normal in distribution (although discrete values are shown). Demand at the lower right side would be roughly lognormal if a continuous function. The sum of each set is unity. For each CAP value there is a probability of combining with any DEM value, and vice versa. These combinations of probabilities are called joint probabilities. As an example, D may combine with 5, so there is a joint probability equal to the product of the probabilities of D and of 5. If $P(D) = 0.40$ and $P(5) = 0.10$, then $P(D,5) = (0.40)(0.10) = 0.04$. As the diagram is drawn the point D, 5 has a DEM/CAP value less than 1 so there would be no damage. However D, 8 would have a DEM/CAP value greater than unity, so some damage would be expected. Its probability, however, would be considerably less than that of point D, 5 as shown by the relative heights of the vertical lines. The probability of severe damage (large DEM/CAP ratios) is very small in this diagram.

With the structural capacity and ground motion established or estimated, there is now a vast computation process involving countless calculations for a large area with many units, zones, and structure classifications. However, with the aid of large computers this computation can be conducted in a very short period of time. More than that, it can be readily repeated with slight variations in the input in order to explore various parameters. The output is dollars of estimated damage for each unit, zone, and classification of structure. Based upon the percentage of estimated damage in each category, there is a clue as to possible safety hazards. These are then further investigated and indicated precautions are recommended.

A simplified idealization of the SMM process follows:

$$D_{zk} = E_{zk} S_z C_z \sum_{i=1}^{13} \sum_{j=1}^{8} P_{ij} F_{ijk} T_{jkz} \quad (14)$$

wherein D_{zk} = the expected damage in zone Z for structure classification K; dollars

E_{zk} = the exposure in zone Z for structure classification K, as defined more fully above; dollars

S_z = the soil factor for zone Z as defined above; dimensionless

C_z = the condition factor for zone Z, as defined above, dimensionless

220
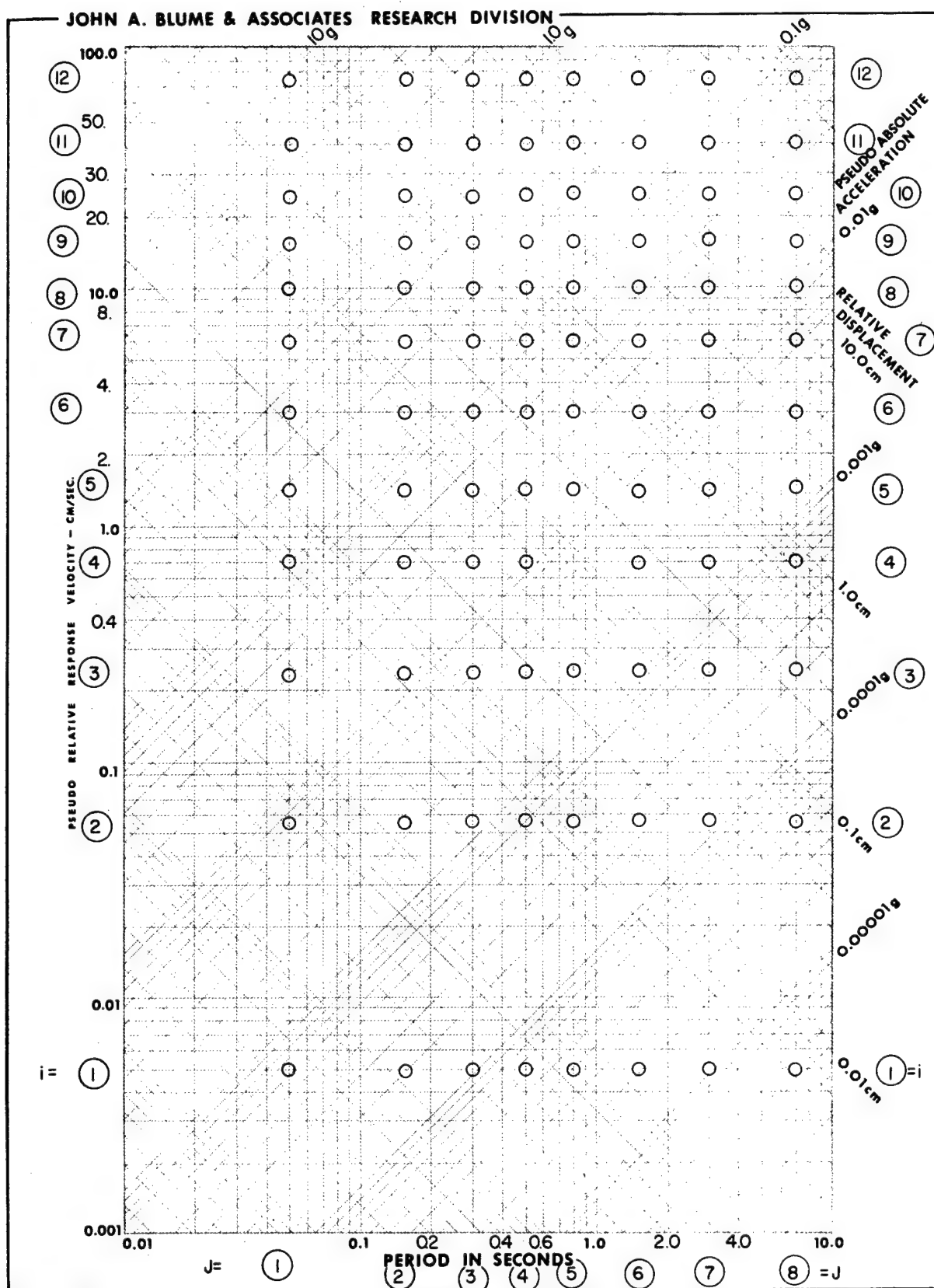
Figure 10.35.   The Spectral Matrix System.

221
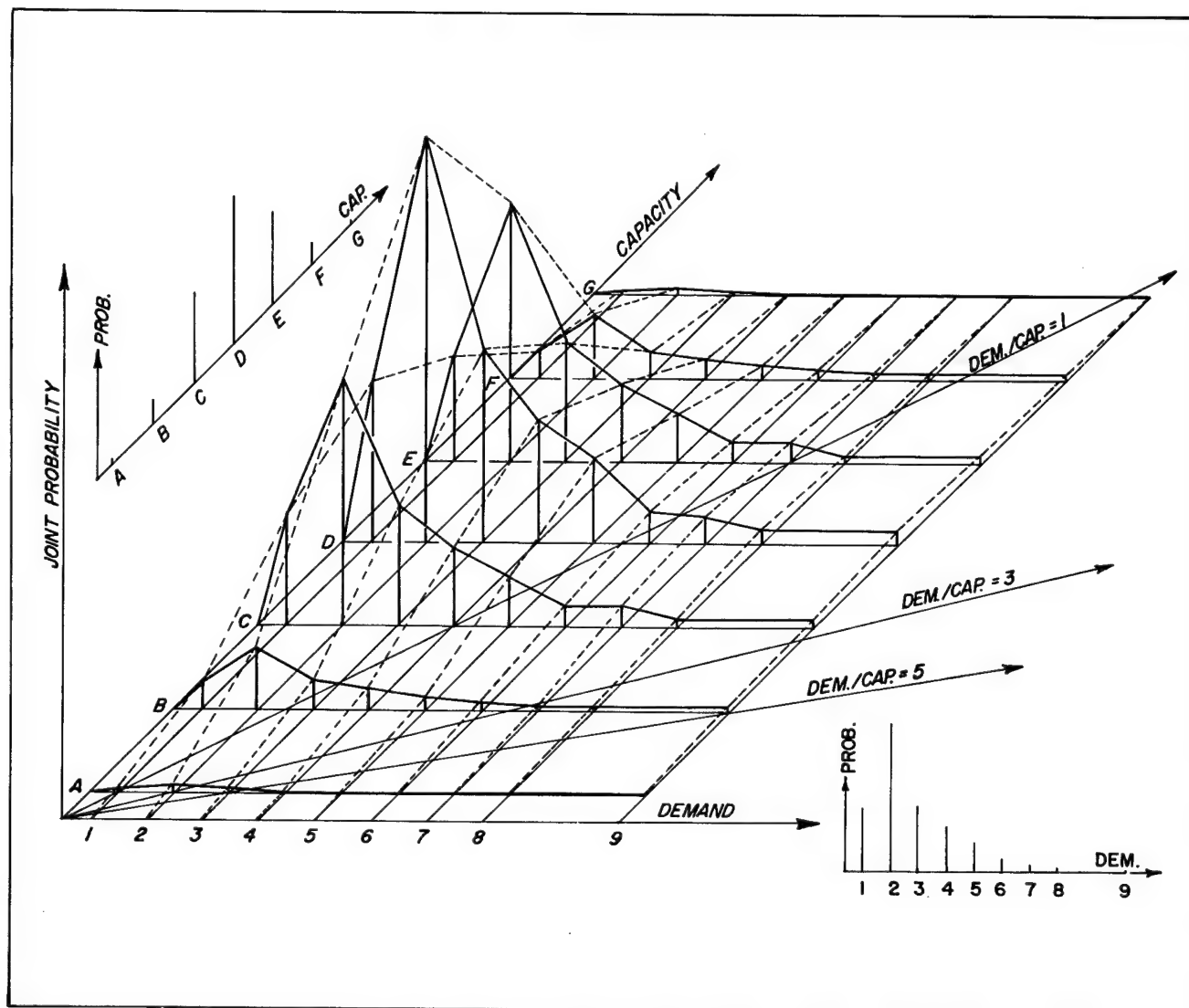
Figure 10.36. Schematic Diagram Joint Probability.

P_{ij} = the probability that damage will occur in matrix element ij as set forth by damage factor, F, given the predicted ground motion, dimensionless

F_{ijk} = the damage factor for structure classification K in matrix element ij; total damage would be represented by $F = 1.00$, and no damage by $F = 0$; dimensionless

T_{jkz} = the ratio of the value of structures of classification K that fall in period band j to that of all the structures in classification K for the zone Z under consideration; dimensionless

Subscripts:

k refers to structure classification K

z refers to zone Z

u refers to unit U

i refers to spectral intensity in terms of 5 percent damped relative response velocity as subsequently defined

j refers to the spectral period band as subsequently defined

The total expected damage in zone Z for all structural classifications K, is determined by

$$D_z = \sum_{k=1}^{all} D_{kz} \qquad (15)$$

and the total expected damage in the entire unit U is determined by

$$D_u = \sum_{z=1}^{all} D_z \qquad (16)$$

LONG-RANGE SAFETY STUDIES

Areas of specific study include the reconciliation of theoretical structural response predictions with the actual behavior of the real structures; the influence of soil dynamic behavior on the response of structures on various types of foundation soils; the determination of elastoplastic behavior boundaries (damage thresholds) for major structural and nonstructural elements and materials; the relationship, if any, between actual motion levels and human perception to motion and the implications with regard to damage complaints; and the development of techniques, including temporary bracing, for minimizing damage from ground motion.

Reconciliation of Theoretical and Actual Structural Response

In order to improve prediction capabilities regarding structural response to ground motion, it is necessary to determine how well the various idealized models used in mathematical analyses correspond to structures as actually built. There is probably not much error in the assumptions pertaining to mass distribution, but there can be considerable error in stiffness and mode shape characteristics and the interrelationships of these parameters.

An ultimate objective is to be able to predict the periods, mode shapes, stiffnesses, stiffness coefficients, damping, and damping coefficients of real buildings without the need of subjecting these buildings to field tests. With such prediction capability, together with the known interrelationships of these parameters, it would be possible to predict the amount, type, and location of damage.

One phase of this long-range program is the continuous acquisition and statistical treatment of empirical data regarding building dynamic properties. Another phase of the work is the reconciliation of the data with theory and the development of new theory where necessary to have acceptable prediction capabilities. A comprehensive study of the interrelationships of periods, mode shapes, stiffness coefficients, and damping coefficients has been in progress throughout the contract life. Several computer programs have been developed and have been tested with idealized systems and with data from real buildings of various types to provide more extensive knowledge about the properties of real buildings.

A second phase of this study includes detailed comparison of predictions of structural response in two 4-story concrete frame test structures with the actual recorded motion of these structures. The recorded motion is that developed in free vibration tests, forced vibration developed by the vibration generator, and incoming ground motion from underground nuclear explosions.

Predicted and actual structural responses from various types of structures are being compared statistically and with the response spectrum technique to evaluate the accuracy of present prediction methods. These are being refined with actual data and with modifications developed from the computer work and from the 4-story test structure results. A comprehensive study on the combined influence of story shear, joint rotation, overall flexure, and movement of the structure base in its foundation soil was completed.

Soil Dynamics and Soil-Structure Interaction Studies

An active program is under way to determine dynamic properties of foundation materials in regions exposed to

223

ground motion from underground nuclear explosions[18 19]. Instrumentation has been placed to conduct soil-structure interaction studies concurrently with the forced vibration testing of the 4-story test structures at the Nevada Test Site[3]. These tests have provided data for preliminary evaluation of the influence of soil-structure interaction for these buildings.

Damage Thresholds for Structural and Nonstructural Elements

The structural dynamics laboratory has conducted tests on a wide variety of partition walls and wall materials, and on plaster wallettes since 1965. Two reports have been submitted on the results of these tests[4,5].

A parallel effort, largely supported by laboratory facilities, has been the design and construction of simple gauges to measure movement in existing cracks in test and other structures. These gauges have been constructed in large quantities and have been installed on real structures at the Nevada Test Site, in communities bordering the Test Site, and in low-rise and high-rise structures in Las Vegas. Other gauges are being installed in buildings in the vicinity of the central Nevada supplementary test site[6]. A continuing survey is in progress to monitor existing conditions and changes in conditions in four rented structures in Las Vegas to evaluate changes occurring during large events. This type of study is also being conducted in the Las Vegas high-rise structures and in structures near the Test Site to make similar evaluations.

Human Perception and Actual Motion

Further study of human perception is planned, both using the shaking platform in the structural dynamics laboratory, and as a concurrent study with the forced vibration testing of the 4-story test structures.

Perception thresholds are being correlated with the incidence and frequency of complaints to determine relationships between actual ground motion parameters and the initiation of damage complaints, if such a relationship exists. Presently it is well established that perception is initiated at some intermediate level. Statistical probability must be considered, however, in assessing the relationships between motion parameters and threshold levels of perception and real damage.

Minimizing Damage

Temporary bracing measures can be employed to minimize damage for isolated structures. These techniques are not likely to be workable if an entire city or populated area is involved. In this event, damage must be minimized by modification of event parameters together with appropriate public relations activities so that necessary preventive measures can be recommended to the public. Other promising methods for the reduction of motion and prevention or minimization of damage in structures are being actively studied and developed.

SUMMARY AND CONCLUSIONS

Our objective in the contract effort has been to develop and improve our capabilities in predicting the response of structures to ground motion from underground nuclear explosions. We have been able to predict structural behavior with reasonable accuracy while conducting a concurrent research program in the refinement of the prediction techniques, and while developing other programs to predict the nature and extent of damage when it does begin to occur.

Reliable predictions of structural response depend primarily upon the extent of knowledge of real structural properties and the accuracy of ground motion predictions. Ground motion predictions, which in order to be of most usefulness have to define the distribution of motion across the frequency range, are dependent upon an accurate foreknowledge of the source of parameters and of the local station effects.

Fortunately for NTS and the central Nevada area program there is a considerable body of evidence and data available for the area influenced by these programs on the characteristics of ground motion from previous events. There is also available much information about the buildings, gathered during the history of the structural response contract. Ground motion predictions including techniques for predicting frequency distribution are becoming quite accurate. Consequently, as long as source parameters can be reliably forecast, a reasonably good prediction of structural response for the area influenced by NTS and central Nevada area programs is within the present capabilities of the safety contractors.

We know from our experience in the testing program and from structural analysis that damage, if and when it occurs, will be generally slight and inconsequential. However, we must continue detailed studies of some structural types and some ground motion conditions which may present a possibility of greater damage. As noted earlier there is always a possibility that unusually high ground motion may be combined with an unusual or susceptible structure to cause more severe damage. To minimize this possibility we keep several experienced engineers active in field inspections of structures within the range of significant ground motion, and intensify these studies just prior to any major event. Using these additional precautions we believe that we can reduce such hazards to their practical minimum. In summary,

then, we believe that the problem of structural response to ground motion developed by NTS and central Nevada area programs is reasonably well understood, and we are confident that the combination of continued close observation of the response of buildings in this area and the continued improvement of prediction methods and data will provide adequate safeguards for these structures.

For new areas, such as the offsite Plowshare events, there is much less information on which to base predictions. In many cases a shot offsite is a one-time affair, so that there will never be any previous experience at such a location to guide prediction efforts. In such cases, safety measures have to be even more conservative. Much more study is needed, relatively, than for an event of equal size at the Nevada Test Site. Normally offsite events are quite small and not of any great potential hazard. Nevertheless, they are handled in about the same manner as a major event at NTS. The extensive safety precautions and very conservative approach used in predictions ensure that the uncertainties inherent in the absence of previous event data are more than compensated.

Planned large offsite events such as those considered for excavation of a new sea level canal across the Isthmus of Panama will have been preceded by extensive studies, including smaller calibration shots at less than damaging levels, which will provide the empirical data needed to substantiate predictions. Here again a conservative approach is used so that safety measures are adequate to compensate for any major uncertainties.

REFERENCES

1. John A. Blume, "Period Determinations and Other Earthquake Studies of a Fifteen-Story Building," Proceedings First World Conference on Earthquake Engineering, June 1956, Earthquake Engineering Research Institute

2. John A. Blume & Associates Research Division, "Structural Condition Survey: Movement of Building Element Cracks in Six Mercury, Nevada Structures," Report NVO-99-20 to the U.S. Atomic Energy Commission, Nevada Operations Office, December 1967

3. John A. Blume & Associates Research Division, "Concrete Test Structures: First Progress Report on Structural Response," Report NVO-99-29 to the U.S. Atomic Energy Commission, Nevada Operations Office, March 1968

4. John A. Blume & Associates Research Division, "First Progress Report on Racking Tests of Wall Panels," Report NVO-99-15 to the U.S. Atomic Energy Commission, Nevada Operations Office, August 1966.

5. John A. Blume & Associates Research Division, "Second Progress Report on Racking Tests of Wall Panels," Report JAB-99-35 to the U.S. Atomic Energy Commission, Nevada Operations Office, July 1968

6. John A. Blume & Associates Research Division, "Report on Structural Condition and Monitoring in Las Vegas, NTS and Southern Nevada Area," Report NVO-99-12 to the U.S. Atomic Energy Commission, Nevada Operations Office, May 1966

7. M. A. Biot, "Analytical and Experimental Methods in Engineering Seismology," Transactions American Society of Civil Engineers, Vol. 108, 1943

8. G. W. Housner, "Behavior of Structures During Earthquakes," Journal, Engineering Mechanics Division, American Society of Civil Engineers, Vol. 85, October 1959

9. N. M. Newmark, "A Method of Computation for Structural Dynamics," American Society of Civil Engineers, Vol. 85, July 1959

10. R. W. Clough, "Dynamic Effects of Earthquakes," Journal, Structural Division, American Society of Civil Engineers, Vol. 86, April 1960

11. J. Penzien, "Elasto-Plastic Response to Idealized Multistory Structures Subjected to a Strong Motion Earthquake," Proceedings Second World Conference on Earthquake Engineering, Vol. 2, Tokyo 1960

12. John A. Blume "Structural Dynamics in Earthquake-Resistant Design," Transactions American Society of Civil Engineers, Vol. 125, 1960

13. L. S. Jacobsen, "Natural Periods of Uniform Cantilever Beams," Transactions American Society of Civil Engineers, Vol. 104, 1939

14. John A. Blume, N. M. Newmark and L. H. Corning, "Design of Multistory Reinforced Concrete Buildings for Earthquake Motions," Portland Cement Association, Chicago 1961

15. John A. Blume & Associates Research Division, "Structural Dynamics of Cantilever-Type Buildings," Report NVO-99-31 to the U.S. Atomic Energy Commission, Nevada Operations Office, January 1968

16. A. S. Veletos and N. M. Newmark, "Effect of Inelastic Behavior on the Response of Simple Systems to Earthquake Motions," Proceedings Second World Conference on Earthquake Engineering, Tokyo 1960

17. International Conference of Building Officials "Uniform Building Code," 1967 Edition, Vol. 1, Pasadena, California 1967

18. John A. Blume & Associates Research Division, "Dynamic Characteristics of Multistory Buildings." Report NVO-99-30 to the U.S. Atomic Energy Commission, Nevada Operations Office, January 1968

19. John A. Blume, "Dynamic Characteristics of Multistory Buildings," Journal, Structural Division, American Society of Civil Engineers, Vol. 94, February 1968

20. John A. Blume & Associates Research Division, "Spectral Response to Ground Displacement at Hattiesburg Resulting from Nuclear Event SALMON," Report NVO-99-27 to the U. S. Atomic Energy Commission, Nevada Operations Office, March 1968

21. John A. Blume & Associates Research Division, "The Spectral Matrix Method of Damage Prediction, Description and Status," Report NVO-99-33 to the U. S. Atomic Energy Commission, Nevada Operations Office, March 1968

Chapter 11

EARTHQUAKES AND AFTERSHOCKS RELATED TO NUCLEAR DETONATIONS

Wendell Weart, *Geophysicist*
Sandia Laboratory, Sandia Corporation, Albuquerque, New Mexico

INTRODUCTION

Small scale seismic tremors have been observed subsequent to nuclear detonations for many years. In nearly all instances, these seismic events have been directly related to the postshot phenomena of cavity collapse and chimney growth. Completion of the chimney growth generally terminates the seismic events. Detonations of higher yield events in the past few years have been accompanied by seismic tremors which originate near the detonation but outside the region involved in chimney growth. Although the seismic events observed to date in no way constitute an offsite hazard to structures or to people, they do focus attention on the general area of concern related to triggering of significant earthquakes as yields increase and other test sites become involved. Consequently, this particular problem has received a great deal of attention in the past year, culminating in an extensive program by various agencies to obtain relevant data on high-yield events.

At this writing, the Benham Event at about 1 megaton yield, (fired December 19, 1968, at Pahute Mesa of the Nevada Test Site) provides the most complete data on the relation between nuclear events and the earthquake aftershock phenomena. A continuing high level of effort to gain understanding concerning all seismic and faulting phenomena related to nuclear detonations is being encouraged by the AEC. Information in this chapter summarizes the present state of knowledge regarding the relationship between seismic and earthquake phenomena and nuclear detonations.

FAULT MOTIONS CAUSED BY NUCLEAR DETONATIONS

Cracking of the earth's surface near ground zero is observed after all nuclear detonations unless the scaled depth of the detonation is much greater than normal containment practices dictate. Cracking associated with most of the events, especially the smaller ones, is circumferential and/or radial to the detonation. This fracturing is related to surface motions caused by the nuclear detonation or to tensile stresses caused by the collapse of the cavity and formation of the collapse crater. Many of the larger yield events (greater than 100 kilotons) and a few smaller yield detonations result in linear fracture trends which follow the lineation of preshot tectonic patterns.

First extensive observations of this effect were associated with the Yucca Fault, a major fault which transects Yucca Flat, the area where most of the underground testing has occurred. (See Figure 11.1.) Cracking and relative movement along this fault as a result of nuclear detonations have been observed over a period of years. Maximum displacements on Yucca Fault due to any event have been less than 3 feet with most faulting showing less than 1 foot displacement. Linear extent of faulting resulting from the largest events in Yucca Flat has been as much as several thousand feet. Other less pronounced faults in Yucca Flat may show relative motion from nearby detonations. As a rule of thumb, a detonation at scaled distances greater than 1000 $kt^{1/3}$ from the fault in question does not cause relative motion along the fault.

Both the displacement and extent of faulting apparently decrease with the detonation of subsequent events of comparable size in the same part of the Flat. This may indicate that prior events have relieved the more critical stress concentrations across these faults. More pronounced (or more observable) faulting has accompanied the high-yield events in Pahute Mesa and the single high-yield event in central Nevada. Maximum fault displacements observed subsequent to any nuclear event were those due to the Faultless Event in central Nevada. Local vertical and horizontal displacements were observed up to 15 feet and 3 feet, respectively. (See Figure 11.2.) The maximum linear extent of faulting was 12,000 feet, and was not part of the fault on which the maximum movement occurred[2].

Two of the largest underground detonations to date, Boxcar and Benham, both at about 1 megaton, produced
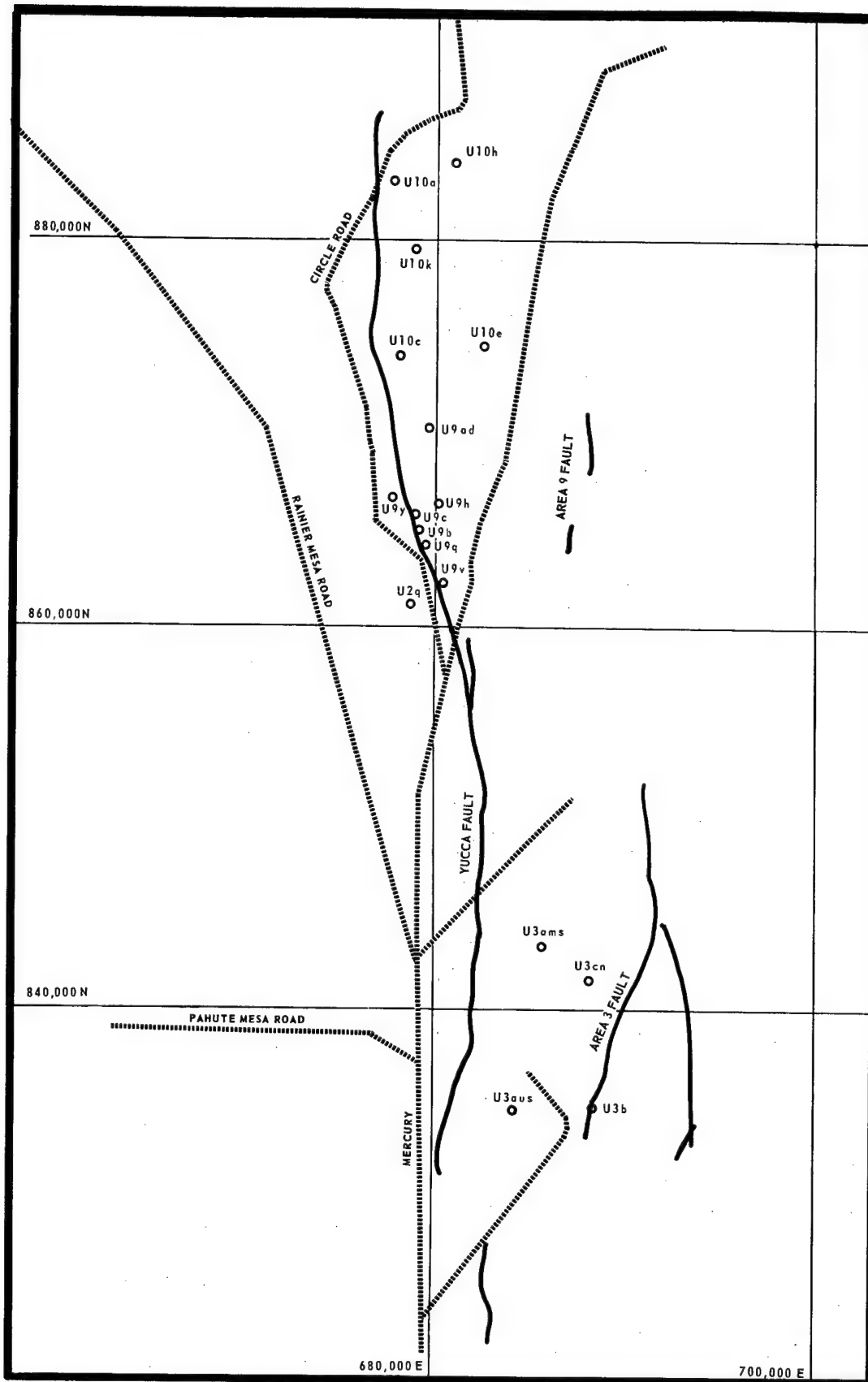
Figure 11.1.   Fault Map of Yucca Valley and Yucca Fault Showing Areas Moved by Detonations [1,7].

EXPLANATION

Lineament on conventional black and white aerial
photographs; bar and ball on downthrown side of
lineaments that are either known or inferred faults

x x x x x x x x x x x x x x x x x x x x x x x x x

Lineament from infrared imagery after Ekren (See
text)

Explosion-produced fracture; heavy line represents
principal fractures along which most displacement
occurred, long dash where discontinuous or gener-
alized; number in block is displacement in feet and
is on downthrown side of fracture; arrows indicate
relative lateral movement

Survey stations; dashed line indicates level line

Ground zero

Figure 11.2.   Fault Map of Faultless Event Showing Areas Moved by Detonations [2].

229

fracturing and faulting about 26,000 feet in linear extent on Pahute Mesa. Maximum displacement for Boxcar was about 3 feet, and for Benham was about 1 foot. (See Figure 11.3.) The data available indicate that fault length may increase linearly with the yield of the detonation. These observations are principally from Pahute Mesa; but the single event in central Nevada, Faultless Event, fits these data.

Shot time photography on a few of the larger yield events indicates these fractures and displacements occur soon after zero time, coincident with passage of the seismic waves. Further photographic and displacement-time studies are necessary to determine whether all of the postshot-mapped fault displacement occurs at one time; but it is evident that most of the motion does occur within seconds of zero time.

NEAR FIELD EARTHQUAKE AND AFTERSHOCK ACTIVITY

Zero Time Fault Displacements

The displacements observed postshot along preexisting fault zones are similar to those surface breaks observed on many moderate earthquakes. It is logical to assume that these pronounced surface breaks are the result of (or result in) an earthquake which occurs shortly after the nuclear event. Seismic waves generated by this early earthquake are generally masked in the latter portions of the seismic waves from the nuclear detonation.

Teleseismic surface waves, both Love and Rayleigh, indicate that a shear source (some form of couple, such as an earthquake slip) is necessary to explain the amplitude and azimuthal variations observed. The assigned surface wave magnitudes for these events are much less than the body wave magnitudes (one of the distinguishing features between earthquakes and explosions), and consequently one may deduce that the magnitude of any zero time earthquake, for events to date, is at least one magnitude unit smaller than the nuclear event. This is so, despite the observed fault lengths which are consistent with lengths associated with magnitude 6 earthquakes.

Since these fault displacements are limited to the region surrounding the nuclear event, they do not constitute an offsite safety hazard as long as the amplitude of seismic waves resulting from the slip remain smaller than those generated by the nuclear source. Further understanding of these phenomena is necessary to permit extension of the present observations to higher yields and especially to other, perhaps more tectonically active, test sites. To achieve the requisite

understanding several programs are underway. Investigation of geodetic and instrumental strain fields imposed by shot time effects to obtain source parameters will be performed. Source mechanism studies utilizing both near field and teleseismic data will provide additional needed information. Location of aftershock hypocenters will also shed light on the three-dimensional extent of shot time faulting.

Location and Frequency of Aftershocks

Following a large nuclear detonation, seismic tremors occur with great frequency in the region surrounding the detonation point. The U. S. Geological Survey (USGS) array of seismic stations, located on Pahute Mesa for the Benham Event, recorded aftershocks at the rate of 12 per minute a few hours after zero time. This activity had decreased to a few dozen shocks per day 1 month after the detonation. Within a 4 week period after the detonation an estimated 10,000 distinguishable events were recorded. This is consistent with the frequency of aftershocks observed by the University of Nevada for the Boxcar Event. For Faultless, Boxcar and Benham a sample of the aftershock events were studied to obtain precise epicenter locations. (See Figures 11.4 through 11.6.) For all three events most of the aftershocks were located close to the detonation, many apparently originating within the region affected by chimney growth.

Of more than 500 events now located for Benham, all but three aftershocks originate within 12 kilometers of surface zero. One aftershock was located 23 kilometers from the detonation and two others 25 kilometers from the detonation. It is not possible to say at this time whether these three small shocks were Benham related. Some of the epicenter determinations by the more remote U. S. Coast & Geodetic Survey (USC&GS) stations are located outside of a 12 kilometer radius from surface zero. These more remote aftershock events are being examined, utilizing the close-spaced seismic array data, to establish whether these epicentral locations do in fact extend out to 20 and 30 kilometer distances.

A sufficient number of Benham aftershocks have been located to establish that many of these tremors have epicenters which lie along a linear trend running north and south and passing about 4 kilometers from surface zero. Postshot observation reveals faulting coincident with this zone of aftershock activity. About 20 days post-Benham there was a marked increase in aftershock activity and a southward extension of about 2 to 3 kilo-
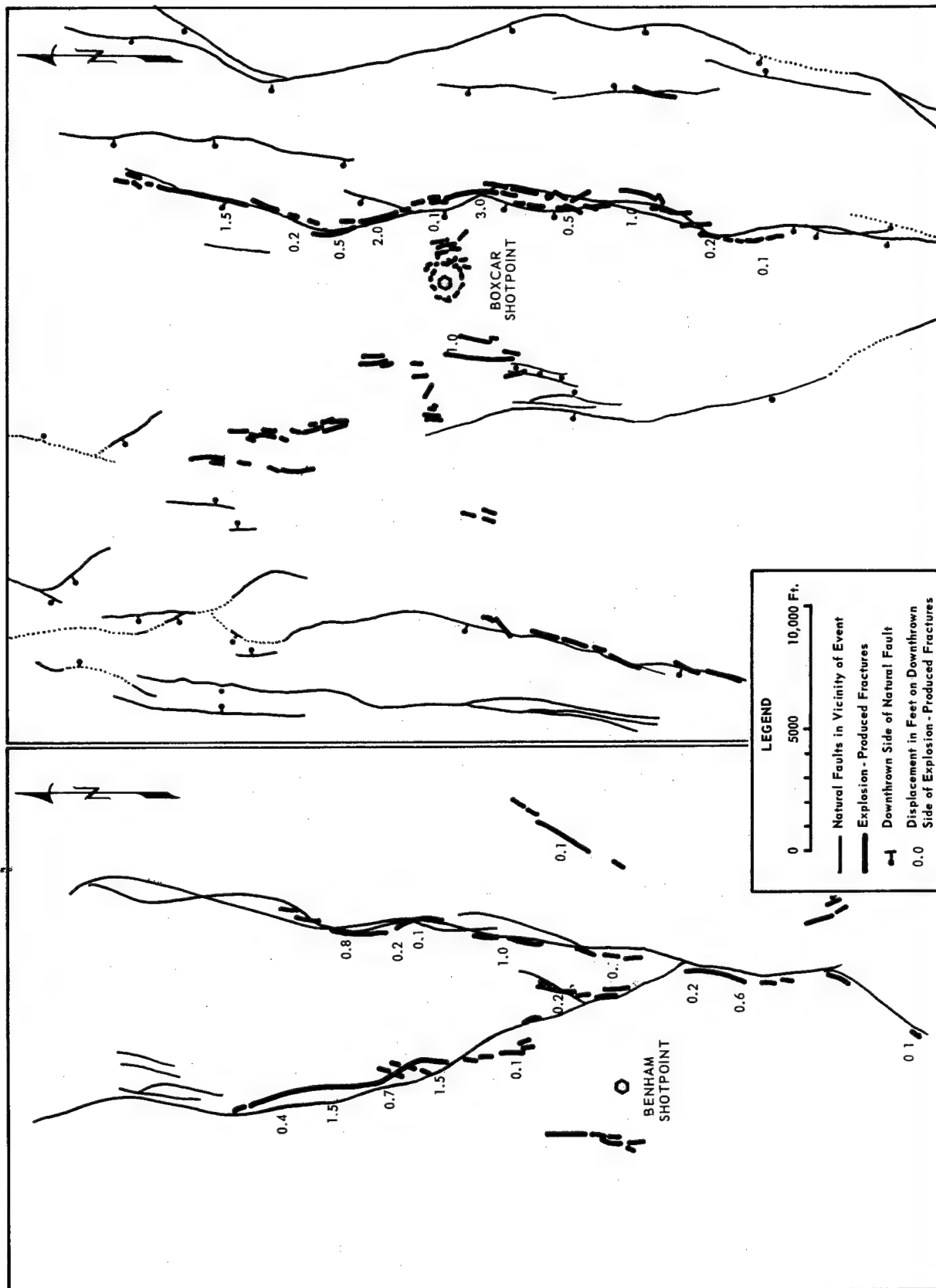
Figure 11.3. Fault Map of Boxcar and Benham Events Showing Areas Moved by Detonations[3].
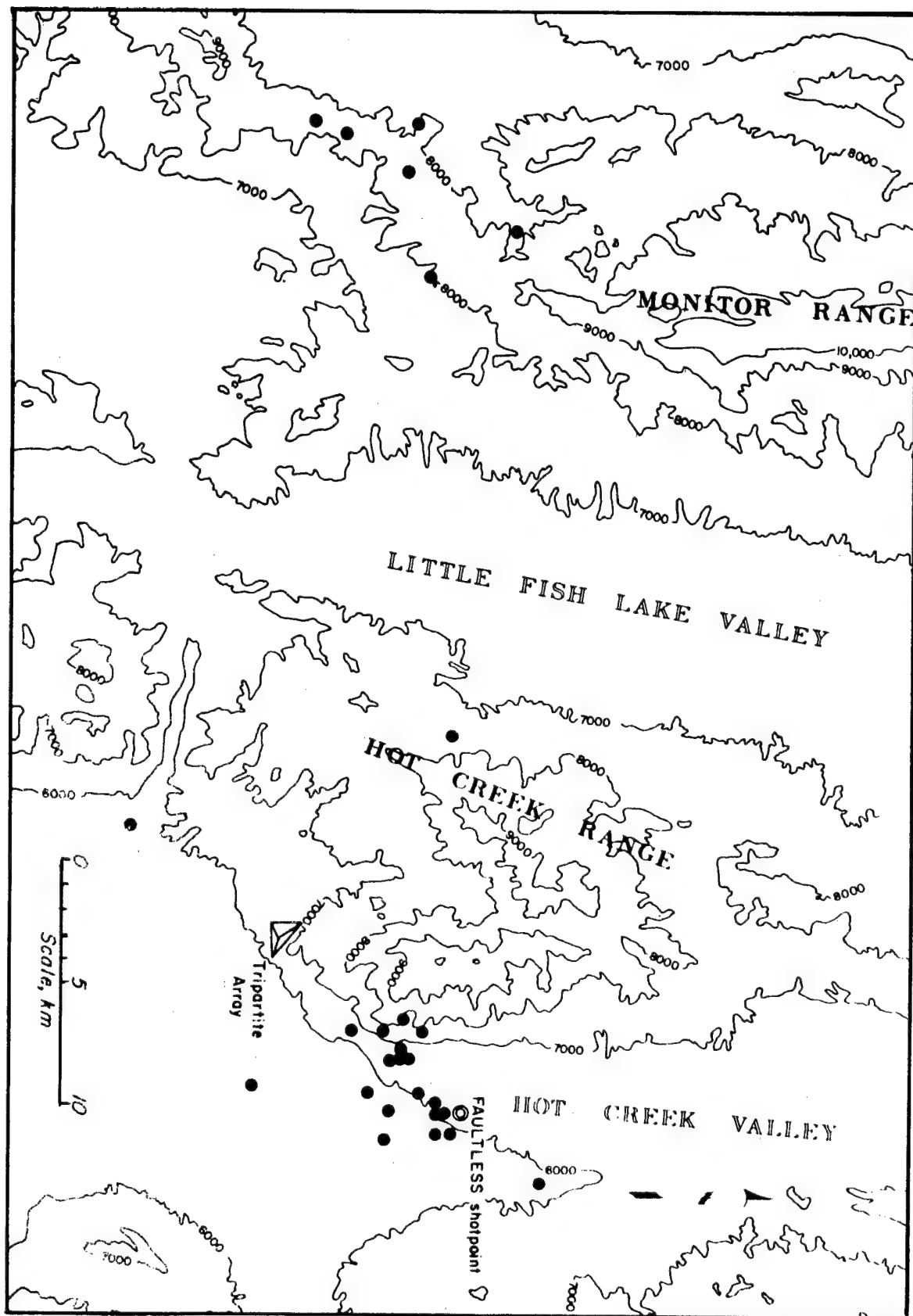
Figure 11.4. Location of Faultless Event Epicenters by University of Nevada, Reno[4].

AFTERSHOCKS DURING 31-DAY PERIOD BEGINNING 5 DAYS
AFTER THE EXPLOSION

AFTERSHOCKS DURING FIRST TWO DAYS AFTER THE EXPLOSION
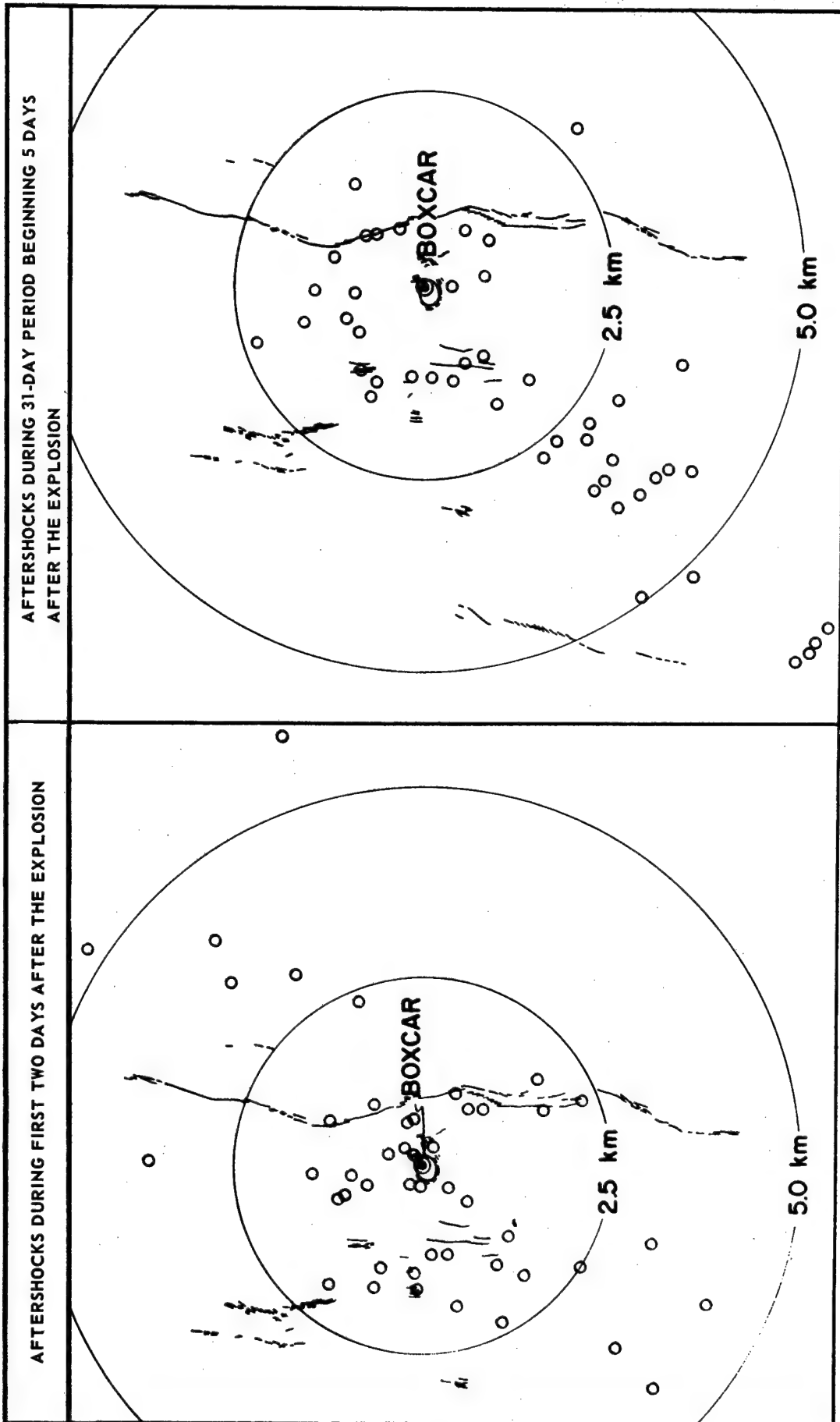
Figure 11.5.   Location of Boxcar Event Epicenters by University of Nevada, Reno[5].

233

37°22' 30''

116°37' 30''

Benham Shot Point

Outline of Pahute Mesa map

37°07' 30''
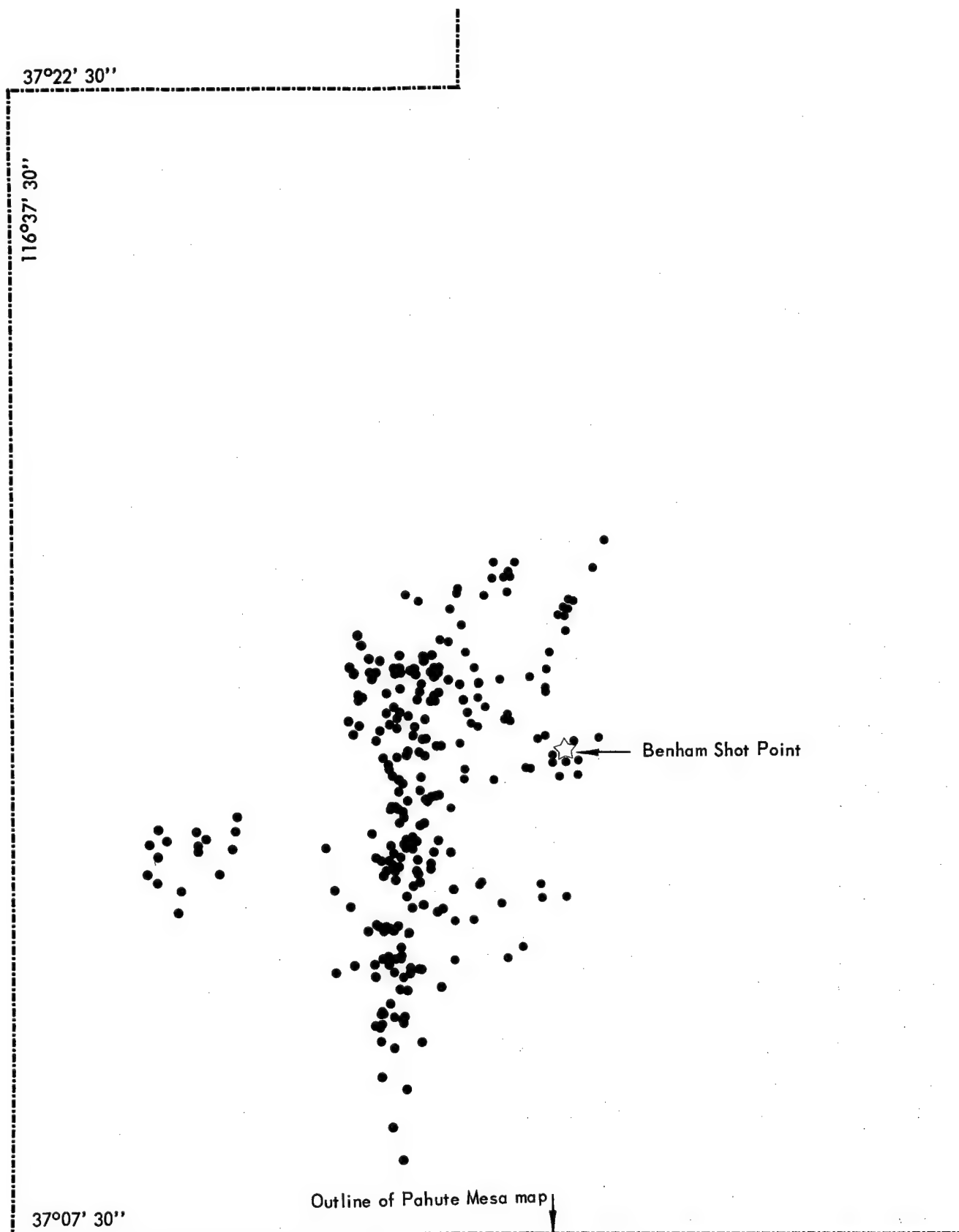
Figure 11.6. Location of Benham Event Epicenters by USGS.

234

meters in the epicenter locations. No seismic activity has been determined to be associated with the more intense faulting to the east of surface zero which occurred at shot time.

Depths of aftershocks have been determined by first arrival methods, using a velocity structure determined from data obtained at a nearby hole on Pahute Mesa. Focal depths are distributed from near surface to about 10 kilometers. No pattern of focal depths has yet been established.

SIZE OF AFTERSHOCKS RELATIVE TO NUCLEAR EVENTS

The largest aftershocks recorded to date from any nuclear event have been two or more magnitudes below the magnitude of the nuclear event. (Unless otherwise stated, magnitudes will refer to body wave magnitudes.) This determination is made by placing the aftershocks and nuclear events on an internally consistent magnitude scale. The frequency of aftershocks as a function of size appears to be similar to that observed for natural aftershocks if one omits the period of time after zero when the chimney forming processes are contributing to the aftershocks. The vast majority of events are detectable only by high gain (magnification greater than or equal to 10^6) seismic arrays. None of the aftershock events have been felt by people outside the test area. Complete statistics on relative size of aftershocks are not yet available, but the number of events reported by teleseismic and offsite stations indicate most are below magnitude 3. Work is proceeding on this aspect of the aftershock investigation.

FAR FIELD EARTHQUAKE STUDIES

STRAIN MEASUREMENTS

Two types of strain data are, or will be, available from the Benham Event. Geodetic control has been established in several selected areas, and instrumental strain meters have been installed at three locations. Geodetic control, reestablished postshot, can detect surface strains greater than 10^{-5} or 10^{-6} depending on whether a geodimeter or geodolite is used in making the survey. Geodetic control nets are established across faults which might be susceptible to movement due to the nuclear events. This susceptibility is established by virtue of proximity to the detonation and an indication of movement in the recent geologic past. Additionally, a survey and level line are established across surface zero, crossing the predominate structural trends and extending for about 6 miles in length.

Strains of 10^{-4} were observed out to 7 miles with local structure exhibiting pronounced control on the amplitude and sense of strain.

Benham postshot results are presently available from one remote geodetic net. The survey across the fault in Jackass Flats, about 30 miles from the detonation, exhibits barely detectable (above survey error) residual strains. Maximum indicated strain is about 5×10^{-4}. The The movement is consistently positive and negative on opposite side of the fault, lending credence to the measurements of low residual strain. Further analysis of this data is in progress as is data reduction for the other geodetic control nets.

Although not installed in conjunction with any nuclear event, creep gages across active fault systems in the Owens Valley, Death Valley, and the San Andreas fault zone have not exhibited any increase in creep rate due to large nuclear detonations.

Instrumental strain installations by the California Institute of Technology (CIT) were located at a distance of 30 kilometers from the Benham Event detonation, and by the Earthquake Mechanism Laboratory/ESSA and the Colorado School of Mines at distances of 28 and 71 kilometers, respectively. These installations are capable of detecting long-period or permanent strain accumulations in addition to measuring transient strains.

All three locations exhibited step-like compressional strain which decay within 1 hour to the preshot strain levels. Amplitude of the strain step was considerably smaller at the CIT installation (3×10^{-8}) 30 kilometers south of the event than for the installations 28 and 71 kilometers to the west. The latter two installations exhibited strain step amplitudes of 1.8×10^{-7} and 0.35×10^{-7}, respectively. It is not known at this time whether these amplitudes represent azimuthal variations or can be explained by strain meter orientation. The CIT installation is not radial to the event as are the other two installations. There is no permanent strain accumulation at these locations from Benham, and in this sense the event differs from the permanent strains induced by earthquakes[6]. The two installations located on the western azimuth support an attenuation with distance which more nearly agrees with earthquake observations ($\epsilon \sim R^{-3/2}$) than dislocation theory ($\epsilon \sim R^{-3}$) for a half-space model. Permanent strain installations located at Isabella, California, Salt Lake City, and Denver did not detect any permanent or long-period strain steps. Instrumental strain appears to offer quantitative data bearing directly on the relation of nuclear detonations to earthquake phenomena and will be expanded for future events.
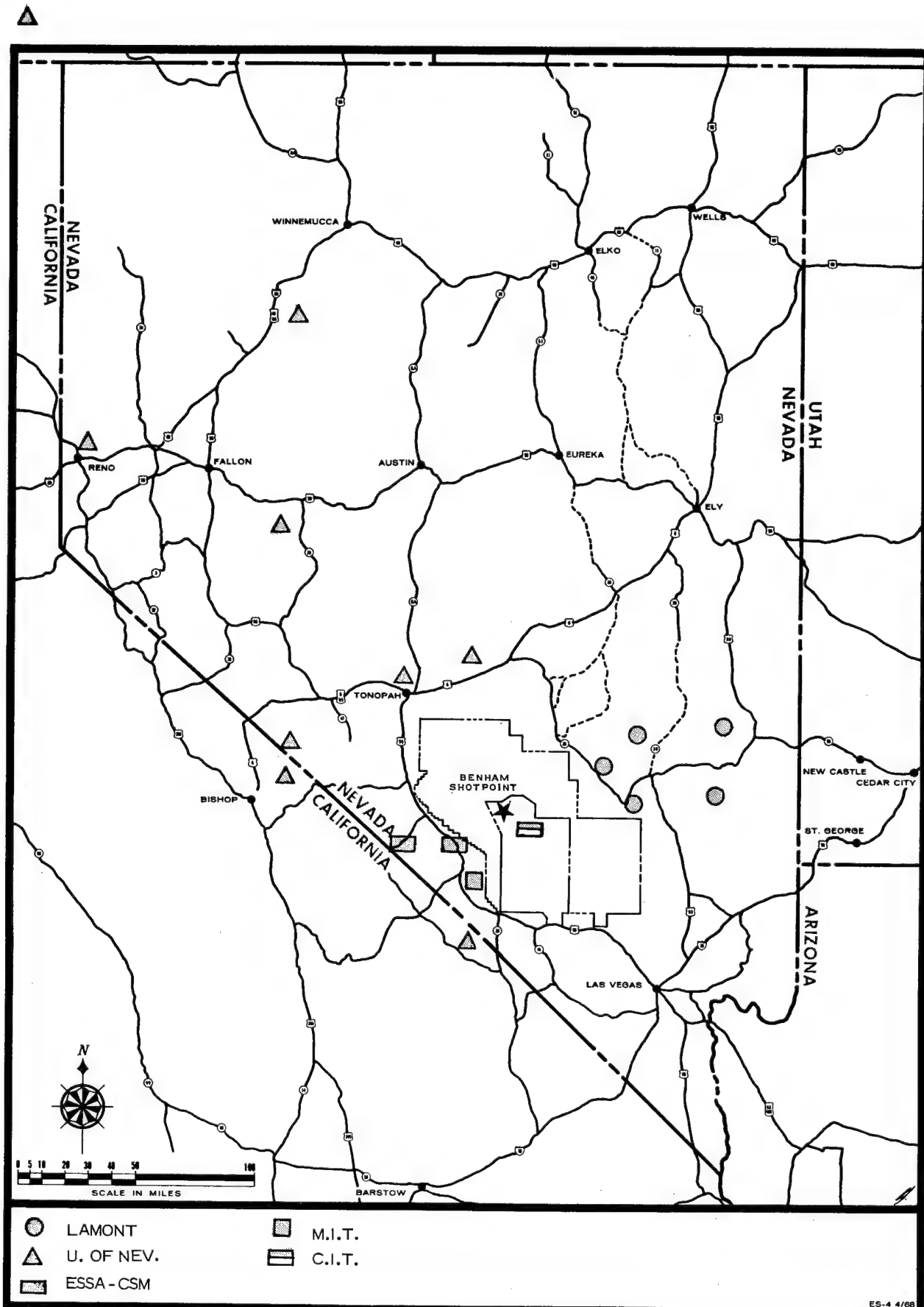
Figure 11.7. Map Showing Location of Microearthquake Station Locations for Benham Explosion.

OFFSITE AFTERSHOCK ACTIVITY RELATED TO BENHAM

Seismic stations, designed specifically to monitor microearthquake activity, were installed at 11 locations throughout Nevada and southern California. (See Figure 11.7.) Locations were selected which normally exhibit local microearthquake activity and, therefore, were more likely to be susceptible to any change in stress-strain field caused by the Benham Event. These stations were installed by University of Nevada, Lamont Geological Observatory, and the USGS[4]. All locations were monitored for a varying period of time pre- and post-Benham. None of the locations instrumented exhibit fluctuations in frequency of microearthquakes which can be related to the Benham Event.

In addition to these microearthquake stations, permanent seismic installations operated by CIT, USGS, and the University of California, Berkeley, and located in southern and central California have been examined. These stations observed no increase in local seismic events which correlated with Benham.

Thus, for Benham as for Boxcar, there is no evidence that changes in the remote strain field were significant enough to affect the level of microearthquake activity, one of the most sensitive indicators of such a change[8].

REGIONAL FAULT MAPPING

Prior to the Benham Event, all faults which showed evidence of recent movement in the region surrounding the Nevada Test Site were covered by aerial photography. If aftershock monitoring indicated any postshot seismicity in these areas, they were to be rephotographed and examined on the ground. None of the suspected areas have shown any seismicity and none of the more highly suspect areas, those with geodetic control, have shown any visible fault motion.

In summary, the following conclusions may be established to date:
1. All earthquake and aftershock activity due to large nuclear detonations has been much smaller in magnitude than the responsible nuclear detonation.
2. Nearly all aftershock activity is confined to a region within 12 kilometers of the detonation. A few very small aftershocks may originate as remote as 20 to 40 kilometers. These few remote events may or may not be part of an already occurring microearthquake pattern, but at this time cannot be conclusively related to the preceding nuclear event.

3. No increase in seismicity related to large nuclear detonations has been noted in normally seismic areas located away from the Nevada Test Site.
4. No permanent strain due to the nuclear detonation is observed at distances of 30 kilometers and greater for the one high-yield event instrumented to date.
5. Additional information and analysis are required, and are proceeding, to gain sufficient understanding of these phenomena to permit increases in yield and utilization of new test locations with confidence that safety of surrounding regions will not be compromised.

REFERENCES

1. F. A. McKeown, D. D. Dickey, and W. L. Ellis, "Maps and Classification of Explosion-Produced Fractures in Yucca Flat, Nevada Test Site," U. S. Geological Survey Tech. Letter: NTS-195, Supp. 1, Dec. 11, 1967 (C/FRD)

2. F. A. McKeown, D. D. Dickey, and W. L. Ellis, "Preliminary Report on The Geologic Effects of the Faultless Event," U. S. Geological Survey Tech. Letter: Central Nevada-16, March 25, 1968

3. D. D. Dickey and W. L. Ellis, "Principal Linear Fractures Resulting From Nuclear Explosions in Pahute Mesa," U. S. Geological Survey Tech. Letter: Special Studies-67, July 22, 1968

4. G. Boucher, A. Ryall, and A. E. Jones, "Triggering of Earthquakes by Underground Nuclear Explosions," Seismological Laboratory, Mackay School of Mines, Univ. of Nevada, Reno, Nevada

5. A. Ryall and W. Savage, "A Comparison of Seismological Effects for the Nevada Underground Test Boxcar and Natural Earthquakes in the Nevada Region," Seismological Laboratory, Mackay School of Mines, Univ. of Nevada, Reno, Nevada, Feb. 1969

6. P. R. Romig, M. W. Major, C. J. Wideman, and D. Touher, "Residual Strains Associated with Benham," Report to the AEC, Las Vegas, Nevada, Jan. 29, 1969

7. F. A. McKeown and D. D. Dickey, "Maps of Explosion-Produced Fractures in Yucca Valley, Nevada Test Site," U. S. Geological Survey Tech. Letter: NTS-195, Supp. 2, Dec. 4, 1968 (C/FRD)

8. Post-Benham Ground Motion and Aftershock Meeting Sponsored by AEC/NVOO, Jan. 29, 1969

Chapter 12

MINE AND WELL INSPECTION PROGRAM

Paul L. Russell, *Research Director,* Denver Mining Research Center,
Bureau of Mines, Denver, Colorado

INTRODUCTION

The Atomic Energy Commission in its concern for the safety of private mines and oil and gas wells in the vicinity of planned nuclear detonations fully recognizes the legal responsibility of the U.S. Geological Survey and the U.S. Bureau of Mines for private operations conducted under lease on Federal lands. The technical competence of these agencies in geology, engineering, and safety fully qualifies them to conduct safety programs relative to other private mines or wells regardless of their location.

The U.S. Bureau of Mines, at the request of the Atomic Energy Commission, has the responsibility for the overall coordination and execution of mine and well examination and safety surveys as defined under this section of the Safety Program.

Purpose of Mine and Well Inspection Program

The purpose of the Mine and Well Inspection Program is to establish a system of controls to assess and evaluate any damage to a mine or oil or gas well alleged to be the result of the detonation of an underground nuclear device. In the event that damage should occur, information from this program would be used to support payment of claims for reasonable compensation. If, on the other hand, claims are made for damage that cannot be attributed to the nuclear explosion, then the same information would be used to refute such claims.

Initial Planning

Conceptual planning of nuclear experiments must include safety measures which assure protection of the public. Under the direction of the Effects Evaluation Division, U.S. Atomic Energy Commission's Nevada Operations Office, a Panel of Safety Consultants, other Government agencies, and contractor organizations are requested to study each project from the standpoint of safeguarding the public and the project participants and preventing or reducing damage to private, industrial, or other facilities. A Mine and Well Inspection Program is proposed by the Director, Effects Evaluation Division, AEC/NVOO, on the basis of information developed by these studies.

Program for Development of Data and Control Procedure

The mine and well examination and safety surveys are conducted before and after a nuclear event. The purpose of the initial survey is to examine and document the preshot condition of mines, wells, and associated surface facilities and, if warranted, develop recommendations to install protective shoring (Figures 12.1 and 12.2), reduce pipeline pressure, or take other measures to prevent or reduce damage potential. The postshot survey includes reexamination of facilities and areas surveyed before the event, the recording of any physical changes, and the determination of the probable cause of such change. At shot time, necessary arrangements are made to insure safety of operating personnel and property.

Work starts long before an event takes place. The earliest work is to document all mines around the proposed shot site based upon the predictions of anticipated ground motions. Generally all mines within a range of 0.01g are included. A "desk survey" using all information that can be found that designates name, location, description, owner, and history of the mine or well is completed. This information is consolidated into a preliminary report for the AEC and U. S. Bureau of Mines use only.

Damage effect calculations (made by others) are then used to estimate the actual effects area around the nuclear shot. A field survey is made to determine the location, ownership, condition, and history of mines and wells in the area where moderate ground motion effects may be expected; this is usually at a range of 0.1g. On the basis of this field survey the actual mines or wells are selected that will be covered by the preshot and postshot surveys. Owners are contacted by AEC or by the U.S. Bureau of Mines for permission to make the planned surveys. Some mines or wells may be included in the survey solely on the basis of a request by the owners or operators to do so.

The scope and magnitude of effort on any particular nuclear test varies in direct ratio to the number of nearby
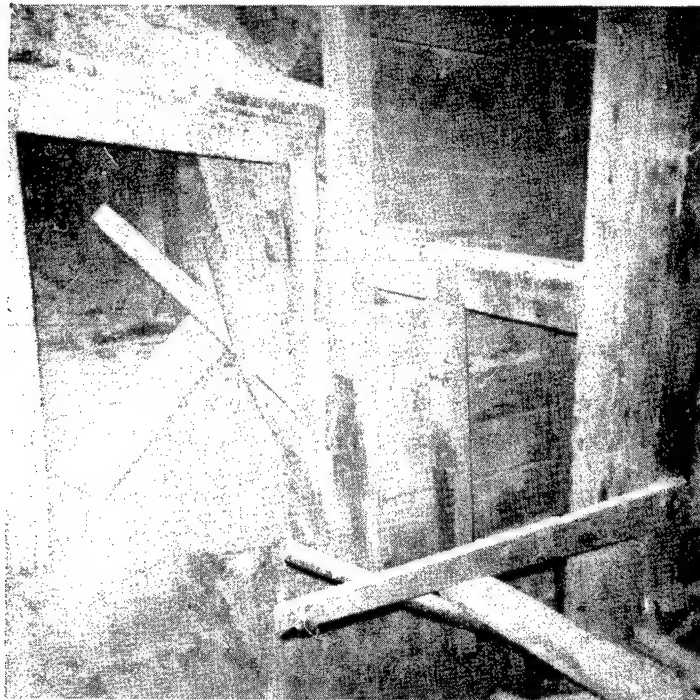
Figure 12.1.   Typical Example of Mine Shaft Before Construction of Protective Shoring.

Figure 12.2.   Cribbing Installed as Protective Shoring in Mine Shaft.

240

mines or oil and gas wells. If the wells and mines are idle the work effort is less than for a highly productive mining operation or well field. The number of people and technical skills required are also a function of location for the nuclear test. The maximum requirements to date have included one or more people from the following agencies: U.S. Geological Survey, U.S. Bureau of Mines, U.S. Coast and Geodetic Survey, U.S. Public Health Service, local State inspector of mines, Sandia Corporation, Holmes & Narver, EG&G, Inc., and representatives of the specific mine or oil and gas well company involved. Each agency provided one or more services within its area of specialization.

Test Environment Studied

The Mine and Well Inspection Program considers only mines, surface and underground; wells, gas and oil, either producing or nonproducing; and oil and gas pipelines used as any part of a collection or distribution system. The surface plant directly connected with either the mine or well is considered a part of the mine or well for the purpose of this survey. Where required, qualified structural or petroleum engineers are provided by either the U.S. Bureau of Mines or other participating agencies for preshot and postshot documentation of any critical surface and underground structures.

Effects of Underground Nuclear Testing on Environment

The preshot and postshot inspection program is designed so that areas considered vulnerable to motions caused by nuclear testing are documented to indicate any changes between preshot and postshot inspection. Such areas are selected by Government engineers and by company engineers, or by both. If damage of any kind should occur, it and its effect upon the company operation is evaluated by those expert in that area.

Company Cooperation

Little, if any, of this Mine and Well Inspection Program could be conducted without the cooperation of mine or well owners and companies involved. In the case of idle or inactive mines or wells, cooperation may consist only of access to records and permission to enter the property. In the case of large operating mines or oil and gas fields, extensive cooperation is desired to obtain mine maps, well logs, details of operation including rate of ore, gas, oil, or other production, types and conditions of wells and shafts; water problems, if any; access to wells and all shafts for detailed inspection; engineering advice concerning mine or well conditions from a structural, geologic, or other viewpoint; knowledge of critical areas;

assistance in locating and installing various types of instrumentation for safety evaluation purposes; and a variety of other information and assistance aimed at providing the best system of controls for use in evaluating any damage that might occur.

Scope of Work

Using the proposed Mine and Well Inspection Program as a basis, meetings are held with each individual mining company or oil and gas well operator that might be affected or concerned by the planned nuclear detonation. Specific problems of each operator are considered. If required, the basic inspection program is modified to include special problem areas of any operator. Thus, in an area where several operating mines and well producers are involved, the inspection program may differ at each facility. A willingness by the Government to modify its program to fit needs expressed by the local operators is essential if industry cooperation for the program is to be obtained.

All Government work is performed on a noninterference basis where possible. However, certain operations, such as inspection of an ore production shaft, may require loss of production as may the need to reduce pressure in a distribution oil or gas line or the closing down of a well or wells during shot time. Often production is on a 24-hour day, 7-day week schedule. In such cases, compensation for lost production may be required, depending on company policy.

Since the problem of mine or well safety is commonly of mutual concern, company cooperation is usually easy to obtain. However, the extent varies with company personnel and with company policy. Diplomacy and tact by the Government agencies involved is a must if the benefits of full cooperation are to be achieved.

DESCRIPTION OF PROGRAM

Obviously a detailed description of each individual type of investigation cannot be given in the space available here. The following briefly describes each major area that may be investigated.

Shaft Inspection

In underground mines, this is the most important single structure of the mine. All men and supplies must enter the mine through the shafts, and all ore reaches the surface through the shafts. Shaft excavation is slow and expensive, with costs ranging from hundreds to thousands of dollars per foot. Shaft linings may seal out underground water that would otherwise prevent mining.

Possibility of damage to shafts is greater than to mine tunnels, and repair is more expensive. Usually a struc-

tural engineer conducts the shaft inspection. A mining engineer or geologist, a photographer and a company engineer ride or climb through every foot of shaft; they note cracks in the lining or in the rock walls, inflows of water and volume, weakness in any timber or steel structural members, and other features that might be affected by the planned nuclear detonation. Preshot and postshot photographs are taken of major features noted. Shaft construction drawings, if available, assist in this work.

At least one and possibly two preshot inspections are made and at least one postshot inspection. A preshot inspection is made as close to shot time as possible and a postshot inspection is made as soon as possible after the nuclear detonation. Inspection notes, maps, and photographs are compared to determine the effect, if any, of the nuclear detonation on the shaft. Pumping records are compared with preshot records for some weeks after the shot to determine if water inflow increases or decreases.

Mine Inspection

Mines examined under this program range from small prospect drifts to very large complex operations producing thousands of tons of ore per day. While the very small mines may be easy to document by detailed examination and photography, such work is seldom warranted. On the other hand, large producing mines contain too much area to permit detailed inspections such as those made in shafts. In all mine inspections, large or small, the objective is to examine and document all working areas or areas deemed critical by mine management. Figures 12.3 through 12.8 are illustrative of preshot and postshot photographic documentation.

Structure Inspection

The surface plant is considered a part of the mine or well for the purpose of this survey. Here again the size of the mining or well-field operation governs the amount of work required. Surface facilities around idle mines or wells may require little work effort, while a large mine and mill surface plant may require several days to examine. A qualified structural engineer is provided by a participating agency and all critical surface and underground structures are documented before and after the detonation.

Ground Surface Surveys

Where underground mining is such that the surface subsides into the underground workings, it is important that this rate of subsidence be controlled. Subsidence rates preshot and postshot may be obtained by ground surface profile surveys. Increase in rate of subsidence may reflect effects of nuclear blasting.

Radiation Surveys

The U.S. Public Health Service provides a radiation monitor to accompany all inspection parties. Many people are not aware of the background radiation count in their area and preshot surveys are made to establish this basic level both on the surface and underground. Following the nuclear test, radiation counts are again made for comparison with preshot data. In some cases, mining companies and miners have expressed concern that radiation might migrate underground from the detonation point into the mines. Where such migration is conceivable monitor surveys may be continued for months, or possibly years.

Seismic Surveys

Seismic instrumentation may be used to record acceleration and displacement on the surface and underground that result from a nuclear detonation. The order-of-magnitude of these measurements is a guide to whether damage might occur. Where a mine is in production, seismic records of normal and well operations are made. These measurements are compared with those measured from the nuclear detonation to assess the effect of the nuclear detonation at that location. In many cases, normal records show higher readings than those made of the nuclear detonation.

Microseismic Surveys

Tests have shown that when rocks are stressed the microseismic rate—that is, the number of microseisms generated per unit of time—increases with the applied stress. The increase in the rate is most pronounced as the ultimate strength is approached.

This characteristic of rock is used to determine the relationship of the stresses produced by normal blasting for ore production in mines with the stress developed in the same test area as a result of nuclear detonation. The microseisms produced by the Gnome nuclear event are shown by Figure 12.9. Note that in the case of this nuclear detonation, both the noise level and the time required to return to normal background level was less than for normal ore blasting.

Stratascope and Roof Sag Instrument Surveys

Convergence stations may be used to measure roof sag and differential roof sag in areas where pillar robbing will ultimately result in caving. The purpose of such stations is to determine normal convergence prior to a nuclear detonation and determine convergence rate change, if any, following the detonation. Holes are drilled upward into the roof stone and visually examined by using a
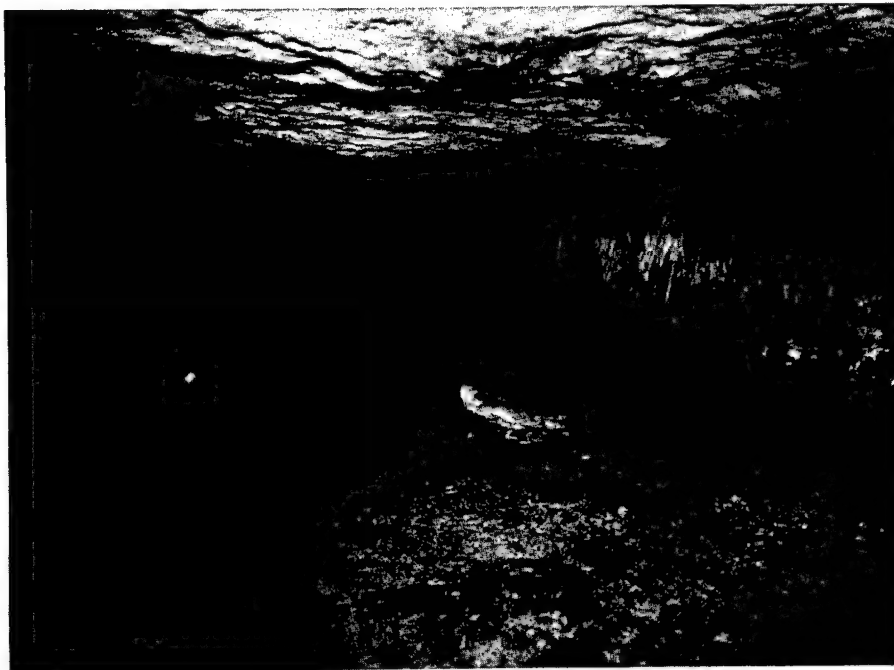
Figure 12.3.   Preshot Stalactites in Idle Mine Section.

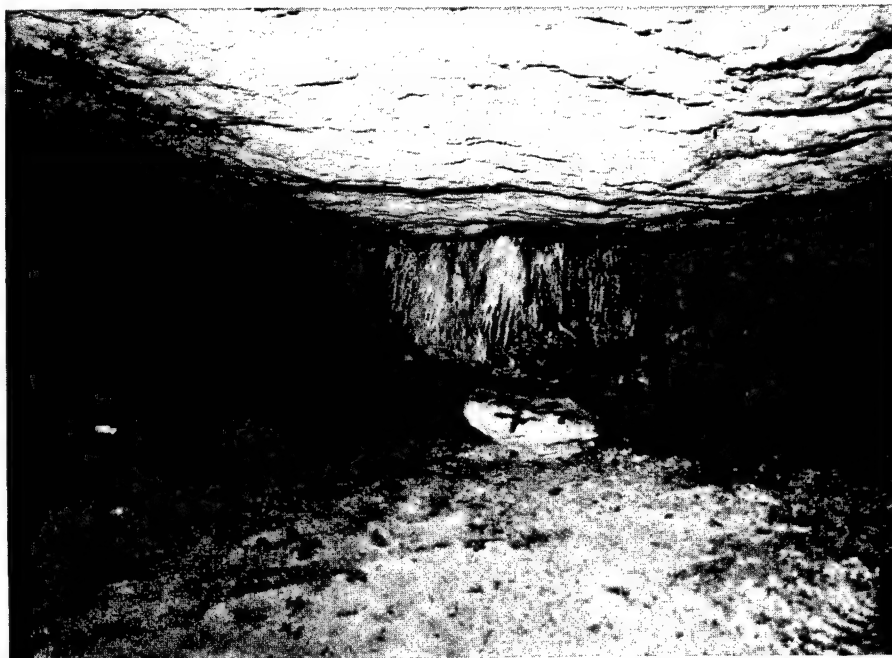Figure 12.4.   Postshot Stalactites in Idle Mine Section.
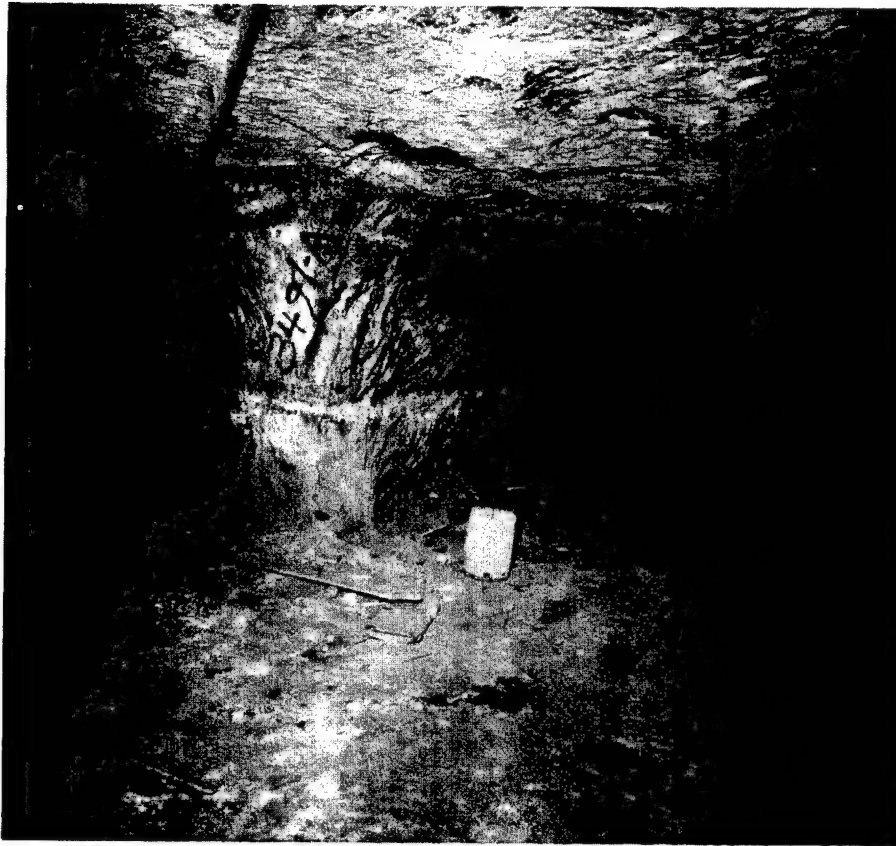
Figure 12.5.   Preshot Support Pillar After Final Mining.
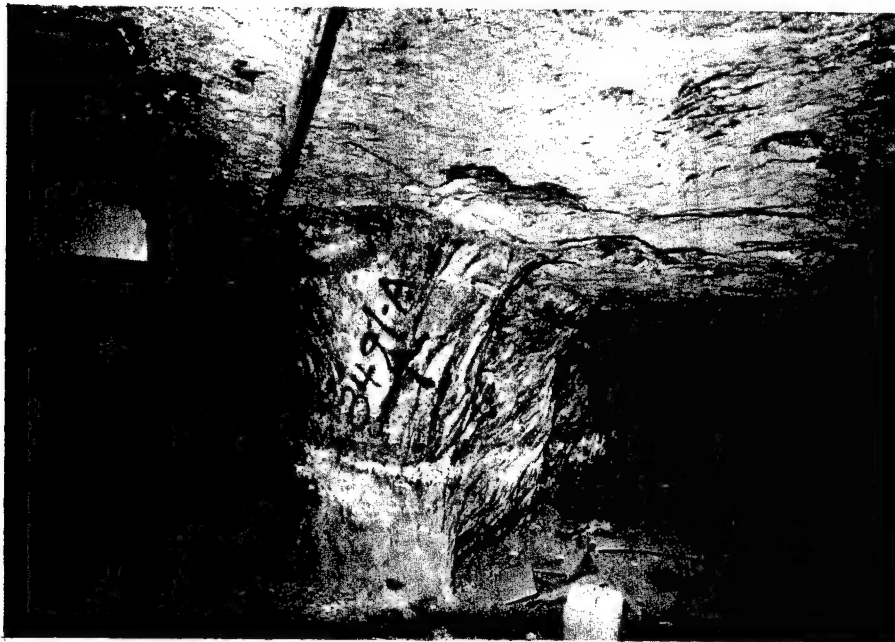
Figure 12.6.   Postshot Support Pillar After Final Mining.
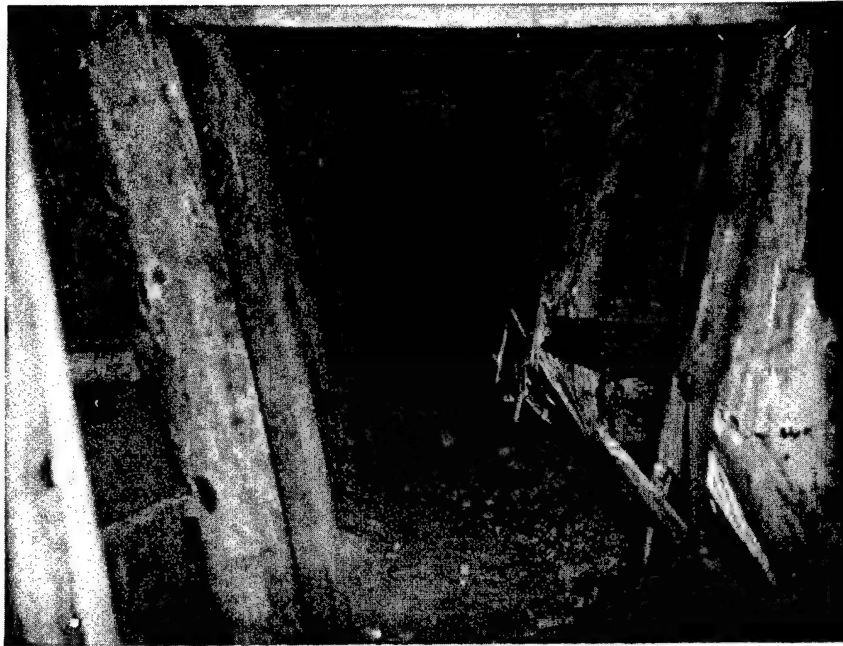
Figure 12.7. Preshot Timber Failure in Stope Area of Sheelite Mine.
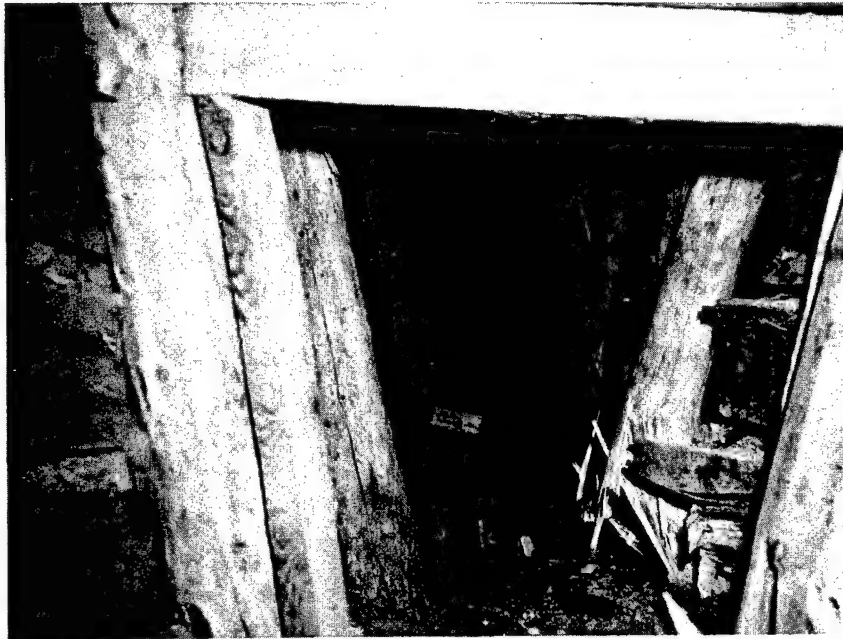
Figure 12.8. Postshot Timber Failure in Stope Area of Sheelite Mine.

245
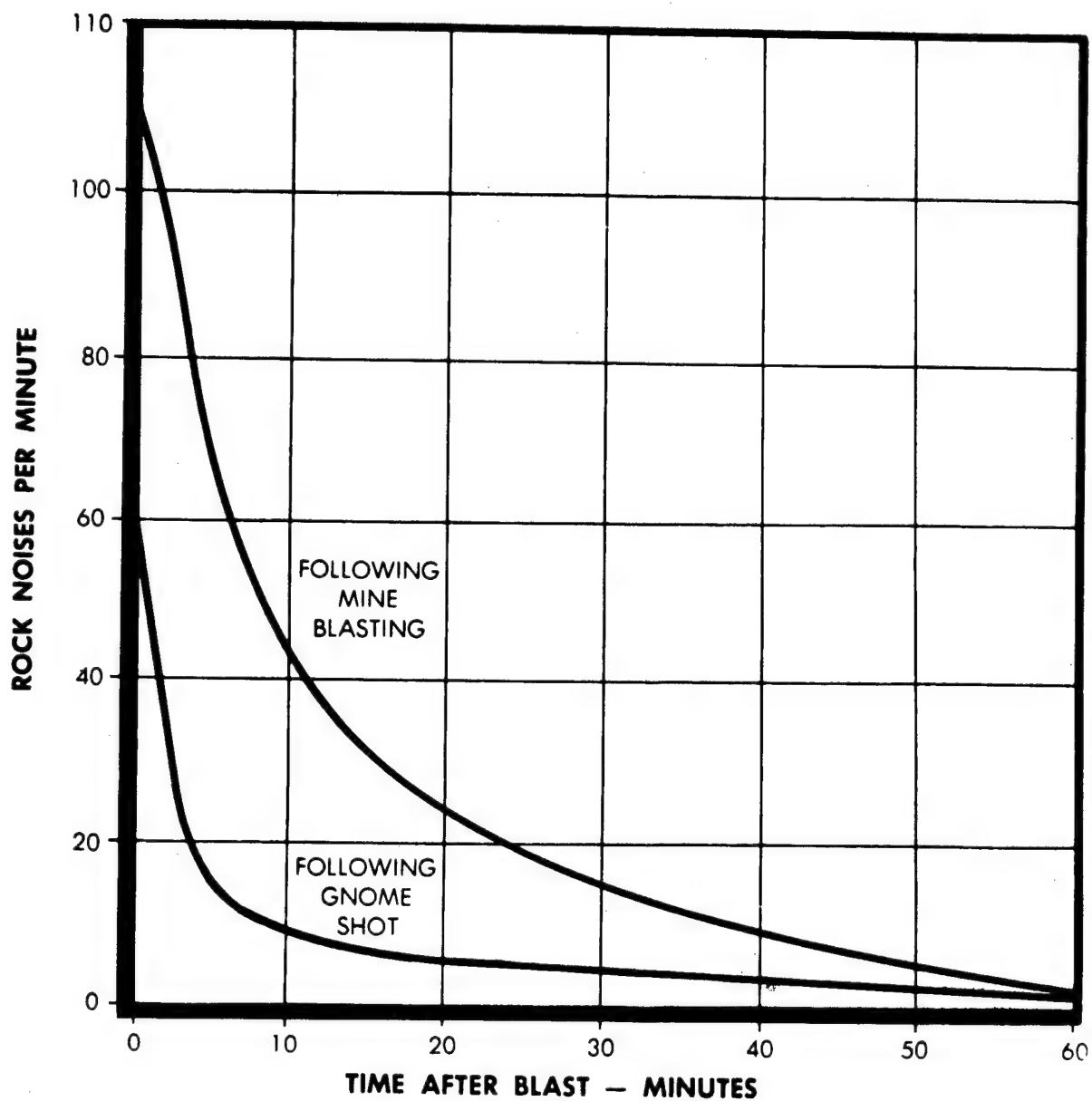
Figure 12.9.   Rock Noise Rate Following Mine Blasting and Gnome Shot.

246

stratascope as shown in Figure 12.10. Using this same instrument, pictures are made of cracks or bedding separations. Using the information obtained, metal measuring points are installed in other holes drilled into the roof and floor (Figure 12.11).

Using an instrument called an extensometer, the distance between roof and floor pins is measured to one-thousandth of an inch, and the rate of convergence or roof sag is calculated. Figure 12.12 shows the roof convergence rate at one of the potash mines in New Mexico for a period before and after the Project Gnome nuclear detonation. No change was noted in convergence rate following the Gnome nuclear test.

Oil or Gas Well Surveys

Documentation of oil or gas wells follows the general pattern for mines. However, since it is not always convenient to the company to inspect a well bore it is necessary to rely more on company records. For wells of special interest (because of known conditions or location in relation to ground zero) geologic logs, details of casing installation and condition, well pressures, and any special features are recorded. Preshot and postshot production records may be made for determining effects. Instruments may be installed where it appears they may be effective. Surface features and equipment are documented. Preshot and postshot radiation counts may be made. In fact every condition that will help in determining nuclear detonation effect upon a well is made and analyzed before and after the detonation.

Water Level Surveys

Measurements of water table levels and rate of flow are recorded in mines and shafts, where possible. Preshot and postshot water level measurements may show that flow has increased or decreased. In either case the effect may have been caused by the nuclear detonation, and further investigations may be made. If flow and level remain stable, it is assumed that the nuclear detonation had little effect to the shaft.

Other Instrument Surveys

Particular conditions in certain areas may require instrumentation of a special nature. An example of one such case was the monitoring of vibrations produced by the Gnome event at a potash refinery in New Mexico. In this case the plant was old and contained a high-pressure boiler plant and numerous high-pressure steam lines. The plant was instrumented to measure vibrations caused by the nuclear test. No damage was noted.

Photographic Documentation

Preshot and postshot photographs are taken of critical areas of mines and wells as determined by company and Government engineers. These photographs provide excellent reference data for use in determining just how any particular area reacted to a nuclear detonation. Photography can be used to record even very minor changes in appearance and is used to document almost every phase of the Mine and Well Inspection Program.

Reentry (Postshot Examination)

Management or union regulations may require that all workmen be removed from underground or surface mines as well as from oil or gas well area and facilities at the time of a nuclear detonation. At company request in such cases, reentry or postshot inspections are performed before men return to work. Special reentry teams make preshot and postshot inspections for the purpose of noting any change that may have resulted from the nuclear detonation. These reentry teams usually consist of representatives of the following agencies: U.S. Bureau of Mines, Safety Division; a State inspector of mines; U.S. Geological Survey; U.S. Public Health Service; structural engineer, and one or more representatives of mine or well company management. These teams make a preshot inspection the day preceding the shot and a postshot inspection immediately following the shot.

PUBLIC AND INDUSTRY ACCEPTANCE

The Mine and Well Inspection Program has been an effective one, and generally well received by the industry. Perhaps too well at times as requests for examinations are often from quite remote areas to the test location.

Often the first reaction from industry is that they really do not expect damage, but why not do this whole thing somewhere else. However, once it is established that there is to be a nuclear test, full cooperation to develop and participate in the Safety Program is usually forthcoming. Public and industry attitude is changing and will change more as experience is gained in the use of nuclear explosives and evidence is demonstrated in the ability to correctly predict effects from such detonations.

CONCLUSIONS

The U.S. Bureau of Mines takes an active part in the Mine and Well Inspection Program and feels that this is a dual role in protection of both Government and industry. This program has been successful to date because of the splendid cooperation received from other participating agencies and from industry.
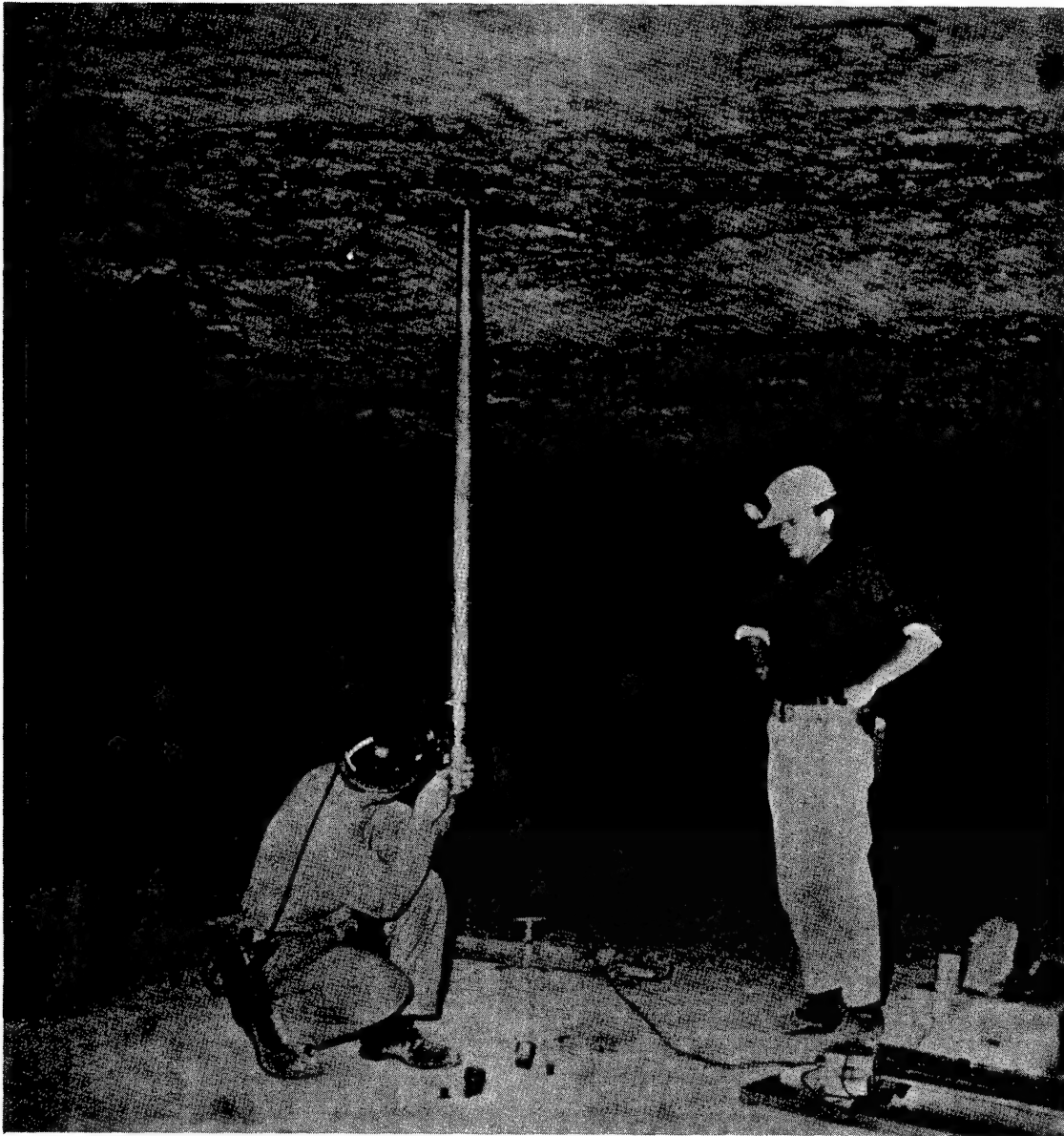
Figure 12.10.   Method of Using Stratascope.

248
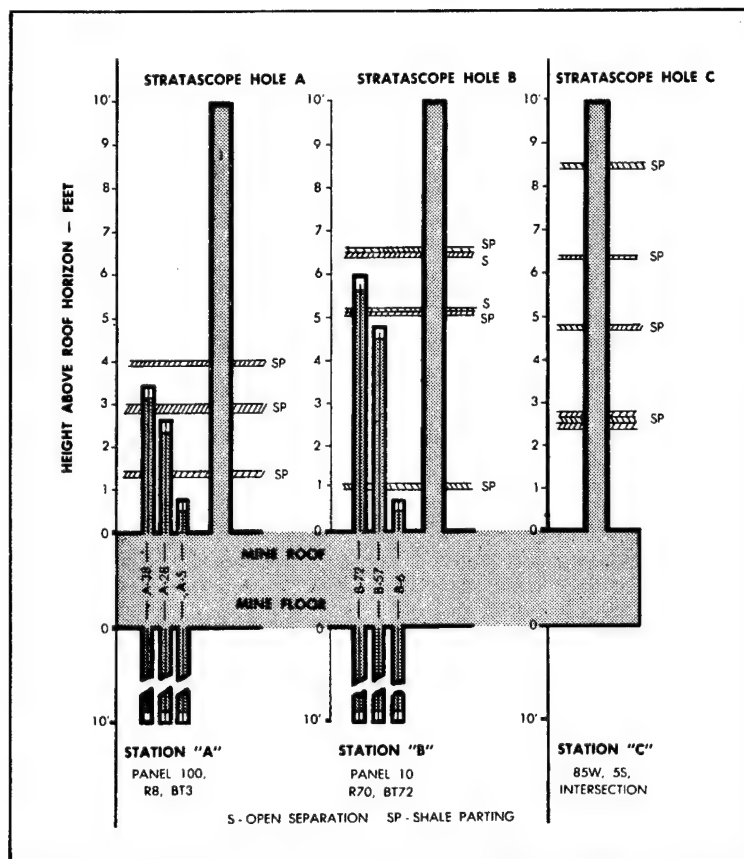
Figure 12.11.　Mine　Section　Showing　Location　of　Sag　Pins.
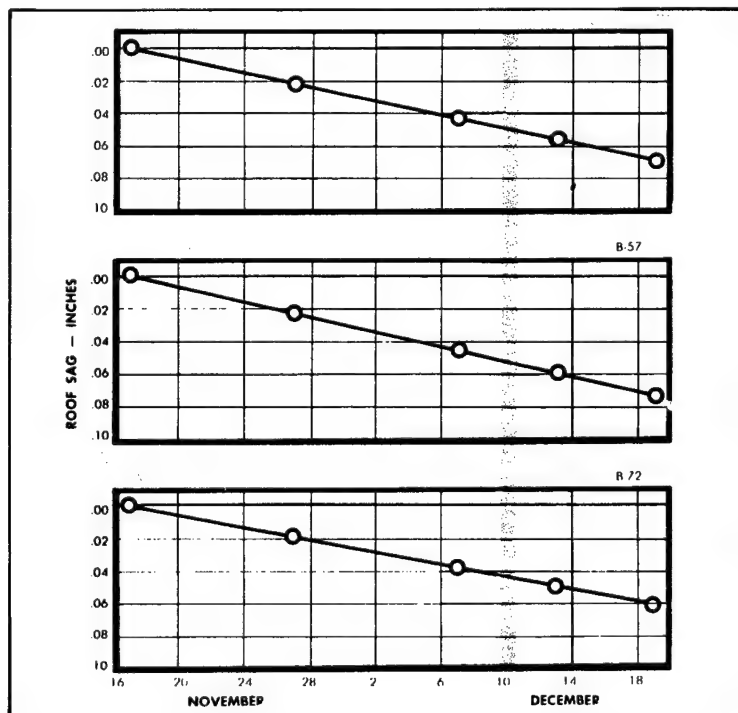
Figure 12.12.　Rock　Sag　Rate　Following　Mine　Blasting　and　Gnome　Shot.

249

Chapter 13

METEOROLOGY AND NUCLEAR DETONATION SAFETY

U.S. Department of Commerce
Environmental Sciences Services Administration Research Laboratories

Part A — Atmospheric Transport of Radioactive Effluents

Phillip W. Allen, *Chief*
Air Resources Laboratory—Las Vegas, Las Vegas, Nevada

ABSTRACT

Airborne radioactive materials are transported and dispersed by atmospheric motions, knowledge of which aids in scheduling nuclear experiments and planning safety actions in such a way as to minimize any radiological hazards. Properties of the atmosphere that influence safety decisions include wind, trajectories, thermal and mechanical turbulence, and precipitation. These and other atmospheric parameters are measured in an appropriately scaled observational network and changes are predicted using conventional numerical techniques and techniques that have been developed for the local area. Some of the more important recent developments in knowledge of air motion and in prediction techniques are described. There are limitations on the accuracy of predictions, and a review is given to the effect of these limitations on nuclear test safety.

INTRODUCTION

In recent years, nearly all underground nuclear tests have either released no radioactive material to the atmosphere or released so little that it could not be found beyond the boundaries of the Government reservation. In each such test, however, the safety organization proceeded as if the worst kind of accidental release would occur, and made its plans for controlling people and activities downstream in such a way as to eliminate human exposure, or if that should prove to be impractical then to minimize it.

The AEC could, without consideration of wind directions or meteorology, prepare to exercise radiological safety measures in all directions to great distances for each test. Instead, to reduce cost and inconvenience to people, the AEC made use of evaluations of radiation hazards that are possible from knowledge of the atmosphere, the probable motion it would give to any debris cloud of released radioactivity, and its ability to dilute and deposit the airborne radioactive materials along that path. The responsibility for evaluating these atmospheric effects has been assigned by the AEC to the Environmental Science Services Administration, which has established the Las Vegas office of its Air Resources Laboratory to provide this service.

The Air Resources Laboratory has studied the meteorology of air pollution, both radioactive and industrial, for more than 20 years. The Las Vegas office (ARL-LV) has been studying the meteorology of radioactive clouds at the Nevada Test Site since 1956, which was during the period of atmospheric testing. It has participated in all continental nuclear explosive tests since that time and some of its personnel have experience with the Pacific test program, which ended in 1962.

ARL-LV handles the hazard evaluation in two closely coordinated technical areas. One is the measurement and prediction of atmospheric processes which is presented in Part A and the other is the evaluation of the effects of these processes on the dilution and deposition of radioactive effluent as given in Part B. The latter area is commonly, but inaccurately, called radiation prediction. The only real prediction into future time that we do is with respect to the atmospheric processes which distribute the radiation. This laboratory thus addresses itself to these questions: Where will any radioactive effluent go and with what maximum radiation intensities and, if a release of radioactivity has occurred, where did the wind actually take it?

METEOROLOGICAL INFORMATION REQUIRED FOR SAFETY

Effective planning for the radiological safety of nuclear explosions begins with the selection of a detonation site, if this is other than the Nevada Test Site. It includes the

251

layout of supporting facilities wherever the test is to occur. Sites and aboveground construction are planned by the AEC with consideration of the frequencies of wind directions and speeds, cloudiness, precipitation and other factors. In some cases it is necessary to decide far in advance that the detonation will occur only when winds meet certain direction or speed criteria, or when certain visibility, cloud height, or precipitation criteria are met. Climatological data are then obtained, either from weather archives or by an observation program, that will indicate the frequency of occurrence of such conditions, their predictability, and hopefully some of the associated radiological problem areas such as frequent shear characteristics, trajectories, or the existence of variable local currents along the desired trajectory.

Nuclear detonations are carefully timed to occur under weather conditions that meet safety requirements or under conditions within which positive and readily attainable emergency measures can be taken to ensure human safety. All detonations can be cancelled or postponed by the Test Manager up to within a few minutes of the detonation time so that late changes in weather can and sometimes have resulted in last-minute schedule changes.

To aid in making final preparations for detonations, safety and weather briefings are held on the afternoon of the day before, and again a few hours prior to the desired detonation time. A final time schedule is decided as a result of the latest briefing, if wind and weather conditions are acceptable. If conditions are not acceptable, the detonation is rescheduled, sometimes by short time increments until acceptable weather is observed in a persistent or regular pattern, at which time the device is fired. Sometimes it is rescheduled to some subsequent date to allow for a major weather change or for some other reason.

The information provided in safety and weather briefings is illustrated schematically in Figure 13.1. Sea level pressure, upper air streamlines, or other charts, not illustrated, provide background information on the current weather. The upper left chart, Panel 1, shows the predicted streamline field at some level above the surface, usually 10,000 feet mean sea level (m.s.l.), for the detonation time. The predicted winds in 1000-foot layers above the surface over the detonation point, showing the expected vertical shear, are in Panel 2 and changes in these winds with time are illustrated in Panel 3. These winds define the initial trajectory of any released radioactive material. The shears are important to the evaluation of radiation levels. A predicted temperature lapse rate over the test area is in Panel 4. Two or more lapse rates are often given to show the changes with time that are expected from solar heating or cooling, and from ad-

vection processes. These lapse rates are used in the radiation computation to determine rates of vertical mixing and diffusion of released debris.

Panel 5 illustrates the local and Panel 6 the long-range scales of trajectory forecasts that are useful to outline the geographical areas that are expected to be traversed by air containing radioactivity. Within the context of this paper such an air mass is referred to as a radioactive cloud, or just cloud. The controls to be exercised over the Test Site and adjacent areas are determined in part from the prediction of the local cloud path.

The maximum radiation levels expected downstream are presented by means of dose versus distance curves illustrated in Panel 7. The presentation in Part B will explain the possible variations in these curves and techniques for arriving at the estimates.

Clouds and precipitation over the southwestern states and especially along and around the expected path of the radioactive cloud are portrayed in Panel 8. When precipitation occurs in or through a radioactive cloud, there is likely to be increased surface deposition, or a hot spot.

MEASUREMENTS AND TECHNIQUES USED IN PREDICTIONS

The atmosphere is a continuous gaseous fluid so that changes in one meteorological element must in some way be related to those in other meteorological elements. For example, one usually does not predict higher local temperatures with predicted north winds because cooler air generally comes from that direction. In practice then, it is not possible to predict each of the required elements entirely separately. The total forecast must be physically consistent. However, it is expedient to describe measurements and prediction techniques separately by weather element. An important contribution to prediction technique for all weather elements comes in the form of extensive forecasting experience on the part of ARL-LV meteorologists. All weather briefers have at least 10 years of experience in this and other geographical areas.

Local Winds and Trajectories

The wind near the surface is measured routinely at more than 15 points over the NTS area. Most sensors are on 30-foot towers and the data are telemetered by wire or radio to detonation Control Point facilities. These sensors measure winds at representative positions in Yucca Flat, Frenchman Flat, Pahute Mesa, and on a mountain north of NTS. Upper level winds are measured routinely at the Yucca Flat Upper Air Station using radar or GMD-1A to track sounding balloons.
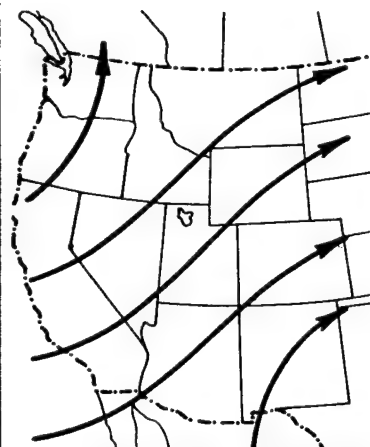
1. STREAMLINES OF AIR MOTION
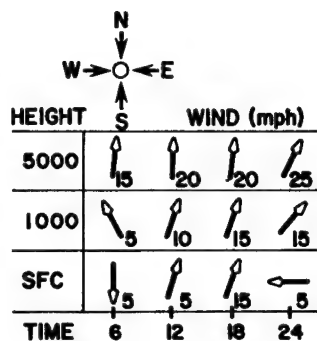
3. CHANGE IN WIND WITH TIME
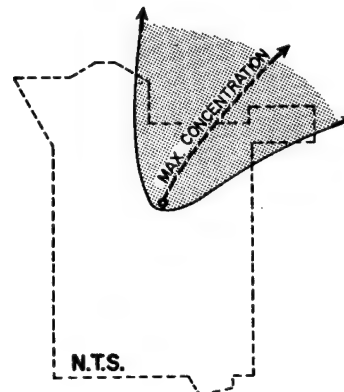
5. LOCAL TRAJECTORY

HT.	DIR.	SPD.
10,000	210	20
8,000	200	15
7,000	200	10
6,000	180	5
5,000	170	5
Surface	010	5

2. WIND AT ALTITUDES OVER
NEVADA TEST SITE
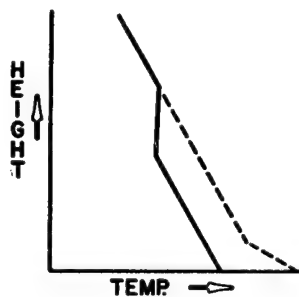
4. HEIGHTS OF VERTICAL MIXING
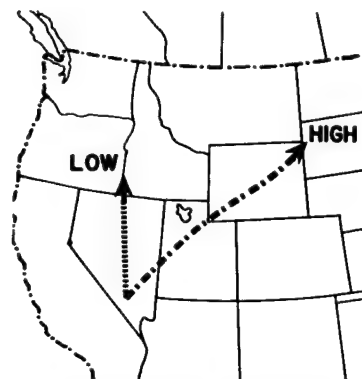
6. LONG RANGE TRAJECTORY
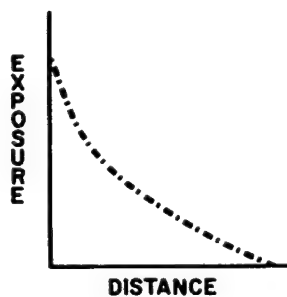
7. MAX. RADIATION EXPOSURE
ALONG TRAJECTORY (EXTERNAL
GAMMA OR AIR CONCENTRATION)
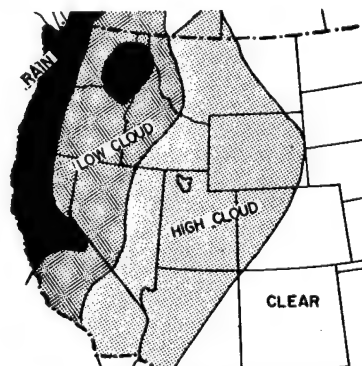
8. WEATHER & PRECIPITATION
LOCALLY & DOWNWIND

Figure 13.1.   Content of Typical Weather Briefing for Radiation Safety.

Special wind measurements are made during final preparations for detonations and continuing after the shot until the risk of leakage has disappeared. These measurements include a tower-mounted telemetered sensor placed within a thousand feet or so of the detonation site, and a network of 4 or more pibal stations encircling the site at distances between 25 and 50 miles. A pibal is a measurement of upper level wind by an optically tracked rising balloon, short for pilot balloon. On tests in which some radiation escape is expected, or the hazard larger than normal for some reason, or when the weather is expected to present unusual problems, additional pibal stations are used. One or more supplementary radars or GMD-1A stations may be placed in the offsite network, usually downstream, to provide more details of irregular circulations and to ensure an all-weather sounding capability. These special soundings are taken at hourly or half-hourly intervals to altitudes of 15 or 20 thousand feet, the data radioed or telephoned to the Control Point, and are all available for study by the test management within 20 to 30 minutes after balloon release.

During the period of a few hours just before a detonation in which final safety decisions are made, local wind data are displayed to show rates of change, presented in hodograph form to facilitate their interpretation in terms of fallout sectors, and sketched in streamline form to identify local flow patterns at several altitudes.

Climatology plays an important role in the prediction of surface winds in the basins at NTS. Figure 13.2 gives the wind direction frequencies for September at BJY, a crossroads in the center of Yucca Flat. Note the pronounced tendency for north winds at night, shifting through east to southerly by noon and southwesterly in the late afternoon. By showing the constancy (lack of variability) of winds by hour and month, Figure 13.3 shows how the time of morning changeover from northerly to southerly wind progresses earlier in the spring and later in the autumn. The afternoon reversal progresses in the opposite sense. Once established, the north winds are fairly constant at night, the south winds even more so in midday during summer. It may help to explain that the percentages are for the ratio of mean speed for the most frequent direction, to the mean speed for all directions.

Several techniques are available to the meteorologist for assistance in predicting local winds and local trajectories, but as of now there is no single prediction process such as a dynamic model that would be appropriate for all weather situations. The NTS Forecaster's Manual is a loose-leaf volume containing statistical relationships that have been prepared and collected over the 12 years of station operation. Relationships exist between atmospheric pressure gradients and changes in surface winds, and between upper level pressure gradients and changes in winds at higher levels. Detailed studies are available of the flow over NTS under various large-scale circulations.[1] These studies are being updated and supplemented as relationships come to light and as time permits.

In recent years a significant improvement has come in the quality of prognostic charts issued by the National Meteorological Center (NMC). Their recent use of the primitive equations of motion in a 6-layer computer model has resulted in predictions of patterns of general flow that are much better than those of only 3 years ago. The task of the NTS forecaster has become mainly one of interpreting from these large-scale patterns what will happen in the local area and in the time frames of the nuclear tests. Orographic effects produce many local variations from the mean flow, ranging from mountain and valley winds in a particular basin such as Yucca Flat, to subsynoptic scale circulations covering portions of southern Nevada but not appearing on the national scale of weather charts. One such small circulation is illustrated in Figure 13.4. Here an anticyclonic vortex is shown moving across the NTS special sounding network. The path of the center of the circulation is indicated by the large arrows, whereas the wind reports or small arrows are placed where there were sounding stations. This eddy was not evident on the NMC charts.

A study done several years ago of local wind prediction accuracy[1] shows 80 percent of frequency-of-direction errors less than 45° in winter, 35° in summer. Median errors were less than 20° in all seasons. These were for 7-hour forecasts of mean winds through the lowest 10,000 feet of atmosphere.

Current efforts to improve local wind and trajectory predictions are along three lines. First, data processing is being gradually converted from manual to electronic computer techniques to speed presentation and reduce errors in information. Second, numerical and statistical models that have been developed at Johns Hopkins University,[2] in the Weather Bureau's Techniques Development Laboratory,[3] and others are being studied in an effort to adapt them to the NTS problem. Third, mesoscale circulations in southern Nevada are being described and trajectories documented through the use of constant volume tetroon tracers tracked by radar. The tetroons are 4-sided mylar balloons of constant volume, which can be inflated to float near a preselected air density surface. They are tracked by M-33 radars. Such tracers have, for example, given information on the distance traveled by nocturnal drainage currents.
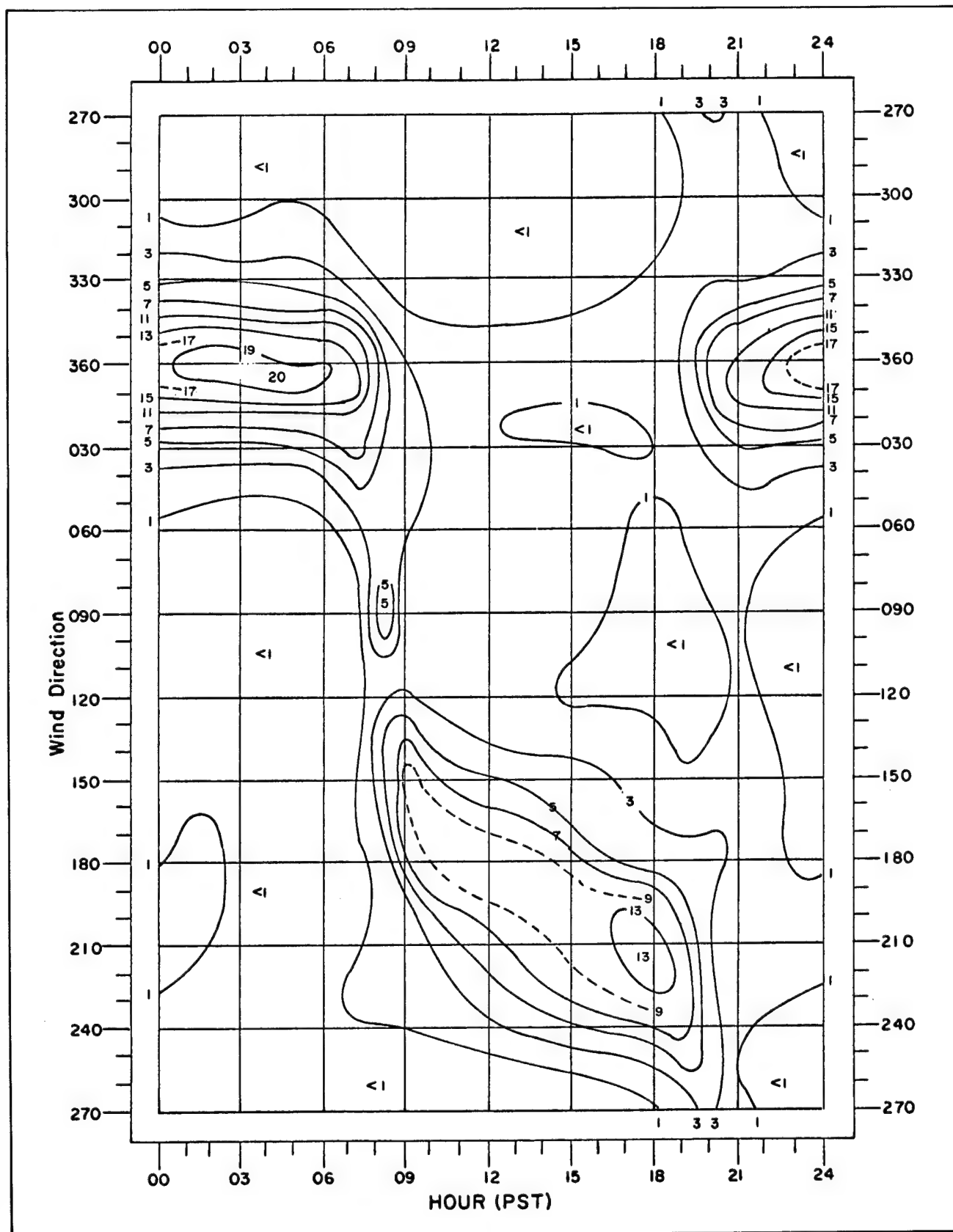
Figure 13.2. Wind Direction Frequency (%) for 10 Degree Increments of Direction. Station: BJY; Month: September.
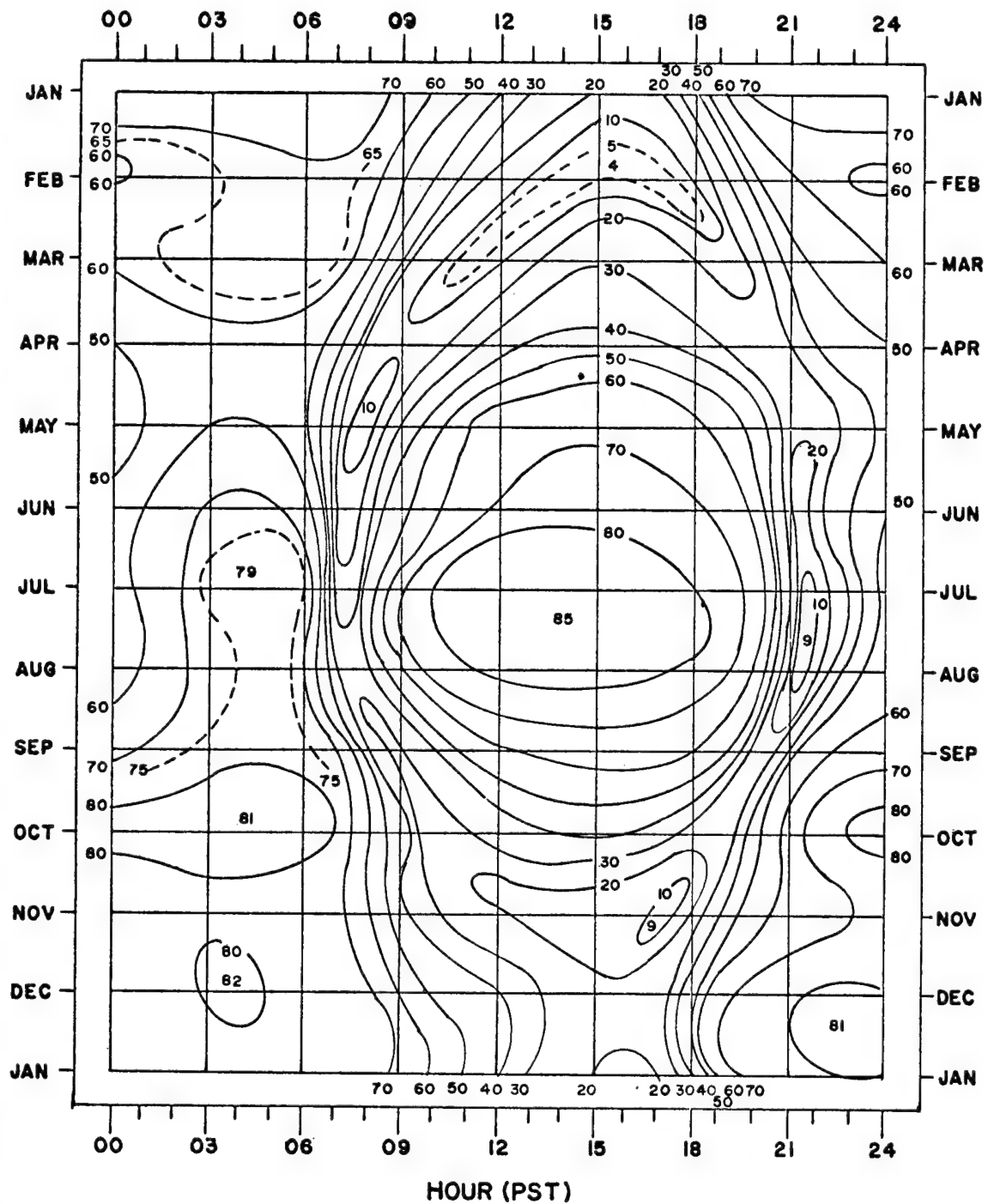
Figure 13.3. Constancy of the Wind Expressed as the Percentage Ratio of the Mean Vector Wind Speed to the Mean Scalar Speed. Station: BJY.
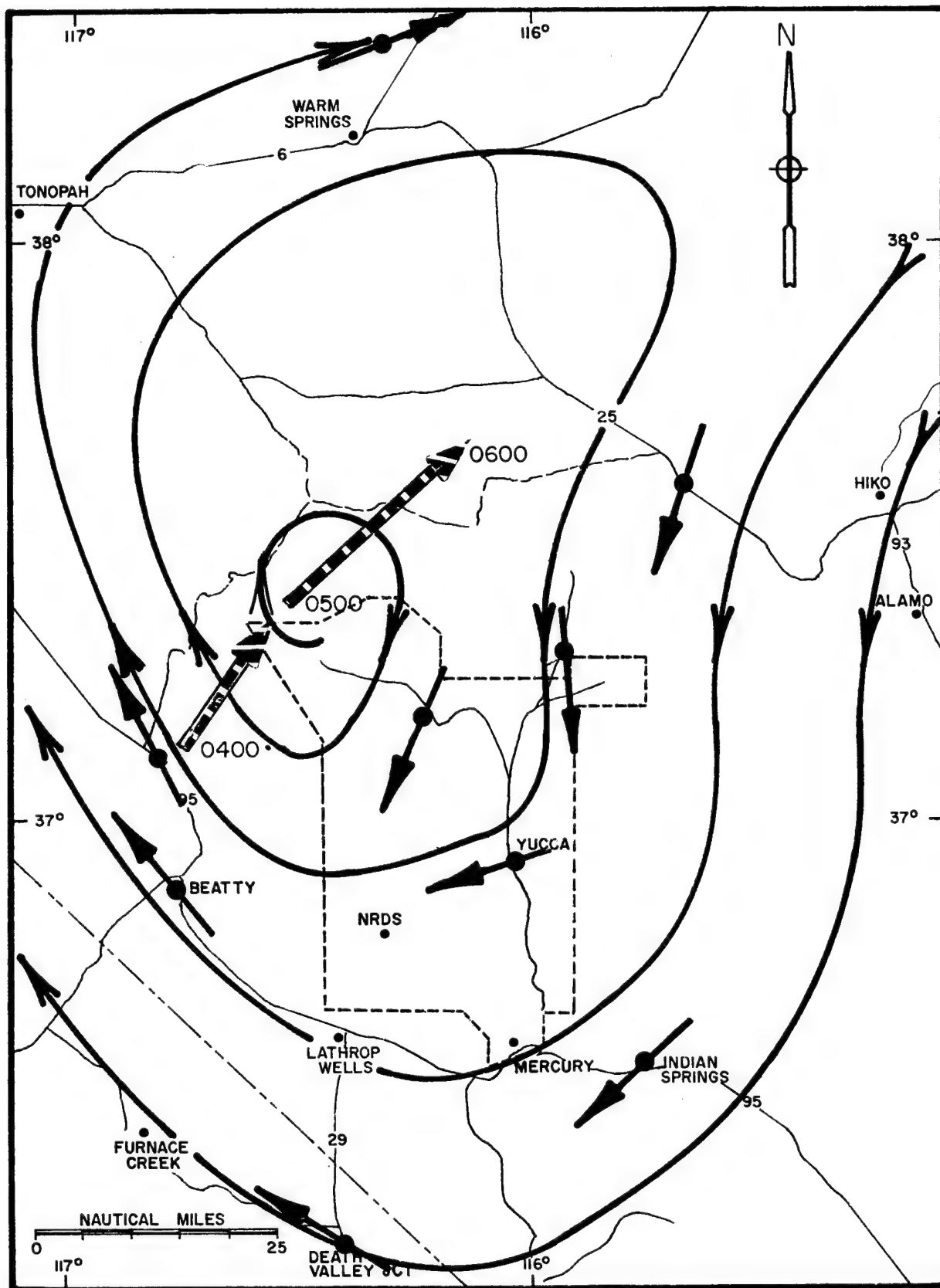
Figure 13.4. 10,000 Ft. (MSL) Streamlines for March 22, 1968, 0500 PST.

Long-Range Trajectories

There exists no entirely satisfactory method of documenting air trajectories over great distances. Various tracer techniques such as radioactive debris, smoke, constant altitude, and constant density balloons have been used but with only limited accuracy or success. Among the more successful efforts has been the ARL-LV tetroon tracking program. The tracers in this effort were tetroons bearing passive radar reflectors. Hundreds of these have been tracked across the western states at altitudes around 12,000 feet m.s.l., using Federal Aviation Agency air traffic control radars. Many of these tetroons have been released in clusters of 3 or 4 and forecasts made of their trajectories. A few of the clusters were tracked for from 12 to 24 hours, but many tetroons were lost at shorter times. The trajectory forecasts were based on prognostic charts obtained routinely from the NMC and on extrapolations into future time of streamlines drawn from local and western U.S. upper wind data. The comparison of forecast trajectories with tetroon tracks is weakened by lack of continuing information on tetroon altitudes and the apparent tendency to obtain long tracks for only those clusters that did not disperse appreciably. In spite of these and other difficulties affecting the validity of the comparison, the information in Table I seems to be the best verification made to date of the accuracy of low altitude trajectory forecasts[4].

TABLE I. VECTOR ERRORS OF FORECAST TRAJECTORIES

Forecast Period (hours)	Number of Cases	Average Travel Distance*	Standard Forecast Vector Deviation*	Percent of Travel Distance
6	129	94	56	59
12	74	186	106	57
18	37	267	148	56
24	20	341	189	55

*nautical miles

Both the forecast and the verification trajectories in this study were line trajectories, whereas a cloud of gas or particles would spread with time and cover a large area. Predicted radioactive cloud trajectories are apparently much more nearly correct, due to cloud size and perhaps the greater effort and care given these forecasts.

Thermal Stability and Mixing Depth

The vertical gradient or lapse rate of air temperature above the surface is measured regularly twice daily by a GMD-1A sounding system at the Yucca Flat station.

For nuclear tests in areas other than Yucca Flat, additional GMD-1A units are employed near the test location with soundings at appropriate times. There is usually only minor horizontal variation or gradient in air temperature at a thousand feet or more above the surface because any such gradient involves density differences that tend to equalize themselves through vertical motion. The temperature at or near the surface, however, can have large gradients from the different radiative characteristics and friction of different orographic slopes. To measure these temperatures, some of the tower-mounted radio-telemetered wind sensors are accompanied by telemetered thermistors. Data from these instruments permit the meteorologist to update the main characteristics of the vertical thermal structure of the boundary layer with relatively few soundings. The diurnal progression of surface temperature is one of the more dependable meteorological elements in the frequently cloudless Nevada desert, and climatological graphs provide excellent prediction tools for the diurnal increase or decrease of surface temperature and the associated diurnal change in mixing depth. A process developed for air pollution potential by Holzworth is helpful to establish the gross characteristics of mixing depth[5]. It is based on the last available sounding of temperature, the adiabatic lapse of temperature with height, and the typical diurnal cycle of surface temperature for the site.

Weather and Clouds

Most of the information used in evaluating present and future moisture cloud distributions downwind along trajectories comes from the Weather Bureau station network. Standard meteorological techniques are used in predicting such cloud cover, including the effects of storm centers, fronts, jet stream, long and short wave patterns, and orography. These have been described for southern Nevada by Booth[6]. NMC provides information on vorticity and vertical velocity distributions, atmospheric moisture distributions, and prognostic weather charts that are very useful.

Predictions of precipitation, either continuous-type or showery-type, are of more than casual interest in safety evaluation because of the ability of precipitation in any form to increase the deposition of airborne radioactive materials. In order to provide the best information possible about the probability of rain or snow relative to a radioactive cloud and to identify where rain has occurred with a radioactive cloud passage, ARL-LV has encouraged Weather Bureau use of the FAA traffic control center radars for weather surveillance, and has arranged for the positions of precipitation areas to be sent

hourly or oftener from the Salt Lake City and Palmdale, California, centers to the NTS by our own facsimile circuit. The areas in which precipitation is watched by these centers are shown in Figure 13.5. The Albuquerque center is expected to join this circuit during 1969, adding areas to the southeast.

Precipitation prediction is not just a matter of watching rain conditions move across the country. Rain can form suddenly in an area without previous recent precipitation history. In order to evaluate the probability of this happening over the southern Nevada area, several local studies have been attempted to give the maximum advance warning of rain. Two of these studies show considerable value: one, for spring rains by Cochrane[7] having been added to the Forecaster's Manual and the other for summer thunderstorms being given its final test this season. Another statistical approach to thunderstorm forecasting is being developed for this area following a technique employed by Travelers Research Center to predict rare meteorological events[8].

EFFECT OF PREDICTION ACCURACY ON SAFETY

The state of any portion of the atmosphere at a particular time may be known only imprecisely. Therefore, a radiological safety program based on forecasts of atmospheric variables needs to provide for large deviations from the forecasts.

At the NTS and most offsite tests, error in predicting the early cloud trajectory is of greatest concern because the plan for clearing personnel and equipment from areas immediately downwind depends on this forecast. At greater distances the longer travel time of any airborne radioactive debris would allow for clearance of additional areas in case of error in the predicted trajectory.

It is a standard practice to provide a large exclusion area around and immediately downwind of each detonation. It is also a major concern at safety briefings to provide adequate capability to react to unpredicted atmospheric behavior as well as to other emergencies.

One essential part of reaction capability is the rapid identification of atmospheric changes. The continuous monitoring of surface winds through telemetered instruments and frequent (half-hourly) soundings of upper level winds provides the most direct measurement of local trajectory changes. Telemetered radiological data and aircraft monitoring provide confirmation that any airborne radioactivity is moving as the measured winds would indicate, or as the predicted flow would suggest. Aircraft tracking of detectable radioactive debris is carried on through a coordinated effort of meteorologists, constructing and predicting trajectories, and aircraft operations, sweeping across areas in which radioactivity could conceivably be present.

Radiological technicians and security forces onsite, and U.S. Public Health personnel offsite, are always alerted by the AEC and prepared to take any necessary actions to assure human safety.

The value of measurements and forecasts of atmospheric behavior is in their contribution to greater human safety in downwind areas and in their use to reduce unnecessary restrictions on human activity in other directions. They also permit limitation of the scope of safety preparations to a reasonable level by indicating sectors and ranges beyond which radiation hazard is within acceptable limits.

SUMMARY

The Air Resources Laboratory-Las Vegas attempts to employ the most effective wind and weather observing and forecasting techniques in its support of the Safety Program for nuclear detonations. It employs modern equipment for wind and weather measurement; and to minimize the chance for surprise trajectories, it provides a dense wind measurement network for each nuclear test. In addition to its staff of experienced forecasting meteorologists, it maintains a small research staff to carry out studies designed to identify and adopt forecasting and observing improvements from other meteorological services, to develop useful meteorological information on the southern Nevada Test Site and other test sites, and to develop new and better prediction techniques for nuclear test application.
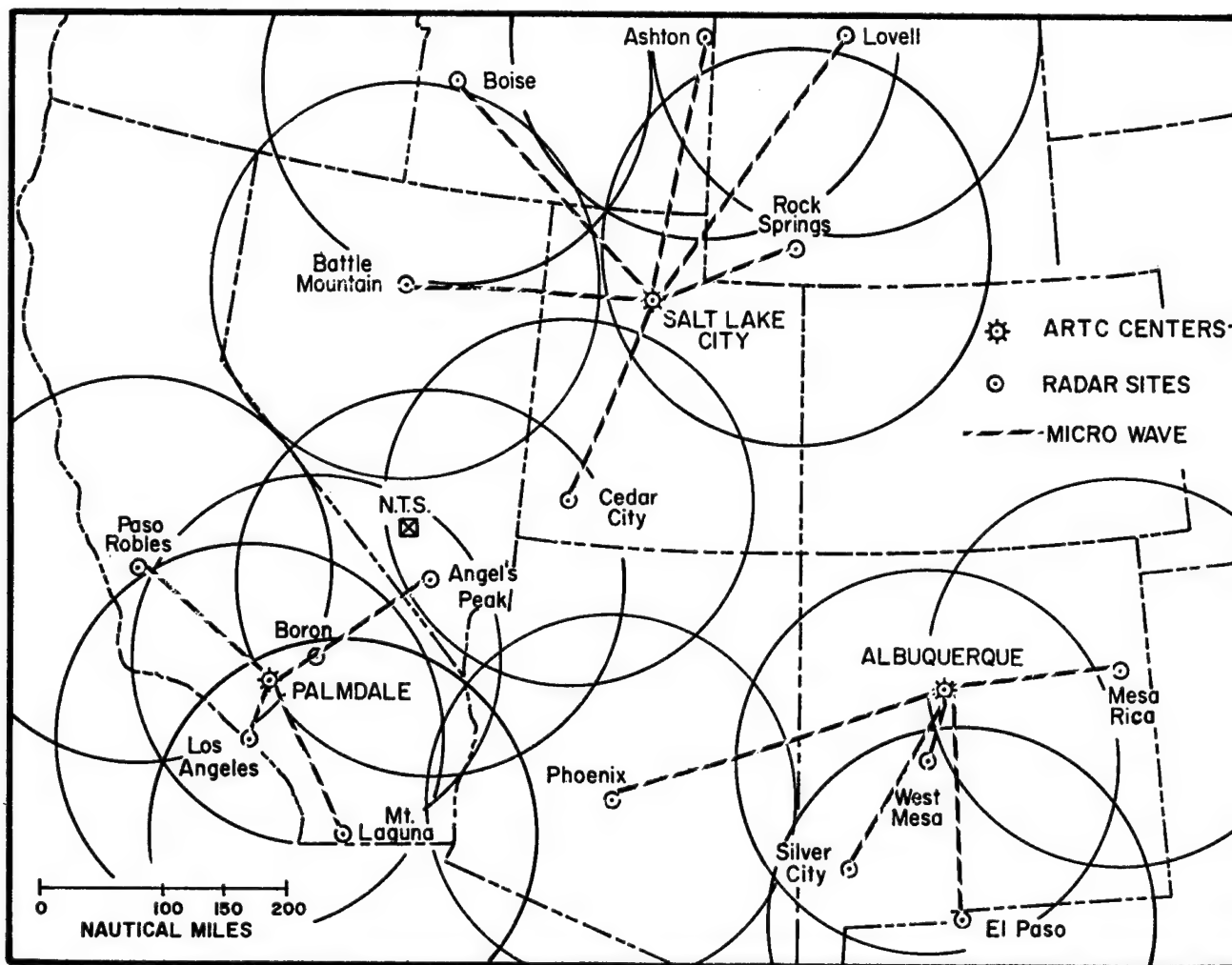
Figure 13.5.   FAA Radar Weather Coverage Used at NTS.

Part B — Local Fallout and Diffusion of Radioactive Material

Harold F. Mueller, *Chief, Radiation Branch*
Air Resources Laboratory—Las Vegas, Las Vegas, Nevada

ABSTRACT

The detonation of a nuclear device requires an appraisal of potential radiological consequences resulting from the expected or accidental release of radioactive material to the atmosphere. Radioactivity production, the manner by which radioactive material may be released to the atmosphere, and source term assumptions for several types of nuclear detonations are briefly described. The use of observed radiological data is discussed. Currently employed prediction techniques are presented and an evaluation of predictive capability is demonstrated for cases where comprehensive radiological data are available.

INTRODUCTION

The detonation of a nuclear device results in the production of radioactive materials. The release of radioactive materials to the atmosphere and their potential interaction with man are matters of concern to all those involved with the safety aspects of nuclear testing. Considerable precaution is taken by the AEC to avoid undesirable radiological consequences. One such precaution is the preshot estimate of maximum air concentrations and deposition of radioactive materials downwind of an expected or accidental release. These estimates are a vital factor in the deliberations of the Test Manager and his safety advisory panel prior to his granting permission to conduct any experiment. Diffusion calculations are performed to estimate downwind air concentrations of predominately gaseous radioactive materials, An analog scaling technique, based on a modification of an ARL (formerly Weather Bureau) fallout model, is employed to predict local fallout of particulate radioactive materials. For the purposes of this paper local fallout may be defined as that fallout deposited within the first 12 hours after detonation.

RADIOACTIVITY PRODUCTION

Radioactivity may be produced as the result of: (1) an energy-producing nuclear reaction, e.g., a fission product activity from a nuclear explosion or from radionuclides produced in a thermonuclear reaction, and (2) the interaction of a product of a nuclear reaction with some other material, e.g., activity from induced radionuclides produced by neutrons from a thermonuclear process interacting with device materials and with the medium surrounding the device. The total radioactivity resulting from a nuclear detonation depends on the device design and on the emplacement medium. The amount of radioactivity produced in a given nuclear detonation is, of course, required input for radioactive effluent predictions. Information on the amount and composition of activity produced is provided by the nuclear laboratory conducting the experiment. The fission yield, or the fission equivalent yield in the case of a thermonuclear reaction, is required for external gamma dose calculations. Quantities of specific radionuclides produced, e.g., iodine-131, can be determined from the fission yield and an appropriate reference on fission product production. A knowledge of the composition of the activity is important when large quantities of induced activities are produced which can considerably alter the decay characteristics of the composite gamma-emitting radionuclides.

RADIOACTIVITY RELEASES

The release of radioactivity to the atmosphere resulting from the underground detonation of a nuclear device may either be expected or accidental. Radioactivity released as the result of a nuclear excavation experiment is expected. A prompt venting or seepage from an underground detonation, designed to completely contain all radioactivity, is accidental. Expected or accidental releases may also occur during postshot operations. Such releases might occur from flaring after gas stimulation detonations or during drillback.

During atmospheric testing at the Nevada Test Site, a great deal of experience was accumulated on the transport and deposition of radioactive materials produced by nuclear detonations at and above the ground surface. Much of the activity produced by these detonations was released to the atmosphere. Today, it is only in the case of nuclear excavation experiments that activity is expected to be released to the atmosphere at the time of detonation. The fractions of the total activity produced which were deposited in local fallout for cratering experiments conducted several years ago were on the order of 50 percent. These devices were detonated at small scaled depths. The scaled depth is a function of the total yield and depth of burial of the nuclear device. The fallout fractions observed with the most recent excavation experiments, where the devices were detonated at greater scaled depths, have been considerably less. For these detonations a much larger fraction of the total activity

produced was found in the crater or on the crater lip. A much smaller fraction than that found in the local fallout pattern remained airborne at later times. During the 1957 Plumbbob and 1958 Hardtack II series at the Nevada Test Site, a number of nuclear devices were detonated at the bottom of drilled holes containing one or more cement plugs between the device and the ground surface. The maximum fraction of the total activity produced by these detonations which was deposited in the local fallout pattern was on the order of 5 percent. Emplacements of nuclear devices detonated at the bottom of drilled holes are now more effectively designed to completely contain all radioactivity by placing the nuclear device deeply underground and completely stemming the hole to the surface. The majority of recent underground detonations released no activity to the atmosphere. Since 1961 a small number of underground detonations have resulted in a prompt release of both gaseous and particulate radioactive debris to the atmosphere. In these few instances, the fraction of the total activity produced which was observed in each local fallout pattern was less than 1 percent. The technology of containment has advanced over the years, and now prompt releases are rare.

For each nuclear detonation, the laboratory conducting the experiment provides both a design yield and a maximum credible yield. The maximum credible yield is routinely used in radioactive effluent predictions.

The total amount of activity produced by a nuclear detonation, when multiplied by an appropriate release fraction, determines the source term used in radioactive effluent predictions. Release fractions assumed for nuclear detonations are based on past experience with various types of emplacement configurations and containment characteristics. Useful estimates can be made of the fraction of the total activity produced in a nuclear excavation detonation which will be deposited in local fallout. These estimates are made on the basis of empirical data relating the fallout fraction to the scaled depth of burial. Figure 13.6 is a graphical representation of this relationship. The graph shows that f, the fraction of total activity produced which is deposited in local fallout, decreases rapidly with increasing scaled depth of burial. There is evidence that f is not merely a function of scaled depth of burial alone. Moisture content of the emplacement medium, for example, appears to be an important factor and much work is being done to gain a better understanding of the basic phenomena involved. Maximum expected fallout fractions, estimated on the basis of experience, are always used when making fallout predictions for nuclear excavation experiments.

Fallout fractions (f) for underground detonations designed to be completely contained are not, at present, explicitly employed. For this type of event radioactive effluent predictions are made on the basis of a maximum credible venting assumption, using our worst venting experience to date. Some criticism can be made for using this approach. Studies currently being conducted by the nuclear laboratories indicate that this may be an unreasonably restrictive assumption, particularly for larger yield events. It is expected that these studies will produce a better understanding of venting phenomenology so that more realistic estimates can be made. For certain experiments, such as the Gasbuggy experiment near Farmington, New Mexico, the device is buried at an extremely large scaled depth. The laboratory which conducted this detonation considered a massive prompt venting to be incredible. Based on both theoretical and empirical considerations the maximum credible release was assumed to be a seepage of radioactive gases. Even this assumption proved to be an over estimate since no prompt seepage resulted from the detonation and only a small release of no more than 1 curie of noble gases occurred during cable cutting.

Thus, the source terms used in radioactive effluent predictions are the product of two conservative estimates, i.e., the maximum credible yield of the device and the maximum expected release fraction or maximum credible venting assumption.

RADIOLOGICAL DATA

Radiological monitoring is conducted for every expected or accidental release of radioactive material to the atmosphere. A detailed analysis of these monitoring data is performed to establish the downwind locations and intensities of radioactive contamination. These results are combined with an analysis of the meteorological conditions existing during the period of detectable cloud transport. These analyses provide the verification of radioactive effluent predictions and additional basis for future predictions. An idealized profile of gamma radiation intensity versus time resulting from the passage of a radioactive cloud composed of both gases and particulates is shown in Figure 13.7. The intensity rises rapidly, as the cloud approaches, from the background value to a peak during the cloud passage and then declines to a value somewhere between the background and peak values at the end of cloud passage. During the period of cloud passage, radioactive particulates are deposited on the ground. Radiation intensities subsequent to cloud passage are a reflection of these residual activities and the decline in intensity reflects the composite decay of the deposited activities. Profiles of this type provide the
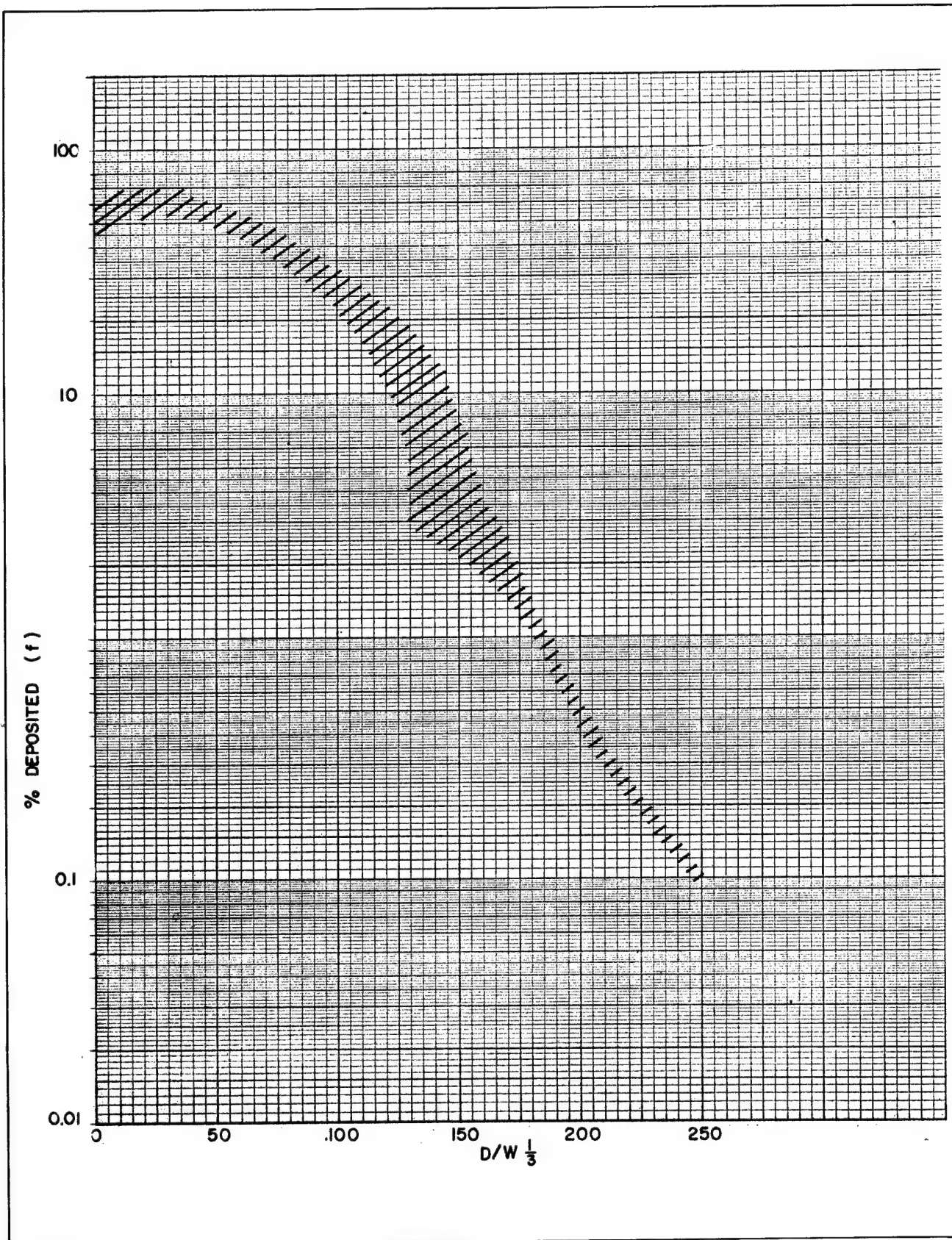
Figure 13.6. Percent of Total Activity Deposited in Local Fallout as a Function of Scaled Depth of Burial.
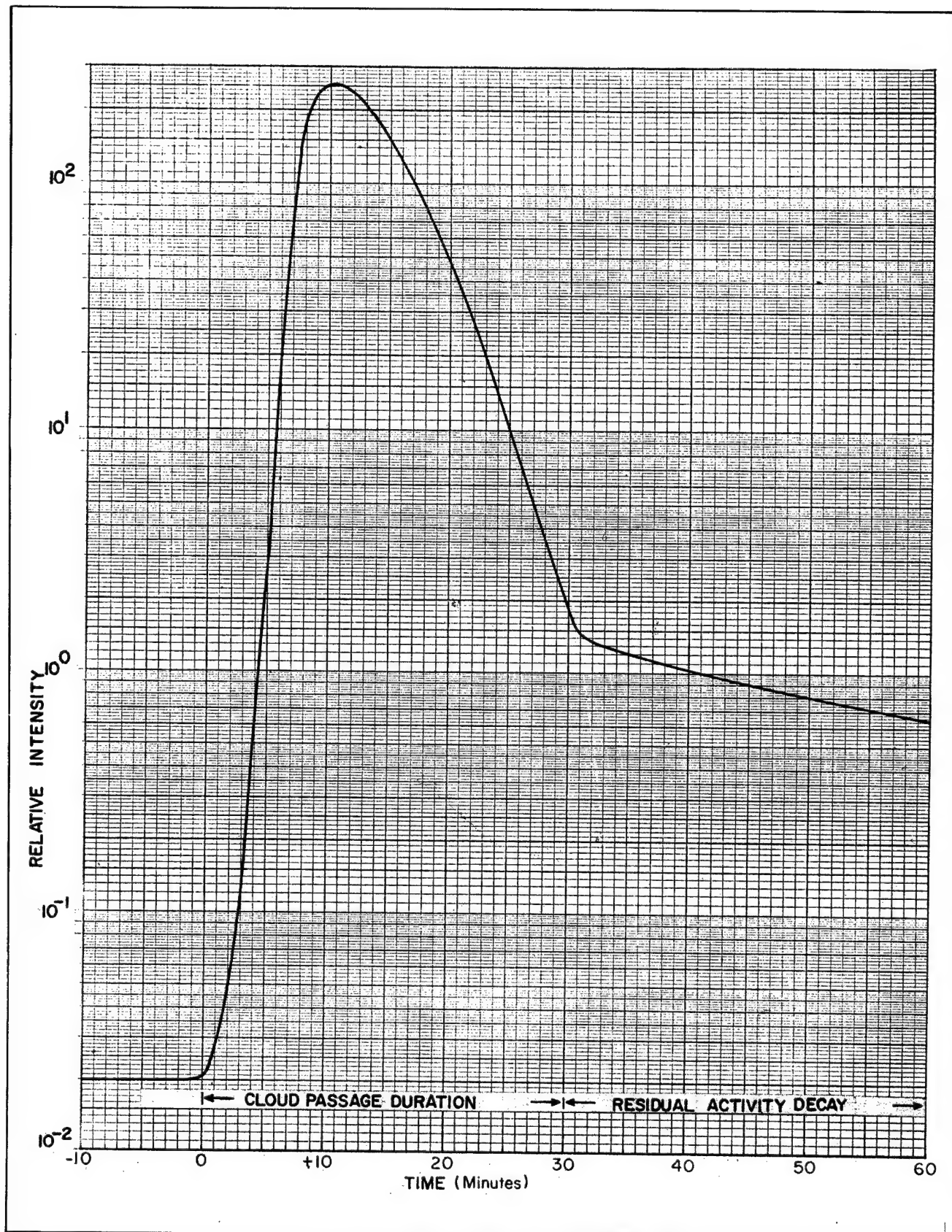
Figure 13.7. Idealized Exposure Rate Profile.

264

data necessary to construct downwind patterns of cloud passage and fallout exposure rates. A fallout pattern, showing contours of gamma radiation intensities, is shown in Figure 13.8. Exposure rates in this particular pattern have been normalized to $H + 12$ hours using the observed decay rate of the deposited activity. The exposure rate pattern can be used to construct a pattern of exposure for any time interval by integrating the exposure rate over the desired time interval. The fraction of the total fission product activity produced by the nuclear detonation which is deposited in the local fallout pattern can also be determined from the exposure rate pattern. This is accomplished by an integration of the $H + 1$ hour exposure rate pattern which yields a number having the units

$$\frac{\text{Roentgens} - \text{Square Mile}}{\text{Hour}}$$

This number is then converted to an equivalent fission yield by using the density conversion factor of

$$\frac{3380 \text{ Roentgens} - \text{Square Mile}}{\text{Hour} - \text{Kiloton}}$$

corrected for backscatter and terrain shielding[9]. This equivalent fission yield when divided by the total fission yield of the device gives the fallout fraction. If significant quantities of gamma-emitting radionuclides are deposited, other than those produced by the fission process, their presence must be accounted for in the determination of the fallout fraction. One method of accomplishing this is to convert the induced gamma activities produced to equivalent fission yields which can then be added to the fission yield of the device.

PREDICTION TECHNIQUES

The type of radioactive effluent prediction technique employed for a specific event depends on the assumed character of the release, the physical composition of the released material, and on past experience with releases of the type assumed. For the current testing program, releases can be considered to be one of the following three types: (1) a seepage of predominately gaseous materials, occurring at or subsequent to the time of detonation; (2) an explosive release of both gaseous and particulate materials from a nuclear excavation experiment; and (3) a massive release of both gaseous and particulate material at or very shortly after the time of detonation. Predictions for type 1 releases are made using a diffusion technique. Predictions for types 2 and 3 releases employ an analog scaling technique.

Numerous diffusion techniques exist for the prediction of downwind air concentration distributions of materials having negligible fall velocities and for the prediction of downwind deposition distributions of materials with significant deposition characteristics. Several of these techniques are similar in a basic assumption that the crosswind and vertical distributions in a plume or cloud of windborne material can be represented by a Gaussian form, and differ primarily in the form of the diffusion coefficients contained in the equations. One such diffusion system, and one currently being employed for type 1 releases, is that proposed by F. Pasquill[10]. This system, on the basis of numerous field experiments, is considered valid out to distances of 100 kilometers from a source. The form of the prediction equation is as follows:

$$C = \frac{2.8 \times 10^{-3} \, Q}{u \, d \, \theta \, h} \tag{1}$$

where: C is the axial or peak concentration at ground level in units/m³ when the release rate (Q) is in units/minute,

or, is the axial total exposure at ground level in units-minutes/m³

when the total release (Q) is in units

u is the wind speed, appropriately determined, (m/sec)

d is the axial downwind distance (km)

θ is the lateral plume spread (degrees)

h is the vertical plume spread (meters)

The lateral (angular) spread θ and the vertical spread h are defined by concentrations one-tenth of the axial or ground values, respectively. Empirical methods are provided for the determination of θ and h. The lateral spread θ is a function of release period, atmospheric stability, and downwind distance from the source. The vertical spread h is a function of atmospheric stability and downwind distance. Stability categories which, in part, determine θ and h are functions of solar insolation and wind speed. An objective method of determining stability categories is available[11]. By this method solar insolation is estimated as a function of solar altitude and modified for conditions of cloud cover and cloud ceiling height. This diffusion equation applies to a ground level release; however, allowance for an elevated source is easily made. The concentration C may be multiplied by an appropriate factor to account for radioactive decay. Ground level exposure rates are obtained by converting air concentrations of activity to exposure rates using an infinite cloud approximation (½ solid angle) and the appropriate mean gamma energy of the composite activity released. Similarly, total exposures may be obtained by converting total integrated air concen-
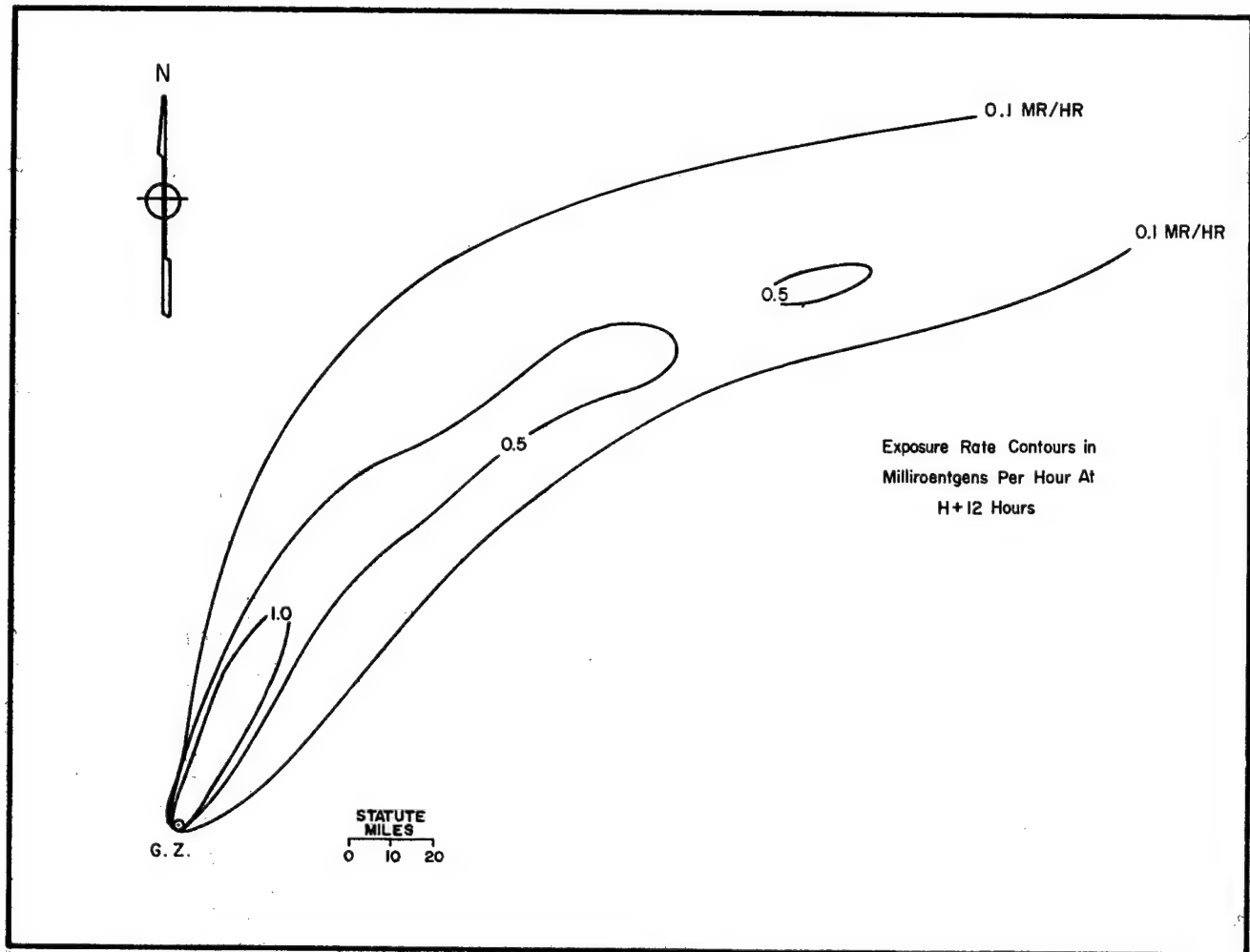
Figure 13.8.   Fallout Pattern.

trations. Potential thyroid doses resulting from the inhalation of the radioiodines can be estimated on the basis of predicted total integrated air concentrations and the appropriate biological conversion factors. Radioiodine contamination of cow's milk can also be estimated on the basis of predicted total integrated air concentrations using appropriate conversion factors for dry deposition.

A number of methods have also been developed by various organizations for the prediction of local fallout. They employ similar fundamental considerations and contain varying degrees of sophistication. One such method was that originally developed by the Special Projects Section, U. S. Weather Bureau, in 1955[12]. The original method was based primarily on fallout data from tower shots in Nevada. The total amount of fallout and the distribution of activity as a function of particle size and height in the initial nuclear cloud must be specified. This method predicts a downwind pattern of fallout intensities. A modification of this method[13] is currently being employed for the prediction of fallout intensities resulting from type 2 and 3 releases. This modified method provides predictions of centerline radiation intensities required for operational application. It is a scaling technique which does not require explicit definition of the distribution of activity as a function of particle size and height in the initial nuclear cloud. Rather, the assumption is made that an appropriate analog event can be chosen whose particle size-activity distribution will closely approximate that of the event for which a prediction is being made. The scaling method consists of a simple ratio technique whereby the parameters which determine the exposure rates and the location of these areas in their respective fallout patterns are related, and then used in conjunction with the empirical results of a previous event for prediction purposes. The exposure rate levels are normalized to 1 hour after the detonation at all downwind distances to account for radioactive decay. The form of the scaling equation, where the unprimed symbols refer to the analog event and the primed symbols refer to the forthcoming event, is as follows:

$$A' = A \left(\frac{\theta}{\theta'}\right)\left(\frac{h}{h'}\right)^2 \left(\frac{V}{V'}\right)^2 \left(\frac{f'Y'}{fY}\right) \quad (2)$$

where:

A, A'   are the exposure rate levels as a function of distance along the fallout centerline for an H + 1 hour reference time (R/hr)

θ, θ' are the directional shears in the wind hodograph from the surface to the top of the cloud at time of stabilization (degrees)

h, h'   are the cloud heights at time of stabilization (feet)

V, V'   are the resultant mean transport speeds from the surface to the appropriate altitude in the cloud (knots)

f, f'   are fractions of the total activity produced which occur as fallout

Y, Y'   are the fission or fission equivalent yields (kilotons)

The exposure rate level (A') when computed, is applicable at a downwind distance determined by the following equation:

$$X' = X \left(\frac{h'}{h}\right)\left(\frac{V'}{V}\right) \quad (3)$$

where:

X, X'   are downwind centerline distances (miles)

For the application of this technique to type 3 releases, an analog event is chosen which is believed to represent the maximum credible venting conditions for the forthcoming event, and it is assumed that f = f'. For type 2 releases f' can be estimated using the procedure previously described.

The scaling technique depends on the careful analysis of exposure rate levels, observed meteorological conditions, and cloud characteristics of past events combined with predicted parameters for the forthcoming event.

EVALUATION OF PREDICTION TECHNIQUES

The value of a prediction technique lies in its ability to reproduce observed radiological data obtained from an actual release of radioactive material. It is, of course, best evaluated in cases where extensive data are available. Although all releases from underground detonations are well documented from a public health point of view, it does not necessarily follow that accidental releases are always sufficiently well documented to provide the data necessary to conduct the comprehensive analysis required for prediction technique evaluation. Radiological monitoring must be conducted at the proper place and time and observations must be of sufficient quantity that cloud passage and fallout exposure patterns can be constructed. The desired quantity and type of documentation is most nearly attained in connection with nuclear excavation experiments. For these experiments a release is expected and comprehensive preparations for radiological documentation are made. Comprehensive data are also available with which to evaluate the meteorological parameters in the prediction equations.

267
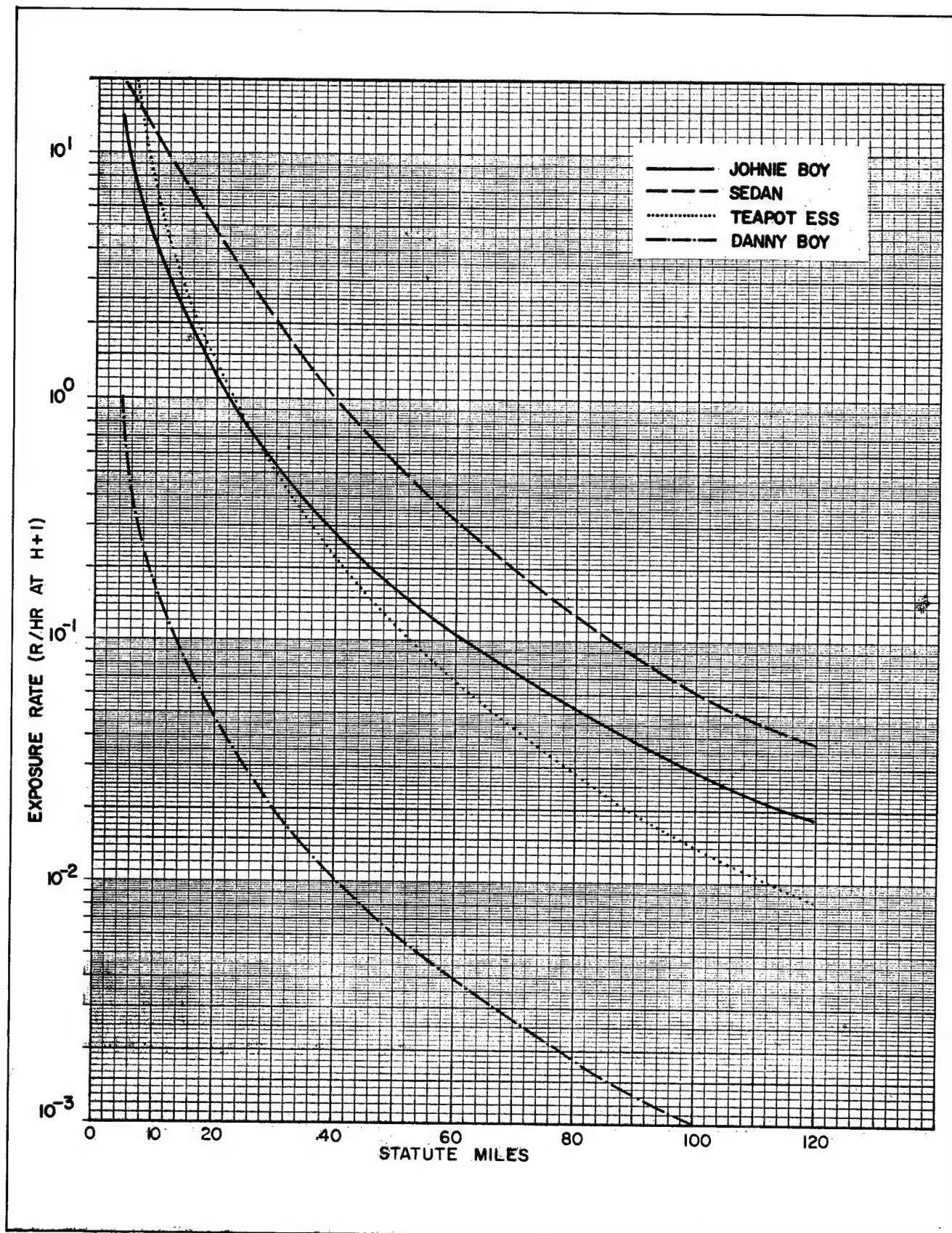
Figure 13.9. Observed Exposure Rate Versus Distance.
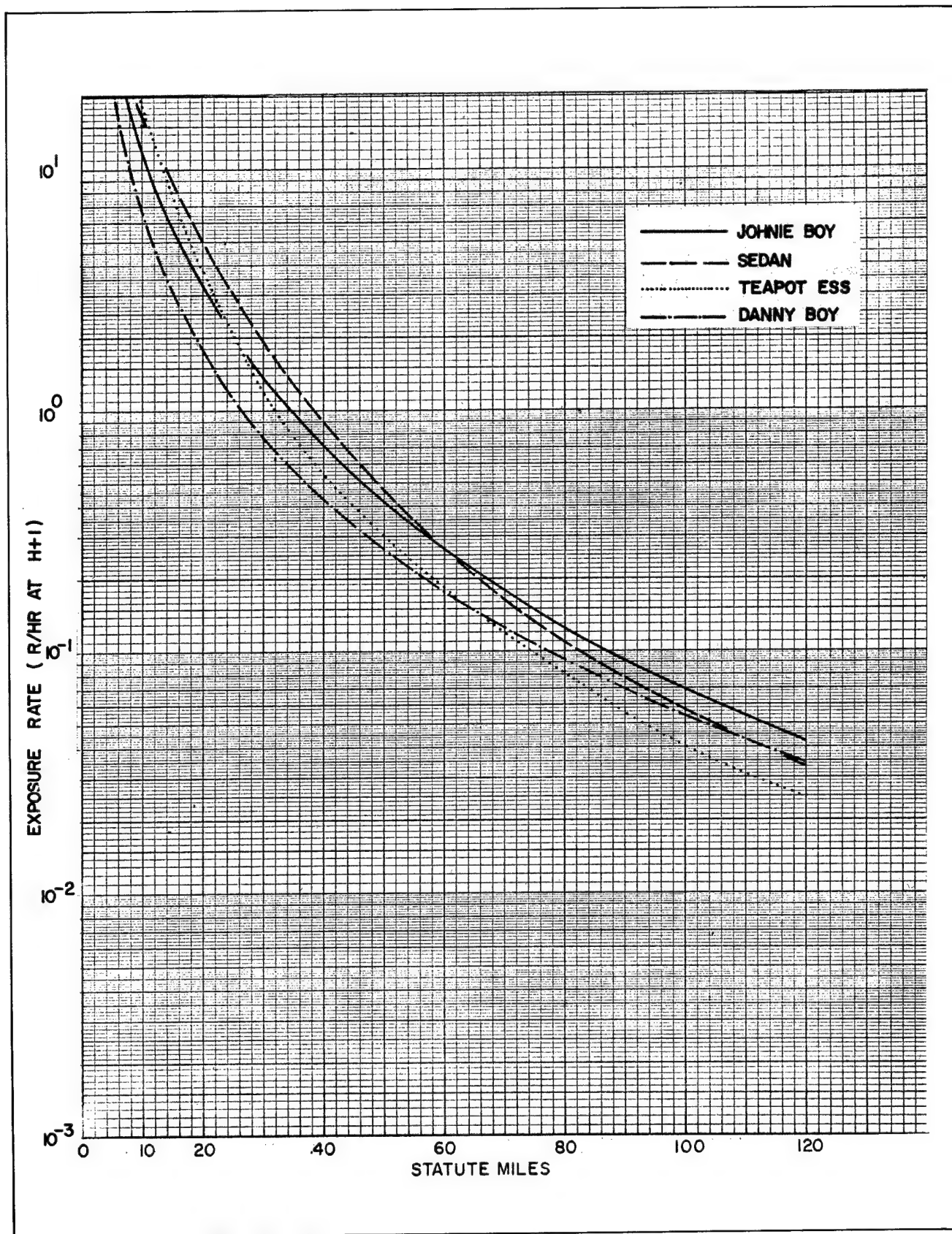
Figure 13.10. Normalized Exposure Rate Versus Distance.

269

Data from several nuclear excavation experiments are presented to demonstrate the validity of the fallout scaling technique. The Sedan, Teapot Ess, Johnie Boy, and Danny Boy observed H+1 hour fallout gamma exposure rates as a function of distances are shown in Figure 13.9. Danny Boy was fired in hard rock (dry basalt) while the others were fired in alluvium. The range in total yield of these detonations is a factor of approximately 240. The range in fallout fraction is approximately a factor of 13. Observed wind speeds, shears, and cloud heights, as expressed in the scaling equations, also varied considerably. Each of these curves has been normalized to a common set of conditions to provide a test of the scaling technique. The results of this scaling normalization are shown in Figure 13.10. If it were possible to account for all factors which contribute to the differences in exposure rates observed for the several events, the normalization would result in a single curve. Although this is not quite the case, it is apparent that the scaling technique performs remarkably well for this series of events. Comparable results can be claimed for accidental venting experience.

The assumptions which were made in the development of the scaling technique appear to account for the major differences in the radiation levels resulting from these excavation detonations. The technique satisfies the requirement for an operationally useful radiation prediction method that can be both rapidly and easily employed. The method requires the minimum of input information essential for any fallout prediction technique and depends realistically on the empirical results of previous detonations as a criteria for radiation prediction.

SUMMARY

The production of radioactivity and the manner by which this activity may be released to the atmosphere have been described. Source terms for several types of nuclear detonations were shown to be based upon conservative estimates of yield and fallout fraction or upon a maximum credible accident assumption. The use of observed radiological data for prediction evaluation was discussed and a predictive capability of useful accuracy was demonstrated for cases where comprehensive radiological data were available.

REFERENCES

1. Francis N. Buck, "Statistical Forecasting Studies for the Nevada Test Site," Unpublished manuscript, USWB Research Station, Las Vegas, 1961

2. R. H. Jones, "Spectral Analysis and Linear Prediction of Meteorological Time Series," Journal of Applied Meteorology, 3, No. 1, pp. 45-52, 1964

3. F. Lewis, "Regression of Complex Variables," Proceedings First Statistical Meteorology Conference, Amer. Meteor. Soc., Hartford, Conn., 1968

4. P. W. Allen, E. A. Jessup, and R. E. White, "Long-Range Trajectories," Proceedings USAEC Meteorological Information Meeting, Chalk River, Ontario, C. A. Mawson, Editor. pp. 176-190, September 11-14, 1967

5. G. C. Holzworth, "Mixing Depths, Wind Speeds, and Air Pollution Potential for Selected Locations in the United States," Journal of Applied Meteorology, 6, No. 6, pp. 1039-1044, 1967

6. H. G. Booth, "Cirrus Forecasting," Unpublished manuscript, Weather Bureau Research Station, Las Vegas, 1958

7. C. T. Cochrane, "Study of Spring Precipitation Types Over Southern Nevada," Unpublished manuscript, Air Resources Laboratory-Las Vegas, 1967

8. J. G. Bryan, J. A. Russo, and G. J. Merriman, "Research on the Prediction of Rare Events to Improve Forecasts of Low Ceiling and Visibility," The Travelers Research Center, Hartford, Conn., Final Report to Techniques Development Laboratory, ESSA Weather Bureau (Cwb-11299), 1967

9. G. Higgins, "Calculation of Radiation Fields from Fallout," Univ. of Calif., Lawrence Radiation Laboratory, UCID-4539, Jan. 1963

10. F. Pasquill, "The Estimation of the Dispersion of Windborne Material," Meteorological Magazine, Vol. 90, 1961

11. D. B. Turner, "A Diffusion Model for an Urban Area," Journal of Applied Meteorology, Vol. 3, No. 1, Feb. 1964

12. K. M. Nagler, L. Machta, and J. F. Pooler, Jr., "A Method of Fallout Prediction for Tower Bursts at the Nevada Test Site," U. S. Weather Bureau, Washington, D.C., June 1955

13. F. D. Cluff and T. R. Palmer, "A Fallout Scaling Model for the Prediction of Gross Gamma Dose Rates from Earth Cratering Detonations," Unpublished manuscript, ESSA, ARFRO, Las Vegas, Nevada, 1964

Chapter 14

OFFSITE RADIOLOGICAL SAFETY PROGRAM

Melvin W. Carter, *Director,* U.S. Public Health Service
Southwestern Radiological Health Service, Las Vegas, Nevada

INTRODUCTION

Charter

The role of the Public Health Service (PHS) in nuclear testing is not a new one. It dates back prior to 1954, the Middle Ages of nuclear testing.

The age of nuclear testing made its dramatic debut with the Trinity Test near Alamogordo, New Mexico, on July 16, 1945. It was not until 1951 that the U.S. nuclear testing program was initiated on a full-scale basis. During the early period of atmospheric testing, radiation measurement and control, both onsite and offsite, were the responsibility of the Los Alamos Scientific Laboratory; although PHS personnel were involved on a limited basis. Manpower assistance was provided by the Army. All available personnel knowledgeable in the respective job categories of this embryonic science were deployed to Nevada during testing. During the intervals between each series of tests, they returned to their home offices.

It was during the intervals between testing series that certain problems were encountered that made it evident to both the Atomic Energy Commission (AEC) and PHS that a continuous surveillance program was necessary. Accordingly, the PHS was assigned the responsibility of conducting an Offsite Radiological Safety Program to be funded by the AEC, in the public areas surrounding the Nevada Test Site and other sites designated by the AEC for testing nuclear devices. The objectives of the PHS program, as outlined in the Memorandum of Understanding between the PHS and AEC, February 1954, are as follows:

1. To verify the offsite radiological situation associated with tests to insure protection of the public from radiological and other effects of nuclear testing. In the event unacceptable situations develop, effectuate measures as prescribed' by the AEC. This requirement includes Project Rover reactor tests conducted at the Nuclear Rocket Development Station (NRDS).

2. To document through radiation monitoring and environmental surveillance the radiation exposure to offsite areas.

3. To assure the public through personal contact, and a program of community relations and public education, that all reasonable safeguards are being employed to protect their health and property from the effects of testing.

4. To investigate incidents involving radiation or its effects which could result in claims against the U.S. Government or create unwarranted adverse public opinion.

In recent years, these objectives have been supplemented with the following:

5. To document any increase of environmental levels of radioactivity due to nuclear testing.

6. To conduct special studies to determine the transport of radioiodine in environmental and biological systems and to determine its effects on man.

7. To assist the U.S. Coast and Geodetic Survey and U.S. Bureau of Mines in the protection of the public from injury due to seismic effects of nuclear tests and from rocket firing activities at the Tonopah Test Range (TTR).

The surveillance program coverage was initially primarily limited to the area within approximately 300 miles of NTS. Subsequently, the program objectives were expanded to include the area encompassed by the 22 contiguous states west of the Mississippi River. States east of the Mississippi, Hawaii, Alaska, and the Central Pacific are also included when nuclear tests are conducted in or adjacent to such areas.

Southwestern Radiological Health Laboratory (SWRHL)

To fulfill these program objectives, the SWRHL staff of PHS has grown from a nucleus of temporary personnel in the early years of testing to the present organization of approximately 250 professional scientists and

engineers, skilled technicians, and other support personnel. This organization occupies a new laboratory complex located on the campus of the University of Nevada, Las Vegas. Although the primary effort of the laboratory is concerned with nuclear test activities and the resulting PHS responsibilities under the Memorandum of Understanding, SWRHL also has responsibility for other PHS programs in public health.

TABLE I. THE ORGANIZATIONAL STRUCTURE OF SWRHL

1. Director	Dr. M. W. Carter
Deputy Director	J. R. McBride
Staff Support	
Programs and Plans	F. N. Buck
Quality Control	R. E. Jaquish
Information Office	G. S. Douglas
Administrative Services	N. Cox
2. Laboratory Programs	
Radiation Medicine	Dr. E. van der Smissen
Environmental Surveillance (Field Operations)	R. D. Coleman
Bioenvironmental Research (Research)	Dr. S. C. Black
Technical Services (Analytical and Electronic Support)	J. W. Mullins
Technical Training and Reports	T. C. Sell

Safety Review Panels

There are numerous review panels, contractors, and consultants in the AEC Safety Program. SWRHL works with these groups and is represented on several panels including the Test Evaluation Panel and the Test Manager's Advisory Panel. These groups are discussed in other presentations.

Scope of Program

The SWRHL program in support of the Memorandum of Understanding may be subdivided into six general categories:

1. Monitoring and Surveillance Programs

2. Population and Milk Cow Statistics and Distribution

3. Community Relations and Public Education

4. Veterinary Investigation

5. Medical Investigation

6. Bioenvironmental Research

The responsibilities of each of these categories are outlined below:

1. Monitoring and Surveillance Programs

   The monitoring and surveillance may be subdivided into:

   - Routine programs conducted on a continuing basis for the determination of and monitoring of environmental levels of radioactivity.

   - Event oriented surveillance performed by mobile teams in conjunction with specific events.

   - National programs which are conducted by the PHS throughout the U.S. and are not specifically related to NTS activities.

   These programs include milk, water, air, and vegetation sampling; aerial tracking; and measurement of gamma exposures. The event oriented program also includes a mine standby program for events where significant ground motion is expected at offsite locations. Further discussion of these programs is given later in this presentation under Methodology.

2. Population and Milk Cow Statistics and Distribution

   Detailed population and milk cow surveys have been conducted throughout the State of Nevada and the parts of California and Utah within a radius of 100 to 200 miles of the NTS boundary. These surveys comprise a census of both humans, including age, and cows. This survey, in addition to a survey of Grade A dairies in Arizona, Utah, southern Idaho and parts of California, is periodically updated. A survey of active mines within approximately 100 miles of the NTS has also been

performed to provide information to be used in the mine standby program.

3. Community Relations and Public Education

Continuous efforts are made to retain good public relations through personal contact, the dissemination of timely information on nuclear tests, and the reassurance of safety. An important part of this program is the day-to-day contact of SWRHL monitors with the people in the performance of their surveillance activities in the offsite area. In addition, SWRHL personnel are not only willing, but volunteer to speak to civic organizations and other social groups.

Also vitally conducive to the success of this program is the SWRHL encouragement of private citizens to participate in surveillance activities. Routine exposure recorder, and air, milk, and water sampling stations are operated by local citizens.

Another facet of this program is the community information center. The centers are located throughout the offsite area for the purpose of providing information concerning the testing program and to announce the schedule for specific events. This program is reserved for those events in and above the intermediate yield range, greater than 200 kilotons, where perceptible ground motion is expected. The centers are staffed by SWRHL personnel several days prior to and after the event.

4. Veterinary Investigation

The veterinary or animal investigation program was established to provide background information to answer inquiries and resolve complaints or claims by livestock raisers, wildlife management personnel, and other groups concerned with the welfare of animals. The program requirements include the following:

• Maintain good veterinary relations with the offsite population.

• Investigate complaints of damage to domestic animals from AEC sponsored activities.

• Determine concentrations of fission and activation products in bovine tissues collected offsite and from the experimental beef herd on the NTS.

• Study wildlife on and adjacent to the NTS, in cooperation with other agencies, to assess the radionuclide content of edible species.

5. Medical Investigation

The primary purpose of the Medical Liaison Officer Network (MLON) is to investigate incidents related to possible or reported injury of persons of the general population resulting from nuclear test activities. The network is comprised of physicians in almost all of the 50 states and PHS Regional Office personnel who are knowledgeable in radiation injury. The Coordinator of MLON is Dr. E. van der Smissen of SWRHL.

As shown in Figure 14.1, a request for investigation of an alleged radiation injury may come to the Coordinator through PHS channels, the AEC, or other sources. On report of an incident, the Coordinator notifies the PHS Regional Office in the area involved and requests that an investigation be initiated. The Regional Office, through the State Health Officer, institutes the investigation which is conducted by the State MLON representative. The State MLON representative initially consults with the patient's physician. Depending on the circumstances of the case, he may elect to examine the patient himself.

Once the investigation is initiated, the MLON representative forwards periodic reports through channels to the Coordinator. A final report of the disposition of the case is made upon completion of the investigation. A summary of the final report is then sent to the AEC and to the agency originating the request for the investigation.

Local investigations in the area immediately surrounding NTS are made by physicians from SWRHL. These physicians follow the same procedural methods as the MLON representatives. Whether the investigation is made by an MLON representative or SWRHL physician, local specialists may be called in on the investigation for consultation or assistance; e.g., for an investigation involving a skin condition, a dermatologist may be consulted.

The philosophy of the MLON is not to state simply that this is or is not a radiation injury, but rather to make a definitive diagnosis so that it can be said, *"This is or is not radiation injury...based on the indicated diagnosis and background information."*

6. Bioenvironmental Research

This program is discussed later in this presentation under Long-Range Safety Program — Radioiodine Program.
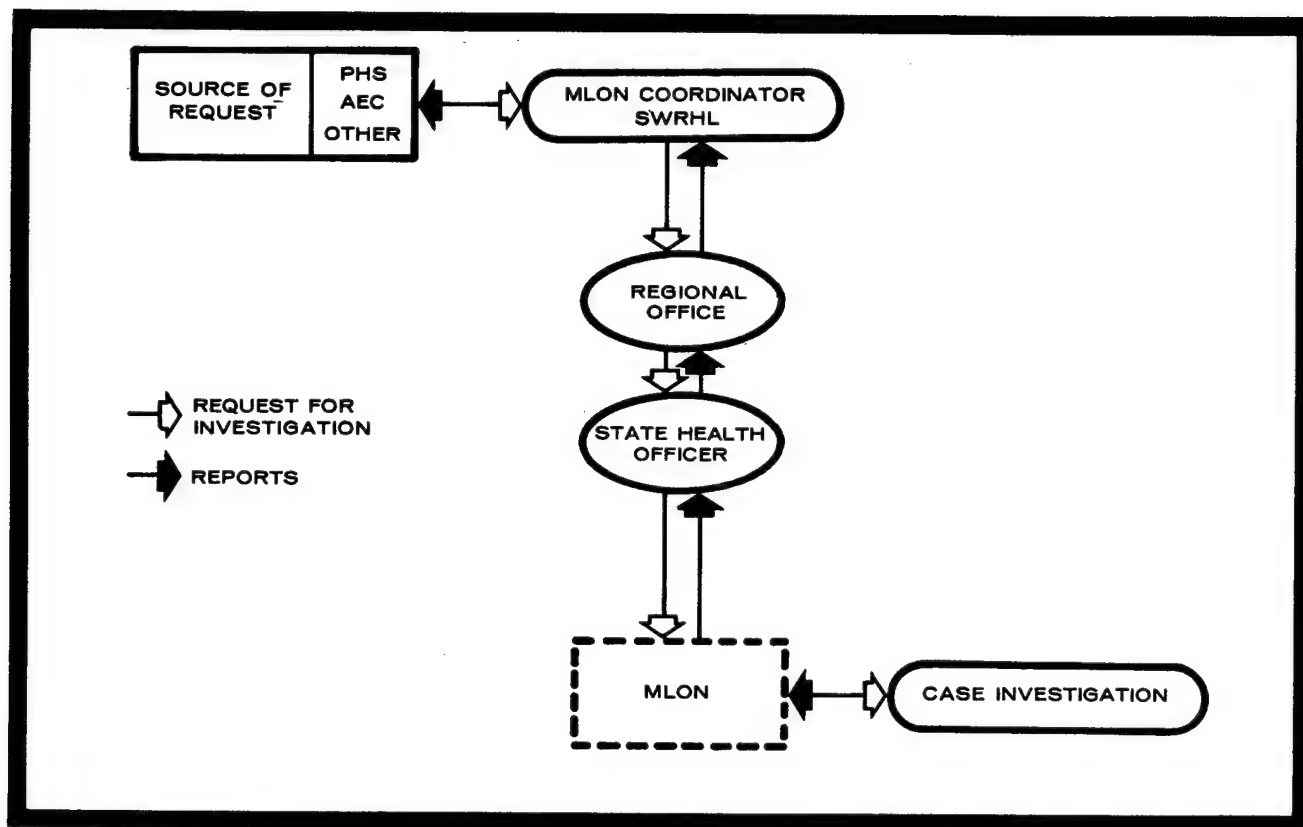
Figure 14.1.   MLON Investigation Flow Chart.

Considered collectively, these programs are complementary. A general operations plan is prepared for all routine events, and for special events these programs are incorporated into an operations plan for the specific event. This operations plan is initially approved by SWRHL and then sent to the AEC for review and concurrence. A copy is also forwarded to the PHS offices, Rockville, Maryland.

Field operations for each event are directed from the Control Point (CP) at NTS via two-way radio. During the period immediately prior to and following the event, all communications are coordinated by a radio controller at the CP. In addition, when releases of radioactivity occur or are anticipated, the Aerial Surveillance Coordination Center (ASCC) is activated by the Test Manager, AEC-Nevada Operations Office (AEC/NVOO). The ASCC, directed by Mr. F. N. Buck of SWRHL, is the clearing point for the release of initial information concerning the event and for coordination of aerial tracking. It is operated continuously while tracking planes are in flight.

The SWRHL Surveillance Information Center provides surveillance information for program planning and evaluation by the Director and his staff. It normally displays information from routine sampling networks and if a radioactive release occurs, it also displays tracking and sampling data for the event.

It is important to note that, although SWRHL as part of PHS has the responsibility for conducting the Offsite Radiological Safety Program in accordance with the Memorandum of Understanding with the AEC, it is first and foremost a public health organization. The SWRHL works continuously for the preservation and improvement of public health with other groups in PHS, the various state health departments, and other agencies. Should significant levels of activity be released from an event, the affected states are notified of the occurrence, surveillance results, and an evaluation of the situation. In addition to contact for specific events, the laboratory has continued programmatic contact with the western states and other states where events are proposed. A specific example is Project Gasbuggy in New Mexico, where state officials from New Mexico and Colorado assisted in the surveillance.

APPLICABLE RADIATION GUIDELINES

Exposure to radiation may produce harmful effects, but so may other things, e.g., electricity, air pollution, automobiles, coffee, cigarettes, etc. Radiation and electricity, etc., also have many beneficial qualities. Throughout life we are faced, consciously or unconsciously, with a risk versus benefit decision. Both the harmful and beneficial effects from the use of radiation and atomic energy have been considered in setting guides. Following is a list of several national and international groups that have been given the responsibility for determining guides; dates shown indicate the year of inception. The guides established by these groups are recommendations rather than regulations.

International Commission on Radiological Protection (ICRP) — 1928

Originated most of the basic guides we have today. Specific reports of interest are ICRP 2, 6, 9.

National Council on Radiation Protection and Measurements (NCRP) — 1929

Considered to be the U.S. equivalent of ICRP. Its early publications appear as National Bureau of Standards Handbooks, while later publications are issued as NCRP Reports.

Federal Radiation Council (FRC) — 1959

The FRC was formed (Public Law 86-373) to provide a Federal policy on human radiation exposure and as an advisory council to the President. Specific reports of interest are FRC 1, 2, 5, and 7.

The recommendations of the NCRP and FRC have been formulated into regulations by the AEC. These are:

For Licensees — Title 10 of the Code of Federal Regulations — notably 10 CFR 20 for licensees.

For AEC Contractors — AEC Manual Chapters — notably AEC Manual Chapter 0524.

Exposures are generally classified into occupational and general population exposures — excluding medical, dental, and natural background exposures. In all cases, the policy of reducing the hazard as much as practicable (minimizing dose) is adhered to. The guides for exposure of individuals in the general population are about 1/10 of those for occupationally exposed individuals.

Following is a summary of the radiation exposure guides for the civilian population under which SWRHL operates in accordance with a memo from the AEC Division of Operational Safety to NVOO, 1962. For purposes of this presentation, the differences between the terms rad, rem, and roentgen are insignificant.

In planning of weapons tests all practicable measures are taken to minimize potential radiation exposures. The criterion used for planning the events is 3.9 roentgens of whole body exposure per year. This includes

any exposure from nonweapons activities, but excludes background and medical x-ray. The criterion of 3.9 roentgens is used in the context that every reasonable effort should be made to keep the radiation exposures as low as practicable. Based on pre-event evaluation, if unanticipated yet credible circumstances could result in estimated exposures in excess of 3.9 roentgens per year, the detonation is postponed until more favorable conditions prevail. Also, to avoid any given community receiving excessive exposure over a period of years, exposures are to be limited to 10 roentgens in any consecutive 10-year period.

Nonweapons nuclear tests are conducted under the guides of AEC Manual Chapter 0524. These guides, summarized below, are compatible with the FRC Radiation Protection Guides (RPG) and are based on an annual average exposure.

TABLE II. RADIATION PROTECTION GUIDES (RADS PER YEAR)

	Individuals	Average of Sample*
Thyroid	1.5	0.5
Whole Body	0.5	0.17

*The value for the average of a suitable sample of the population stems from the FRC concept that the maximum exposure of individuals within a population class will be unlikely to exceed 3 times the average of a suitable sample. Also, when groups that are large compared to total population are exposed, the value of 0.17 rads whole body or gonad exposure should be used (genetic effects).

The ICRP, in Report No. 9, points out that exposures above the general population guide are not an indication of hazard or potential harm, but rather an indication that the methods of source control are inadequate or have broken down. With similar philosophy, the FRC in Reports 5 and 7 compiled the Protective Action Guides (PAG). These PAG's are the criteria for consideration of enactment of protective action in the event of accidents as distinguished from the RPG's for normal operations. Applicable only to incidents that are not likely to occur more than once in several years, these PAG's represent the basis for weighing the effects of a potential radiation exposure against the detrimental effects of instituting protective action; i.e., upsetting diets, distribution of food, etc. Following is the PAG for radioiodine:

TABLE III. PROTECTIVE ACTION GUIDES (RADS)

	Individuals	Average of Sample
Thyroid	30	10

The basic guides are formulated in terms of radiation doses to various body organs. Internal exposures, which are often more limiting than external exposures, result primarily from ingestion or inhalation of radioactive material. Thus, as an operational convenience, the guides are often converted to concentrations of specific radionuclides in various environmental media, notably air, water, and milk; i.e., activity per unit volume. But, in the use of these concentration guides, it is imperative that assumptions be applicable to the situation. An air concentration guide based on continuous exposure for a year should not be used to evaluate a concentration that prevailed for only several hours.

The operating philosophy of SWRHL and the AEC is not only to keep all exposures within the appropriate guides, but to keep them as low as practicable.

EVALUATION OF LIMITING EXPOSURE MECHANISMS

The evaluation of public health implications of nuclear events requires the consideration of many parameters. In summary these are:

- Source Term

  Quantity and form of the various radionuclides produced and released to the environment.

- Environmental Transport

  Transport of radionuclides from the point of release to where they are a source of exposure to the general population (atmospheric and water transport).

- Ecological Transport

  Transport through the environment to an individual, e.g., the milk-food chain, etc.

- Dose to Man

  Determination of the resulting dose to man from the various radionuclides via inhalation, ingestion, or external exposure.

The SWRHL is primarily concerned with the last two factors. Although the others are considered in program

276

planning, they are primarily the responsibility of other organizations in the AEC Safety Program.

The complete process of determining the limiting exposure (the radionuclide and/or media most likely to exceed the guide) to the public from nuclear tests is too voluminous to present in this paper. Decisions of this nature are based on theoretical studies as well as empirical results. In essence, the potential doses to the various organs of the body from various radionuclides, for various modes of biological uptake, based on the resulting contamination of the environment from nuclear events, are considered. Then, a comparison of the potential doses with the various radiation protection guides indicates which radionuclides and modes of human exposure are most important.

The following illustrates the technique of a dose calculation. First, the calculation of dose due to a quantity of material in the body is considered, and then the evaluation of a potential exposure based on radioiodine in milk is presented.

$$\text{Dose} = \frac{\text{Energy Deposited}}{\text{Mass of Tissue}} \times K \quad (1)$$

$$\text{Energy Deposited} = \left[\begin{array}{c}\text{Quantity}\\\text{of}\\\text{Material}\end{array} \times \text{Energy}\right]\left[\frac{\text{Effective}}{\text{Half-life}}{0.693}\right]$$

Mass of
Tissue = weight of critical organ

K = units conversion constant

$$\text{Dose} = \frac{\left[\begin{array}{c}\text{Quantity}\\\text{of}\\\text{Material}\end{array} \times \text{Energy}\right]\left[\frac{\text{Effective}}{\text{Half-life}}{0.693}\right]\left[K\right]}{\text{mass of tissue}} \quad (2)$$

Equation (1) indicates the units and definition of dose; i.e., energy deposited per unit mass of irradiated material at the place of interest. Equation (2) indicates the dose calculation. The quantity of radioactive material is normally expressed in curies, where a curie equals 3.7×10^{10} disintegrations per second. Thus, the result of multiplying this by the energy deposited per disintegration equals the rate of energy deposition — the first term in the equation. Then, rate per unit mass times the effective half-life divided by 0.693 equals dose. The last term is a units conversion constant.

Radioactive material decays with time; when taken into the body it not only decays, but is removed by biological processes. Thus, the quantity of any given radionuclide must be expressed as a function of time and integrated with respect to time. This gives rise to the second term

in equation (2) — the effective time the quantity of material is present (half-life/0.693).

The relative hazard of various radionuclides can be assessed by use of equation (2). Radioiodines are important because they are concentrated in a small organ in the body, and because the phenomena of environmental transport are such that significant quantities of radioiodine can reach man via the milk-food chain.

The BASIS and ASSUMPTIONS for the calculation of the potential dose from ^{131}I in milk resulting from an acute deposition of ^{131}I on the cow's feed are cited below. Similar calculations can be performed for inhalation, ingestion of vegetables, etc. It is well to note that an article in the May 1968 issue of the "Health Physics Journal" reports that up to 40 percent of thyroid exposure from ^{131}I can be from consumption of fresh vegetables. This is true for adults. However, the critical receptor for ^{131}I, due to the ratio of thyroid weight to intake parameters, is a young child or infant for whom the contribution from fresh vegetables is minor. A similar statement can be made with regard to inhalation; in that, although it is a source of exposure, the contribution of ^{131}I uptake via milk is much more significant.

BASIS:

1. Peak concentration in milk of 1,000 pCi/liter.

2. Child with 2-gram thyroid drinking 1 liter of milk per day.

3. Using FRC 5 and ICRP 2 parameters for the above equation, the following factor is calculated:

   10^3 pCi of ^{131}I in thyroid = 55.7 mrad/2 gram

ASSUMPTIONS:

1. Biological effective half-life in milk of 5 days for ^{131}I.

2. For cows feeding on fresh feed, 25 percent of the total ^{131}I intake via milk occurs prior to the time of peak concentration.

3. 30 percent of the iodine ingested is deposited in the thyroid (f = 0.3).

Equation (3) shows a simplified statement of the intake of ^{131}I from milk. The concentration of radioiodine in milk is not constant. As the cow eats contaminated feed, the ^{131}I concentration in milk builds up and then decreases with time. The concentration must be integrated with respect to time to obtain the total intake of ^{131}I.

$$\begin{array}{c}\text{Quantity}\\\text{of}\\\text{Material}\end{array} = (1 \text{ 1/day}) (\text{concentration pCi/1}) (\text{time}) f \quad (3)$$

REPRESENTATION OF MILK CONCENTRATION VERSUS TIME
(Not to scale)
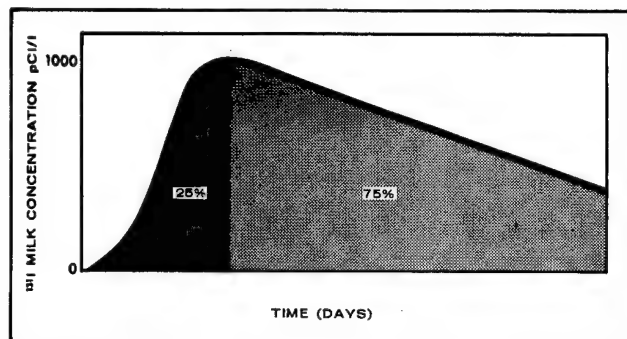
Figure 14.2. Determination of Intake.

The graph in Figure 14.2 indicates the concentration in milk as a function of time. The ordinate is a log scale so that the plot gives a straight line — exponential decay. Summation of the area under the curve indicates that the total intake is about 9.6 times the peak concentration (based on FRC Report 5). Equation (4) presents the calculation for the quantity of ^{131}I deposited in the thyroid. Equation (5) shows the product of this quantity times the dose conversion parameter — giving an estimate of the resulting dose if this milk were consumed.

Quantity
of $= 1 \ 1/\text{day} \times 1,000 \ \text{pCi}/1 \times$
Material $9.6 \ \text{days} \times 0.3 = 2,880 \ \text{pCi}$ (4)

Dose $= (2,880 \ \text{pCi}) (55.7 \ \text{mrad}/10^3$
           $\text{pCi}) = 160 \ \text{mrad}$ (5)

In summary:

1. Although under certain conditions some exposure to the public may occur, every reasonable effort is made to reduce any radiation exposure to a minimum. The methods employed to minimize exposure include: requesting people to remain under cover during passage of the radioactive cloud, substitution of clean for contaminated feed to limit the concentration of radioiodine in milk, and diverting of contaminated milk supplies to reduce the exposure to the public.

2. It is not necessary to sample everything that moves and analyze it for every radionuclide. The radiological situation can be adequately assessed with a reasonable amount of effort by determining the following:

   • critical receptor

   • critical radionuclides

   • critical environmental media and food chains

Experience indicates that whole body exposures and radioiodine exposure to the thyroid are generally the most limiting exposures from fission product releases at the NTS. Thus, effort is focused principally in that direction; although consideration is given to other situations, such as tritium in ground water. The SWRHL program provides analyses for many radionuclides including fission and/or activation products with half-lives ranging from several hours to many years. In addition, analyses may be performed for certain naturally occurring radionuclides. Although primary emphasis is given to those radionuclides considered to be biologically significant, the program is continuously reviewed to determine any necessary reorientation. Later in this report, several of the long-range safety studies conducted by SWRHL will be noted.

METHODOLOGY — MONITORING AND SURVEILLANCE PROGRAMS

This description of operational techniques is oriented towards monitoring and surveillance for events, but also includes the routine surveillance programs. Results from these latter programs are used to detect any increase in long-term background values due to testing or to detect unknown or unexpected releases, as well as to supplement the event monitoring results.

Aerial Tracking and Surveillance

Prior to the detonation of each nuclear event, an Air Force U-3A airplane, with two PHS monitors with monitoring instruments aboard, orbits near ground zero (GZ). Subsequent to the detonation, the aircraft makes low passes over GZ to determine whether or not any radioactivity is released. If there is a release, the crew reports to the CP via radio. This information supplements that obtained by an arc of onsite air samplers and the Remote Area Monitoring System. Should there be a release, the aircraft determines the following information:

1. Peak exposure rate in the cloud at various distances downwind. These data are used to estimate the general magnitude of the release and the resulting environmental contamination.

2. Cloud trajectory and boundaries at various points in time.

Two Turbo-Beech aircraft, operated by SWRHL, are also used for aerial tracking and sampling as well as initial detection of releases. The responsibilities of these planes are:

1. Assist in near-in tracking.

278

2. Cloud sampling — Sample results from which cloud inventory can be calculated are obtained by flying a prearranged flight plan with various transects of the cloud while taking both sequential and continuous samples (particulate filter, charcoal bed, and gas samples). The inventory is subdivided into its isotopic composition: radioiodine, tritium, carbon-14, noble gases, etc. Cloud concentrations at various points in time along the trajectory are also determined. The aerial estimate of cloud inventory is useful because it is the true source term for downwind projections (i.e., release minus near-in deposition).

3. Long-range tracking — Sophisticated tracking gear, including air samplers and sensitive scintillation counting equipment, are used for long-range tracking of the effluent to distances of hundreds of miles.

The aerial tracking has two immediate uses:

1. Determine cloud trajectory for positioning of ground monitors.

2. Initial, "real-time," assessment of hazard.

External Exposure Measurements

1. Routine Networks

   The following networks are operated on a continuous basis:

   RM-11

   RM-11 continuous exposure rate recorders are operated at the locations indicated on Figure 12.3. The recorder is essentially a Geiger-Mueller (GM) instrument recording on a 4-decade strip chart (0.01-100 mR/hr) recorder. The charts are changed daily and mailed to SWRHL.

   Film Badges and TLD's

   Figure 14.4 shows the locations of film badges and thermoluminescent dosimeters (TLD's) which are used to document any variations in gamma background levels. These are collected monthly. The Du Pont 545 film badges have a minimum sensitivity of about 30 mR and an upper range of 2 R. Increased emphasis is currently being placed on the use of TLD's because of their sensitivity for measuring low exposure and resistance to environmental effects. The SWRHL uses the CaF_2-Mn TLD developed by EG&G, which has good exposure-equivalent energy response characteristics from 50 Kev to several Mev and has linear dose response from several mR to 5,000 R. The film badges are analyzed by Reynolds Electrical and Engineering Company whereas the TLD's are analyzed at SWRHL.

2. Event Monitoring.

   The information from the following program is also supplemented with that from the routine stations:

   TLD

   TLD's are placed on roads forming general arcs across the predicted downwind trajectory from GZ. The minimum sensitivity on these TLD's, which remain in the field for only several days, is about 2 mR net gamma exposure.

   Mobile Monitors

   Figure 14.5 shows a SWRHL monitoring unit in the field. The monitors utilize two-way radio equipped vehicles, portable air samplers, radiation survey instruments, and containers for environmental samples. The monitors are in continuous contact with the CP, ASCC, and SWRHL via two-way radio. The SWRHL conducts a monitor certification program to insure availability of qualified personnel to perform necessary monitoring duties. The SWRHL can field about 20 fully equipped monitoring units with 20 supplementary units staffed by certified monitors. Additional personnel are available to assist in monitoring or for other duties. All monitors are equipped with survey meters, calibrated with ^{137}Cs and capable of measuring radiation levels from hundredths of an mR/hr to 50 R/hr - scintillation: low level; GM: intermediate level; and ionization chamber: high level. There are also 50 portable exposure rate recorders for positioning at unmanned locations to supplement the data compiled by the monitors. These are GM survey meters with strip chart recorders.

   The number of monitors deployed to the field is determined by the magnitude of the event. The positioning of these monitors is determined by project control personnel at the CP.

   For events where significant ground motion is anticipated, the monitors or other individuals from SWRHL are stationed at mines and susceptible structures in the area of concern during the event. They are in constant contact with the CP and advise people of the time schedule for the event and recommend that they remain outside the structures during time of detonation. Subsequent to the shot, they conduct visual inspections of the structures to gauge any hazard to personnel reentering the structure.
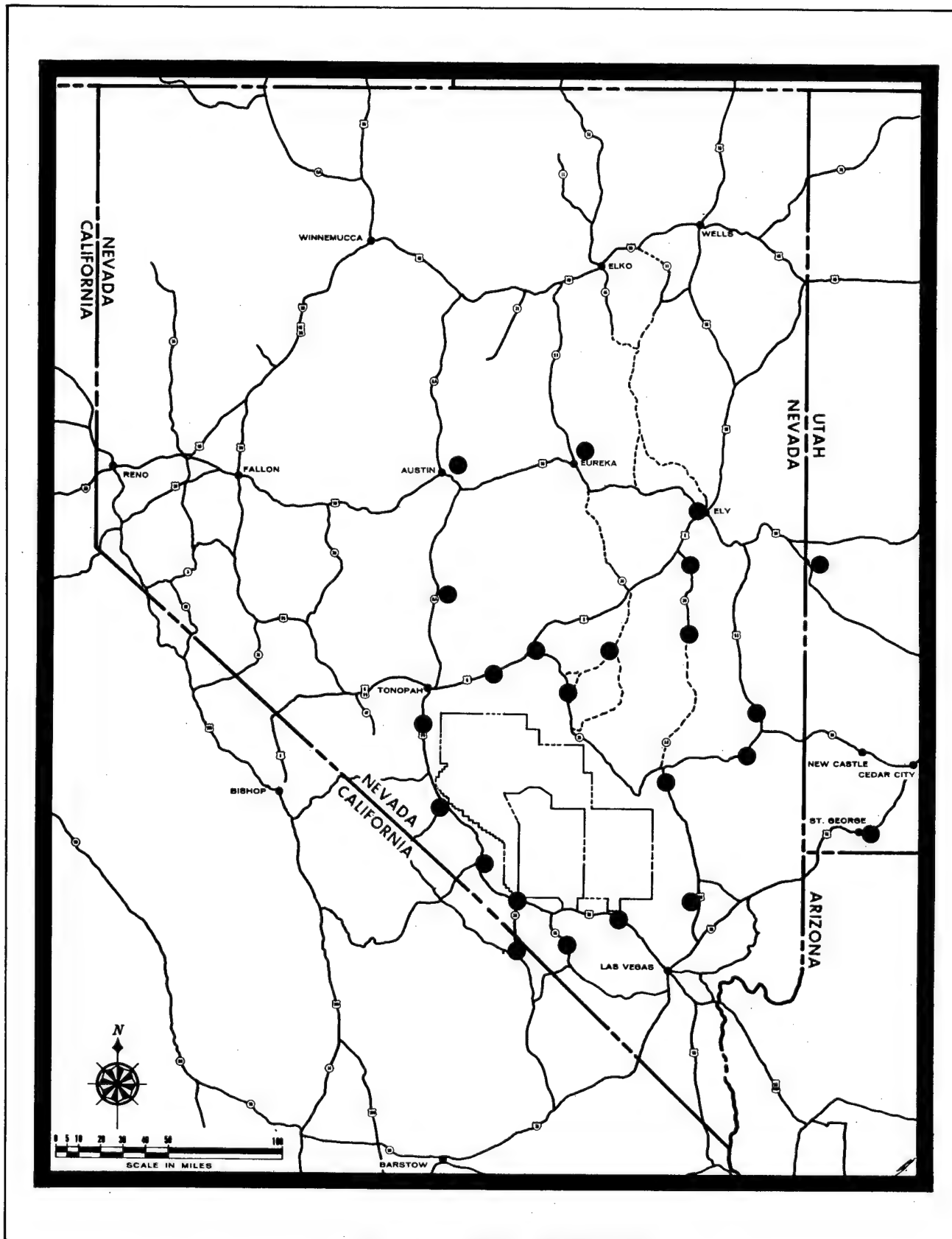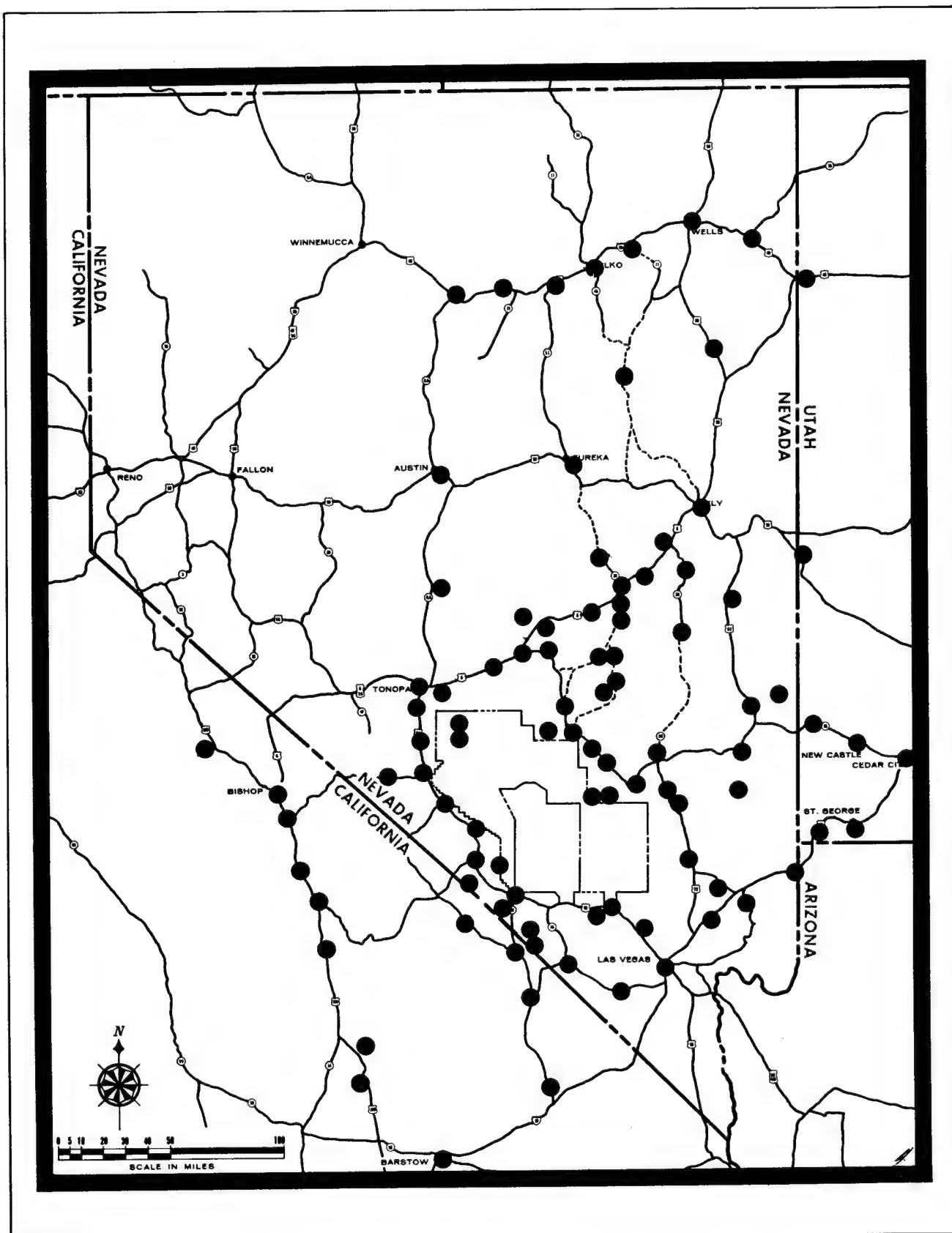
279

Figure 14.3. RM-11 Locations.

Figure 14.4. Film Badge and TLD Stations.

281

Figure 14.5. SWRHL Monitors in the Field.

Environmental Sampling

Environmental surveillance results indicate the extent of contamination of the environment, and may be used to determine the potential for ingestion or inhalation of radioactivity.

1. Routine Programs

   Air

   Figure 14.6 shows air sampling station locations; where daily samples are taken on a continuous basis using Gelman Tempest samplers operated on commercial power. The sampling medium is a 4-inch diameter Gelman Type E prefilter backed with an MSA, Part 46727, charcoal cartridge (impregnated with stable iodine and NaI for high organic iodine collection efficiency). These samplers are operated by private citizens who mail the samples to SWRHL for analysis.

   Prefilters are routinely analyzed for gross beta activity, and the charcoal cartridges are gamma scanned. If activities are above the normal background levels, the samples are analyzed for specific nuclides by gamma spectrum analysis.

   Milk

   Figure 14.7 shows milk sampling stations where samples are collected monthly. Samples are analyzed at SWRHL for specific radionuclides by gamma spectroscopy and radiochemistry.

   Water

   Figure 14.8 shows water sampling stations where samples are collected monthly. These samples are taken from both surface and underground water supplies and are analyzed at SWRHL for gross beta activity and for specific radionuclides by gamma spectroscopy. Selected samples are analyzed for ^{226}Ra, ^{238}U, and ^{3}H.

2. Special Event Sampling

   Special event sampling is performed in suspected areas of cloud passage. The effluent trajectory is determined by aerial surveillance, ground monitoring, and evaluation of surveillance sample results. Aircraft are often used for transporting samples to the laboratory to decrease the time required to assess the effects of an event. The analysis of the samples is similar to that for routine samples.

   Air

   Mobile monitors operate portable air samplers similar to the samplers for the routine network. These samples are analyzed the night of the event to determine the area of cloud passage and general ground level effluent concentrations. The concentrations of radionuclides in air are used to estimate potential inhalation doses and the concentration of radioiodine in milk.

   Vegetation

   Both natural vegetation and cow feed samples are collected. Their results are used to determine the area and center line of cloud passage and projected milk concentrations.

   Water

   Water samples are taken from all open sources of potable water and from milk sampling locations in the effluent trajectory.

   Milk

   Milk sampling locations in the area of cloud passage are selected from information based on the previously described census of Nevada locations and the standby network shown as Figure 14.9. The standby network was established with the assistance of numerous state and federal agencies. By prior arrangement, persons at the stations, when alerted by telephone, collect and mail in milk samples representative of their local areas.

   Samples are taken at these locations for approximately a week following the time of detonation or until milk concentrations return to background levels. Sampling locations are continuously revised on the basis of results; keeping in mind that the peak concentration of ^{131}I in milk does not occur prior to 2 to 5 days if the cow's intake was by ingestion of contaminated food, or about 1 day if the cow's intake was by inhalation.

Dose Assessment

The surveillance and monitoring results are continuously scrutinized to determine the possibility that there was or will be significant ingestion or inhalation of radioactivity. If so, the following techniques are used to determine the burden of internally deposited radioactivity. It should be noted that SWRHL monitors and aircraft crews, who are more directly exposed to the effluent cloud than the general population, are routinely assayed by these techniques. This furnishes an additional indication of the levels to which the population may have been exposed.

1. In Vivo Analysis

   The term in vivo stems from using an instrument to determine quantities of radionuclides inside individuals. The individual is the sample to be analyzed, thus a nondestructive technique, gamma
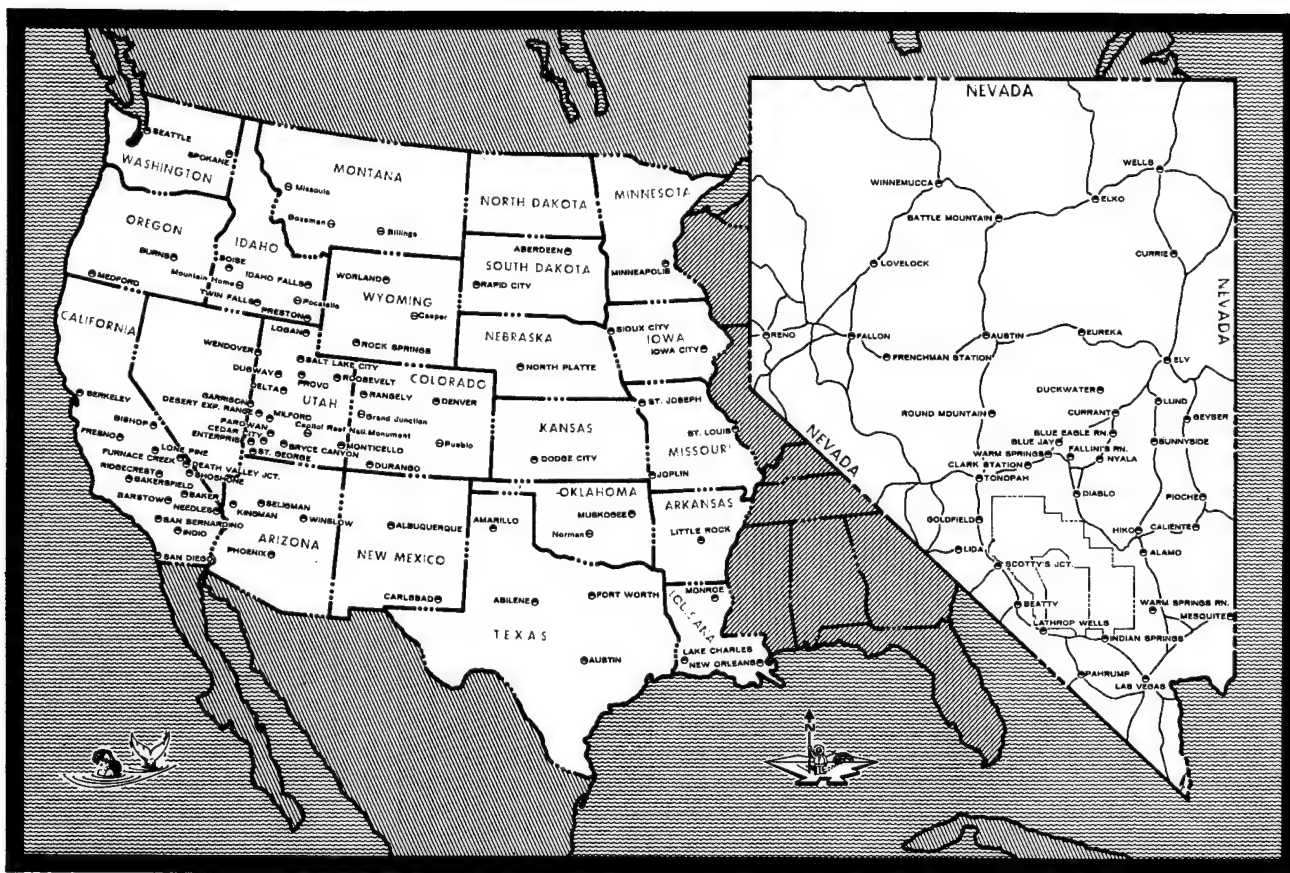
Figure 14.6. Air Surveillance Network Stations.
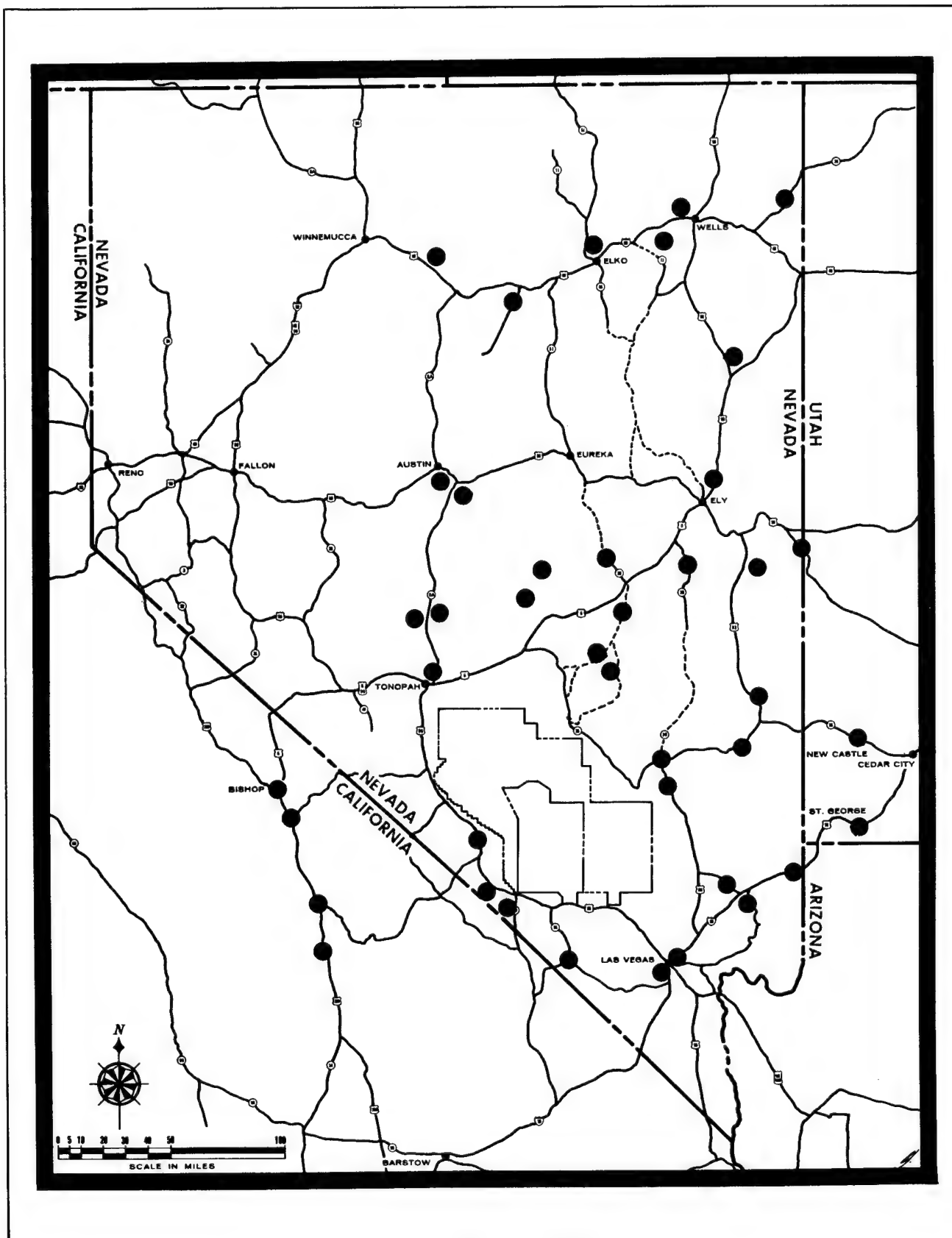
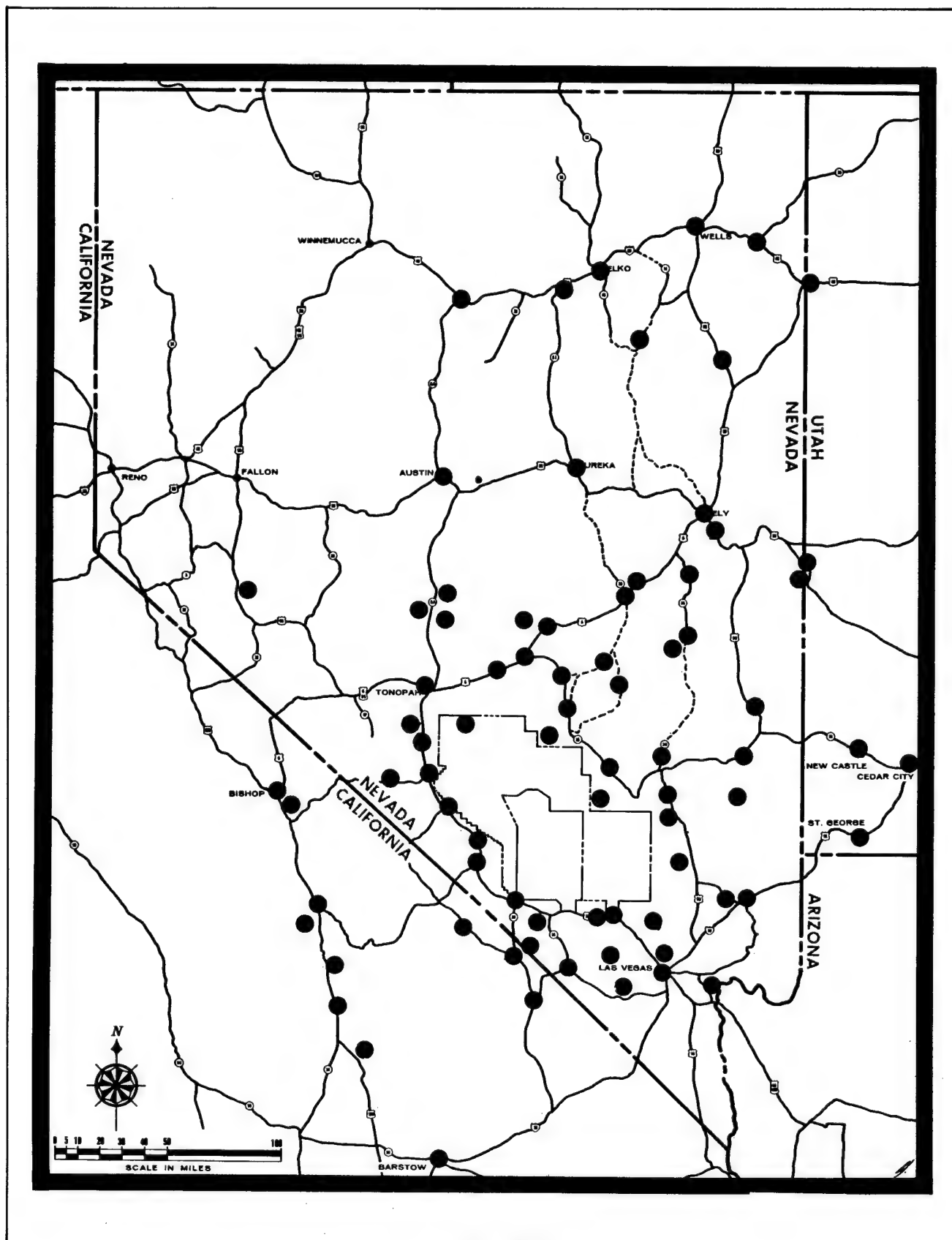Figure 14.7.   Milk Sampling Stations.

Figure 14.8.   Water Sampling Stations.
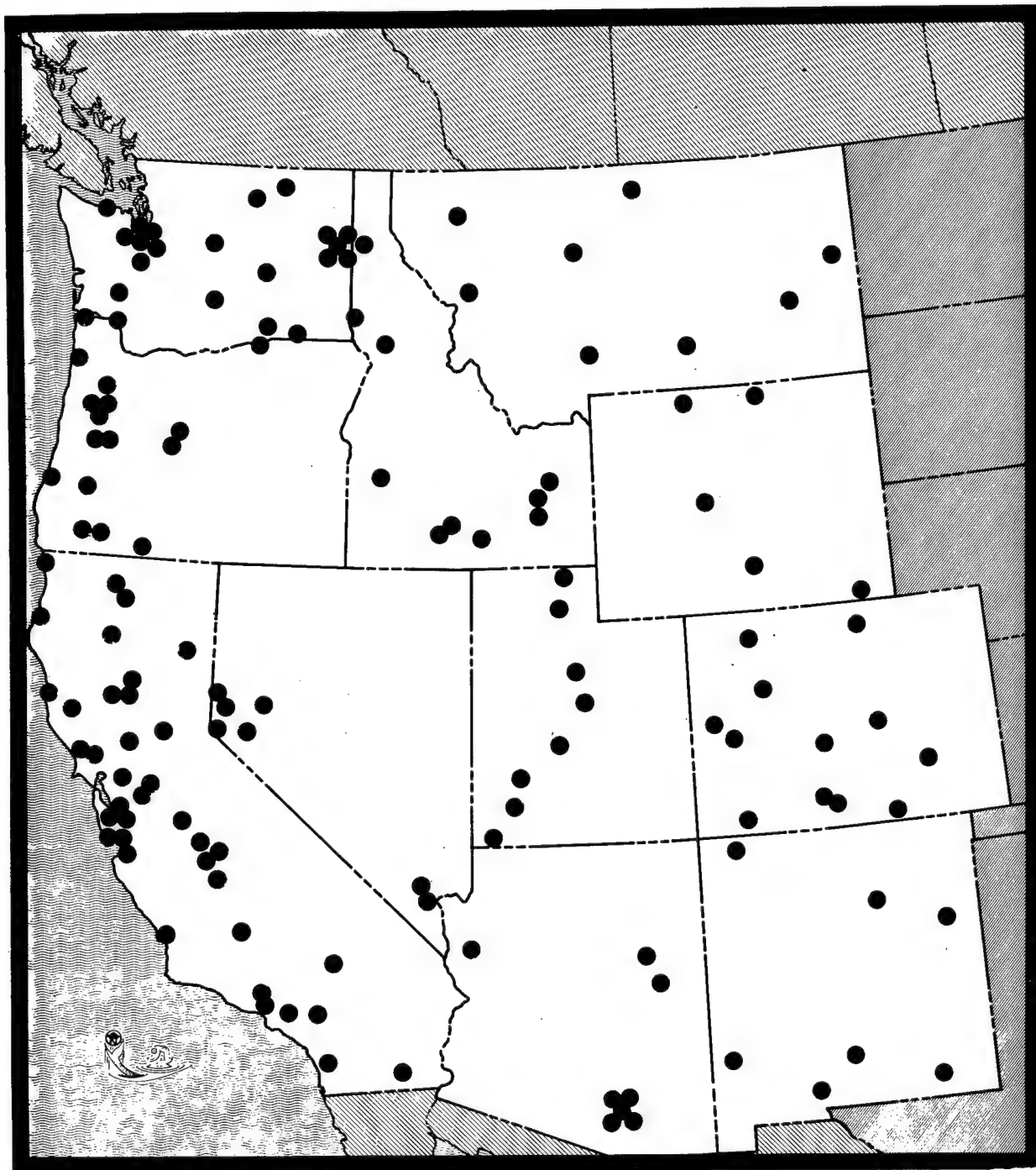
Figure 14.9.   Standby Milk Surveillance Network.

spectroscopy, is used. The technique is applicable to radionuclides such as ^{137}Cs which are uniformly distributed in the body as well as to radionuclides such as ^{131}I that are localized in a specific organ.

The subject is placed in what is often termed a whole body counter in close proximity to the detector, NaI crystal. The gamma spectra obtained is analyzed by techniques similar to those used for spectra obtained from environmental samples. The results include both the identity and quantity of gamma emitting radionuclides that are present. Figure 14.10 shows the trailer containing the SWRHL portable whole body counter. Figure 14.11 shows a subject being counted. The major items of interest are (1) the analyzer, (2) the detector, and (3) the couch. This system is specially designed for detection of radioiodine contained in the thyroid.

A more sophisticated in vivo detection system is located at SWRHL. It is designed to locate and determine the quantity of gamma emitting radionuclides contained in the body. This system is underground and contains special shielding to lower the background from external radiation, thus increasing its detection capabilities.

2. Bioassay

Samples of body excreta, such as urine and feces, are analyzed to determined the quantities of various radionuclides present. Using information concerning the rate of excretion of the nuclides, it is possible to determine the body burden of such nuclides as tritium and plutonium.

These in vivo and bioassay techniques determine the amount of various radionuclides deposited in the body. On the other hand, environmental surveillance indicates the amount of radioactivity available for ingestion. Based on information from either of these sources, together with an estimate of the weight of the organ in which the activity is deposited and estimates of when the activity was ingested, the dose to the individual can be calculated.

RESULTS

The following summary of results from the Pin Stripe event is atypical and was selected to give an example of the upper magnitude of levels resulting from NTS releases and as an indication of the type of results obtained.

Pin Stripe was an underground test which released radioactivity to the atmosphere. It was conducted on April 25, 1966, at 1138 PDT. Figure 14.12 indicates the locations

of GZ and some of the sampling stations for this test. Table IV gives a summary of the gamma results. The highest gamma exposure rate at a populated location was 1.5 mR/hr measured at Hiko, Nevada, during cloud passage.

TABLE IV. PIN STRIPE GAMMA EXPOSURES

Location	Distance Miles from GZ	Time	Net mR/hr*	Comments
18 mi NE of Groom Lake	40	1405	8	Unpopulated
Hiko	65	1600	1.5	
Caliente	95	1814	0.02	
Pioche	110	1850	0.05	
*Measured with E-500 B.				

A summary of milk results is listed in Table V. The highest milk concentration was 4800 pCi/1 at the Schofield Dairy at Hiko. At the request of the AEC, whose decision was in part based on a PHS recommendation, hay was substituted for fresh feed for all but 4 cows at this dairy. The milk from these 4 cows was used in a field study and was not consumed by humans. This substitution was made on about D+3, about the time of the peak concentration. It reduced the potential ^{131}I dose by about 70 percent. The milk from the other cows at this dairy was picked up by tank truck and transported to Las Vegas for processing. The peak concentration after dilution by the milk in the truck was 100 pCi/1. There was no radioiodine detected in processed milk in the Las Vegas area.

TABLE V. PIN STRIPE MILK RESULTS

Location	Distance (Miles)	Date	^{131}I pCi/1	Comment
Hiko, Schofield	65	4/27/66	4800	
Hiko, Davis	65	4/27/66	3500	All milk taken for sample
Ursine, Donahue	125	4/28/66	1100	All milk taken for sample
Alamo, Sharp	55	4/28/66	2100	All milk taken for sample
Caliente, Charlton	95	4/28/66	130	
Panaca, Lee	105	4/30/66	170	

Cow feeding practices varied during this period of time. Generally, the higher results are from locations where cows were on fresh feed.

Figure 14.10.   In Vivo Thyroid Counting Trailer.
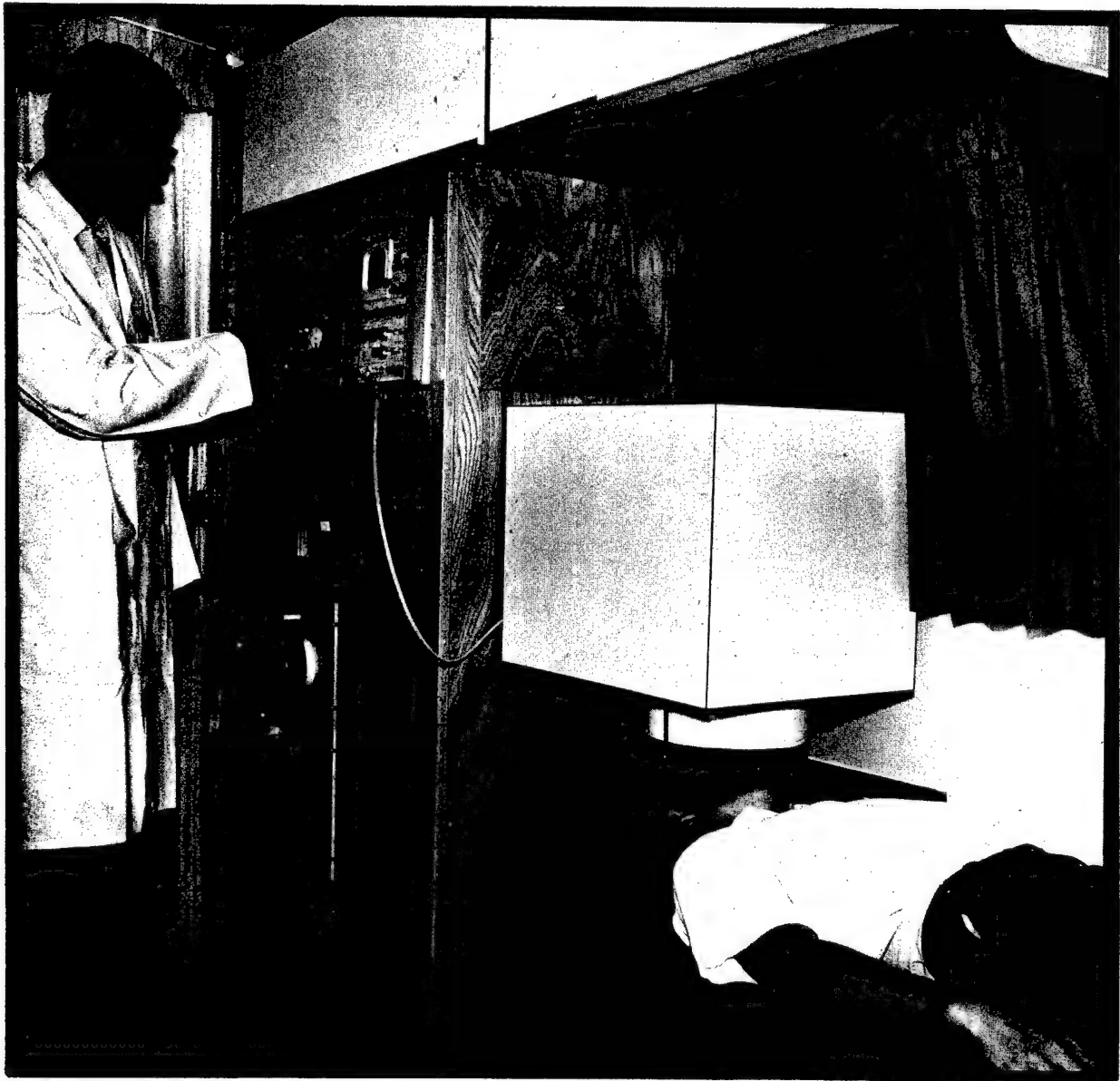
Figure 14.11. Thyroid Counting.
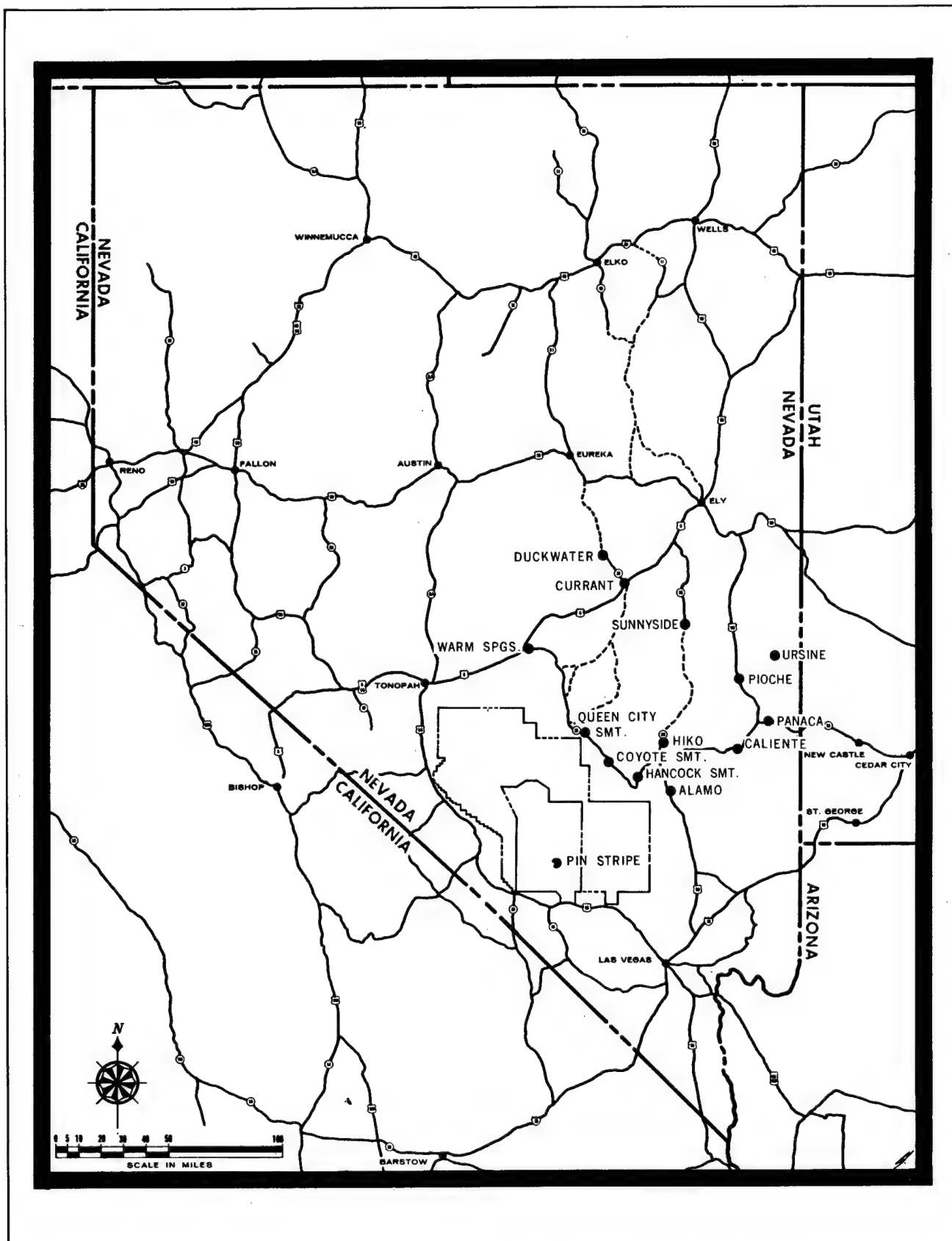
Figure 14.12. Pin Stripe — Map of Nevada.

TABLE VI. PIN STRIPE AIR RESULTS

Location	End of Collection	Running Time**	Collector	131I pCi/m³	131I pCi-sec*/m³	133I pCi/m³	133I pCi-sec*/m³
6.5 mi W of Hancock Summit	25/1700	3.1	P	3500	4.1E7	4100	5.1E7
			C	150		500	
Ash Springs	25/1755	3.3	P	5300	6.5E7	5600	7.0E7
			C	130		290	
Hiko	25/1800	10.9	P	510	2.2E7	650	3.1E7
			C	39		150	
Pioche	25/1925	3.9	P	1100	1.6E7	350	0.8E7
			C	53		250	

*pCi-sec/m³ = Air concentration in pCi/m³ times the time of exposure in seconds. E7 = 10⁷.
**Metered running time in hours.
P = Prefilter; C = Charcoal Cartridge.

Table VI gives a summary of the air results. The integrated air concentration is a summation of pCi/m³ times time.

Table VII indicates the estimated thyroid doses as determined from the ^{131}I and ^{133}I thyroid burdens. The indicated ranges are maximum doses based on conservative assumptions, i.e., assumed exposure resulted from inhalation rather than ingestion.

TABLE VII. PIN STRIPE THYROID COUNTING RESULTS

Location	Distance (Miles)	BKG	<50 mrad	50-150 mrad	150-300 mrad	Total People
Pioche	110	1	0	0	0	1
Panaca	105	5	0	0	0	5
Ursine	125	4	1	0	0	5
Alamo	55	10	17	6	0	33
Hiko	65	5	19	8	2	34

Number of people within given range of computed thyroid dose.

The results from Hiko are comparable with the following estimate based on environmental samples:

^{131}I Inhalation	23 mrad
^{133}I Inhalation	9 mrad
^{131}I Ingestion via milk	254 mrad
^{133}I Ingestion via milk	184 mrad

The total estimated dose is about 470 mrad (assuming an infant with a 2 gram thyroid, drinking 1 liter of milk per day and breathing 6m³ of air per day).

This estimate of 470 mrad compares favorably with the thyroid counting results of two of the children who received an estimated 150-300 mrad. The thyroid weights for the subject children based on their ages were greater than 5 grams.

The values of ^{131}I in milk at Hiko were less than 1/10 of the PAG; thus, the substitution of feed at Schofield's Dairy was done in large part to investigate the operational procedures and effectiveness of protective actions. Also, early results had indicated that values would be higher than those that actually occurred and, considering the apparent ease of instituting the protective action, it was deemed prudent to do so. This action complied with the philosophy of avoiding unnecessary exposure.

Normally the dose contribution from ^{133}I ingestion via milk is much smaller than that for ^{131}I. In this case, due to the protective action taken, the dose from ^{133}I relative to ^{131}I became significant. Due to the short half-life of ^{133}I, its dose contribution was about 90 percent complete by the time protective action was instituted.

The RPG's were not exceeded in this example. The exposures were within the guides for an average of a sample of the general population. Although in the case of the higher exposures, the monitoring was sufficiently detailed that the individual guides were applicable.

The SWRHL routine surveillance results indicate that in recent years effluent from the test site activities has not produced any significant long term increases in the offsite background radioactivity levels. This statement is based on our routine isotopic; e.g., ^{3}H, ^{90}Sr, and ^{137}Cs results for water, air, and milk; and gamma exposure results from film badges, monitoring instruments, and in recent years TLD's.

PROTECTIVE ACTION

The potential requirements for taking protective action to eliminate or reduce public exposure to radioactive contaminants exist in connection with all nuclear experiments. Pre-event planning must examine this potential with respect to both the predicted or potential concentrations and exposure rates to which the general public may be subjected as well as the possibility of after the fact information indicating the requirement for emergency action. In general, the lack of a satisfactory protective action plan is sufficient grounds for recommending delay or cancellation of an experiment.

Figure 14.13 indicates some of the generalized types of protective action which have been (may be) taken by the Offsite Radiological Safety Program in cooperation with various state agencies and the general public following previous nuclear experiments. As can be seen, evacuation of an area prior to the event is by far the most effective method of reducing the external whole body exposure. Because general safety considerations would limit the necessity for this type of action to an area relatively close to the site of the experiment, the estimation of the effectiveness of reduction of dose due to deposition has been based on an arrival time of H+1 hour for the radioactive cloud. It also includes the further assumption that the exposure is due to fission products. The combined effect of evacuation prior to cloud arrival and return from 24 to 48 hours later not only reduces the total dose due to cloud passage and deposition by a factor of 3 or 4, it also eliminates the problem of inhalation exposure during cloud passage. By contrast, keeping individuals indoors during cloud passage is estimated to be only about 50 percent effective in reducing both the whole body and inhalation exposures. Unless additional constraints are imposed beyond the time of cloud passage, significant exposure due to deposition can still occur.

Evacuation following cloud passage would obviously be an example of an emergency response. There would be no affect on the dose due to cloud passage which might normally be expected to represent 50 percent or less of the total dose, and its effectiveness in reducing the dose due to deposition will be a rapidly decreasing function of time.

A second area in which protective action is both feasible and effective is the reduction of dose to the thyroid resulting from drinking milk contaminated with radioactive iodine. While it is recognized that milk may not be the only significant source of radioiodine for adults, it does represent the only significant source for the critical receptor (young child). The most effective method of dose reduction in this case is to remove the milk from general availability and replace it with milk from an uncontaminated supply. Where large dairies or major producers are involved, this is unattractive from both the economic and public relations standpoint. A special form of this technique, applicable to the individual family milk cow, removes the milk by taking it for analysis and replacing it with uncontaminated milk. This method which serves the double purpose of providing analytical data and effectively reducing thyroid dose, is utilized regularly by the Offsite Radiological Safety Program.

Diverting milk to cheese processing, rather than consumption as whole milk, introduces a time delay which normally permits the decay of the radioiodine to 25 percent or less of its initial concentration.

When predictions indicate that unacceptable concentrations of radioiodine could occur in milk, it may be desirable to protect stored feed from contamination by covering it. Feeding this to milk cows rather than permitting them to graze on pasture, or to feed on contaminated material will significantly reduce the concentration of radioiodine in their milk. The method is not 100 percent effective due to exposure of the cows from inhalation, possibly from open drinking water supplies, and other general contamination of the area.

Replacement of contaminated feed by an uncontaminated supply can be used to produce a rapid reduction in milk concentrations of ^{131}I. The normal effective half-life for ^{131}I in milk resulting from an acute deposition on pasture is 5 days. Introducing uncontaminated feed as the sole diet can be expected to reduce this half-life to 1 to 2 days. Figure 14.13 indicates the effect on the total dose of replacing feed. For ease of calculation, it was assumed that action was initiated at or after the peak concentration had been reached and continued to the same end point (10 days after the peak). Initiating action before the peak has been reached will have a substantially greater effect. For this reason, the development of accurate prediction techniques to estimate the peak concentrations of ^{131}I in milk assume major importance. These methods must include techniques to be applied during the planning stages before an event, as well as development of the probable relationships between milk, air concentrations, and level of pasture contamination for application to actual event data.

The graph in Figure 14.14 is a representation (not to exact scale) of the milk concentration at Schofield's Dairy, Hiko, Nevada (See Typical Results for more details.), which resulted from the Pin Stripe event. A peak concentration in milk of 4800 pCi/1 of ^{131}I occurred the second day after the event and it was decided to substitute stored uncontaminated feed for the contaminated green chop which the cows were being fed (third day). The area under the curve has been divided into three areas (A, B, and C) where:

A. Reduce External Dose

1. Due to Cloud Passage

> EVACUATE PRIOR TO CLOUD ARRIVAL
> KEEP UNDER COVER

2. Due to Deposition
(H+1 Hr. Arrival)
    a) Evacuate Prior—
    b) Evacuate After
       Cloud Passage

> RETURN AFTER: 1 DAY   2   5 10

      1 Hour
      5 Hours
      1 Day

> RETURN AFTER: 1   2   5 10
> 1 DAY   2   5 10
> 1   2 10

ACTION AT OR AFTER THE PEAK (COWS ON FRESH FEED)

B. Reduce Thyroid Dose
(Milk Contamination)
    Dump or Divert

> REMOVE & REPLACE FOR 2 WEEKS
> DIVERT TO CHEESE
> PEAK TO + 10 DAYS

    Replace Feed

> PEAK +1 TO +10
> +2 TO +10
> +5

    Cover Stored Feed

> PRIOR TO CONTAMINATION

0   .50   1.00

MAXIMUM POTENTIAL DOSE REDUCTION

Figure 14.13   Generalized Protective Action.

Effectiveness Of
--Changing Cows Feed
--Normal Dilution
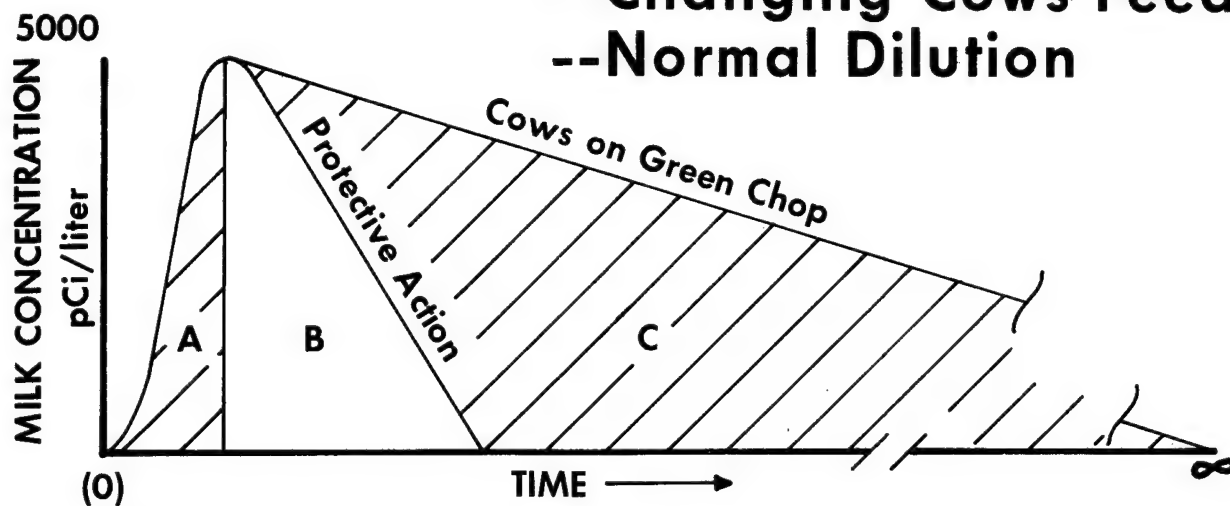
DESCRIPTION	AREA	FRACTION	% DOSE SAVED
Total Area (no P.A.)	A+B+C	A+B+C/A+B+C	————
Total Dose Saved	C	C/A+B+C	70%
Projected Dose Saved	C	C/B+C	85%
Dilution in Tank Truck	Reduced Peak From 5000 to 100 pCi/liter		
Processed Milk	Radioiodine Not Detectable		

Figure 14.14.   Pin Stripe Protective Action.

Area A — Integrated milk concentration prior to the peak.

Area B and C — Integrated milk concentration after the peak if no action had been taken. This is based on several cows which were fed contaminated green chop all the time.

Area C — The integrated milk concentration saved by the protective action.

The milk concentration integrated over time (the area under the curve) is proportional to the dose to the thyroid if the milk had been consumed. Thus, the relative areas are related to doses or fractions of dose.

Figure 14.14 indicates the effectiveness of the various actions taken. The only countermeasure was the substitution of feed. The dilution of the Schofield milk by other milk in the transport tank truck and additional dilution and reduction of the radioiodine concentrations due to processing were a result of normal operation procedures, not countermeasures.

The effect of sampling procedures at the Davis, Donahue, and Sharp Ranches (Table V) (which could be termed countermeasures) where the contaminated milk (family cows versus dairies) was removed by sampling are not included in the figure. The effectiveness of this procedure is determined by how early sampling is initiated and its intensity and duration. The protective action at Schofield following Pin Stripe was taken primarily to gain experience rather than because of necessity. The experiment indicated that the substitution of stored feed was an effective measure.

LONG-RANGE SAFETY PROGRAM— RADIOIODINE PROGRAM

Scope

In the spring of 1963, the AEC sponsored a meeting to examine all aspects of potential radioiodine doses which could result to humans from the release of mixed fission products into the biosphere. Four areas, summarized in Figure 14.15, were considered.

In brief, the meeting attendees concluded that a coordinated major research effort was needed in the areas of transport, environmental monitoring, and biological studies. The AEC amended the Memorandum of Understanding to provide that the PHS would mount a Long-Range Safety Program to conduct the appropriate studies. This included U.S. Weather Bureau support to assist in the transport phases of the studies. The Bioenvironmental Research Program of SWRHL was initiated on July 1, 1963, with the mission of conducting the required research studies to obtain the needed information.

Problem Definition

The approach conceived constituted problem oriented systems research. Figure 14.16 depicts the principal elements in the system under study.

The systems approach used consists of measuring pertinent input parameters to each system, and then measuring the output of interest. With this approach, it is not necessary to fully define all the inner workings and detailed mechanisms which function within a system. However, as knowledge of the input-output relationships of the major systems grows, it is planned to intensify research in the smaller subsystems in order to gain a working knowledge of the mechanisms.

Approach

In general, there are two separate types of situations for which field experiments were designed and conducted. These are:

1. All nuclear tests in which there is a reasonable probability that radioactivity will be released to the atmosphere. An example of this is a nuclear cratering experiment or Project Rover reactor test.

2. A nuclear test in which radioactivity is inadvertently and unexpectedly released to the atmosphere.

The approach for the type 1 situation is to establish stations in the predicted fallout pattern. Air samplers, fallout trays, film badges, lactating dairy cows, and dairy cow forage of various types are located at these stations. Subsequent to the test, environmental surveys are made at each station. Many different types of samples are collected and analyzed for radionuclides. Air uptake of radionuclides by lactating dairy cows in the fallout pattern is studied by measuring the secretion of radionuclides in their milk. The contaminated forage is removed from the area, transported to the dairy barn, and fed to different groups of experimental lactating cows. Radioactive uptake from the contaminated forage is also studied by measuring the secretion of radionuclides in milk. Quantitative relations are then established for forage-to-milk radionuclide ratios, for time after beginning ingestion of contaminated forage for the radionuclide concentrations to reach a peak in the milk, for disappearance rate of the radionuclides from the milk after the peak has been reached, and for the percentage of the radionuclides on the forage which subsequently appear in the milk.

The approach for type 2 situations involves organizing an "after-the-fact" study at one or more existing dairy farms in the fallout pattern. The exact nature of the study depends upon the extent of cooperation established with the dairy farm managers. An attempt is made to de-
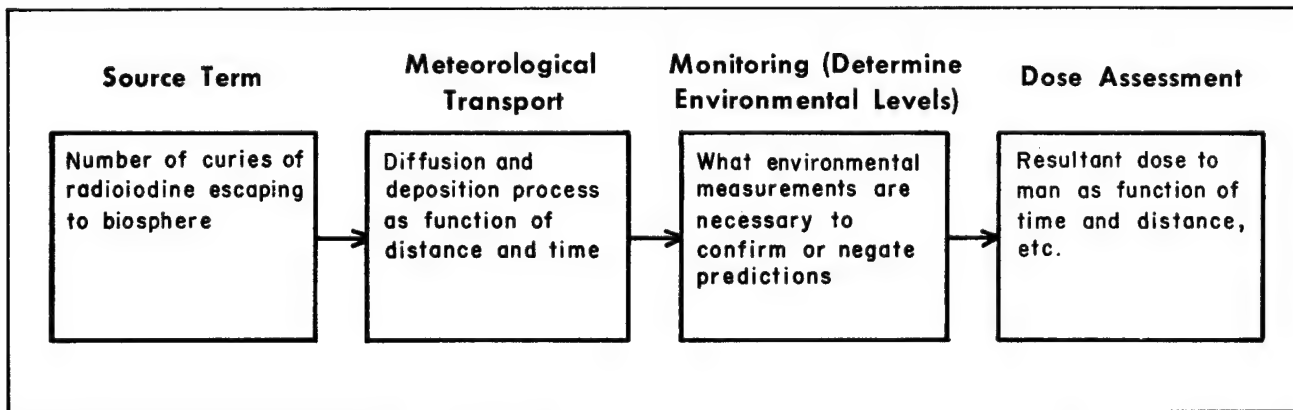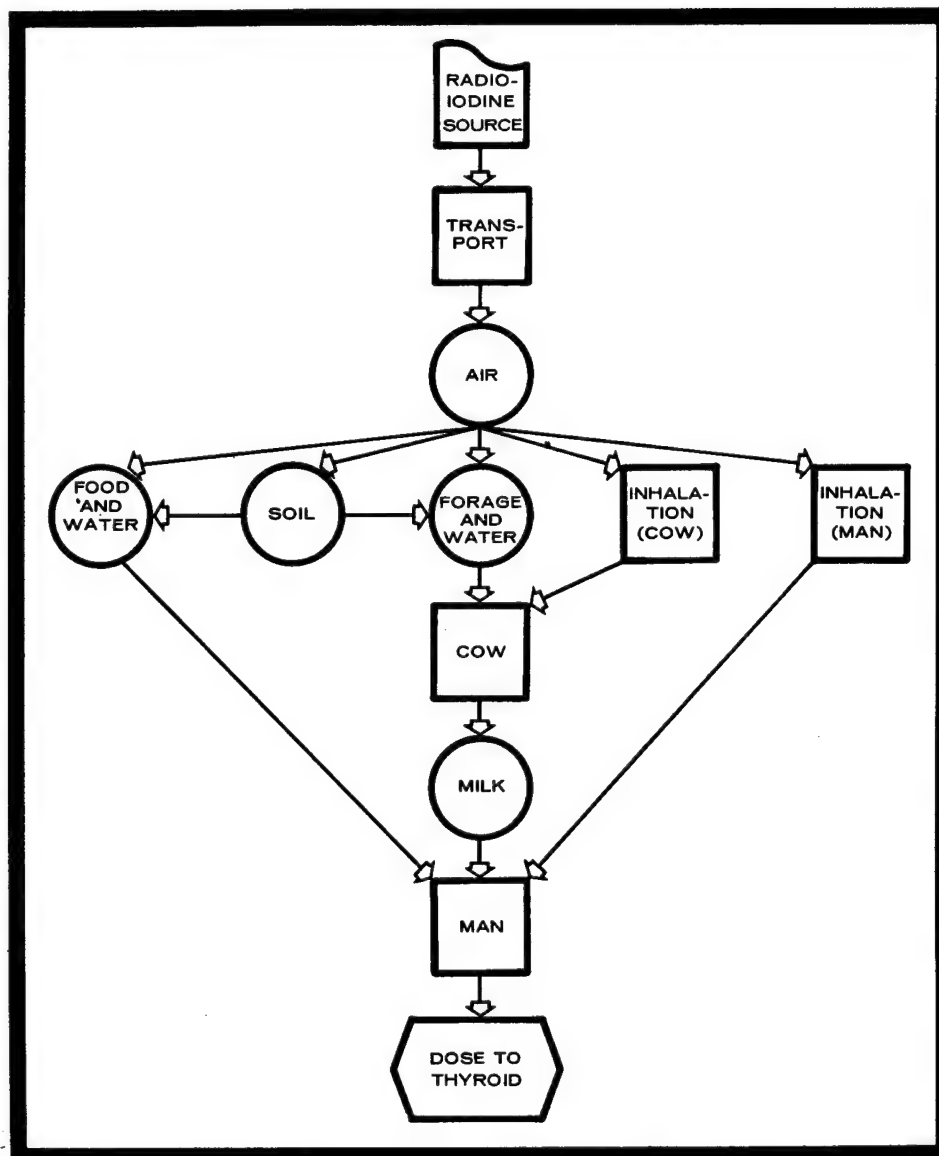
Figure 14.15. Study Areas for Radioiodine.

Figure 14.16   Radioiodine — Source to Man.

297

termine the same relationship among air-forage-milk as is done in the type 1 approach.

In addition to the studies described above, controlled releases of radionuclides over growing forage crops, at the PHS experimental farm on NTS, are conducted. In general, these studies correspond closely to those of type 1, above. To date there have been five such controlled releases.

Both the Radioiodine Program and the Offsite Radiological Safety Program complement each other for both type 1 and 2 events. This is apparent in that results from the Safety Program are used in a decision to initiate the type 2 study.

Results

The first of the type 2 studies followed the Pike event and took place at two neighboring Las Vegas, Nevada, dairy farms. In summary, the results of this study indicated that the peak ^{131}I concentration in milk for cows on stored or dry feed was 1/6 of that for cows fed fresh feed (green chop). The half-life for ^{131}I in milk for the two feeding conditions was 3.5 days for fresh feed and 6.5 days for stored feed.

As previously cited, a similar study was conducted at two dairies in the Alamo-Hiko area following the Pin Stripe event. The effective half-lives at the two locations for ^{131}I in milk (cows eating contaminated fresh green forage) were 4 and 5.6 days, respectively.

As an experimental countermeasure, one group of cows was fed uncontaminated hay after 3 days on the fresh forage. This countermeasure reduced the potential thyroid dose from ^{131}I to humans drinking the milk by about 70 percent.

In addition to the two previous studies, type 1 field studies have been conducted in association with the Transient Nuclear Test of a Kiwi Reactor; Projects Sulky, Palanquin, Cabriolet, and Buggy I, all Plowshare cratering experiments; and five studies involving controlled releases of ^{131}I. These latter studies included three releases with different diameter dry aerosols, one with gaseous iodine, and one using an aerosol mist; it was found that the ^{131}I appeared more biologically available as the dry particle size decreased.

To summarize these studies, radioiodines are secreted in cows' milk following intake by either inhalation or ingestion of various types of contaminated feed. Generally ingestion is the most significant source of uptake of radioiodine by the cow. The biological availability of radioiodines, as measured by the milk-to-forage ratio,

is a function of several variables, including:

1. The type of forage.
2. The particle size distribution and gaseous-to-particulate ratio of the contaminating effluent.

Future Direction

Future research will be concentrated on iodine metabolism in the cow, using various types of ingesta, and on the air-forage link in the food chain. Particular emphasis will be placed on *post facto* estimation of fallout characteristics, such as the gaseous-particulate ratio, particle size distribution, and soil-to-plant transfer. The metabolism studies will include various types of ingesta, or combinations of them, containing various particle size distributions of radioiodine.

It is anticipated that by mid-1969, it will be possible to predict, to an accuracy of a factor of 2 at the 90 percent confidence level, the average peak levels of radioiodine in the milk of dairy cows fed feed from a fallout area—when the source of radioiodine and the meteorological conditions are known.

The Radioiodine Program is not the only long-range safety study conducted at SWRHL. The program concerned with long-lived radionuclides is particularly worthy of mention. The SWRHL is also in the process of establishing a program to assess the significance of radionuclides that may be found in natural gas as a result of nuclear stimulation of gas wells.

CONCLUSION

The efforts and achievements of SWRHL represent many man-years of study and experience in Radiological Safety Programs. Many millions of dollars are spent on research, field studies, and operational safety. The PHS-SWRHL policy, in conjunction with that of the AEC, is to protect the general public from exposure to needless or excessive quantities of radiation. That is the professional responsibility of the PHS.

A large amount of the effort in the offsite safety program is applied to events that do not release radioactivity to the offsite area, but — this information comes through hindsight — the effort must be made to insure adequate protection should there be a radioactive release. The results from the small number of underground events that have released radioactivity to the offsite area since the Limited Test Ban Treaty resulted in doses below the FEC and AEC guides.

298

To the best of our knowledge and belief, there has never been any radiation injury to offsite residents as a result of continental nuclear testing. It is the job of the PHS-SWRHL to assist in preserving this status quo. The employees of the SWRHL and their families give testimony to confidence in the Safety Program by residing in the offsite area.

Several facets of our program, specifically analytical techniques, are covered in more detail in NVO-28, *Safety Involving Detonation of Nuclear Devices*. Our laboratory reports are available through the Oakridge DTIE. Event summary reports are published in the U.S. Health, Education and Welfare publication, *Radiological Health Data and Reports*.

Chapter 15

BIOENVIRONMENTAL SAFETY

R. G. Fuller, *Ecologist* and W. E. Martin, *Radioecologist*
Battelle Memorial Institute, Columbus Laboratories, Columbus, Ohio

INTRODUCTION

The Columbus Laboratories of Battelle Memorial Institute have been assigned the responsibility for planning and carrying out applied ecology studies required by NVOO in connection with underground nuclear detonations. The safety programs discussed in other chapters of this publication are primarily aimed at protecting people from direct injury, and man-made structures from direct damage, during testing of nuclear explosives. The bioenvironmental safety program is concerned with the more subtle and indirect consequences of such tests: the potential exposure of people to internal radiation via food chains, direct or indirect damage to wildlife populations, and environmental disturbances that may lead to undesirable ecosystem changes. As noted in Chapter 14 of this publication, certain aspects of bioenvironmental safety are included in the responsibilities of the U. S. Public Health Service. For example, USPHS collects demographic data, and monitors offsite atmospheric radiation levels and radioisotope levels in milk. Other investigations at the NTS, supported by the AEC Division of Biology and Medicine, or conducted by AEC laboratories, include basic research on the effects of radioactivity on natural vegetation, and the cycling of radionuclides in ecological systems. These studies generate information useful to the NVOO bioenvironmental safety program, which is largely a mission-oriented effort directed to the needs of specific test events at sites other than the NTS.

The bioenvironmental safety program deals with the potential impact of such shot-related perturbations as air blast, ground motion, and radionuclide release on the ecosystem. In addition it considers the ecological consequences of construction, site preparation, and drillback activities associated with the execution of the detonation. Such ancillary operations may sometimes have more influence on the ecological system than detonation of the nuclear device. Within the context of the safety philosophy, it is the aim of NVOO to avoid or to minimize detrimental ecological changes due to nuclear detonations, whether such changes arise from human occupancy of the site, construction activities, or from the detonation itself. The bioenvironmental safety program is specifically designed to assist NVOO in achieving that aim, as well as to protect humans from exposure to radiation through indirect environmental pathways.

OBJECTIVES

Bioenvironmental safety studies are directed toward four principal objectives: (1) prediction of the potential effects of any given detonation on the surrounding ecosystem and, via indirect routes, on humans; (2) recommendation of courses of action to avoid or to minimize harmful test consequences; (3) post-event documentation and evaluation of the ecological effects, if any, of the test; and (4) recommendation of corrective action if harmful consequences ensue.

The detonation of any nuclear device will inevitably disturb the ecological system to some degree, just as will the building of a highway, or the damming of a river. The responsible approach in planning a nuclear event is to estimate, in advance of the event, what the significant ecological consequences are likely to be. By reference to such an assessment, AEC/NVOO program planners are able to weigh any predicted detrimental effects against the benefits to be gained and to determine objectively whether "the detonation can be accomplished without injury to people, either directly or indirectly, and without unacceptable damage to the ecological system . . . ." Objective prediction of the ecological effects and the indirect radiological health hazards, if any, of any test under consideration therefore becomes a primary goal of the bioenvironmental safety studies.

Prediction of probable environmental disturbances is also the first step toward planning courses of action that will reduce undesirable effects to a minimum. Bioenvironmental studies are directed toward identifying those elements of the ecosystem that are most sensitive to disturbance and those environmental pathways

by which radionuclides might be transported to man. Vulnerability of many components of an ecological system is likely to be strongly dependent on seasonal factors; an understanding of this dependency may suggest ways to minimize hazards. For example, a proposed test site may have a dense wildlife population at one season of the year, and a relatively sparse population at another season. In a similar manner, the potential for transfer of radionuclides to humans via certain food chains may be high during one season but of little significance during another. Knowledge of such seasonal variations in ecosystem dynamics at a particular site can provide the basis for scheduling detonations during periods when detrimental consequences will be minimal.

Finally, when a nuclear shot is carried out, the bioenvironmental safety program must document the ecological consequences of the event. If a release of radioactivity occurs, immediate post-event bioenvironmental activities will be concerned with collection and analysis of samples of the biota and of environmental media such as soil and water. This effort will indicate (1) whether any components of the biota are accumulating radionuclide burdens that may be hazardous either to populations or to individuals and (2) whether radionuclides accumulated by species at the lower trophic levels are likely to reach man in significant amounts after passage through food chains. Early post-event surveys must also consider any prompt effects that ground motion and related disturbances may have had on plants and animals and on their habitats. Longer range post-event studies of radionuclide transport through the ecosystem (if radionuclide release occurs) and of direct effects on habitats and biota may be required to ensure human safety and to detect more subtle, but not necessarily unimportant, ecological changes. The post-event documentation of bioenvironmental consequences not only provides a necessary check on the reliability of pre-event predictions, but will also lead to improved predictive capabilities for subsequent events.

Bioenvironmental safety studies will vary widely in complexity, and consequently in time and manpower requirements, depending on the site location, the complexity and productivity of the ecosystem, and the nature of the nuclear detonation or series of detonations planned for the site. Deeply emplaced detonations, for which the probability of radionuclide release to the environment is considered low, may require relatively little attention to problems of nuclide transfer to man by environmental pathways, or radiation damage to the ecosystem. This is not to say that these prob-

lems can be completely ignored, since the escape of some radioactivity to the environment must be considered as a possibility.

On the other hand, deeply emplaced nuclear events, if of sufficiently high yield, may require a fairly detailed study of the ecosystem, directed mainly to evaluating its susceptibility to physical disturbance by ground motion, overpressure pulses in nearby water masses, and terrain alteration by formation of collapse craters.

Some of the kinds of bioenvironmental safety studies that may be required for different types of sites and nuclear detonations are discussed below. It is only in exceptional situations, such as a major nuclear construction project, that all of the types of studies mentioned might be employed.

DEVELOPING A BIOENVIRONMENTAL SAFETY PROGRAM

Because the problems to be dealt with are related to both the site and the event, bioenvironmental studies are planned and conducted with specific reference to each site and each event. However, it is possible to outline in a general way the approaches followed in organizing a bioenvironmental safety study. Figure 15.1 shows schematically the sequence of steps followed in planning and carrying out a typical program.

Whenever possible, bioenvironmental considerations enter into the site selection process, and sites are chosen that appear, on preliminary examination, to present the fewest bioenvironmental safety problems. However, site selection is likely to be made to a large degree on the basis of other factors, and after the choice is made it becomes the task of the bioenvironmental safety contractor to make a more detailed assessment of the potential ecological cost of the proposed event or events.

Absolute boundaries limiting the extent of the bioenvironmental safety investigations generally cannot be set at the start; approximate limits are arbitrarily taken, and they are constantly reevaluated as ecological data are collected and more refined predictions of physical effects are developed. The initial limits for the ecological studies are determined by evaluating the information available on such pertinent factors as site topography, land usage, and demography. Such factors as the proposed yield and emplacement of the device to be exploded are also taken into account. An estimate is obtained of the kinds and amounts of radionuclides that might be released. Preliminary estimates are made (or obtained from appropriate sources) of
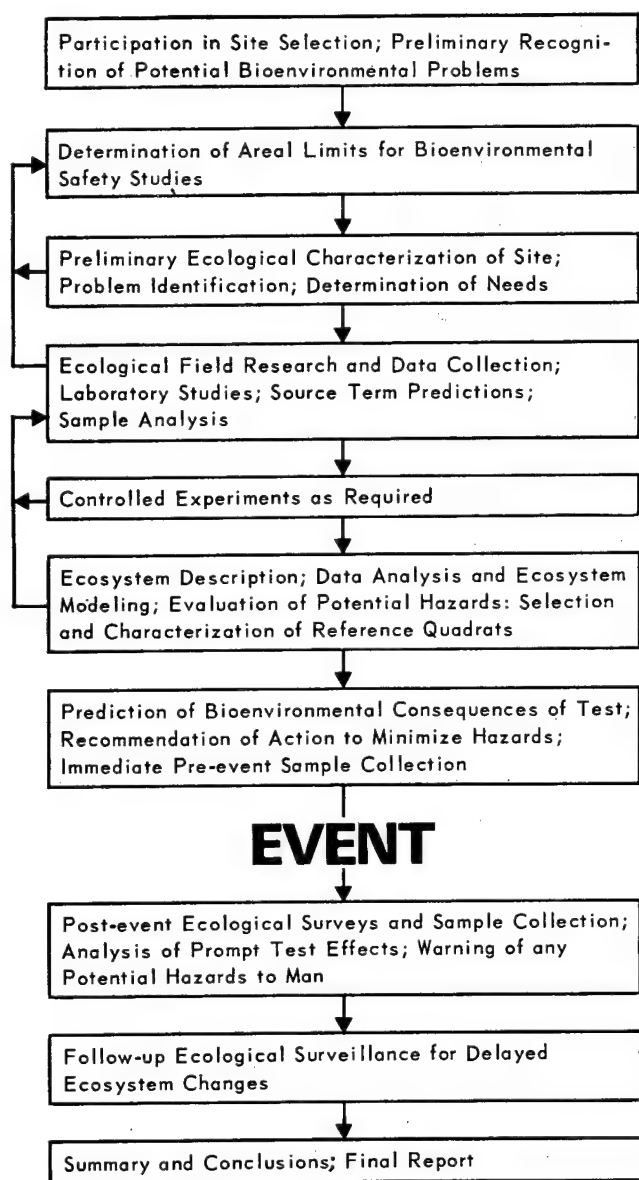
Figure 15.1. Steps in Organizing and Conducting a Bioenvironmental Safety Program.

Flowchart boxes (top to bottom):

- Participation in Site Selection; Preliminary Recognition of Potential Bioenvironmental Problems
- Determination of Areal Limits for Bioenvironmental Safety Studies
- Preliminary Ecological Characterization of Site; Problem Identification; Determination of Needs
- Ecological Field Research and Data Collection; Laboratory Studies; Source Term Predictions; Sample Analysis
- Controlled Experiments as Required
- Ecosystem Description; Data Analysis and Ecosystem Modeling; Evaluation of Potential Hazards: Selection and Characterization of Reference Quadrats
- Prediction of Bioenvironmental Consequences of Test; Recommendation of Action to Minimize Hazards; Immediate Pre-event Sample Collection

EVENT

- Post-event Ecological Surveys and Sample Collection; Analysis of Prompt Test Effects; Warning of any Potential Hazards to Man
- Follow-up Ecological Surveillance for Delayed Ecosystem Changes
- Summary and Conclusions; Final Report

ground shock, air blast, and probable areal distribution of fallout. Wherever available, input from other safety programs and from AEC laboratories is utilized in arriving at realistic estimates of these parameters. On the basis of these considerations it is possible to predict the approximate area that may be affected by the proposed event or events.

Once the study area is defined, the ecology of the area is characterized by field reconnaissance, literature study, and consultation with scientists personally acquainted with the region. This assessment brings into focus the relative importance of the various components of the ecosystem and helps to identify specific aspects of the system that require special study. Typical questions to which answers are sought illustrate the approach followed:

What are the habitats (for example, evergreen or deciduous forest, grassland, lakes and ponds, bogs or marshes, sea shore, inshore ocean waters, open ocean, etc.) found within the area of concern?

What principal types of plants, wildlife, and domestic animals occupy these habitats as year-round inhabitants or as migrants?

Which components of the natural biota are utilized by man and in what ways?

What agricultural crops and domestic animals are raised in the area of concern, and what are the seasonal production patterns?

Which of these biotic components or agricultural products are most likely to accumulate radionuclides and to what extent?

Is the area a habitat for any plant or animal species considered to be rare or threatened with extinction?

What is the general pattern of materials transfer within the area of interest, and what exchanges take place with adjacent areas?

Collection and analysis of existing information on these and similar questions help to identify critical problems and gaps in essential information that can only be filled by field and laboratory investigations.

An understanding of the dynamics of materials transport within and between the ecosystems of interest is basic to any meaningful prediction of the radiological consequences of a nuclear test. Radionuclides and their stable element counterparts tend to follow the same pathways and to undergo the same degree of dilution or concentration, and certain pathways may lead to man, thus resulting in his exposure to internal radiation if radionuclide release occurs.

In some instances it may be advantageous to use appropriate mathematical models that can simulate the transfer and cycling of materials in ecosystems. It is thus possible, by using a large digital computer and generalized ecosystem models, to predict radionuclide transport to man via environmental pathways. Similarly, mathematical models may be useful in assessing the potential impact of physical habitat disturbance on the biotic populations occupying the habitat. In applying computer simulation to hazards evaluation a practical approach consistent with the nature and location of the particular event is followed. A relatively sim-

ple model may suffice for a deeply emplaced shot designed for complete containment. On the other hand, a high-yield detonation within a complex environmental situation would require a much more sophisticated model to realistically estimate internal dosages to man. The required degree of sophistication is an unknown until at least some of the relevant factors are measured and their effect in the model evaluated.

The initial planning phase (determining areal limits for the bioenvironmental safety studies, making a general ecological characterization of the area and exploring hazards evaluation approaches) is followed by mission-oriented field research. The extent of this field effort may vary from a few site visits by ecologists skilled in the applicable disciplines, to intensive data collection programs extending through one or more years. Efforts are focused on those aspects of the ecological system judged most likely to be significantly affected by the proposed nuclear detonation, and on those components most likely to play a major role in the transfer of radionuclides to humans in the event of accidental release. Field investigations utilizing standard ecological techniques are conducted to obtain the data required to describe the composition and food chain dynamics of the important ecosystems and to determine which ecosystem components and processes are most sensitive to physical disturbance. These studies lead to objective estimates of the probable consequences of the nuclear detonation for the ecosystem and for man.

Since a bioenvironmental safety program involves not only prediction but also documentation of effects, the field studies provide detailed descriptive data on the pre-event status of representative sample areas within the larger areas of interest. Comparison of the pre- and post-event condition of these sample areas provides a direct basis for detecting and assessing the ecological effects of the test. If radionuclide release occurs, analysis of selected pre- and post-event reference samples from the test area is required to document any change in radionuclide burden due to the detonation.

A bioenvironmental safety investigation oriented to a given site may require the participation of specialists in several scientific disciplines. Biologists with various special fields of competence may play a major role in the investigations; the particular types of biological disciplines involved will depend on the site — on what habitat types and what biotic components predominate in the area of study. Along with the biologists, the bioenvironmental study team may include physicists, chemists, photogrammetrists, mathematicians, and systems analysts. The contributions required from each will be determined by the problems encountered at the particular site and by the nature of the events planned. Planning and interpretive functions are the responsibility of a technical management group with an ecological and systems analysis orientation. This approach is used because bioenvironmental safety studies deal with complex ecosystems in which natural processes can greatly alter the initial distribution of radionuclides, to the extent that man may be exposed to harmful levels of internal radiation. Effects on the ecosystem itself are also of concern, and a systems analysis approach may prove useful in estimating whether or not the system can withstand predicted perturbations without sustaining permanent or long-lasting damage.

METHODS OF INVESTIGATION

A bioenvironmental safety study comprises two major phases: (1) data collection and ecosystem description, and (2) data analysis and interpretation. These phases are not usually carried out in sequence, since in practice it is more productive to pursue both efforts simultaneously, with a gradual shift in emphasis toward Phase 2 as the investigation progresses. Some representative methods used in carrying out a program are cited below. Of course, not all of these methods will necessarily be required for every event.

The ecological description of any site at which it is proposed to carry out a nuclear detonation must include both the physicochemical setting and its associated complex of living organisms. The description must take into account both the dynamic and the static aspects of the ecosystem. It is essential for the ecologist to know which important plant and animal species are present in the area of concern and where they are located with respect to the site of the proposed shot. It is also necessary to determine how the various members of the biotic community interact with each other and with the physical environment. To the extent that release of radioactivity is considered probable, particular attention must be given to elucidating the pathways and rates by which chemical elements circulate through the ecosystem — the pathways by which man, as a consumer organism, could be exposed to internal radiation from radionuclides that may be released into the environment by a nuclear detonation, or by which other components of the biota may receive harmful radiation dosages.

An ecological description of the site will attempt to identify those ecosystem components that are most susceptible to the effects of site occupancy and preparation and the physical effects propagated from the

detonation. It will likewise indicate seasonal changes in the vulnerability of the biota or the physical environment to disturbance, thus enabling the scheduling of test events to minimize ecological effects.

DATA COLLECTION AND ECOSYSTEM DESCRIPTION

The methods employed in developing an ecological description of any site will depend on what kinds of existing habitat types and biotic communities are considered important in the area of interest. At an inland site, the ecosystem will characteristically include a terrestrial and possibly a freshwater phase. Different kinds of expertise and different techniques and equipment are required for investigation of these two aspects of the ecosystem. A site located on an island or near a seashore might include a marine phase as well, requiring still different scientific skills, equipment, and logistic support.

Terrestrial studies are concerned first of all with the distribution and composition of the major natural plant communities in the area of interest and, if any of the area is under cultivation, the distribution of forage and food crops. Knowledge of the vegetation becomes especially important if any release of radioactivity to the environment is anticipated. Depending on the degree of ground cover at event time, a substantial amount of fallout may be intercepted by plant foliage, and thereafter ingested directly by herbivorous animals. Fallout radionuclides reaching the soil may also become available to plants, and thence to herbivores, by entering the soil solution or becoming fixed on clay minerals or organic complexes in the soil.

Literature and Field Surveys

For many areas where detonations may be planned, the distribution of native and cultivated vegetation can be ascertained in considerable detail from the literature and from files of various state and federal agencies. The same is often true for relevant soil properties such as nutrient status, exchange capacity, and leaching characteristics. In such instances, only a minimal level of onsite surveys and field studies may be required to check the reliability of published information. In those few regions where the vegetation and soil have not been adequately characterized — certain parts of the tropics, for example — much more field work by plant ecologists and soil scientists may be necessary before the bioenvironmental safety of a proposed detonation or series of detonations can be adequately assessed.

If any considerable area is expected to be stripped of living plant cover by site preparation activities, or by postevent operations, the plant ecologist may need to ascertain what pioneering plant species are available to invade the denuded area, and how rapidly plant cover may be reestablished. This can be important because vegetational cover plays such an important role in regulating runoff of rainwater and snow melt in preventing erosion by wind and water, and in protecting watershed values.

To characterize the terrestrial ecosystem, other ecologists may need to collect information on the populations of vertebrate and invertebrate animals that occupy the different habitats in the area of interest. Many of these animals constitute the principal components in food chains leading to man. The technical literature can generally provide some information on what important species occupy the area, and on seasonal shifts in population density, migration patterns, and breeding habits of these species. To whatever extent the published sources are inadequate, field investigations may be required, utilizing appropriate study methods.

Important food chains, and particularly those in which humans are the ultimate consumers, must be identified and investigated. This involves tracing the food chain or food web through successively lower levels, finally leading to identification of the plant species that constitute the primary production. Chemical analyses of samples taken from different segments of the chain can provide data for modeling radionuclide transport through the ecological system, if this degree of sophistication in hazards evaluation becomes necessary.

For obvious reasons, attention must be focused mainly on those species that are eaten by man, or those that otherwise constitute important economic resources. However, any "rare" or "endangered" species occupying habitats that might be adversely affected by the proposed detonation are identified, so that special measures can be taken to avoid further endangering such species. Similar considerations, of course, apply in determining where emphasis is to be placed in the investigation of the freshwater and marine ecosystems.

The freshwater habitats of a site, if considered important, are studied in much the same way as the terrestrial phase, but the equipment and sampling methods are, of course, different. The production of organic matter by phytoplankton in lakes and ponds (net primary productivity) can be estimated indirectly by determining the total chlorophyll content of water samples. A

more precise measure of productivity may be obtained directly by determining the amount of carbon fixed per unit of time in a bottled sample of water exposed in the lake or pond from which it was taken. A comparable sample, with light excluded, is exposed for comparison. This is the standard "light and dark bottle" method; ^{14}C is frequently used in the samples to provide a convenient method for measuring carbon fixation. Other methods are used for determining the contribution of rooted aquatic plants to the system. Since the overall productivity is limited by primary productivity, the net primary production of a system gives an index to the system's potential ability to sustain populations of primary and secondary consumers (herbivores and carnivores). In addition, it provides an estimate of rates at which certain materials can be exchanged between the producers (plants) and their environment (in this case, water). Thus, measuring productivity is a simple, easy way to obtain preliminary estimates of potentially critical ecological parameters.

Population estimates of fish and invertebrates are made by the freshwater ecologist or fisheries biologist, using a variety of sampling techniques. Spawning areas are identified by field observation, and seasonal sequences of spawning and egg hatching are determined by periodic examination of suitable spawning sites. Food chain relationships are studied in essentially the same way as in the terrestrial phase, by analyzing the stomach contents of species eaten by man, and working down to successively lower trophic levels when such detail appears to be justified.

Water chemistry has a bearing on the uptake of elements by the aquatic biota, and hence would influence the uptake of any radionuclides introduced into the freshwater system. Samples are collected and analyzed for selected chemical elements, such as those that influence productivity (N, P, K, and certain trace nutrients), or those that have radioactive isotopes or counterparts that might be released by the nuclear detonation. Chemical analysis of selected samples may also be required to detect nonradioactive water pollutants that may be introduced as a result of construction or site preparation activities.

In situations where the bioenvironmental safety studies require investigation of a marine system, the complementary disciplines of physical oceanography and marine biology are employed. Information on currents, volume transport rates, mixing processes and turbulent diffusivities are obtained for the area under consideration, by reference to oceanographic data centers,

or by vessel cruises if necessary. These data are then utilized in a physical transport model to estimate dispersion and dilution rates for any radionuclides that may be vented or otherwise released into the marine environment by a nuclear detonation.

Marine ecology studies, if judged to be needed in a bioenvironmental safety program for a given site, are similar in approach to those described for the terrestrial and freshwater systems. Primary attention is given to the biology of marine species eaten by man, and especially to commercially important species that are harvested on a large scale. In some instances it may be sufficient to review catch statistics to ascertain seasons of the year when a venting accident would be least likely to affect a commercial fishery resource. By executing the event during one of those seasons, maximum time would be allowed for any radioactivity reaching the sea to become diluted to acceptable levels.

For detonations at sites very close to a seacoast, the potential effects of ground motion and water overpressures on marine life and habitats in the nearshore waters may have to be considered. Studies in the intertidal zone and shallow littoral waters, most likely to be affected by such forces, can be carried out from shore or from small boats.

Experimentation

Pre-event field or laboratory experimentation may sometimes be the most economical means for getting the data required for predicting ecological consequences of an event or for making hazards evaluations. For example, in considering the feasibility of conducting a series of deeply emplaced detonations, the potential effects of shock-generated water overpressure pulses on the inshore marine fauna of a nearby seacoast can be evaluated experimentally. Equipment has been designed and constructed to simulate the anticipated type of overpressure pulse, and has been used to ascertain the response of selected marine species to such overpressure.

Also, when a series of nuclear detonations is carried out at a given test site, each event offers an opportunity for planned experiments that will improve capabilities for effects predictions relative to subsequent events. Many such event-related ecological experiments have already been conducted and are being continued at NTS by such organizations as U. S. Public Health Service, Lawrence Radiation Laboratory, and the Civil Effects Test Organization. The bioenvironmental safety program may propose and conduct such experiments

for events at sites other than the NTS when it appears that they will contribute to the objectives of the program.

DATA ANALYSIS AND INTERPRETATION

The data collected from the literature, from field surveys, and from experiments must be systematically analyzed and interpreted to yield useful predictions regarding the consequences of the nuclear detonation under consideration. As will be seen from the discussion that follows, the interpretive function is to a large extent an application of the techniques of systems analysis. It should be emphasized that this procedure not only serves to utilize the available data in the most effective manner but also provides guidance as to the types of data and samples that need to be collected. At the other extreme, when bioenvironmental safety problems appear to be simple and few, the ecologist may be able to make adequate predictions without recourse to systems analysis methods.

Mathematical techniques are utilized as required to predict (1) the potential internal dosage to man and the potential radiological burden of important wildlife species from possibly released radionuclides, and (2) the effects on a population of a given wildlife species through either radiation, direct shock, or other environmental disturbance. Statistical techniques are employed to interpret the adequacy of the data being obtained.

Potential Internal Radiation Dose to Man

Mathematical simulation models may be used to predict the rates and quantities of radionuclide transfer through the environmental and food-chain pathways leading to man. The predicted rates and quantities of radionuclide ingestion by an individual or population are then used to estimate potential internal radiation doses to individuals, critical organs, critical population groups, and so forth. The generalized model for estimating internal (or external) dose due to a particular radionuclide is

$$D_i = Y_i f_i \int_{t_1}^{t_2} C_i(t) \, P_i(t) \, dt \text{ (rem)} \qquad (1)$$

The subscript i indicates the dependence of dose on a particular radionuclide and a particular exposure pathway.

The fallout input term $Y_i f_i$ (radionuclide yield x fraction deposited at a particular location) should be provided for each radionuclide of interest in units of radioactivity per unit area of surface. Predictions of radionuclide production, venting, fractionation, and initial fallout deposition patterns are required to estimate these values.

The dose commitment, $C_i(t)$, is the dose rate due to a unit intake of the ith radionuclide. It is shown as a function of time because the interval t_1 to t_2 may extend over a period of years during which parameters such as organ size, assimilation rates, elimination rates, and so forth, may vary as a function of age. For many potentially important radionuclides, the age-dependent parameter values required to calculate $C_i(t)$ are not readily available, but C_i values for most radionuclides can be normalized to Standard Man on the basis of data tabulated in the ICRP Report of Committee II.[1]

The investigation of exposure pathway terms, $P_i(t)$, is a major objective of any program designed to provide realistic estimates of potential internal radiation doses to man or to other organisms, either wild or domesticated. The potentially critical pathways of internal exposure are (1) inhalation and (2) ingestion of contaminated food and water. Usually, inhalation can be avoided by operational procedures which exclude people from areas in the direct line of fallout. In most cases, ingestion is the most important general pathway of internal exposure.

A network of ingestion pathways can be established by first analyzing the dietary habits of the populations of interest, and then identifying the ecosystem or ecosystems which serve as sources of the drinking water, foods, and other ingested materials (herb medicines for example) which comprise the total diet. The third step in this procedure is to define the trophic-dynamic position of each food source (such as plant, animal, or source of drinking water) in its ecosystem of origin. In cases where all but a small fraction of the potential internal dose can be attributed to a few radionuclides and a few exposure pathways, this may take the form of a simple food-chain analysis: pasture plants→cow →milk→man, or lichen→caribou→man, for example. In more complex cases, or in the initial phases of a comprehensive study, the analysis of trophic-dynamics with respect to items ingested by man involves the development of a network diagram showing the major pathways of material transfer between the major components in the specific ecosystems involved at the event site.

Figure 15.2 shows a preliminary network diagram developed for an area in which the human populations obtain their water from streams and their food supply from various ecosystems that can be classified as forest, agricultural (including domestic animals), marine
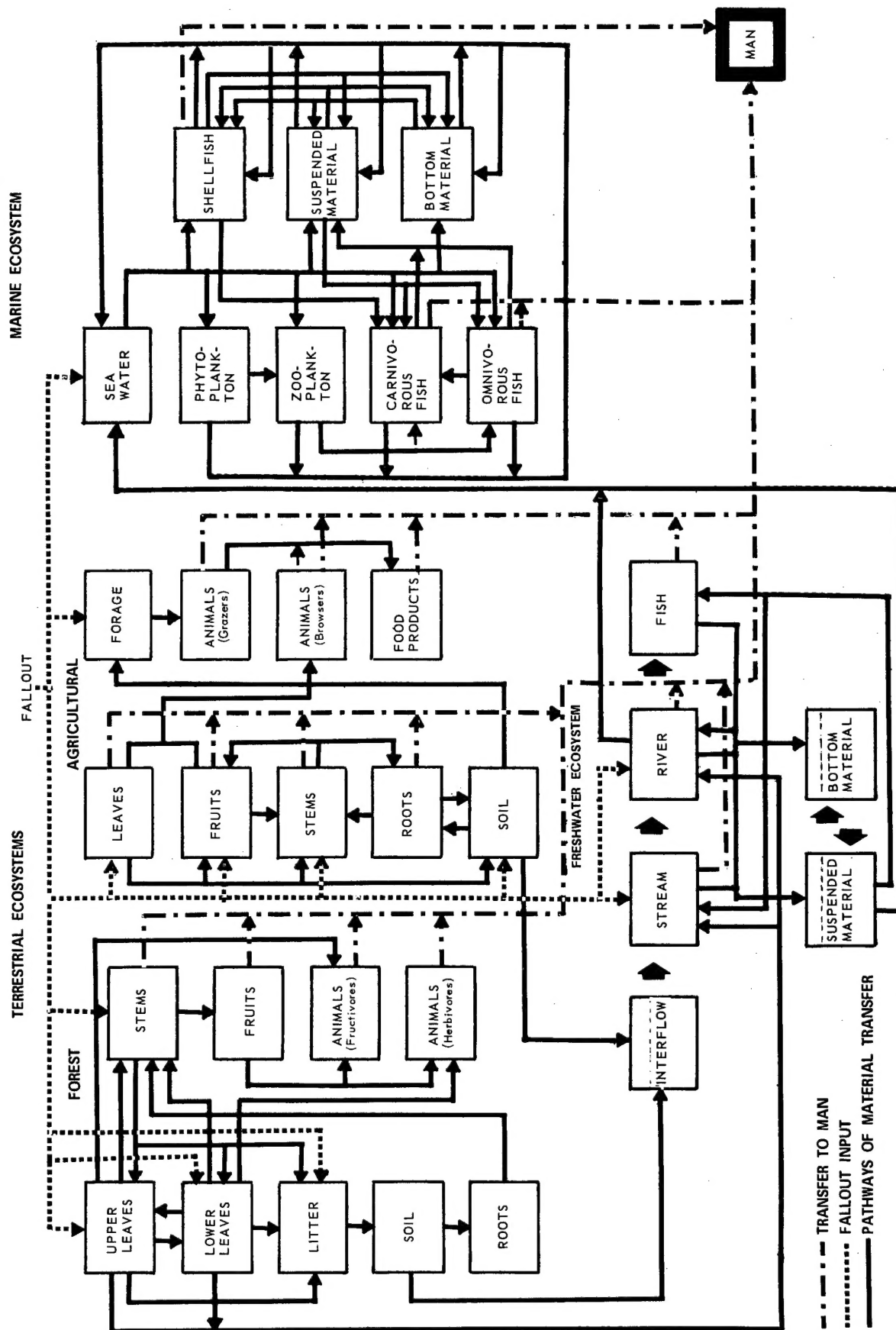
307

Figure 15.2. Generalized Materials Transfer Program.

(including estuarine), or fluvial. The compartments (boxes) in this diagram are generalized to show the more important interconnecting pathways within ecosystems and the principal output pathways to man. To avoid unnecessary complexity, minor or relatively unimportant pathways have been omitted from the diagram. In practice, each compartment is defined with reference to a particular dietary component and a particular human population. This means, in effect, that the specific network used to formulate a simulation model will depend on the cultural, demographic, and dietary data that characterize the population of reference and on the trophic-dynamic structure of the ecosystems which are the sources of dietary components.

Within the framework of the system depicted by the network diagram, the formulation of a simulation model is built up from knowledge of the transport mechanisms involved in different transfer pathways. Considering the whole network as a "black box", the fallout prediction provides input data, $Y_i f_i$, in units of radioactivity per unit area for different radionuclides while the output can be expressed as the amount of radionuclide ingested as a function of time, $\sum P_i(t)$, or as potential internal dose as a function of time, $D_i(t)$, after fallout.

For the food-chain transfers, it is reasonable to assume initially that the rate of elimination from a given compartment will follow a simple exponential law, equation (2), if the input to that compartment were suddenly reduced to zero, that is:

$$\frac{dX_j}{dt} = -\lambda_{jj} X_j \qquad (2)$$

where

X_j is the concentration of the ith radionuclide in the jth compartment, and

λ_{jj} is the elimination rate coefficient (d^{-1}) for the ith radionuclide from the jth compartment.

This assumption is employed by the ICRP Report of Committee II[1], and by various other groups attempting to deal with such problems. For example, see NAS-NRC Publication 985[2].

The net flux of a radionuclide (or other material) to a given biological compartment in the network can now be formulated as shown by equation (3).

$$\frac{dX_k}{dt} = \sum_{j=o}^{n} \lambda_{jk} X_j - \sum_{j=o}^{n} \lambda_{kj} X_k \qquad (3)$$
$$j \neq k$$

where,

Compartment K is the compartment of reference and all other compartments are designated j:

jk is an input pathway,

kj is an output pathway,

X_j and X_k are the concentrations of the same radionuclide or other material in the jth and k^{th} compartments,

λ_{jk} and λ_{kj} are input and output transfer coefficients having dimensions of reciprocal days.

On the basis of equation (3) the transfer of a radionuclide or other material through the network of coupled compartments can be simulated mathematically by a system of simultaneous ordinary differential equations. Sensitivity analysis will then identify the critical parameters and critical pathways providing, simultaneously, a basis for simplifying the network and for guiding field studies to concentrate on those measurements which are most needed to improve the accuracy of the simulation model.

Reference to Figure 15.2 will suggest that there are some intercompartmental pathways involving physical transport mechanisms — and the same may be true of certain predator-prey and soil-plant relations — which may not be adequately represented by the linear model, equation (3). Since the actual simulations are accomplished by numerical computer techniques, it is quite feasible to include nonlinear functions in the model — if the experimental evidence so requires — and comparisons between linear and nonlinear models will indicate the sensitivity of the results to the kind of model employed.

The application of a comprehensive model such as the one outlined above requires a considerable knowledge of the human populations and ecosystems of reference. When based on data collected in the particular area of reference, the general model can be made quite specific, and realistic estimates of potential dose can be obtained for a wide variety of possible circumstances. In many cases, a much simpler approach may be justified and sufficient. If the probability of radionuclide release to the biosphere is very low, and if the maximum amounts of radionuclides that could be released are very small, a simple model based on ultraconservative assumptions may suffice. For example, one can estimate the maximum specific activities of vented material and assume that man obtains his daily mineral requirements from food with the same specific activities. This, of course, is an unduly conservative assumption, and calculations based on it will yield unrealistically high estimates of potential dose; but if

these estimates fall within the acceptable range, it is obvious that no further refinement is necessary. The assessment of potential radiological hazards related to a nuclear test or application involving a high probability that large quantities of radionuclides will be released to the bioenvironment will require the use of more sophisticated models to provide more realistic estimates of potential dose. If the populations and ecosystems of reference are not well known, more field and laboratory study may be required to identify the potentially critical pathways, to determine the transport mechanisms involved, and to obtain estimates of the parameter values required to formulate realistic simulation models.

Potential Effects on Ecosystems and Animal Populations

The potential effects of a nuclear detonation on populations or communities of plants and animals (other than man) and on their physical environments (habitats) can probably be attributed (1) to releases of radioactive materials to the environment, and (2) to ancillary activities such as site preparation or drilling operations. This is obviously a much wider range of potential effects than usually considered in assessing the potential consequences to man. However, the geographical range of effects implied by item (2) is mostly confined to close-in onsite areas, and as a consequence the study area for predicting effects of this type is relatively small.

The potential radiation doses to plant and animal populations can be estimated by the same general model as that outlined for man. Doses to plants and animals are likely to be higher than those to man because (1) the plants may occur in areas of high initial concentration from which man can be excluded, and (2) fallout intercepted by plant foliage becomes directly available to herbivorous animals. Most presently available information suggests that plants and many animals are less sensitive than man to radiation effects, although exceptions to this generalization no doubt exist. Radiation protection standards such as those established for humans have not been recognized for plants and animals, and it would be unrealistic to devote the same degree of effort to protecting individual plants or animals that is accorded to protecting individual humans. On the other hand, the bioenvironmental safety program takes cognizance of any potential hazards to entire species or to rare or commercially valuable plant and animal populations.

Methods for assessing potential ecological effects of environmental disturbance due to the detonation per se

or to ancillary activities are more difficult to describe precisely. As mentioned above, these effects are usually confined to close-in areas and therefore not of as wide concern even though the local disturbance may be drastic. No generalized modeling has been attempted for this kind of problem for the simple reason that it can take a wide variety of forms, each of which should be analyzed on the basis of its own merits.

One generalization that may be of some value in planning is related to the concept of ecosystem stability. It is a common observation, for example, that animal populations in ecosystems characterized by a large number of species and trophic levels and by environmental conditions that are relatively uniform (tropical rain forest, for example) are more stable than in ecosystems characterized by a small number of species and, by more severe or more variable environmental conditions (arctic tundra, for example). In this sense, ecosystem stability has been related to the pattern of interaction among the species comprising the biotic portion of the ecosystem and the number of equally probable pathways by which energy and materials may move from one population or trophic level to another[3]. Thus, a system composed of many species at each trophic level, each species having a wide variety of food species, will be more stable than one composed of few species, each of which feeds on only one or a few other species. In the present frame of reference, the significant implication of this concept is the expectation that the effects of environmental disturbance on plant and animal populations are likely to be most severe in ecosystems of the second kind (few species, severe environmental conditions) and least severe in ecosystems of the first kind (many species, mild environmental conditions). In less rigorous terms, perturbation of an apparently simple ecosystem may result in drastic population responses and slow recovery following the disturbance. An equal perturbation of an apparently complex system may result in only minor population responses and be followed by rapid recovery after disturbance.

In many situations, the important problems will be so obvious to the ecologist that sophisticated analyses of population and/or community stability will not be required. In areas characterized by slow-growing vegetation and poor soils, disturbance leading to denudation will probably be followed by slow recovery and, in some cases at least, specific efforts to hasten revegetation should be considered. As noted above, potential effects of shock waves or other physical forces on individuals of important wildlife species can some-

times be assessed directly by experimentation, if there is any reasonable basis for suspecting that there may be significant damage. Potential effects on animal populations are more difficult to assess because the significant responses may be delayed, and they may come about indirectly due to habitat destruction or disturbances that may be detrimental to the food supply of the species or beneficial to its natural enemies (diseases, parasites, or predators). In general, we can anticipate that species having a limited choice of food species and a narrow range of habitat requirements are most likely to be adversely affected by environmental disturbance.

Unless the species or a local population of the species is virtually confined to areas relatively close to the shot point, it can be anticipated that the only long-term effects of any consequence to the population as a whole will be a reduction of maximum population size proportional to the extent of habitat destruction.

CONCLUSION

In the testing of nuclear devices, bioenvironmental safety investigations are concerned with direct and indirect effects of tests, including engineering and related activities, on the environment, and with potential exposure of people to radiation via indirect environmental pathways. Objectives include preshot prediction of effects, recommendation of courses of action to mitigate significant adverse effects, and postshot documentation of ecological consequences.

The methods used to achieve these objectives are the usual techniques of applied ecology: mission-oriented ecological surveys, analysis of ecosystem dynamics, experimentation when required, and application of relevant ecosystem models for predictive purposes. These concepts are equally applicable to any type of nuclear detonation, but the bioenvironmental safety problems encountered will vary with the location and with the type of event. In general, the safety standards and the basic approaches to ensure that detonations meet those standards will remain the same. As the use of nuclear explosives advances from the testing phase into practical utilization in engineering projects, mining, and related uses, the same type of bioenvironmental safety efforts will be required, and the methods now being developed and used will be adaptable to future needs.

REFERENCES

1. International Commission on Radiological Protection (ICRP), "Report of Committee II on Permissible Dose for Internal Radiation," Pergamon Press, Oxford, 1959

2. National Academy of Sciences - National Research Council, "Disposal of Low-Level Radioactive Waste into Pacific Coastal Waters," NAS-NRC Publication 985, Washington, D. C., 1962

3. MacArthur, Robert, "Fluctuations of Animal Populations, and a Measure of Community Stability," Ecology 36, pp. 533-536, 1955